

Effects of heat shock, hypoxia, post-mortem interval and glioma disease state on heat shock gene *HSPA* expression

by

Glenda Maria Beaman

A thesis submitted in partial fulfilment for the requirements of the degree of
Doctor of Philosophy at the University of Central Lancashire

May 2012

Student Declaration

I declare that while registered as a candidate for the research degree, I have not been a registered candidate or enrolled student for another award of the University or other academic or professional institution.

I declare that no material contained in the thesis has been used in any other submission for an academic award and is solely my own work.

Signature of Candidate

Type of Award **Doctor of Philosophy**

School **School of Forensic and Investigative Sciences**

Abstract

Heat shock protein 70 (*HSPA/HSP70*) gene expression is induced by a wide range of cellular stress conditions. This study investigated *HSPA/HSP70* expression in human cell lines exposed to hypoxic conditions, in cancerous and non-cancerous brain tissue specimens from 18 patients (gliomas and normal conditions), and in post mortem rat brain samples exposed to heat shock.

Three human glioma cell lines were chosen for this study, each representing various types of glioma: (astrocytoma, oligodendroglioma and glioblastoma), with a normal human astrocyte cell line used as a control. In addition, 18 clinical brain tissue samples were also examined. *HSPA* RNA transcripts and proteins were examined in these samples using qRT-PCR, immunofluorescence and flow cytometry techniques.

The average *HSPA* mRNA copy numbers detected in glioblastoma tissue were 1.8 and 8.8 fold higher respectively than in lower grade glioma and control tissues, which is suggestive of a grade related transcription profile. Similar patterns of grade related expression were also observed in corresponding cell lines. The percentage of cells showing positive for *HSPA* protein in normal cell lines increased from 0 to 33% immediately after exposure to hypoxia, and gradually declined to 11% 24 h after treatment. However, the effects of hypoxia were marginal in glioma cells, due to the already elevated levels of *HSPA*. Although hypoxia induced *HSPA* expression in normal cells, it did not achieve the same level of induction in cancer cells, suggesting that there are other factors which contribute to the induction of *HSPA*. These results suggest that *HSPA* is induced in cancer cells, not only by hypoxia, but also by other factors. In addition, this study indicated for the first time that *HSPA* expression in

glioma cells may possibly be grade related, and thus may have value as a prognostic marker. However a greater sample size is needed to validate such findings.

This study showed that *HSPA* is expressed at low levels in normal brain tissue, but was more highly expressed in brain tissue subjected to mild heat shock. The levels of *HSPA* transcripts in heat shocked post mortem brain tissue showed a marked increase in *HSPA* expression.

GAPDH was used as a control gene for these studies, and exhibited a consistent level of expression in normal and tumourous cell lines and tissue samples under normal and hypoxic conditions, and also in post mortem tissues exposed to heat shock. For *Homo sapiens GAPDH*, the average transcript numbers for normal and tumourous cell lines and brain tissue samples were approximately 145,000 copies per sample. For *Rattus norvegicus GAPDH*, levels were higher than for human samples, at an average of 268,300 copies per sample. The consistency of these results confirms that *GAPDH* was a suitable candidate gene for the purpose of this study.

Early in the post-mortem period, *HSPA* is expressed more highly in tissues subjected to single and multiple heat shocks compared to controls. However, later post-mortem intervals of between 3 - 24 h demonstrated inconsistent and irregular results, with no predictive or reproducible patterns. Therefore, although there is demonstrable *de novo* expression of *HSPA* in post mortem brain tissue in response to heat shock, it is difficult to predict the full parameters of this induction, probably as a result of other forms of cellular stress affecting these tissues under our experimental methodology. These initial studies indicate that the use of *HSPA* with the methodologies employed here are not suitable as an accurate indicator of post-mortem interval.

Table of Contents

STUDENT DECLARATION	2
ABSTRACT	3
ACKNOWLEDGEMENTS	27
ABBREVIATIONS	28
CHAPTER 1	39
INTRODUCTION	39
1.1 MOLECULAR CHAPERONES AND HEAT SHOCK PROTEINS	40
1.2 HEAT SHOCK PROTEINS	68
1.2.1 Heat Shock Protein 27 (HSPB).....	68
1.2.2 Heat Shock Protein 40 (DNAJ).....	71
1.2.3 Heat Shock Protein 60 (HSPD).....	74
1.2.4 Heat Shock Protein 90 (HSPC).....	76
1.2.5 Heat Shock Protein 70 (HSPA).....	78
1.2.5.1 Polymorphisms in HSP70 genes	88
1.3 ACTIVATION OF HSPA/HSP70	91
1.3.1 Heat shock.....	91
1.3.1 Glioma.....	93
1.3.2 Hypoxia	101
1.3.3 Post-mortem conditions	103
1.4 AIMS OF RESEARCH	111
CHAPTER 2	113
MATERIALS AND METHODS	113
2.1 CELL CULTURE	114

2.1.1	Tissue samples, cell lines and culture conditions	114
2.1.2	Media and Reagents	116
2.1.3	Preparation of Media.....	116
2.1.4	Resuscitation of Cells.....	117
2.1.5	Subculture	118
2.1.6	Hypoxia Treatment.....	118
2.1.7	Trypsinisation.....	118
2.1.8	Cell Quantification	119
2.2	MRNA ISOLATION.....	120
2.2.1	Quantification of nucleic acids by UV spectrophotometry.....	124
2.2.2	Analysis of Nucleic acid by agarose gel electrophoresis	124
2.3	COMPLIMENTARY DNA SYNTHESIS (CDNA).....	125
2.4	PRIMER PREPARATION.....	128
2.5	REAL-TIME QUANTITATIVE REVERSE TRANSCRIPTASE POLYMERASE CHAIN REACTION (QRT-PCR).....	128
2.6	ANALYSIS OF QRT-PCR.....	134
2.6.1	Agarose gel electrophoresis	134
2.7	QUANTIFICATION ANALYSIS OF QRT-PCR.....	134
2.8	IMMUNOFLUORESCENCE	134
2.9	FLOW CYTOMETRY	135
2.10	<i>RATTUS NORVEGICUS</i> BRAIN TISSUE	137
2.11	TREATMENT	138
2.11.1	Induction of mild heat shock.....	138
2.11.2	Induction of multiple heat shock.....	138
2.12	DNA EXTRACTION.....	139
2.12.1	Quantification of nucleic acids.....	141

2.12.2. Analysis of Nucleic acid by agarose gel	142
2.12.3. Quantification analysis of qRT-PCR	142
2.14 mRNA ISOLATION	142
2.15 COMPLIMENTARY DNA SYNTHESIS (cDNA)	144
2.16 PRIMER PREPARATION	144
2.17 REAL-TIME QUANTITATIVE REVERSE TRANSCRIPTASE POLYMERASE CHAIN REACTION (QRT-PCR)	144
2.18 QUANTIFICATION ANALYSIS OF QRT-PCR	148
2.19 CRYOSTAT	148
2.20 IMMUNOFLUORESCENCE	148
2.21 STATISTICAL ANALYSIS	148
CHAPTER 3	150
DEVELOPMENTAL WORK	150
3.1 DEVELOPMENTAL WORK	151
3.2 TISSUE SAMPLES AND CELL LINES	151
3.3 INTRODUCTION AND HISTORY OF BIOINFORMATICS	152
3.4 CANDIDATE GENES	153
3.5 GENE LOCATION	155
3.6 NUCLEOTIDE SEQUENCES	156
3.7 PRIMER DESIGN	157
3.7.1 Primer Specificity.....	157
3.7.2 Primer Length.....	157
3.7.3 Primer Melting (Annealing) Temperature (T _m)	158
3.7.4 Primer GC content	158
3.7.5 Product Length (Amplicon Size)	159
3.7.6 Experimental design of Primers	159

3.8 SEQUENCE HOMOLOGY FOR <i>HSP70</i> BETWEEN <i>HOMO SAPIENS</i> AND <i>RATTUS NORVEGICUS</i>	160
3.9 SPECTROPHOTOMETRY	163
3.10 OPTIMIZATION OF PRIMER CONCENTRATIONS	165
3.11 REAL-TIME REVERSE TRANSCRIPTION POLYMERASE CHAIN REACTION (RT-PCR)	166
3.11.1 Detection Chemistry used in RT-PCR	166
3.11.2 Melting Curve Analysis	167
3.12. STANDARD CURVE FOR HOUSE KEEPING GENE <i>GAPDH</i>	169
3.13 REFERENCE GENES	178
3.14 REAL TIME PCR ASSAY	179
CHAPTER 4	180
HSPA GENE EXPRESSION IN GLIOMA CELLS AND BRAIN TISSUE...	180
4.1 GENE EXPRESSION	181
4.2 CONSTITUTIVE EXPRESSION	183
4.2.1 Glioma Cell lines	184
4.2.2 Statistical Analysis	185
4.2.3 Brain Tissue Samples	189
4.2.4 Statistical Analysis	195
4.3 IMMUNOFLUORESCENCE	202
4.4 FLOW CYTOMETRY	208
4.4.1 Statistical Analysis	211
CHAPTER 5	218
EFFECTS OF HYPOXIA ON <i>HSPA</i> GENE EXPRESSION IN GLIOMA ..	218
5.1 GENE EXPRESSION	219

5.2	CONSTITUTIVE EXPRESSION	221
5.2.1	Glioma Cell lines	221
5.2.2	Statistical Analysis	225
5.3	IMMUNOFLUORESCENCE	230
5.4	FLOW CYTOMETRY	256
5.4.1	Statistical Analysis	259
CHAPTER 6	284
EFFECTS OF HEAT SHOCK TREATMENT ON <i>HSPA</i> GENE EXPRESSION IN RAT BRAIN TISSUE.....		
6.1	GENE EXPRESSION	285
6.2	CONSTITUTIVE EXPRESSION	287
6.2.1	Rat Brain tissue	287
6.2.2	Statistical Analysis	301
6.2.3	Rat Brain tissue - thermotolerance.....	313
6.2.4	Statistical Analysis	324
6.3	IMMUNOFLUORESCENCE	335
CHAPTER 7	349
DISCUSSION	349
7.1.	DISCUSSION.....	35049
7.1.1	Chapter 3 results.....	350
7.1.2	Chapter 4 and 5 results.....	356
7.1.3	Chapter 6 results.....	361
7.2	SUMMARY	368
CHAPTER 8	376
REFERENCES	376

8.1 REFERENCES	377
8.2 WEBSITES	429
CHAPTER 9	431
APPENDIX	431

List of Figures

Figure 1.1. Representation of a light microscope image of <i>Ritossa</i> 's chromosomal puffs, which are characterised by localized swellings of specific regions of a polytene chromosome.	44
Figure 1.2. Diagram showing the conditions that induce heat shock in response to environmental, physiological and non-stressful conditions	54
Figure 1.3 Schematic diagram showing the stress defence mechanism mediated by heat shock proteins.	56
Figure 1.4. Regulation of transcription of heat shock protein genes by heat shock factor.	61
Figure 1.5. The general structural and regulatory features of HSFs.	63
Figure 1.6. Heat shock factor regulation	65
Figure 1.7. Regulation of the heat shock response and the HSF cycle.	67
Figure 1.8 Chaperone-assisted protein folding	80
Figure 1.9. Phylogenetic tree of 17 human HSPA proteins	83
Figure 1.10. Localization of the three <i>HSPA</i> genes (H = HSPA1L, 1 = HSPA1A, 2 = HSPA1B).	87
Figure 1.11. Magnetic resonance imaging showing features of pilocytic astrocytomas	94
Figure 1.12. Magnetic resonance imaging showing features of a diffuse astrocytomas	95
Figure 1.13. Magnetic resonance imaging showing features of an anaplastic astrocytomas.....	96
Figure 1.14. Magnetic resonance imaging features of glioblastoma multiforme.....	97
Figure 1.15. The temperature-time of death relating nomogram	105
Figure 2.1 A diagrammatic representation of the principals involved in extracting mRNA from culture cells and tissue using the mRNA	123
Figure 3.1 Locations of human genes used in this study	155

Figure 3.2 An example of a melting (dissociation) curve produced for rat <i>GAPDH</i> ...	168
Figure 3.3 Quantification Curve of known concentrations of rat DNA.....	173
Figure 3.4 Standard curve produced from quantification curve of known concentrations of rat DNA.....	174
Figure 3.5 Quantification Curve of known concentrations of human DNA	176
Figure 3.6 Standard curve produced from quantification curve of known concentrations of human DNA.....	177
Figure 4.1 <i>HSPA</i> and <i>GAPDH</i> transcript levels in NHA, 1321N1, GOS-3 and U87-MG cell lines.	184
Figure 4.2 <i>HSPA</i> mRNA copy number in 18 brain tissue samples.....	192
Figure 4.3 <i>GAPDH</i> mRNA in 18 brain tissue samples.....	193
Figure 4.4 Histogram showing the mean <i>HSPA</i> mRNA copy number in brain tissues grouped by: Glioblastomas (n = 12), low grade gliomas (n = 3) and normal tissues (n = 3).	194
Figure 4.5 <i>HSPA</i> protein levels assessed using immunofluorescence in untreated NHA cells.	204
Figure 4.6 <i>HSPA</i> protein levels assessed using immunofluorescence in untreated 1321N1 cells.	205
Figure 4.7 <i>HSPA</i> protein levels assessed using immunofluorescence in untreated GOS-3 cells	206
Figure 4.8 <i>HSPA</i> protein levels assessed using immunofluorescence in untreated U87-MG cells.....	207
Figure 4.9 Average percentages of cells showing positive for <i>HSPA</i>	210
Figure 4.10 2D scatter plots and fluorescence intensity histograms of <i>HSPA</i> protein levels for the NHA cell lines.....	213

Figure 4.11 2D scatter plots and fluorescence intensity histograms of HSPA protein levels for the 1321N1 cell lines.....	214
Figure 4.12 2D scatter plots and fluorescence intensity histograms of HSPA protein levels for the GOS-3 cell lines.	215
Figure 4.13 2D scatter plots and fluorescence intensity histograms of HSPA protein levels for the U87-MG cell lines.	216
Figure 5.1 Levels of <i>HSPA</i> mRNA transcripts in pre- and post-hypoxia treated NHA, 1321N1, GOS-3 and U87-MG cells.....	223
Figure 5.2 Levels of <i>GAPDH</i> mRNA transcripts in pre and post hypoxia treated NHA, 1321N1, GOS-3 and U87-MG cells.....	224
Figure 5.3 HSPA protein levels assessed using immunofluorescence for negative control of un-treated NHA cells.	232
Figure 5.4 HSPA protein levels assessed using immunofluorescence in untreated NHA cells.	233
Figure 5.5 HSPA protein levels assessed using immunofluorescence in in post hypoxia treated NHA cells after 0 h recovery.....	234
Figure 5.6 HSPA protein levels assessed using immunofluorescence in in post hypoxia treated NHA cells after 3 h recovery.....	235
Figure 5.7 HSPA protein levels assessed using immunofluorescence in in post hypoxia treated NHA cells after 6 h recovery.....	236
Figure 5.8 HSPA protein levels assessed using immunofluorescence in in post hypoxia treated NHA cells after 24 h recovery.....	237
Figure 5.9 HSPA protein levels assessed using immunofluorescence for negative control of un-treated 1321N1 cells.....	238
Figure 5.10 HSPA protein levels assessed using immunofluorescence in untreated 1321N1 cells.	239

Figure 5.11 HSPA protein levels assessed using immunofluorescence in in post hypoxia treated 1321N1 cells after 0 h recovery.	240
Figure 5.12 HSPA protein levels assessed using immunofluorescence in in post hypoxia treated 1321N1 cells after 3 h recovery.	241
Figure 5.13 HSPA protein levels assessed using immunofluorescence in in post hypoxia treated 1321N1 cells after 6 h recovery.	242
Figure 5.14 HSPA protein levels assessed using immunofluorescence in in post hypoxia treated 1321N1 cells after 24 h recovery.	243
Figure 5.15 HSPA protein levels assessed using immunofluorescence for negative control of un-treated GOS-3 cells.	244
Figure 5.16 HSPA protein levels assessed using immunofluorescence in untreated GOS-3 cells.	245
Figure 5.17 HSPA protein levels assessed using immunofluorescence in in post hypoxia treated GOS-3 cells after 0 h recovery.	246
Figure 5.18 HSPA protein levels assessed using immunofluorescence in in post hypoxia treated GOS-3 cells after 3 h recovery.	247
Figure 5.19 HSPA protein levels assessed using immunofluorescence in in post hypoxia treated GOS-3 cells after 6 h recovery.	248
Figure 5.20 HSPA protein levels assessed using immunofluorescence in in post hypoxia treated GOS-3 cells after 24 h recovery.	249
Figure 5.21 HSPA protein levels assessed using immunofluorescence for negative control of un-treated U87-MG cells.	250
Figure 5.22 HSPA protein levels assessed using immunofluorescence in untreated U87-MG cells.	251
Figure 5.23 HSPA protein levels assessed using immunofluorescence in in post hypoxia treated U87-MG cells after 0 h recovery.	252

Figure 5.24 HSPA protein levels assessed using immunofluorescence in in post hypoxia treated U87-MG cells after 3 h recovery.....	253
Figure 5.25 HSPA protein levels assessed using immunofluorescence in in post hypoxia treated U87-MG cells after 6 h recovery.....	254
Figure 5.26 HSPA protein levels assessed using immunofluorescence in in post hypoxia treated U87-MG cells after 24 h recovery.....	255
Figure 5.27 Average percentage of cells showing positive for HSPA in pre and post hypoxia treatment.....	258
Figure 5.28 2D scatter plots and fluorescence intensity histograms of HSPA protein levels for the NHA cell lines pre hypoxia treatment.....	263
Figure 5.29 2D scatter plots and fluorescence intensity histograms of HSPA protein levels for the NHA cell lines post hypoxia treatment after 0 h recovery.....	264
Figure 5.30 2D scatter plots and fluorescence intensity histograms of HSPA protein levels for the NHA cell lines post hypoxia treatment after 3 h recovery.....	265
Figure 5.31 2D scatter plots and fluorescence intensity histograms of HSPA protein levels for the NHA cell lines post hypoxia treatment after 6 h recovery.....	266
Figure 5.32 2D scatter plots and fluorescence intensity histograms of HSPA protein levels for the NHA cell lines post hypoxia treatment after 24 h recovery.....	267
Figure 5.33 2D scatter plots and fluorescence intensity histograms of HSPA protein levels for the 1321N1 cell lines pre hypoxia treatment.....	268
Figure 5.34 2D scatter plots and fluorescence intensity histograms of HSPA protein levels for the 1321N1 cell lines post hypoxia treatment after 0 h recovery.....	269
Figure 5.35 2D scatter plots and fluorescence intensity histograms of HSPA protein levels for the 1321N1 cell lines post hypoxia treatment after 3 h recovery.....	270
Figure 5.36 2D scatter plots and fluorescence intensity histograms of HSPA protein levels for the 1321N1 cell lines post hypoxia treatment after 6 h recovery.....	271

Figure 5.37 2D scatter plots and fluorescence intensity histograms of HSPA protein levels for the 1321N1 cell lines post hypoxia treatment after 24 h recovery.....	272
Figure 5.38 2D scatter plots and fluorescence intensity histograms of HSPA protein levels for the GOS-3 cell lines pre hypoxia treatment.	273
Figure 5.39 2D scatter plots and fluorescence intensity histograms of HSPA protein levels for the GOS-3 cell lines post hypoxia treatment after 0 h recovery.	274
Figure 5.40 2D scatter plots and fluorescence intensity histograms of HSPA protein levels for the GOS-3 cell lines post hypoxia treatment after 3 h recovery.	275
Figure 5.41 2D scatter plots and fluorescence intensity histograms of HSPA protein levels for the GOS-3 cell lines post hypoxia treatment after 6 h recovery.	276
Figure 5.42 2D scatter plots and fluorescence intensity histograms of HSPA protein levels for the GOS-3 cell lines post hypoxia treatment after 24 h recovery.	277
Figure 5.43 2D scatter plots and fluorescence intensity histograms of HSPA protein levels for the U87-MG cell lines pre hypoxia treatment.....	278
Figure 5.44 2D scatter plots and fluorescence intensity histograms of HSPA protein levels for the U87-MG cell lines post hypoxia treatment after 0 h recovery.....	279
Figure 5.45 2D scatter plots and fluorescence intensity histograms of HSPA protein levels for the U87-MG cell lines post hypoxia treatment after 3 h recovery.....	280
Figure 5.46 2D scatter plots and fluorescence intensity histograms of HSPA protein levels for the U87-MG cell lines post hypoxia treatment after 6 h recovery.....	281
Figure 5.47 2D scatter plots and fluorescence intensity histograms of HSPA protein levels for the U87-MG cell lines post hypoxia treatment after 24 h recovery.	282
Figure 6.1 Transcription levels of <i>HSPA</i> mRNA in non-heat shock and heat shocked rat brain tissue at 0 h PMI.	291
Figure 6.2 Transcription levels of <i>HSPA</i> mRNA in non-heat shock and heat shocked rat brain tissue at 3 h PMI.	292

Figure 6.3 Transcription levels of <i>HSPA</i> mRNA in non-heat shock and heat shocked rat brain tissue at 6 h PMI.	293
Figure 6.4 Transcription levels of <i>HSPA</i> mRNA in non-heat shock and heat shocked rat brain tissue at 12 h PMI.	294
Figure 6.5 Transcription levels of <i>HSPA</i> mRNA in non-heat shock and heat shocked rat brain tissue at 24 h PMI.	295
Figure 6.6 Transcription levels of <i>GAPDH</i> mRNA in non-heat shock and heat shocked rat brain tissue at 0 h PMI.	296
Figure 6.7 Transcription levels of <i>GAPDH</i> mRNA in non-heat shock and heat shocked rat brain tissue at 3 h PMI.	297
Figure 6.8 Transcription levels of <i>GAPDH</i> mRNA in non-heat shock and heat shocked rat brain tissue at 6 h PMI.	298
Figure 6.9 Transcription levels of <i>GAPDH</i> mRNA in non-heat shock and heat shocked rat brain tissue at 12 h PMI.	299
Figure 6.10 Transcription levels of <i>GAPDH</i> mRNA in non-heat shock and heat shocked rat brain tissue at 24 h PMI.	300
Figure 6.11 Estimated marginal means of <i>HSPA</i> transcript copy numbers at 0 h PMI	303
Figure 6.12 Estimated marginal means of <i>HSPA</i> transcript copy numbers at 3 h PMI.	304
Figure 6.13 Estimated marginal means of <i>HSPA</i> transcript copy numbers at 6 h PMI.	305
Figure 6.14 Estimated marginal means of <i>HSPA</i> transcript copy numbers at 12 h PMI.	306
Figure 6.15 Estimated marginal means of <i>HSPA</i> transcript copy numbers at 24 h PMI.	307

Figure 6.16 Transcription levels of <i>HSPA</i> mRNA in non-heat shock and heat shocked rat brain tissue at 0 h PMI.	316
Figure 6.17 Transcription levels of <i>HSPA</i> mRNA in non-heat shock and heat shocked rat brain tissue at 3 h PMI.	317
Figure 6.18 Transcription levels of <i>HSPA</i> mRNA in non-heat shock and heat shocked rat brain tissue at 6 h PMI.	318
Figure 6.19 Transcription levels of <i>HSPA</i> mRNA in non-heat shock and heat shocked rat brain tissue at 24 h PMI.	319
Figure 6.20 Transcription levels of <i>GAPDH</i> mRNA in non-heat shock and heat shocked rat brain tissue at 0 h PMI.	320
Figure 6.21 Transcription levels of <i>GAPDH</i> mRNA in non-heat shock and heat shocked rat brain tissue at 3 h PMI.	321
Figure 6.22 Transcription levels of <i>GAPDH</i> mRNA in non-heat shock and heat shocked rat brain tissue at 6 h PMI.	322
Figure 6.23 Transcription levels of <i>GAPDH</i> mRNA in non-heat shock and heat shocked rat brain tissue at 24 h PMI.	323
Figure 6.24 Estimated marginal means of <i>HSPA</i> transcript copy numbers at 0 h PMI.	326
Figure 6.25 Estimated marginal means of <i>HSPA</i> transcript copy numbers at 3 h PMI.	327
Figure 6.26 Estimated marginal means of <i>HSPA</i> transcript copy numbers at 6 h PMI.	328
Figure 6.27 Estimated marginal means of <i>HSPA</i> transcript copy numbers at 24 h PMI.	329
Figure 6.28 HSPA protein levels assessed using immunofluorescence in non-heat shocked rat brain tissue, PMI 0 h.	337

Figure 6.29 HSPA protein levels assessed using immunofluorescence in non-heat shocked rat brain tissue, PMI 3 h.	338
Figure 6.30 HSPA protein levels assessed using immunofluorescence in non-heat shocked rat brain tissue, PMI 6 h.	339
Figure 6.31 HSPA protein levels assessed using immunofluorescence in non-heat shocked rat brain tissue, PMI 12 h.	340
Figure 6.32 HSPA protein levels assessed using immunofluorescence in non-heat shocked rat brain tissue, PMI 24 h.	341
Figure 6.33 HSPA protein levels assessed using immunofluorescence in heat shocked rat brain tissue, PMI 0 h.	342
Figure 6.34 HSPA protein levels assessed using immunofluorescence in heat shocked rat brain tissue, PMI 3 h.	343
Figure 6.35 HSPA protein levels assessed using immunofluorescence in heat shocked rat brain tissue, PMI 6 h.	344
Figure 6.36 HSPA protein levels assessed using immunofluorescence in heat shocked rat brain tissue, PMI 12 h.	345
Figure 6.37 HSPA protein levels assessed using immunofluorescence in heat shocked rat brain tissue, PMI 24 h.	346
Figure 7.1 Histogram showing the average <i>HSPA</i> transcript levels from experiments using in control, glioma cell lines and v glioma brain tissue samples.	369
Figure 7.2 Histogram showing the average <i>HSPA</i> transcript levels in control and glioma cell lines under pre and post hypoxia conditions.	370

List of Tables

Table 1.1 Major Heat Shock Proteins.....	50
Table 1.2. Revised nomenclature for the heat shock protein families.....	52
Table 1.3. Characterization of heat shock factors across species.....	58
Table 1.4. Expression and location of the human HSPA genes	81
Table 1.5. Single nucleotide polymorphisms in three human HSPA genes	90
Table 1.6. WHO grading and survival of gliomas	93
Table 1.7. Summary of inducible <i>HSPA/HSP70</i> expression in select brain tumour cell lines	99
Table 1.8. Empiric corrective factors of the body weight	106
Table 2.1 Media and supplements for each cell line used in this thesis.....	116
Table 2.2 Reagents and chemicals used in cell culture.	117
Table 2.3. Reagents, composition and quantity provided mRNA isolation Kit.....	120
Table 2.4. Volumes of reagents used for mRNA isolation as per manufacturers' protocol.	122
Table 2.5 Reagents, composition and quantity of each reagent provided within the First Strand cDNA Synthesis Kit for RT-PCR.....	125
Table 2.6 The quantities of reagents required for each cDNA synthesis reaction using those provided within the First Strand cDNA Synthesis Kit for RT-PCR (AMV).....	127
Table 2.7 The composition and quantity of each reagent provided within the LightCycler® FastStart DNA MasterPLUS SYBR Green I kit.	129
Table 2.8 The quantities of reagents required for each RT-PCR reaction using those provided within the LightCycler® FastStart DNA MasterPLUS SYBR Green I kit. ..	129
Table 2.9 LightCycler program utilising FastStart DNA MasterPLUS SYBR Green Kit	132

Table 2.10. The <i>HSPA</i> and <i>GAPDH</i> for <i>Homo sapiens</i> and <i>Rattus norvegicus</i> primers	133
Table 2.11. Reagents, components and quantity provided of each in the DNeasy® Blood and Tissue Kit (Qiagen).	139
Table 2.12. Volumes of reagents used for DNA extraction as per manufacturers‘ protocol.	141
Table 2.13 LightCycler program utilising FastStart DNA MasterPLUS SYBR Green Kit.....	147
Table 3.1. Table showing gene and amino acid sequence homology between genes and species.	162
Table 3.2 An example of the obtained spectrophotometric readings and the subsequent concentrations of the mRNA isolated from all four cell lines used in this study.....	163
Table 3.3 An example of the obtained spectrophotometric readings and the subsequent concentrations of the mRNA isolated from rat brain tissue at 0, 3, 6, 12 and 24 hour post mortem interval used in this study.	164
Table 3.4 Table showing final concentration of genomic DNA required for serial dilution.	171
Table 3.5 Table showing calculation for serial dilution of known copy numbers.	172
Table 3.6 Known concentrations of Genomic human DNA corresponding to the average Ct value and copy number.	175
Table 4.1 Descriptive statistics showing the mean expression levels of <i>HSPA</i> for each cell line.....	185
Table 4.2. Statistical data from Tukey’s HSD test showing significance of <i>HSPA</i> gene expression between cell lines.....	186
Table 4.3 Descriptive statistics showing the mean transcript levels of <i>GAPDH</i> in each cell line.....	187

Table 4.4. Statistical data from Tukey’s HSD test showing significance of <i>GAPDH</i> gene expression between cell lines.	188
Table 4.5 Tissues used in this study are in chronological order.....	189
Table 4.6 Descriptive statistics showing the mean transcript copy numbers of <i>HSPA</i> and <i>GAPDH</i> expression in brain tissue sample	199
Table 4.7 Statistical data from Tukey’s HSD test showing significance of <i>HSPA</i> transcript copy numbers between brain tissue sample groups. ...	200
Table 4.8 Descriptive statistics showing the mean for <i>HSPA</i> protein levels for each cell line.	211
Table 4.9. Statistical data from Tukey’s HSD test showing significance of <i>HSPA</i> protein levels between cell lines.	212
Table 5.1. Descriptive statistics showing the mean mRNA copy numbers for <i>HSPA</i> and <i>GAPDH</i> gene expression for untreated and treated cell lines.	228
Table 5.2. Statistical data from Tukey’s HSD test showing significance of <i>HSPA</i> transcript copy numbers in treated and untreated cell lines.	229
Table 5.3. Descriptive statistics showing the mean <i>HSPA</i> protein levels for untreated and treated cell lines.....	259
Table 5.4. Statistical data from Tukey’s HSD test showing significance of <i>HSPA</i> protein levels in treated and untreated cell lines.	262
Table 6.1. Descriptive statistics showing the mean <i>HSPA</i> transcript copy numbers for untreated and treated brain tissue.....	310
Table 6.2. Descriptive statistics showing the mean <i>GAPDH</i> transcript copy numbers for untreated and treated brain tissue.....	311
Table 6.3. Statistical data from Tukey’s HSD test showing significance of <i>HSPA</i> transcript copy numbers between PMI.....	312
Table 6.4. Descriptive statistics showing the mean <i>HSPA</i> transcript copy numbers for untreated and treated brain tissue.....	332

Table 6.5. Descriptive statistics showing the mean *GAPDH* transcript copy numbers for untreated and treated brain tissue..... 333

Table 6.6. Statistical data from Tukey's HSD test showing significance of *HSPA* transcript copy numbers between PMI..... 334

List of Appendices

Appendix 9.1 Amino acid and gene sequence for <i>HSPA1A Homo sapiens</i> adapted from NCBI.....	432
Appendix 9.2 Amino acid and gene sequence for <i>HSPA1B Homo sapiens</i> adapted from NCBI.....	434
Appendix 9.3 Amino acid and gene sequence for <i>HSPA1L Homo sapiens</i> adapted from NCBI.....	437
Appendix 9.4 Amino acid and gene sequence for <i>HSPA1A Rattus norvegicus</i> adapted from NCBI	440
Appendix 9.5 Amino acid and gene sequence for <i>HSPA1B Rattus norvegicus</i> adapted from NCBI	443
Appendix 9.6 Amino acid and gene sequence for <i>HSPA1L Rattus norvegicus</i> adapted from NCBI	447
Appendix 9.7 Amino acid and gene sequence for <i>GAPDH Homo sapiens</i> adapted from NCBI.....	450
Appendix 9.8 Amino acid and gene sequence for <i>GAPDH Rattus norvegicus</i> adapted from NCBI	452
Appendix 9.9 Output page generated from Primer3 for <i>HSPA1A Homo sapiens</i> (adapted from Primer3).....	454
Appendix 9.10 Output page generated from Primer3 for <i>HSPA1B Homo sapiens</i> (adapted from Primer3).....	455
Appendix 9.11 Output page generated from Primer3 for <i>HSPA1A Rattus norvegicus</i> (adapted from Primer3).....	456
Appendix 9.12 Output page generated from Primer3 for <i>GAPDH Homo sapiens</i> (adapted from Primer3).....	457

Appendix 9.13 Output page generated from Primer3 for <i>GAPDH Rattus norvegicus</i> (adapted from Primer3)	458
Appendix 9.14 Gene Sequence Alignment for <i>HSPA1A</i> (1), <i>HSPA1B</i> (2) and <i>HSPA1L</i> (3) <i>Homo sapiens</i>	459
Appendix 9.15 Amino Acid Sequence Alignment for <i>HSPA1A</i> (1), <i>HSPA1B</i> (2) and <i>HSPA1L</i> (3) <i>Homo sapiens</i>	465
Appendix 9.16 Gene Sequence for <i>HSPA1A</i> (1), <i>HSPA1B</i> (2) and <i>HSPA1L</i> (3) <i>Rattus</i> <i>norvegicus</i>	467
Appendix 9.17 Amino Acid Sequence for <i>HSPA1A</i> (1), <i>HSPA1B</i> (2) and <i>HSPA1L</i> (3) <i>Rattus norvegicus</i>	475
Appendix 9.18 Gene Sequence Alignment for <i>HSPA1A Homo sapiens v Rattus</i> <i>norvegicus</i>	477
Appendix 9.19 Amino Acid Sequence for <i>HSPA1A Homo sapiens v Rattus norvegicus</i>	483
Appendix 9.20 Gene Sequence Alignment for <i>HSPA1B Homo sapiens v Rattus</i> <i>norvegicus</i>	485
Appendix 9.21 Amino Acid Sequence for <i>HSPA1B Homo sapiens v Rattus norvegicus</i>	493
Appendix 9.22 Gene Sequence Alignment for <i>HSPA1L Homo sapiens v Rattus</i> <i>norvegicus</i>	495
Appendix 9.23 Amino Acid Sequence for <i>HSPA1L Homo sapiens v Rattus norvegicus</i>	497
Appendix 9.24 Gene Sequence Alignment for <i>GAPDH Homo sapiens v Rattus</i> <i>norvegicus</i>	500
Appendix 9.25 Amino Acid Sequence for <i>GAPDH Homo sapiens v Rattus norvegicus</i>	503

Appendix 9.26 BLAST analysis showing sequences producing significant alignments
for *HSPAJA*504

Appendix 9.27 BLAST analysis showing sequences producing significant alignments
for *HSPA* designed primers505

Acknowledgements

It is a pleasure to convey my sincere thanks and gratitude to the many people who have made this thesis possible.

I cannot overstate my gratitude to Dr Lee Chatfield – PhD supervisor, friend, philosopher and guide. During my time at UCLan Lee has been a constant source of good advice and encouragement. His mentorship has been paramount in providing excellent research experience allowing me to develop as an experimentalist and an independent thinker.

Many sincere thanks are due to several academics within UCLan who have given me excellent advice, terrific support and unconditional periods of their valuable time. I am especially grateful to Professor Jaipaul Singh, Dr Amal Shervington, Dr Sarah Dennison, Dr Paul Taylor, Dr Nicola Bridges and Dr Simarjit Singhrao.

Collectively and individually, I am indebted to good friends and colleagues from UCLan for providing a stimulating environment to learn and develop. I am especially grateful to Helen Godfrey, Robin Moll, Shahid Nazir, Sophie Poole Dr Julie Shorrocks and Dr Christopher Platt for their emotional support and camaraderie they have so willingly provided, especially through difficult times.

Most of all, I wish to express my deep and sincere thanks to my family, especially my mum, Marion, my late father, Trevor, my daughter Samantha, my son Jonathan and to my loving husband, Ed, for their absolute confidence, unconditional love, support and encouragement. To them I dedicate this thesis.

Abbreviations

μl	Microlitres
μg	Micrograms
1321N1	Grade I astrocytoma cell line
A	Adenosine
A172	Adult malignant glioma cell line
aa-tRNA	Amino acid transfer ribonucleic acid
ABM	Astrocyte Basal Medium
AKT1	RAC-alpha serine/threonine protein kinase
AM	Astrocyte medium
AMV	Avian Myeloblastosis Virus
ADP	Adenosine diphosphate
ARNT	Aryl hydrocarbon receptor nuclear translocator
ATCC	American Type Culture Collection
ATP	Adenosine triphosphate
BAG-1	Bcl-2-associated athanogene-1
bHLH	Basic helix loop helix
bp	Base Pairs
BSA	Bovine Serum Albumen
C	Cytosine
c-CND1	Condensin, non-SMC subunit
c-FOS	FBJ osteosarcoma oncogene
c-MYC	Myelocytomatosis oncogene

cDNA	Complimentary DNA
CHIP	Carboxy-terminus OH Hsp70 Interacting Protein
COOH	Carboxylic acid
CNS	Central Nervous System
Ct	Cycle threshold
CT	Computed tomography
CYR61	Cysteine-rich, angiogenic inducer, 61
D341MG	Pediatric medulloblastoma cell line
D392MG	Adult malignant glioma cell line
D54MG	Adult malignant glioma cell line
dATP	Deoxyadenosine triphosphate
DAXX7	Cellular death associated protein
DBD	DNA binding domain
dCTP	Deoxycytidine triphosphate
DDBJ	DNA Data Bank of Japan
dGTP	Deoxyguanosine triphosphate
DMEM	Dulbeccos Modified Eagles Medium
DMSO	Dimethylsulphoxide
DMSZ	Deutsche Sammlung von Mikroorganismen und Zellkulturen
DNA	Deoxyribonucleic Acid
DNAJ	Heat shock protein 40
dsDNAs	Double Stranded DNA
dTTP	Deoxythymidine triphosphate

DTT	Dithiothreitol
EBI	European Bioinformatics Institute
ECACC	European Collection of Cell Cultures
EDTA	Ethylenediaminetetraacetic Acid
EMBL	European Molecular Biology Laboratory
EMEM	Eagles Minimum Essential Medium
EPO	Erythropoietin
ER	Endoplasmic Reticulum
ESTs	Expression Sequence Tags
EXP	Exponential
F	F-distribution = mean squares between effects / mean squares within effects
FBS	Foetal Bovine Serum
FITC	Fluorescein Isothiocyanate
G	Guanine
GA-1000	Amphotericin-B
GAPDH	Glyceraldehyde-3-phosphate dehydrogenase
GBM	Glioblastoma Multiforme
GENBANK	NIH genetic sequence database
Glu	Glutamic acid
GLUT-2	Glucose transporter 2
GOS-3	Grade II/III oligodendroglioma cell line
Grp75	Heat shock 70kDa protein 9 (mortalin)
H	Hours

H ₂ O	Water
HDJ1	DnaJ (Hsp40) homolog
HepG2	Hepatocellular carcinoma cell line
HIF-1 α	Hypoxia-inducible factor 1 alpha
HIF-2 α	Hypoxia-inducible factor 2 alpha
HIF-3 α	Hypoxia-inducible factor 3 alpha
HIF-1 β	Hypoxia-inducible factor 1 beta
HNF-3/fork	Hepatocyte nuclear factor 3/fork
HR	Heptad repeats
HR-A	Heptad repeats amino terminal
HR-B	Heptad repeats carboxy terminal
HR-C	Heptad repeats N terminus
HRE	Hypoxia responsive element
HSBP1	Heat shock factor binding protein 1
HSEs	Heat shock elements
HSF	Heat shock factor
HSF1	Heat shock factor 1
HSF2	Heat shock factor 2
HSF3	Heat shock factor 3
HSF4	Heat shock factor 4
HSP10	Heat shock protein 10
HSP22	Heat shock protein 22
HSP23	Heat shock protein 23
HSP26	Heat shock protein 26
HSP27	Heat shock protein 27

HSP40	Heat shock protein 40
HSP60	Heat shock protein 60
HSP68	Heat shock protein 68
HSP70	Heat shock protein 70
HSP70-1	Heat shock protein 70-1
HSP70-2	Heat shock protein 70-2
HSP70-hom	Heat shock protein 70-hom
HSP75	Heat shock protein 75
HSP90	Heat shock protein 90
HSP90 α	Heat shock protein 90 alpha
HSP90 β	Heat shock protein 90 beta
HSP90N	Heat shock protein 90kDa alpha (cytosolic), class A member 1
HSPA	Heat shock protein 70
HSPA1A	Heat shock 70kDa protein 1A
HSPA1B	Heat shock 70kDa protein 1B
HSPA1L	Heat shock 70kDa protein 1L
HSPA2	Heat shock 70kDa protein 2
HSPA3	Heat shock 70kDa protein 3
HSPA4	Heat shock 70kDa protein 4
HSPA4L	Heat shock 70kDa protein 4-like
HSPA5	Heat shock 70kDa protein 5
HSPA6	Heat shock 70kDa protein 6
HSPA7	Heat shock 70kDa protein 7
HSPA8	Heat shock 70kDa protein 8

HSPA9	Heat shock 70kDa protein 9
HSPA9B	Heat shock 70kDa protein 9 (mortalin)
HSPA12A	Heat shock 70kDa protein 12A
HSPA12B	Heat shock 70kDa protein 12B
HSPA14	Heat shock 70kDa protein 14
HSPB	Family of small heat shock proteins
HSPB1	Heat shock protein 27
HSPC	Heat shock protein 90
HSPC1A	Heat Shock Protein 90 alpha
HSPC2A	Heat Shock Protein 90 beta
HSPC3A	Heat shock protein 90kDa alpha (cytosolic), class A member 1
HSPC5A	Heat shock protein 75, TNFR-associated protein 1
HSPD	Heat shock protein 60
HSPE	Heat shock protein 10
HSPH1	Heat shock 105kDa/110kDa protein 1
HSR	Heat Shock Response
HYOU1	Hypoxia up-regulated protein 1
IDDM	Insulin Dependant Diabetes Mellitus
IgG	Immunoglobulin G
IgM	Immunoglobulin M
i-NOS	Inducible nitric oxide synthase
KCL	Potassium chloride
KDa	Kilo Dalton

L-G	L-Glutamine
LiCl	Lithium Chloride
Lys	Lysine
M	Molar
MAP-KAPK-2	Map kinase activated protein 2
MAP-KAPK-3	Map kinase activated protein 3
MD	Mean Differences
Met	Methionine
mg	Milligrams
MgCl ₂	Magnesium Chloride
MHC-III	Major Histocompatibility Complex Class 3 Region
min	minutes
ml	Milli-litres
mM	Micro molar
MRI	Magnetic Resonance Imaging
mRNA	Messenger RNA
mtDNA	Mitochondrial DNA
NaOH	Sodium hydroxide
NBD	N-Terminal Binding ATPase Domain
NCBI	National Centre for Biotechnology Information
NEAA	Non essential amino acids
NEF	Nucleotide Exchange Factor
ng	Nanograms

-NH ₂	Amine group
NHA	Normal Human Astrocyte cell line
NIDDM	Non-Insulin Dependent Diabetes Mellitus
NTC	No Template Control
OCT	Optimal Cutting Temperature
OD	Optical density
P	Significant value between 0.0 and 1.0
P7056k	P70 S6 kinase
PAS	Acronym for Per, ARNT and Sim
PBS	Phosphate Buffered Saline
PCK7	YE1389 putative serine protease
PCR	Polymerase chain reaction
Per	Period homolog
pg	Picograms
Phe	Phenylalanine
PI	Propidium Iodide
PKD1	Polycystin-1
PMI	Post Mortem Interval
qRT-PCR	Quantitative RT-PCR
rhEGF	Recombinant Human Epidermal Growth Factor
RNA	Ribonucleic Acid
RPM	Revolutions per minute
rRNA	Ribosomal Ribonucleic Acid
RT-PCR	Real Time Polymerase Chain Reaction

s	Seconds
SBD	Substrate Binding Domain
SD	Standard deviation
Sim	Single minded homolog
SMA560	Murine anaplastic astrocytoma cell line
SMPs	Streptavidin Coated Magnetic Particles
SNPs	Single nucleotide Polymorphisms
snRNP	Small Nuclear Ribonucleoproteins
ssDNA	Single stranded DNA
ssRNA	Single Stranded RNA
STCH	Heat shock protein 70kDa family, member 13
STZ	Streptozotocin
SwissProt	Part of the Swiss Institute of Bioinformatics (SIB)
T98G	Human glioblastoma cell line
t	$T \text{ value} = (\text{mean} - 1) / (\text{SD} / \text{square root of the number of samples})$
T	Tyrosine
TAE	Tris-acetate-EDTA
<i>Taq</i>	<i>Thermus aquaticus</i>
TBE	Tris-borate-EDTA
Thr	Threonine
Tm	Melting temperature
TNF- α	Tumour Necrosis Factor Alpha

Trap1	TNFR-associated protein 1
tRNA	Transfer Ribonucleic Acid
U87-MG	Grade IV glioblastoma cell line
UTR	Untranslated Region
UV	Ultra Violet
v/v	Volume/volume
w/v	Weight/volume
VEGF	Vascular endothelial growth factor
VHL	Von hippel-lindau
WHO	World Health Organisation
WWW	World Wide Web

Chapter 1

Introduction

1.1 Molecular Chaperones and Heat Shock Proteins

Protein synthesis is a complex molecular process which has been reviewed recently by Babitzke *et al*, (2009); Braakman and Bulleid, (2011) and Zamecnik, (2005). Translation involves interactions between three major groups of RNA molecules; ribosomal ribonucleic acid (rRNA), transfer ribonucleic acid (tRNA) and messenger ribonucleic acid (mRNA) templates, and a large number of accessory protein factors. Eukaryotic protein synthesis occurs in the cytoplasm at ribosomes, where the genetic information encoded by mRNA molecules is translated, according to the genetic code, into a corresponding sequence of amino acids to form a polypeptide.

Amino acids are brought to the peptide site of a ribosome by charged tRNA molecules, and the complementary anticodon in the tRNA specifically binds to the codon in the mRNA. Protein factors or initiation factors are required during the initiation phase of protein synthesis, interacting with the ribosome-mRNA complex, and dissociate when polypeptide chain synthesis is initiated. After the initiation complex has formed, elongation of the polypeptide chain proceeds. Elongation begins when the carboxyl, (–COOH) group of an amino acid carried by a charged aminoacyl-tRNA (aa-tRNA), binds to the peptidyl site of the ribosome with the amino, (NH₂) group of the amino acid of another aa-tRNA in the aminoacyl site. The peptidyl tRNA translocates from the aminoacyl site to the peptide site where the tRNA disassociates from the peptide to the exit site. This process repeats until a nonsense codon is reached. Termination of this process requires specific protein release factors which recognise nonsense codons, causing the nascent polypeptide chain to release from the peptidyl tRNA and the ribosome.

The polypeptide that emerges from the ribosome is inactive and must undergo protein folding, one of four post translation processes, before taking on its functional role in the cell.

Proteins are generally considered to have four distinct levels of structural organization.

The primary structure of a protein is formed by the linkage of amino acids via covalent peptide bonds to form a linear polypeptide chain. The two ends of the polypeptide chain are chemically distinct; the start of the polypeptide chain has a free amino group which is referred to as the N-terminus, and the other end of the polypeptide chain has a free carboxyl group, termed the C-terminus (Braakman and Bulleid, 2011).

The secondary structure of proteins describes the folding and twisting of the linear polypeptide chain into specific conformations, such as α -helix and β -pleated sheet structures. The α -helix structure is formed by intramolecular hydrogen bonding between the -NH groups of one amino acid and the -COOH groups of an amino acid that is four amino acids away within the chain. Repeated formation of this bonding results in the helical coiling of the polypeptide chain. The β -pleated sheet structure is formed by intermolecular hydrogen bonding between the amide hydrogen of one chain to the amide oxygen of a neighbouring chain resulting in a zigzag or pleated formation (Braakman and Bulleid, 2011).

Tertiary structures are formed through the folding of secondary structure into three-dimensional structures determined by a variety of bonding interactions, including hydrogen bonding (Arunan *et al*, 2011), salt bridges (Kumar and Kussinov, 2002), disulphide bonds (Sevier and Kaiser, 2002) and non-polar hydrophobic interactions (Rose *et al*, 2006) between the -side chains on the amino acids (Braakman and Bulleid, 2011).

The quaternary structure is formed by the clustering of two or more proteins linking together to form a multi-subunit protein, but it is worth noting that not all proteins exhibit quaternary structures. Again, a variety of bonding interactions, including hydrogen bonding, salt bridges, and disulphide bonds, hold the protein in its final structural shape, but also allow the proteins to revert back to their component polypeptide or change their subunit composition, depending on their functional requirement (Braakman and Bulleid, 2011).

Folding of newly synthesized proteins requires the interaction of numerous protein cofactors, referred to as molecular chaperones. Molecular chaperones ensure that polypeptide chains are not damaged during the transport and assembly stages of protein production. These proteins are not part of the final proteins with which they are associated. They are a diverse family of largely unrelated proteins (Ellis and Hemmingsen, 1989; Ellis and van der Vies, 1991; Feder, 1999; Hartl *et al*, 2011). Molecular chaperones maintain newly synthesized polypeptides in an unfolded state for translocation across intracellular membranes and hence recognise and selectively bind to new polypeptide chains and to partially folded intermediates of proteins (Atalay *et al*, 2009; ; Jolly and Morimoto 2000; Welch *et al*, 1993). They also prevent the aggregation and misfolding of newly synthesized proteins, prevent non-productive interactions with other cell components, direct the assembly of larger proteins and multiprotein complexes, and cause previously folded proteins to unfold during exposure to stressful conditions (Atalay *et al*, 2009; Ellis, 1993; Jolly and Morimoto, 2000; Welch *et al*, 1993).

Molecular chaperones play a crucial protective role under conditions of cellular stress and damage, preventing the appearance of folding intermediates that lead to either

misfolded or damaged protein molecules. When their production or activity is induced in response to either acute or chronic stress, molecular chaperones capture folding intermediates and prevent their misfolding or premature aggregation. They are also implicated in the control of cellular apoptosis (Ellis, 1993; Jolly and Morimoto, 2000; Welch *et al*, 1993).

Molecular chaperones are highly conserved groups of proteins, which comprise a number of unrelated families, and most are classified as heat shock (stress) proteins. They are highly ubiquitous and are found in both prokaryotic and eukaryotic cells, where they can be found localized in the cytoplasm, nucleus, endoplasmic reticulum or the mitochondria. The existence of these proteins, and their associated genes, was discovered from studies of the response to cells to heat shock, first reported by Ferruccio Ritossa in 1962. This was first observed in the salivary gland cells of the fruit fly *Drosophila busckii*, which were exposed to an elevated temperature of 37°C for 30 min, followed by recovery at their normal temperature of 25°C. Ritossa described a unique set of chromosomal ‘puffs’ (Figure 1.1) observed after exposure of these cells to heat, together with the increased production of then unknown proteins with molecular masses of 70 and 26 KDa (Ritossa, 1962; Ritossa, 1963; Trivedi *et al*, 2010). The polytene chromosomes present in *Drosophila* salivary gland cells allowed the observation of ‘puffing’ of specific regions of the chromosomes in response to heat shock, which resulted from high levels of transcription of heat shock genes.

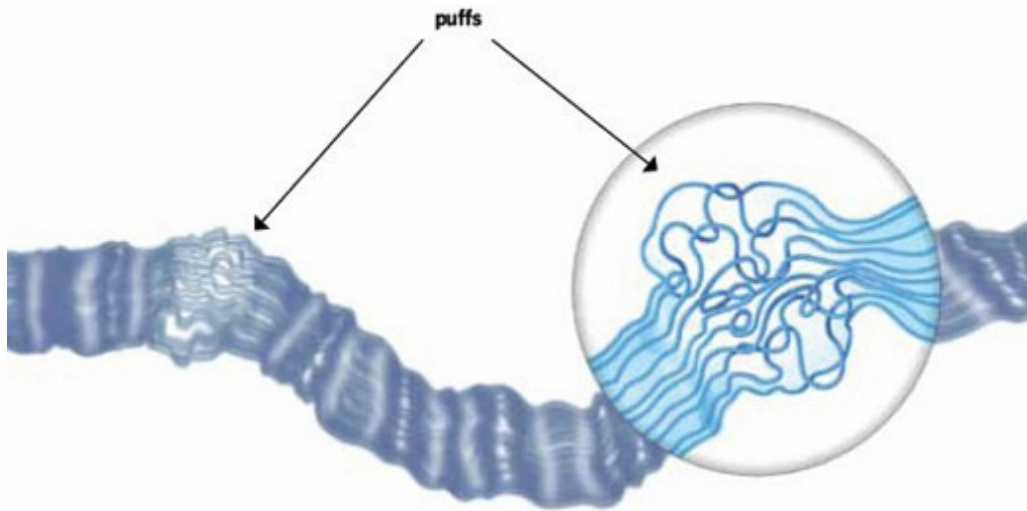


Figure 1.1. Representation of a light microscope image of *Ritossa*'s chromosomal puffs, which are characterised by localized swellings of specific regions of a polytene chromosome. These 'puffs' result from localised synthesis of RNA, resulting from high levels of transcription of heat shock genes at each chromosomal location (Morimoto, 2010).

Over the next decade, further studies showed that these chromosomal puffs were also induced by a variety of other cellular treatments, such as exposure to dinitrophenol, sodium salicylate (Ritossa, 1962), actinomycin D (Berendes, 1968), or anoxia (Ashburner, 1970); these treatments all resulted in cellular stress. The production of puffing was shown to be associated with newly synthesized RNA, indicating that these resulted from high levels of gene expression (Leenders and Berendes, 1972; Ritossa, 1962) and that the response was rapidly induced, as puffs were produced within a few minutes of treatment (Ashburner, 1970; Berendes, 1968). The phenomenon was also found in other *Drosophila* species such as *Drosophila melanogaster*, *Drosophila hydei* and *Drosophila similans* (Berendes, 1965; Ritossa, 1964). Later studies by Guttman and Gorovsky, (1979); Kelly and Schlesinger (1982); McAlister *et al*, (1979); Miller *et al*, (1979) and Neidhardt *et al*, (1984) showed that this was a wide-spread phenomenon in most other organisms, indicating that heat shock response was a fundamental cellular function. It was discovered that heat and various other types of stress could induce the synthesis of similar proteins in yeast (McAlister *et al*, 1979; Miller *et al*, 1979); cultured avian cells (Kelly and Schlesinger, 1982); tetrahymena (Guttman and Gorovsky, 1979) and *Escherichia coli* (Neidhardt *et al*, 1984). Studies undertaken by Ashburner and Berendes (1978); Choa and Guild, (1986) and Huet *et al*, (1993) have shown sequential activation of early and late puffs in the polytene chromosomes in multiple gene sets during heat shock. Early puffs are active for approximately 4 hours and then regress, during which time late puff sets become active (Ashburner, 1970; Ashburner and Berendes, 1978; Berendes, 1968; Leenders and Berendes, 1972). In *Drosophila melanogaster*, nine puffs induced by heat shock in polytene nuclei were identified on different chromosomes; the left arm of chromosome 2 loci 33B, left arm of chromosome 3 loci 63BC, 64EF, 67B, right arm of chromosome 3 loci 70A, 87A, 87C, 93D and 95D (Ashburner, 1970; Mukherjee and Lakhotia,

1979). The first gene products resulting from these chromosomal puffs were identified some 12 years later and subsequently termed –heat shock proteins| (Neuer *et al*, 2000; Tissiere *et al*, 1974). In both eukaryotic and prokaryotic organisms, heat shock protein genes are scattered at various chromosomal locations, with some related genes clustered or, if unrelated, interspersed with independently regulated genes. On the right arm of chromosome three, five copies per haploid genome for the gene HSP70 are present, two at locus site 87A and three at locus site 87C, also the gene for HSP68 is present at locus site 95D (Holmgren *et al*, 1979). On the left arm of chromosome three, four of the small heat shock proteins are encoded at locus site 67B, in the order HSP27, HSP23, HSP26 and HSP22 (Corces *et al*, 1980; Craig and McCarthy, 1980; Voellmy *et al*, 1981) and also HSP83 coding sequences are located at locus 63BC.

The normal growth temperature for *Drosophila* cells is 25°C. When the cells are subjected to heat shock with temperatures between 29 – 38°C, heat shock proteins are induced with a maximum response by temperatures between 36 – 37°C (Lindquist, 1980). Within minutes of temperature elevation, heat shock mRNAs appear in the cytoplasm and are translated immediately with high efficiency (Lindquist, 1980). Within an hour of heat shock, several thousand heat shock transcripts are found in each cell (Lindquist, 1980). During this time, translation of pre-existing messages (Kelly and Schlesinger, 1982; Lindquist, 1981) and transcription of previously active genes are repressed (Berendes, 1968; Findly and Pederson, 1981; Lindquist, 1986). If the cells are maintained at elevated temperatures, heat shock proteins will continue to be the primary products of protein synthesis. If the cells are returned to their normal growth temperature, normal protein synthesis will be gradually resumed, the timing of which is dependent on the severity of the heat shock induced (DiDomenico *et al*, 1982).

In other organisms, induction of heat shock protein genes is equally rapid. However, the maximum induction temperature varies depending on the physiological growth temperature. For example, in humans, with a normal physiological temperature of 37°C, the maximum response temperature is 42°C; in yeast, with a normal physiological temperature of 30 – 37°C, the maximum response temperature is 39 - 40°C (Lindquist *et al*, 1982), in salmon/trout, with a normal physiological temperature of 5 – 15°C (Kothary and Candido, 1982), the maximum response temperature is 28°C and in *E.coli*, with an optimal growth temperature of 37°C, the maximum response temperature is 45 – 50°C (Neidhardt *et al*, 1984; Yamamori *et al*, 1978). In organisms that grow over a broad range of temperatures, the maximum response temperature is generally 10 – 15°C above the optimum physiological temperature, whereas for organisms/species that grow over a more restricted temperature range, the maximum response temperature is generally 5°C above the optimum physiological temperature (Lindquist, 1986).

In some organisms, heat shock response appears to be either transient or sustained. For example, in *E.coli* heat shock response is transient when the normal growth temperature is raised to 42°C but is sustained when the temperature is raised to 45 - 50°C (Neidhardt *et al*, 1984; Yamamori *et al*, 1978). In most organisms heat shock will be transient at moderate temperatures where normal growth will be resumed, and sustained at higher temperatures until the cells slowly begin to die (Lindquist, 1986).

The majority of cells in multicellular organisms respond to heat shock. For example, cells respond identically in different tissues of *Drosophila* such as the malpighian tubules, imaginal wing discs, brain, salivary glands, and tissue cultured cells (Tissiere *et al*, 1974), and in *Rattus norvegicus* heart, brain, liver, lung, kidney, thymus and adrenal gland tissues, the same phenomenon is observed (White and Currie, 1982). However,

there are some exceptions. For example, in *Rattus norvegicus*, *Hsp70* cannot be induced in the brain until three weeks postpartum (Tissiere *et al*, 1974).

It is worth noting that, due to the inconsistency in nomenclature that has been used for heat shock genes and their products in published literature, regarding abbreviations, gene and protein symbols in different species, there was a need for standardization. The use of different names for these genes and proteins make comparison of different studies very difficult. For the purposes of this thesis, nomenclature for human and non-human primates has been based on the Guidelines for Human Nomenclature (Show *et al*, 1987). Other species-based nomenclature, such as mouse, rat and chicken species, has been based on the Rules for Nomenclature of Genes (<http://www.informatics.jax.org/>).

For human / non-human primates and other species, nomenclature for proteins will be non-italicized and in lower case, and will be italicized if referring to genes. Gene symbols for humans and non-human primates are designated by a combination of italicized upper case letters and Arabic letters, e.g. *HSPA*. Protein designations are the same as for the gene symbol but not italicized and all in upper case e.g. HSPA.

For mouse, rat and chicken, nomenclature will be non-italicized and in lower case, and will be italicized if referring to genes. Gene symbols are designated by a combination of italicized letters and Arabic letters, the first letter in upper case and the rest lower case: e.g. *HSPA*. Protein designations are the same as for the gene symbol, but not italicized and all in upper case: e.g. HSPA.

In mammalian cells, heat shock proteins function as either molecular chaperones or proteases (Jolly and Morimoto, 2000) and are classified into five major families, according to their molecular size or function. These are HSP90, HSP70, HSP60, HSP40 and HSP27 (Table 1.1 Craig *et al*, 1994; Jolly and Morimoto, 2000; Kampinga *et al*, 2009; Lindquist and Craig, 1988; Morimoto *et al*, 1994; Powers *et al*, 2007; Sreedhar *et al*, 2004). These families are described in more detail later in this chapter in section 1.3.

Table 1.1 Major Heat Shock Proteins (Taken from Craig *et al*, 1994; Jolly and Morimoto, 2000; Kampinga *et al*, 2009; Lindquist and Craig, 1988; Morimoto *et al*, 1994; Powers *et al*, 2007; Sreedhar *et al*, 2004)

Heat shock protein Families	Co-chaperones or Isoforms	Expression	Localization	Activity / Function
HSP27	Various	Constitutive /Inducible	Cytoplasm/ Nucleus	Prevent heat denaturation protein aggregation via ATP-independent formation of high molecular weight oligomers; phosphorylation of HSP27 monomers/dimers regulate microfilament polymerization.
HSP40	Hdj1 and Hdj2	Constitutive /Inducible	Cytoplasm/ Nucleus	Cochaperone activity with HSP70 proteins. Regulates adenosine triphosphate (ATP) activity and substrate release.
HSP60	mtHsp60/HSP10-mito	Constitutive /Inducible	Mitochondria	Folds newly imported mitochondrial proteins.
	TRIC/CCT	Constitutive /Inducible	Cytoplasm	Folds approx. 10% of cytosolic polypeptide chains downstream of the Hsp70 machinery.
HSP70	HSC70	Constitutive /Inducible	Cytoplasm /Nucleus	Cognate form assists constitutive folding and transport of proteins to organelles.
	HSP70.1	Constitutive /Inducible	Cytoplasm	Induced upon heat shock and mediate similar functions in response to stress-induced increase in protein misfolding and aggregation
	HSP70.2	Constitutive	Cytoplasm	
	HSP70.3	Constitutive	Cytoplasm	
	mtHsp70/Grp75	Constitutive	ER/Cytoplasm	Protein folding and translocation in mitochondria
	Bip/Grp78	Constitutive /Inducible	ER/Cytoplasm	Binds folding and translocation intermediates to prevent aggregation
HSP90	HSP90- α	Inducible	Cytoplasm /Nucleus	Growth promotion, cell cycle regulation, stress induced cytoprotection, signal transduction
	HSP90- β	Constitutive	Cytoplasm /Nucleus	Cellular transformation, signal transduction, cytoskeletal stabilization, long term cell adaption
	HSP-N	Constitutive /Inducible	Cytoplasm /Nucleus	Cellular transformation
	HSP75 1TRAP-1	Constitutive /Inducible	Mitochondria	Cell cycle regulation

Due to the expanding number of members of the human heat shock protein families and the inconsistency in their nomenclature, it was suggested that a more consistent and standardized nomenclature should be assigned. In recently reviewed literature names used for the human heat shock protein family members have been inconsistent with a number of different names and symbols being used for the same gene product.

In 2009, the nomenclature for human heat shock protein families and the human chaperonin families were revised from previous designations (Kampinga *et al*, 2009). The new guidelines for the nomenclature propose HSPC (HSP90), HSPA (HSP70), DNAJ (HSP40), HSPB (small HSP) and HSPD/E (HSP60/HSP10) respectively. The new nomenclature is mainly based on the systematic gene symbols that have been assigned by the HUGO Gene Nomenclature Committee that are used as primary identifiers in gene databases such as the National Centre of Biotechnology Information (NCBI), Entrez Gene and Ensembl.

Throughout this thesis, the new nomenclature described above for (example HSPA/HSP70) has been used for all the heat shock protein families reported (Table 1.2).

Table 1.2. Revised nomenclature for the heat shock protein families used in this study (taken from Kampinga *et al*, 2009)

Family	Gene	Protein Name	Previous Nomenclature
HSPB			Small heat shock proteins
	<i>HSPB1</i>	HSPB1	HSP27
DNAJ			HSP40
	<i>DNAJA1</i>	DNAJA1	Hdj2, HSP40
	<i>DNAJB1</i>	DNAJB1	Hdj1, HSP40
HSPD			HSP60
	<i>HSPD1</i>	HSPD1	HSP60
HSPA			HSP70
	<i>HSPA1A</i>	HSPA1A	HSP70-1, HSP72, HSP70.3
	<i>HSPA1B</i>	HSPA1B	HSP70-2
	<i>HSPA5</i>	HSPA5	BIP, GRP78
	<i>HSPA8</i>	HSPA8	HSC70, HSP71, HSP71, HSP73
	<i>HSPA9</i>	HSPA9	GRP75, mtHSP70
HSPC			HSP90
	<i>HSPC1a</i>	HSPC1	HSP90- α
	<i>HSPC2a</i>	HSPC2	Hsp90- β
	<i>HSPC3a</i>	HSPC3	HSP-N
	<i>HSPC5a</i>	HSPC5	HSP75, TRAP-1

Each family of heat shock proteins contains members which are expressed either constitutively or which are induced in response to stimuli and are targeted to different sub-cellular compartments (Garrido *et al*, 2006; Powers *et al*, 2009). Both constitutive and inducible heat shock proteins carry out numerous functions including: nascent protein folding; prevention of the formation of protein aggregates; assisting in the re-folding of denatured proteins; facilitation of degradation of irreparable proteins; modulation of the assembly or disassembly of protein complexes and assisting in the translocation of proteins across cellular membranes (Calderwood *et al*, 2006; Mosser and Morimoto, 2004; Powers *et al*, 2009). In addition to the above roles, heat shock proteins also play a strong part in cytoprotection and allow cells to adapt to gradual changes in their environment and to survive under hostile or otherwise lethal conditions (Calderwood *et al*, 2006; Mosser and Morimoto, 2004; Parcellier *et al*, 2003; Powers *et al*, 2009). The expression and functions of heat shock protein genes have been extensively studied in a wide variety of tissues and cell types that have been exposed to a range of stress conditions. Although the production of heat shock proteins results in the protection of cells from the effects of further stresses, they are deemed toxic if present in the cells for any prolonged period (Theodorakis *et al*, 1999).

Heat shock proteins are thus a family of highly conserved ubiquitous proteins encoded by genes which are activated, not only in response to various physiological and environmental stress conditions (Figure 1.2.), but also in cells affected by various diseases, such as cancer, Alzheimer's, Parkinson's and Huntington's diseases and diabetes, and by fever or inflammation (Jolly and Morimoto, 2000; Lindquist, 1986; Morimoto, 1993).

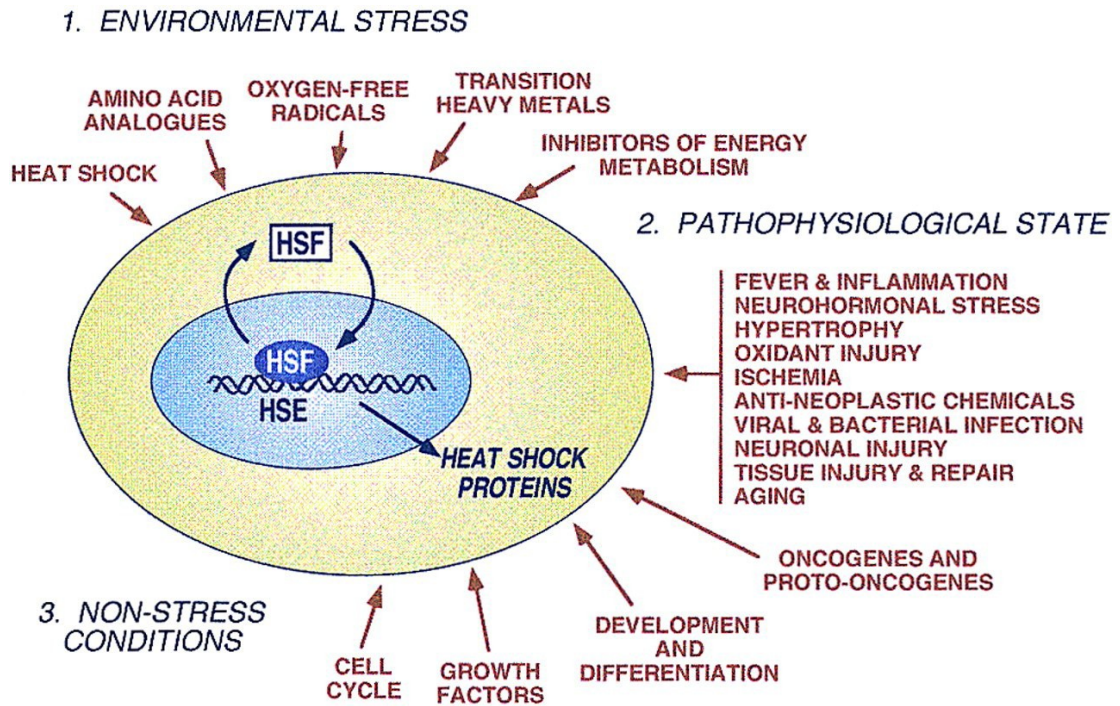


Figure. 1.2. Diagram showing the conditions that induce heat shock in response to environmental, physiological and non-stressful conditions (Taken from Morimoto, 1998).

Heat shock proteins achieve this by recognizing nascent polypeptides, partially and misfolded regions of proteins and exposed hydrophobic regions of amino acids (Figure 1.3) (Bakau and Horwich, 1998; Jolly and Morimoto, 2000; Morimoto, 1998; Nollen and Morimoto, 2002; Parsell and Lindquist, 1993). Under normal growth conditions nearly all heat shock proteins are constitutively expressed at relatively low but constant levels, as their normal cellular function is to maintain protein homeostasis by regulating correct protein folding (Hartl and Hayer-Hartl, 2002; Nollen and Morimoto, 2002). However, under conditions of stress, induction of heat shock gene expression results in heat shock proteins being produced at much higher levels to prevent incorrect polypeptide aggregation and protein denaturation during physiochemical insults to enhance cell survival. Constitutive heat shock proteins perform housekeeping functions by acting as molecular chaperones. They assist polypeptides to achieve their proper conformation by binding to nascent proteins via their C-terminal domain (Mosser and Morimoto, 2004; Parsell and Lindquist, 1994).

The response of cells to such stress conditions is dependent on the concentration of heat shock proteins in the cell prior to stress, and on the severity of the stress, based upon its intensity and duration. The outcome of such stress events is either cell survival or apoptotic or necrotic cell death (Mosser and Morimoto, 2004). Thus, heat shock proteins play a role in the cell cycle. Elevated levels of heat shock proteins are seen in cells recovering from induced stress, and these cells are in a cytoprotected state, protecting them from further exposures to stress conditions (Nollen and Morimoto, 2002). Cells initiating apoptosis after induced stress also elicit the production of heat shock proteins. This continues until such time as heat shock protein levels in the cell have returned to normal (Mosser and Morimoto, 2004; Parsell and Lindquist, 1993).

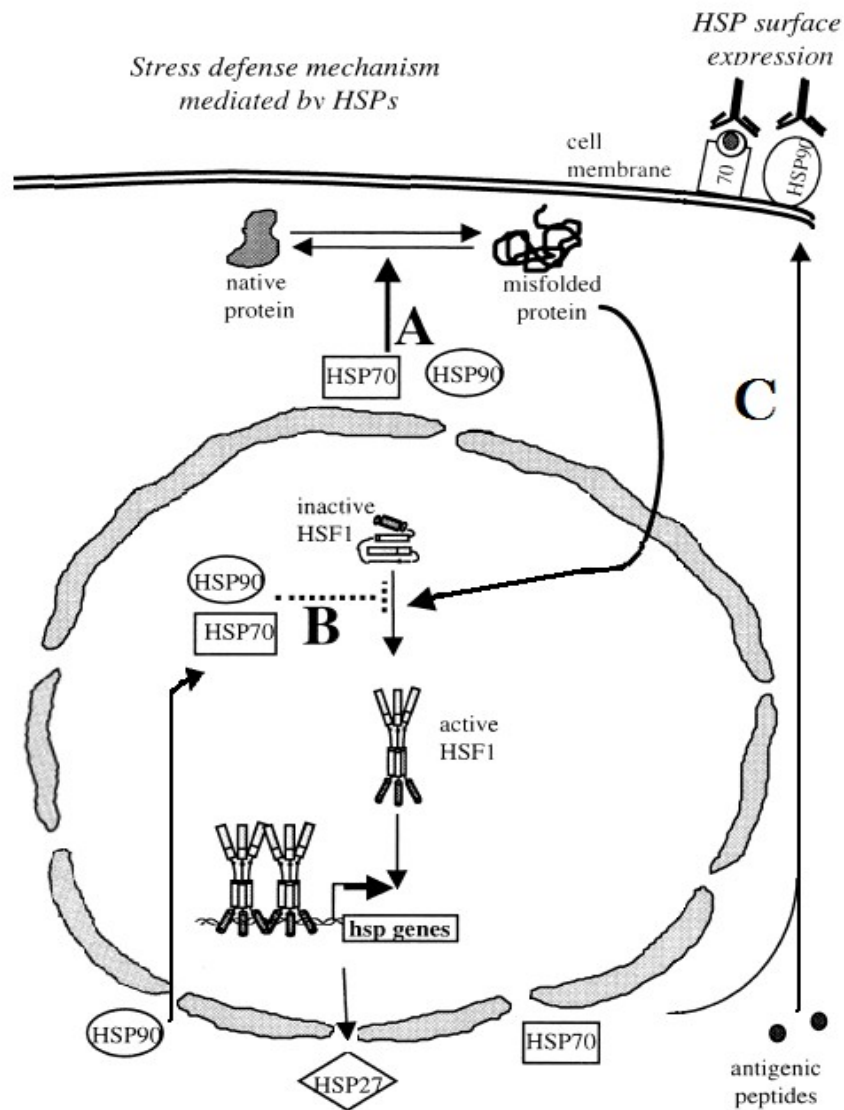


Figure 1.3 Schematic diagram showing the stress defence mechanism mediated by heat shock proteins. Stress such as heat shock, hypoxia, post-mortem and cancer are associated with the emergence of misfolded proteins. Initially heat shock proteins will assist misfolded proteins and folded intermediates to obtain a native state (pathway A), resulting in the activation of the heat shock transcription factor in the nucleus, which activates the transcription of heat shock protein genes (pathway B). Heat shock proteins are also involved in the negative regulation of their own synthesis by autoregulation (pathway B). In some tumour cells heat shock proteins have been shown to be expressed at the cell surface (pathway C) (Taken from Jolly and Morimoto, 2000).

The induction of heat shock gene expression in response to stress conditions is dependent on a specific DNA sequence, termed the heat-shock element (HSE). The HSE is a stress responsive operator element located in the promoter regions of heat shock genes (Fernandes *et al*, 1994; Morimoto *et al*, 1994; Wu *et al*, 1994). It consists of a series of inverted pentameric units with the nucleotide sequence 5' nGAAn 3' (Santoro, 2000). Inducible transcription of heat shock protein genes require the *de novo* binding of the HSE by a heat shock transcription factor (HSF), which is constitutively produced.

In mammalian cells, the HSF gene family consists of the four members *HSF1*, *HSF2*, *Hsf3* and *HSF4* (Table 1.3), of which three (*HSF1*, *HSF2* and *HSF4*) have been characterized in human cells. The HSF1 protein is ubiquitously synthesised and plays a major role in the stress induced expression of heat shock protein genes (de Thonel *et al*, 2011). The HSF2 protein is activated during specific stages of cell development and is associated with development of the brain and reproductive organs (de Thonel *et al*, 2011). The HSF4 protein acts as an inhibitor of stress-induced gene expression (de Thonel *et al*, 2011; Jolly and Morimoto, 2000; Morimoto, 1993; Wu, 1995). The *Hsf3* gene has only been characterized in avian species and more recently identified in mouse as an orthologue of the chicken *Hsf3* gene (de Thonel *et al*, 2011; Nakai, 1999; Nakai and Morimoto, 1993; Tanabe *et al*, 1998). In mouse and avian species the HSF3 protein has been identified as a redundant heat shock responsive factor which is co-expressed with HSF1 suggesting that both HSF1 and HSF3 are involved in the activation of heat shock protein genes during heat shock (Tanabe *et al*, 1998).

Table 1.3. Characterization of heat shock factors across species (adapted from de Thonel *et al*, 2011; Morimoto, 1998).

	HSF1		HSF2		HSF3		HSF4^(a)
Species	<i>Homo sapiens, Mus musculus, Rattus norvegicus, Gallus gallus</i>		<i>Homo sapiens, Mus musculus, Rattus Norvegicus, Gallus gallus</i>		<i>Mus musculus, Gallus gallus</i>		<i>Homo sapiens Mus musculus, Rattus Norvegicus, Gallus gallus</i>
Homology between species	92%		92%				
Tissue Specific Location	Ubiquitous		Ubiquitous		Ubiquitous		Tissue specific – heart, brain, pancreas, skeletal muscle
In vivo conditions	37°C	42°C heat shock	37°C	42°C heat shock	37°C	42°C heat shock	37°C
Protein size							
Native (KDa)	70	178	127	127			
Denatured (KDa)	70	85	72	72	69	69	55
Localization	Cytoplasmic / Nuclear	Nuclear	Cytoplasmic and Nuclear	Cytoplasmic and Nuclear	Cytoplasmic	Nuclear	Constitutively Nuclear
Oligomeric State	Monomer	Trimer	Dimer	Dimer	Dimer	Trimer	Trimer
DNA-binding		+	-	-	-	+	Constitutive DNA binds but lacks transcriptional activity

(a) DNA – binding activity is lost *in vitro* upon heat shock

Heat shock protein synthesis is regulated at the transcriptional level by heat shock factors (HSF) which assist, not only in the long term induction of heat shock protein genes, but also in the regulation of gene expression and developmental processes (Morimoto, 1998; Sreedhar *et al*, 2004). All members of the heat shock factor protein family share two evolutionary conserved structural functional domains: a conserved DNA-binding domain (DBD) at the amino terminus and an oligomerization domain (Figure 1.4). The heat shock factor DBD is a member of the winged helix-turn-helix hepatocyte nuclear factor 3/fork (HNF-3/fork) transcription factors (de Thonel *et al*, 2011; Harrison *et al*, 1994, Vuister *et al*, 1994). The oligomerization domain comprises arrays of hydrophobic heptad repeats (HRs) which are divided into two subdomains: the amino terminal HR-A and the carboxy-terminal HR-B, both of which are essential for trimer formation (de Thonel *et al*, 2011; Peteranderl and Nelson, 1992; Shamovsky and Nudler, 2008; Soger and Nelson, 1989). A third HR domain (HR-C) is also located in *Drosophila* HSF and mammalian HSF1 which maintains heat shock factors in a monomeric state by suppressing trimer formation through interactions with HR-A/B. (de Thonel *et al*, 2011; Green *et al*, 1995; Shamovsky and Nudler, 2008; Shi *et al*, 1995; Wisniewski *et al*, 1996; Zuo *et al*, 1995).

Heat shock response involves the functional activation of heat shock factor 1 (HSF1), in response to damage to other cellular proteins which requires the action of molecular chaperones. HSF1 is present in both stressed and unstressed cells. Under normal conditions, HSF1 exists in the cytoplasm as an inert monomer, which is unable to bind to DNA and does not show any transcriptional activity (Pockley, 2003; Santoro 2000). HSF1 is constitutively phosphorylated and lacks the ability to bind to the cis-acting heat shock elements within the promoter regions of the heat shock protein genes (Wang *et al*, 2003, Wu, 1995). In a stressed state, when non-native or damaged proteins are

detected, induction of transcriptional activity by heat shock factor 1 requires that the inactive HSF1 monomer is converted to phosphorylated trimers which have the capacity to bind to DNA, and which also translocate from the cytoplasm to the nucleus (Baler *et al*, 1993; Pockley, 2003; Santoro 2000; Sarge *et al*, 1993; Westwood *et al*, 1993).

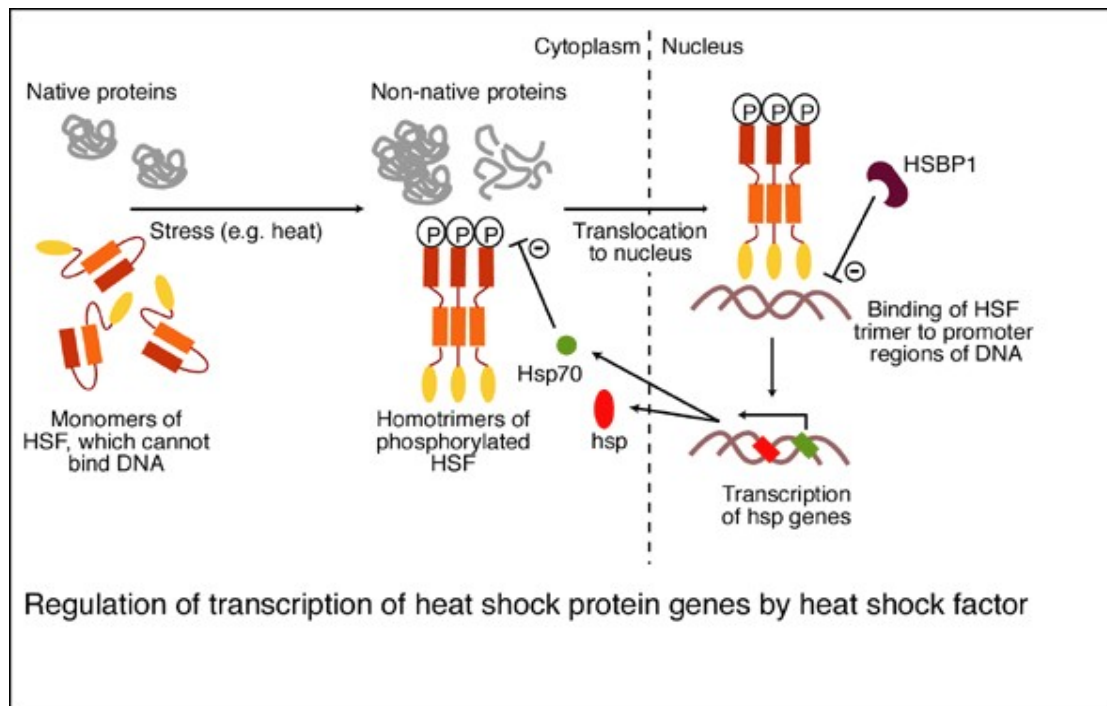


Figure 1.4. Regulation of transcription of heat shock protein genes by heat shock factor. Heat shock factor (HSF) is present in the cytoplasm in a monomeric state that is unable to bind to DNA. Under conditions of stress such as heat shock, the flux of non-native proteins leads to phosphorylation and trimerisation of HSFs. The trimers translocate to the nucleus, bind the promoter regions of heat shock protein genes and mediate heat shock protein gene transcription (Adapted from Pockley, 2003).

Activation induced trimerization of HSF1 occurs by the intermolecular coiled-coil interaction of the HR-A/B and HR-C domains (Figure 1.5) (Rabindran *et al*, 1993), which is mediated by leucine zipper domains (three hydrophobic heptad repeats of HR-A/B) in the N-terminus, which is in turn subject to intramolecular negative regulation by a fourth leucine zipper (hydrophobic heptad repeat of HR-C) in the C-terminus. The phosphorylated HSF1 binds to the heat shock element, thereby allowing transcription of the target genes (Santoro, 2000).

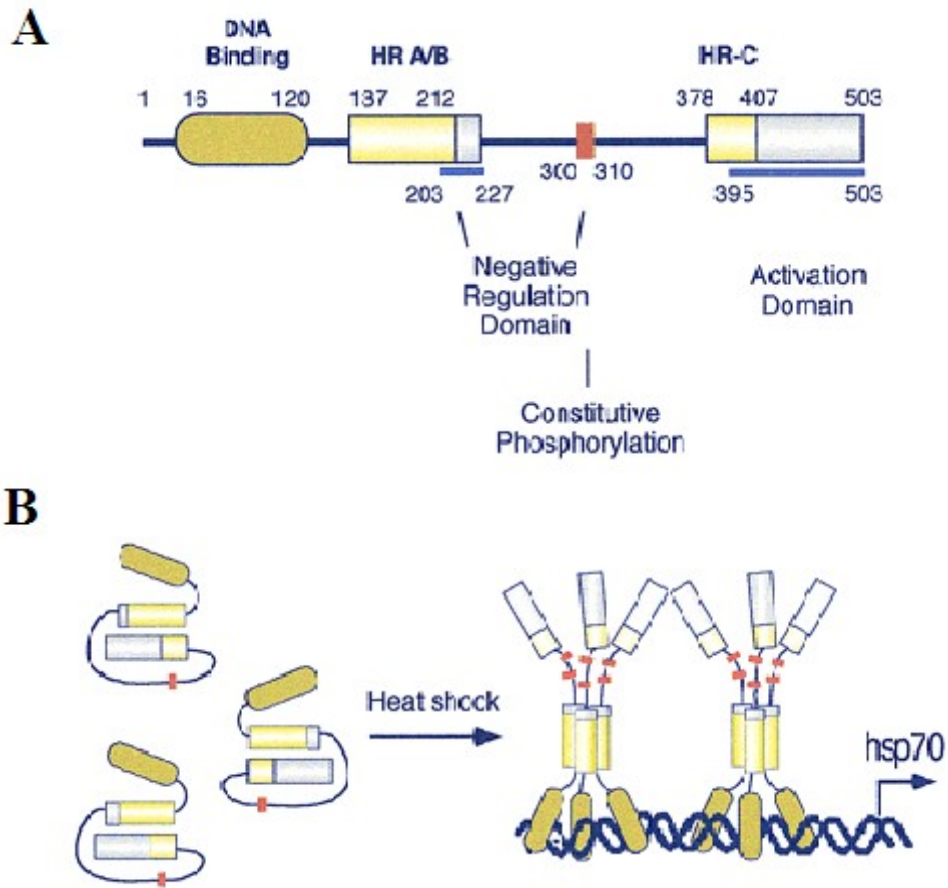


Figure 1.5. The general structural and regulatory features of HSFs. (A) A schematic representation of HSF1 structural motifs corresponding to the DNA-binding domain (DBD), hydrophobic heptad repeats (HR-A, HR-B and HR-C), the carboxyl-terminal transcriptional activation domain and the negative regulatory domains all of which influence HSF1 activity. (B) A schematic representation of the intramolecular negatively regulated monomer which, upon exposure to stress, becomes activated to form homotrimers with DNA-binding activity (adapted from de Thonel *et al*, 2011 and Santoro, 2000).

Various mechanisms for HSF binding and regulation of heat shock protein gene transcription have been proposed, and these are described here with respect to heat shock protein 70 gene (*HSPA/HSP70*) (Abravaya *et al*, 1992; Morimoto, 1993). In the absence of stress in cells, HSF is present in both the cytoplasm and the nucleus and is maintained in a non-DNA binding monomeric state through transient interactions with *HSPA/HSP70*, which prevents the activation of HSF (Abravaya *et al*, 1992; Morimoto, 1993). During heat shock, denatured and misfolded proteins accumulate and prevent new substrates for *HSPA/HSP70* which compete for *HSPA/HSP70* binding with HSF (Abravaya *et al*, 1992). This results in the release of HSF from *HSPA/HSP70*. The released HSF proteins oligomerises into a trimeric state which binds to the HSE sequence within the heat shock gene promoter region and becomes inducibly phosphorylated by active protein kinases, such as protein kinase A (PKAca) , at serine residues in the carboxyl-terminal domain, thus activating stress induced transcription (Abravaya *et al*, 1992; Morimoto, 1993; Zhang *et al*, 2011). Activated HSF induces transcription of the heat shock protein genes resulting in increased levels of synthesis of heat shock proteins within the cell. This eventually results in the formation of a new HSF-*HSPA/HSP70* complex (Abravaya *et al*, 1992), which the HSF-*HSPA/HSP70* complex dissociates from the HSE resulting in the cessation of transcription (Figure 1.6) (Abravaya *et al*, 1992; Morimoto. 1993).

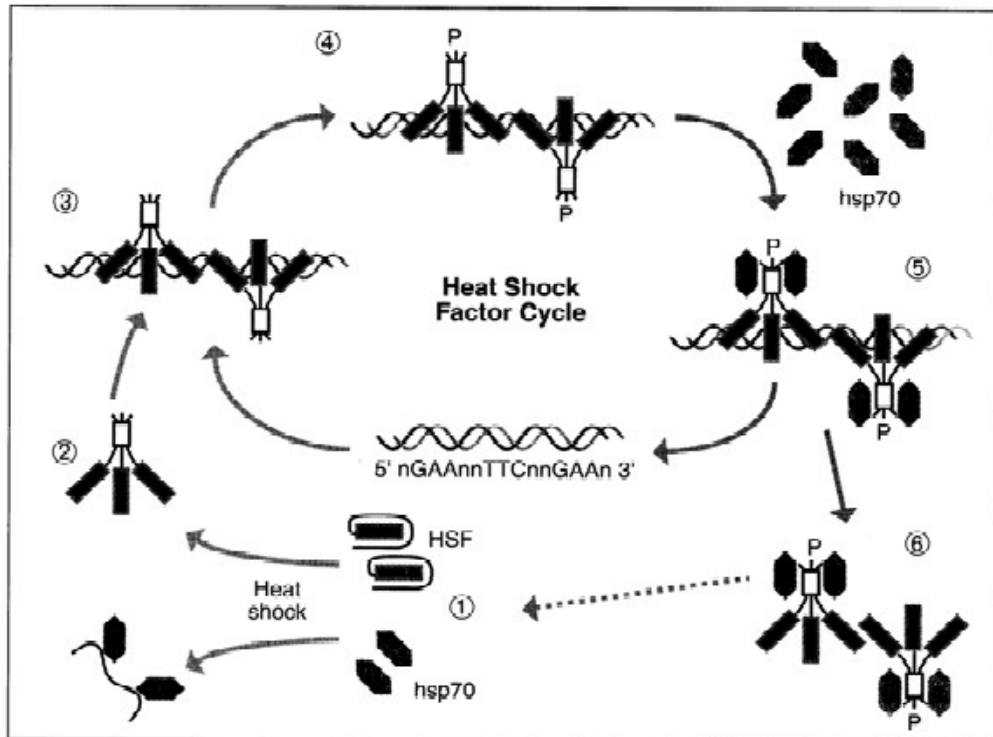
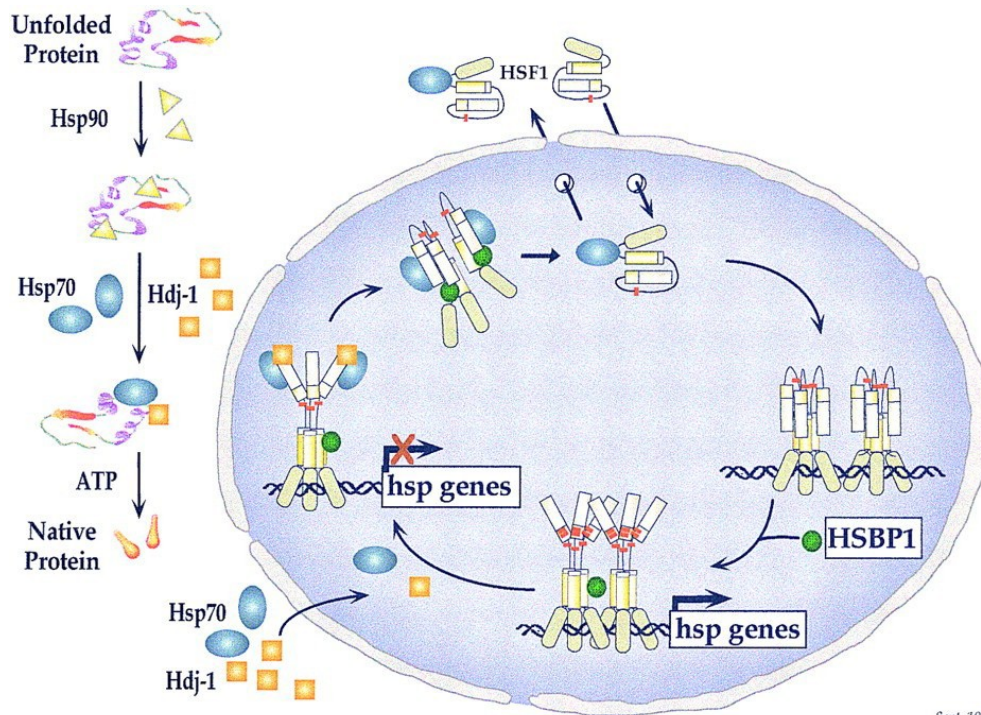


Figure 1.6. Heat shock factor regulation (adapted from Morimoto. 1993). In the absence of stress in cells, HSF is maintained in a non-DNA binding monomeric state (1). Following stress, HSF oligomerises into a trimeric state (2). HSF binds to specific sequences, HSE, in heat shock gene promoters (3), and becomes phosphorylated (4). Transcriptional activation of heat shock genes increases the levels of HSPA/HSP70 which forms a HSF-HSPA/HSP70 complex (5). HSF dissociates from the DNA and reverts back to a non-DNA binding monomer (Morimoto. 1993).

Complexes of HSPA/HSP70 and HSF trimers have been detected in cells and are consistent with the role of chaperones during attenuation of the heat shock transcriptional response (Abravaya *et al*, 1992; Baler *et al*, 1992; Morimoto, 1998). In the absence of stress, overexpression of *HSPA/HSP70* or *DNAJ/HSP40* prevents the inducible transcription of heat shock genes (Morimoto, 1998; Mosser *et al*, 1993; Shi *et al*, 1998). These molecular chaperones bind directly to the HSF1 transactivation domain. However, HSPA/HSP70 chaperones and associated co-chaperones, such as DNAJ/HSP40, which participates in the function of HSPA/HSP70, alone are insufficient to prevent the appearance of HSF1 trimers, suggesting that the acquisition of transcriptional activity is a separate process from that of the regulation of trimer formation (Figure 1.7) (Morimoto, 1998)



Sept. 1998

Figure 1.7. Regulation of the heat shock response and the HSF cycle. HSF1 exists in a controlled state as an inert monomer in either the cytoplasm or the nucleus through transient interactions with a number of chaperones such as HSPA/HSP70, HSPC/HSP90 and DNAJ/HDJ1. In response to heat shock the transcriptional activity of HSF1 is suppressed by direct binding of HSPA/HSP70 and HDJ1. The heat shock factor binding protein 1 (HSBP1), which is a conserved protein of 76 amino acids containing an extended hydrophobic heptad repeat interacts and binds to the hydrophobic heptad repeats of both HSF1 and HSPA/HSP70. These events lead to the appearance of HSF1 inert monomers and the dissociation of HSF1 trimers. (Taken from Morimoto, 1998).

1.2 Heat shock proteins

It is necessary to describe the main heat shock protein families found in eukaryotic cells. However, due to the diversity of the heat shock protein families, which cover approximately five hundred client proteins, this section will focus on the five heat shock proteins studied examples.

1.2.1 Heat Shock Protein 27 (HSPB)

The ubiquitous heat shock protein 27 (HSPB/HSP27) has a molecular weight of 27 KDa and is a member of the small heat shock protein family. HSPB/HSP27 is highly conserved amongst all species and has high homology with the eye lens α -crystallin proteins (Ciocca *et al*, 1993). α -crystallin proteins are water soluble structural proteins that are present in high concentrations in the cytoplasm of eye lens fibre cells (de Jong *et al*, 1989). α -crystallin proteins exhibit chaperone-like properties, which include the ability to prevent the acceleration of denatured proteins; an increase in cellular tolerance to stress and assist in the maintenance of lens transparency and prevention of cataracts (Augusteyn, 2004; de Jong *et al*, 1989). HSPB/HSP27 production is induced by stimuli similar to those of the larger molecular weight heat shock proteins (Garrido *et al*, 1997; Garrido *et al*, 2006; Parcellier *et al*, 2003). It is constitutively expressed in a variety of tissues and this expression is up-regulated under conditions of stress, including disease (Kappe *et al*, 2003).

HSPB/HSP27 contains a homologous and highly conserved amino acid sequence the α -crystallin domain at the C-terminus. These sequences consist of ~ 100 residues with a homology between 20-60 % and which forms β sheets which are necessary for the formation of stable dimers. It also possesses a less conserved proline/phenylalanine rich region containing one or two WF/EPF motifs, tryptophan, phenylalanine / glutamic

acid, proline, phenylalanine, at the NH₂-terminus which are essential for protection, maintenance of the oligomeric structure and chaperone activity of the protein (Kim *et al*, 1998; Theriault *et al*, 2004, von Montfort *et al*, 2001). HSPB/HSP27 acts as an ATP-independent molecular chaperone which inhibits protein aggregation and stabilises partially denatured proteins, which ensures protein refolding by the HSPA/HSP70 complex (Ehrnsperger *et al*, 1997; Parcellier *et al*, 2003). Also, HSPB/HSP27 assists in cytoprotection, by protecting cells against apoptosis under stress conditions (Charette *et al*, 2000; Pandley *et al*, 2000; Paul *et al*, 2002). Apoptosis is inhibited by interactions with the cellular death associated protein DAXX7, facilitating the activation of protein kinase B, AKT, (Rane *et al*, 2003) and blocking the formation of the apoptosome, a multisubunit protein complex involved in the activation of apoptosis, (Pandley *et al*, 2000; Paul *et al*, 2002). HSPB/HSP27 has been shown to interact with different cytoskeletal elements affecting actin polymerization (Ehrnsperger *et al*, 1997), to modulate intracellular reactive oxygen species content, to prevent apoptotic cell death activated by various stimuli including heat, serum deprivation, tumour necrosis factor alpha (TNF- α) and many commonly used anti-cancer drugs such as etoposide, doxorubicin, vincristine and cisplatin (Garrido, 2002; Huott *et al*, 1991; Oesterreich *et al*, 1996; Parcellier *et al*, 2003).

Studies have shown HSPB/HSP27 to be phosphorylated in response to a number of extracellular-derived signals such as TNF- α , thrombin, and also under conditions of stress arising from heat shock, oxidative stress and disease (Charette *et al*, 2000; Landry *et al*, 1992). Phosphorylation of HSPB/HSP27 occurs at three serine residues, Ser-15, Ser-78 and Ser-82 (Landry *et al*, 1992; Stokoe *et al*, 1992), and is activated by a number of protein kinases including MAPKAPK-2, MAPKAPK-3, PKAC α , p7056k, PKD1,

AKT1 and PCK7 (Butt *et al*, 2001; Doppler *et al*, 2005; Landry *et al*, 1992; Rane *et al*, 2003; Stokoe *et al*, 1992).

Overexpression of *HSPB/HSP27* in disease states, such as cancer, facilitates the adaptation of cells to stressful conditions by assisting in the suppression of apoptosis, leading to a more aggressive disease phenotype (Aldrian *et al*, 2002). Therefore, overexpression of *HSPB/HSP27* correlates with poor patient prognosis in a variety of cancers such as include: colorectal, prostate, testis, breast, and ovarian cancers (Ciocca *et al*, 2005; Garrido *et al*, 1998; Garrido *et al*, 1997; Oesterreich *et al*, 1993; Richards *et al*, 1996). *In vivo*, *HSPB/HSP27* has also been implicated in cellular thermotolerance, although the expression of *HSPB/HSP27* alone is insufficient to induce this state and requires the assistance of higher molecular weight heat shock proteins (Trautinger *et al*, 1997).

1.2.2 Heat Shock Protein 40 (DNAJ)

The heat shock protein 40 (DNAJ/HSP40) family, with an average molecular weight of 40 KDa, is a large protein family consisting of over 100 members. Members of the DNAJ/HSP40 family have been classified into three subtypes in relation to their domain structures, (subfamily A, Type I; subfamily B, Type II; subfamily C, Type III) (Cheetham and Caplan, 1998; Ohtsuka and Hata, 2000; Uchiyama *et al*, 2006). All subfamilies contain a highly conserved J domain of ~ 78 residues (Fink, 1999; Laufen *et al*, 1998). In subfamilies I and II the J-domain is located at the N-terminus, whereas in subfamily III, the J-domain may be located at any position within the protein sequence. Both subfamilies I and II have a peptide-binding fragment located at the C-terminus of the proteins. The N-terminal J-domains are connected to the peptide-binding fragments via a Gly/Phe rich linker in subfamilies I and II. Subfamily I members, for example the human member HDJ2, contain two Zinc finger motifs between the J-domain and the C-terminal peptide-binding fragment. In contrast, subfamily II members, such as the human member HDJ1, lack this feature (Caplan *et al*, 1992; Cyr *et al*, 1994; Zhong and Arndt, 1993). Subfamily III members, as mentioned above, contain the J-domain, but this may be located at any position within the protein and therefore lack the other conserved domains found in subfamily I and II members.

The main role of DNAJ/HSP40 is that of a cochaperone, which specifies the cellular action of HSPA/HSP70 proteins. DNAJ/HSP40 plays an important role in protein folding, unfolding, translation, translocation and degradation, primarily by stimulating the ATPase activity of HSPA/HSP70 proteins (Fink *et al*, 1999, Minami *et al*, 1996; Qiu *et al*, 2006). DNAJ/HSP40 in both eukaryotic and prokaryotic cells interacts with HSPA/HSP70 in the presence of ATP suppressing protein aggregation (Cyr, 1994; Fink *et al*, 1999). It has been suggested that DNAJ/HSP40 binds to the non-native polypeptide first and then delivers the non-native polypeptide to HSPA/HSP70 for

folding (Bukau and Horwich, 1998; Gething and Sambrook, 1992; Hartl, 1996). The main function of Dnaj/HSP40 is to regulate adenosine triphosphate (ATP) dependent polypeptide binding by HSPA/HSP70 protein (Fan *et al*, 2003; Hartl and Hayer-Hartl, 2009; Szabo *et al*, 1994). Dnaj/HSP40 strongly accelerates the hydrolysis of ATP to adenosine diphosphate (ADP) resulting in the closing of the α -helical lid of the peptide binding domain and tight binding of the peptide substrate by HSPA/HSP70. Dnaj/HSP40 dissociates from HSPA/HSP70 (Hartl and Hayer-Hartl, 2009). Interaction of the substrate with HSPA/HSP70 is mediated by the J domain, which is present in all Dnaj/HSP40s (Hartl and Hayer-Hartl, 2009; Mayer *et al*, 2000). Dnaj/HSP40 also directly interacts with unfolded polypeptides and can convert HSPA/HSP70 to protein substrates (Hartl and Hayer-Hartl, 2009; Young *et al*, 2003). Following ATP-hydrolysis, a number of nucleotide exchange factors (NEF), such as Bag, and HSPBP1, bind to the HSPA/HSP70 ATPase domain and catalyse ADP-ATP exchange, which results in the opening of the α -helical lid and release of the substrate (Hartl and Hayer-Hartl, 2009). The released substrate either folds to a native state; or is transferred to downstream chaperones, such as HSPC/HSP90, or rebinds to HSPA/HSP70 (Hartl and Hayer-Hartl, 2009).

The J domain, which is common to all Dnaj/HSP40 family members, is responsible for the regulation of HSPA/HSP70 ATPase activity. Interactions of HSPA/HSP70 proteins with Dnaj/HSP40 proteins produce HSPA/HSP70-Dnaj/HSP40 heterodimers which assist certain processes at specific locations within a cell (Fan *et al*, 2003; Liu *et al*, 1998). Dnaj/HSP40 also functions as homodimers which interact with non-native polypeptides of at least six residues in length, through hydrophobic interactions (Cyr, 1994; Fan *et al*, 2003; Fink *et al*, 1999; Li *et al*, 2009). The peptide-binding site of Dnaj/HSP40 also serves as the binding site for the C-terminal EEVD motif of

HSPA/HSP70 through charge-charge interactions (Freeman *et al*, 1995; Li *et al*, 2009; Qian *et al*, 2002).

The overexpression of *DNAJ/HSP40* and *HSPA/HSP70* has been observed in colorectal (Kanazawa *et al*, 2003) and gastric tumour tissues (Isomoto *et al*, 2003). However, immunohistochemical analysis has shown only a small proportion of samples which were positive for *DNAJ/HSP40* in gastric cancer tissues (Isomoto *et al*, 2003). *HSPA/HSP70* and *DNAJ/HSP40* were shown to be down-regulated in undifferentiated cancers, suggesting that HSPA/HSP70-DNAJ/HSP40 chaperone systems could have a role in tumour differentiation (Isomoto *et al*, 2003; Kanazawa *et al*, 2003).

1.2.3 Heat Shock Protein 60 (HSPD)

The heat shock protein 60 family (HSPD/HSP60) is named after the average molecular weight of its members of 60 KDa. Their genes are either moderately stress inducible or are highly expressed constitutively (Jindal *et al*, 1989; Neuer *et al*, 2000). Although the majority of HSPD/HSP60 is located in the mitochondria, ~ 15 -20% of cellular HSPD/HSP60 is located in extramitochondrial sites, such as the cytosol, peroxisomes, endoplasmic reticulum and at the cell surface (Gupta *et al*, 2002; Pfister *et al*, 2005; Stefano *et al*, 2009; Stetler *et al*, 2010). They are responsible for the synthesis, transportation and refolding of essential proteins from the cytoplasm into the mitochondrial domain. Their main function is the ATP-dependant folding and/or refolding of approximately 15-30% of total cellular proteins and they also assist in the folding of linear amino acid chains into their respective tertiary structures (Ranford *et al*, 2000; Trivedi *et al*, 2010; Urushibara *et al*, 2007).

HSPD/HSP60 has two main roles in relation to mitochondrial protein transport: the catalysis of the folding of proteins destined for the mitochondrial matrix and maintenance of proteins in an unfolded state for transmembrane transportation (Koll *et al*, 1992). *In vitro* HSPD/HSP60 has been identified as a single-stranded DNA (ssDNA) binding protein that simulates DNA replication (Smiley *et al*, 1992). HSPD/HSP60 has been found to associate with ssDNA regions and to bind to ssDNA of active sequences with high specificity for the template of a putative origin of mitochondrial DNA (mtDNA) replication in a strand specific manner (Kaufman *et al*, 2003; Kaufman *et al*, 2000).

Under normal physiological conditions, HSPD/HSP60 is located typically in the mitochondria, but can also be found in the cytoplasm (Itoh *et al*, 2002; Jindal *et al*, 1989; Neuer *et al*, 2000). HSPD/HSP60 is composed of monomers that form a double heptameric ring structure (Cheng *et al*, 1990) comprised of a large central cavity whereby unfolded proteins bind via hydrophobic interactions (Fenton *et al*, 1994). Each subunit of HSPD/HSP60 contains three domains: the apical domain, the equatorial domain, which contains the binding site for ATP, and the intermediate domain which links the apical and equatorial domains (Ranford *et al*, 2000).

HSPD/HSP60 proteins play an important role in preventing apoptosis in the cytoplasm and are also associated with the immune response and cancer (Hansen *et al*, 2003; Itoh *et al*, 2002). The cytoplasmic HSPD/HSP60 forms a complex with various other proteins that are responsible for apoptosis and regulates their activity (Itoh *et al*, 2002). HSPD/HSP60 has been shown to influence apoptosis in the immune response (Hansen *et al*, 2003) and in cancer cells (Itoh *et al*, 2002).

In cancer, *HSPD/HSP60* expression appears either to inhibit apoptotic and necrotic cell death or plays a role in the activation of apoptosis, dependent on the tumour type (Capello *et al*, 2006; Urushibara *et al*, 2007). A loss of *HSPD/HSP60* expression in bladder carcinomas, –indicates a poor prognosis and the risk of developing tumour infiltration, (Lebret *et al*, 2003). In the initial stages of ovarian cancer, *HSPD/HSP60* is over-expressed with a decrease in expression as the disease progresses, associated also with tumour aggressiveness (Lebret *et al*, 2003; Schnieder *et al*, 1999). These changes in *HSPD/HSP60* expression levels have the potential to be –new useful biomarkers for diagnostic and prognostic purposes (Capello *et al*, 2006).

1.2.4 Heat Shock Protein 90 (HSPC)

The heat shock protein 90 family (HSPC/HSP90) has an average molecular weight of 90 KDa and is one of the most abundant of the heat shock proteins, comprising approximately 1 - 2% of total cellular proteins under unstressed conditions (Csermely *et al*, 1998). HSPC/HSP90 plays an important role in the folding of newly synthesized proteins and the stabilization and refolding of denatured proteins after stress conditions; intracellular protein transport; protein degradation; facilitation of cell signalling and in suppressing the aggregation of numerous client/substrate proteins (Buchner, 1999; Jakob *et al*, 1995; Miyata and Yahara, 1992; Wiech *et al*, 1992).

The HSPC/HSP90 family consists of both inducible and constitutive isoforms, with the two major cytoplasmic isoforms being HSPC1a/HSP90 α (the inducible isoform and HSPC2a/HSP90 β (the constitutive isoform) (Chen *et al*, 2006; Csermely *et al*, 1998). A further identified isoform of the HSPC/HSP90 family is HSPC3a/HSP90N, a constitutive protein associated with cellular transformation (Grammatikakis *et al*, 2002; Sreedhar *et al*, 2004). A number of HSPC/HSP90 analogues have also been reported: HSPA9/Grp75, localized in the endoplasmic reticulum (ER) and HAPC5a/HSP75/TRAP1, localized in the mitochondrial matrix (Csermely *et al*, 1998; Sreedhar *et al*, 2004).

All members of the HSPC/HSP90 family contain three structural domains: a highly conserved N-terminal nucleotide binding pocket ~ 25 KDa in length which possesses a high affinity ATP binding site (Chadli *et al*, 2000; Pearl and Prodromou, 2000; Prodromou *et al*, 1997; Prodromou and Pearl, 2003), a central domain ~ 40 KDa in length which is involved in substrate protein folding and ATPase activity

(Grammatikakis *et al*, 2002; Meyer *et al*, 2003) and a C-terminal domain ~ 12 KDa in length, which acts as a second ATP binding site when the N-terminal domain is occupied (Garnier *et al*, 2002; Marcu *et al*, 2000; Soti *et al*, 2002).

HSPC/HSP90 expression can be associated with various types of cancers. *HSPC/HSP90* in cancer cells exists in a hyperactive state in the diseased tissue compared to that of the normal surrounding tissue (Kamel *et al*, 2003). In this highly active state *HSPC/HSP90* influences various other proteins that contribute to the pathogenesis of the disease. These include cell growth promotion, evasion of apoptosis and stimulation of angiogenesis (Kamel *et al*, 2003). Over-expression of *HSPC1a/HSP90α* has been associated with poor prognosis of leukaemia (Yufu *et al*, 1992), pancreatic carcinoma (Gress *et al*, 1994) and breast cancer (Jameel *et al*, 1992).

A study undertaken by Ogata *et al*, (2000) in pancreatic carcinoma tissue showed over-expression of *HSPC1a/HSP90α* compared to pancreatitis and normal pancreas tissue. In contrast, *HSPC2a/HSP90β* was constitutively over-expressed in pancreatic carcinoma, pancreatitis and normal pancreatic tissues. These results suggest that *HSPC2a/HSP90β* is correlated to structural conformation by forming complexes with tubulin and actin which constitute the cytoskeleton, and that *HSPC1a/HSP90α* is directly or indirectly involved with cell proliferation and carcinogenesis (Ogata *et al*, 2000).

1.2.5 Heat Shock Protein 70 (HSPA)

The heat shock protein 70 (HSPA/HSP70) family is the most conserved group of the heat shock proteins (Oehler *et al*, 2000). HSPA/HSP70 is an anti-apoptotic protein which blocks a number of steps in the stress-induced apoptotic pathway (Kang *et al*, 2009; Lanneau *et al*, 2007). Its functions include the folding and assembly of newly synthesized proteins, refolding of misfolded and aggregated proteins, regulation of apoptosis, membrane translocation of organellar and secretory proteins, and controlling the activity of regulatory proteins (Figure 1.8) (Beckman *et al*, 1990; Kang *et al*, 2009; Mayer and Bukau, 2005; Seidberg *et al*, 2003).

During stress conditions, HSPA/HSP70 is induced at high levels through a combination of transcriptional activation, preferential translation and mRNA stabilization. It inhibits cell death by preventing the aggregation of cell proteins (Calderwood *et al*, 2005; Lindquist and Craig, 1988). HSPA/HSP70 proteins are weak ATPases which cycle through high and low affinity substrate binding states by nucleotide hydrolysis. An ATP bound HSPA will bind substrates with low affinity, whereas an adenosine 5' diphosphate (ADP) bound HSPA will bind substrates with high affinity (Schmid *et al*, 1994; Shaner and Morano, 2007).

An extensive literature and database search undertaken by Brocchieri *et al*, (2008) identified 130 human HSPA/HSP70 proteins. Subsequent analysis revealed 86 groups of non-identical sequences which were further analysed and clustered into 13 groups. A representative sequence was selected from each of the 13 groups to query the human genome using NCBI Build 36.1 and to identify conserved and diverged sequences. This process yielded 47 loci, which included coding HSPA/HSP70-like sequences, of which

seventeen corresponded to known genes recognized in the genome annotation (Table 1.4). Included within the latter seventeen was *HSPA 7*, which is considered to be a pseudogene.

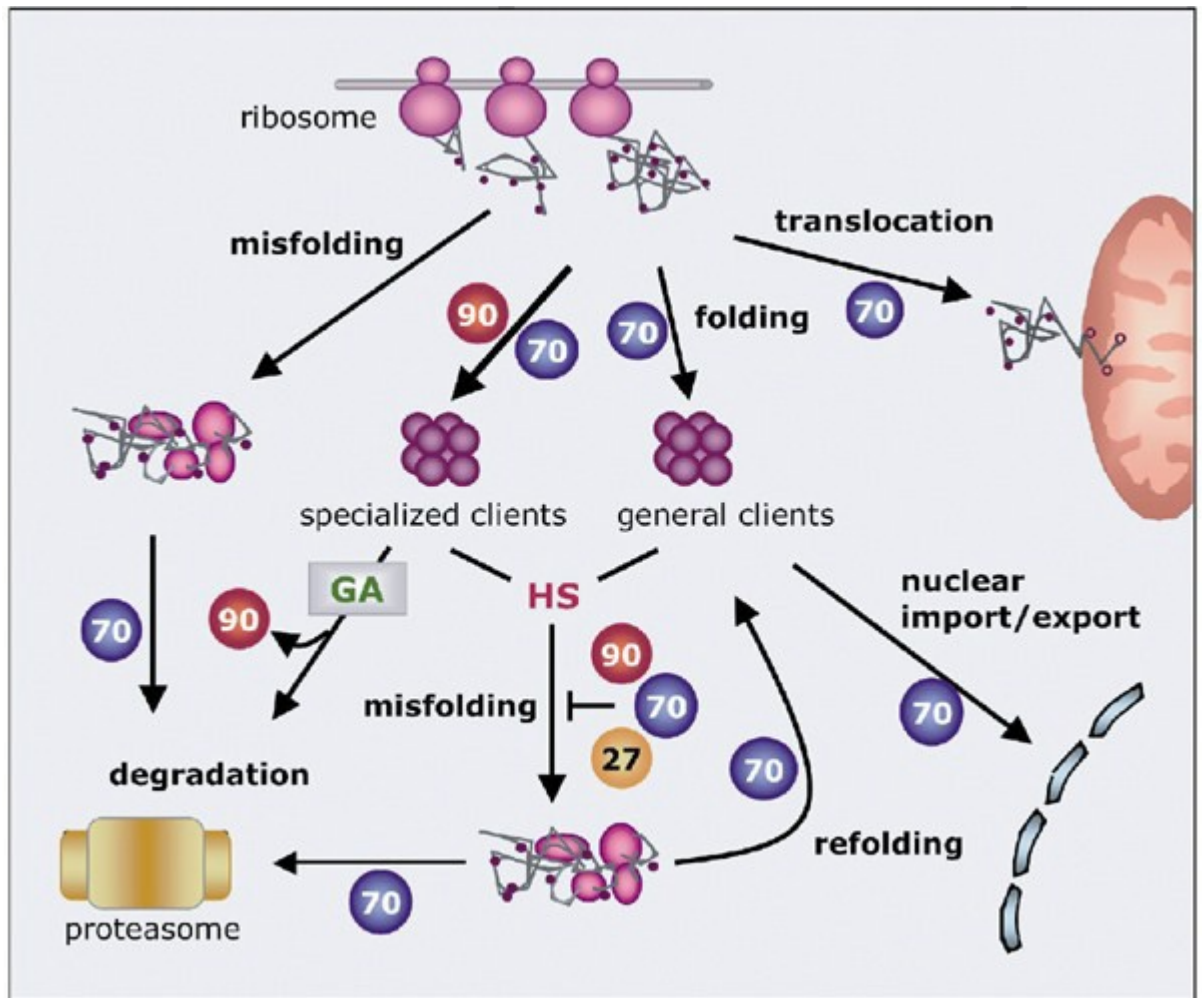


Figure 1.8 Chaperone-assisted protein folding (taken from Mosser and Morimoto, 2004). HSPA/HSP70 is required for the productive folding of newly synthesized proteins, translocation across intracellular membranes and import into and export of the nucleus. Heat shock and other protein damaging stresses cause protein misfolding and aggregation, which can be limited by heat shock proteins. These misfolded proteins can be rescued by the folding activity of HSPA/HSP70. Proteins that cannot be refolded are targeted to the proteasome for degradation.

Table 1.4. Expression and location of the human HSPA genes (Taken from Brocchieri *et al*, 2008)

Gene	Cell Locale	Tissue	Expression	Location
<i>HSPA8</i>	Cytosol	All tissues highly expressed	Constitutive. Moderately induced by heat shock.	11q24.1
<i>HSPA12A</i>	NK	Brain/kidney/muscle	Constitutive. Induced by stress.	10q25.3
<i>HSPA12B</i>	NK	Skeletal/heart muscle	Constitutive. Induced by stress.	20p13
<i>HSPA9B</i>	Mitochondria/ER/Cytosol/cystolic vesicles/membrane surface	Many tissues	Constitutive	5q31.2
<i>HSPA4</i>	Cytosolic	Most tissues	Constitutive. Not induced by heat shock.	5q31.1
<i>HSPA4L</i>	Cytosol	Testis	Constitutive. Induced by heat shock.	4q28.1
<i>HSPH1</i>	Cytosol	Most tissues	Constitutive. Induced by heat shock.	13q12.3
<i>HYOU1</i>	ER/Cytosol	Liver/pancreas	Induced by ER stressors	11q23.3
<i>HSPA14</i>	Cytosol, associated ribosomes	Many tissues	Undetermined	10p13
<i>STCH</i>	Microsomas	All tissues	Constitutive	21q11.2
<i>HSPA2</i>	Nucleus	Testis/skeletal and heart muscles/oesophagus/brain	Constitutive	14q23.3
<i>HSPA1A</i>	Cytosol	All tissue	Strongly induced by heat shock	6p21.33
<i>HSPA1B</i>	Cytosol	All tissue	Strongly induced by heat shock	6p21.32
<i>HSPA1L</i>	Cytosol	Spermatides	Constitutive. Not induced by heat shock.	6p21.33
<i>HSPA6</i>	Cytosol/Nucleus	Most tissues	Induced by heat shock	1q23.3
<i>HSPA7</i>				1q23.3
<i>HSPA5</i>	ER	All tissue	Induced by ER stressors	9q33.3

The human *HSPA* genes encode proteins which have been clustered into seven major distinct evolutionary groups (Figure 1.9), with noticeable subgroups relating to phylogenetic and other related data, including pseudogenes, exon-intron and protein features (Brocchieri *et al*, 2008).

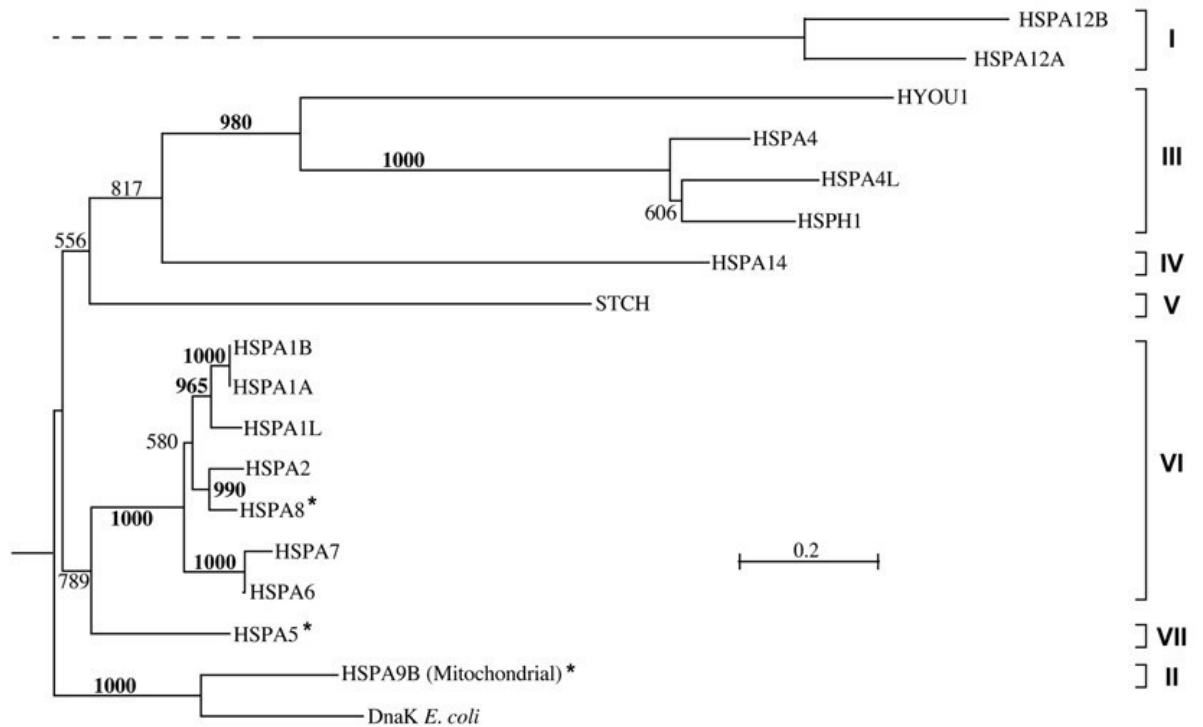


Figure 1.9. Phylogenetic tree of 17 human HSPA proteins. This is based on the alignment of their protein products defined by bootstrap support values over 85 %. Group I refers to HSPA12B and HSPA12A, Group II, HSPA9B AND DnaK, Group III, HYOU1, HSPA4, HSPA4L and HSPH1, Group IV, HSPA14, Group V, STCH, Group VI, HSPA1B, HSPA1A, HSPA1L, HSPA2, HSPA8, HSPA7 and HSPA6 and Group VII, HSPA5. The distance scale of 0.2 = 20% represents the differences between sequences. The branch lengths are proportional to the scale, so two sequences with longer branches are more diverged than sequences with shorter branches (taken from Brocchieri *et al*, 2008).

Group I is characterised by two similar, but diverged, sequences, HSPA12A and HSPA12B. Both sequences possess identical exon-intron structures and 12 exons have been located within their coding regions. Group II includes the mitochondrial protein HSPA9B, encoded by a nuclear gene which possesses 17 exons, and the DnaK sequence from *E. coli*. Group III proteins include three closely related 105/110 KDa proteins whose genes all have a common structure of 18 – 19 exons. These Group III proteins include HSPA4L, HSPA4 and HSPH1, which all occur as two isoforms. Also contained within Group III is the distantly related sequence HYOU1, which encodes the 170 KDa protein, Grp170, known to exist in three isoforms, and whose genes possess 16, 24 or 25 exons respectively (Brocchieri *et al*, 2008).

Group IV includes the sole sequence HSPA14, of which two isoforms exist, possessing 4 and 14 exons respectively. Although closely associated with Group III, cluster analysis showed a bootstrap support value of 81% for HSPA14, which is below the bootstrap threshold value of 85% and therefore the latter protein is allocated a separate evolutionary group. Group V also comprises a single sequence, STCH, which has 5 exons within the coding region and is weakly related to Group III and Group IV, having a bootstrap support value of 55.6% (Brocchieri *et al*, 2008).

Group VI contains seven sequences, each with bootstrap values of 100%, which have been divided into three distinct subgroups. Subgroup one includes the intronless sequences for HSPA1A, HSPA1B and HSPA1L, which are positioned within the MHC-III region on the short arm of chromosome 6. Subgroup two contains HSPA2 and HSPA8, existing as two isoforms which possess 7 – 8 exons, whilst subgroup three comprises HSPA6 and HSPA7. Finally, Group VII contains one sequence HSPA5,

which has 8 exons within the coding region and is closely related to Group VI having a bootstrap support value of 78.9% (Brocchieri *et al*, 2008).

The HSPA family share significant similarities in sequence and structure, based on highly conserved bipartite domain structure (Shaner and Morano, 2007). This structure comprises three major functional domains, including a highly conserved N-terminal ATPase domain (NBD) with a molecular mass of ~ 44 KDa which controls the closing and opening of the peptide domain. An adjacent well-conserved substrate binding domain (SBD), with a molecular mass of ~ 18kD, contains a hydrophobic pocket and lid-like structure over the pocket and a conserved C-terminal domain, with a molecular mass of ~ 10 KDa, which chaperones denatured proteins and peptides (Fiege and Polla, 1994; Hartl, 1996; Hartl and Hayer-Hartl, 2002; Mao *et al*, 2006; Mayer and Bukau, 2005; Mosser and Morimoto, 2004; Osipiuk *et al*, 1999; Wisniewska *et al*, 2010). When non-active, HSPA/HSP70 is usually in an ATP bound state. As newly synthesized proteins emerge, the SBD of HSPA/HSP70 recognizes and interacts with sequences of hydrophobic amino acid residues, stimulating the ATPase activity of HSPA/HSP70 and increasing ATP hydrolysis. As ATP is hydrolyzed to ADP, the hydrophobic pocket tightly closes, binding the peptides to the SBD (Hartl, 1996; Hartl and Hayer-Hartl, 2002; Mao *et al*, 2006; Mayer and Bukau, 2004; Mosser and Morimoto, 2004). In the case of partially synthesized peptide sequences, HSPA/HSP70 will prevent aggregation, allowing them to re-fold correctly. All three domains play important roles in tumour immunity, not only by enabling intracellular HSPA/HSP70 to prevent tumour apoptosis, but also to promote the generation of stable complexes with cytoplasmic tumour antigens stimulating anti-tumour immunity (Calderwood *et al*, 2005; Schmitt *et al*, 2007). Under normal conditions, HSPA/HSP70 functions as an ATP dependent molecular chaperone and is found mainly in the cytosol. Various stress

conditions such as heat shock, hypoxia and cancer increase the synthesis of HSPA/HSP70, and also cause it to migrate to the nucleus and associate with nuclear proteins (Santoro, 2000).

Heat shock proteins can be toxic if present in cells for any prolonged period of time and must therefore be stringently regulated. Theodorakis *et al*, (1999) examined the expression of *HSPA/HSP70* after heat shock in thermotolerant (heat resistant) and non-thermotolerant human hepatoblastoma cells. During and after heat shock, *HSPA/HSP70* transcriptional activity in both thermotolerant and non-thermotolerant cells was very similar. mRNA stability and expression of *HSPA/HSP70* was reduced in thermotolerant cells, compared to the non-thermotolerant cells after heat shock, suggesting that the thermotolerant cells possibly limit *HSPA/HSP70* expression to avoid cytotoxic effects.

The *HSPA/HSP70* gene family is of particular interest with regard to three members (*HSPA1A/HSP70-1*, *HSPA1B/HSP70-2* and *HSPA1L/HSP70-Hom*; Milner and Campbell, 1990). The nomenclature now used is specific to the allelic level of the genes, whose genes are located within the major histocompatibility complex class III region (MHC-III) on the short arm of chromosome 6 (6p21.3), and are intronless (Figure 1.10).

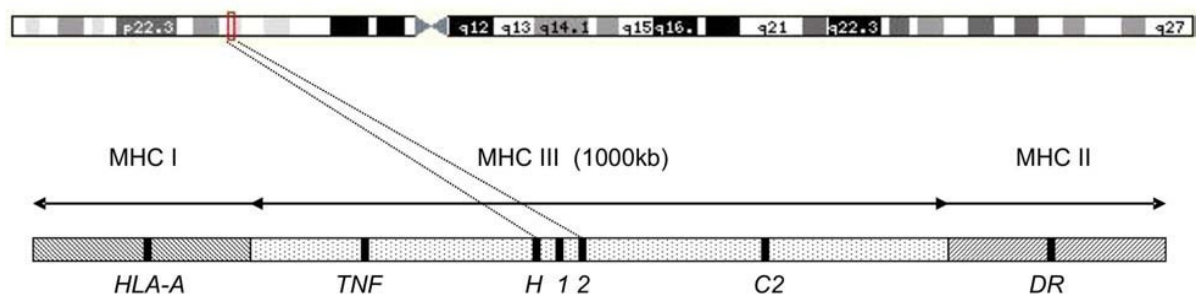


Figure 1.10. Localization of the three HSPA genes (H = HSPA1L, 1 = HSPA1A, 2 = HSPA1B). *HSPA1A* and *HSPA1B* are 11 kb apart and *HSPA1L* is 4 kb telomeric to *HSPA1A*. (Taken from Singh *et al*, 2007)

Although these three genes have similar sequences, they differ in their regulation. Both *HSPA1A* and *HSPA1B* have been shown to encode identical protein products of 641 amino acids, and *HSPAIL* has been identified at a location 4 kb telomeric to *HSPA1A* with a 90% similarity in amino acid sequence (Sargent *et al*, 1989a, Sargent *et al*, 1989, Milner and Campbell, 1990). Both *HSPA1A* and *HSPA1B* have been shown to be highly expressed in mammalian cells that have been subjected to heat shock at 42°C. *HSPA1A* is also constitutively expressed at low levels. *HSPAIL*, which has no heat shock consensus sequence, has been shown to be expressed at low levels both constitutively and after heat shock at 42°C, with no comparable difference in levels (Milner and Campbell, 1990).

1.2.5.1. Polymorphisms in HSP70 genes

The term polymorphism relates to the presence of multiple allelic variants of a gene and is a significant part of the genetic variation that exists in a population. The MHC region is one of the most highly polymorphic regions in the human genome. Single nucleotide polymorphisms (SNPs) are the most common type of genetic variation within the human genome. They involve variation between two sequences by a single base pair, often due to a base-pair substitution, of which two subtypes exist: transitions, whereby a purine or pyrimidine base is substituted by another and transversions, whereby a purine is substituted by a pyrimidine or vice versa (Singh *et al*, 2007).

Four different polymorphic locations have been described in *HSPA1A* (Table 1.5). Three lie within the 5' flanking region of the gene, which is not transcribed into RNA and the 5' untranslated region (UTR). They are located at positions -110 (A to C transversion), 120 (T to C transition) and 190 (G to C transversion). The fourth

polymorphic location is found in the coding region of the gene at the position 438 (C to T transition) (Singh *et al*, 2007).

The *HSPA1B* gene also has four different polymorphic locations (Table 1.5). One lies within the 5' flanking region of the gene at the position 145 (C to T transition), and two lie within the coding region of the gene at positions 1267 (A to G transition) and 2074 (C to G transversion). The fourth polymorphism is located in the 3' UTR region at the position 2257 and is a result of a duplication of the pentameric sequence AAGTT which gives rise to two alleles (183bp and 188bp) differing in 5bp (Singh *et al*, 2007).

Four different polymorphic sites have also been discovered in *HSPA1L* (Table 1.5). These lie within the coding region of the gene at positions 1097 (C to T transition), 2180 (G to A transition), 2437 (C to G transition) and 2763 (G to A transition). The polymorphisms at position 2437 and 2763 lead to amino acid substitutions at position 493 from Methionine (Met) to Threonine (Thr) and position 602 from Glutamic acid (Glu) to Lysine (Lys) respectively (Singh *et al*, 2007).

Table 1.5. Single nucleotide polymorphisms in three human HSPA genes (taken from Singh *et al*, 2007)

SNP position	Nucleotide Change	
<i>HSPA1A</i>		
-110 (5' flanking)	A to C transversion	
120 (5' UTR)	T to C transition	
190 (5' UTR)	G to C transversion	
438 (coding)	C to T transition	
<i>HSPA1B</i>		
145 (5' flanking)	C to T transition	
1267 (coding)	A to G transition	Generates a <i>Pst I</i> site giving rise to two alleles, L allele (8.5 kb) and U allele (9.0 Kb) identified according to their length
2074 (coding)	C to G transition	
2257 (3'UTR)	Penta-duplication of the sequence AAGTT	This gives rise to two alleles A1 (183 bp) and A2 (188 bp) differing in 5 bp.
<i>HSPA1L</i>		
1097 (coding)	C to T transition	
2180 (coding)	G to A transition	
2437 (coding)	C to T transition (aa substitution)	An AA change at position 493 from a non-polar hydrophobic Methionine (Met) to a polar neutral Threonine (Thr). The change of AA could be associated with altered peptide binding specificity and efficiency of HSP70.
2763 (coding)	G to A transition (aa substitution)	An AA change at position 602 from Glutamic acid (Glu) to Lysine (Lys). This change lies within the <i>Nco I</i> restriction site

Due to the diversity of heat shock protein families, which cover approximately five hundred client proteins, the present study will only focus on HSPA/HSP70.

1.3 Activation of HSPA/HSP70

1.3.1 Heat shock

As stated previously, heat shock proteins are up-regulated in response to a variety of stressful conditions, including thermal stress (Tolson and Roberts, 2005; Welch, 1993). Environmental temperatures have an impact on the cellular stress response and determine how cells adapt to subsequent changes in temperature. This is referred to as thermotolerance, a cellular adaptation resulting from a single severe non-lethal exposure to heat which allows cells to better survive subsequent potentially lethal heat stress episodes. The accumulation of stress-induced heat shock proteins in cells is associated with thermotolerance and is responsible for their ability to survive not only lethal heat stress, but also a variety of other stresses. The characteristics for thermotolerance are dependant on survival of the cell(s) exposed to an otherwise lethal heat stress, synthesis of heat shock proteins and a short duration of the thermotolerant state (Moseley, 1997).

As discussed previously, Theodorakis *et al.*, (1999) compared the expression and mRNA degradation in thermotolerant (cells that had been subjected to an initial heat shock) and non-thermotolerant (cells under normal conditions that had not been subjected to an initial heat shock) human liver hepatocellular carcinoma (HepG2) cells after heat shock. The normal physiological temperature for human cells is 37°C. Induction of heat shock protein genes occurs when heat shock is applied just above the normal growth temperature. Cells were made thermotolerant by the application of a nonlethal heat shock (43°C for 1.5 h) followed by a recovery period of 24 h at 37°C. Both thermotolerant and non-thermotolerant cells were thermally stressed at 43°C for 1.5 h, followed by a 6 h recovery period at 37°C. Results showed limited expression of

HSPA/HSP70 in thermotolerant cells, compared with non-thermotolerant cells after heat shock. It was suggested that this was due to both a decrease in *HSPA/HSP70* transcription and an increase in *HSPA/HSP70* mRNA degradation, thus increasing cellular levels of this protein in the recovery period, during which cells returned to non-heat shock conditions 37°C (Theodorakis *et al*, 1999). In contrast, during the heat shock period, no significant differences were observed in the levels of *HSPA/HSP70* transcription in thermotolerant and non-thermotolerant cells. *HSPA/HSP70* mRNA was observed to be less stable in thermotolerant cells, with a half-life in non-thermotolerant cells of approximately 1 h and approximately half an hour in thermotolerant cells. However, the half-life of *HSPA/HSP70* has previously been reported to be longer in comparison to the recovery period after stress (Theodorakis and Morimoto, 1987). The explanation suggested for this is that, under normal conditions, levels of *HSPA/HSP70* mRNA are unstable, but during heat shock the mRNA becomes more stable because its degradation is affected by stress. In thermotolerant cells subjected to heat shock, mRNA degradation begins immediately after returning to normal conditions, and therefore it is suggested that mRNA degradation is accelerated in thermotolerant cells resulting in a reduced *HSPA/HSP70* mRNA half-life.

1.3.1 Glioma

Gliomas, in the form of astrocytomas, anaplastic astrocytomas and glioblastomas, are the most common primary brain tumours and comprise about 2% of all newly diagnosed cancers every year in the UK (Chandana *et al*, 2008; Khalil, 2007). Gliomas are defined as tumours of the central nervous system (CNS), the majority of which arise from glial cells displaying histological, immunohistochemical and ultrastructural evidence of glial differentiation (Khalil, 2007). The classification of brain tumours is based upon cell morphology and the degree of malignant behaviour, which is in turn dependent on nuclear atypia, mitoses, microvascular proliferation and necrosis (Behin *et al*, 2003). The World Health Organization (WHO) classifies brain tumours into various subtypes such as astrocytoma, oligodendroglioma, oligoastrocytoma and ependymoma and into four malignancy grades; Grade I pilocytic astrocytoma, Grade II diffuse astrocytoma (including oligodendroglioma), Grade III anaplastic astrocytomas and Grade IV glioblastoma (Table 1.6) (Khalil, 2007; Kleihues *et al*, 2002; Louis *et al*, 2007).

Table 1.6. WHO grading and survival of gliomas (adapted in part from Christine *et al*, 2005).

WHO Grade	Glioma	Histological Features	Survival
I	Pilocytic astrocytoma	Rosenthal fibres	+10 years
II	Diffuse astrocytoma/ oligodendroglioma/ mixed oligoastrocytoma	Moderate hypercellularity with occasional nuclear atypia	+5 years
III	Anaplastic astrocytoma / oligodendroglioma/ oligoastrocytoma	Increased hypercellularity, Nuclear atypia with high mitotic activity, microvascular proliferation	2-3 years
IV	Glioblastoma multiforme	Marked nuclear atypia, mitotic activity, prominent endothelial proliferation and tumour necrosis	9-12 months

Pilocytic astrocytomas are defined as Grade I tumours and characterised by their slow growth rate and regressive nature and are often considered as benign tumours. Pilocytic astrocytomas generally develop in young children and young adults (Behin *et al*, 2003; Parsa and Givard, 2008). They usually originate in the optic tracts, hypothalamus or basal ganglia and in the cerebellum and brainstem (posterior fossa) but they may occur in any area where astrocytes are present, such as the spinal cord and the cerebral hemispheres (Behin *et al*, 2003; Kleihues & Cavenee, 2000). Imaging using MRI and CT scans show pilocytic astrocytomas as solid, cystic, well circumscribed and contrast-enhancing tumours (Figure 1.11) (Behin *et al*, 2003).

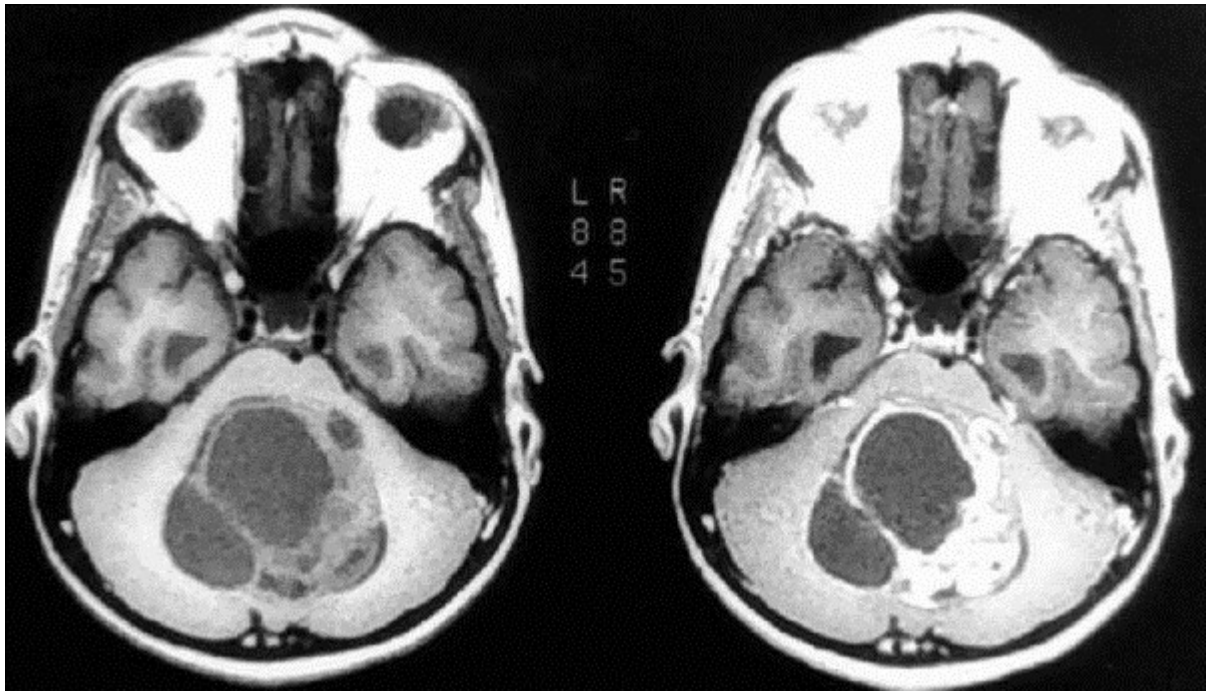


Figure 1.11. Magnetic resonance imaging showing features of pilocytic astrocytomas (rad.usuhs.mil/rad/who/JPA.html). Post-contrast image reveals a large irregular, multilobulated shape, in the enhancing mass in the cerebellar hemisphere.

Diffuse astrocytomas, referred to as Grade II tumours, such as oligodendrogliomas, are well differentiated tumours that are most prevalent in young adults, commonly located in the frontal, temporal and insular regions within the cerebral hemispheres (Behin *et al*, 2003; Huang *et al*, 2000). They originate from oligodendrocytes, which are the myelin-forming cells of the central nervous system, and which play a crucial role in the normal functioning of the brain (Jiang *et al*, 2007). Although slow growing, they have the potential for malignant progression and to develop into anaplastic astrocytomas (Grade III tumours) and eventually into glioblastomas (Grade IV tumours) (Behin *et al*, 2003; Huang *et al*, 2000). Contrast enhancement, whereby the contrast between normal and cancerous tissue is enhanced, is generally absent in MRI and CT images (Figure 1.12). However, presence of contrast enhancement would suggest malignant transformation into a higher grade of tumour (Behin *et al*, 2003).

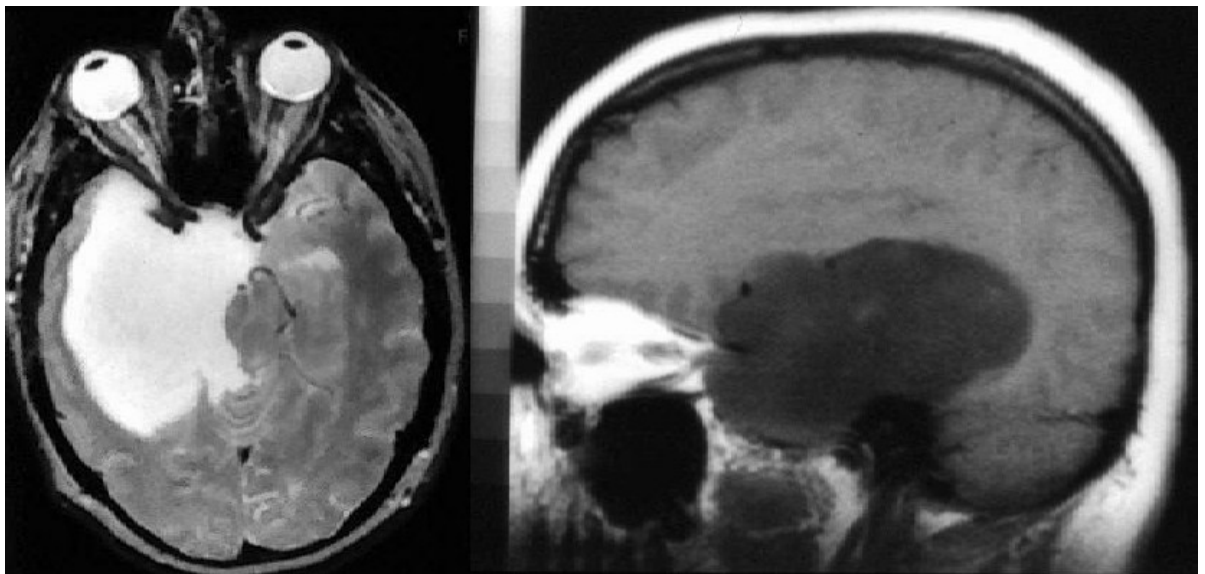


Figure 1.12. Magnetic resonance imaging showing features of a diffuse astrocytomas (rad.usuhs.mil/rad/who/JPA.html) post-contrast image reveals a large enhancing irregular, mass in the left frontal lobe.

Anaplastic astrocytomas, defined as Grade III tumours, may originate either *-de novo* without previous indication of a malignant lesion or as a transition from low grade lesions (Kleihues & Cavenee, 2000). The latter types of tumours are less common and generally represent a short-term intermediate lesion during malignant transition from Grade II to Grade IV tumour status (Behin *et al*, 2003; Huang *et al*, 2000). Histological astrocyte and anaplastic features include pleomorphism, increased tumour cellularity, high mitotic activity, microvascular activity, nuclear atypia and necrosis (Brat *et al*, 2008). On MRI and CT images (Figure 1.13) they present as an irregular hypodense lesion with varying degrees of contrast enhancement and oedema (Behin *et al*, 2003).

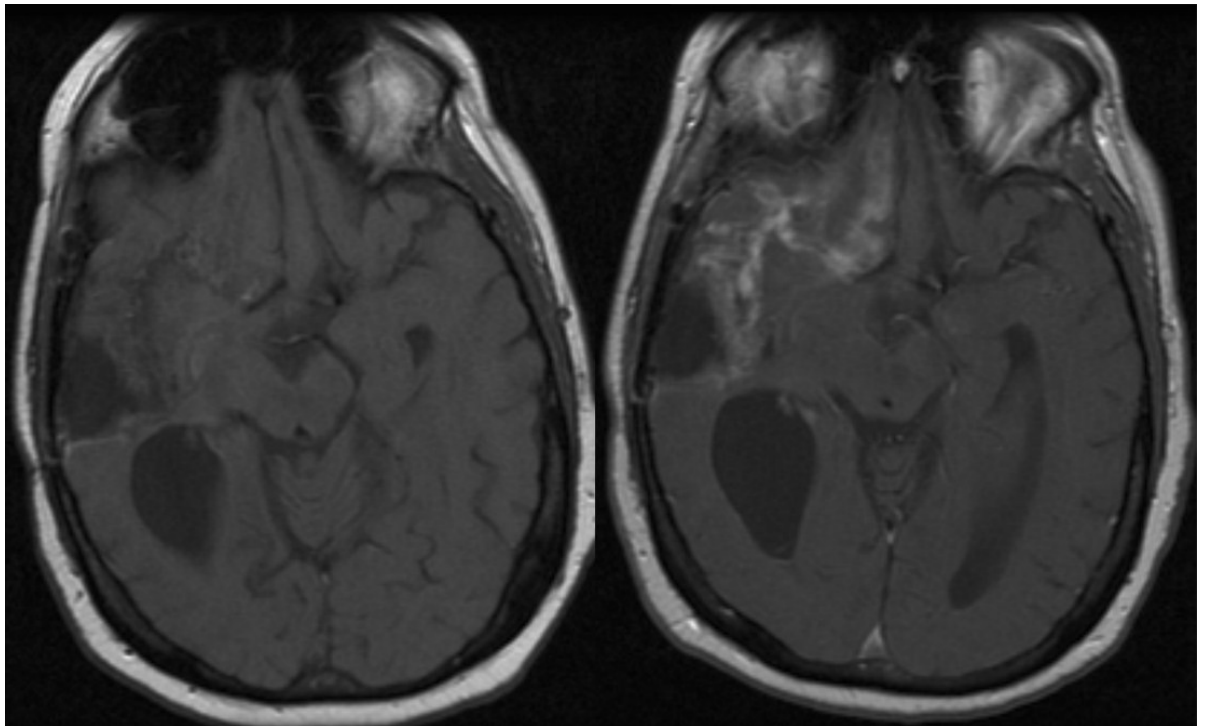


Figure 1.13. Magnetic resonance imaging showing features of an anaplastic astrocytomas (rad.usuhs.mil/rad/who/JPA.html) post-contrast image reveals a large enhancing irregular, mass in the left temporal lobe

Glioblastoma multiforme (GBM) tumours are defined as Grade IV and are amongst the most common glioma tumours. They can arise in one of two ways, either spontaneously without prior indication of a malignant lesion, or as a malignant progression from a lower grade lesion (Kleihues & Cavenee, 2000; Tso *et al*, 2006). GBMs are most prevalent in older adults (45-60 years), and usually arise in the frontal, temporal and insular regions of the cerebral hemispheres, although they occasionally may be located in the brainstem or cerebellum (Behin *et al*, 2003; Brat *et al*, 2008). GBMs are normally represented in MNR images as a grossly irregular hypodense heterogeneous mass, with various degrees of contrast-enhancement and vasogenic oedema (Figure 1.14). The most common presentation is as a ring-like enhancement surrounding a necrotic center (Behin *et al*, 2003, Brat *et al*, 2008).

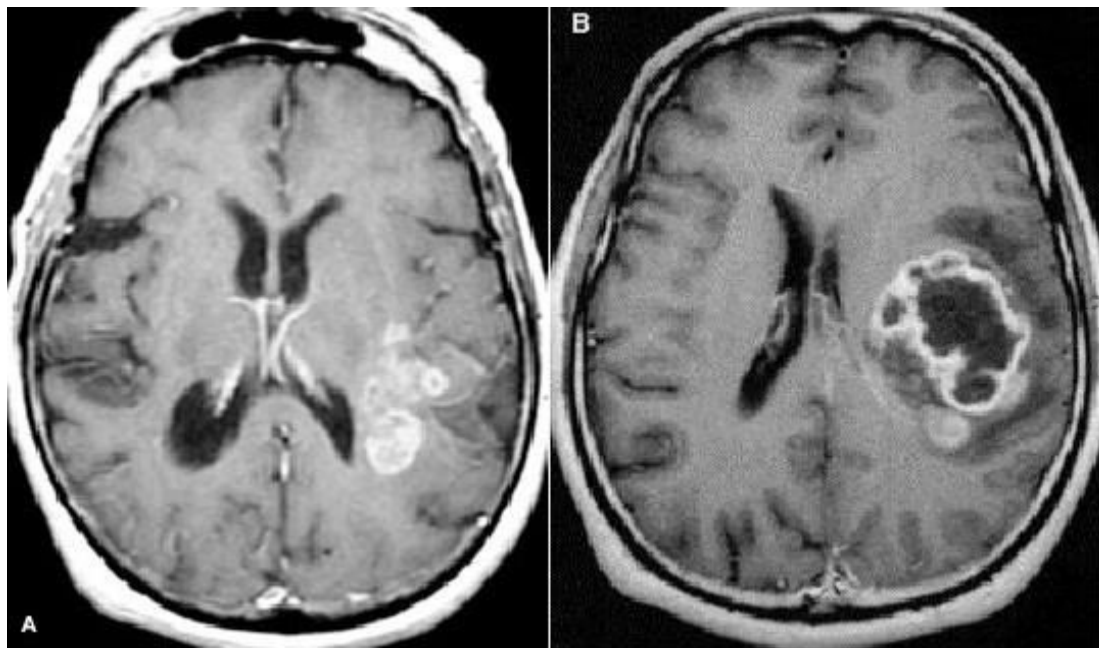


Figure 1.14. Magnetic resonance imaging features of glioblastoma multiforme (rad.usuhs.mil/rad/who/JPA.html) (A) post-contrast image revealing a multilobulated, enhancing mass in the right temporal lobe. (B) glioblastoma; tumour is an irregularly shaped, heterogeneous mass with central necrosis and ring-like contrast enhancement surrounded by oedema.

Cancerous tissues generally contain high levels of stress proteins, particularly members of the chaperone and heat shock protein families (Ciocca and Calderwood, 2005; Graner *et al*, 2007). The response of cells to such stress conditions is in part dependent on the concentration of heat shock proteins in the cell prior to stress. The intensity and duration of the stress will have an influence on the eventual outcome for the cell of either survival, apoptosis or necrosis (Mosser and Morimoto, 2004; Multhoff, 2007). During a stress response, while total protein synthesis is inhibited, the synthesis of specific heat shock proteins is elevated in recovering cells (cytoprotected state) (Lindquist and Craig, 1988). Initiation of apoptosis induces the expression of heat shock proteins, which continues until protein synthesis ceases (Mosser and Morimoto, 2004; Parsell *et al*, 1994).

Protein-damaging environmental and physiological stresses induce the expression of heat shock proteins that are often constitutively over-expressed in various cancer cells and are also involved in tumour cell proliferation, cellular death, metastasis and differentiation, suggesting that they may be a contributing factor in tumourigenesis (Calderwood *et al*, 2006, Ciocca and Calderwood, 2005; Graner *et al*, 2007; Mosser and Morimoto, 2004; Powers *et al*, 2007). It has been widely reported that elevated levels of *HSPA/HSP70*, *HSPB/HSP27* and *HSPC/HSP90*, either as combinations or individually, have been observed in breast, uterine, renal, brain, endometrial and osteosarcoma cancers (Graner *et al*, 2007; Jolly and Morimoto, 2000).

Numerous publications have studied heat shock protein expression and heat stress characterization in a wide range of tumour cell types (Calderwood *et al*, 2006; Ciocca and Calderwood, 2005; Li and Lee, 2006) However, studies are rare in different types of brain tumours (Fuse, 1991; Hermisson *et al*, 2000; Wang *et al*, 2006). A study

undertaken by Graner *et al*, (2007) examined changes in heat shock protein gene expression and localization of heat shock proteins in a number of brain tumour cell lines both at intracellular and cell surface/extracellular levels under normal conditions and the effect of heat shock on expression and localisation (Table 1.7).

Table 1.7. Summary of inducible HSPA/HSP70 expression in select brain tumour cell lines (relative to unstressed cells or to non-heat shock protein expression such as actin) (adapted from Graner *et al*, 2007).

Cell Line	HSPA/HSP70 expression (Western blot)		Cell surface HSPA/HSP70 expression (flow cytometry)		Extracellular HSPA/HSP70 release (ELISA)	
	Constitutive	Heat Stress	Constitutive	Heat Stress	Constitutive	Heat Stress
D54MG Adult malignant	+	++	+	++	+	++
D392MG Adult malignant glioma	+/-	+++	++	+++	++	+++
D341MED Pediatric medulloblastoma	++	+/-	+	++	+	+++
SMA560 Murine anaplastic astrocytoma	+/-	++++	+/-	++	+	++++

(+/-, Detectable expression; +, moderate expression; ++ →++++, high to very high expression)

Although a number of heat shock proteins were examined, the most significant effects of heat shock related to HSPA/HSP70, and a clear increase in *HSPA/HSP70* expression following heat shock was reported by these authors. Western blot analysis showed no consistent correlation between the different cell lines regarding *HSPA/HSP70* expression as a result of heat shock. D392MG (adult malignant glioma) (Ostrowski *et al*, 1991) and SMA560 (a murine anaplastic astrocytoma) (Sampson *et al*, 1997; Serano *et al*, 1980) cell lines showed significantly higher levels of *HSPA/HSP70* gene expression compared to D54MG (derived from line A172, adult malignant glioma) (Giard, 1973) and D341MED (pediatric medulloblastoma) (Friedman *et al*, 1988) after heat shock, while the converse was observed in untreated cells. In most cell lines,

HSPA/HSP70 was present on the surfaces of the cells at normal temperature, and increased when the cells were exposed to heat shock and allowed to recover for a period of 24h. The fold increases ranged from ~1.5- to ~20-fold after heat shock. The results from the spent media (media that the cells were grown in) for HSPA/HSP70 is between 1.5 – 10 fold higher after heat shock, which could not be attributed to cell death as the number of viable cells was the same before and after heat shock (Graner *et al*, 2007). Previous work by Guzhova *et al*, (2001), examined the release of HSPA/HSP70 into culture media in human glioblastoma T98G cells and found a greater release from cells subjected to heat shock, compared to that from cells under normal conditions.

Stress induced by heat shock produced a substantial variation in heat shock responses in different brain tumour cells, some of which showed a significantly higher level of expression after heat shock while, conversely, expression in some brain tumour cells was high in the absence of heat shock (Calderwood *et al*, 2006).

The overexpression of heat shock proteins in numerous cancers, including glioma, is associated with tumour cell proliferation, metastasis, invasion, differentiation and death (Nylandsted *et al*, 2000). In some cancers, the overexpression of heat shock protein genes is correlated with poor prognosis and a reduced positive response to therapy (Calderwood *et al*, 2006). HSPA/HSP70 has been associated with higher cell proliferation, with the worst prognosis in patients suffering from breast cancer (Ciocca *et al*, 2003). Overexpression of heat shock proteins requires the activation of heat shock transcription factor 1 (HSF1), which is also upregulated in cancer cells and is involved in invasion and metastasis (Ciocca and Calderwood, 2005).

1.3.2 Hypoxia

Hypoxia is a condition resulting from decreased cellular oxygen levels in tissues, and is associated with many diseases, such as pulmonary disease, heart disease, vascular disease and cancer. Research has shown that regions of acute/chronic hypoxia exist within the majority of solid tumours (Williams *et al*, 2001). In cellular hypoxia, tumours require additional blood vessels, a condition which is evident in many neoplasms. Hypoxia induces transcriptional activation of many genes that affect cellular metabolism and also promotes neoangiogenesis (the formation of new or recent blood vessels) (Duffy *et al*, 2003). Cells are able to sense and respond to decreased oxygen levels through the conserved hypoxic response pathway involved in tumourigenesis. Exposure to decreased oxygen levels initiates the hypoxic response pathway by the regulated expression of hypoxia inducible transcription factor-1 (HIF-1). HIF-1 is a transcription factor which, under hypoxic conditions, specifically binds to the region 5' – RCGTG- 3' of the hypoxia-responsive element (HRE) in the promoter of various hypoxia-inducible genes such as heat shock protein gene families, erythropoietin (EPO); vascular endothelial growth factor (VEGF) (Simiantonaki *et al*, 2008) and von hippel-lindau (VHL) (Baird *et al*, 2006; Gombos *et al*, 2011; Huang and Bunn, 2003). HIF-1 is a member of the basic-helix-loop-helix (bHLH)-PAS family. PAS is an acronym for the first three members recognised, being period homolog (Per), aryl hydrocarbon receptor nuclear translocator (ARNT) and single minded homolog (Sim) (Huang and Bunn, 2003). HIF-1 is a heterodimer composed of one of three subunits, HIF-1 α ~120 KDa, HIF-2 α ~118 KDa and ~72 KDa HIF-3 α subunits and a 91 – 94 KDa HIF-1 β /ARNT subunit (Baird *et al*, 2006; Gombos *et al*, 2011; Huang and Bunn, 2003). Under normal oxygen conditions (normoxia), both HIF-1 α and HIF-1 β mRNAs and proteins are constitutively expressed (Baird *et al*, 2006; Wang *et al*, 1995).

Many of the hypoxia-inducible genes are up-regulated during hypoxia, thus increasing oxygen transport to hypoxic tissues by promoting angiogenesis and also promoting cell proliferation and survival. However, failure to adapt to decreased oxygen levels will ultimately result in cell death via apoptosis (Bruick, 2003). Angiogenesis is associated with metastasis, and as tumours grow, some cells become detached from the tissues nutrient supply limiting the delivery of oxygen and nutrients to those cells (Duffy *et al*, 2003). This results in cellular hypoxia and metabolic stress inducing changes in transcriptional regulation, promoting growth of highly permeable blood vessels and facilitating the passage of tumour cells into the circulatory system. The response of cancer to hypoxia not only maintains the survival and growth of tumours, but promotes tissue invasion and metastasis through angiogenesis (Duffy *et al*, 2003).

Activation of heat shock proteins plays a crucial role in adaptation by cells to hypoxic conditions and in tolerating the oxidative stress of reoxygenation (Baird *et al*, 2006; Semenza 1999). Heat shock proteins are regulated by heat shock factors and are linked to the oxygen-sensing and heat shock pathways. The activity of the heat shock pathway is controlled by the trimerization and post translational modification of heat shock factor protein subunits (Baird *et al*, 2006; Orosz *et al*, 1996). Transcription of heat shock factors is controlled by HIF-1 which is increased during hypoxia, increasing the cellular abundance of heat shock factors and the sensitivity of the heat shock pathway, thus maximising the production of protective heat shock proteins (Baird *et al*, 2006). During hypoxia, heat shock factors are up-regulated due to the direct binding by HIF-1 to HIF-1 response elements. The up-regulation of heat shock factors are essential for the increase of heat shock protein transcripts during hypoxia and reoxygenation (Baird *et al*, 2006).

1.3.3 Post-mortem conditions

In cases of unexplained death, one of the most important investigative factors is the accurate and precise determination of the time interval since death occurred, which is usually referred to as the post-mortem interval (PMI). There has been much debate as to the precise moment when death actually occurs. Various methods involving many different scientific disciplines, such as forensic medicine, anthropology, physiology, molecular biology and entomology have been employed in determining an accurate post-mortem interval, and the application of these methods largely depend on whether the PMI is assumed to be short (hours/days), medium (weeks) or long term (years) (Mathur and Agrawal, 2011). To date, the precise time of death cannot be determined with complete accuracy or certainty. Broadly speaking, there are two phases of death: somatic death, which is the cessation of the integrated functioning of an individual at a physiological level, and molecular or cellular death, which is the cessation of respiration and the normal metabolic activity in the tissues and cells. However, there has been much debate surrounding cellular death as to when this actually occurs. Various methods are currently employed in determining PMI. These include temperature measurements made post-mortem (Henssge and Madea, 2004), the use of biochemical markers such as protein fractions and enzymes (Fountoulakis *et al*, 2001; Sabucedo and Furton, 2003), potassium concentration in the vitreous humor of the eye (Madea and Rodig, 2006) eye temperature decrease (Kaliszan *et al*, 2010) and post-mortem muscle proteolysis (the relaxation of muscles following rigor mortis) (Madea and Henssge, 1990).

The most commonly used method for the determination of short term PMI by pathologists is based on the cooling of the body and involves the measurement of the

body core temperature at various time points. This requires the direct measurement of the intra-abdominal temperature and applying this to Newton's law of cooling (Besson, 2010; Newton, 1701) which states –the rate of cooling of a body is determined by the difference between the temperature of the body and that of its environment‖ (Henssge, 1988; Henssge and Madea, 2004; Marshall and Hoare, 1962). Various algorithm / nomogram models have been suggested for its use, and the current preferred model is the –temperature time of death relating nomogram‖ (Figure 1.15) developed on the basis of physical considerations, and the two-exponential term of Marshall and Hoare (1962).

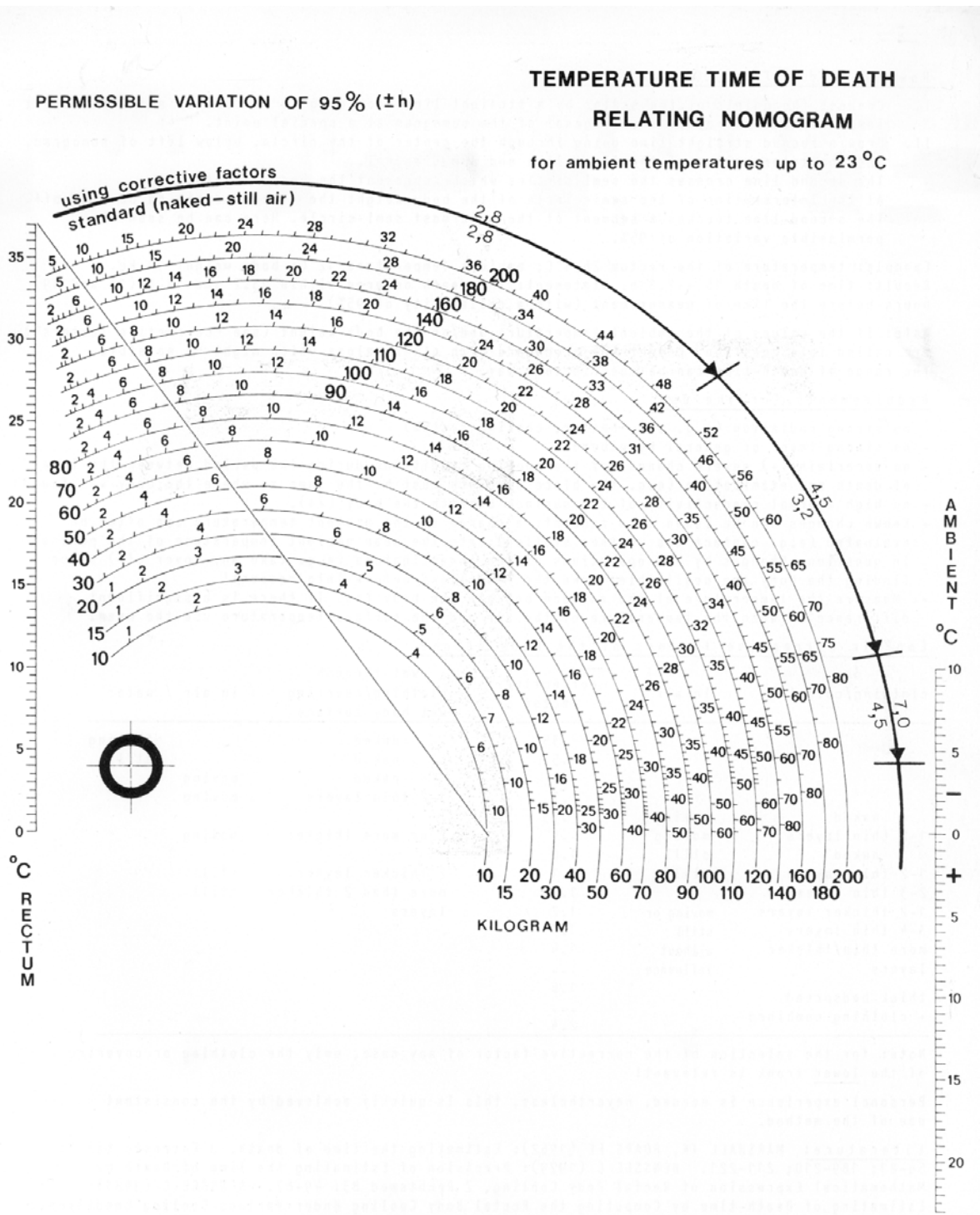


Figure 1.15. The temperature-time of death relating nomogram (adapted from Hessenge and Madea, 2004).

Death-time (t) is expressed by:

$$\frac{T_{\text{rectum}} - T_{\text{ambient}}}{37.2 - T_{\text{ambient}}} = 1.25 \exp(Bt) - .25 \exp(5Bt); B = -1.2815 (\text{kg}^{-.625}) + .0284$$

The nomogram is related to the chosen standard of a naked body lying in still air. Cooling conditions that differ from the chosen standard may be proportionally adjusted by corrective factors as shown in Table 1.8 of the real body weight (Hessenge and Madea, 2004).

Table 1.8. Empiric corrective factors of the body weight (adapted from Hessenge and Madea, 2004).

Dry clothing / covering	In air	Corrective Factor	Wet clothing / covering wet body surfaces	In air / water
		3.5	Naked	Flowing
		.5	Naked	Still
		.7	Naked	Moving
		.7	1-2 thin layers	Moving
Naked	Moving	.75		
1-2 thin layers	Moving	.9	2 or more thicker	Moving
Naked	Still	1.0		
1-2 thin layers	Still	1.1	2 thicker layers	Still
2-3 thin layers		1.2	More than 2 thicker layers	still
1-2 thicker layers	Moving or still	1.2		
3-4 thin layers		1.3		
More thin/thicker layers	Without influence	1.45		
Thick bedspread & clothing		1.8		
combined		2.4		

Although this is the preferred method, there are still factors that cause much controversy and doubts regarding the complete accuracy of this method. This method assumes a constant ambient temperature, but it has been suggested by Althaus and Henssge (1999) that, if there is a rapid increase or decrease in ambient temperature, the PMI based on this method would not be totally reliable.

One area that has not been fully investigated with regards to PMI is the persistence of gene transcripts in post mortem tissue. In the period immediately following death there are a number of cellular functions that persist, such as continued cell division, continued reactivity of muscle fibres to stimuli, mechanical or electrical stimulation (Jones *et al*, 1995; Madea 1992; Schleyer, 1963) and continuation of enzymatic activities such as adenylyl cyclase which has conserved basal activity in neural tissue up to 48h after death (Palego *et al*, 1999). During the early post mortem period, the amount of RNA in cells rapidly changes depending on pathophysiological changes of the microenvironments involved in the death process (Maeda *et al*, 2010). However, some genetic reactions continue during the early post-mortem period, such as supravital reactions, the reactions that occur within the body from somatic to cell death, which result in either an increase or decrease in mRNA transcripts, which may modify the biological status at time of death (; Ikematsu *et al*, 2008; Maeda *et al*, 2010).

In general, the cause of death is determined by evaluating functional and morphological changes of the viscera (internal organs), tissues and cells following a fatal insult (Maeda *et al*, 2010). Death due to a functional mechanism such as fatal disease, injury or chemical insult, may produce few morphological changes, however the status of cell functions may be preserved in the mRNA pattern indicated by precise up / down regulations of gene expression which occurs rapidly after death (Maeda *et al*, 2010;

Zhao *et al*, 2009). Studies undertaken by Ikematsu *et al* (2008) have demonstrated a significant tissue- specific increase or decrease in mRNA levels in the early post mortem period of < 12h. The study was undertaken using mechanically asphyxiated mouse lung and brain after somatic death, for the detection of early response genes including myelocytomatosis oncogene, C-MYC, inducible-nitric oxide synthase 2, i-NOS, and FBJ osteosarcoma oncogene, C-FOS (Ikematsu *et al*, 2008). Rapid changes in mRNA levels, depending on the pathophysiology of death could be useful to investigate acute violent deaths such as electrocution, asphyxiation or in cases of sudden death.

The measurement of gene expression at the mRNA level in post-mortem tissue can potentially provide useful information relevant to the determination of a more accurate post-mortem interval and the possible circumstances, mechanisms and diagnosis surrounding or leading to the cause of death.

Studies by Anderson *et al*, (2005); Bauer *et al*, (2003) and Maarti, (2004) have shown that RNA remains largely intact for a considerable time period (up to 24 to 48 h) after death under appropriate ambient conditions. Furthermore, assessing mRNA levels by RT-PCR is believed to produce more accurate results than other techniques, such as comparison with levels of ribosomal 18S and 28S rRNAs. Therefore, measurement of cellular mRNA levels could provide information about RNA quality in tissues of relevance to PMI determination as well for research or diagnostic purposes, such as wound age determination.

A number of recent studies (Anderson *et al*, 2005; Bauer *et al*, 2003; Maarti, 2004) have shown that there is the potential to determine post-mortem interval in a forensic context by measuring the levels of total RNA populations and the transcripts of specific genes

in the early post-mortem period. These studies were specifically undertaken in relation to the identification of body fluids, the age of blood and semen stains, the age of wounds (Anderson *et al*, 2005; Bauer *et al*, 2003) and the functional status of cells and organs for the purpose of forensic pathology (Maarti, 2004). Studies have also demonstrated, across a wide range of both human and rat tissue types, that the molecular integrity of RNA (the 28S and 18S ribosomes) and targeted gene transcripts can remain relatively high in post-mortem tissue for up to periods of 148 h (brain tissue; Inoue *et al*, 2002); 48 h (bone, Kuliwaba *et al*, 2005); 72 h (lungs, heart and muscle tissue, De Paepe *et al*, 2002; Heinrich *et al*, 2007; Inoue *et al*, 2002); and 24 h (liver, kidney and spleen tissue, Heinrich *et al*, 2007; Inoue *et al*, 2002). The results were all obtained under ambient temperatures or at 4°C using real time quantitative reverse transcription polymerase chain reaction (RT-PCR).

Gopee and Howard (2007) demonstrated that, over a time course of post-mortem intervals up to 60 min, skin excised from 10 month old hairless mice showed minimal variation in terms of the integrity of total RNA and also the mRNA of the genes C-MYC, CYR61, HIF-1 α , C-CND1 and one housekeeping gene 18S ribosomal RNA.

Overall these studies indicate that the cellular integrity of mRNA is unlikely to change significantly in the early post-mortem period, thereby allowing the opportunity to elicit *de novo* gene expressions of specific target genes in response to mild heat shock.

A study undertaken by Pardue *et al*, (2007) compared the induction and the levels of HSPA/HSP70 and heat shock cognate HSPA8/HSC70 proteins and mRNAs in human brain (in cases of sudden or unexpected death with no known agonal stresses pre-mortem) with those in brains of non-stressed and heat shocked rats. Post-mortem

intervals ranged from 3.5 – 22 h in human brain samples, 3 h for non-stressed rat brain at room temperature and 0 – 24 h for rat brains that were subjected to heat shock at 3, 5, 8, 12 and 24 h. Results indicated that the levels of HSPA/HSP70 proteins were 43-fold higher in human brain than those in non-stressed rat brain and 14-fold higher than those subjected to heat shock. HSPA8/HSC70 results were less dramatic, showing only a 1.5-fold increase in that of human brain samples compared to that of non-stressed rat brain. Consistent with the presence of the HSPA/HSP70 protein, *HSPA/HSP70* mRNA levels were also found to be 8.5-fold higher in human brain than in non-stressed rat brain. Clearly, the overall conclusion is that HSPA/HSP70 protein levels are significantly higher in humans who die suddenly and are not subjected to agonal stresses pre-mortem than in rats either non-stressed pre-mortem or subjected to heat shock post-mortem.

HSPA/HSP70 has been linked with post-mortem events due to its association with BAG-1 (Bcl-2-associated athanogene-1) and CHIP (carboxyl terminus of the Hsc70-interacting protein). BAG-1 contains a domain within HSPA/HSP70 nucleotide-exchange activity that is presumed to assist molecular chaperones in the removal of aberrant proteins from the cytosol (Curcio *et al*, 2006; Lanneau *et al*, 2007; McClellan *et al*, 2005). BAG-1 has a capacity to inhibit apoptosis and modulates the chaperone activity of HSPA/HSP70 and heat shock cognate 70 (HSPA8/HSC70) by binding to their ATPase domains (Luders *et al*, 2000b; Seidberg *et al*, 2003; Stuart *et al*, 1998; Takayama *et al*, 1997;). BAG-1 appears to alleviate cellular stress by joining HSPA/HSP70 and other chaperones to the ubiquitin proteasome system facilitating degradation of oligomeric species. However, during the agonal state linking of BAG1 and HSPA/HSP70 to the ubiquitin proteasome system can be affected by various pre and post-mortem variables (Curcio *et al*, 2006).

1.4 Aims of the Research

The expression of *HSPA/HSP70* is up-regulated by various cellular stress factors, including cancer, hypoxia and post-mortem conditions. The main research aims of this project were to explore and measure the effects of these factors further, using human and rat tissues and cell lines. Experiments were devised to characterise *HSPA/HSP70* expression in normal and glioma cell lines, and under hypoxic conditions. Expression was also characterised in post mortem tissues at different stages of the early post mortem interval, to determine whether *HSPA/HSP70* was capable of *-de novoll* expression in response to cellular signals for its use as an early post-mortem marker to estimate PMI. In terms of the potential for clinical application, this research also attempted to assess the possible use of *HSPA/HSP70* as a prognostic marker.

To provide structure to the presentation of results in this thesis, these objectives can be individually summarised as follows:

1. To characterize the level of *HSPA* expression in normal human cell lines and normal human brain tissue, compared to that of glioma cell lines and tumourous brain tissue;
2. To characterize the level of *HSPA* transcription in response to hypoxia in normal and glioma cell lines;
3. To characterize the level of *HSPA* transcription in post-mortem brain tissue ;
4. To characterize the level of *HSPA* transcription in response to heat shock applied to the brain tissue in the early post-mortem period;

5. To characterize the level of *HSPA* transcription in response to multiple heat shocks applied to the brain tissue in the early post-mortem period; and
6. To determine the potential for *HSPA* to be used as an early post-mortem marker.

Chapter 2

Materials and Methods

2.1 Cell Culture

2.1.1 Tissue samples, cell lines and culture conditions

Tumour and normal (control) brain tissue samples were obtained from patients admitted to the Royal Preston Hospital, UK. Ethical approval from both the North Manchester Research Ethics Committee Ref: 06/Q1406/104 and the Ethics Committee at the University of Central Lancashire were obtained prior to work being carried out on tissue samples. Tumour tissue samples were obtained from glioma cancer patients, and normal (control) tissue samples were obtained from patients who required resection of normal brain for purposes other than primary glioma treatment. Written consent was obtained prior to tissue samples being used in this investigation. For each patient, brain tissues samples were surgically dissected and immediately frozen at -80°C and stored for analysis (performed by neurosurgeons and the pathology department at the Royal Preston Hospital, UK). In total, 18 tissue samples were used in this study.

Human brain cell lines grade I astrocytoma, 1321N1 from European Collection of Cell Cultures, ECACC, (UK), grade II/III oligodendroglioma GOS-3 from Deutsche Sammlung von Mikroorganismen und Zellkulturen GmbH, DMSZ, (Germany), grade IV glioblastoma, U87-MG from ECACC (UK) and normal human astrocytes, NHA from Lonza (UK) were used in this study. 1321N1 and GOS-3 cells were routinely cultured in Dulbecco's modified Eagle's medium (DMEM; Sigma) supplemented with 10% foetal bovine serum (FBS) and with 2 mM and 4 mM L-glutamide respectively, while U87-MG cells were cultured in Eagle's minimum essential medium (EMEM; Sigma) supplemented with 2 mM L-glutamide, 10% FBS, 1 mM sodium pyruvate and 1% (v/v) nonessential amino acids, NEAA, (Sigma). NHA cells were cultured in astrocyte

medium (AM) supplemented with 15 ml (3%) of FBS, 0.5 ml (0.1%) ascorbic acid, 0.5 ml recombinant human epidermal growth factor, rhEGF, 0.5 ml gentamicin amphotericin-B, GA-1000, 1.25 ml insulin and 5 ml L-glutamide.

All cells were of human origin without infectious viruses or toxic products. Routine mycoplasma testing was performed at the University of Central Lancashire on all cell lines and strains used in the study. Cells were received as frozen ampoules in 1 ml plastic cryotubes containing cells suspended in appropriate freezing medium and 10 % (v/v) dimethyl sulphoxide (DMSO), as supplied by commercial laboratories.

2.1.2 Media and Reagents

Complete medium for cell growth was aseptically prepared for each cell line according to the supplier's recommendations with the addition of specific supplements (Table 2.1).

Table 2.1 Media and supplements for each cell line used in this thesis.

Cell Line	Medium	Supplements
1312N1	Dulbecco's Modified Eagle's Medium (DMEM)	10% FBS 2 mM L-glutamine
GOS-3	Dulbecco's Modified Eagle's Medium (DMEM)	10% FBS 4 mM L-glutamine
U87-MG	Eagle's Minimum Essential Medium (EMEM)	10% FBS 2 mM L-glutamine 2 mM non-essential amino acids 1 mM sodium pyruvate
NHA	Astrocyte Basal Medium (ABM)	0.5 ml recombinant human epidermal growth factor (rhEGF) 1.25 ml insulin 0.5 ml ascorbic acid 0.5 ml gentamicin amphotericin-B (GA-1000) 5.0 ml L-glutamine 3% FBS

2.1.3 Preparation of Media

The media for cell lines were prepared according to the individual cell line requirements, based on the ECACC / DMSZ / Lonza recommendations and all additional supplements were added in accordance with the supplier's recommendations. Supplemented media were labeled with date of preparation and stored for up to a maximum of two weeks at 4°C. All reagents and chemicals used for cell culture are

listed in Table 2.2. Prior to inoculation of the complete media with the cell lines, the complete medium for each cell line was pre-incubated overnight to ensure that no contaminants, mycoplasma or toxic products were present.

Table 2.2 Reagents and chemicals used in cell culture.

Reagents	Supplier	Components
Foetal bovine serum	Gibco BRL	Heat inactivated foetal bovine serum
Non-essential amino acid	Sigma	100x non-essential amino acid
Trypsin EDTA	Sigma	0.5 g porcine trypsin 0.2 g EDTA
L-glutamine	Sigma	200 mM L-glutamine
Phosphate buffer saline 0.1M	Sigma	8 g/l sodium chloride 0.2 g/l potassium chloride
DMSO	Sigma	Dimethyl sulfoxide 99.5%
Trypan blue (0.4% v/v)	Sigma	0.81% w/v sodium chloride 0.06% w/v potassium phosphate dibasic

2.1.4 Resuscitation of Cells

Complete media for cell lines were pre-warmed to 37°C before the frozen ampoules containing the cells were added and thawed rapidly in a 37°C water bath. Thawed cells were immediately rinsed by resuspension in 4 ml of appropriate growth medium to remove the freezing medium and centrifuged at 150 g for 5 min. The supernatant was discarded and the cells were resuspended in 3 ml of the appropriate medium and then aliquoted into 2 x 25 cm² flasks together with 5 ml of the appropriate medium and mixed manually. Flasks were suitably labeled with the cell line, passage number and then incubated at 37°C with 5% CO₂ in 95% filtered air.

2.1.5 Subculture

Following overnight incubation, the cells were observed using a phase contrast microscope for a monolayer growth of approximately 70–80% confluency and to confirm the absence of bacterial and fungal contaminants. Depending on observations, cells were either trypsinised or subjected to hypoxia treatment. However, for slow growing cell lines, the medium was changed every 48 h after incubation to ensure sufficient nutrients for cell growth.

2.1.6 Hypoxia Treatment

Cells were cultured in 75 cm² tissue culture-treated polystyrene flasks (Sigma). Hypoxic conditions were induced by exposing confluent cells to nitrogen (100 %) for 30 min (Kay *et al*, 2007). After treatment, the cells were collected at various recovery periods (0, 3, 6 and 24 h) for experiments concerning gene expression, immunofluorescence and flow cytometry assays.

2.1.7 Trypsinisation

The culture medium was removed and the cells were washed once with 5 ml of 1 x phosphate buffered saline (PBS) (0.1 M, pH 7.4) to remove any excess culture medium. Trypsin EDTA 1 x (1ml/ 25cm² flask, 2ml/ 75cm² flask) was added to each flask and cells were incubated under normal conditions for 5-10 min at 37°C (atmosphere of 95% O₂, 5% CO₂). The cells were examined using a phase contrast microscope to ensure that all the cells had detached and were floating. Cells were resuspended in 2ml/ 25cm² flasks or 4ml/ 75cm² flasks of the appropriate medium to inactivate the trypsin. The cell suspension was transferred to a 15 ml centrifuge and centrifuged (ALC PK120) at

1000 rpm for 5 min. The supernatant was discarded and the pellet resuspended in 1 ml of medium followed by gentle pipetting to aid resuspension.

2.1.8 Cell Quantification

Cell quantification involved first adding 20 μ l of the cell suspension and 80 μ l of trypan blue (Freshney, 1987) (1:5 dilutions) to a 1.5 ml microfuge tube and the suspension mixed by gently pipetting. Cells were observed and cell concentration calculated by the use of a Neubauer haemocytometer. Samples were prepared by attaching a cover slip using slight pressure until Newton's refraction rings appeared (rainbow-like rings under the cover-slip). Both sides of the chamber were filled (approx. 10 μ l) with cell suspension / trypan blue solution, ensuring no air bubbles were present, and samples viewed under a light microscope using x 20 magnification. The number of viable cells (seen as bright cells) were counted in the central square (gridded 5 x 5 squares) and the 4 squares above and below, left and right of the central square, followed by calculation of the average number of cells per large square. This number = $\times 10^4$ and equalled the number of cells per ml within the cell suspension / trypan blue solution. During this calculation, it was noted that, due to the addition of trypan blue, the number of cells had to be $\times 5$ to correct for the dilution. The cell suspension was then diluted to a concentration of 1×10^5 cells/ml. The dilution factor was calculated using the following equation:

$$\text{Dilution factor} = \frac{\text{Concentration of original cell suspension}}{\text{Concentration of required cell suspension}} \times \text{Volume}$$

2.2 mRNA Isolation

mRNA was isolated using mRNA Isolation Kit (Roche-applied-science, Germany Cat. No. 11 741 985 001). Reagents were mixed according to the manufacturer's instructions using a vortex mixer and briefly centrifuged prior to commencing this procedure. This kit works on the basis that the poly (A) tail of mRNA hybridises to a biotin-labelled oligo(dT) probe. Streptavidin-coated magnetic particles capture the biotinylated hybrids and, with the aid of a magnetic separator, the magnetic particles are captured. The fluid is then removed by washing the particles with washing buffer and finally the mRNA is eluted from the particles by incubation with redistilled water.

Table 2.3. Reagents, composition and quantity provided mRNA isolation Kit (Roche).

Reagent	Composition	Quantity
Lysis Buffer	0.1 M tris buffer, 0.3 M lithium chloride (LiCl), 10 mM ethylenediaminetetraacetic acid (EDTA), 1% lithium dodecylsulphate, 5 mM dithiothreitol (DTT) pH 7.5	1 x 100 ml
Streptavidin-coated magnetic particles (SMP's)	10mg/ml in 50 mM hepes, 0.1% bovine serum albumin, 0.1% chloracetamide, 0.01% methylisothiazolone, pH 7.4	1 x 1.7 ml
Oligo(dT) ₂₀ probe biotin labelled	100 pmol biotin labelled oligo(dT) ₂₀ per µl of redistilled water	1 x 66 µl
Washing buffer	10 mM tris buffer, 0.2 M LiCl, 1 mM EDTA, pH 7.5	1 x 50 ml
Double redistilled water, RNase free	RNase-free H ₂ O	1 x 4 ml
Storage buffer	10 mM tris buffer, 0.1% chloracetamide, 0.01% methylisothiazolone, pH 7.5	1 x 7 ml

mRNA was isolated from 2×10^6 cells following the manufacturer's protocol as shown in the schematic diagram (Figure 2.1). The volumes and composition of each reagent and buffers provided within the kit are detailed in Table 2.3, whilst the specific measures used during each extraction procedure are shown in Table 2.4.

Cells were washed by suspension in $3 \times 500 \mu\text{l}$ of ice cold Phosphate Buffer Saline (PBS, 0.1 M) to remove excess media which could potentially interfere with UV spectrophotometric measurements. The suspension was centrifuged at 10,000 g for 3 min at room temperature and the supernatant discarded. To the cell pellet, 500 μl of lysing buffer (0.1 M Tris buffer, 0.3 M LiCl, 10 mM EDTA, 1% (w/v) lithium dodecylsulphate, 5 mM dithiothreitol, DTT, pH 7.5) was added, followed by mechanical shearing of cells, achieved by passing samples through a 21 gauge needle (six times). An aliquot of 0.5 μl biotin labelled oligo(dT)₂₀ probe (100 pmol biotin-labelled oligo(dT)₂₀ per μl of molecular biology grade H₂O) was added to the cell lysate and allowed to hybridise with mRNA for 10 min at room temperature. Simultaneously, 50 μl of streptavidin magnetic particles (10 mg/ml of suspension in 50 mM Hepes, 0.1% (w/v) bovine serum albumin, 0.1% (w/v) chlorace tamide, 0.01% (w/v) methylisothiazolone, pH 7.4) was aliquoted into a 1.5 ml sterile microfuge tube and separated from the storage buffer by placing in a magnetic separator, after which the storage buffer was discarded. The particles were cleansed by resuspension in 70 μl of lysing buffer (0.1 M Tris buffer, 0.3 M LiCl, 10 mM EDTA, 1% (w/v) lithium dodecylsulphate, 5 mM DTT, pH 7.5). Following magnetic separation and disposal of the supernatant, the prepared particles were resuspended in the dT-mRNA hybrid mixture; after brief vortexing, the resultant suspension was incubated for 5 min at 37°C to achieve immobilisation. Following incubation, the hybrid-linked particles were magnetically separated from this fluid and the supernatant was discarded. The remaining particles were then washed by resuspension in $3 \times 200 \mu\text{l}$ of washing buffer

(10 mM Tris buffer, 0.2 M LiCl and 1 mM EDTA, pH 7.5). Upon disposal of the final supernatant, mRNA was eluted from the particles by resuspension in 10 μ l of redistilled water, mixing and incubation for 2 min at 65°C. After magnetically separating the particles from the fluid, the resulting supernatant (mRNA) was stored at -20°C in an RNase free microfuge tube ready for quantification and analysis.

Table 2.4. Volumes of reagents used for mRNA isolation as per manufacturers' protocol.

	Amount of Tissue (mg)		Number of Cells				
	200	50-100	1×10^8	2×10^7	1×10^7	2×10^6	2×10^5
Volume of lysis buffer	3 ml	1.5 ml	15 ml	3 ml	1.5 ml	0.5 ml	0.1 ml
Volume of streptavidin magnetic particles	300 μ l	150 μ l	1.5 ml	300 μ l	150 μ l	50 μ l	50 μ l
Volume of lysis buffer: streptavidin magnetic particle preparation	500 μ l	250 μ l	2.5 ml	500 μ l	250 μ l	70 μ l	70 μ l
Volume of oligo(dT) ₂₀ probe biotin labelled	3 μ l	1.5 μ l	15 μ l	3 μ l	1.5 μ l	0.5 μ l	0.5 μ l
Volume of washing buffer	3 x 500 μ l	3 x 250 μ l	3 x 2.5 ml	3 x 500 μ l	3 x 250 μ l	3 x 200 μ l	3 x 200 μ l
Volume of redistilled water	50 μ l	25 μ l	250 μ l	50 μ l	25 μ l	10 μ l	5 μ l

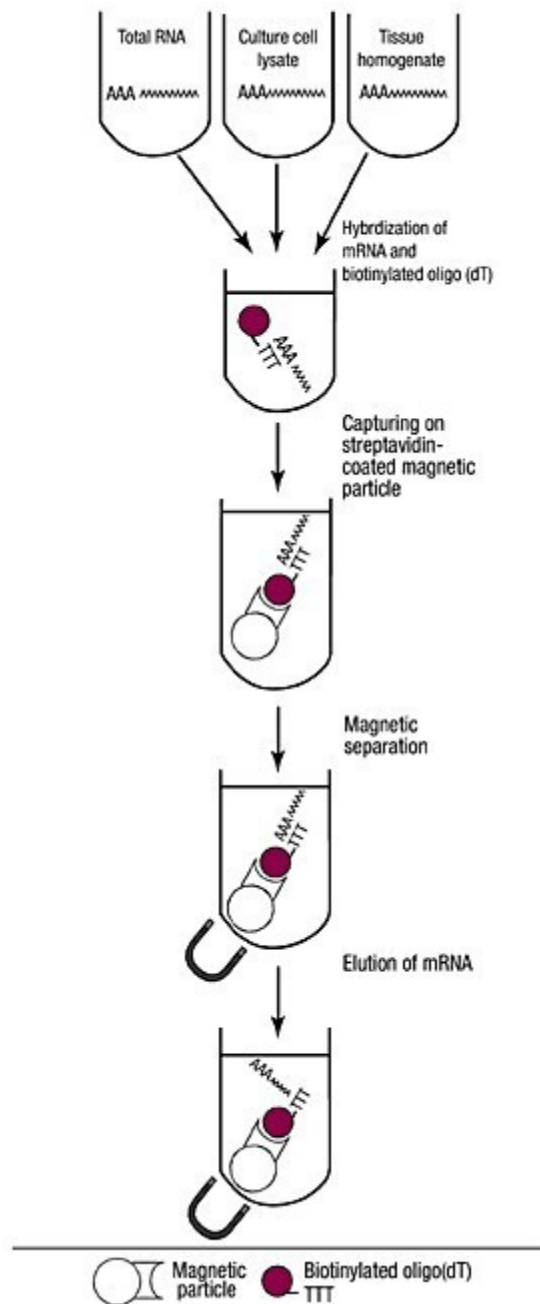


Figure 2.1 A diagrammatic representation of the principals involved in extracting mRNA from culture cells and tissue using the mRNA Isolation Kit (adapted from Roche mRNA Isolation Kit instruction manual).

2.2.1 Quantification of nucleic acids by UV spectrophotometry

Isolated mRNA was quantified by measurement of absorbance using the thermo spectrophotometer Helios gamma (Thermospectronics, UK) at wavelengths of 260 nm and 280 nm. Samples of mRNA (2 µl) were combined with 500 µl of TAE (Tris-acetate-EDTA) buffer (400 mM Tris, 0.01 M EDTA; pH 8.0). Spectrophotometric measurements were obtained and mRNA concentrations were calculated. The standard formula was based on an absorbance of one optical density (OD) unit at 260 nm = 50 µg/ml for dsDNA and 40 µg/ml for ssRNA. The ratio of absorbance at 260 nm and 280 nm was used to assess the purity of isolated nucleic acids. A ratio of 1.8 - 2.0 indicated the presence of pure single-stranded (ss) RNA. The concentrations of the isolated mRNA were calculated as follows

$$\text{Concentration mRNA } (\mu\text{g/ml}) = A_{260} \text{ reading} \times \text{dilution factor (250)} \times 40 \text{ (ssRNA)}$$

2.2.2 Analysis of Nucleic acid by agarose gel electrophoresis

Isolated mRNA was visualized on 2% agarose gels to determine whether RNA was intact or degraded. The 2% gel was prepared using 0.6 g of agarose powder (Geneflow, UK) dissolved in 30 ml TAE buffer (400mM Tris, 0.01 M EDTA; pH 8.3) and heated in a domestic microwave until a clear transparent solution had formed. The solution was poured into a prepared electrophoresis gel tank, combs inserted and left to solidify. TAE buffer was used to completely submerge the gel before the samples and a 100 bp ladder, as a molecular weight marker, were loaded into appropriate wells. Each sample loaded comprised 10 µl of extracted mRNA mixed with 2 µl of loading dye (0.25% w/v bromophenol blue, 0.25% w/v xylene cyanol and 40% w/v sucrose), together with 2 µl of 100 bp ladder mixed with 5 µl of loading dye. The gel was electrophoresed at 100 V for 25 min, followed by staining in 0.4 µg/ml ethidium bromide for 45 min and then

destained in distilled H₂O for approximately 10 min. The banding patterns were then visualized using a GENE GENIUS Bioimaging system and Gensnap software (Syngene, UK).

2.3 Complimentary DNA Synthesis (cDNA)

mRNA was reverse transcribed using First Strand cDNA Synthesis Kit, which harnesses enzymes isolated from Avian Myeloblastosis Virus (Roche-applied-science, Germany Cat. 11 483 188 001). The composition and volumes of all reagents provided are shown in Table 2.5, whilst the specific quantities required by each cDNA synthesis reaction are shown in Table 2.6. All reagents were kept on ice, mixed using a vortexer and briefly centrifuged prior to commencing this procedure.

Table 2.5 Reagents, composition and quantity of each reagent provided within the First Strand cDNA Synthesis Kit for RT-PCR (AMV) (Roche).

Reagent	Composition	Quantity
10 X Reaction Buffer	100 mM tris buffer, 500 mM KCl; pH 8.3	1.05 ml
MgCl ₂	25 mM MgCl ₂	3 ml (3 vials; 1 ml in each)
Deoxynucleotide Mix	dATP, dCTP, dTTP, dGTP; 10 mM each	210 µl
Gelatine	0.5 mg/ml (0.05% [w/v]) gelatine	210 µl
Oligo-p(dT) ₁₅ primer	0.02 A ₂₆₀ U/µl (0.8 µg/µl) oligo-p(dT) ₁₅ primer sequence	60 µl
Random primer p(dN) ₆	0.04 A ₂₆₀ U/µl (2 µg/µl) primer sequence	60 µl
RNase inhibitor	50 U/µl RNase inhibitor	30 µl
AMV Reverse Transcriptase	AMV reverse transcriptase	24 µl
Control Neo pa RNA	0.2 µg/µl RNA sample; 1.0 kb in length with an additional 19-base 3'-poly(A) tail	25 µl
Molecular biology-grade H ₂ O	RNase-free H ₂ O	2 ml (2 vials; 1 ml in each)

A master mix of 2 μ l of 10 X reaction buffer (500 mM KCl; pH 8.3), 4 μ l of $MgCl_2$ (25 mM), 2 μ l of deoxynucleotide mix (dATP, dCTP, dGTP and dTTP; 10 mM each in sterile double distilled water, pH 8.5), 2 μ l of oligo-p(dT)₁₅ primer (0.02 A260 units/ μ l (0.8 μ g/ μ l)), 1 μ l of RNase inhibitor (50 U/ μ l) and 0.8 μ l of AMV reverse transcriptase (25 U/ μ l) was made, to which the appropriate amount of mRNA (100 ng) was added, along with the relevant volume of molecular biology-grade H₂O, to make a total volume of 20 μ l, as shown in Table 2.6. The reaction mixture was briefly vortexed and centrifuged followed by an incubation period of 10 min at 25°C to allow the oligo-(dT)₁₅ primer to anneal to the mRNA. The reaction mixture was then further incubated for 60 min at 42°C, during which the mRNA template was reverse transcribed into single-stranded cDNA. As a final step, AMV Reverse Transcriptase was denatured by further incubating the reaction mixture for 5 min at 99°C, followed by cooling on ice for 5 min. The synthesised cDNA sample was then stored at -20°C until required.

Table 2.6 The quantities of reagents required for each cDNA synthesis reaction using those provided within the First Strand cDNA Synthesis Kit for RT-PCR (AMV).

Reagent	Quantity
10 X reaction buffer	2 μ l
MgCl ₂	4 μ l
Deoxynucleotide (dNTP) Mix	2 μ l
Oligo-p(dT) ₁₅ primer	2 μ l
RNase inhibitor	1 μ l
AMV reverse transcriptase	0.8 μ l
mRNA sample †	
Molecular biology-grade H ₂ O ‡	
Total reaction volume	20 μl

† The volume of mRNA sample added to each reaction was determined by its concentration following extraction. Since 50–100 ng of mRNA is typically required for successful cDNA synthesis, 100 ng of extracted mRNA was added to each sample reaction.

‡ Following the addition of 100 ng of extracted mRNA sample, the total reaction volume was made up to a final volume of 20 μ l using molecular biology-grade H₂O.

2.4 Primer Preparation

HSPA and *GAPDH* sequence-specific primers were designed using Primer3 software and commercially synthesised by TIB MOLBIOL syntheselabor (Berlin, Germany). Primers were received in a powdered form and collected by centrifugation at 10,000 g for 1 min at room temperature. Molecular biology-grade H₂O (250 µl) was added to each primer to create 20 µM stock solutions. Finally, 20 µl of the sense and antisense primer stock solutions were combined to generate a 10 µM PCR primer mix, which was then stored at -20°C until required. Table 2.10 portrays the sequences of the primers used in this study.

2.5 Real-time quantitative reverse transcriptase polymerase chain reaction (qRT-PCR)

Polymerase chain reaction (PCR) is a method that allows logarithmic amplification of short DNA sequences (usually 100 to 600 bases) within longer double stranded DNA molecules. qRT-PCR allows detection of very low copies of mRNA that would otherwise not show up if other analytical techniques such as northern blotting was used. The levels of *HSPA* and *GAPDH* (reference genes used in RT-PCR reaction, Olsvik *et al*, 2005) within all the cell lines used in this study were measured by performing real-time qRT-PCR (Ball *et al*, 2003) using the LightCycler 2.0 system (Roche Diagnostics Ltd, Germany) and LightCycler[®] FastStart DNA Master^{PLUS} SYBR Green I kit, according to the manufacturer's instructions. The composition and volumes of all reagents provided are shown in Table 2.7, whilst the specific quantities used during the amplification procedure shown in Table 2.8. All samples and reagents were kept on ice throughout the procedure.

Table 2.7 The composition and quantity of each reagent provided within the LightCycler® FastStart DNA MasterPLUS SYBR Green I kit.

Reagent	Reagent Composition	Quantity
Enzyme (1a)	FastStart Taq DNA Polymerase	1 vial
Reaction mix (1b)	Reaction buffer, dNTP mix (with dUTP instead of dTTP), SYBR Green I dye and MgCl ₂	3 vials
Molecular biology-grade H ₂ O	RNase-free H ₂ O	2 ml (2 vials; 1 ml in each)

Table 2.8 The quantities of reagents required for each RT-PCR reaction using those provided within the LightCycler® FastStart DNA MasterPLUS SYBR Green I kit.

Reagent	Quantity
Molecular biology-grade H ₂ O	12 µl
PCR primer mix	2 µl
Master Mix*	4 µl
Single-stranded cDNA template	2 µl
Total reaction volume	20 µl

* The Master Mix was formed by transferring 14 µl of enzyme (Table 2.7) into the vial of reaction mix (Table 2.7).

Prior to using hot-start PCR, an enzyme reaction mix was prepared by transferring 14 µl of LightCycler® FastStart Enzyme (1a) into the LightCycler® FastStart Reaction Mix SYBR Green vial (1b) (Table 2.8). Each reaction capillary contained a total reaction volume of 20 µl, comprising 4 µl of the ready to use hot-start reaction mix, 12 µl of molecular biology-grade H₂O, 2 µl of 10 µM PCR primer mix (generated from section 2.4 for each specific gene) and 2 µl of single stranded cDNA template. A further 20 µl of template-free reaction mix was prepared as a negative control (in which molecular biology-grade H₂O was substituted for cDNA). Prior to qRT-PCR being carried out, the definitive annealing temperature for each gene was established (Table 2.10). The LightCycler protocol for use with FastStart DNA Master^{PLUS} SYBR Green Kit 1 utilised the program, shown in Table 2.9.

Quantitative real-time PCR was used to evaluate the expression of *HSPA* (predicted amplicon size of 213 bp) and glyceraldehyde-3-phosphate dehydrogenase (*GAPDH*) as a control (predicted amplicon size of 238 bp) using FastStart DNA Master^{PLUS} SYBR Green 1 (Roche, UK). Primers used for *HSPA* were 5' CGACCTGAACAAGAGCATCA 3' (sense) and 5' AAGATCTGCGTCTGCTTGGT 3' (antisense) and for *GAPDH* primers were 5' GAGTCAAGCGATTTGGTCGT 3' (sense) and 5' TTGATTTTGGAGGGATCTCG 3' (antisense). All primers were designed using Primer3 software and manufactured by TIB MOLBIOL. The PCR protocol involved a hot start induction, with the FastStart *Taq* DNA polymerase enzyme activated by pre-incubating the reaction mixture at 95°C for 10 min. Hot start is an essential step which prevents non-specific elongations and increases PCR sensitivity, specificity and yield (Dang and Jayasena, 1996). The single stranded cDNA template was then subjected to 35 amplification cycles, each possessing the following parameters: denaturation at 95°C for 10 s, annealing at the primer dependant temperature 57°C (*HSPA*) and 56°C (*GAPDH*) for 15 s and extension at 72°C for 25 bp /

s (amplicon dependant, *HSPA* 9 s, *GAPDH* 10 s) (Patel *et al*, 2008). At the end of each cycle, the fluorescence emitted was measured in a single step in channel F1 (gain1) to obtain data for quantification analysis (Shervington *et al*, 2007b, Mohammed and Shervington, 2007). After the 35th cycle, the amplicons were prepared for melting curve analysis, heated to 95°C (denaturation) and then rapidly cooled to the previously used annealing temperature (+10°C) for 40 s. All heating and cooling steps were performed with a slope of 20°C / s. To obtain the data for the melting curve analysis, the temperature was subsequently raised to 95°C with a slope of 0.1°C / s and the emitted fluorescence was measured continuously (channel F1, gain1). Melting curve analysis was used to assess the specificity of the amplified PCR product and allow for discrimination between primer-dimers and specific product. At the final step, the generated amplicons were cooled to 40°C for 30 s and stored at -20°C until required for further analysis. All PCR reactions were performed in triplicate and a negative control included, which contained primers but no DNA.

Table 2.9 LightCycler program utilising FastStart DNA MasterPLUS SYBR Green Kit

Cycles	Analysis Mode	Target Temperature	Hold Time	
1	None	95°C	10 min	Pre-incubation
35	None	95°C	15 s	Denaturation
35	Quantification	57°C <i>HSPA</i> 56°C <i>GAPDH</i>	15 s	Annealing, amplification and real time analysis
35		72°C	9 sec <i>HSPA</i> 10sec <i>GAPDH</i>	Extension
	Melting Curve analysis	95°C		Denaturation
1		67°C <i>HSPA</i> 66°C <i>GAPDH</i>	40 s	
1		95°C		Melting
1	None	40°C	30 s	Cooling

Table 2.10. The *HSPA* and *GAPDH* for *Homo sapiens* and *Rattus norvegicus* primers [designed using Primer3 software and commercially synthesised by TIB MOLBIOL syntheselabor (Berlin, Germany)] utilised in real-time RT-PCR.

Gene	Primer Sequences	Annealing Temperature (°C)				Expected amplicon size (bp)	Extension time (s) (amplicon dependant - 25bp/s)
		Primer3	TIB MOLBIOL	GC / AT rule*	Experimental temperature		
<i>HSPA Homo sapien</i>	Sense: 5' - CGACCTGAACAAGAGCATCA - 3' Antisense: 5' - AAGATCTGCGTCTGCTTGGT - 3'	59.98 60.02	55.50 56.80	60.00 60.00	57	213	9
<i>GAPDH Homo sapien</i>	Sense: 5' - GAGTCAACGGATTTGGTCGT - 3' Antisense: 5' - TTGATTTTGGAGGGATCTCG - 3'	59.97 60.01	56.20 54.80	60.00 58.00	56	238	10
<i>HSPA Rattus norvegicus</i>	Sense: 5' - GTGTGGAGAGCCAAGAGGAG - 3' Antisense: 5' - TTTCCAAACTGGATCGAAGG - 3'	59.99 60.04	56.50 55.60	64.00 58.00	56	156	7
<i>GAPDH Rattus norvegicus</i>	Sense: 5' - AGTGCCAGCCTCGTCTCATA - 3' Antisense: 5' - GGATCTCGCTCCTGGAAGAT - 3'	60.97 60.70	57.10 56.00	62.00 62.00	57	265	11

* GC / AT rule: A method of calculating the primer annealing temperature using the formula: $T = 2^{\circ} (A + T) + 4^{\circ} (G + C)$, where A, C, G and T represent the number of adenine, cytosine, guanine and thymine bases respectively in the primer sequence concerned.

2.6 Analysis of qRT-PCR

2.6.1 Agarose gel electrophoresis

The amplicons from qRT-PCR were visualized on 2% agarose gels as described in section 2.2.2.

2.7 Quantification analysis of qRT-PCR

Genomic DNA of known concentrations was used as a standard to amplify *GAPDH* gene using the LightCycler instrument (Shervington *et al*, 2007b). A standard curve was produced using the crossing points shown in section 3.11.1, Figure 3.35 generated from five concentrations of genomic DNA in duplicate: 0.005, 0.05, 0.05, 5 and 50 ng with known copy numbers shown in section 3.11.1, Table 3.6. The equation generated ($y = -1.3124\ln(x) + 32.058$) was rearranged to $(=EXP ((Ct \text{ value} -32.058/-1.3124))$ and used to determine copy numbers of *HSPA* and *GAPDH* mRNA expression throughout this thesis.

2.8 Immunofluorescence

The cell culture medium was removed by gentle aspiration from the chamber slides and the cells were washed three times with warm PBS (0.1 M) before fixation. The fixation procedure involved incubation of the cells for 10 min at room temperature with freshly made 4% paraformaldehyde (w/v) in PBS (0.1 M) and 0.1 M, NaOH (sodium hydroxide). The excess paraformaldehyde was removed and the cells were washed again three times with warm PBS (0.1 M). The cells were permeabilized using 0.3 % (w/v) Triton X-100 in PBS and incubated for 7 min at room temperature on a shaker. Bovine Serum Albumin (BSA) blocking solution (1% w/v in PBS) was added to prevent

any non-specific binding and samples were incubated for 30 min at room temperature. After incubation, the blocking solution was removed by gentle aspiration. The primary antibody HSPA (Anti-Hsp70 antibody [BRM-22]) diluted in blocking solution, (dilution factor 1:200) (Abcam, UK, Cat No. ab6535) was added to each chamber and incubated at 4°C overnight. The primary antibody was removed by gentle aspiration followed by three consecutive washes with warm PBS (0.1 M). The cells were incubated with light sensitive Anti-mouse IgG FITC (fluorescein isothiocyanate) conjugated secondary antibody (Goat polyclonal Secondary Antibody to Mouse IgG - H&L FITC, Abcam, UK, Cat. No. ab6785) diluted in blocking solution (dilution factor 1:128) for a further 60 min at room temperature on a shaker in a dark room. The secondary antibody was removed by gentle aspiration, followed by three consecutive washes with warm PBS (0.1 M). The sections were mounted under a cover slip using VECTASHIELD PI (0.01 M) (Propidium Iodide, Vector, USA) mounting medium. The cells were then visualized and scanned using an Axiovert 200 LSM 510 laser scanning confocal microscope (Carl Zeiss, USA). Negative control cells from each sample underwent identical preparations for immunofluorescence staining, except that the primary antibody was omitted. Routinely 500 cells were analysed per sample.

2.9 Flow Cytometry

Cells were washed once in 0.1% BSA in PBS (500 µl), centrifuged for 5 min at 1000 rpm, and the supernatant was removed. Triton X-100 0.1% (100 µl) was added and samples incubated on ice for 15 min. Following incubation, the suspension was centrifuged for 5 min at 1000 rpm, and the supernatant was removed. Cells were washed once in 0.1% BSA in PBS (500 µl) and samples centrifuged for 5 min at 1000 rpm, after which the supernatant was removed. Goat serum (5% in PBS) and 0.1% BSA (50 µl) was added to each sample, which were then incubated on ice for 30 min. Following incubation, the suspension was centrifuged for 5 min at 1000 rpm, and the

supernatant was removed. Primary antibody (HSPA) (Anti-Hsp70 antibody [BRM-22], Abcam,UK) in PBS, 0.1% BSA and goat serum 5% (50 μ l) was added and incubated on ice for 30 min. Following incubation, the suspension was centrifuged for 5 min at 1000 rpm, before the supernatant was removed. Cells were washed once in 0.1% BSA in PBS (500 μ l) and centrifuged for 5 min at 1000 rpm, and the supernatant was removed. Fluorescein isothiocyanate (FITC) conjugated secondary antibody (Goat polyclonal Secondary Antibody to Mouse IgG - H&L FITC, Abcam, UK,) in PBS, 0.1% BSA and goat serum 5% (50 μ l) was added to each sample and they were then incubated on ice for 30 min. Following incubation, the suspension was centrifuged for 5 min at 1000 rpm, and the supernatant removed. Cells were washed twice in 0.1% BSA in PBS (500 μ l) and centrifuged for 5 min at 1000 rpm, and the supernatant was again removed. Cells were resuspended in 0.1% BSA in PBS (300 μ l) and filtered into FACS tubes. Becton Dickinson FACSAria flow cytometry equipment was used to count and distinguish between cells for the presence or absence of HSPA.

2.10 *Rattus norvegicus* Brain Tissue

Studies were undertaken using post-mortem brain tissue samples from aged-matched male Wistar rats (obtained from the Physiology Laboratory, University of Central Lancashire). All procedures conformed to the –UK Animals (Scientific Procedures) Act 1986¹ according to the –Principles of Laboratory Animal Care, 1985¹. The work had the relevant ethical clearance from the Ethics Committee for the University of Central Lancashire under Home Office Licence PIL50/00824. Animals were housed in groups under institutional regulations at standard vivarium conditions, granted free access to water and commercial chow, exposed to a 12 h light / 12 h dark cycle and monitored for any signs of stress. Rats were humanely killed by cervical dislocation and the brain removed, either immediately or at the given post-mortem interval.

Brain tissue samples weighing approximately 50 mg – 100 mg and no less than 0.5 cm in thickness, were excised using a sterile scalpel at timed intervals of 0, 3, 6, 12 and 24 h and maintained at room temperature. Excised samples after sacrifice were immediately weighed and snap-frozen by immersion into liquid nitrogen, followed by grinding of the tissue to a fine powder using a pestle and mortar under liquid nitrogen. Samples were transferred to new sterile 1.5 ml RNase free microfuge tubes and stored at -80°C.

2.11 Treatment

2.11.1 Induction of mild heat shock

Additional brain tissue excised at 0, 3, 6, 12 and 24 h post sacrifice was subjected to mild heat shock. This was performed by placing the brain tissue into sterile 1.5 microfuge tubes and immersion in a heated water bath at 42°C for a period of 10 min, after which samples were stored at room temperature. Samples weighing approximately 30 mg – 50 mg, and no greater than 0.5 cm in thickness, were excised using a sterile scalpel at timed intervals of 0, 3, 6, 12 and 24 h post sacrifice. Excised samples were immediately weighed and snap-frozen, by immersion in liquid nitrogen followed by grinding of the tissue to a fine powder using a sterile pestle and mortar, again under liquid nitrogen, before transfer to sterile 1.5 ml RNase free microfuge tubes and storage at -80°C.

2.11.2 Induction of multiple heat shocks

Additional rat brain tissue excised at 0, 3, 6, and 24 h post sacrifice was subjected to mild heat shock at 0 h and again at 3, 6 and 24 h time course periods. This was performed by placing the brain tissue into sterile 1.5 microfuge tubes and immersion in a heated water bath at 42°C for a period of 10 min, after which samples were stored at room temperature. Samples weighing approximately 30 mg – 50 mg, and no greater than 0.5 cm in thickness, were excised using a sterile scalpel at timed intervals of 0, 3, 6, and 24 h post sacrifice. Excised samples were immediately weighed and snap-frozen, by immersion in liquid nitrogen followed by grinding of the tissue to a fine powder using a sterile pestle and mortar, again under liquid nitrogen, before transfer to sterile 1.5 ml RNase free microfuge tubes and storage at -80°C.

2.12 DNA Extraction

DNA was extracted from brain tissue using DNeasy[®] Blood and Tissue Kit (Qiagen, UK. Cat. No. 69504) and RNase A (Qiagen, UK. Cat. No. 19101). Prior to commencing this procedure, 25 ml and 30 ml ethanol (96 -100%) was added to 95 ml of AW1 and 66 ml of AW2 buffer concentrates respectively.

Table 2.11. Reagents, components and quantity provided of each in the DNeasy[®] Blood and Tissue Kit (Qiagen).

Reagent / Component	Quantity
DNeasy Mini Spin Columns in 2 ml Collection Tubes	50
Collection Tubes 2 ml	100
Buffer ATL	10 ml
Buffer AL	12 ml
Buffer AW1 (concentrate)	19 ml
Buffer AW2 (concentrate)	13 ml
Buffer AE	22 ml
Proteinase K	1.25 ml
RNase A (17,500 U)	2.5 ml (100mg/ml; 7000 units/ml solution)

DNA was isolated from 25 mg of ground brain tissue following the manufacturer's protocol. The volumes of each reagent and buffers provided within the kit are detailed in Table 2.11, whilst the specific measures used during each extraction procedure are

shown in Table 2.12. Initially, 180 μ l of Buffer ATL was added to 25 mg of ground brain tissue with 20 μ l of Proteinase K. Samples were vortexed thoroughly and incubated overnight at 56°C. Following overnight incubation, 4 μ l of RNase A (100 mg/ml) was added to each sample and mixed by vortexing before incubating for 2 min at room temperature. After incubation, the lysed samples were vortexed for 15 s and 200 μ l of Buffer AL was added and mixed thoroughly by vortexing, followed by the addition of 200 μ l of ethanol (100%) which was again mixed thoroughly by vortexing. The lysis solution was pipetted into a DNeasy mini-spin column placed in a 2 ml collection tube and centrifuged at 6000 g (8000 rpm) for 1 min. The flow-through and the collection tube were discarded. The DNeasy mini-spin column was placed in a new 2 ml collection tube, 500 μ l of Buffer AW1 was added and centrifuged at 6000 g (8000 rpm) for 1 min. The flow-through and the collection tube were again discarded. The DNeasy mini-spin column was placed in a new 2 ml collection tube 500 μ l of Buffer AW2 was added and centrifuged at 20000 g (14000 rpm) for 3 min, before the flow-through and the collection tube were discarded. The DNeasy mini-spin column was placed in a new 1.5 ml micro-centrifuge tube and 200 μ l of Buffer AE was added directly onto the DNeasy membrane, incubated at room temperature for 1 min and centrifuged at 6000 g (8000 rpm) for 1 min. The resulting supernatant (DNA) was stored at -20°C ready for quantification and analysis.

Table 2.12. Volumes of reagents used for DNA extraction as per manufacturers' protocol.

Amount of Tissue	25 mg
Buffer ATL	180 μ l
Buffer AL	200 μ l
Buffer AW1 (concentrate)	500 μ l
Buffer AW2 (concentrate)	500 μ l
Buffer AE	200 μ l
Proteinase K	20 μ l
RNase A (17,500 U)	4 μ l
Ethanol 100%	200 μ l

2.12.1 Quantification of nucleic acids

Extracted DNA was quantified by measurement of absorbance of samples using the Thermo Scientific NanoDrop™ 1000 spectrophotometer at wavelengths of 260 nm and 280 nm. A 2 μ l DNA sample was pipetted onto the end of a fiber optic cable (the receiving fiber). A second fiber optic cable (the source fiber) was then brought into contact with the liquid sample, causing the liquid to bridge the gap between the fiber optic ends. A pulsed xenon flash lamp provide the light source and a spectrometer utilizing a linear CCD array was used to analyse the light passing through the sample (<http://www.nanodrop.com/Library/nd-1000-v3.7-users-manual-8.5x11.pdf>). The ratio of 260 nm to 280 nm was used to determine the purity of the extracted DNA. A ratio of ~ 1.8 was generally accepted as indicative of pure DNA.

2.12.2. Analysis of Nucleic acid by agarose gel

Extracted DNA was visualized on 2% agarose gels to determine whether DNA was intact or degraded as per section 2.2.2.

2.12.3. Quantification analysis of qRT-PCR

Extracted *Rattus norvegicus* genomic DNA was used as a standard to amplify *GAPDH* gene using the LightCycler instrument. A standard curve was produced using the crossing points (section 3.11.1, Figures 3.33) generated from five concentrations of genomic DNA in duplicate: 0.005, 0.05, 0.05, 5 and 50 ng with known copy numbers (section 3.11.1, Table 3.5). The equation generated ($y = -1.3124\text{Ln}(x) + 32.058$) was rearranged to $(=EXP ((Ct \text{ value} - 32.058 / -1.3124))$ and used to determine copy numbers of *HSPA* and *GAPDH* mRNA expression throughout this thesis.

2.14 mRNA Isolation

mRNA was isolated using mRNA Isolation Kit (Roche-applied-science, Germany Cat. No. 11 741 985 001). Reagents were mixed using a vortex mixer and briefly centrifuged prior to commencing this procedure.

mRNA was isolated from 50 mg of ground brain tissue following the manufacturer's protocol as shown in the schematic diagram Figure 2.1. The volumes and composition of each reagent and buffers provided within the kit are detailed in Table 2.3, whilst the specific measures used during each extraction procedure are shown in Table 2.4.

Initially, 1.5 ml of lysis buffer (0.1 M Tris buffer, 0.3 M LiCl, 10 mM EDTA, 1% (w/v) lithium dodecylsulphate, 5 mM DTT (dithiothreitol) pH 7.5) was chilled to $\leq 0^{\circ}\text{C}$ in a

sodium chloride-ice water bath, after which 50 mg of ground brain tissue was added followed by mechanical shearing of tissue achieved by passing through a 21 gauge needle (four). The suspension was centrifuged at 11,000 g for 30 s between 0°C and -4°C. The supernatant was captured and transferred into a 1.5 ml sterile microfuge tube and placed on ice. An aliquot of 1.5 µl of biotin labelled oligo(dT)₂₀ probe (100 pmol biotin-labelled oligo(dT)₂₀ per µl of molecular biology grade H₂O) was added to the tissue lysate and allowed to hybridise with mRNA for 10 min at room temperature. Simultaneously, 150 µl of streptavidin magnetic particles (10mg/ml of suspension in 50 mM Hepes, 0.1 % (w/v) bovine serum albumin, 0.1 % (w/v) chlorace tamide, 0.01 % (w/v) methylisothiazolone, pH 7.4) was aliquoted into a 1.5 ml sterile microfuge tube and separated from the storage buffer by placing in a magnetic separator, after which the storage buffer was discarded. The particles were cleansed by re-suspension in 250 µl of lysing buffer (0.1 M Tris buffer, 0.3 M LiCl, 10 mM EDTA, 1% (w/v) lithium dodecylsulphate, 5 mM (dithiothreitol) DTT pH 7.5). Following magnetic separation and disposal of the supernatant, the prepared particles were resuspended in the dT-mRNA hybrid mixture. After briefly vortexing, the resultant suspension was incubated for 5 min at 0°C to achieve immobilisation. Following incubation, the hybrid-linked particles were magnetically separated from this fluid and the supernatant was discarded. The remaining particles were then washed by resuspension in 3 × 200 µl of washing buffer (10 mM Tris buffer, 0.2 M LiCl and 1 mM EDTA, pH 7.5). Upon disposal of the final supernatant, mRNA was eluted from the particles by resuspension in 10 µl of redistilled water, mixed and incubated for 2 min at 65°C. After magnetically separating the particles from the fluid, the resulting supernatant (mRNA) was stored at -20°C in an RNase free microfuge tube ready for quantification and analysis.

2.15 Complimentary DNA Synthesis (cDNA)

mRNA was reversed transcribed using First Strand cDNA Synthesis Kit harnessing AMV enzymes as per section 2.3. The composition and volumes of all reagents provided are shown in Table 2.5, whilst the specific quantities required by each cDNA synthesis reaction are shown in Table 2.6. Reagents were mixed using a vortex mixer and briefly centrifuged prior to commencing this procedure.

2.16 Primer Preparation

Rattus norvegicus GAPDH and *HSPA* sequence-specific primers were designed using Primer3 software and commercially synthesised by TIB MOLBIOL syntheselabor (Berlin, Germany). Primers were received in a powdered form and collected by micro-centrifugation at 10,000 g for 1 min at room temperature. Molecular biology-grade H₂O (250 µl) was added to each primer to create 20 µM stock solutions. Finally, 20 µl of the sense and antisense primer stock solutions were combined to generate a 10 µM PCR primer mix, which was then stored at -20°C until required. Table 2.10 portrays the sequences of the primers corresponding to each gene.

2.17 Real-time quantitative reverse transcriptase polymerase chain reaction (qRT-PCR)

The levels of *HSPA* and *GAPDH* RNA sequences (*GAPDH* reference gene used in RT-PCR reaction, Olsvik *et al*, 2005) for all tissue samples were measured by performing real-time qRT-PCR (Ball *et al*, 2003) using the LightCycler 2.0 system (Roche Diagnostics Ltd, Germany) and LightCycler[®] FastStart DNA Master^{PLUS} SYBR Green I kit according to the manufacturer's instructions. The composition and volumes of all reagents provided are shown in Table 2.7, whilst the specific quantities used during the

amplification procedure shown in Table 2.8. All samples and reagents were kept on ice throughout the procedure.

Prior to using the hot-start PCR an enzyme reaction mix was prepared by transferring 14 µl of LightCycler[®] FastStart Enzyme (1a) into the LightCycler[®] FastStart Reaction Mix SYBR Green vial (1b) (Table 2.8). Each reaction capillary contained a total reaction volume of 20 µl, comprising 4 µl of the ready to use hot-start reaction mix, 12 µl of molecular biology-grade H₂O, 2 µl of 10 µM PCR primer mix (generated from section 2.4 for each specific gene) and 2 µl of single stranded cDNA template. A further 20 µl of template-free reaction mix was prepared as a negative control (in which molecular biology-grade H₂O substituted for cDNA). Prior to qRT-PCR being carried out, the definitive annealing temperature for each gene was established (Table 2.10). LightCycler protocol for use with FastStart DNA Master^{PLUS} SYBR Green Kit 1 utilised the program shown below in Table 3.13.

Quantitative real-time PCR was used to evaluate the expression of *HSPA* (predicted amplicon size of 156 bp) and glyceraldehyde-3-phosphate dehydrogenase (*GAPDH*) (predicted amplicon size of 207 bp) using FastStart DNA Master^{PLUS} SYBR Green 1 (Roche, UK). Primers used for *HSPA* were 5' GTGTGGAGAGCCAAGAGGAG 3' (sense) and 5' TTTCCAAACTGGATCGAAGG 3' (antisense) and for *GAPDH* primers were 5' AGACAGCCGCATCTTCTTGT 3' (sense) and 5' CTTGCCGTGGGTAGAGTCAT 3' (antisense). All primers were designed using Primer3 software and manufactured by TIB MOLBIOL. The PCR protocol involved a hot start induction, with the FastStart *Taq* DNA polymerase enzyme activated by pre-incubating the reaction mixture at 95°C for 10 min. Hot start includes a step which prevents non-specific elongations and increases PCR sensitivity, specificity and yield (Dang and Jayasena, 1996). The single stranded cDNA template was then subjected to

35 amplification cycles, each with the following parameters: denaturation at 95°C for 10 s, annealing at the primer dependant temperature 56°C (*HSPA*) and 57°C (*GAPDH*) for 15 s and extension at 72°C for 25 bp / s (amplicon dependant, *HSPA* 7 s, *GAPDH* 9 s) (Patel *et al*, 2008). At the end of each cycle, the fluorescence emitted was measured in a single step in channel F1 (gain1) to obtain data for quantification analysis (Shervington et al, 2007b, Mohammed and Shervington, 2007). After the 35th cycle, the amplicons were prepared for melting curve analysis, heated to 95°C (denaturation) and then rapidly cooled to the previously used annealing temperature (+10°C) for 40 s. All heating and cooling steps were performed with a slope of 20°C / s. To obtain the data for the melting curve analysis, the temperature was subsequently raised to 95°C (melting) with a slope of 0.1°C / s and the emitted fluorescence was measured continuously (channel F1, gain1). Melting curve analysis was used to assess the specificity of the amplified PCR product and allow for discrimination between primer-dimers and specific product. At the final step, the generated amplicons were cooled to 40°C for 30 s and stored at -20°C until required for further analysis. All PCR reactions were performed in triplicate with a negative control included, which contained primers but no DNA.

Table 2.13 LightCycler program utilising FastStart DNA MasterPLUS SYBR Green Kit

Cycles	Analysis Mode	Target Temperature	Hold Time	
1	None	95°C	10 min	Pre-incubation
35	None	95°C	15 s	Denaturation
35	Quantification	56°C <i>HSPA</i> 57°C <i>GAPDH</i>	15 s	Annealing, amplification and real time analysis
35		72°C	7 s <i>HSPA</i> 9 s <i>GAPDH</i>	Extension
	Melting Curve analysis	95°C		Denaturation
1		66°C <i>HSPA</i> 67°C <i>GAPDH</i>	40 s	
1		95°C		Melting
1	None	40°C	30 s	Cooling

2.18 Quantification analysis of qRT-PCR

Genomic DNA of known concentrations was used as a standard to amplify *GAPDH* gene using the LightCycler instrument. A standard curve was produced using the crossing points as shown in section 3.11.1, Figure 3.33 generated from five concentrations of genomic DNA in duplicate: 0.005, 0.05, 0.05, 5 and 50 ng with known copy numbers shown in section 3.11.1, Table 3.6. The equation generated ($y = -1.3124\ln(x) + 32.058$) was rearranged to $(=EXP((Ct\ value - 32.058)/-1.3124))$ and used to determine copy numbers of *HSPA* and *GAPDH* mRNA expression throughout this thesis.

2.19 Cryostat

Frozen sections of brain tissue were placed onto a chuck containing OCT (optimal cutting temperature) compound (10.24% polyvinyl alcohol, 4.26% polyethylene glycol, 85.5% non-reactive ingredient) and placed in liquid nitrogen. Once the OCT compound had turned solid and white, the frozen samples on the chuck were placed in the Bright's cryostat for cutting. The samples were coarsely trimmed until a full flat face was visible. Sections were then cut at 10 μ (microns) thickness and carefully placed on a charged slide. A few drops of 5% acetic acid was added to the cut sections and allowed to fix for a few seconds. Slides were kept at -20°C until required for immunofluorescent experiments.

2.20 Immunofluorescence

The tissue sections were initially fixed in freshly made 4% Paraformaldehyde (w/v) in PBS (0.1 M) for 15 min at room temperature, after which the excess paraformaldehyde was removed. The fixed tissue sections were permeabilized using Trypsin (0.025%) in

aqueous calcium chloride (CaCl₂) (0.1%, pH 7.8), incubated for 45 min at 37°C, and then washed three times in warm PBS (0.1M). The sections were then incubated in blocking solution (0.1% PBS, 0.5% Tween 20, 0.1% Goat serum) for 30 min at room temperature, followed by overnight incubation at 4°C in the primary antibody for HSPA (Anti-Hsp70 antibody [BRM-22], Abcam,UK, dilution 1:200) to allow the antibody to bind, and for saturation to take place. After overnight incubation, the sections were washed with PBS three times for 5 min and incubated in a solution of a light sensitive Anti-mouse IgG FITC (Fluorescein Isothiocyanate) conjugated secondary detection antibody (Goat polyclonal Secondary Antibody to Mouse IgG - H&L FITC, Abcam, UK, dilution 1:200) diluted in blocking solution for 1h at room temperature. The secondary antibody was removed followed by three consecutive washes with warm PBS (0.1 M). The sections were mounted under a cover slip using VECTASHIELD PI (0.01 M) (Propidium Iodide, Vector, USA) mounting medium. The tissue sections were then examined and images recorded using an Axiovert 200 LSM 510 laser scanning confocal microscope (Carl Zeiss, USA). Negative control cells from each sample encountered identical preparations for immunofluorescence staining, except that the primary antibody was omitted.

2.21 Statistical Analysis

For analysis of *HSPA*, *GAPDH* mRNA copy number and protein levels, all quantitative data was presented as the mean \pm SD of three separate experiments and subjected to either a one-way ANOVA between groups of analysis of variance test, a two-way factorial mixed ANOVA analysis of variance test, a three-way factorial mixed ANOVA analysis of variance or an independent-samples t-test using IBM SPSS statistics 19 software.

Chapter 3

Developmental Work

3.1 Developmental Work

During the course of this programme of research, initial developmental work was required to gain experience and establish the validity of the techniques and primer sequences for use in PCR experimentation. This chapter will focus on these areas of developmental work, to enable subsequent results chapters to focus on the results obtained. It will also describe the biological samples used for experimental work, and standard methodologies used.

3.2 Tissue samples and cell lines

Work undertaken throughout this study involved the use of the following samples:

- a) Tumour and normal (control) brain tissue samples were obtained from patients admitted to the Royal Preston Hospital, UK (section 4.2.3, Table 4.5). Work on these samples was carried out with ethical approval from the North Manchester Research Ethics Committee (Ref: 06/Q1406/104) and the Ethics Committee at the University of Central Lancashire.

- b) Human brain cell line grade I astrocytoma, 1321N1 was obtained from European Collection of Cell Cultures, ECACC, (UK), grade II/III oligodendroglioma GOS-3 from Deutsche Sammlung von Mikroorganismen und Zellkulturen GmbH, DMSZ, (Germany), grade IV glioblastoma, U87-MG from ECACC (UK) and normal human astrocytes, NHA from Lonza (UK) (section 2.1.2, Table 2.1).

- c) Post-mortem brain tissue samples were obtained from aged-matched male Wistar rats from the Physiology Laboratory, University of Central Lancashire.

Due to difficulties in obtaining post-mortem human brain tissue for all experiments, rat brain tissue was chosen for some experiments in this thesis. These samples were readily accessible from the Physiology Laboratory, University of Central Lancashire under the Home Office Licence PIL50/00824. Sequence homology between *Homo sapiens* and *Rattus norvegicus* for the target genes used indicated 73% homology for *HSPA/HSP70* nucleotide sequences, 96% homology for *HSPA/HSP70* amino acid sequences, 84% homology for the control *GAPDH* nucleotide sequence and 93% homology for *GAPDH* amino acid sequence (Table 3.1).

3.3 Introduction and history of bioinformatics

Bioinformatics is an essential computational tool in molecular biology, enabling the storage, retrieval, analysis and distribution of biological data (Kamel 2003; Kim, 2000; Singh and Kumar, 2001). It is defined as –the field of science in which biology, computer science and information technology merge into a single discipline (National Centre for Biotechnology Information, NCBI). Broadly speaking, this discipline consists of three main areas:

- the development of new algorithms and statistics in order to determine relationships amongst members of large data sets,
- the analysis and interpretation of various types of data, such as nucleotide and amino acid sequences, protein domains and structures, and

- the development of tools that enable the efficient access and management of different types of information.

To date, bioinformatics encompasses a wide variety of biological data, such as protein structures, gene and protein functional data, metabolic pathways and genomes. Due to the huge amount of data involved, much work has been concerned with the development of databases such as GenBank (Genetic Sequence Databank, USA), EMBL Nucleotide Sequence Database (Europe), DDBJ (DNA Database Japan), SwissProt (Switzerland), and with the associated software required for the analysis of the stored sequence information, primarily DNA, RNA and protein sequence data from the human and other genome sequencing projects (Fenstermacher, 2005). The management and accessibility of this data has been directly attributable to the development of the World Wide Web (WWW), which has facilitated access to this data by researchers, regardless of country or in-house research facilities.

3.4 Candidate Genes

Heat shock proteins are a family of highly conserved ubiquitous proteins encoded by genes which are activated not only in response to various physiological and environmental stress conditions, but also in cells affected by various diseases, such as cancer, Alzheimer's, Parkinson's and Huntington's diseases and diabetes, or by fever or inflammation (Jolly and Morimoto, 2000; Lindquist, 1986; Morimoto, 1993). However, in contrast to the diversity of the heat shock protein families, which cover approximately five hundred client proteins, the present study will only focus on HSPA/HSP70.

The *HSPA/HSP70* gene family is one of the most predominant heat shock protein gene families and is of particular interest due to three well-characterized members; *HSPA1A/HSP70-1*, *HSPA1B/HSP70-2* and *HSPA1L/HSP70-Hom*; (Milner and Campbell, 1990). Genes for these members are located within the major histocompatibility complex class III region (MHC-III), for *Homo sapiens* located on the short arm of chromosome 6 (6p21.3), and are intronless and for *Rattus norvegicus* located on the short arm of chromosome 20 (20p12), and again are intronless.

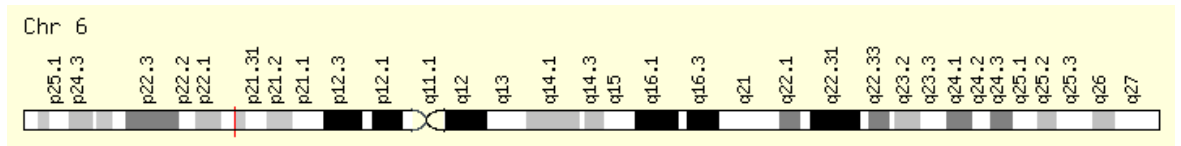
Although these three genes have similar nucleotide sequences, they differ in their regulation. Both *HSPA1A* and *HSPA1B* have been shown to encode identical protein products of 641 amino acids, and *HSPA1L* has been identified at a location 4 kb telomeric to *HSPA1A* with a 90% similarity in amino acid sequence (Milner and Campbell, 1990; Sargent *et al*, 1989a; Sargent *et al*, 1989). Both *HSPA1A* and *HSPA1B* have been shown to be highly expressed in mammalian cells that have been subjected to heat shock at 42°C (Milner and Campbell, 1990). *HSPA1A* is also constitutively expressed at low levels (Milner and Campbell, 1990). *HSPA1L*, which has no associated regulatory heat shock consensus sequence, has been shown to be expressed at low levels both constitutively and after heat shock at 42°C, with no comparable difference in levels (Milner and Campbell, 1990).

GAPDH was chosen as the preferred housekeeping gene to be used throughout this study. *GAPDH* is ubiquitously expressed in cells and has been shown to remain relatively constant in RNA and protein levels in normal and tumorous brain tissue (Barber *et al.*, 2005; Said *et al*, 2007).

3.5 Gene location

The genomic locations of the human genes *HSPA1A*, *HSPA1B*, *HSPA1L* and *GAPDH* were (Figure 3.1) obtained from GeneCards (<http://www.genecards.org>).

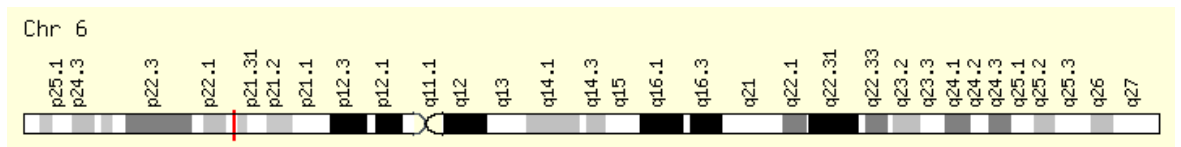
A. *HSPA1A*



B. *HSPA1B*



C. *HSPA1L*



D. *GAPDH*

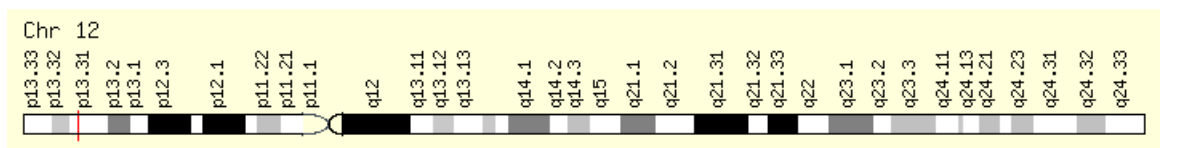


Figure 3.1 Locations of human genes used in this study. A. Chromosome 6 *HSPA1A*, B. *HSPA1B*, C. *HSPA1L* D. Chromosome 12 *GAPDH*. Location is denoted by the red bar (taken from GeneCards database <http://www.genecards.org>).

3.6 Nucleotide sequences

Nucleotide sequences for those genes of interest in this study were located using public databases, such as GenBank, SwissProt and EMBL which are held by the National Centre for Biotechnology Information (NCBI, Unigene). The NCBI database contains a collection of Expression Sequence Tags (ESTs), small sub-sequences derived from cDNA sequences (approx. 200 – 500 bp in length) that are generated by sequencing either one or both ends of RNA transcripts. ESTs are mapped to corresponding genomes, providing information regarding putative genes that have been located through analysis of biocomputational techniques.

The mRNA sequences used for this study were accessed from NCBI at:

<http://www.ncbi.nlm.nih.gov/entrez/query.fcgi?db=nucleotide&cmd=search&term>

The sequences obtained are shown in Appendix 9.1 (*HSPA1A Homo sapiens*), 9.2 (*HSPA1B Homo sapiens*), 9.3 (*HSPA1L Homo sapiens*), 9.4 (*HSPA1A Rattus norvegicus*), 9.5 (*HSPA1B Rattus norvegicus*), 9.6 (*HSPA1L Rattus norvegicus*), 9.7 (*GAPDH Homo sapiens*) and 9.8 (*GAPDH Rattus norvegicus*).

3.7 Primer Design

3.7.1 Primer Specificity

One of the most critical parameters for successful PCR is the design of amplification primers (Kamel *et al*, 2003). The efficacy, specificity and sensitivity of PCR depend largely on the efficiency of these primers (Dieffenbach *et al*, 1993; He *et al*, 1994). The sequence of each of the designed primers in a pair determines their specificity, melting temperature, G/C content and product length. There are numerous bioinformatic software programs available, such as primer-Blast (<http://www.ncbi.nlm.nih.gov/tools/primer-blast>) and Primer 3 (<http://frodo.wi.mit.edu/primer3/>), which assist in the design of effective PCR primers from a template DNA sequence (Dieffenbach *et al*, 1993; Kamel *et al*, 2003).

3.7.2 Primer Length

For RT-PCR, the most efficient primers are between 18 and 24 nucleotides in length (Dieffenbach *et al*, 1993; He *et al*, 1994; Kamel *et al*, 2003). In general, primers between 18 and 24 nucleotides in length tend to be very specific, particularly if the annealing temperature is set within a few degrees of the primer melting temperature (Dieffenbach *et al*, 1993). Depending on the size of the genome for the organism being studied, there is a minimum optimal primer length. For each additional nucleotide, the primer becomes four times more specific and hence the minimum primer length used in most applications is 18 nucleotides (Dieffenbach *et al*, 1993). Primers longer than 24 nucleotides in length may have a tendency to form secondary structures, which can

result in primer dimer formation and hence decrease PCR efficiency (Dieffenbach *et al*, 1993; He *et al*, 1994; Kamel *et al*, 2003).

3.7.3 Primer Melting (Annealing) Temperature (T_m)

Primer melting temperature (T_m) is important in determining the optimal PCR annealing temperature, which is in turn determined by primer sequence, primer concentration, salt concentration and magnesium chloride (MgCl₂) concentration. Ideally, both forward and reverse primers should have similar optimal melting temperatures, within the range of 52 – 62°C (Dieffenbach *et al*, 1993; He *et al*, 1994; Kamel *et al*, 2003). As a rule of thumb, most primer design programs use the following 4 + 2 rule, based purely on primer GC content, to calculate the optimal primer melting temperature:

$$T_m = 4 * (G + C) + 2 * (A + T)$$

The T_m is calculated by counting the numbers of guanine or cytosine residues and adenine or thymine residues in both the forward and reverse primers and substituting this information in the above equation. Each G/C effectively represents 4°C and A/T represents 2°C of the calculated melting temperature.

3.7.4 Primer GC content

For most PCR applications, the primer G/C content should be within the range of 45 – 60% of the total sequence (Dieffenbach *et al*, 1993; Kamel *et al*, 2003). If the G/C content is too low, then this could result in decreased PCR efficiency and poor primer

binding. Alternatively, if the G/C content is too high, this could result in mispriming through the formation of a stably annealed duplex with non-target templates (Dieffenbach *et al*, 1993; Kamel *et al*, 2003).

3.7.5 Product Length (Amplicon Size)

For accurate quantification and PCR efficiency, the product length should be within the range of 100 – 250 bp. Products longer than 250 bp will lead to decreased PCR efficiency (Dieffenbach *et al*, 1993; Kamel *et al*, 2003). The primers were designed using Primer 3 software, accessible at the website (http://frodo.wi.mit.edu/cgi-bin/primer3/primer3_www.cgi) to produce amplicons in this size range.

3.7.6 Experimental design of Primers

All primers were ordered and commercially synthesised by TIB MOLBIOL syntheselabor (Berlin, Germany). All primers were rehydrated in molecular biology grade H₂O (250 µl) to create 20 µM stock solutions which were stored at -20°C until required. Primers were designed using Primer 3 software using the following design parameters: primer length 20 ± 2 bp; G/C content between 45 – 60%; primer melting temperature between 52 – 62°C; and avoidance of the GC-rich 3' end (4 or more G's or C's in a row). Any potential hairpin formation, (i.e. self-complementarity of primers) was checked using the oligonucleotides properties calculator (<http://www.basic.northwestern.edu/biotools/oligocalc.html>). Section 2.7, Table 2.10 portrays the sequences of the primers used in this study.

Nucleotide sequences obtained from NCBI for *HSPA1A*, *HSPA1B*, *HSPA1L* and *GAPDH*, for both *Homo sapiens* and *Rattus norvegicus*, (appendices 9.1 – 9.8) were copied and pasted into a software program Primer3, which designs primers required for real time qRT-PCR (http://frodo.wi.mit.edu/cgi-bin/primer3/primer3_www.cgi). The program generated a number of possible forward and reverse primers, identifying primer location and length, amplicon size, GC % and suggested annealing temperature. The primers selected for this study were chosen based on the above parameters. Product lengths were between 156 – 238 bp, G/C content was between 45 – 60%, melting temperatures was between 59 – 61°C, primers contained no GC-rich 3' ends and did not contain any hairpin formations (appendices 9.9 – 9.13). A Basic Local Alignment Search Tool (BLAST) analysis was performed to find regions of local similarity between sequences. The program compares nucleotide or protein sequences to sequence databases and calculates the statistical significance of matches (NCBI) (Appendix xx).

3.8 Sequence Homology for HSP70 between *Homo sapiens* and *Rattus norvegicus*

General purpose multiple sequence alignment programs were used to determine sequence homology between the human and rat genes used in this study. This provides information useful in identifying conserved sequence regions and can also show multiple alignments for nucleic acid and protein sequences between species. Alignment of sequences can be carried out either along the entire length (global alignment) or restricted to certain regions (local alignment); (Kulikova *et al*, 2004) European Bioinformatics Institute (EBI) (<http://www.ebi.ac.uk>). The best matches for selected sequences are calculated and aligned so that identities, similarities and differences may be observed (Chenna *et al*, 2003).

The nucleotide and amino acid sequences obtained from NCBI for *HSPA1A*, *HSPA1B*, *HSPA1L* and *GAPDH* for both *Homo sapiens* and *Rattus norvegicus* (appendices 9.1 to 9.8) were copied and pasted into the software programme ClustalW2 <http://www.ebi.ac.uk/clustalw/>. Results for gene sequence and amino acid sequence homology by species and between species are shown in appendices 9.14 -9.25 and Table 3.1.

For *Homo sapiens*, results indicated 90%, 64% and 61% homology for *HSPA1A* v *HSPA1B*, *HSPA1A* v *HSPA1L* and *HSPA1B* v *HSPA1L* nucleotide sequences respectively, and 100%, 90% and 89% homology for amino acid sequences respectively. For *Rattus norvegicus*, results indicated 78%, 73% and 74% homology for *HSPA1A* v *HSPA1B*, *HSPA1A* v *HSPA1L* and *HSPA1B* v *HSPA1L* nucleotide sequences respectively, and 100%, 80% and 80% homology for amino acid sequences respectively. Sequence homology between *Homo sapiens* and *Rattus norvegicus* indicated 73%, 78%, 78% and 84% homology for *HSPA1A*, *HSPA1B*, *HSPA1L* and *GAPDH* nucleotide sequences respectively and 96%, 96%, 94% and 93% homology for *HSPA1A*, *HSPA1B*, *HSPA1L* and *GAPDH* amino acid sequences respectively.

Table 3.1. Table showing gene and amino acid sequence homology between genes and species.

Species	Gene	Gene Sequence Homology %	Amino Acid Sequence Homology %
<i>Homo sapiens</i>			
	<i>HSPA1A v HSPA1B</i>	90	100
	<i>HSPA1A v HSPA1L</i>	64	90
	<i>HSPA1B v HSPA1L</i>	61	89
<i>Rattus norvegicus</i>			
	<i>HSPA1A v HSPA1B</i>	78	100
	<i>HSPA1A v HSPA1L</i>	73	80
	<i>HSPA1B v HSPA1L</i>	74	80
<i>Homo sapien v Rattus norvegicus</i>			
	<i>HSPA1A</i>	73	96
	<i>HSPA1B</i>	78	96
	<i>HSPA1L</i>	78	94
	<i>GAPDH</i>	84	93

Results from Clustal W2 indicated for *Homo sapiens*, 90%, 64% and 61% homology for *HSPA1A v HSPA1B*, *HSPA1A v HSPA1L* and *HSPA1B v HSPA1L* nucleotide sequences and 100%, 90% and 89% homology for amino acid sequences respectively. For *Rattus norvegicus*, results indicated 78%, 73% and 74% homology for *HSPA1A v HSPA1B*, *HSPA1A v HSPA1L* and *HSPA1B v HSPA1L* nucleotide sequences and 100%, 80% and 80% homology for amino acid sequences respectively. Results between species indicated 73%, 78%, 78% and 84% homology for *HSPA1A*, *HSPA1B*, *HSPA1L* and *GAPDH* nucleotide sequences and 96%, 96%, 94% and 93% homology for *HSPA1A*, *HSPA1B*, *HSPA1L* and *GAPDH* amino acid sequences respectively.

3.9 Spectrophotometry

Spectrophotometry was conducted on the extracted mRNA samples obtained from each cell line and from rat brain tissue samples, to establish the purity and yield of nucleic acids. The absorbance of samples was measured at wavelengths of 260 and 280 nm, and the concentration of mRNA present in each cell line was calculated as described in Section 2.2.1. Examples of typical results obtained from mRNA samples are presented below in Table 3.2.

Table 3.2 An example of the obtained spectrophotometric readings and the subsequent concentrations of the mRNA isolated from all four cell lines used in this study.

Cell line	A ₂₆₀ reading	A ₂₈₀ reading	A ₂₆₀ / A ₂₈₀ ratio	Concentration (µg/ml)
1321N1	0.010	0.005	2.000	100
U87- MG	0.013	0.007	1.857	130
GOS-3	0.062	0.032	1.938	620
NHA	0.015	0.008	1.875	150

Aliquots (2ul) from mRNA samples from each of the cell lines were electrophoresed on a 2% agarose gel. Visualisation of the agarose gels typically showed that intact mRNA was obtained from each of the cell lines. Typically, no running streaks were observed on the gels, indicating that there was little or no degradation of the extracted mRNA. The purity of the mRNA (as assessed by the A₂₆₀ / A₂₈₀ ratio) is an important factor to be considered in these experiments because the contaminating presence of cellular proteins can reduce the efficiency of the first strand cDNA synthesis reaction. The A₂₆₀ / A₂₈₀ ratios of all the mRNA samples used in this study were between 1.8 and

2.0, to ensure that the mRNA samples were of an appropriate quality for use in PCR experimentation.

Table 3.3 An example of the obtained spectrophotometric readings and the subsequent concentrations of the mRNA isolated from rat brain tissue at 0, 3, 6, 12 and 24 hour post mortem interval used in this study.

Post-mortem Interval	A₂₆₀ reading	A₂₈₀ reading	A₂₆₀ / A₂₈₀ ratio	Concentration (ng/μl)
0 hr	2.249	1.434	1.57	89.9
3 hr	1.563	0.872	1.79	62.5
6 hr	2.683	1.594	1.68	107.3
12 hr	1.086	0.662	1.64	43.4
24 hr	0.533	0.312	1.68	21.3

The isolated mRNA samples from each of the brain tissue samples were run on a 2% agarose gel. Results indicated that intact mRNA was obtained from each of the brain tissue samples. The A₂₆₀ / A₂₈₀ ratios of all the mRNA used in this study were between 1.57 and 1.79. Although this was lower than the cell lines, the results of downstream assays were not affected.

3.10 Optimization of Primer concentrations

The efficiencies of sets of primers in PCR are dependent on their concentrations in each PCR reaction mixture (Ponchel *et al*, 2003). Primer concentrations that give the lowest threshold cycle (Ct) value should be selected since lower Ct values correspond to more efficient production of PCR products (Fraga *et al*, 2008).

Primer concentration in an amplification reaction should be between 0.1 and 0.5 μM . Primer concentrations which are too high can result in mispriming, whereby subsequent extension of misprimed molecules results in non-specific PCR products, or may lead to the production of non-specific products such as primer dimers (Fraga *et al*, 2008). The primer concentrations used in this study were based on the manufacturer's protocol and no additional optimization was required.

Cycling parameters were based on the manufacturer's guidelines and optimized empirically. No additional optimization was required.

Magnesium chloride is generally used in all RT-PCR reactions, with a concentration ranging between 1.5 and 3.0 mM. Although the kits used in this study contained magnesium chloride further optimization was performed using different combinations of template and primers, however results indicated no difference, therefore no further optimization was required.

3.11 Real-Time Reverse Transcription Polymerase Chain Reaction (RT-PCR)

Real time PCR is a highly sensitive, rapid and accurate method which can be used to monitor small changes in gene expression. Quantitative measurements are taken during the exponential phase when the fluorescence produced is proportional to the accumulation of PCR product. Absolute quantification of a target amplicon may be expressed as a copy number. A positive reaction in real time PCR is detected through the accumulation of a fluorescent signal, referred to as the cycle threshold (Ct), which reflects the number of cycles required for the fluorescent signal to cross a cycle threshold, and hence exceeds the background level. Fluorescence values are recorded during every cycle and represent the amount of amplified product. The more template that is present at the start of the reaction, the fewer number of cycles it will take to reach a point at which a fluorescent signal will be first recorded.

3.11.1 Detection Chemistry used in RT-PCR

The most commonly used methodologies for the detection of amplicons by RT-PCR involves fluorescent dyes. One of the most frequently used dyes, which was employed in this study, is SYBR Green I (Roche). SYBR Green I, when free in solution, displays relatively low fluorescence, but when bound to ds-DNA, its fluorescence increases by 1000 fold. The more ds-DNA that is present, the more binding sites there are for the dye, and hence fluorescence increases in proportion to ds-DNA concentration. As the target sequence is amplified, the increase in concentration of the ds-DNA can be directly measured by the corresponding increase in fluorescence signal.

Measurement of fluorescence at the end of the elongation step of every PCR cycle is performed to monitor the increasing amount of amplified DNA. Following the amplification reaction, PCR products are denatured and SYBR Green fluorescence decreases. If the PCR products consist of molecules of homogeneous length, then only a single thermal transition will be detected. Correlation of fluorescence with the temperature curve (often referred to as a dissociation curve) can be used to differentiate between specific and non-specific amplicons, based on the melting temperature of the reaction end products. Together with a melting curve analysis performed under the same PCR conditions, the SYBR Green I format provides an excellent tool for specific product identification and quantification.

3.11.2 Melting Curve Analysis

Melting curve analysis is performed after the amplification stage, when it is used to assess the dissociation-characteristics of double-stranded DNA during heating. For SYBR Green based detection of amplicons, it is important to run a dissociation curve following the real time PCR, because SYBR Green will detect any double stranded DNA, including primer-dimers, contaminating DNA, and PCR products arising from misannealed primers. By viewing a dissociation curve, as shown in Figure 3.2, it is possible to gain confidence that only the desired amplicon is being detected. Melting curve analysis can be used to identify different reaction products, including nonspecific products and primer-dimers. This is valuable because the presence of secondary nonspecific products and primer-dimers can severely reduce the amplification efficiency and accuracy of the data obtained from the experiment. Primer-dimers can also limit the dynamic range of the desired standard curve through competition for reaction components during amplification. After completion of the amplification reaction, a melting curve is generated by increasing the temperature in small increments and

monitoring the fluorescent signal at each step. As the dsDNA in the reaction denatures, the fluorescence decreases rapidly and significantly. A plot of the negative first derivative of the change in fluorescence ($-dF/dT$, the rate of change of fluorescence) vs. temperature has distinct peaks that correspond to the melting temperature (T_m) of each product.

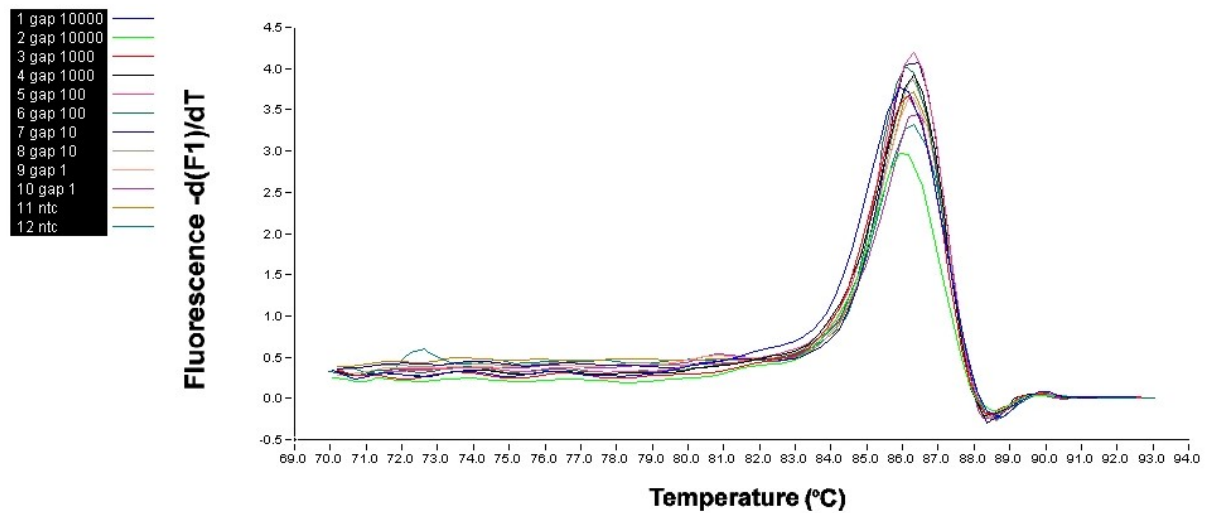


Figure 3.2 An example of a melting (dissociation) curve produced for rat GAPDH. The single peak indicates the presence of one PCR products, no presence of primer-dimers.

3.12. Standard Curve for house keeping gene *GAPDH*

A standard curve is a useful tool for quantifying mRNA and DNA of unknown amounts, and this process is referred to as absolute quantification. Absolute quantification is used to determine how much (number of copies, ng, etc.) of a target gene is present in a particular sample without reference to other samples. In absolute quantification, the quantity of the unknown sample is interpolated from a range of standards of known quantity. To construct a standard curve, a template with known concentration is required. This template is diluted to create a range of standard concentrations.

Absolute quantification is relatively simple and the mathematical calculations are easy to perform. It involves comparing the C_T values of test samples to those of standards of known quantity plotted on a standard curve. Usually, the quantity is normalized to a unit amount of sample, such as the number of cells in the original sample material, volume, or the total amount of nucleic acid. The standard curve constructed from the diluted standard template can then be used to determine the target quantity in the unknown sample by interpolation, in a similar way to that by which molecular size standards are used to determine the molecular size of an unknown DNA band on an agarose gel.

To establish a standard curve, a sample of human and rat genomic DNA was extracted from brain tissue. The size of the human genome was determined as 3,400,000,000 bp and the size of the rat genome was determined as 2,900,000,000 bp from the Database of Genome Sizes (DOGS): <http://www.cbs.dtu.dk/databases/DOGS/index.html>.

For example using the calculation from Applied Biosystems protocol for mass of the rat haploid genome;

(http://www6.appliedbiosystems.com/support/tutorials/pdf/quant_pcr.pdf)

$$M = n \times 1.096 \times e^{-21}$$

Where:

M = Mass of the haploid genome

N = Genome size (bp)

$$e^{-21} = 10^{-21}$$

$$M = 2.9e^9 \times 1.096 \times e^{-21}$$

$$M = 3.1784e^{-12} \text{ g}$$

Convert from g (grams) to pg (picograms)

$$3.1784e^{-12} \text{ g} \times 1e^{12} \text{ pg}$$

$$M = 3.1784 \text{ pg}$$

The mass of the haploid genome was determined as 3.1784 pg. The target gene *GAPDH* exists as a single copy gene per haploid genome and thus two copies per cell (Ponchel *et al*, 2003), and therefore it was calculated that 3.1784 pg of rat genomic DNA contained 1 copy of *GAPDH*. The A_{260} reading was 1.026, and thus the quantity of DNA per μl of original sample was 51,300 pg/ μl . From this, it was calculated that 19.49 μl contained 1 million copy numbers of the *GAPDH* gene sequence.

Table 3.4 Table showing final concentration of genomic DNA required for serial dilution.

Copy Numbers	Mass of Haploid Genome	Mass of gDNA Needed (pg)	PCR Reaction Volume (μ l)	Final Conc. Of gDNA (pg/ μ l)
10,000	x 3.1784	31784	/ 2	15892
1,000		3178.4		1589.2
100		317.84		158.92
10		31.784		15.892
1		3.1784		1.5892

Using the data from Table 3.4, a serial dilution was carried out to give samples containing 1, 10, 100, 1000 and 10,000 copy numbers. The serial dilution was prepared using the formula:

$$C1 \times V1 = C2 \times V2$$

Where:

C1 = Initial Concentration of gDNA (pg/ μ l)

V1 = Volume of gDNA (μ l)

V2 = Final Volume (μ l)

C2 = Final Conc. of Dilution (pg/ μ l)

Table 3.5 Table showing calculation for serial dilution of known copy numbers.

Source of gDNA	Initial Conc. (pg/ μ l)	Volume of gDNA (μ l)	Volume of Diluent (μ l)	Final Volume (μ l)	Final Conc. of Dilution (pg/ μ l)	Resulting Copy No. GAPDH / 2 μ l
	C1	V1		V2	C2	
Stock	51300	31	69	100	15892	10,000
Dilution 1	15892	10	90	100	1589.2	1,000
Dilution 2	1589.2	10	90	100	158.92	100
Dilution 3	158.92	10	90	100	15.892	10
Dilution 4	15.892	10	90	100	1.5892	1

A standard curve was produced using RT-PCR utilising the conditions as described in section 2.5 and 2.17, using the crossing points (Figures 3.3 and 3.5) generated from five copy number concentrations of genomic DNA, in triplicate : 1, 10, 100, 1,000 and 10,000 copies with known concentrations (Table 3.5 and 3.6). The equation generated for *GAPDH* for *Rattus norvegicus* ($y = -1.192\ln(x) + 30.35$) (Figure 3.4) was rearranged to $(=EXP ((Ct \text{ value } -30.35/-1.192))$ and for *GAPDH Homo sapiens* ($y = -1.312\ln(x) + 32.05$) (Figure 3.6) was rearranged to $(=EXP ((Ct \text{ value } -32.05/-1.312))$. These were then used to determine copy numbers of *HSPA* and *GAPDH* mRNA expression for rat brain tissue, human cell lines and brain tissue throughout this thesis.

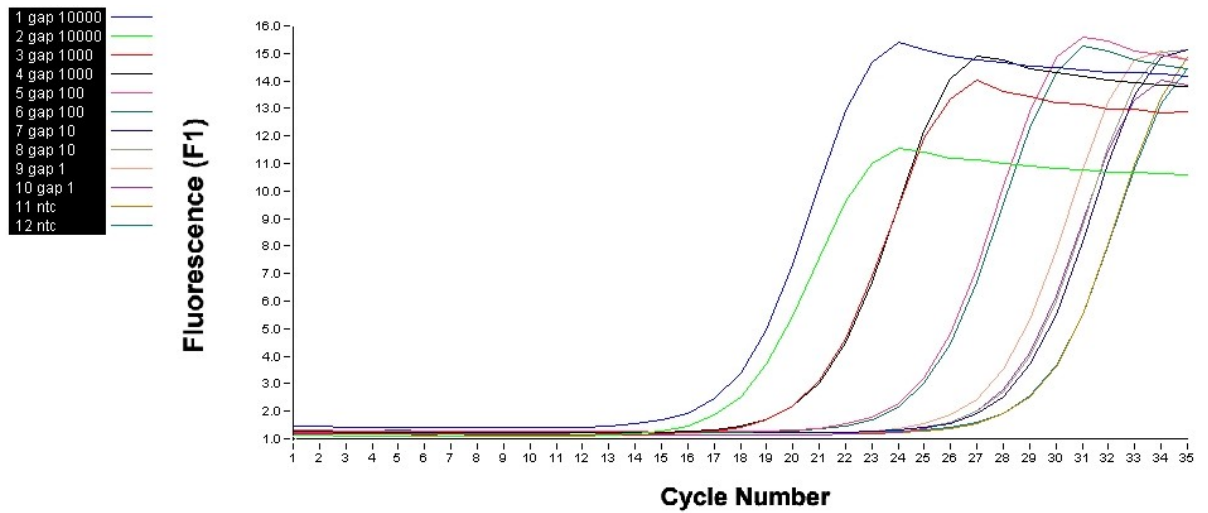


Figure 3.3 Quantification Curve of known concentrations of rat DNA. Standards used to generate the copy numbers of *HSPA*. LightCycler quantification curve generated when known concentration of Genomic rat DNA was amplified, which shows that the higher the concentration the lower the Ct value i.e. earlier detection of fluorescence. The negative control (primer alone, NTC) showed no detection of fluorescence until after 30 Ct (straight line).

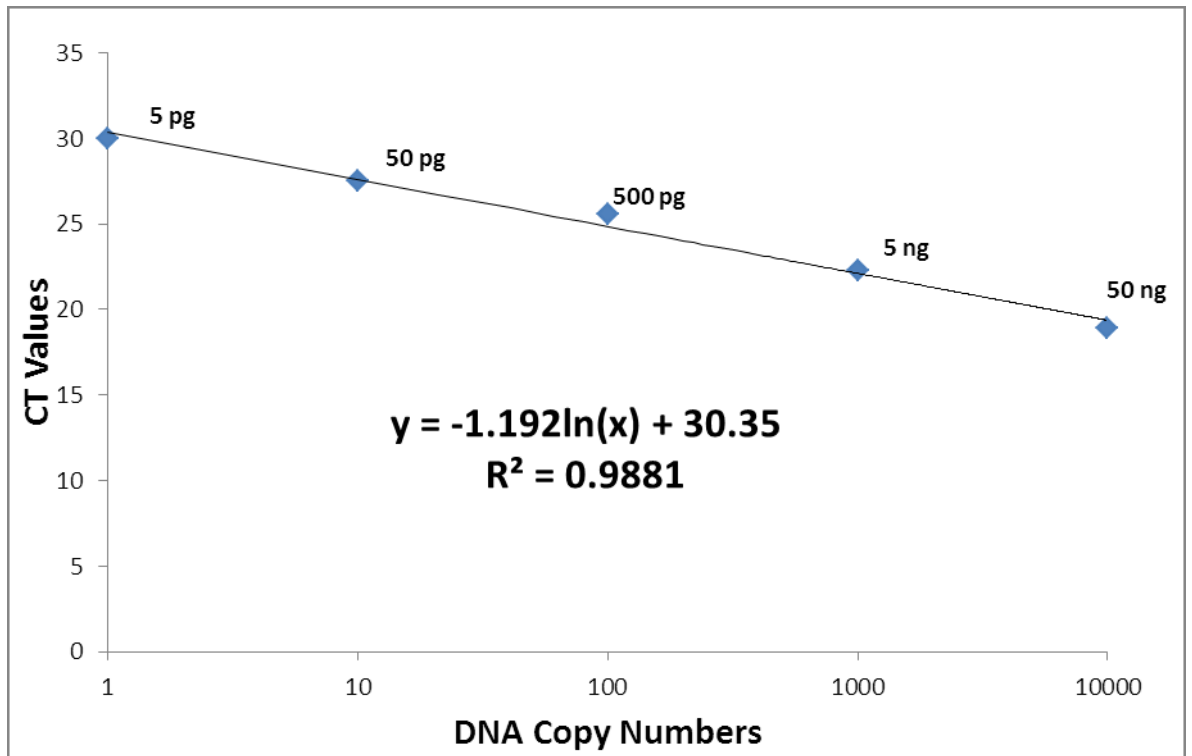


Figure 3.4 Standard curve produced from quantification curve of known concentrations of rat DNA. The standard curve generated from the crossing points showing the relationship between Ct values and copy numbers of the amplified Genomic rat DNA using *GAPDH* reference gene.

Table 3.6 Known concentrations of Genomic human DNA corresponding to the average Ct value and copy number.

Concentration of Genomic DNA (ng)	Average Ct	Copy number
0.005	30.15	1.7
0.05	29.1	17
0.5	26.42	170
5	22.6	1700
50	18.3	17000

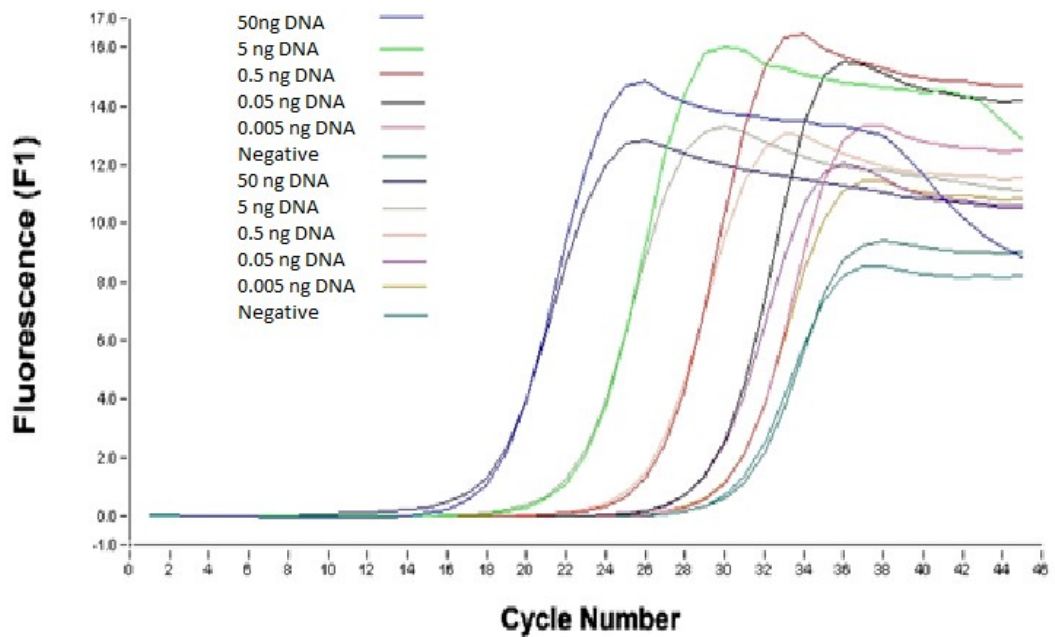


Figure 3.5 Quantification Curve of known concentrations of human DNA. Standards used to generate the copy numbers of *HSPA*. LightCycler quantification curve generated when known concentration of Genomic human DNA was amplified, which shows that the higher the concentration the lower the Ct value i.e. earlier detection of fluorescence. The negative control (primer alone, NTC) showed no detection of fluorescence until after 30 Ct (straight line) (adapted from Mohammed, 2007).

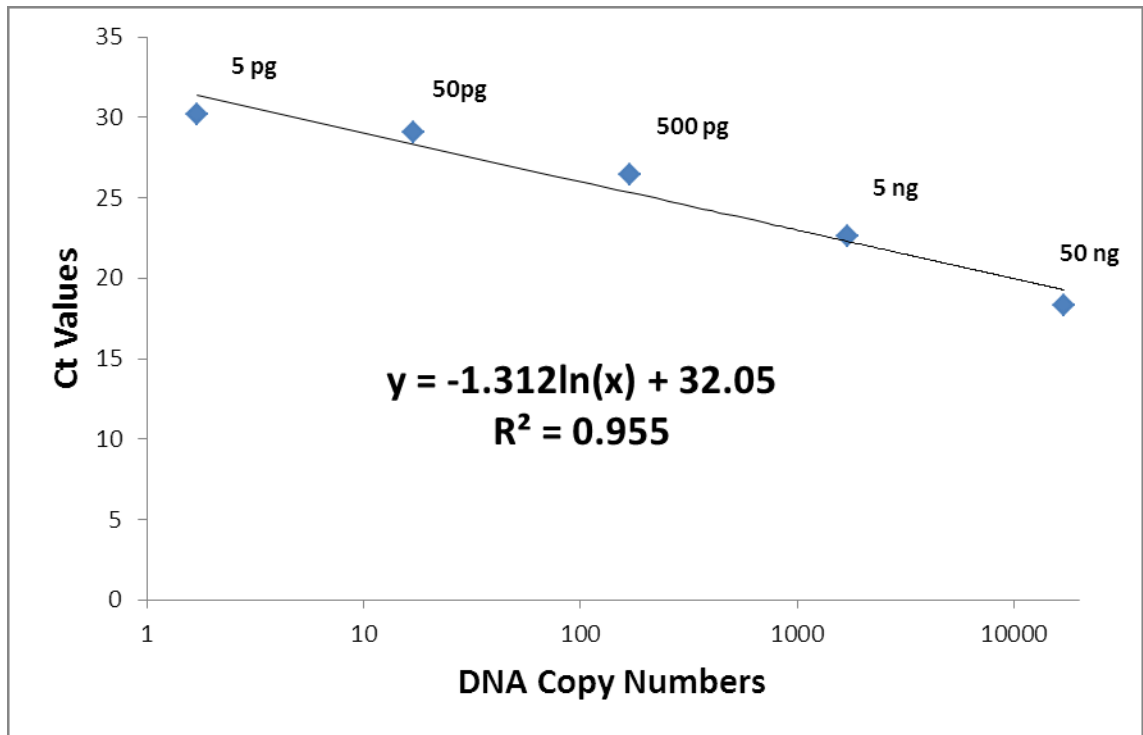


Figure 3.6 Standard curve produced from quantification curve of known concentrations of human DNA. The standard curve generated from the crossing points showing the relationship between Ct values and copy numbers of the amplified Genomic human DNA using *GAPDH* reference gene (adapted from Mohammed, 2007).

3.13 Reference Genes

Control genes, which are often referred to as housekeeping genes, are frequently used to normalise mRNA levels between different tissue types, such as those obtained from normal and diseased cells. The levels of expression of these genes may vary among tissues or cells and may change under certain circumstances (Barber *et al*, 2005; Silver *et al*, 2006). Quantitative studies are commonly used in biomedical research to compare RNA populations under different experimental or clinical conditions. In order to control experimental variations in the amount of RNA used in qRT-PCR, reference (housekeeping) genes are used for the normalization of target gene expression data, such as glyceraldehyde-3-phosphate dehydrogenase (*GAPDH*), β -actins, and 16S rRNA (Barber *et al*, 2005; Silver *et al*, 2006; Thellin *et al*, 1999). It is assumed that the expression of these genes will remain constant in the cells or tissues under investigation. Although some exceptions to this assumption have been well documented, housekeeping genes are of general value in fully characterized systems. The variability in the expression of the most commonly used housekeeping genes has shown that there is no -one-size-fits-all gene that can be used for normalization of gene expression data (Barber *et al*, 2005; Silver *et al*, 2006). A study undertaken by Barber (2005) has shown that, by providing copy numbers of *GAPDH* mRNA expression, the data can be used as a factor for the normalization of gene expression between tissues types, where *GAPDH* is used as the housekeeping control gene. Results indicated differences in *GAPDH* mRNA expression in different tissue types however, the data provided no evidence that there was any effect by age or gender and in most tissues the influence of delay in processing surgical and post-mortem tissues was negligible (Barber *et al*, 2005). Due to the findings within this study, and given that *GAPDH* is one of the most commonly used housekeeping genes used in comparisons of gene expression data, *GAPDH* was chosen as the preferred housekeeping gene to be used throughout this study.

3.14 Real time PCR assay

The Roche LightCycler 2.0 instrument with the LightCycler® FastStart^{PLUS} DNA Master SYBR Green I kit was used for quantitative analysis of *HSPA* and *GAPDH* mRNA by real-time PCR. Initial assays were carried out according to the manufacturer's conditions utilising the following optimum parameters: the primer concentration was 1 µM, the annealing temperature for the amplification of *Homo sapien HSPA* and *GAPDH* was 57°C and 56°C respectively and *Rattus norvegicus HSPA* and *GAPDH* 56°C and 57°C was respectively. Confirmation of PCR products was performed by incorporating a melting curve analysis step to ensure that only the target genes were amplified and detected.

Chapter 4

***HSPA* gene expression in glioma**

cells and brain tissue

4.1 Gene Expression

HSPA expression is up-regulated in cancer cells (Graner *et al*, 2007; Jolly and Morimoto, 2000), and thus the main research aim of work presented in this chapter was to measure and compare *HSPA* expression in normal and glioma cell lines and normal and cancerous brain tissue. A significant difference between these tissues might allow assessment of its possible use as a prognostic marker for grade related brain tumours.

Tumour and normal brain tissue samples were obtained from patients admitted to the Royal Preston Hospital, UK. Informed consent and ethical approval was obtained prior to this investigation. Tissues were dissected and immediately frozen to -80°C and stored for analysis. In total 18 tissue samples were used in this study (Table 4.5). Human brain cell lines GOS-3 (grade II/III oligodendroglioma) from DMSZ (Germany), U87-MG (grade IV glioblastoma) from ECCAC (UK) and NHA (normal human astrocytes) from Lonza (UK) were also used in this study. GOS-3 cells were routinely cultured in Dulbecco's modified Eagle's medium (DMEM) (Sigma) supplemented with 10% FBS and with 4 mM L-glutamide, while U87-MG cells were cultured in Eagle's minimum essential medium (EMEM) (Sigma) supplemented with 2 mM L-glutamide, 10% FBS and 1% (v/v) nonessential amino acids (Sigma). The NHA cells were cultured in astrocyte medium (AM) supplemented with 15 ml of FBS, 0.5 ml Ascorbic Acid, 0.5 ml rhEGF (astrocyte growth supplement) 0.5 ml GA100 1.25 ml Insulin and 5 ml L-glutamide.

mRNA was isolated from all four cell lines, 15 human glioma brain tissues and three normal (control) brain tissues using mRNA Isolation Kit (Roche, UK) following the manufacturer's protocol. The concentration and purity of mRNA was determined by ultraviolet spectrophotometry. Isolated mRNA (100 ng) was transcribed to cDNA using

1st Strand cDNA Synthesis Kit for RT-PCR (AMV) (Roche, UK) following the manufacturer's protocol, which was then used as a template for qRT-PCR. Quantitative real-time PCR was used to evaluate the expression of *HSPA*, and *GAPDH* as a control using FastStart DNA Master^{PLUS} SYBR Green 1 (Roche, UK). Primers used for *HSPA* were 5' CGACCTGAACAAGAGCATCA 3' (sense) and 5' AAGATCTGCGTCTGCTTGGT 3' (antisense). For *GAPDH*, primers were 5' GAGTCAAGCGATTTGGTCGT 3' (sense) and 5' TTGATTTTGGAGGGATCTCG 3' (antisense). All primers were designed using Primer3 software and manufactured by TIB MOLBIOL. After an initial denaturation at 95°C for 10 min, the samples were subjected to 35 cycles of RT-PCR 95°C for 10 s, annealing temperature 57°C (*HSPA*) and 56°C (*GAPDH*) for 15 s, and 72°C for 15 s (Patel *et al.*, 2008). At the end of each cycle, the fluorescence emitted was measured in a single step in channel F1 (gain1). After the 35th cycle, the specimens were heated to 95°C and rapidly cooled to 65°C for 15 s. All heating and cooling steps were performed with a slope of 20°C / s. The temperature was subsequently raised to 95°C with a slope of 0.1°C / s and fluorescence was measured continuously (channel F1, gain1) to obtain data for the melting curve analysis. All PCR reactions were performed in triplicate and a negative control included, which contained primers with no DNA. All PCR products were analysed using gel electrophoresis stained and visualised using a gel analyser (SynGene, UK).

Expression of *HSPA* was compared between the three glioma cell lines (1321N1, GOS-3 and U87-MG) and in a normal (control) human astrocyte cell line (NHA), and also in 15 glioma and 3 normal brain tissue samples. *GAPDH* was used as an internal standard throughout all RT-PCR experiments (Barber *et al.*, 2005).

4.2 Constitutive Expression

4.2.1 Glioma Cell lines

Copy numbers of *HSPA* and *GAPDH* transcripts were determined using RT-PCR in the three glioma cell lines (1321N1, GOS-3 and U87-MG), and in the normal human astrocyte cell line (NHA). The primers and optimal temperatures used for the amplification of both genes are documented in Table 2.10 in section 2.5. All PCR experiments were carried out in triplicate for consistency and repeatability. For each gene analysed, a quantification graph was produced to confirm gene amplification. The resulting amplicons for *HSPA* and *GAPDH* were also visualized using agarose gel electrophoresis, each being represented by bands of 213 and 238 bp, respectively. The three glioma cell lines transcribed *HSPA* at higher levels than the normal astrocyte cell line NHA (Figure 4.1). *GAPDH* transcript levels were consistent in all glioma and normal cell lines, confirming comparability of *HSPA* results (Figure 4.1). The mRNA copy number for both genes was calculated for each cell line to monitor the gene expression level. For *HSPA*, mRNA copy numbers per 100 ng of extracted mRNA confirmed that 1321N1, produced approximately 7,500 copies, GOS-3 contained approximately 8,900 copies and U87-MG contained approximately 8,200 copies of this transcript. Glioma cell lines expressed *HSPA* at a higher level than normal human astrocyte NHA, with approximately 1,400 copies, indicating that *HSPA* is expressed at lower levels in normal cells but is highly expressed in cancer cells (Table 4). For *GAPDH*, mRNA copy numbers per 100 ng of extracted mRNA were relatively consistent, NHA produced approximately 146,500 copies, 1321N1 contained approximately 144,500 copies, GOS-3 contained approximately 147,500 copies and U87-MG contained approximately 147,500 copies, again confirming comparability of *HSPA* results (Table 4.1).

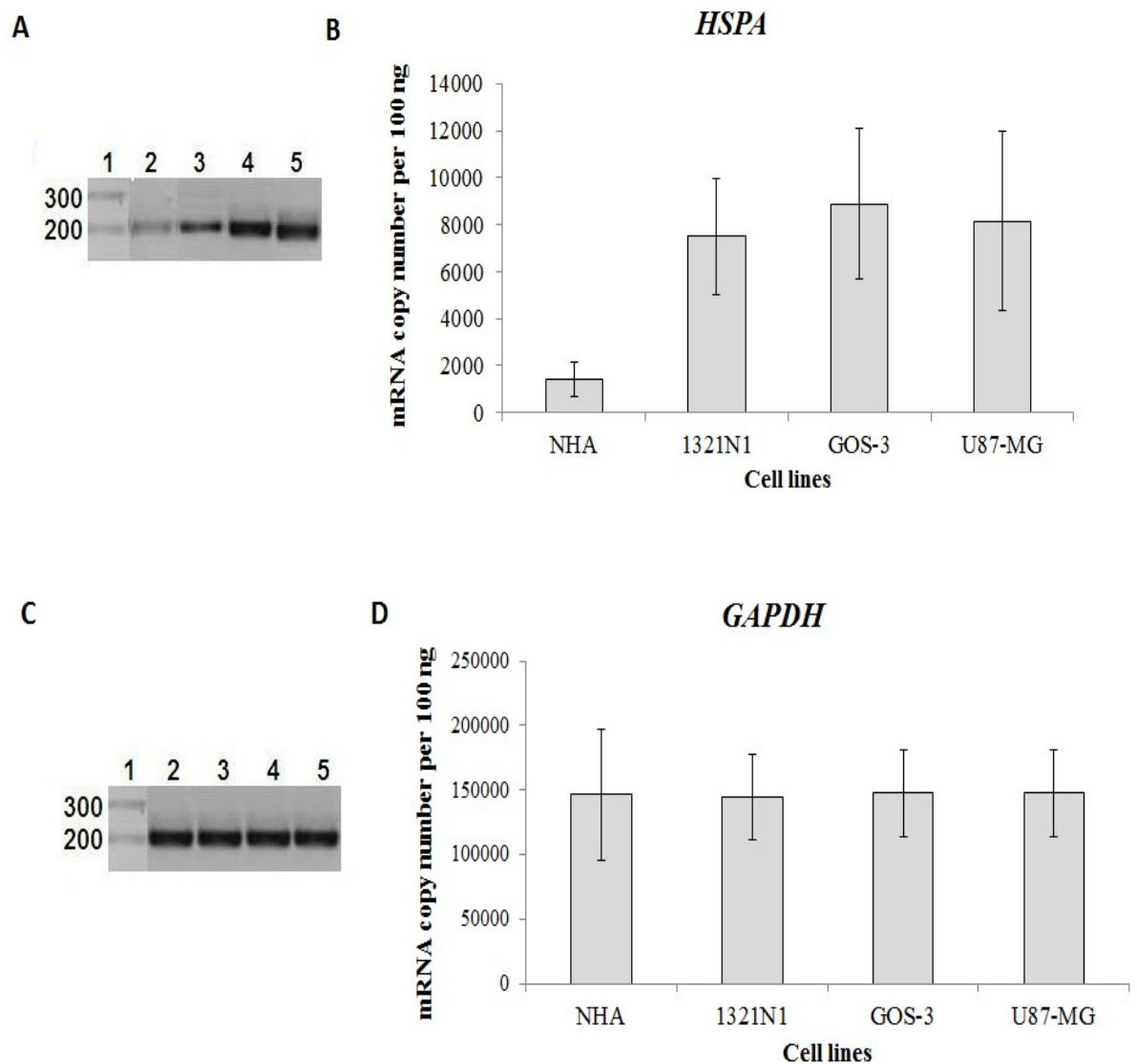


Figure 4.1 *HSPA* and *GAPDH* transcript levels in NHA, 1321N1, GOS-3 and U87-MG cell lines. A (*HSPA*) and C (*GAPDH*), show agarose gel electrophoresis of samples. Lane 1 represents the 100 bp molecular ladder, lanes 2 – 5 represents amplicons from NHA, 1321N1, GOS-3 and U87-MG respectively. B and D histograms represent mRNA copy numbers per 100 ng of extracted mRNA of *HSPA* (B) and *GAPDH* (D) in the same cell lines. Data values are the mean of three independent experiments, and the standard deviation from this mean is shown by the error bars.

4.2.2 Statistical Analysis

A one-way ANOVA test between groups of analysis of variance was conducted to analyse results of the previous experiments of *HSPA* and *GAPDH* gene expression in normal (control) and glioma cell lines in three independent experiments. For this statistical analysis, the cell lines comprised of four groups: group 1 NHA, group 2 1321N1, group 3 GOS-3 and group 4 U87-MG. The means and standard deviations are presented in Table 4.1 (*HSPA*) and Table 4.3 (*GAPDH*).

Table 4.1 Descriptive statistics showing the mean expression levels of *HSPA* for each cell line.

Cell Line	N	Mean <i>HSPA</i> transcript copy number	Std Deviation
NHA	3	1419.63	708.76
1321N1	3	7491.67	2495.20
GOS-3	3	8879.29	3210.83
U87-MG	3	8158.12	3816.44

There was a significant difference in *HSPA* transcript copy number between the four cell line groups [$F(3,8) = 5.157, P = 0.028$]. The effect size, calculated using eta squared indicated a large effect of 0.659.

Table 4.2. Statistical data from Tukey’s HSD test showing significance of *HSPA* gene expression between cell lines. Any significant differences are highlighted in bold.

(I) Cell	J (Cell)	Mean Difference between copy number (I – J)	Std. Error	Sig.
NHA	1321N1	6072.04	2133.21	0.083
NHA	GOS-3	7459.67	2133.21	0.033
NHA	U87-MG	6738.49	2133.21	0.053
1321N1	GOS-3	1387.62	2133.21	0.912
1321N1	U87-MG	666.45	2133.21	0.989
GOS-3	U87-MG	721.17	2133.21	0.986

Post-hoc analyses using Tukey’s HSD test indicated significantly lower *HSPA* gene expression in group 1, NHA than in group 3, GOS-3 (MD = 7459.67, P = 0.033). All other differences between groups failed to reach significance (Table 4.2). Significance \leq 0.05.

Table 4.3 Descriptive statistics showing the mean transcript levels of *GAPDH* in each cell line.

Cell Line	N	Mean <i>GAPDH</i> transcript copy number	Std Deviation
NHA	3	146468.91	50836.00
1321N1	3	144546.62	18955.42
GOS-3	3	147541.72	19549.02
U87-MG	3	147541.72	19549.02

There was no significant difference in *GAPDH* gene expression between the four cell line groups [$F(3,8) = 0.004$, $P > .05$]. The effect size, calculated using eta squared indicated a small effect of 0.001.

Table 4.4. Statistical data from Tukey’s HSD test showing significance of *GAPDH* gene expression between cell lines.

(I) Cell	J (Cell)	Mean Difference between copy number (I – J)	Std. Error	Sig.
NHA	1321N1	1922.29	31504.52	1.000
NHA	GOS-3	1072.82	31504.52	1.000
NHA	U87-MG	1072.82	31504.52	1.000
1321N1	GOS-3	2995.10	31504.52	1.000
1321N1	U87-MG	2995.10	31504.52	1.000
GOS-3	U87-MG	0.00	31504.52	1.000

Post-hoc analyses using Tukey’s HSD test indicated no significant difference in *GAPDH* gene expression between any of the four groups (Table 4.4). Significance \leq 0.05.

4.2.3 Brain Tissue Samples

The expression of *HSPA* and *GAPDH* were analysed in eighteen brain tissue specimens, of which fifteen were glioma tissues and three were normal (control) brain tissue samples. RNA populations were again analysed by RT-PCR, with the mRNA copy number for each gene being calculated for each sample, sections 2.7 and 3.11.

Table 4.5 Tissues used in this study.

	Diagnosis	Grade	Age	Gender	Survival from diagnosis to death
G1	glioblastoma	IV	16	F	(Alive) 13+ months
G2	glioblastoma	IV	23	F	10 months
G3	glioblastoma	IV	38	M	8 months
G4	glioblastoma	IV	38	M	10 months
G5	glioblastoma	IV	46	F	11 months
G6	glioblastoma	IV	60	F	10 months
G7	glioblastoma	IV	62	M	11 months
G8	glioblastoma	IV	63	M	10 months
G9	glioblastoma	IV	64	M	11 months
G10	glioblastoma	IV	67	F	12 months
G11	glioblastoma	IV	68	M	8 months
G12	glioblastoma	IV	28	F	10 months
G13	recurrent anaplastic ependymoma	III	34	F	8 months
G14	anaplastic oligodendroglioma III	III	56	M	11 months
G15	anaplastic oligoastrocytoma III	III	62	F	11 months
G16	normal		39	F	Alive
G17	normal		38	F	Alive
G18	normal		66	M	Alive

The results showed that tissue samples from 8 of the 12 glioblastoma patients showed high levels, (> 2000 copies), of *HSPA* transcripts, with approximate copy numbers per 100 ng of extracted mRNA ranging between 2,100 and 3,300, while the remaining tissue samples from the 4 glioblastoma patients showed lower levels, (< 900 copy numbers), of *HSPA* transcripts, with approximate copy numbers per 100 ng of extracted mRNA ranging between 300 and 870 (Figure 4.2 and Table 4.6). The tissue sample from the ependymoma patient showed high levels of *HSPA* transcripts, approximate copy number per sample, G13 2,000, whilst the tissue samples from the oligodendroglioma III patient, and from the oligoastrocytoma III patient, had low but detectable *HSPA* transcript levels, with approximate copy numbers per 100 ng of extracted mRNA of G14 750 and G15 350 respectively (Figure 4.2 and Table 4.6). The three control samples also showed relatively low or barely detectable levels of *HSPA* transcripts, with approximate copy numbers per 100 ng of extracted mRNA ranging between 100 and 400 (Figure 4.2 and Table 4.6). *HSPA* transcription in glioma samples was independent of age or gender. The mRNA copy numbers of *HSPA* were averaged for the twelve glioblastomas and compared against similar average data from the three low grade gliomas and three control brain tissues samples (Figure 4.4). Significantly higher *HSPA* transcription was observed in the glioblastoma tissues compared to low grade tissue samples, (approximately 1.75-fold higher), and the control tissue samples, (approximately 9-fold higher). Significantly higher *HSPA* transcription was observed in the low grade tissue samples compared to control tissue samples, (approximately 5-fold higher); (Figure 4.4).

As seen in the glioma cell lines, section 4.2.1, more *HSPA* transcripts were observed in the glioma tissues, (approximately 6-fold higher), than in control brain tissue, confirming that *HSPA* expression is consistently up-regulated in some cancer cells. For

GAPDH, mRNA copy numbers per 100 ng of extracted mRNA were relatively consistent in all brain tissue samples, with approximately 143,700 copies per 100 ng of extracted mRNA, giving confidence in the comparability of *HSPA* experiments (Figure 4.3 and Table 4.6).

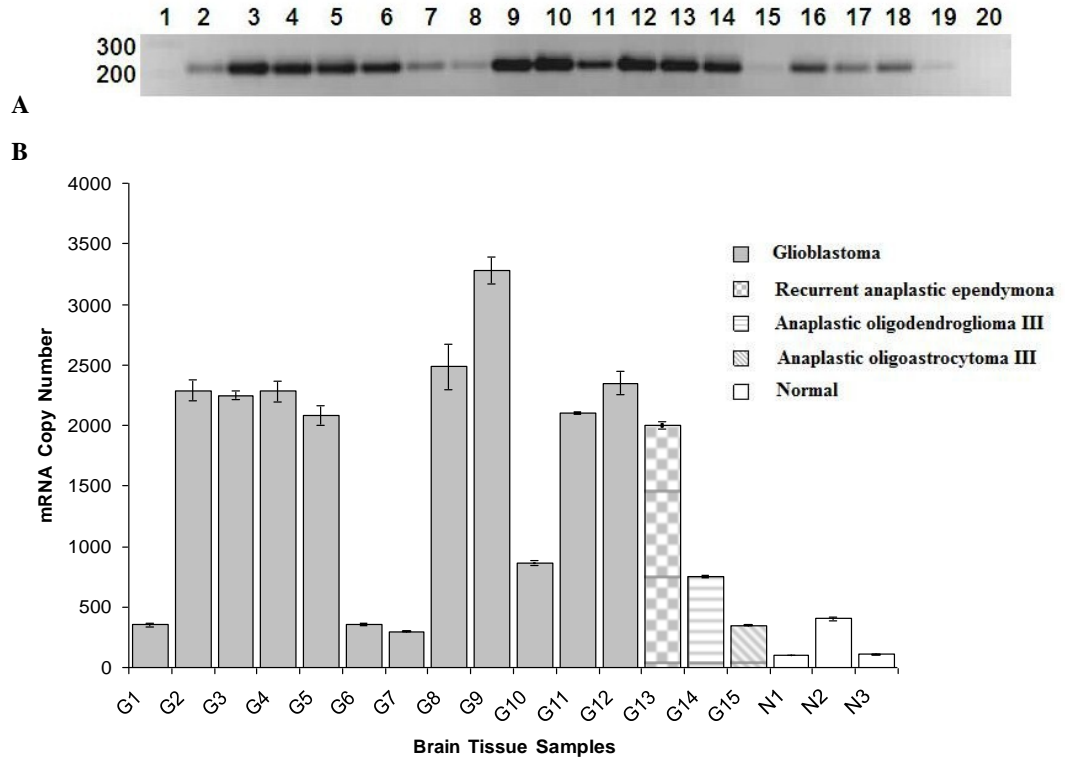


Figure 4.2 *HSPA* mRNA copy number in 18 brain tissue samples. A. Agarose gel electrophoresis: Lane 1 represents the 100 bp molecular ladder; lanes 2 - 13 represent amplicons from glioblastoma tissues; lanes 14 - 16 represent amplicons from ependymoma, oligodendroglioma III and oligoastrocytoma III tissues respectively; lanes 17 - 19 represent amplicons from normal brain tissues and lane 20 is a no template control. B. Histogram representing mRNA copy numbers per 100 ng of extracted mRNA of *HSPA* in tissues. Data values are the mean of three independent experiments, and the standard deviation from this mean is shown by the error bars. G1 - G12 represents the brain tissue of individual patients with glioblastoma, G13 represents the brain tissue from an individual patient with ependymoma, G14 represents the brain tissue from an individual patient with oligodendroglioma III, G15 represents the brain tissue from an individual patient with oligoastrocytoma III and N1 - N3 represents the normal (control) brain tissue from individual .

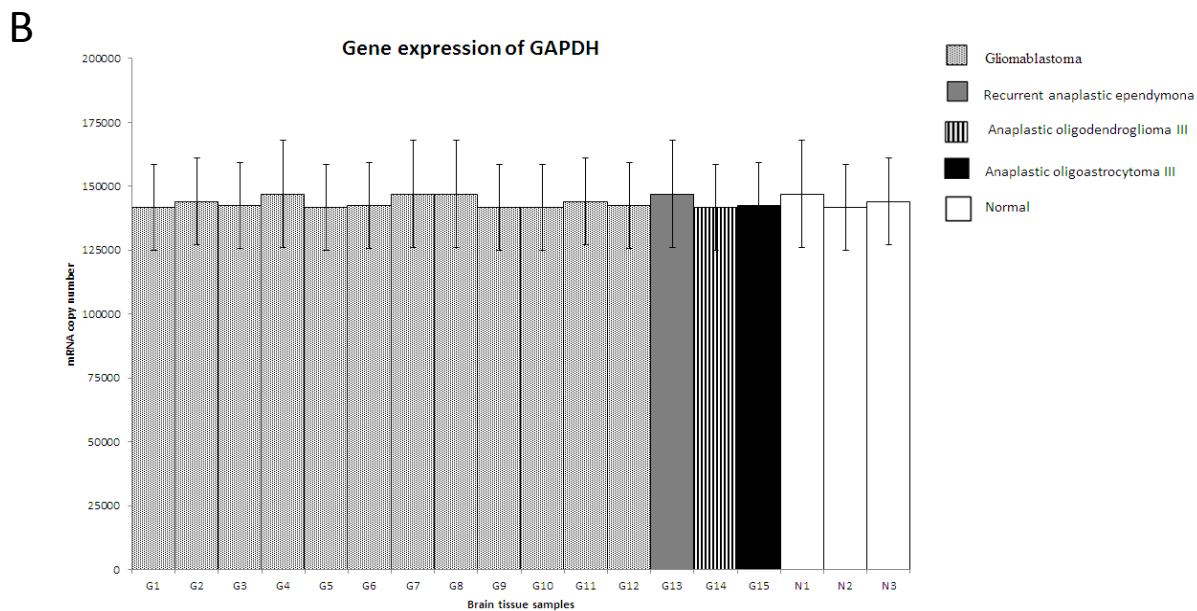
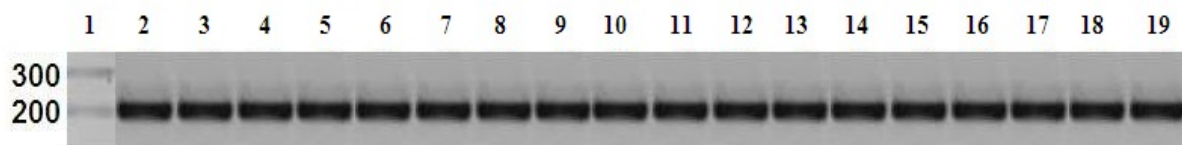


Figure 4.3 *GAPDH* mRNA in 18 brain tissue samples. A. Agarose gel electrophoresis: Lane 1 represents the 100 bp molecular marker; lanes 2 - 13 represent amplicons from glioblastoma tissues; lanes 14 - 16 represent amplicons from ependymoma, oligodendroglioma III and oligoastrocytoma III tissues respectively; lanes 17 - 19 represent amplicons from normal brain tissue. B. Histogram representing mRNA copy numbers per 100 ng of extracted mRNA of *GAPDH* in tissues. Data values are the mean of three independent experiments, and the standard deviation from this mean is shown by the error bars. G1 - G12 represents the brain tissue of individual patients with glioblastoma, G13 represents the brain tissue from an individual patient with ependymoma, G14 represents the brain tissue from an individual patient with oligodendroglioma III, G15 represents the brain tissue from an individual patient with

oligoastrocytoma III and N1 – N3 represents the normal (control) brain tissue from individual .

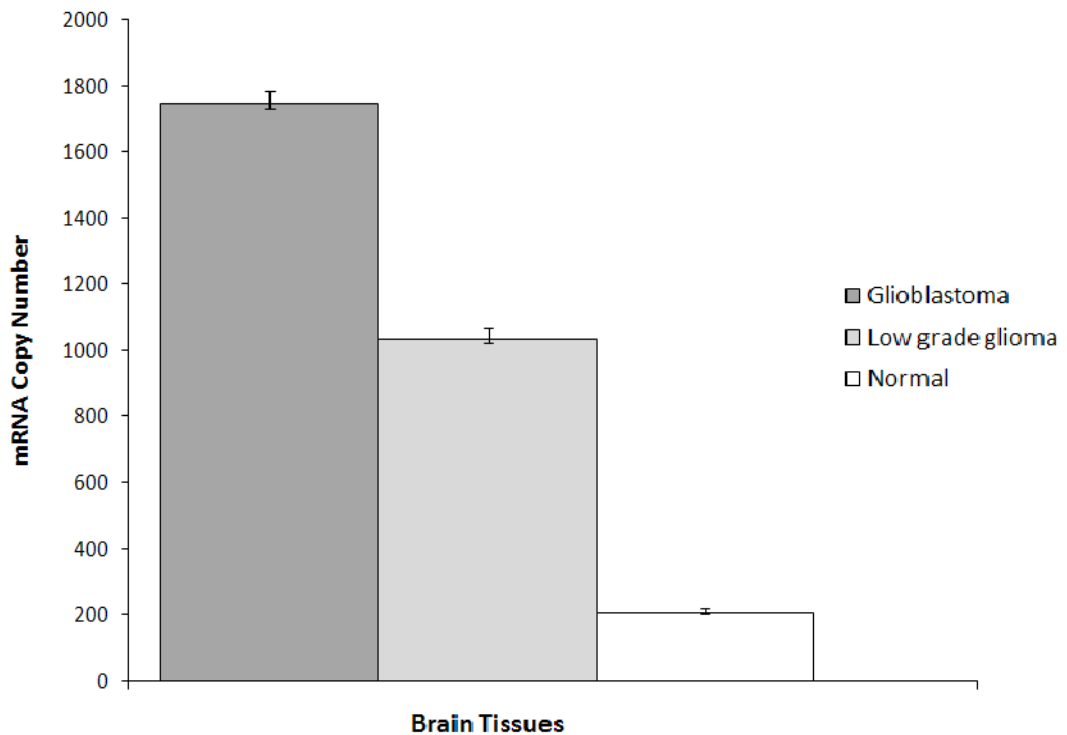


Figure 4.4 Histogram showing the mean *HSPA* mRNA copy numbers in brain tissues grouped by: Glioblastomas (n = 12), low grade gliomas (n = 3) and normal tissues (n = 3). mRNA copy number data from 12 glioblastoma tissues were averaged and compared against the three low grade gliomas and the three normal brain tissues. Data values are the mean of three independent experiments, and the standard deviation from this mean is shown by the error bars.

As can be seen in Figure 4.4 *HSPA* transcripts are approximately 9-fold higher in the glioblastoma tissues compared to the control tissue samples. *HSPA* transcripts are also approximately 5-fold higher in the low grade tissue samples than in control tissue samples.

4.2.4 Statistical Analysis

A one-way ANOVA test between groups of analysis of variance was conducted to analyse results of the previous experiments of *HSPA* and *GAPDH* gene expression in normal (control) and glioma brain tissue in three independent experiments. For this statistical analysis, the brain tissue samples comprised eighteen groups: groups G1 – G12, glioblastomas; group G13, recurrent anaplastic ependymoma; group G14, anaplastic oligodendroglioma III; G15, anaplastic oligoastrocytoma III and groups N1 - N3 normal brain tissue. The means and standard deviations for *HSPA* and *GAPDH* results are presented in Table 4.6.

There was significant differences in *HSPA* transcript copy numbers between the eighteen brain tissue groups [$F(17,36) = 719.138$, $P < 0.001$]. The effect size, calculated using eta squared indicated a large effect of 0.997.

Data obtained from post-hoc analyses using Tukey's HSD test indicated significantly lower *HSPA* transcript copy numbers in G1 than in: G2 (MD = 1935.13, $P < .05$); G3 (MD = 1893.88, $P < .05$); G4 (MD = 1929.31, $P < .05$); G5 (MD = 1729.89, $P < .05$); G8 (MD = 2132.44, $P < .05$); G9 (MD = 2928.44, $P < .05$); G10 (MD = 514.00, $P < .05$); G11 (MD = 1750.16, $P < .05$); G12 (MD = 1994.21, $P < .05$); G13 (MD = 1651.22, $P < .05$); G14 (MD = 397.09, $P < .05$) and N1 (MD = 247.85, $P < .05$) (Table 4.7).

There was significantly lower *HSPA* transcript copy numbers in G2 than in: G6 (MD = 1935.24, $P < .05$); G7 (MD = 1991.97, $P < .05$); G9 (MD = 993.31, $P < .05$); G10 (MD = 1421.12, $P < .05$); G13 (MD = 283.90, $P < .05$), G14 (MD = 1538.03), G15 (MD = 1937.91, $P < .05$); N1 (MD = 2182.97, $P < .05$), N2 (MD = 1883.25, $P < .05$) and N3 (MD = 2180.54, $P < .05$) (Table 4.7).

There was significantly lower *HSPA* transcript copy numbers in G3 than in: G6 (MD = 1893.99, $P < .05$); G7 (MD = 1950.73, $P < .05$); G8 (MD = 238.58, $P < .05$); G9 (MD = 1034.55, $P < .05$); G10 (MD = 1379.88, $P < .05$); G13 (MD = 242.66, $P < .05$); G14 (MD = 1496.79, $P < .05$); G15 (MD = 1896.67, $P < .05$); N1 (MD = 2141.73, $P < .05$); N2 (MD = 1842.01, $P < .05$) and N3 (MD = 2139.30, $P < .05$) (Table 4.7).

There was significantly lower *HSPA* transcript copy numbers in G4 than in: G6 (MD = 1929.42, $P < .05$); G7 (MD = 1986.15, $P < .05$); G9 (MD = 999.13, $P < .05$); G10 (MD = 1415.31, $P < .05$); G13 (MD = 278.09, $P < .05$); G14 (MD = 1532.22, $P < .05$); G15 (MD = 1932.10, $P < .05$); N1 (MD = 2177.16, $P < .05$); N2 (MD = 1877.44, $P < .05$) and N3 (MD = 2174.72, $P < .05$) (Table 4.7).

There was significantly lower *HSPA* transcript copy numbers in G5 than in: G6 (MD = 1730.00, $P < .05$); G7 (MD = 1786.74, $P < .05$); G8 (MD = 402.55, $P < .05$); G9 (MD = 1198.54, $P < .05$); G10 (MD = 1215.89, $P < .05$); G12 (MD = 264.32, $P < .05$); G14 (MD = 1332.80, $P < .05$), G15 (MD = 1732.68, $P < .05$), N1 (MD = 1977.74, $P < .05$), N2 (MD = 1678.02, $P < .05$) and N3 (MD = 1975.31, $P < .05$) (Table 4.7).

There was significantly lower *HSPA* transcript copy numbers in G6 than in: G8 (MD = 2132.55, $P < .05$); G9 (MD = 2928.55, $P < .05$); G10 (MD = 514.11, $P < .05$); G11 (MD = 1750.27, $P < .05$); G12 (MD = 1994.32, $P < .05$); G13 (MD = 1651.33, $P < .05$); G14 (MD = 397.20, $P < .05$); N1 (MD = 247.74, $P < .05$) and N3 (MD = 245.31, $P < .05$) (Table 4.7).

There was significantly lower *HSPA* transcript copy numbers in G7 than in: G8 (MD = 2189.28, $P < .05$); G9 (MD = 2985.28, $P < .05$); G10 (MD = 570.85, $P < .05$); G11 (MD = 1807.00, $P < .05$); G12 (MD = 2051.06, $P < .05$); G13 (MD = 1708.07, $P < .05$) and G14 (MD = 453.94, $P < .05$) (Table 4.7).

There was significantly lower *HSPA* transcript copy numbers in G8 than in: G9 (MD = 796.00, $P < .05$); G10 (MD = 1618.44, $P < .05$); G11 (MD = 382.28, $P < .05$); G13 (MD = 481.22, $P < .05$); G14 (MD = 1735.35, $P < .05$); G15 (MD = 2135.23, $P < .05$); N1 (MD = 2380.29, $P < .05$); N2 (MD = 2080.57, $P < .05$) and N3 (MD = 2377.85, $P < .05$) (Table 4.7).

There was significantly lower *HSPA* transcript copy numbers in G9 than in: G10 (MD = 2414.43, $P < .05$); G11 (MD = 1178.28, $P < .05$); G12 (MD = 934.26, $P < .05$); G13 (MD = 1277.21, $P < .05$); G14 (MD = 2531.24, $P < .05$); G15 (MD = 2931.22, $P < .05$); N1 (MD = 3176.28, $P < .05$); N2 (MD = 2876.56, $P < .05$) and N3 (MD = 3173.85, $P < .05$) (Table 4.7).

There was significantly lower *HSPA* transcript copy numbers in G10 than in: G11 (MD = 1236.16, $P < .05$); G12 (MD = 1480.21, $P < .05$); G13 (MD = 1137.22, $P < .05$); G15 (MD = 526.79, $P < .05$); N1 (MD = 761.85, $P < .05$); N2 (MD = 462.13, $P < .05$) and N3 (MD = 759.41, $P < .05$) (Table 4.7).

There was significantly lower *HSPA* transcript copy numbers in G11 than in: G12 (MD = 244.05, $P < .05$); G14 (MD = 1353.07, $P < .05$); G15 (MD = 1752.95, $P < .05$); N1 (MD = 1998.01, $P < .05$); N2 (MD = 1698.29, $P < .05$) and N3 (MD = 1995.57, $P < .05$) (Table 4.7).

There was significantly lower *HSPA* transcript copy numbers in G12 than in: G13 (MD = 342.99, $P < .05$); G14 (MD = 1597.12, $P < .05$); G15 (MD = 1997.00, $P < .05$); N1 (MD = 2242.06, $P < .05$); N2 (MD = 1942.34, $P < .05$) and N3 (MD = 2239.62, $P < .05$) (Table 4.7).

There was significantly lower *HSPA* transcript copy numbers in G13 than in: G14 (MD = 1254.13, $P < .05$); G15 (MD = 1654.01, $P < .05$); N1 (MD = 1899.07, $P < .05$); N2 (MD = 1599.35, $P < .05$) and N3 (MD = 1896.64, $P < .05$) (Table 4.7).

There was significantly lower *HSPA* transcript copy numbers in G14 than in: G15 (MD = 399.88, $P < .05$); N1 (MD = 644.94, $P < .05$); N2 (MD = 345.22, $P < .05$) and N3 (MD = 642.51, $P < .05$) (Table 4.7).

There was significantly lower *HSPA* transcript copy numbers in G15 than in: N1 (MD = 245.06, $P < .05$) and N3 (MD = 242.63, $P < .05$) (Table 4.7).

There was significantly lower *HSPA* transcript copy numbers in N1 than in N2 (MD = 299.72, $P < .05$) (Table 4.7).

There was significantly lower *HSPA* transcript copy numbers in N2 than in N3 (MD = 297.29, $P < .05$) (Table 4.7).

All other difference between groups failed to reach significance (Table 4.7).

There was a significant difference in *GAPDH* transcript copy numbers between the eighteen brain tissue groups [$F(17,36) = 0.43$, $P = >.05$]. The effect size, calculated using eta squared indicated a small effect of 0.02.

Post-hoc analyses using Tukey's HSD test indicated no significant difference ($P > .05$) in *GAPDH* transcript copy numbers between any of the eighteen groups.

Table 4.6 Descriptive statistics showing the mean transcript copy numbers of *HSPA* and *GAPDH* expression in brain tissue sample.

Tissue sample	N	Mean <i>HSPA</i> gene expression	Std Deviation	Mean <i>GAPDH</i> gene expression	Std Deviation
G1	3	352.86	13.44	141748.41	16746.50
G2	3	2287.99	87.40	143942.85	16976.61
G3	3	2246.74	34.24	142468.77	16727.43
G4	3	2282.17	86.93	146885.07	20948.44
G5	3	2082.76	79.34	141748.41	16746.50
G6	3	352.75	8.06	142468.77	16727.43
G7	3	296.02	4.51	146885.07	20948.44
G8	3	2485.30	189.23	146885.07	20948.44
G9	3	3281.30	112.51	141748.41	16746.50
G10	3	866.86	19.81	141748.41	16746.50
G11	3	2103.02	9.26	143942.85	16976.61
G12	3	2347.07	98.28	142468.77	16727.43
G13	3	2004.08	30.54	146885.07	20948.44
G14	3	749.95	11.43	141748.41	16746.50
G15	3	350.07	8.00	142468.77	16727.43
N1	3	105.01	.800	146885.07	20948.44
N2	3	404.73	15.42	141748.41	16746.50
N3	3	107.45	1.64	143942.85	16976.61

Table 4.7 Statistical data from Tukey's HSD test showing significance of *HSPA* transcript copy numbers between brain tissue sample groups. Any significant differences ($P \leq 0.05$) between groups are highlighted bold.

	G1	G2	G3	G4	G5	G6	G7	G8	G9	G10	G11	G12	G13	G14	G15	N1	N2	N3
G1		M1935.12 Sig .000	M1893.88 Sig .000	M1929.31 Sig .000	M1729.89 Sig .000	M.109 Sig 1.0	M56.84 Sig 1.0	M2132.44 Sig .000	M2928.44 Sig .000	M514.00 Sig .000	M1750.16 Sig .000	M1994.21 Sig .000	M1651.22 Sig .000	M397.09 Sig .000	M2.79 Sig 1.0	M247.85 Sig.008	M51.87 Sig 1.0	M245.41 Sig.009
G2	M1935.12 Sig .000		M41.24 Sig 1.0	M5.82 Sig 1.0	M205.23 Sig .056	M1935.24 Sig .000	M1991.97 Sig .000	M197.31 Sig .078	M993.31 Sig .000	M1421.12 Sig .000	M184.97 Sig .129	M59.08 Sig 1.0	M283.90 Sig .001	M1538.03 Sig .000	M1937.91 Sig .000	M2182.97 Sig .000	M1883.25 Sig .000	M2180.54 Sig .000
G3	M1893.88 Sig .000	M41.24 Sig 1.0		M35.43 Sig 1.0	M163.99 Sig .271	M1893.99 Sig .000	M1950.73 Sig .000	M238.56 Sig .012	M1034.55 Sig .000	M1379.88 Sig .000	M143.72 Sig .483	M100.33 Sig .925	M242.66 Sig .010	M1496.79 Sig .000	M1896.67 Sig .000	M2141.73 Sig .000	M1842.01 Sig .000	M2139.30 Sig .000
G4	M1929.31 Sig .000	M5.82 Sig 1.0	M35.43 Sig 1.0		M199.42 Sig .072	M1929.42 Sig .000	M1986.15 Sig .000	M203.13 Sig .061	M999.13 Sig .000	M1415.31 Sig .000	M179.15 Sig .160	M64.90 Sig .999	M278.09 Sig .002	M1532.22 Sig .000	M1932.10 Sig .000	M2177.16 Sig .000	M1877.44 Sig .000	M2174.72 Sig .000
G5	M1729.89 Sig .000	M205.23 Sig .056	M163.99 Sig .271	M199.42 Sig .072		M1730.00 Sig .000	M1786.74 Sig .000	M402.55 Sig .000	M1198.54 Sig .000	M1215.89 Sig .000	M20.26 Sig 1.0	M264.32 Sig .003	M1378.67 Sig .991	M1332.80 Sig .000	M1732.68 Sig .000	M1977.74 Sig .000	M1678.02 Sig .000	M1975.31 Sig .000
G6	M.109 Sig 1.0	M1935.24 Sig .000	M1893.99 Sig .000	M1929.42 Sig .000	M1730.00 Sig .000		M56.74 Sig 1.0	M2132.55 Sig .000	M2928.55 Sig .000	M514.11 Sig .000	M1750.27 Sig .000	M1994.32 Sig .000	M1651.33 Sig .000	M397.20 Sig .000	M2.68 Sig 1.0	M247.74 Sig .008	M51.98 Sig 1.0	M243.30 Sig .009
G7	M56.84 Sig 1.0	M1991.97 Sig .000	M1950.73 Sig .000	M1986.15 Sig .000	M1786.74 Sig .000	M56.74 Sig 1.0		M2189.28 Sig .000	M2985.28 Sig .000	M570.85 Sig .000	M1807.00 Sig .000	M2051.05 Sig .000	M1708.07 Sig .000	M453.94 Sig .000	M54.06 Sig 1.0	M191.00 Sig .101	M108.72 Sig .868	M188.57 Sig .112
G8	M2132.44 Sig .000	M197.31 Sig .078	M238.56 Sig .012	M203.13 Sig .061	M402.55 Sig .000	M2132.55 Sig .000	M2189.28 Sig .000		M796 Sig .000	M1618.44 Sig .000	M382.28 Sig .000	M138.23 Sig .548	M481.22 Sig .000	M1735.35 Sig .000	M2135.23 Sig .000	M2380.29 Sig .000	M2080.57 Sig .000	M2377.85 Sig .000
G9	M2928.44	M993.31	M1034.55	M999.13	M1198.54	M2928.55	M2985.28	M796		M2414.43	M1178.28	M934.23	M1277.21	M2531.34	M2931.22	M3176.28	M2876.56	M3173.85

	G1	G2	G3	G4	G5	G6	G7	G8	G9	G10	G11	G12	G13	G14	G15	N1	N2	N3
	Sig .000		Sig .000															
G10	M514.00 Sig .000	M1421.12 Sig .000	M1379.88 Sig .000	M1415.31 Sig .000	M1215.89 Sig .000	M514.11 Sig .000	M570.85 Sig .000	M1618.44 Sig .000	M2414.43 Sig .000		M1236.16 Sig .000	M1480.21 Sig .000	M1137.22 Sig .000	M116.91 Sig .794	M516.79 Sig .000	M761.85 Sig .000	M462.13 Sig .000	M759.41 Sig .000
G11	M1750.16 Sig .000	M184.97 Sig .129	M143.72 Sig .483	M179.15 Sig .160	M20.26 Sig 1.0	M1750.27 Sig .000	M1807.00 Sig .000	M382.28 Sig .000	M1178.28 Sig .000	M1236.16 Sig .000		M244.05 Sig .009	M98.93 Sig .932	M1353.07 Sig .000	M1752.94 Sig .000	M1998.01 Sig .000	M1698.29 Sig .000	M1995.57 Sig .000
G12	M1994.21 Sig .000	M59.08 Sig 1.0	M100.33 Sig .925	M64.90 Sig .999	M264.32 Sig .003	M1994.32 Sig .000	M2051.05 Sig .000	M138.23 Sig .548	M934.23 Sig .000	M1480.21 Sig .000	M244.05 Sig .009		M342.99 Sig .000	M1597.12 Sig .000	M1997.00 Sig .000	M2242.06 Sig .000	M1942.34 Sig .000	M2239.62 Sig .000
G13	M1651.22 Sig .000	M283.90 Sig .001	M242.66 Sig .010	M278.09 Sig .002	M78.67 Sig .991	M1651.33 Sig .000	M1708.07 Sig .000	M481.22 Sig .000	M1277.21 Sig .000	M1137.22 Sig .000	M98.93 Sig .932	M342.99 Sig .000		M1254.13 Sig .000	M1654.01 Sig .000	M1899.07 Sig .000	M1599.35 Sig .000	M1896.64 Sig .000
G14	M397.09 Sig .000	M1538.03 Sig .000	M1496.79 Sig .000	M1532.22 Sig .000	M1332.80 Sig .000	M397.20 Sig .000	M453.94 Sig .000	M1735.35 Sig .000	M2531.34 Sig .000	M116.91 Sig .794	M1353.07 Sig .000	M1597.12 Sig .000	M1254.13 Sig .000		M399.88 Sig .000	M644.94 Sig .000	M345.22 Sig .000	M642.51 Sig .000
G15	M2.79 Sig 1.0	M1937.91 Sig .000	M1896.67 Sig .000	M1932.10 Sig .000	M1732.68 Sig .000	M2.68 Sig 1.0	M54.06 Sig 1.0	M2135.23 Sig .000	M2931.22 Sig .000	M516.79 Sig .000	M1752.94 Sig .000	M1997.00 Sig .000	M1654.01 Sig .000	M399.88 Sig .000		M245.06 Sig .009	M54.66 Sig 1.0	M242.63 Sig .010
N1	M247.85 Sig .008	M2182.97 Sig .000	M2141.73 Sig .000	M2177.16 Sig .000	M1977.74 Sig .000	M247.74 Sig .008	M191.00 Sig .101	M2380.29 Sig .000	M3176.28 Sig .000	M761.85 Sig .000	M1998.01 Sig .000	M2242.06 Sig .000	M1899.07 Sig .000	M644.94 Sig .000	M245.06 Sig .009		M299.72 Sig .001	M2.43 Sig 1.0
N2	M51.87 Sig 1.0	M1883.25 Sig .000	M1842.01 Sig .000	M1877.44 Sig .000	M1678.02 Sig .000	M51.98 Sig 1.0	M108.72 Sig .868	M2080.57 Sig .000	M2876.56 Sig .000	M462.13 Sig .000	M1698.29 Sig .000	M1942.34 Sig .000	M1599.35 Sig .000	M345.22 Sig .000	M54.66 Sig 1.0	M299.72 Sig .001		M297.28 Sig .001
N3	M245.41 Sig .009	M2180.54 Sig .000	M2139.30 Sig .000	M2174.72 Sig .000	M1975.31 Sig .000	M245.30 Sig .009	M188.57 Sig .112	M2377.85 Sig .000	M3173.85 Sig .000	M759.41 Sig .000	M1995.57 Sig .000	M2239.62 Sig .000	M1896.64 Sig .000	M642.51 Sig .000	M242.63 Sig .010	M2.43 Sig 1.0	M297.28 Sig .001	

4.3 Immunofluorescence

Under normal conditions HSPA protein in cells is localized in the cytoplasm, however under conditions of stress HSPA migrates to the nucleus. Immunofluorescence detection staining was carried out utilising a monoclonal primary HSPA antibody to identify the presence and localization of HSPA protein in the NHA and the three glioma cells lines, 1321N1, GOS-3 and U87-MG for any comparable differences between normal (unstressed) and cancerous cells (stressed).

Cells cultured on chamber slides were fixed using 4% paraformaldehyde (BDH, UK) for 10 min then incubated with 0.3% Triton X-100 (BDH) in PBS for 7 min after hypoxia treatment. Slides were incubated in blocking solution containing 1% BSA (Sigma,UK) and PBS for 30 min. HSPA1A primary antibody (1:200) (Abcam, UK) was diluted in the blocking solution and applied to the cells for 1 h at room temperature. After three washes in PBS, cells were incubated with light sensitive Anti-Mouse IgG FITC conjugated secondary antibody (1:200) (Sigma, UK) diluted in blocking solution for 1 h at room temperature. All slides were washed three times in PBS and counter stained with VECTASHIELD® (1.5 µg/ml) mounting medium with Propidium iodide (PI; Vector, USA) for 10 min. Cells were visualized and scanned on an Axiovert 200M LSM 510 laser scanning confocal microscope (Carl Zeiss Ltd, UK) as described by Shervington *et al.*, (2009).

HSPA antigens detected using an Anti-mouse IgG FITC conjugated secondary antibody were predominantly identified in both the nucleus and the cytoplasm in the three glioma cell lines; 1321N1, GOS-3 and U87-MG. HSPA protein was detected in the cytoplasm

in the normal astrocyte cell line, NHA, with only limited fluorescence emitted from the nucleus of the cells. (Figures 4.5, 4.6, 4.7 and 4.8).

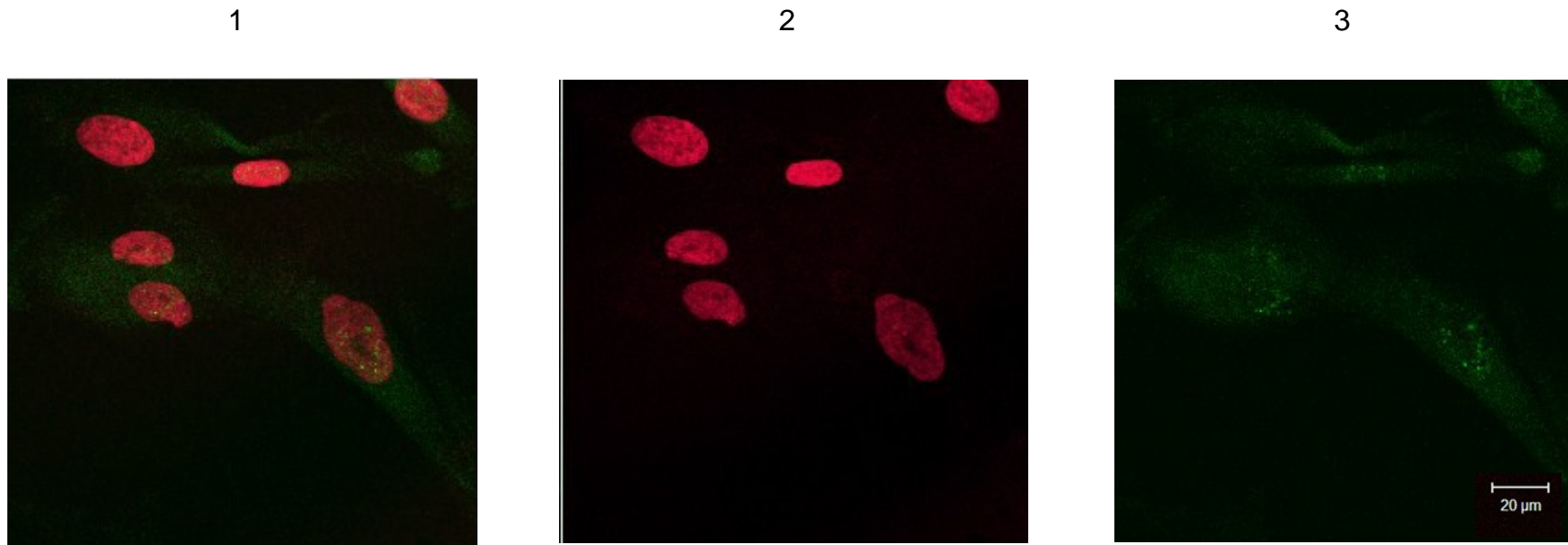


Figure 4.5 HSPA protein levels assessed using immunofluorescence in untreated NHA cells. (1) combined nuclei labelled with propidium iodide (red) and primary antibody HSPA detected with Anti-mouse IgG FITC conjugated secondary antibody (green); (2) nuclei staining labelled with propidium iodide (red) and (3) primary antibody HSPA detected with Anti-mouse IgG FITC conjugated antibody (green). Objective = x 40 magnification. Scale bar = 20μm.

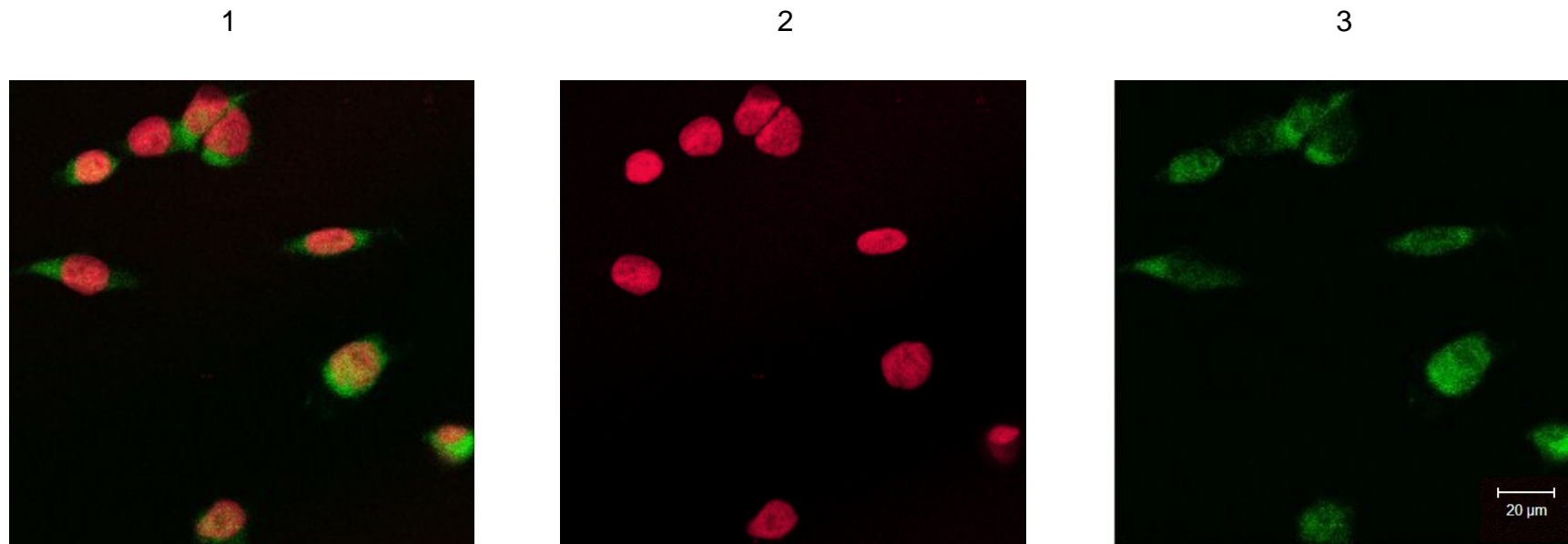


Figure 4.6 HSPA protein levels assessed using immunofluorescence in untreated 1321N1 cells. (1) combined nuclei labelled with propidium iodide (red) and primary antibody HSPA detected with Anti-mouse IgG FITC conjugated secondary antibody (green); (2) nuclei staining labelled with propidium iodide (red) and (3) primary antibody HSPA detected with Anti-mouse IgG FITC conjugated antibody (green). Objective = x 40 magnification. Scale bar = 20μm.

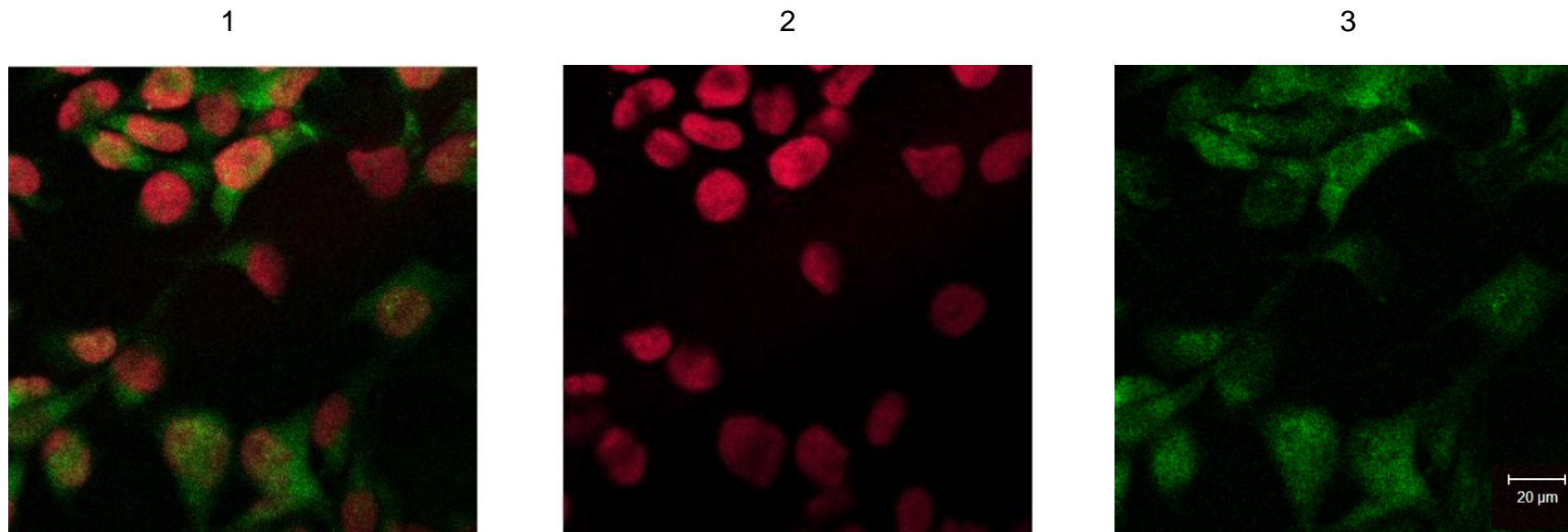


Figure 4.7 HSPA protein levels assessed using immunofluorescence in untreated GOS-3 cells. (1) combined nuclei labelled with propidium iodide (red) and primary antibody HSPA detected with Anti-mouse IgG FITC conjugated secondary antibody (green); (2) nuclei staining labelled with propidium iodide (red) and (3) primary antibody HSPA detected with Anti-mouse IgG FITC conjugated antibody (green). Objective = x 40 magnification. Scale bar = 20μm.

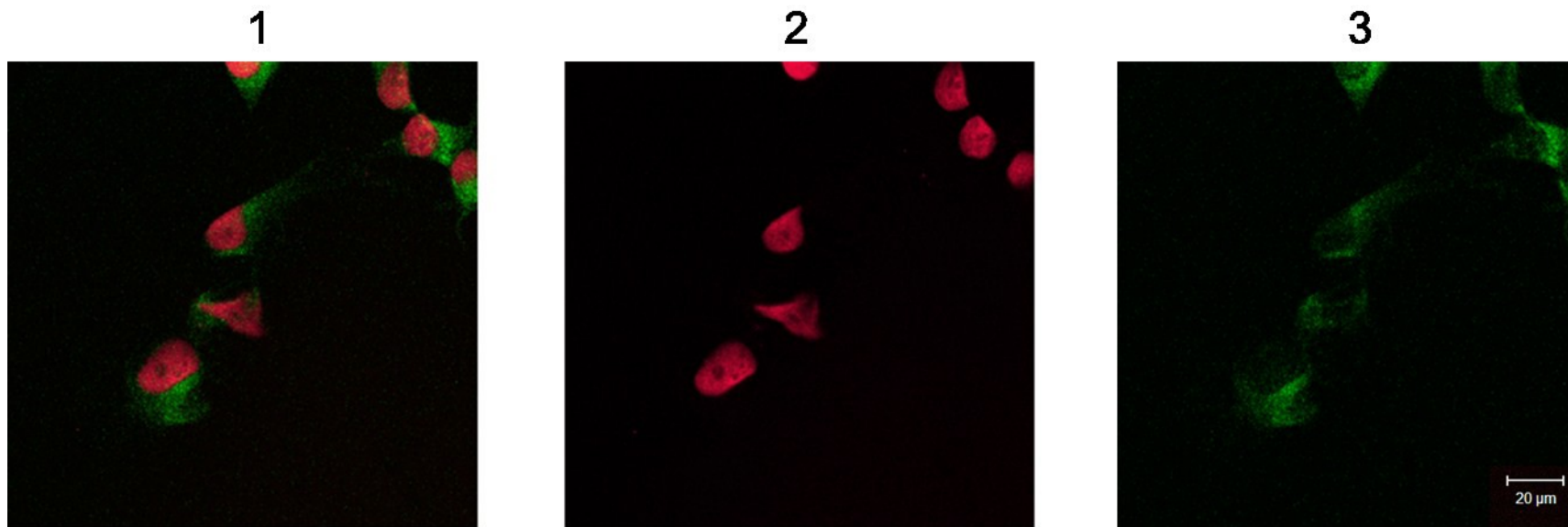


Figure 4.8 HSPA protein levels assessed using immunofluorescence in untreated U87-MG cells. (1) combined nuclei labelled with propidium iodide (red) and primary antibody HSPA detected with Anti-mouse IgG FITC conjugated secondary antibody (green); (2) nuclei staining labelled with propidium iodide (red) and (3) primary antibody HSPA detected with Anti-mouse IgG FITC conjugated antibody (green). Objective = x 40 magnification. Scale bar = 20µm.

4.4 Flow Cytometry

To accurately quantify the presence of HSPA protein, flow cytometry analysis was carried out. The data obtained from flow cytometry was used to produce fluorescence intensity histograms, which depict the distribution of cell surface antigen densities within the population under study, and provide a molecular fingerprint of protein distribution. Comparisons of HSPA protein production were made between the different cell lines.

Flow cytometry involves the use of fluorescent labelled antibodies and fluorescent detectors to analyse large numbers of cells sequentially. Antibodies bind to their respective target molecule or antigen in a one-to-one ratio, such that the number of antibodies bound to a cell and the number of fluorescent molecules present, will in general be proportional to the level of production of that protein on the cell.

Cultured cells were stained and subjected to flow cytometry, briefly 1×10^6 were washed once in 0.1% BSA in PBS before being re-suspended in 0.1% Triton X-100 for 15 min. Following incubation cells were collected and washed once with 0.1% BSA in PBS before being blocked in 5% goat serum in 0.1% BSA in PBS for 30 min. HSPA primary antibody (1:200) diluted in blocking solution was applied for 30 min. Cells were then washed with 0.1% BSA in PBS and light sensitive Anti-Mouse IgG FITC conjugated secondary antibody (1:200) diluted in blocking solution was added for 30 min. Following incubation cells were washed twice in 0.1% BSA in PBS before finally being re-suspended in an aliquot 0.1% BSA in PBS and filtered into FACS tubes. All incubation steps were performed on ice.

As expected, analysis showed high relative fluorescence intensity, with approximately 98% of the 1321N1 cell population showing positive, approximately 89% of GOS-3 cell population showing positive, and 97% of the U87-MG cell population showing positive compared to little or no fluorescence intensity in the NHA cell line, approximately 0.13% showing positive for HSPA. This is taken to indicate that HSPA protein is barely detectable in normal cells, but is present at significantly higher levels in cancer cells; approximately 97-fold higher in 1321N1, 89-fold higher in GOS-3 and 97-fold higher in U87-MG (Figures 4.9, 4.10, 4.11, 4.12 and 4.13).

A

Cell Line	Total % of cells +ve for HSPA
NHA	0
1321N1	97.1
GOS-3	89.2
U87-MG	96.9

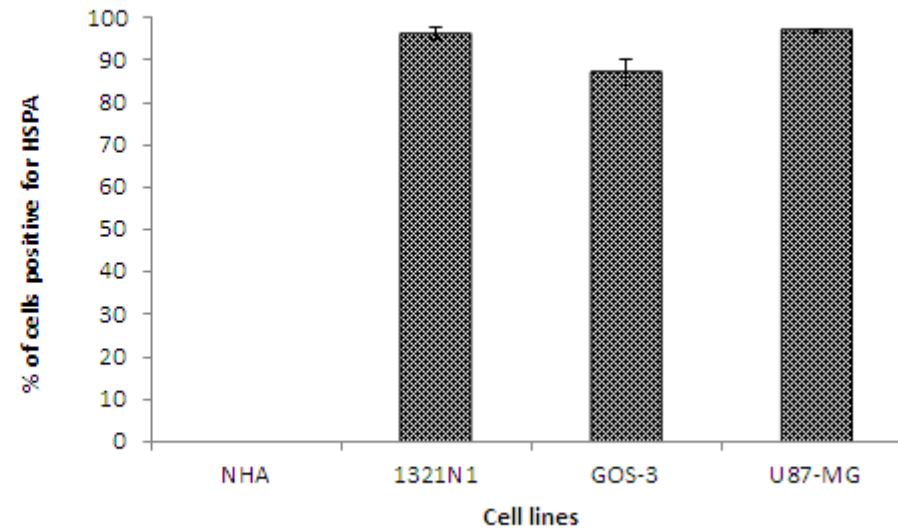
B

Figure 4.9 Average percentages of cells showing positive for HSPA. (A) Average percentage of normal and glioma cells positive for HSPA protein detected by flow cytometry, considering 10,000 events per sample. (B) Histogram showing the mean percentage of cells evaluated by flow cytometry of three independent experiments, and the standard deviation from this mean is shown by the error bars. No column was shown on the histogram for NHA as the value = 0.

4.4.1 Statistical Analysis

A one-way ANOVA test between groups of analysis of variance was conducted to access HSPA protein production in normal and glioma cell lines in three independent experiments. The cell lines comprised of four groups: group 1 NHA, group 2 1321N1, group 3 GOS-3 and group 4 U87-MG. The means and standard deviations are presented in Table 4.8.

Table 4.8 Descriptive statistics showing the mean for HSPA protein levels for each cell line.

Cell Line	N	Mean % of HSPA protein levels	Std Deviation
NHA	3	0.133	0.057
1321N1	3	96.87	0.321
GOS-3	3	89.15	0.050
U87-MG	3	96.85	0.050

There was significant difference in HSPA protein levels for the four cell line groups [$F(3,8) = 239590$, $P < 0.001$]. The effect size, calculated using eta squared indicated a large effect of 0.999.

Table 4.9. Statistical data from Tukey’s HSD test showing significance of HSPA protein levels between cell lines. Any significant differences $P \leq 0.05$ are highlighted in bold.

(I) Cell	J (Cell)	% Mean Difference (I – J)	Std. Error	Sig.
NHA	1321N1	96.73	0.136	0.000
NHA	GOS-3	89.02	0.136	0.000
NHA	U87-MG	96.72	0.136	0.000
1321N1	GOS-3	7.72	0.136	0.000
1321N1	U87-MG	0.0168	0.136	0.999
GOS-3	U87-MG	7.70	0.136	0.000

Post-hoc analyses using Tukey’s HSD test indicated significantly lower HSPA protein levels in group 1, NHA than in: group 2, 1321N1 (MD = 96.73, $P < .05$); group 3, GOS-3 (MD = 89.02, $P < .05$) and group 4, U87-MG (MD = 96.72, $P < .05$) (Table 4.9).

There was a significantly lower HSPA protein levels in group 2, 1321N1 than in group 3, GOS-3 (MD = 7.72, $P < .05$) (Table 4.9).

There was a significantly lower HSPA protein levels in group 3, GOS-3 than in group 4, U87-MG (MD = 7.70, $P < .05$) (Table 4.9).

All other differences between groups failed to reach significance (Table 4.9).

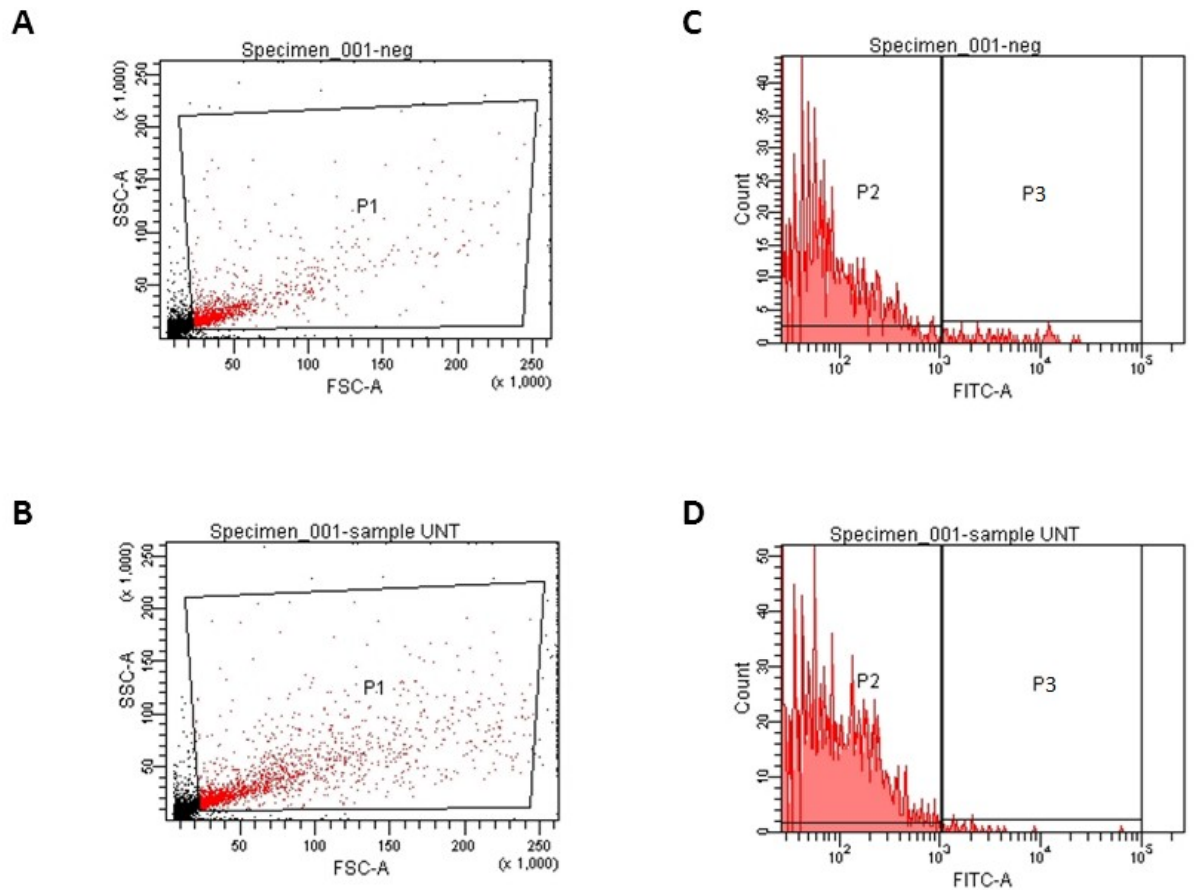


Figure 4.10 2D scatter plots and fluorescence intensity histograms of HSPA protein levels for the NHA cell lines. No fluorescence intensity was observed in the NHA cell line (A, negative, primary antibody omitted and B, sample) 2D scatter plot showing cell population of interest (P1), (C, negative, D, sample) fluorescent intensity histogram showing cells positive (P3) and negative (P2) for HSPA. Data values are for three independent experiments considering 10,000 events per sample.

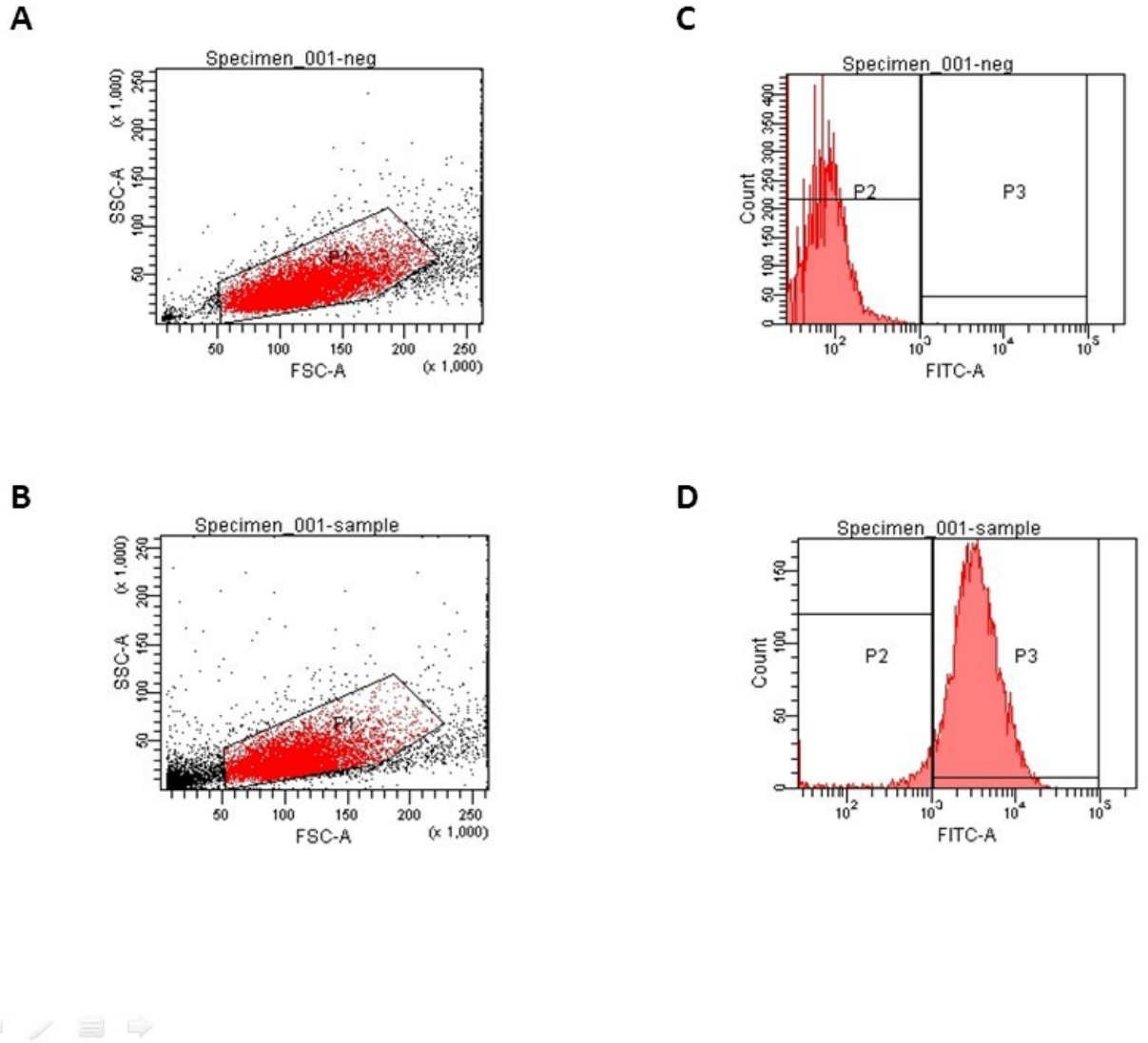


Figure 4.11 2D scatter plots and fluorescence intensity histograms of HSPA protein levels for the 1321N1 cell lines. Approximately 97% of 1321N1 glioma cells showed positive for HSPA. (**A**, negative, primary antibody omitted and **B**, sample) 2D scatter plot showing cell population of interest (P1), (**C**, negative, **D**, sample) fluorescent intensity histogram showing cells positive (P3) and negative (P2) for HSPA. Data values are for three independent experiments considering 10,000 events per sample.

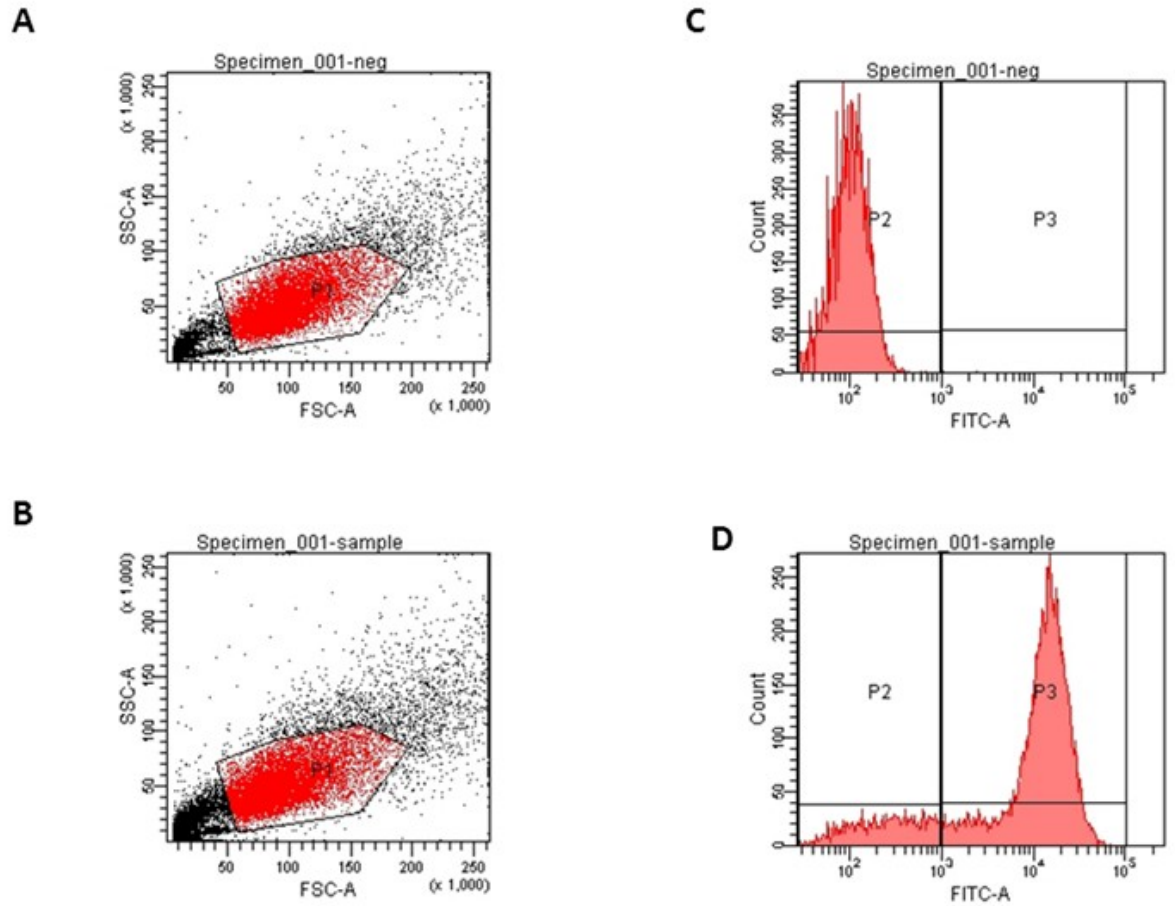


Figure 4.12 2D scatter plots and fluorescence intensity histograms of HSPA protein levels for the GOS-3 cell lines. Approximately 89% of GOS-3 glioma cells showed positive for HSPA. (**A**, negative, primary antibody omitted and **B**, sample) 2D scatter plot showing cell population of interest (P1), (**C**, negative, **D**, sample) fluorescent intensity histogram showing cells positive (P3) and negative (P2) for HSPA. Data values are for three independent experiments considering 10,000 events per sample.

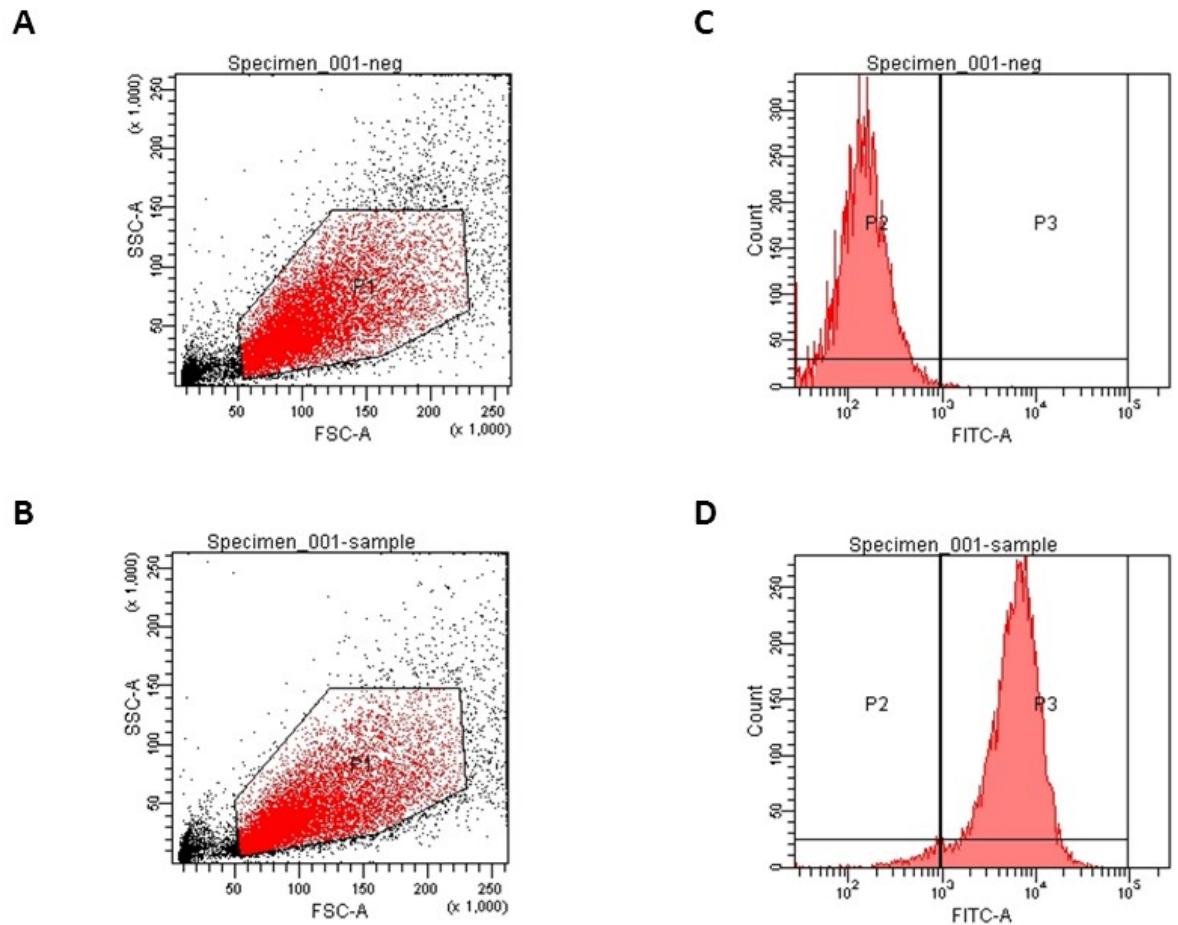


Figure 4.13 2D scatter plots and fluorescence intensity histograms of HSPA protein levels for the U87-MG cell lines. Approximately 97% of U87-MG glioma cells showed positive for HSPA. (A, negative, primary antibody omitted and B, sample) 2D scatter plot showing cell population of interest (P1), (C, negative, D, sample) fluorescent intensity histogram showing cells positive (P3) and negative (P2) for HSPA. Data values are for three independent experiments considering 10,000 events per sample.

Taken together, the results from these experiments show that *HSPA* is expressed at low levels in normal cells and normal brain tissue, but is more highly expressed in cancer cell lines and brain tumours. The average *HSPA* mRNA copy numbers in the three glioma cell lines were approximately 6 fold higher than the normal cell line, and the average *HSPA* mRNA copy numbers in glioblastoma tissue were approximately 1.8 and 9 fold higher than the low grade glioma and normal tissue respectively, suggesting a grade-related transcription profile.

As with *HSPA* mRNA, high levels of HSPA protein were detected in the three glioma cell lines compared to low/barely detectable levels in the NHA cell line, indicating a direct correlation between *HSPA* mRNA and HSPA protein levels in glioma cell lines.

These results suggest that *HSPA* mRNA and HSPA protein levels in glioma may possibly be grade related, and therefore may be useful as a possible prognostic marker.

As expected, given that cancer is a form of cellular stress, HSPA protein was detected in both the cytoplasm and the nucleus of the three glioma cell lines. HSPA protein was detected predominantly in the cytoplasm in the normal astrocyte cell line, NHA with only limited fluorescence emitted from the nucleus of the cells.

Chapter 5

Effects of hypoxia on *HSPA* gene

expression in glioma

5.1 Gene Expression

HSPA expression is up-regulated in cells by cancer and also in response to hypoxia, and the main research aim of this chapter was to measure and compare *HSPA* expression in normal and glioma cell lines under pre- and post-hypoxic conditions, with a view to characterising the expression of *HSPA*. The potential correlation between *HSPA* expression and hypoxia was investigated using three glioma cell lines (1321N1, GOS-3 and U87-MG) and the normal human astrocyte cell line (NHA). Expression of *HSPA* was compared between the three glioma cell lines (1321N1, GOS-3 and U87-MG) and with a normal (control) human astrocyte cell line (NHA), under pre- and post-hypoxia conditions. *GAPDH*, was used as an internal standard throughout all RT-PCR experiments (Barber *et al*, 2005).

Human brain cell lines GOS-3 (grade II/III oligodendroglioma) from DMSZ (Germany), U87-MG (grade IV glioblastoma) from ECCAC (UK) and NHA (normal human astrocytes) from Lonza (UK) were used in this study. GOS-3 cells were routinely cultured in Dulbecco's modified Eagle's medium (DMEM) (Sigma) supplemented with 10% FBS and with 4 mM L-glutamide, while U87-MG cells were cultured in Eagle's minimum essential medium (EMEM) (Sigma) supplemented with 2 mM L-glutamide, 10% FBS and 1% (v/v) nonessential amino acids (Sigma). The NHA cells were cultured in astrocyte medium (AM) supplemented with 15 ml of FBS, 0.5 ml Ascorbic Acid, 0.5 ml rhEGF (astrocyte growth supplement) 0.5 ml GA100 1.25 ml Insulin and 5 ml L-glutamide.

Hypoxic conditions were induced by exposing confluent cells to nitrogen (100 %) for 30 min (Kay *et al*, 2007). After treatment, the cells were collected at various recovery

periods (0, 3, 6 and 24 h) for experiments concerning gene expression, immunofluorescence and flow cytometry.

mRNA was isolated from all four cell lines, using mRNA Isolation Kit (Roche,UK) following the manufacturer's protocol. The concentration and purity of mRNA was determined by ultraviolet spectrophotometry. Isolated mRNA (100 ng) was transcribed to cDNA using 1st Strand cDNA Synthesis Kit for RT-PCR (AMV) (Roche, UK) following the manufacturer's protocol, which was then used as a template for qRT-PCR. Quantitative real-time PCR was used to evaluate the expression of *HSPA* and *GAPDH* as a control using FastStart DNA Master^{PLUS} SYBR Green 1 (Roche, UK).

Primers used for *HSPA* were 5' CGACCTGAACAAGAGCATCA 3' (sense) and 5' AAGATCTGCGTCTGCTTGGT 3' (antisense). For *GAPDH*, primers were 5' GAGTCAAGCGATTTGGTCGT 3' (sense) and 5' TTGATTTTGGAGGGATCTCG 3' (antisense). All primers were designed using Primer3 software and manufactured by TIB MOLBIOL.

After an initial denaturation at 95°C for 10 min, the samples were subjected to 35 cycles of RT-PCR 95°C for 10 s, annealing temperature 57°C (*HSPA*) and 56°C (*GAPDH*) for 15 s, and 72°C for 15 s (Patel *et al.*, 2008). At the end of each cycle, the fluorescence emitted was measured in a single step in channel F1 (gain1). After the 35th cycle, the specimens were heated to 95°C and rapidly cooled to 65°C for 15 s. All heating and cooling steps were performed with a slope of 20°C / s. The temperature was subsequently raised to 95°C with a slope of 0.1°C / s and fluorescence was measured continuously (channel F1, gain1) to obtain data for the melting curve analysis. All PCR reactions were performed in triplicate and a negative control included, which contained primers with no DNA. All PCR products were analysed using gel electrophoresis stained and visualised using a gel analyser (SynGene, UK).

5.2 Constitutive Expression

5.2.1 Glioma Cell lines

Transcript copy numbers of *HSPA* and *GAPDH* were determined using RT-PCR for three glioma cell lines; 1321N1, GOS-3 and U87-MG and in the normal human astrocyte cell line NHA, under pre- and post-hypoxia treatment. The primers and optimal temperatures used for the amplification of both genes are documented in Table 2.10 in section 2.5. All PCR experiments were carried out in triplicate for consistency and repeatability. For each gene analysed, a quantification graph was produced to confirm gene amplification. The resulting amplicons for *HSPA* and *GAPDH* were then visualized using agarose gel electrophoresis, each being represented by bands of 213 and 238 bp respectively.

The mRNA copy number per 100 ng of extracted mRNA for both genes was calculated for each cell line. High levels of *HSPA* mRNA expression were observed in 1321N1, GOS-3 and U87-MG glioma cell lines pre-hypoxia treatment, with approximate copy numbers of each of 7,500, 8,900, 8,200 respectively and post-hypoxia treatment after 0 h recovery, with approximate copy numbers of each of 8,200, 7,300, 8,100 respectively; after 3 h recovery, with approximate copy numbers of each of 8100, 7,500, 7,800 respectively; after 6 h recovery, with approximate copy numbers of each of 8,100, 7,500, 8,200 respectively and after 24 h recovery, with approximate copy numbers of each of 7,800, 7,800, 8,200 respectively (Figure 5.1 and Table 5.1). In contrast, the normal human astrocyte cell line showed low but detectable levels of *HSPA* mRNA in pre hypoxia treatment, with an approximate copy number of 1,400 and slightly raised levels of *HSPA* mRNA in post hypoxia treatment after 0 h recovery, with an approximate copy number of 2,500, after 3 h recovery, with an approximate copy

number of 1,100, after 6 h recovery, with an approximate copy number of 590 and after 24 h recovery, with an approximate copy number of 350 (Figure 5.1 and Table 5.1).

For *GAPDH*, mRNA copy numbers per 100 ng of extracted mRNA were relatively consistent for NHA, with approximate copy numbers of 148,300, for 1321N1, with approximate copy numbers of 147,400, for GOS-3, with approximate copy numbers of 147,400 and for U87-MG, with approximate copy numbers of 147,300, again confirming comparability of HSPA results (Figure 5.2 and Table 5.1).

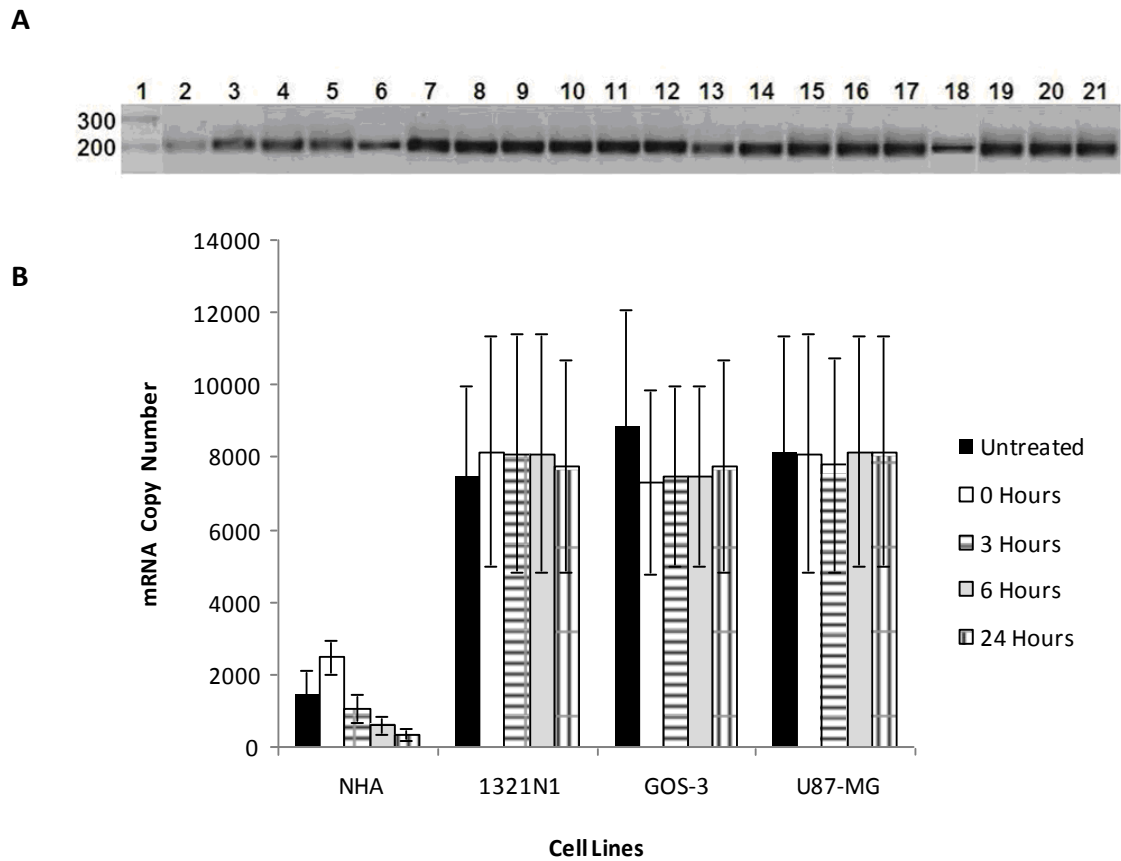


Figure 5.1 Levels of *HSPA* mRNA transcripts in pre- and post-hypoxia treated NHA, 1321N1, GOS-3 and U87-MG cells. (A) agarose gel electrophoresis: Lane 1 represents the 100 bp molecular ladder; lanes 2 - 6 represent amplicons from NHA: pre-hypoxia, post-hypoxia after 0, 3, 6 and 24 h recovery, lanes 7 - 11 represent amplicons from 1321N1: pre-hypoxia, post-hypoxia after 0, 3, 6 and 24 h recovery, lanes 12 - 16 represent amplicons from GOS-3: pre-hypoxia, post-hypoxia after 0, 3, 6 and 24 h recovery and lanes 17 - 21 represent amplicons from U87-MG: pre-hypoxia, post-hypoxia after 0, 3, 6 and 24 h recovery. (B) Histogram showing *HSPA* mRNA copy numbers per 100 ng of extracted mRNA for pre and post hypoxia 0, 3, 6 and 24 h treated cell lines. Data values are the mean of three independent experiments, and the standard deviation from this mean is shown by the error bars.

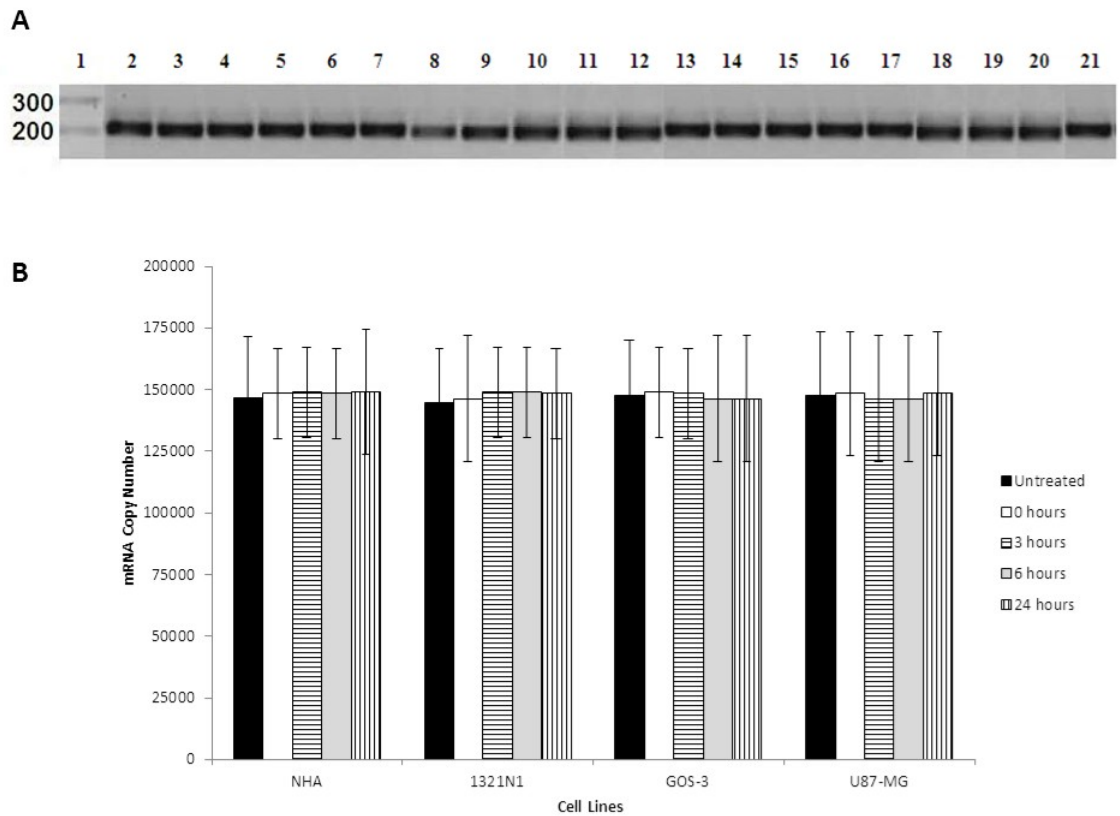


Figure 5.2 Levels of *GAPDH* mRNA transcripts in pre and post hypoxia treated NHA, 1321N1, GOS-3 and U87-MG cells. (A) agarose gel electrophoresis: Lane 1 represents the 100 bp molecular ladder; lanes 2 - 6 represent amplicons from NHA: pre-hypoxia, post-hypoxia after 0, 3, 6 and 24 h recovery, lanes 7 - 11 represent amplicons from 1321N1: pre-hypoxia, post-hypoxia after 0, 3, 6 and 24 h recovery, lanes 12 - 16 represent amplicons from GOS-3: pre-hypoxia, post-hypoxia after 0, 3, 6 and 24 h recovery and lanes 17 - 21 represent amplicons from U87-MG: pre-hypoxia, post-hypoxia after 0, 3, 6 and 24 h recovery. (B) Histogram showing *HSPA* mRNA copy numbers per 100 ng of extracted mRNA for pre and post hypoxia 0, 3, 6 and 24 h, treated cell lines. Data values are the mean of three independent experiments, and the standard deviation from this mean is shown by the error bars.

5.2.2 Statistical Analysis

A two-way factorial mixed 4 (cell line: NHA, 1321N1, GOS-3, U87-MG) x 5 (treatment: untreated, 0, 3, 6 and 24 h recovery after hypoxia treatment) ANOVA analysis of variance test was performed to investigate differences of *HSPA* and *GAPDH* gene expression. The means and standard deviation are presented in Table 5.1.

For *HSPA* gene expression there was a non-significant effect for: cell line [F(15,11.44) = .832, P = 0.637]; Wilks' Lambda = 0.131; partial eta squared = 0.493 and treatment [F(4,5) = 1.692; P = 0.287], Wilks' Lambda = 0.425, partial eta squared = 0.575. The interaction between treatment and cell line also failed to reach significance [F(12,13.52) = 1.0; P = 0.496], Wilks' Lambda = 0.186, partial eta squared = 0.429.

There was a statistically significant main effect in *HSPA* transcript copy numbers for cell lines on the combined variables: [F(3,8) = 6.544, P = .015]; partial eta squared (η_p^2) = 0.710.

When the results for the dependent variables were considered separately, there was a statistical significance in untreated [F(3,8) = 5.157, P = .028]; partial eta squared (η_p^2) = 0.659.

Post-hoc analyses using Tukey's HSD test indicated significantly lower *HSPA* transcript copy numbers in untreated NHA than in untreated, GOS-3 (MD = 7459.67, P = 0.033). All other differences between groups failed to reach significance (Table 5.2).

There was a non statistical significance after 0 h recovery [F(3,8) = 3.187, P = .084]; partial eta squared (η_p^2) = 0.544. Posthoc analyses using Tukey's HSD indicated that all differences between groups failed to reach significance (Table 5.2)

There was a statistical significance after 3 h recovery [F(3,8) = 5.260, P = .027]; partial eta squared (η_p^2) = 0.664. Posthoc analyses using Tukey's HSD indicated significantly

lower *HSPA* transcript copy numbers after 3 h recovery in NHA than in: 1321N1 (MD 7042.05, $P < .05$) and U87-MG (MD = 6730.03, $P < .05$). All other differences between groups failed to reach significance (Table 5.2).

There was a statistical significance after 6 h recovery [$F(3,8) = 5.910$, $P = .020$]; partial eta squared (η_p^2) = 0.689. Posthoc analyses using Tukey's HSD indicated significantly lower *HSPA* transcript copy numbers after 6 h recovery in NHA than in: 1321N1 (MD 7510.99, $P < .05$); GOS-3 (MD = 6901.49, $P < .05$) and U87-MG (MD = 7567.85, $P < .05$). All other differences between groups failed to reach significance (Table 5.2).

There was a statistical significance after 24 h recovery [$F(3,8) = 6.232$, $P = .017$]; partial eta squared (η_p^2) = 0.700.

Posthoc analyses using Tukey's HSD indicated significantly lower *HSPA* transcript copy numbers after 24 h recovery in NHA than in: 1321N1 (MD 7414.30, $P < .05$); GOS-3 (MD = 7414.30, $P < .05$) and U87-MG (MD = 7807.93, $P < .05$). All other differences between groups failed to reach significance (Table 5.2).

For *GAPDH* transcript copy numbers, there was a non significant effect for: cell line [$F(15,11.44) = 0.005$, $P > .05$]; Wilks' Lambda = 0.980, partial eta squared = 0.007 and treatment [$F(4,5) = .003$; $P > .05$], Wilks' Lambda = 0.998, partial eta squared = 0.002. The interaction between treatment and cell line also failed to reach significance [$F(12,13.52) = .007$; $P > .05$], Wilks' Lambda = .983, partial eta squared = 0.006.

There was a non significant main effect in *GAPDH* gene expression for cell lines on the combined variables: [$F(3,8) = .001$, $P > .05$]; partial eta squared (η_p^2) = 0.000.

When the results for the dependent variables were considered separately, there was a non statistical significance in untreated [$F(3,8) = .004$, $P > .05$]; partial eta squared (η_p^2)

= 0.002. Posthoc analyses using Tukey's HSD indicated that all differences between groups failed to reach significance.

There was a non statistical significance after 0 h recovery [$F(3,8) = .005$, $P > .05$]; partial eta squared (η_p^2) = 0.002. Posthoc analyses using Tukey's HSD indicated that all differences between groups failed to reach significance.

There was a non statistical significance after 3 h recovery [$F(3,8) = .004$, $P > .05$]; partial eta squared (η_p^2) = 0.002. Posthoc analyses using Tukey's HSD indicated that all differences between groups failed to reach significance.

There was a non statistical significance after 6 h recovery [$F(3,8) = .007$, $P > .05$]; partial eta squared (η_p^2) = 0.003. Posthoc analyses using Tukey's HSD indicated that all differences between groups failed to reach significance.

There was a non statistical significance after 24 h recovery [$F(3,8) = .005$, $P > .05$]; partial eta squared (η_p^2) = 0.002. Posthoc analyses using Tukey's HSD indicated that all differences between groups failed to reach significance.

Table 5.1. Descriptive statistics showing the mean mRNA copy numbers for *HSPA* and *GAPDH* gene expression for untreated and treated cell lines.

Treatment	Cell Line	N	Mean <i>HSPA</i> transcript copy number	STD. Dev.	Mean <i>GAPDH</i> Transcript copy number	STD. Dev.
Pre-hypoxia	NHA	3	1419.63	708.76	146468.91	50836.00
	1321N1	3	7491.67	2495.20	144546.62	32831.75
	GOS-3	3	8879.29	3210.84	147541.72	33859.90
	U87-MG	3	8158.12	3204.01	147541.72	33859.90
0 h recovery after hypoxia treatment	NHA	3	2463.77	488.26	148473.30	18197.56
	1321N1	3	8158.12	3204.01	146112.84	25188.06
	GOS-3	3	7286.28	2548.80	148927.19	46355.40
	U87-MG	3	8101.26	3299.79	148439.75	24974.58
3 h recovery after hypoxia treatment	NHA	3	1059.21	401.35	148927.19	46355.40
	1321N1	3	8101.26	3299.79	148927.19	46355.40
	GOS-3	3	7491.67	2495.20	148473.30	18197.56
	U87-MG	3	7789.23	2955.70	146112.84	25188.06
6 h recovery after hypoxia treatment	NHA	3	590.27	233.87	148473.30	18197.56
	1321N1	3	8101.26	3299.79	148927.19	46355.40
	GOS-3	3	7491.67	2495.20	146112.84	25188.06
	U87-MG	3	8158.12	3204.01	146112.84	25188.04
24 h recovery after hypoxia treatment	NHA	3	350.19	167.09	148927.19	46355.40
	1321N1	3	7764.50	2930.96	148473.30	18197.56
	GOS-3	3	7764.50	2930.96	146112.84	25188.06
	U87-MG	3	8158.12	3204.01	148439.75	24974.58

Overall inspection of the mean scores for *HSPA* transcript copy numbers indicated that untreated and treated 1321N1; GOS-3 and U87-MG cell lines were considerably higher than the NHA cell line.

Overall inspection of the mean scores for *GAPDH* transcript copy numbers indicated no significant differences in untreated and treated NHA, 1321N1, GOS-3 and U87-MG cell lines.

Table 5.2. Statistical data from Tukey’s HSD test showing significance of *HSPA* transcript copy numbers in treated and untreated cell lines. Any significant differences are highlighted in bold. Significance ≤ 0.05 .

Treatment	Cell Line	NHA		1321N1		GOS-3		U87-MG	
		Mean Diff \pm STD error	SIG.						
Pre-hypoxia	NHA			6072.04 \pm 2311.21	.083	7459.67 \pm 2133.21	.033	6738.49 \pm 2133.21	.053
	1321N1	6072.04 \pm 2133.21	.083			1387.62 \pm 2311.21	.912	666.45 \pm 2311.21	.989
	GOS-3	7459.67 \pm 2133.21	.033	1387.62 \pm 2311.21	.912			721.17 \pm 2311.21	.986
	U87-MG	6738.49 \pm 2133.21	.053	666.45 \pm 2311.21	.989	721.17 \pm 2311.21	.986		
0 h recovery after hypoxia treatment	NHA			5694.35 \pm 2155.96	.110	4822.51 \pm 2155.96	.193	5637.49 \pm 2155.96	.114
	1321N1	5694.35 \pm 2155.96	.110			871.84 \pm 2155.96	.976	56.86 \pm 2155.96	1.000
	GOS-3	4822.51 \pm 2155.96	.193	871.84 \pm 2155.96	.976			814.98 \pm 2155.96	.980
	U87-MG	5637.49 \pm 2155.96	.114	56.86 \pm 2155.96	1.000	814.98 \pm 2155.96	.980		
3 h recovery after hypoxia treatment	NHA			7042.05 \pm 2082.14	.039	6432.46 \pm 2082.14	.059	6730.03 \pm 2082.14	.048
	1321N1	7042.05 \pm 2082.14	.039			609.59 \pm 2082.14	.991	312.02 \pm 2082.14	.999
	GOS-3	6432.46 \pm 2082.14	.059	609.59 \pm 2082.14	.991			297.57 \pm 2082.14	.999
	U87-MG	6730.03 \pm 2082.14	.048	312.02 \pm 2082.14	.999	297.57 \pm 2082.14	.999		
6 h recovery after hypoxia treatment	NHA			7510.99 \pm 2138.34	.032	6901.40 \pm 2138.34	.048	7567.85 \pm 2138.34	.031
	1321N1	7510.99 \pm 2138.34	.032			609.59 \pm 2138.34	.991	56.86 \pm 2138.34	1.000
	GOS-3	6901.40 \pm 2138.34	.048	609.59 \pm 2138.34	.991			666.45 \pm 2138.34	.989
	U87-MG	7567.85 \pm 2138.34	.031	56.86 \pm 2138.34	1.000	666.45 \pm 2138.34	.989		
24 h recovery after hypoxia treatment	NHA			7414.30 \pm 2139.86	.035	7414.30 \pm 2139.86	.035	7807.93 \pm 2139.86	.027
	1321N1	7414.30 \pm 2139.86	.035			0.0 \pm 2139.86	1.000	393.62 \pm 2139.86	.998
	GOS-3	7414.30 \pm 2139.86	.035	1.0 \pm 2139.86	1.000			393.62 \pm 2139.86	.998
	U87-MG	7807.93 \pm 2139.86	.027	393.62 \pm 2139.86	.998	393.62 \pm 2139.86	.998		

5.3 Immunofluorescence

Under normal conditions HSPA protein in cells is localized in the cytoplasm, however under conditions of stress HSPA migrates to the nucleus. Immunofluorescence detection staining was carried out utilising a monoclonal primary HSPA antibody to identify the presence and localization of HSPA protein in the NHA and the three glioma cells lines, 1321N1, GOS-3 and U87-MG for any comparable differences between normal (unstressed) and cancerous cells (stressed) under pre and post hypoxic conditions.

Cells cultured on chamber slides were fixed using 4% paraformaldehyde (BDH, UK) for 10 min then incubated with 0.3% Triton X-100 (BDH) in PBS for 7 min after hypoxia treatment. Slides were incubated in blocking solution containing 1% BSA (Sigma,UK) and PBS for 30 min. HSPA primary antibody (1:200) (Abcam, UK) was diluted in the blocking solution and applied to the cells for 1 h at room temperature. After three washes in PBS, cells were incubated with light sensitive Anti-Mouse IgG FITC conjugated secondary antibody (1:200) (Sigma, UK) diluted in blocking solution for 1 h at room temperature. All slides were washed three times in PBS and counter stained with VECTASHIELD® (1.5 µg/ml) mounting medium with Propidium iodide (PI; Vector, USA) for 10 min. Cells were visualized and scanned on an Axiovert 200M LSM 510 laser scanning confocal microscope (Carl Zeiss Ltd, UK) as described by Shervington *et al.*, (2009).

HSPA antigens detected using an Anti-mouse IgG FITC conjugated secondary antibody were identified, pre- and post-hypoxic treatment, in both the nucleus and the cytoplasm of the three glioma cell lines; 1321N1 (Figures 5.7 – 5.14), GOS-3 (Figures 5.15 – 5.20) and U87-MG (Figures 5.21 – 5.26). As with mRNA expression in the three glioma cell

lines, HSPA protein was detected pre-and post-hypoxia treatment in both the cytoplasm and the nucleus.

HSPA protein was detected in the cytoplasm in the normal astrocyte cell line, NHA with only limited fluorescence emitted from the nucleus of the cells. However, post-hypoxia, fluorescence was observed in both the cytoplasm and the nucleus (Figures 5.3 – 5.8). HSPA protein had migrated into the nucleus during hypoxia treatment, which correlates with the increased *HSPA* transcript levels, as shown in Figure 5.1.

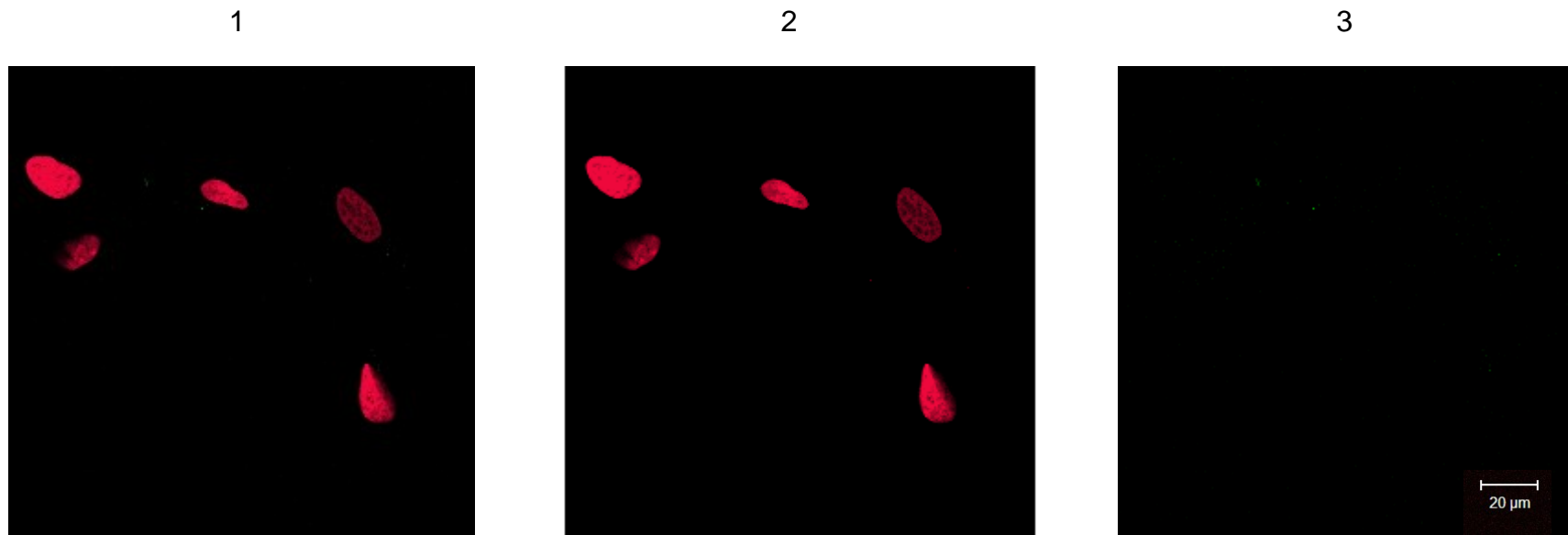


Figure 5.3 HSPA protein levels assessed using immunofluorescence for negative control of un-treated NHA cells. (1) Negative control whereby primary antibody HSPA has been omitted, Anti-mouse IgG FITC conjugated secondary antibody (green), no staining, nuclei labelled with propidium iodide (red); (2) nuclei staining labelled with propidium iodide (red) and (3) Anti-mouse IgG FITC conjugated secondary antibody (green), no staining. Objective = x 40 magnification. Scale bar = 20µm.

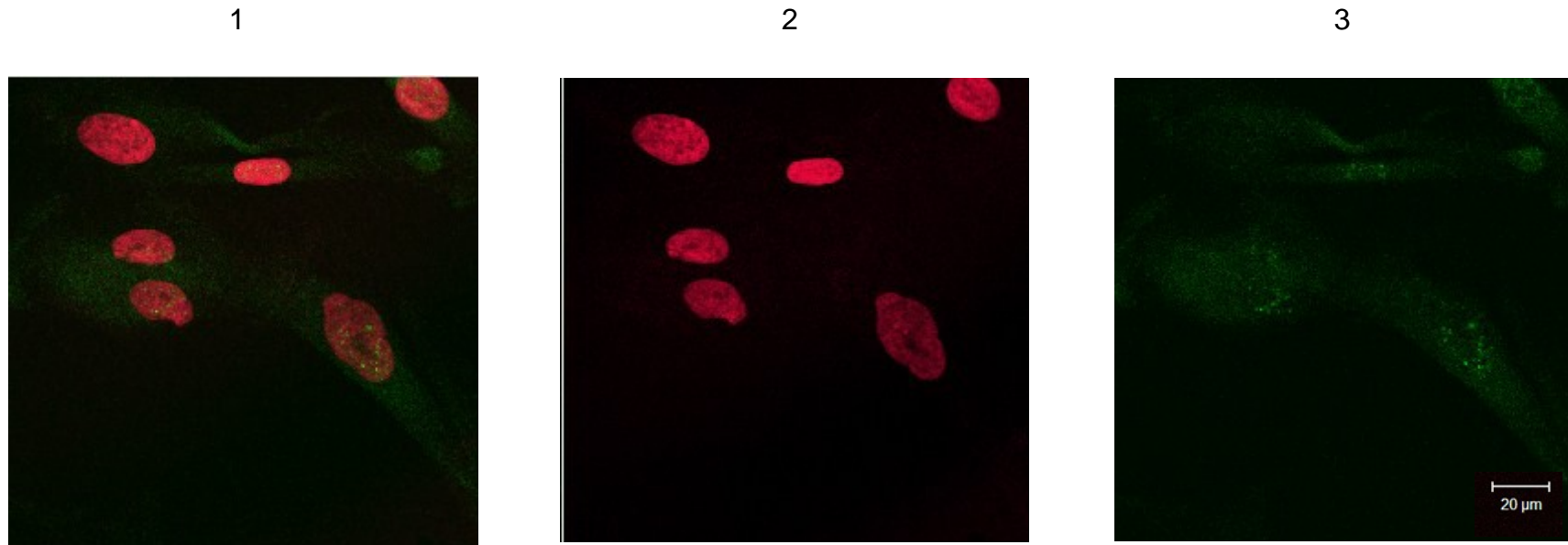


Figure 5.4 HSPA protein levels assessed using immunofluorescence in untreated NHA cells. (1) combined nuclei labelled with propidium iodide (red) and primary antibody HSPA detected with Anti-mouse IgG FITC conjugated secondary antibody (green); (2) nuclei staining labelled with propidium iodide (red) and (3) primary antibody HSPA detected with Anti-mouse IgG FITC conjugated antibody (green). Objective = x 40 magnification. Scale bar = 20μm.

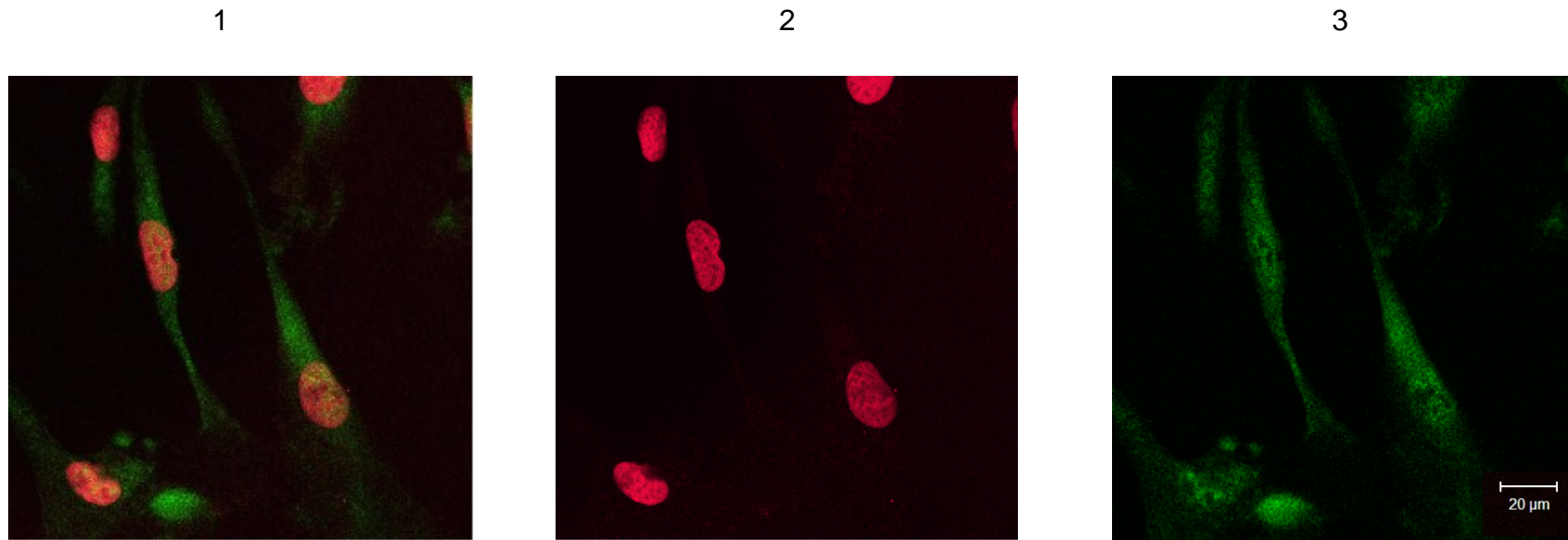


Figure 5.5 HSPA protein levels assessed using immunofluorescence in in post hypoxia treated NHA cells after 0 h recovery. (1) combined nuclei labelled with propidium iodide (red) and primary antibody HSPA detected with Anti-mouse IgG FITC conjugated secondary antibody (green); (2) nuclei staining labelled with propidium iodide (red) and (3) primary antibody HSPA detected with Anti-mouse IgG FITC conjugated antibody (green). Objective = x 40 magnification. Scale bar = 20µm.

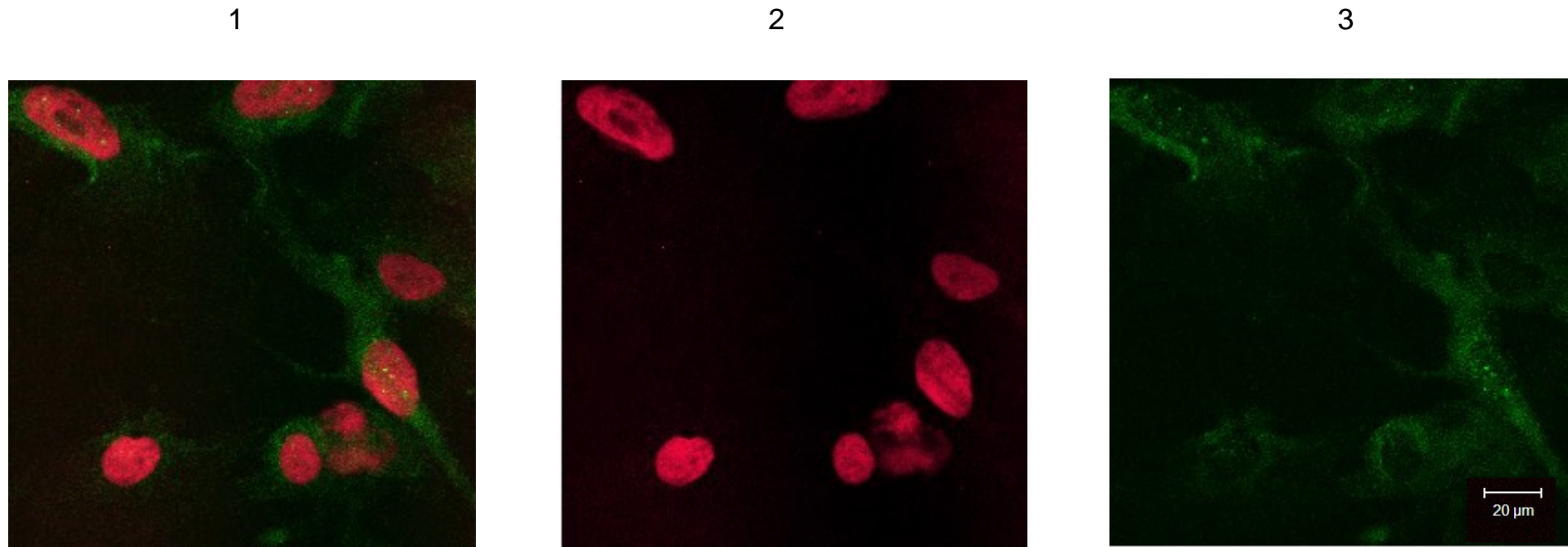


Figure 5.6 HSPA protein levels assessed using immunofluorescence in in post hypoxia treated NHA cells after 3 h recovery. (1) combined nuclei labelled with propidium iodide (red) and primary antibody HSPA detected with Anti-mouse IgG FITC conjugated secondary antibody (green); (2) nuclei staining labelled with propidium iodide (red) and (3) primary antibody HSPA detected with Anti-mouse IgG FITC conjugated antibody (green). Objective = x 40 magnification. Scale bar = 20 μ m.

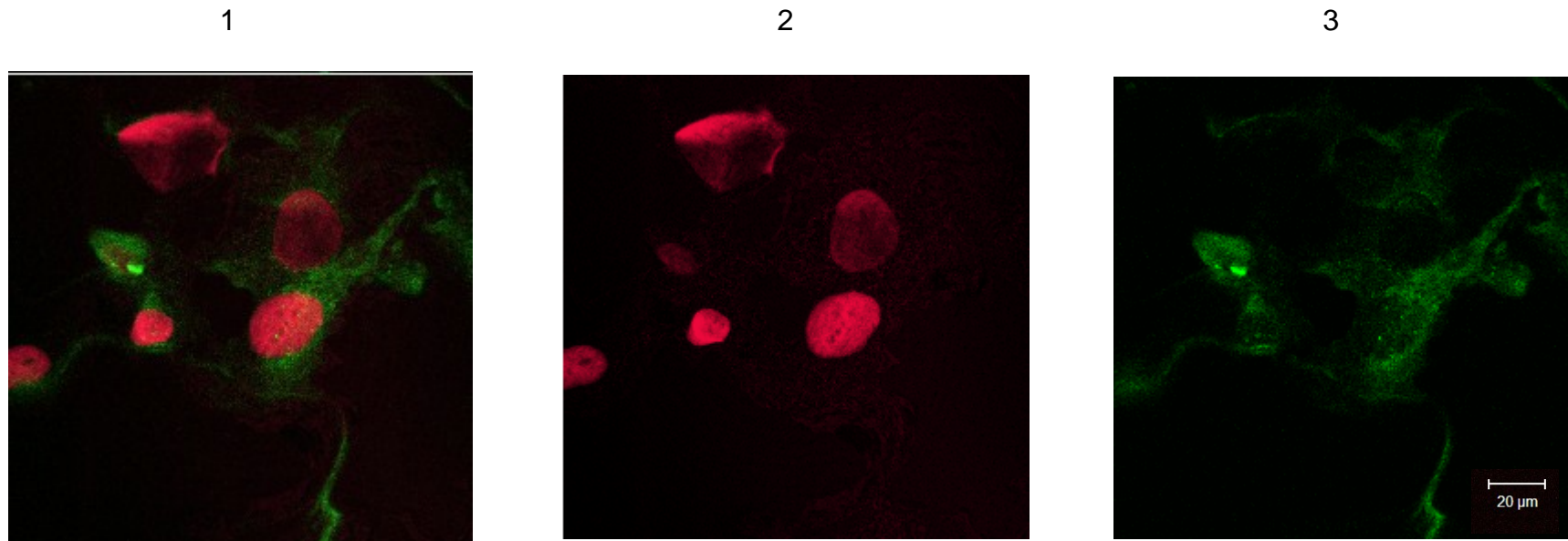


Figure 5.7 HSPA protein levels assessed using immunofluorescence in in post hypoxia treated NHA cells after 6 h recovery. (1) combined nuclei labelled with propidium iodide (red) and primary antibody HSPA detected with Anti-mouse IgG FITC conjugated secondary antibody (green); (2) nuclei staining labelled with propidium iodide (red) and (3) primary antibody HSPA detected with Anti-mouse IgG FITC conjugated antibody (green). Objective = x 40 magnification. Scale bar = 20µm.

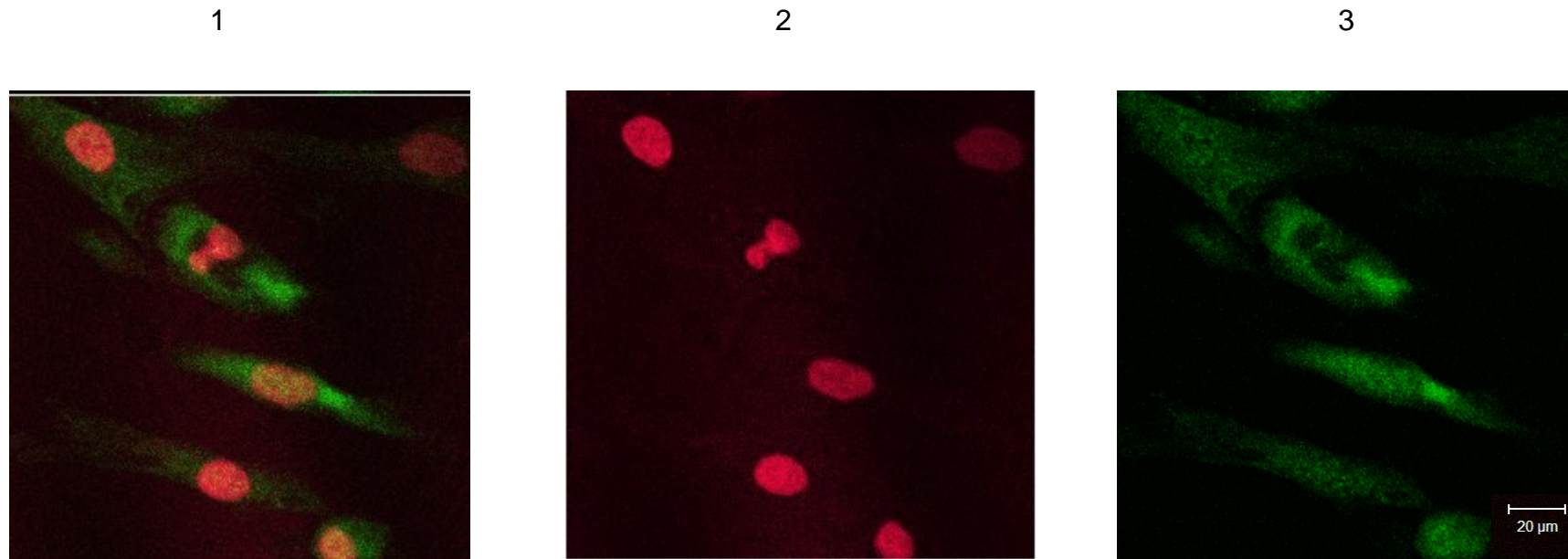


Figure 5.8 HSPA protein levels assessed using immunofluorescence in in post hypoxia treated NHA cells after 24 h recovery. (1) combined nuclei labelled with propidium iodide (red) and primary antibody HSPA detected with Anti-mouse IgG FITC conjugated secondary antibody (green); (2) nuclei staining labelled with propidium iodide (red) and (3) primary antibody HSPA detected with Anti-mouse IgG FITC conjugated antibody (green). Objective = x 40 magnification. Scale bar = 20μm.



Figure 5.9 HSPA protein levels assessed using immunofluorescence for negative control of un-treated 1321N1 cells. (1) Negative control whereby primary antibody HSPA has been omitted, Anti-mouse IgG FITC conjugated secondary antibody (green), no staining, nuclei labelled with propidium iodide (red); (2) nuclei staining labelled with propidium iodide (red) and (3) Anti-mouse IgG FITC conjugated secondary antibody (green), no staining. Objective = x 40 magnification. Scale bar = 20µm.

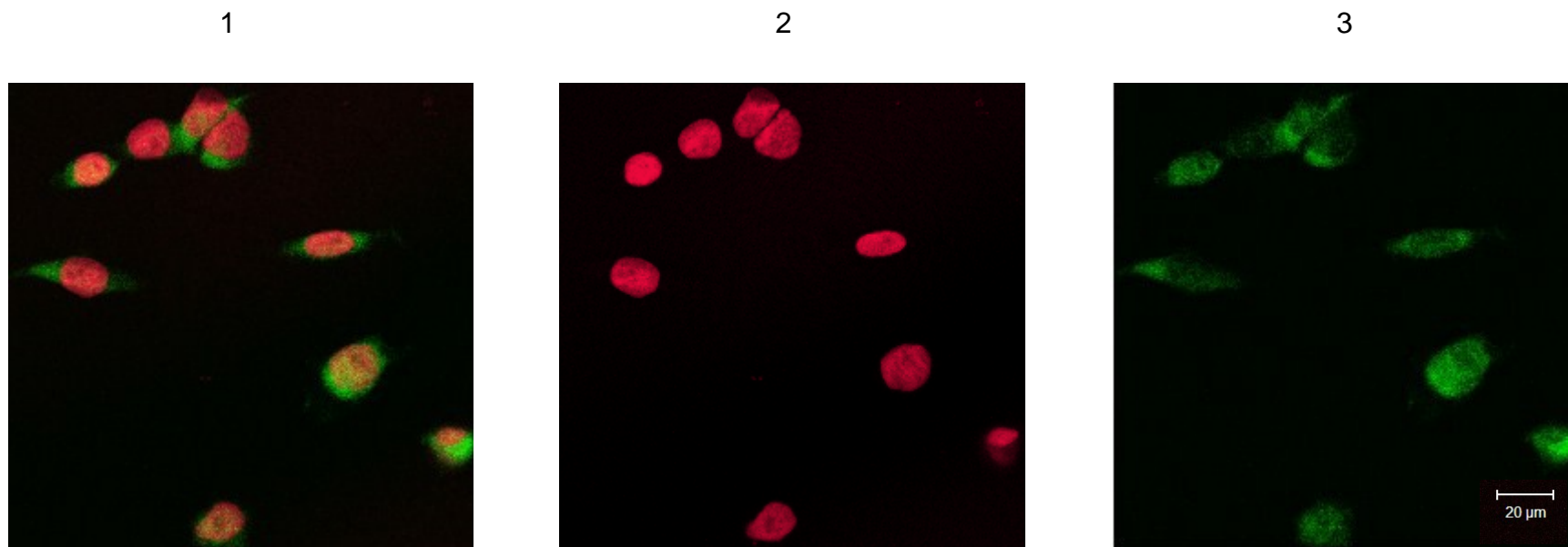


Figure 5.10 HSPA protein levels assessed using immunofluorescence in untreated 1321N1 cells. (1) combined nuclei labelled with propidium iodide (red) and primary antibody HSPA detected with Anti-mouse IgG FITC conjugated secondary antibody (green); (2) nuclei staining labelled with propidium iodide (red) and (3) primary antibody HSPA detected with Anti-mouse IgG FITC conjugated antibody (green). Objective = x 40 magnification. Scale bar = 20 μ m.

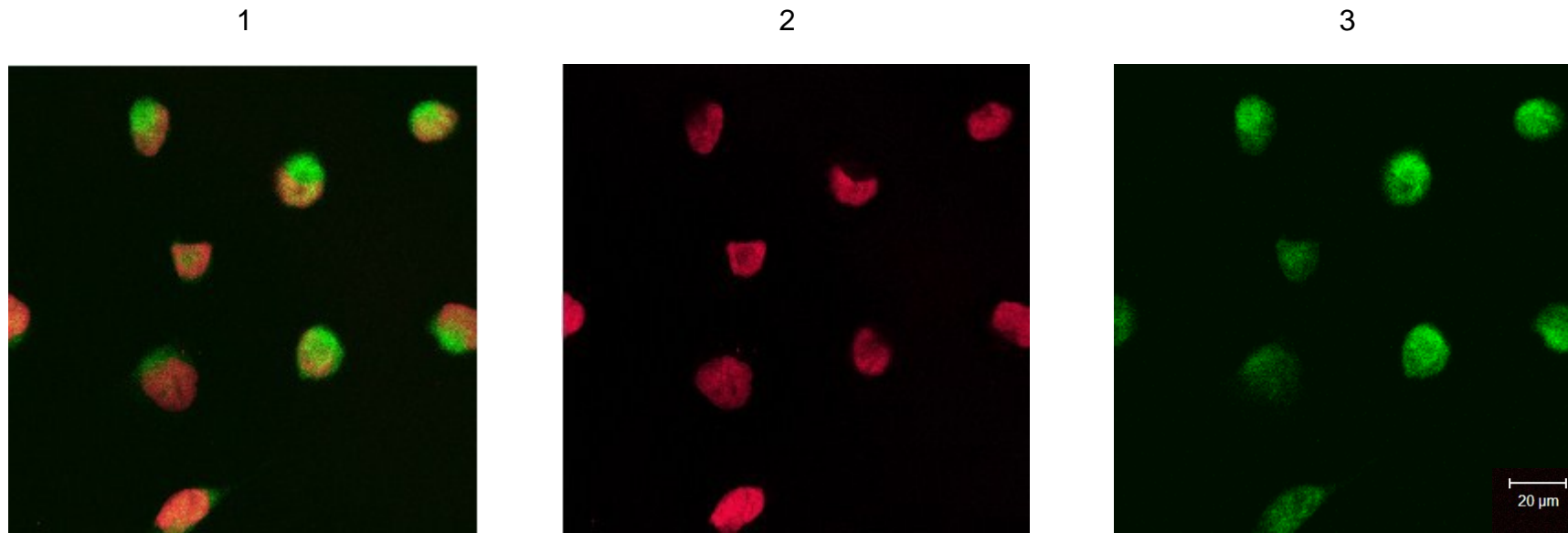


Figure 5.11 HSPA protein levels assessed using immunofluorescence in in post hypoxia treated 1321N1 cells after 0 h recovery. (1) combined nuclei labelled with propidium iodide (red) and primary antibody HSPA detected with Anti-mouse IgG FITC conjugated secondary antibody (green); (2) nuclei staining labelled with propidium iodide (red) and (3) primary antibody HSPA detected with Anti-mouse IgG FITC conjugated antibody (green). Objective = x 40 magnification. Scale bar = 20 μ m.

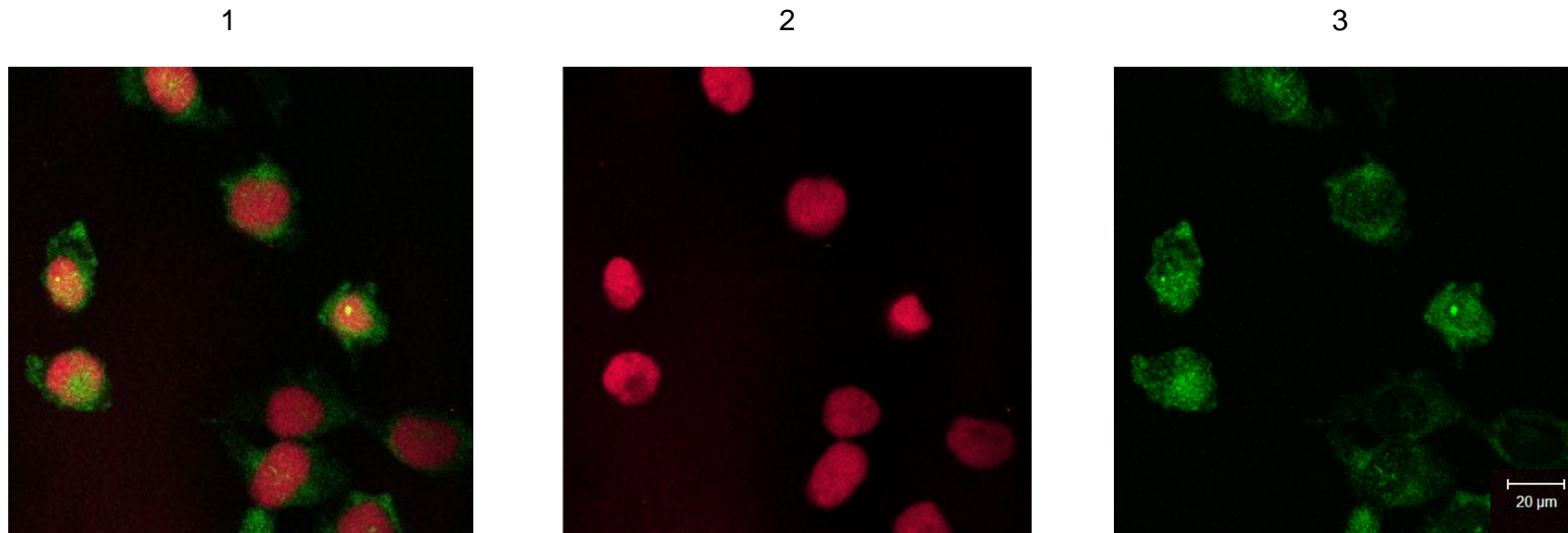


Figure 5.12 HSPA protein levels assessed using immunofluorescence in in post hypoxia treated 1321N1 cells after 3 h recovery. (1) combined nuclei labelled with propidium iodide (red) and primary antibody HSPA detected with Anti-mouse IgG FITC conjugated secondary antibody (green); (2) nuclei staining labelled with propidium iodide (red) and (3) primary antibody HSPA detected with Anti-mouse IgG FITC conjugated antibody (green). Objective = x 40 magnification. Scale bar = 20 μ m.

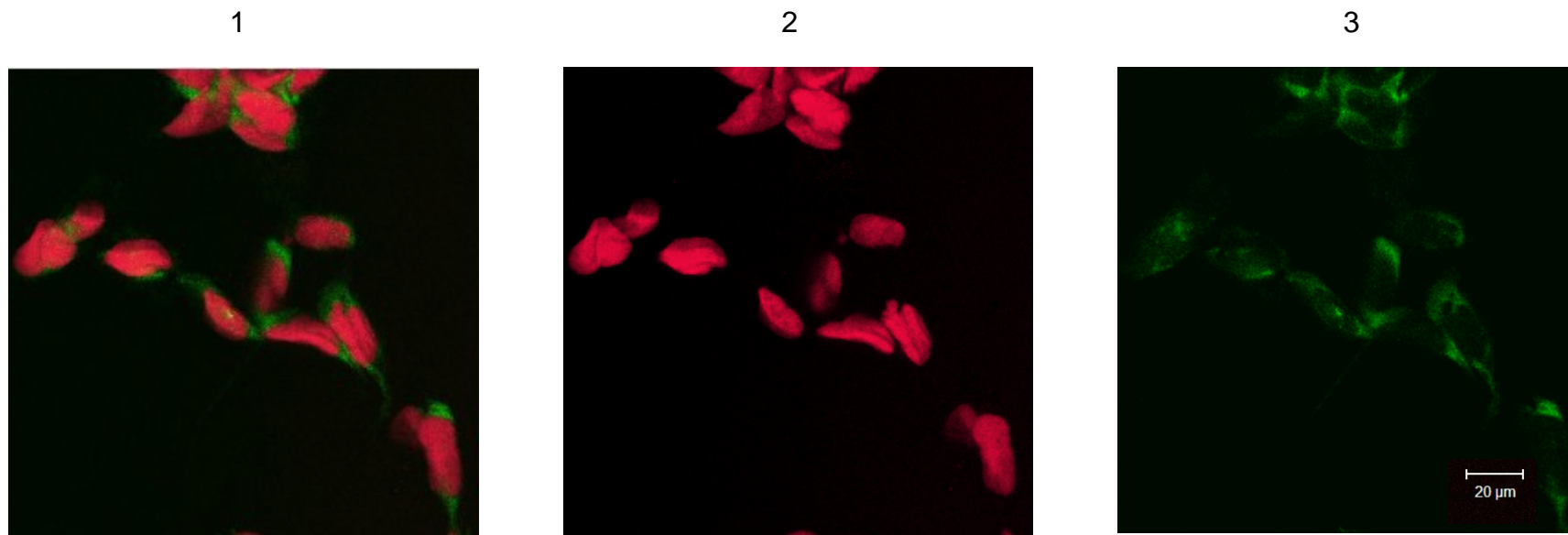


Figure 5.13 HSPA protein levels assessed using immunofluorescence in in post hypoxia treated 1321N1 cells after 6 h recovery. (1) combined nuclei labelled with propidium iodide (red) and primary antibody HSPA detected with Anti-mouse IgG FITC conjugated secondary antibody (green); (2) nuclei staining labelled with propidium iodide (red) and (3) primary antibody HSPA detected with Anti-mouse IgG FITC conjugated antibody (green). Objective = x 40 magnification. Scale bar = 20 μ m.

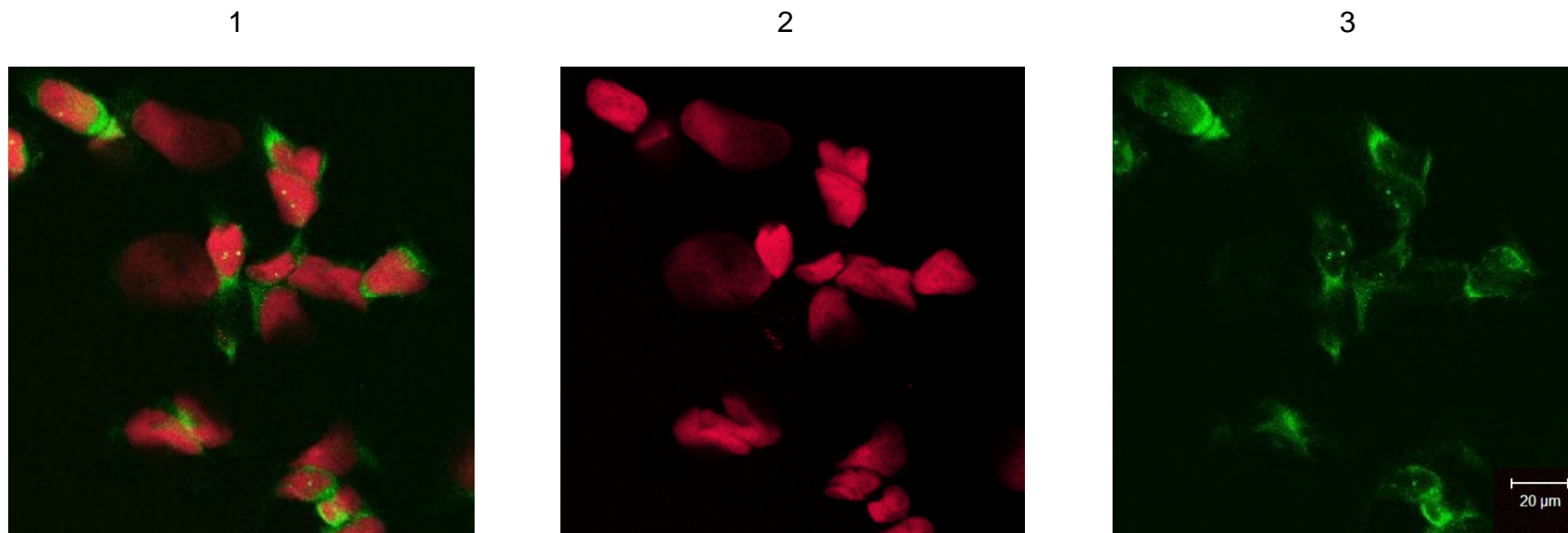


Figure 5.14 HSPA protein levels assessed using immunofluorescence in in post hypoxia treated 1321N1 cells after 24 h recovery. (1) combined nuclei labelled with propidium iodide (red) and primary antibody HSPA detected with Anti-mouse IgG FITC conjugated secondary antibody (green); (2) nuclei staining labelled with propidium iodide (red) and (3) primary antibody HSPA detected with Anti-mouse IgG FITC conjugated antibody (green). Objective = x 40 magnification. Scale bar = 20 μ m.

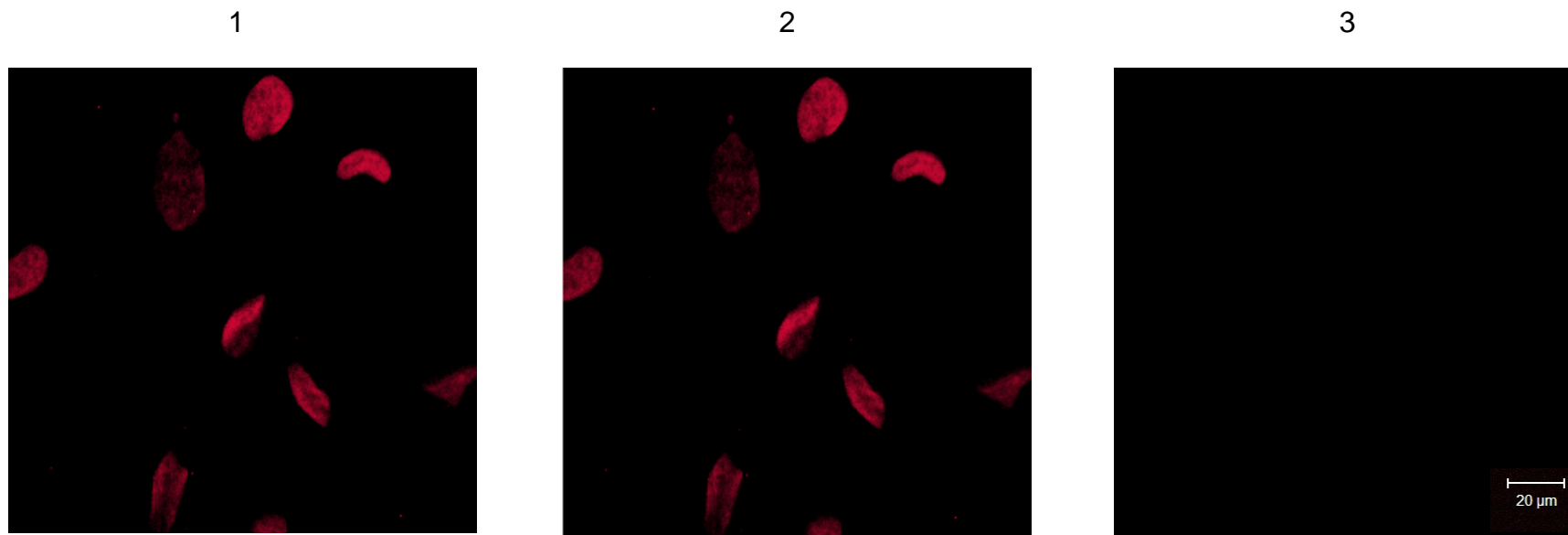


Figure 5.15 HSPA protein levels assessed using immunofluorescence for negative control of un-treated GOS-3 cells. (1) Negative control whereby primary antibody HSPA has been omitted, Anti-mouse IgG FITC conjugated secondary antibody (green), no staining, nuclei labelled with propidium iodide (red); (2) nuclei staining labelled with propidium iodide (red) and (3) Anti-mouse IgG FITC conjugated secondary antibody (green), no staining. Objective = x 40 magnification. Scale bar = 20µm.

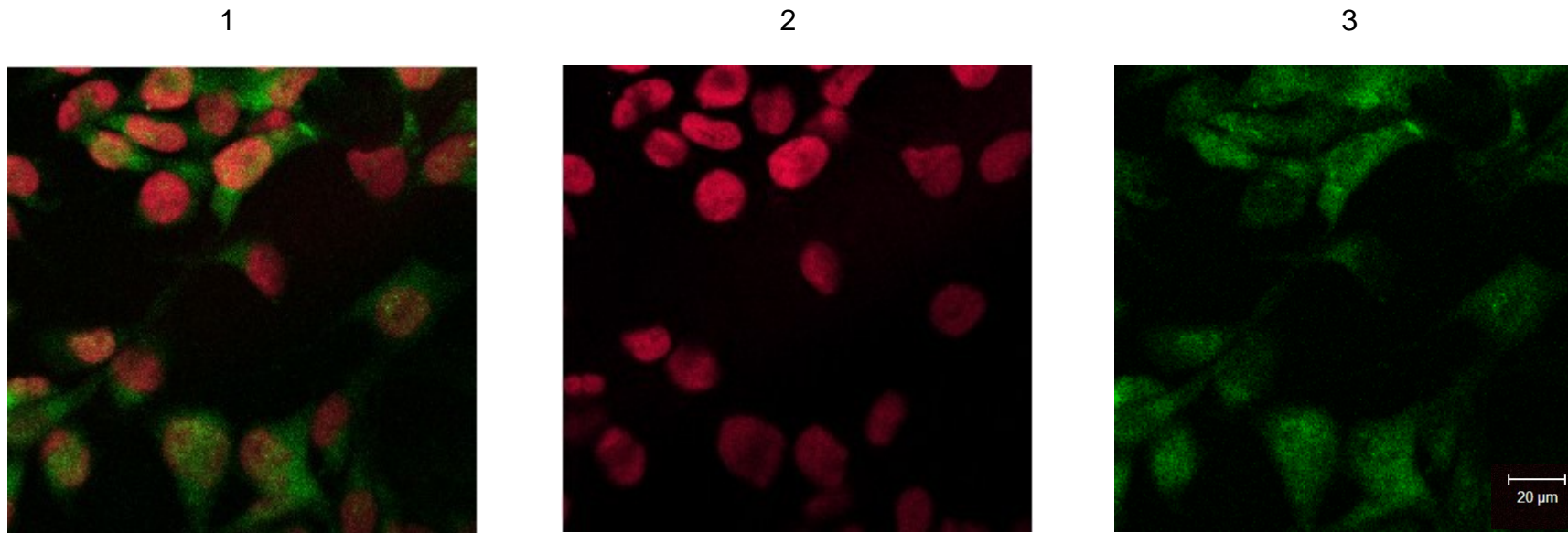


Figure 5.16 HSPA protein levels assessed using immunofluorescence in untreated GOS-3 cells. (1) combined nuclei labelled with propidium iodide (red) and primary antibody HSPA detected with Anti-mouse IgG FITC conjugated secondary antibody (green); (2) nuclei staining labelled with propidium iodide (red) and (3) primary antibody HSPA detected with Anti-mouse IgG FITC conjugated antibody (green). Objective = x 40 magnification. Scale bar = 20μm.

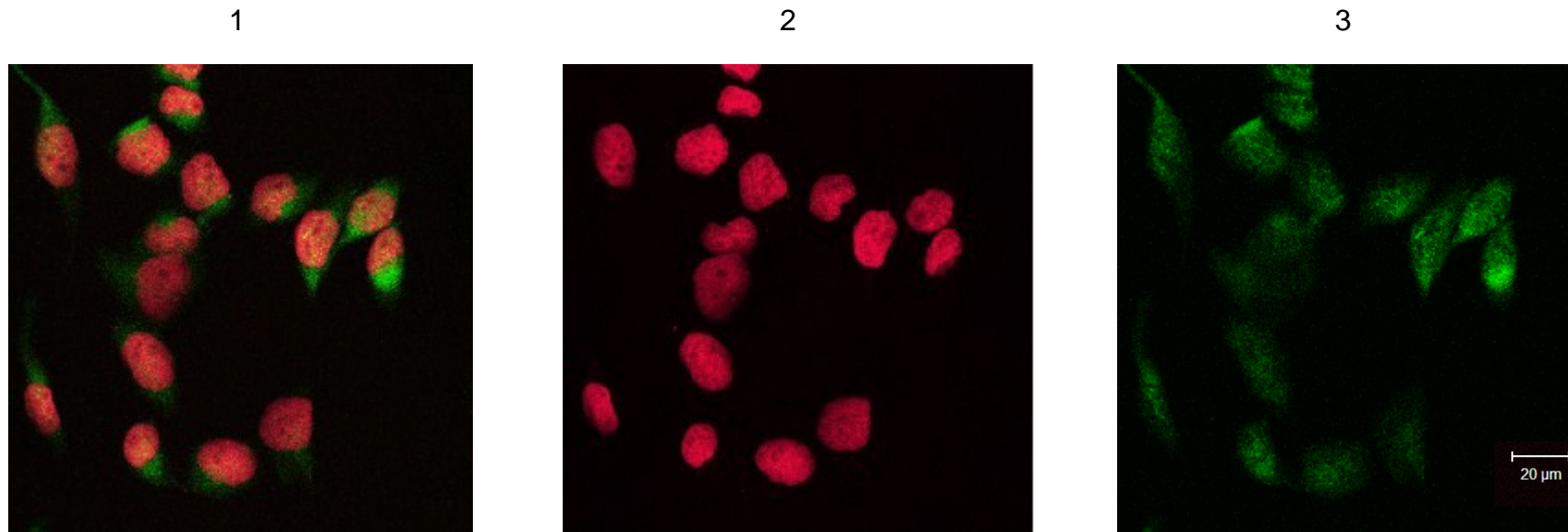


Figure 5.17 HSPA protein levels assessed using immunofluorescence in in post hypoxia treated GOS-3 cells after 0 h recovery. (1) combined nuclei labelled with propidium iodide (red) and primary antibody HSPA detected with Anti-mouse IgG FITC conjugated secondary antibody (green); (2) nuclei staining labelled with propidium iodide (red) and (3) primary antibody HSPA detected with Anti-mouse IgG FITC conjugated antibody (green). Objective = x 40 magnification. Scale bar = 20µm.

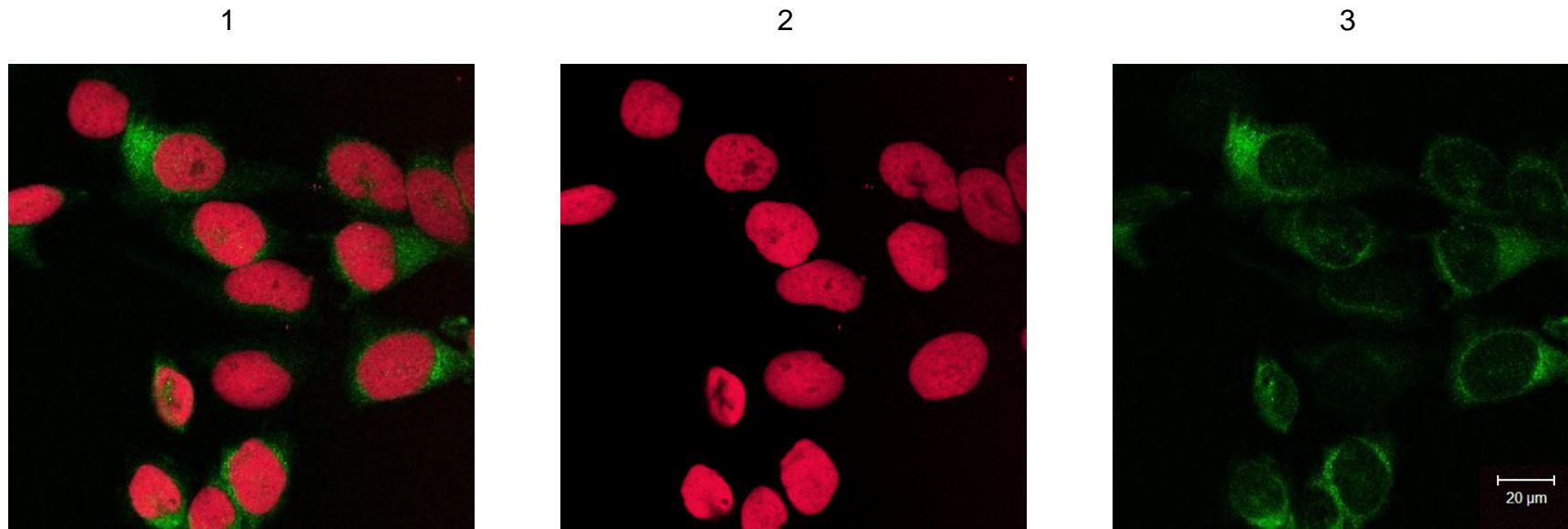


Figure 5.18 HSPA protein levels assessed using immunofluorescence in in post hypoxia treated GOS-3 cells after 3 h recovery. (1) combined nuclei labelled with propidium iodide (red) and primary antibody HSPA detected with Anti-mouse IgG FITC conjugated secondary antibody (green); (2) nuclei staining labelled with propidium iodide (red) and (3) primary antibody HSPA detected with Anti-mouse IgG FITC conjugated antibody (green). Objective = x 40 magnification. Scale bar = 20µm.

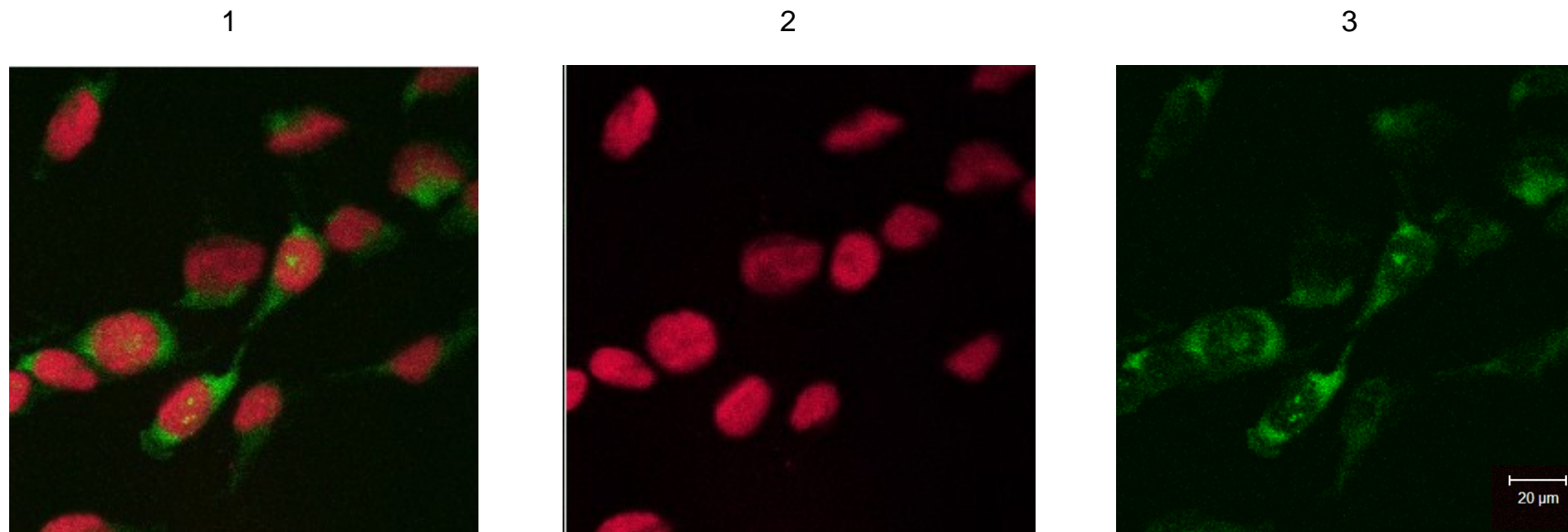


Figure 5.19 HSPA protein levels assessed using immunofluorescence in in post hypoxia treated GOS-3 cells after 6 h recovery. (1) combined nuclei labelled with propidium iodide (red) and primary antibody HSPA detected with Anti-mouse IgG FITC conjugated secondary antibody (green); (2) nuclei staining labelled with propidium iodide (red) and (3) primary antibody HSPA detected with Anti-mouse IgG FITC conjugated antibody (green). Objective = x 40 magnification. Scale bar = 20µm.

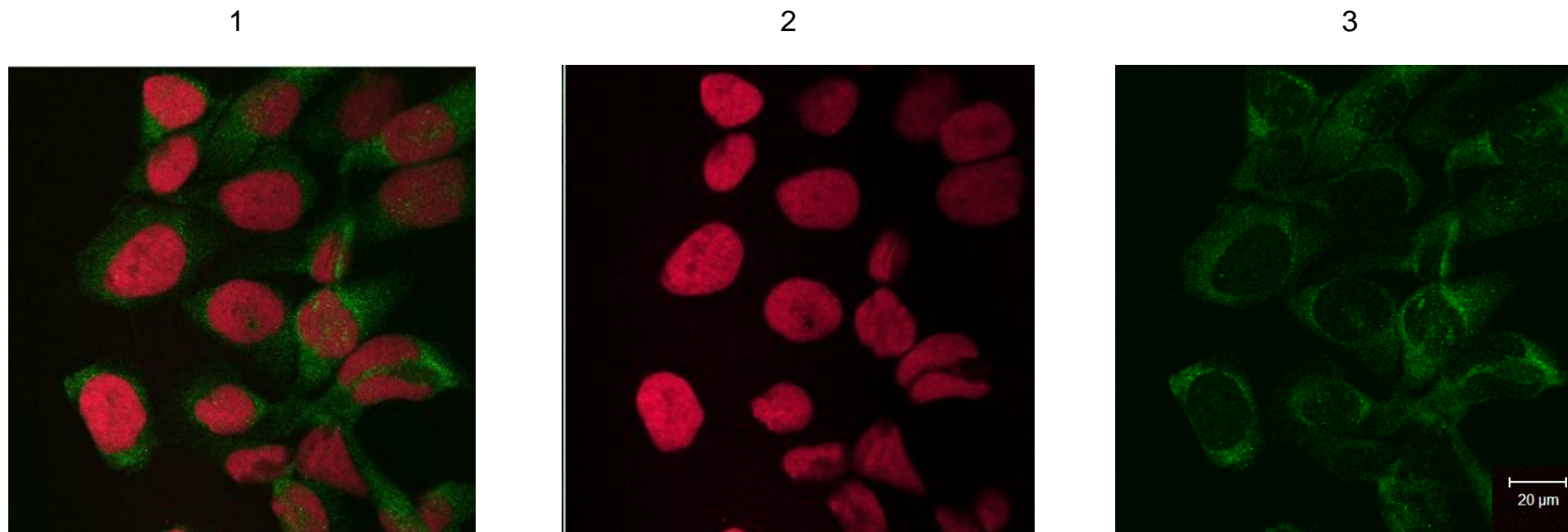


Figure 5.20 HSPA protein levels assessed using immunofluorescence in in post hypoxia treated GOS-3 cells after 24 h recovery. (1) combined nuclei labelled with propidium iodide (red) and primary antibody HSPA detected with Anti-mouse IgG FITC conjugated secondary antibody (green); (2) nuclei staining labelled with propidium iodide (red) and (3) primary antibody HSPA detected with Anti-mouse IgG FITC conjugated antibody (green). Objective = x 40 magnification. Scale bar = 20µm.

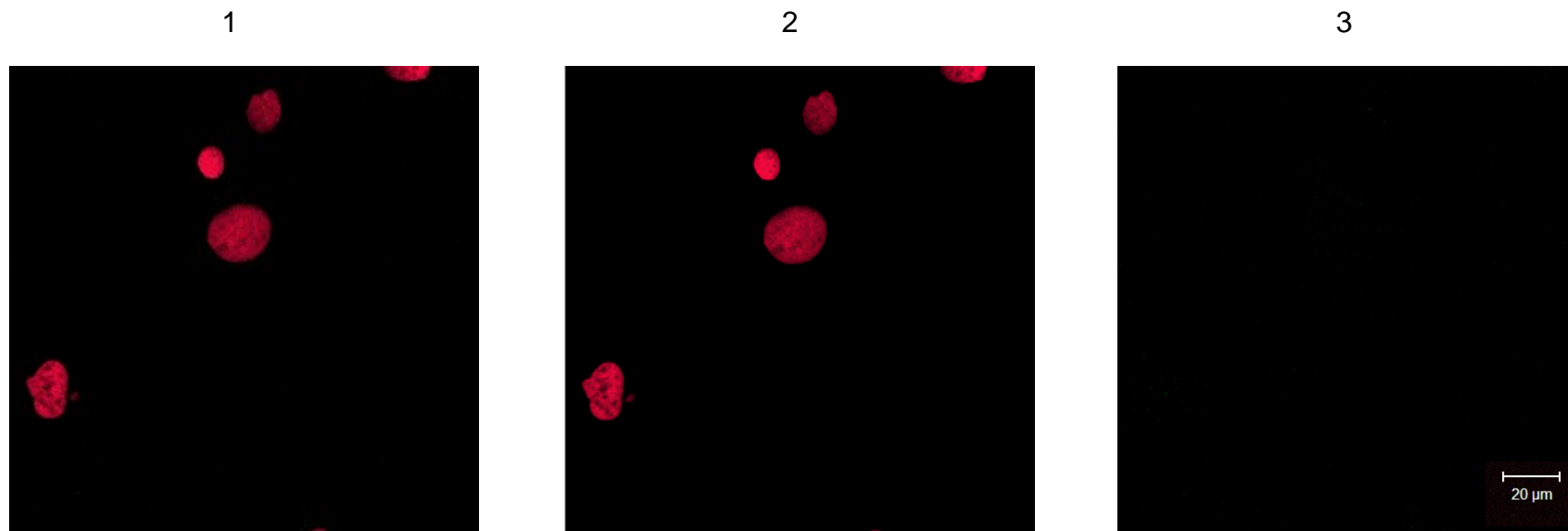


Figure 5.21 HSPA protein levels assessed using immunofluorescence for negative control of un-treated U87-MG cells. (1) Negative control whereby primary antibody HSPA has been omitted, Anti-mouse IgG FITC conjugated secondary antibody (green), no staining, nuclei labelled with propidium iodide (red); (2) nuclei staining labelled with propidium iodide (red) and (3) Anti-mouse IgG FITC conjugated secondary antibody (green), no staining. Objective = x 40 magnification. Scale bar = 20 μ m.

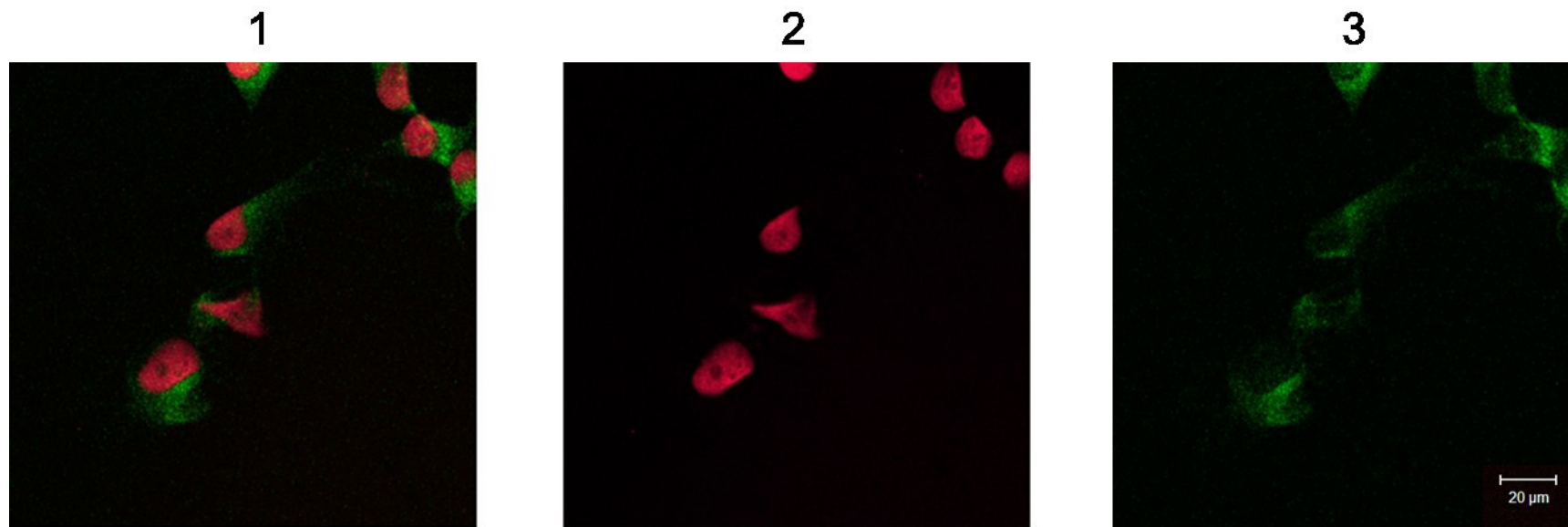


Figure 5.22 HSPA protein levels assessed using immunofluorescence in untreated U87-MG cells. (1) combined nuclei labelled with propidium iodide (red) and primary antibody HSPA detected with Anti-mouse IgG FITC conjugated secondary antibody (green); (2) nuclei staining labelled with propidium iodide (red) and (3) primary antibody HSPA detected with Anti-mouse IgG FITC conjugated antibody (green). Objective = x 40 magnification. Scale bar = 20µm.

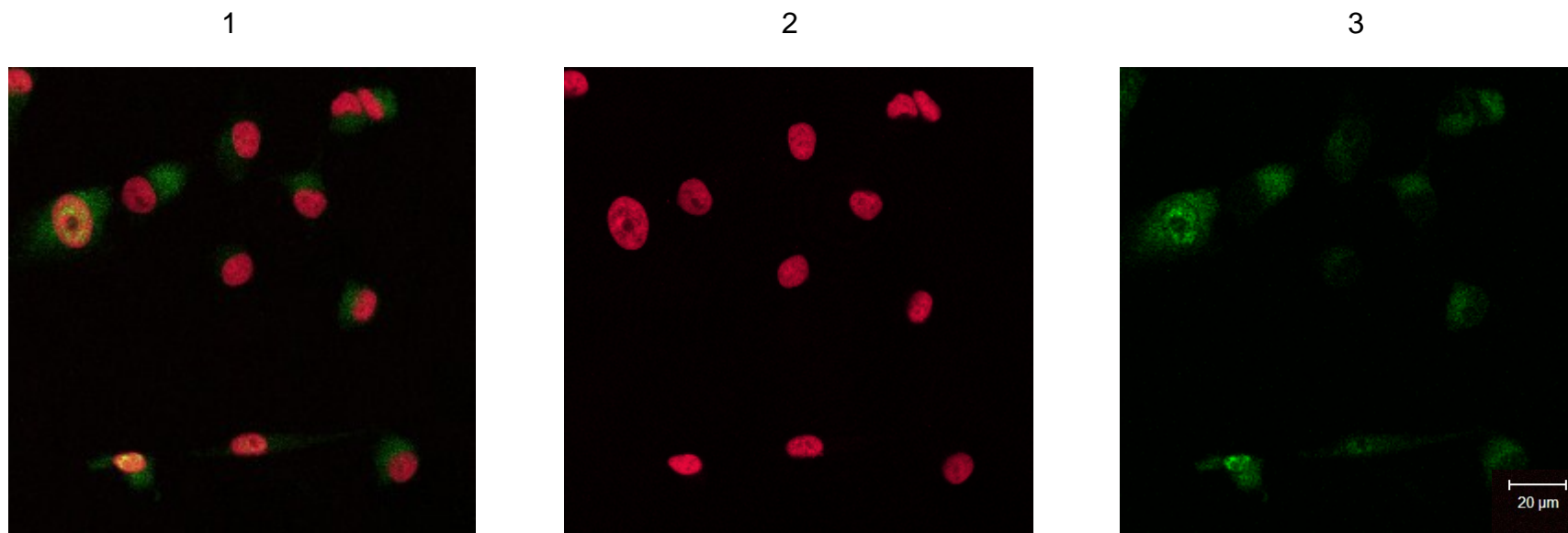


Figure 5.23 HSPA protein levels assessed using immunofluorescence in in post hypoxia treated U87-MG cells after 0 h recovery. (1) combined nuclei labelled with propidium iodide (red) and primary antibody HSPA detected with Anti-mouse IgG FITC conjugated secondary antibody (green); (2) nuclei staining labelled with propidium iodide (red) and (3) primary antibody HSPA detected with Anti-mouse IgG FITC conjugated antibody (green). Objective = x 40 magnification. Scale bar = 20µm.

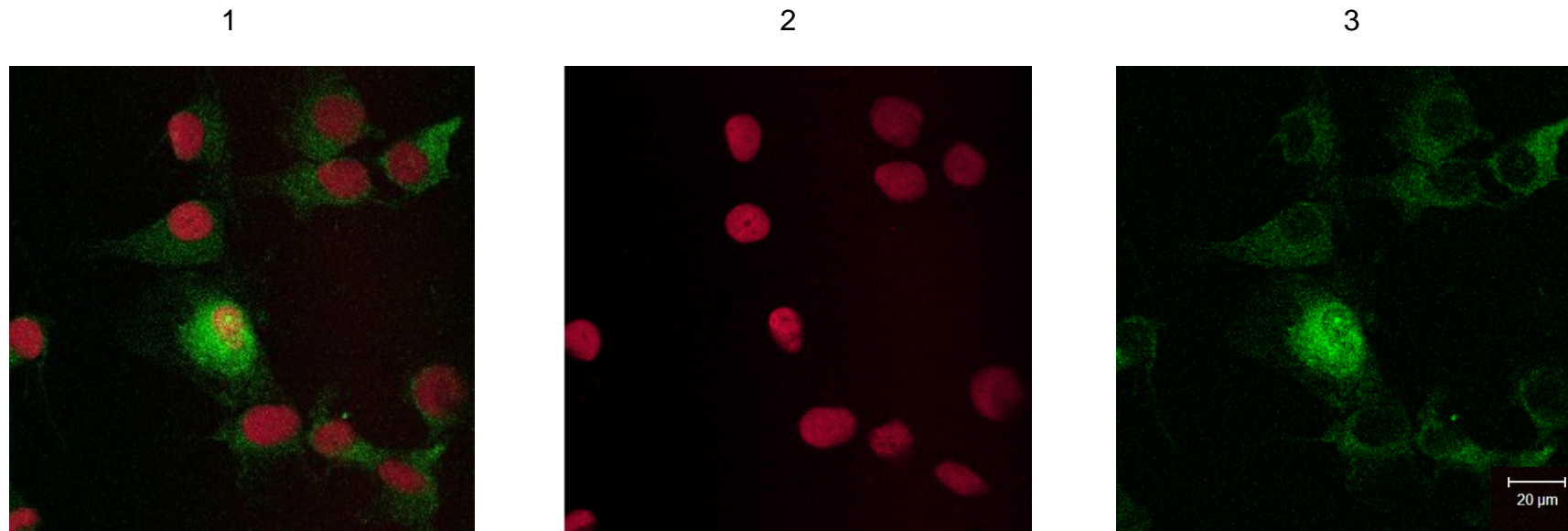


Figure 5.24 HSPA protein levels assessed using immunofluorescence in in post hypoxia treated U87-MG cells after 3 h recovery. (1) combined nuclei labelled with propidium iodide (red) and primary antibody HSPA detected with Anti-mouse IgG FITC conjugated secondary antibody (green); (2) nuclei staining labelled with propidium iodide (red) and (3) primary antibody HSPA detected with Anti-mouse IgG FITC conjugated antibody (green). Objective = x 40 magnification. Scale bar = 20µm.

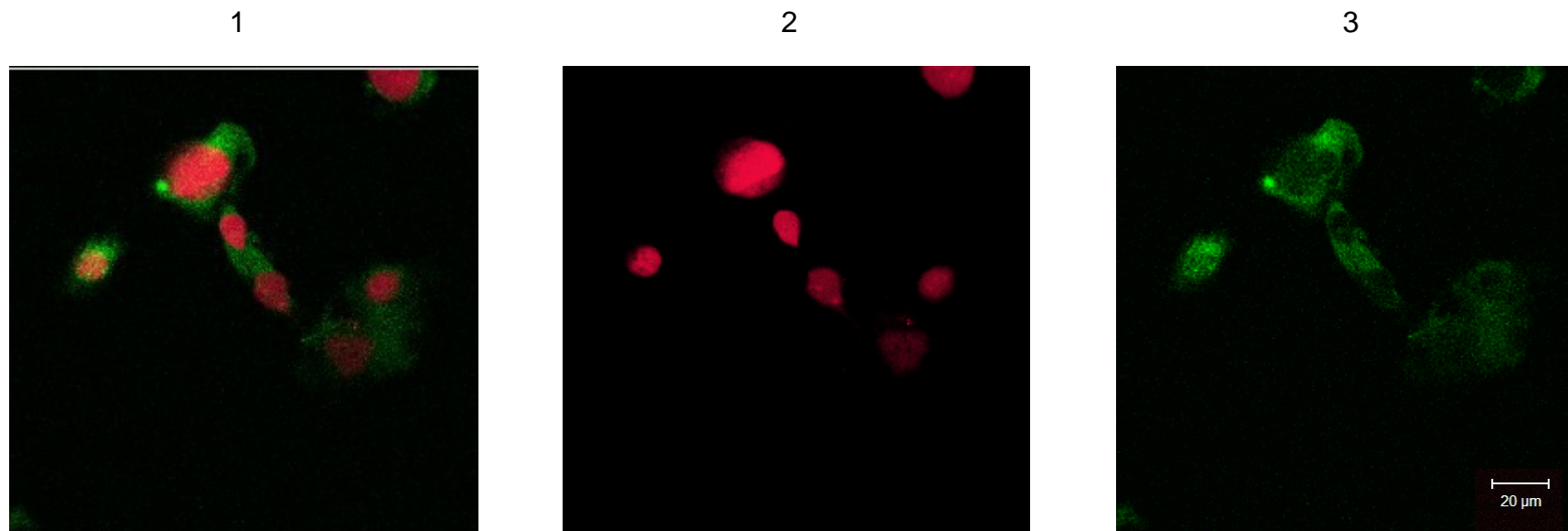


Figure 5.25 HSPA protein levels assessed using immunofluorescence in in post hypoxia treated U87-MG cells after 6 h recovery. (1) combined nuclei labelled with propidium iodide (red) and primary antibody HSPA detected with Anti-mouse IgG FITC conjugated secondary antibody (green); (2) nuclei staining labelled with propidium iodide (red) and (3) primary antibody HSPA detected with Anti-mouse IgG FITC conjugated antibody (green). Objective = x 40 magnification. Scale bar = 20 μ m.

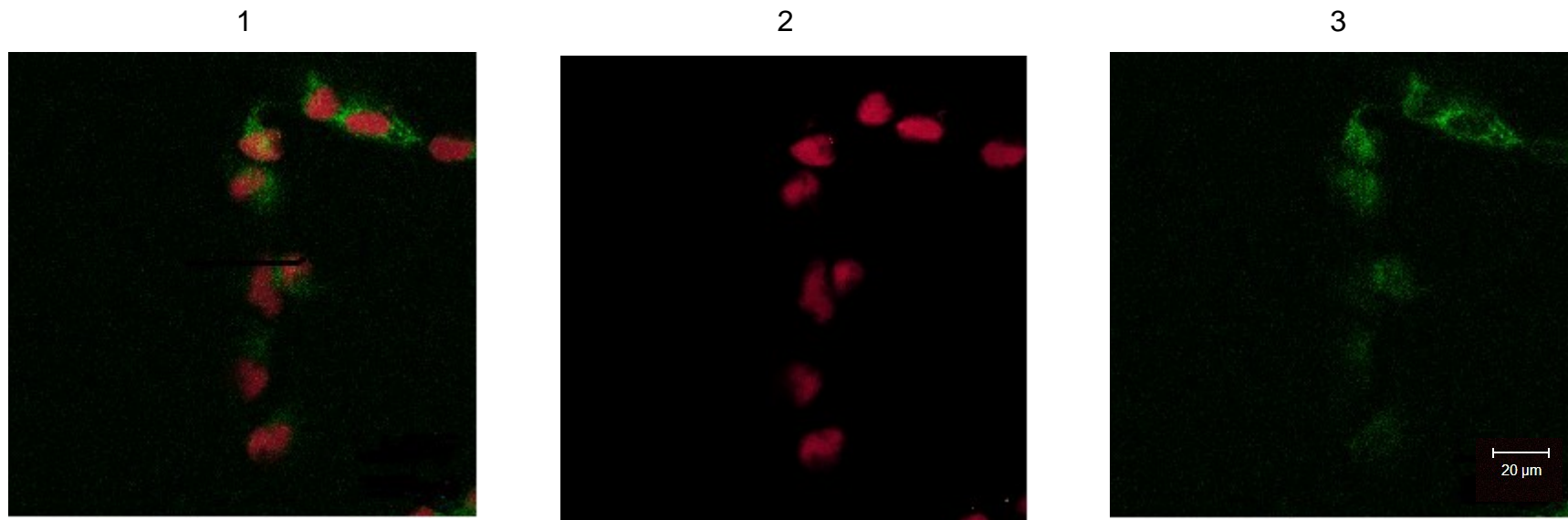


Figure 5.26 HSPA protein levels assessed using immunofluorescence in in post hypoxia treated U87-MG cells after 24 h recovery. (1) combined nuclei labelled with propidium iodide (red) and primary antibody HSPA detected with Anti-mouse IgG FITC conjugated secondary antibody (green); (2) nuclei staining labelled with propidium iodide (red) and (3) primary antibody HSPA detected with Anti-mouse IgG FITC conjugated antibody (green). Objective = x 40 magnification. Scale bar = 20 μ m.

5.4 Flow Cytometry

To accurately quantify production of the protein HSPA in cells, flow cytometry analysis was carried out using the same four cell lines for pre- and post-hypoxia conditions as in previous sections of this chapter. Cultured cells were stained and subjected to flow cytometry, briefly 1×10^6 were washed once in 0.1% BSA in PBS before being re-suspended in 0.1% Triton X-100 for 15 min. Following incubation cells were collected and washed once with 0.1% BSA in PBS before being blocked in 5% goat serum in 0.1% BSA in PBS for 30 min. HSPA primary antibody (1:200) diluted in blocking solution was applied for 30 min. Cells were then washed with 0.1% BSA in PBS and light sensitive Anti-Mouse IgG FITC conjugated secondary antibody (1:200) diluted in blocking solution was added for 30 min. Following incubation cells were washed twice in 0.1% BSA in PBS before finally being re-suspended in an aliquot 0.1% BSA in PBS and filtered into FACS tubes. All incubation steps were performed on ice.

This analysis showed a higher relative fluorescence intensity in hypoxic 1321N1, GOS-3 and U87-MG cell lines (approximately 3-fold) compared to NHA, reflecting a higher level of production of HSPA protein (Figures 5.28 – 5.32, NHA, 5.33 – 5.37, 1321N1, 5.38 – 5.42, GOS-3, 5.43 – 5.47, U87-MG). In pre and post hypoxia treated 1321N1, GOS-3 and U87-MG glioma cells, HSPA protein levels were relatively high, with approximately 97%, 89% and 97% respectively showing positive for HSPA in pre hypoxia treatment, with approximately 99%, 73% and 84% respectively showing positive for HSPA in post hypoxia treatment after 0 h recovery, with approximately 99%, 92% and 91% respectively showing positive for HSPA in post hypoxia treatment after 3 h recovery with approximately 99%, 92% and 96% respectively showing positive for HSPA in post hypoxia treatment after 6 h recovery, and approximately

94%, 97% and 96% respectively showing positive for HSPA in post hypoxia treatment after 24 h recovery compared to the NHA cells showing positive for HSPA pre hypoxia treatment approximately 0.10% and post hypoxia treatment after 0 h recovery, approximately 33%; after 3 h recovery approximately 31%; after 6 h recovery approximately 25% and after 24 h recovery approximately 11% (Figure 5.27 and Table 5.3).

In GOS-3 and U87-MG glioma cells, hypoxic treatment resulted in a transient decrease in HSPA protein at 0 h recovery period from, approximate percentage level: 89 to 73 for GOS-3 and from 97 to 84 for U87-MG. After a three hour recovery period, HSPA protein levels increased to pre-hypoxic levels and remained relatively constant up to 24 h. HSPA protein synthesis in the NHA cell line reached maximal levels of approximately 33% at the 0 h recovery period after hypoxia treatment, followed by a progressive decrease in HSPA protein levels up to the 24 h recovery period (Figure 5.27). A shift of the HSPA detection peak was observed from 1×10^2 to 1×10^4 in the NHA cell line (Figures 5.28 – 5.32), however, no such shift was observed in 1321N1, GOS-3 and U87-MG glioma cell lines.

A

Cell Line	Pre-hypoxia	Post-hypoxia (Hours)			
		0	3	6	24
NHA	0	33.0	30.8	24.7	11.3
1321N1	97.1	99.6	99.1	99.0	93.6
GOS-3	89.2	73.4	91.9	92.0	96.6
U87-MG	96.9	83.7	90.9	96.5	96.3

B

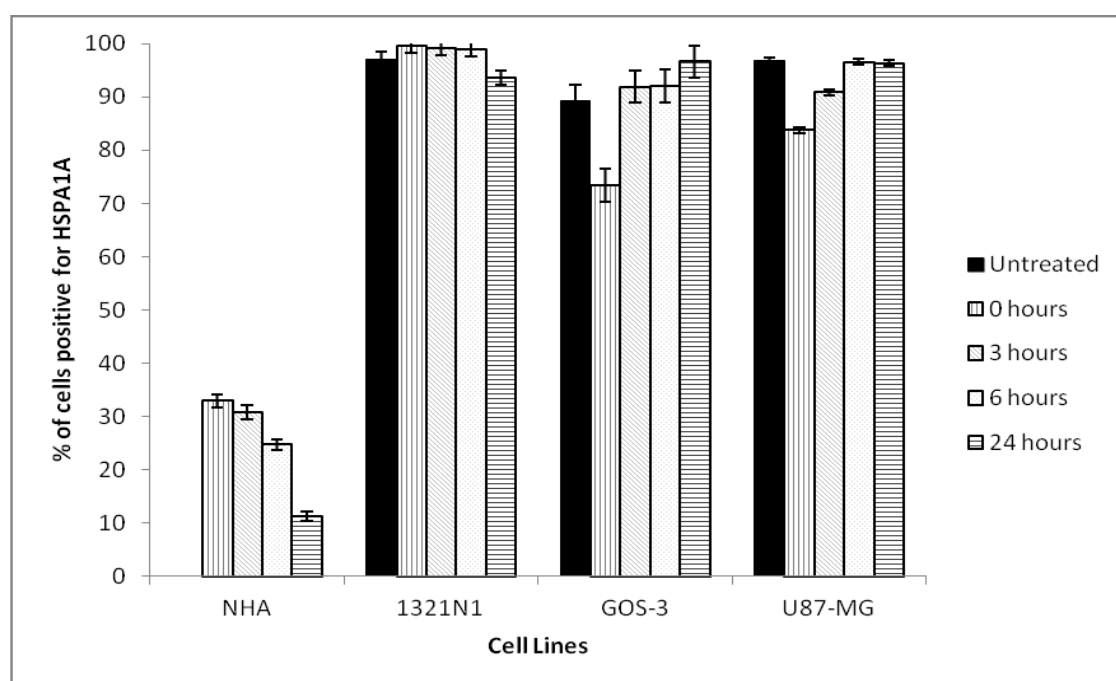


Figure 5.27 Average percentage of cells showing positive for HSPA in pre and post hypoxia treatment. (A) Average percentage of normal and glioma cells positive for HSPA pre and post hypoxia detected by flow cytometry, considering 10,000 events per sample. (B) Histogram showing the mean percentage of cells evaluated by flow cytometry of three independent experiments, and the standard deviation from this mean is shown by the error bars. No column was shown on the histogram for NHA as the value = 0.

5.4.1 Statistical Analysis

A two-way factorial mixed 4 (cell line: NHA, 1321N1, GOS-3, U87-MG) x 5 (treatment: untreated, 0, 3, 6 and 24 h recovery after hypoxia treatment) ANOVA analysis of variance test was performed to investigate differences of HSPA protein levels. The means and standard deviation are presented in Table 5.3.

Table 5.3. Descriptive statistics showing the mean HSPA protein levels for untreated and treated cell lines.

Treatment	Cell Line	N	Mean HSPA protein level	STD. Deviation
Pre-hypoxia	NHA	3	.13	.058
	1321N1	3	96.87	.322
	GOS-3	3	89.15	.050
	U87-MG	3	96.85	.050
0 h recovery after hypoxia treatment	NHA	3	32.50	.500
	1321N1	3	99.55	.050
	GOS-3	3	73.38	.076
	U87-MG	3	83.6	.100
3 h recovery after hypoxia treatment	NHA	3	30.83	.153
	1321N1	3	99.05	.050
	GOS-3	3	91.85	.050
	U87-MG	3	90.85	.050
6 h recovery after hypoxia treatment	NHA	3	24.72	.126
	1321N1	3	99.03	.061
	GOS-3	3	91.83	.764
	U87-MG	3	96.45	.050
24 h recovery after hypoxia treatment	NHA	3	11.30	.095
	1321N1	3	93.53	.060
	GOS-3	3	96.62	.076
	U87-MG	3	96.33	.058

Overall inspection of the mean scores for HSPA protein levels indicated that untreated and treated 1321N1; GOS-3 and U87-MG cell lines were considerably higher than the NHA cell line (Table 5.3).

There was a significant effect for: cell line [$F(15,11.44) = 32736$; $P < 0.001$]; Wilks' Lambda = 0.000, partial eta squared = 1.000; a significant effect for treatment [$F(4,5) = 6262.1$; $P < 0.001$], Wilks' Lambda = 0.000, partial eta squared = 1.000. There was a significant effect in the interaction between treatment and cell line, [$F(12,13.52) = 5234.5$; $P < 0.001$], Wilks' Lambda = 0.000, partial eta squared = 0.999.

There was a statistically significant main effect for cell lines on the combined variables: [$F(3,8) = 406583$, $P < .001$]; partial eta squared (η_p^2) = 1.0.

When the results for the dependent variables were considered separately, there was a statistically high significance in untreated [$F(3,8) = 239590$, $P < .000$]; partial eta squared (η_p^2) = 1.000. Post-hoc analyses using Tukey's HSD test indicated significantly lower HSPA protein levels in untreated NHA than in: 1321N1 (MD = 96.73, $P < .05$); GOS-3 (MD = 89.02, $P < .05$) and U87-MG (MD = 96.72, $P < .05$). There was significantly lower HSPA protein levels in untreated 1321N1 than in GOS-3 (MD = 7.72, $P < .05$). There was significantly lower HSPA protein levels in untreated GOS-3 than in U87-MG (MD = 7.70, $P < .05$). All other differences between groups failed to reach significance (Table 5.4).

There was a statistically high significance after 0 h recovery [$F(3,8) = 36603$, $P < .000$]; partial eta squared (η_p^2) = 1.000. Post-hoc analyses using Tukey's HSD test indicated significantly lower HSPA protein levels after 0 h recovery in NHA than in: 1321N1 (MD = 67.05, $P < .05$); GOS-3 (MD = 40.88, $P < .05$) and U87-MG (MD = 51.10, $P < .05$). There were significantly lower HSPA protein levels after 0 h recovery in 1321N1 than in: GOS-3 (MD = 7.72, $P < .05$) and U87-MG (MD = 15.95, $P < .05$). There was significantly lower HSPA protein levels after 0 h recovery in GOS-3 than in U87-MG (MD = 10.22, $P < .05$) (Table 5.4).

There was a statistically high significance after 3 h recovery [$F(3,8) = 392388$, $P < .000$]; partial eta squared (η_p^2) = 1.000. Post-hoc analyses using Tukey's HSD test indicated significantly lower HSPA protein levels after 3 h recovery in NHA than in: 1321N1 (MD = 68.22, $P < .05$); GOS-3 (MD = 61.02, $P < .05$) and U87-MG (MD = 60.02, $P < .05$). There were significantly lower HSPA protein levels after 3 h recovery in 1321N1 than in: GOS-3 (MD = 7.20, $P < .05$) and U87-MG (MD = 8.20, $P < .05$). There was significantly lower HSPA protein levels after 3 h recovery in GOS-3 than in U87-MG (MD = 1.00, $P < .05$) (Table 5.4).

There was a statistically high significance after 6 h recovery [$F(3,8) = 25196$, $P < .000$]; partial eta squared (η_p^2) = 1.000. Post-hoc analyses using Tukey's HSD test indicated significantly lower HSPA protein levels after 6 h recovery in NHA than in: 1321N1 (MD = 74.31, $P < .05$); GOS-3 (MD = 67.12, $P < .05$) and U87-MG (MD = 71.73, $P < .05$). There were significantly lower HSPA protein levels after 6 h recovery in 1321N1 than in: GOS-3 (MD = 7.20, $P < .05$) and U87-MG (MD = 2.58, $P < .05$). There was significantly lower HSPA protein levels after 6 h recovery in GOS-3 than in U87-MG (MD = 4.62, $P < .05$) (Table 5.4).

There was a statistically high significance after 24 h recovery [$F(3,8) = 972016$, $P < .000$]; partial eta squared (η_p^2) = 1.000. Post-hoc analyses using Tukey's HSD test indicated significantly lower HSPA protein levels after 24 h recovery in NHA than in: 1321N1 (MD = 82.23, $P < .05$); GOS-3 (MD = 85.31, $P < .05$) and U87-MG (MD = 85.03, $P < .05$). There were significantly lower HSPA protein levels after 24 h recovery in 1321N1 than in: GOS-3 (MD = 3.09, $P < .05$) and U87-MG (MD = 2.80, $P < .05$). There was significantly lower HSPA protein levels after 24 h recovery in GOS-3 than in U87-MG (MD = .283, $P < .05$) (Table 5.4).

Table 5.4. Statistical data from Tukey’s HSD test showing significance of HSPA protein levels in treated and untreated cell lines. Any differences that are not significant are highlighted in bold. Significance ≤ 0.05 .

Treatment	Cell Line	NHA		1321N1		GOS-3		U87-MG	
		Mean Diff \pm STD error	SIG.	Mean Diff \pm STD error	SIG.	Mean Diff \pm STD error	SIG.	Mean Diff \pm STD error	SIG.
Untreated	NHA			96.73 \pm .136	.000	89.02 \pm .136	.000	96.72 \pm .136	.000
	1321N1	96.73 \pm .136	.000			7.72 \pm .136	.000	0.017 \pm .136	.999
	GOS-3	89.02 \pm .136	.000	7.72 \pm .136	.000			7.70 \pm .136	.000
	U87-MG	96.72 \pm .136	.000	0.017 \pm .136	.999	7.70 \pm .136	.000		
0h recovery	NHA			67.05 \pm .212	.000	40.88 \pm .212	.000	51.1 \pm .212	.000
	1321N1	67.05 \pm .212	.000			26.17 \pm .212	.000	15.95 \pm .212	.000
	GOS-3	40.88 \pm .212	.000	26.17 \pm .212	.000			10.22 \pm .212	.000
	U87-MG	51.1 \pm .212	.000	15.95 \pm .212	.000	10.22 \pm .212	.000		
3h recovery	NHA			68.21 \pm .072	.000	61.02 \pm .072	.000	60.02 \pm .072	.000
	1321N1	68.21 \pm .072	.000			7.20 \pm .072	.000	8.20 \pm .072	.000
	GOS-3	61.02 \pm .072	.000	7.20 \pm .072	.000			1.0 \pm .072	.000
	U87-MG	60.02 \pm .072	.000	8.20 \pm .072	.000	2.0 \pm .072	.000		
6h recovery	NHA			74.31 \pm .318	.000	67.12 \pm .318	.000	71.73 \pm .318	.000
	1321N1	74.31 \pm .318	.000			7.20 \pm .318	.000	2.58 \pm .318	.000
	GOS-3	67.12 \pm .318	.000	7.20 \pm .318	.000			4.62 \pm .318	.000
	U87-MG	71.73 \pm .318	.000	2.58 \pm .318	.000	4.62 \pm .318	.000		
12h recovery	NHA			82.23 \pm .060	.000	85.31 \pm .060	.000	85.03 \pm .060	.000
	1321N1	82.23 \pm .060	.000			3.09 \pm .060	.000	2.80 \pm .060	.000
	GOS-3	85.31 \pm .060	.000	3.09 \pm .060	.000			.283 \pm .060	.007
	U87-MG	85.03 \pm .060	.000	2.80 \pm .060	.000	.283 \pm .060	.007		

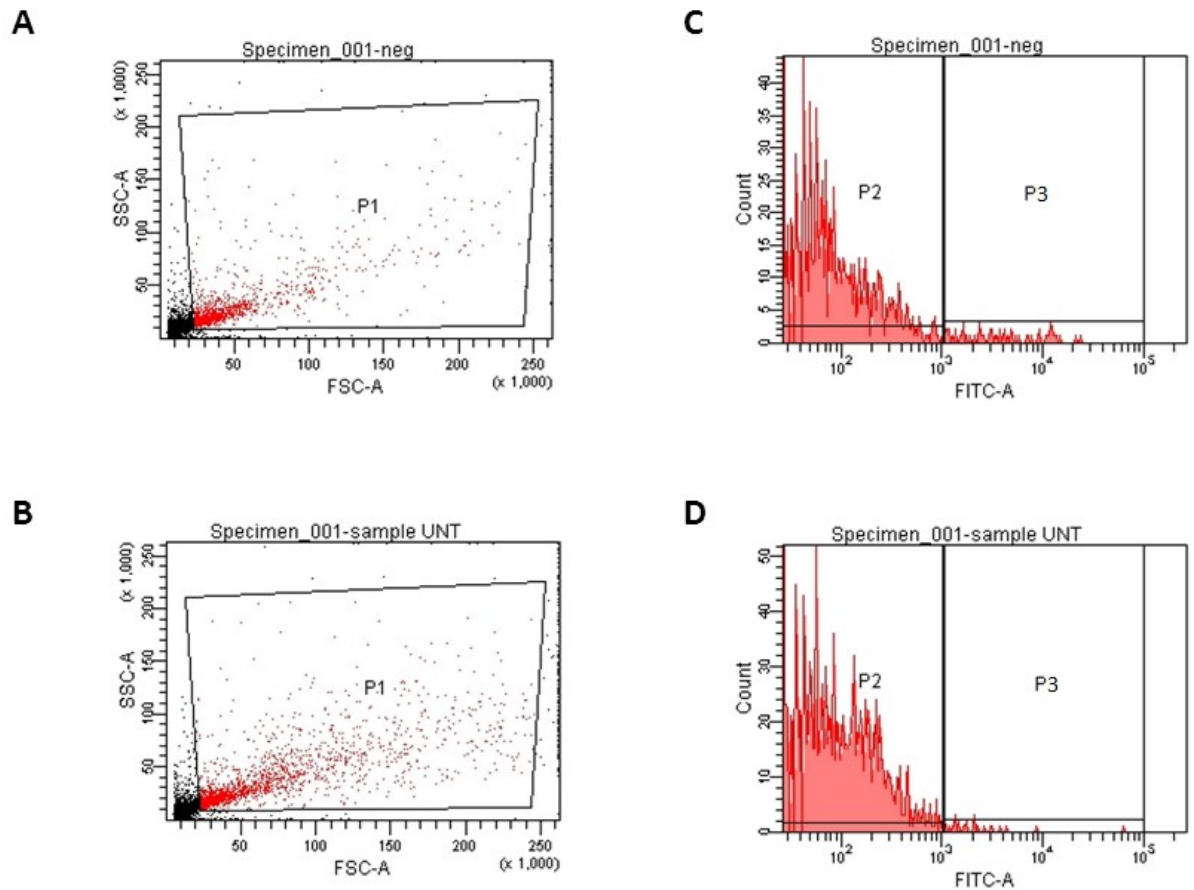


Figure 5.28 2D scatter plots and fluorescence intensity histograms of HSPA protein levels for the NHA cell lines pre hypoxia treatment. No fluorescence intensity was observed in the NHA cell line (**A**, negative, primary antibody omitted and **B**, sample) 2D scatter plot showing cell population of interest (P1), (**C**, negative, **D**, sample) fluorescent intensity histogram showing cells positive (P3) and negative (P2) for HSPA. Data values are for three independent experiments considering 10,000 events per sample.

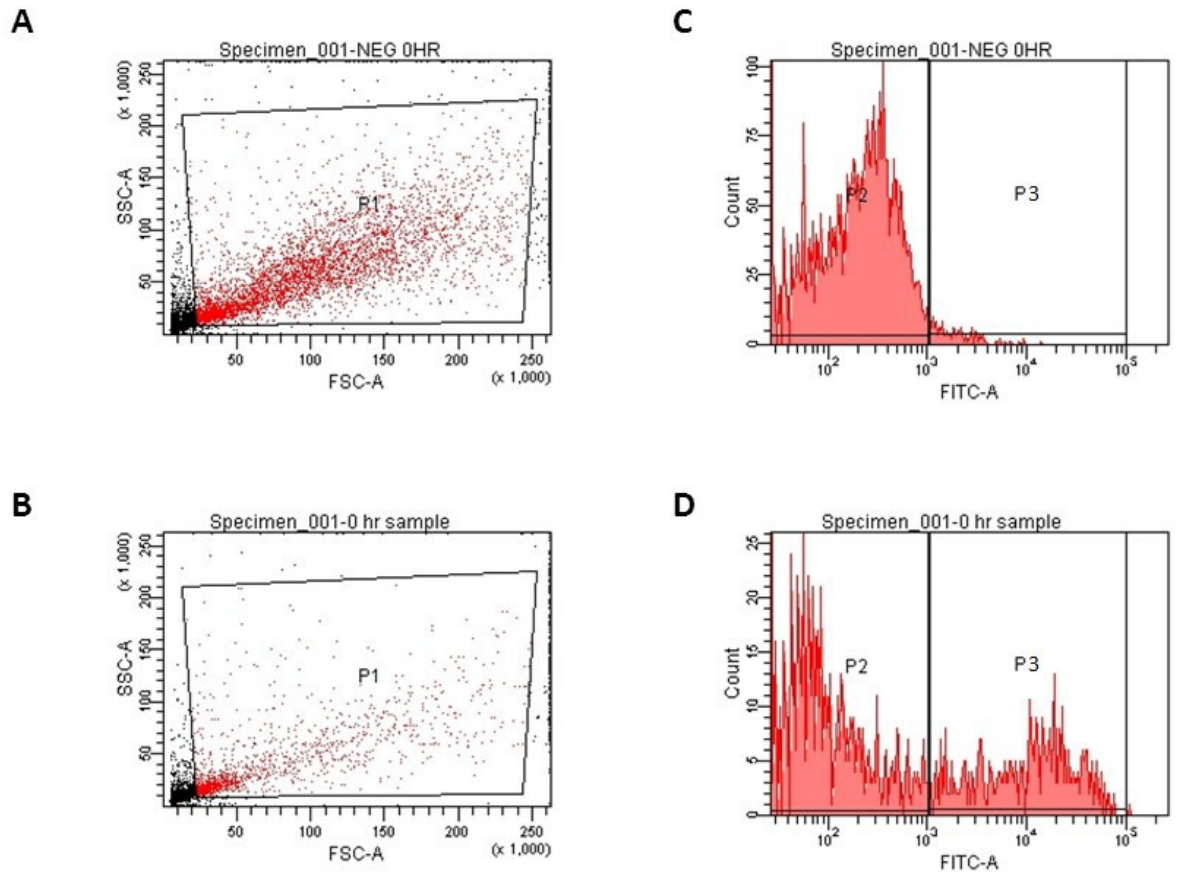


Figure 5.29 2D scatter plots and fluorescence intensity histograms of HSPA protein levels for the NHA cell lines post hypoxia treatment after 0 h recovery. Approximately 33% of NHA cells showed positive for HSPA. (**A**, negative, primary antibody omitted and **B**, sample) 2D scatter plot showing cell population of interest (P1), (**C**, negative, **D**, sample) fluorescent intensity histogram showing cells positive (P3) and negative (P2) for HSPA. Data values are for three independent experiments considering 10,000 events per sample.

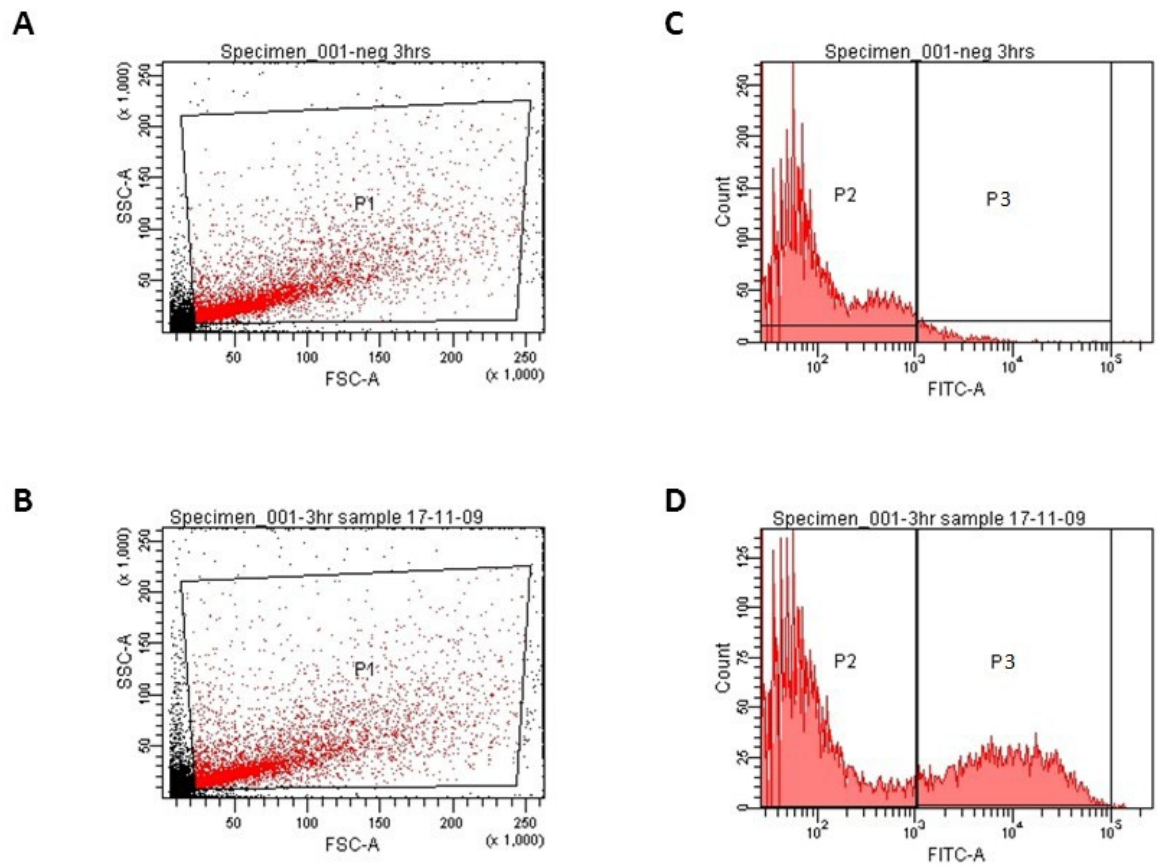


Figure 5.30 2D scatter plots and fluorescence intensity histograms of HSPA protein levels for the NHA cell lines post hypoxia treatment after 3 h recovery. Approximately 31% of NHA cells showed positive for HSPA. (**A**, negative, primary antibody omitted and **B**, sample) 2D scatter plot showing cell population of interest (P1), (**C**, negative, **D**, sample) fluorescent intensity histogram showing cells positive (P5) and negative (P2) for HSPA. Data values are for three independent experiments considering 10,000 events per sample.

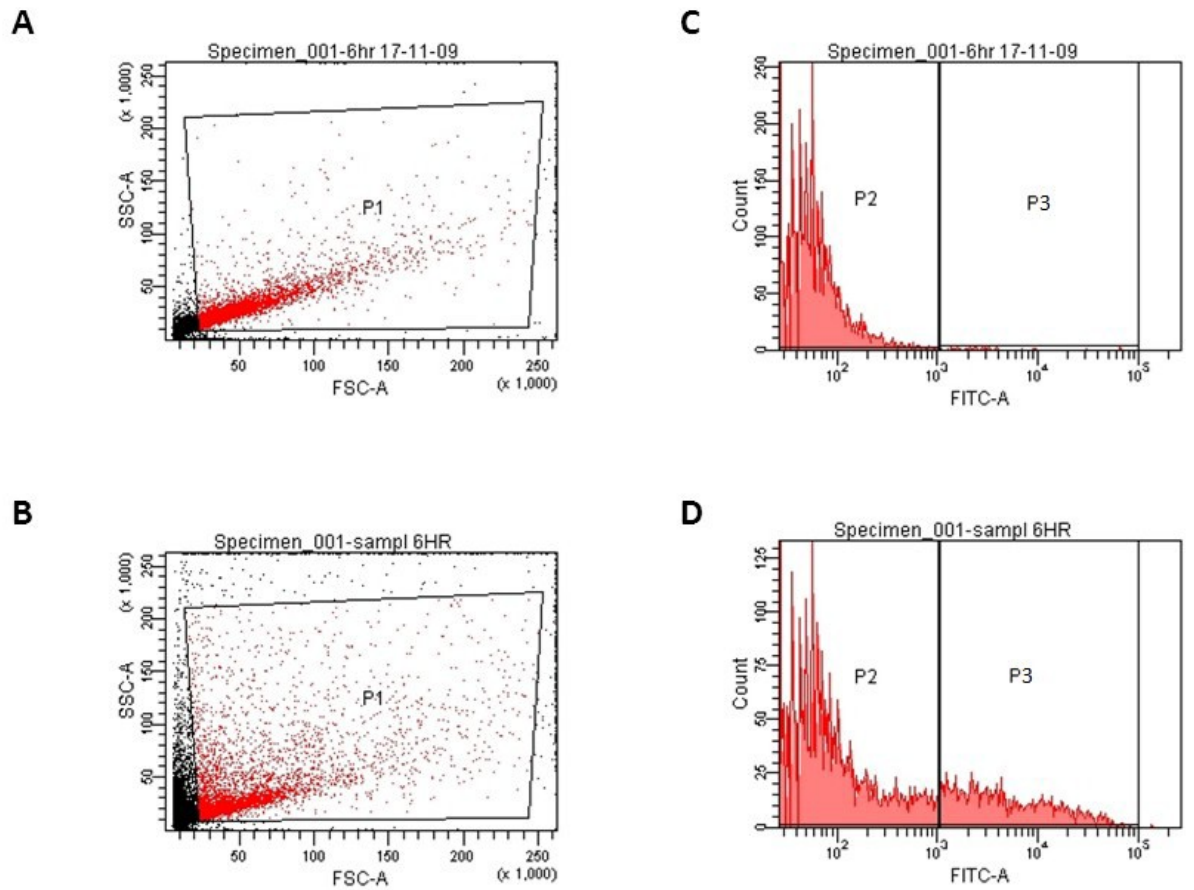


Figure 5.31 2D scatter plots and fluorescence intensity histograms of HSPA protein levels for the NHA cell lines post hypoxia treatment after 6 h recovery. Approximately 25% of NHA cells showed positive for HSPA. (**A**, negative, primary antibody omitted and **B**, sample) 2D scatter plot showing cell population of interest (P1), (**C**, negative, **D**, sample) fluorescent intensity histogram showing cells positive (P3) and negative (P2) for HSPA. Data values are for three independent experiments considering 10,000 events per sample.

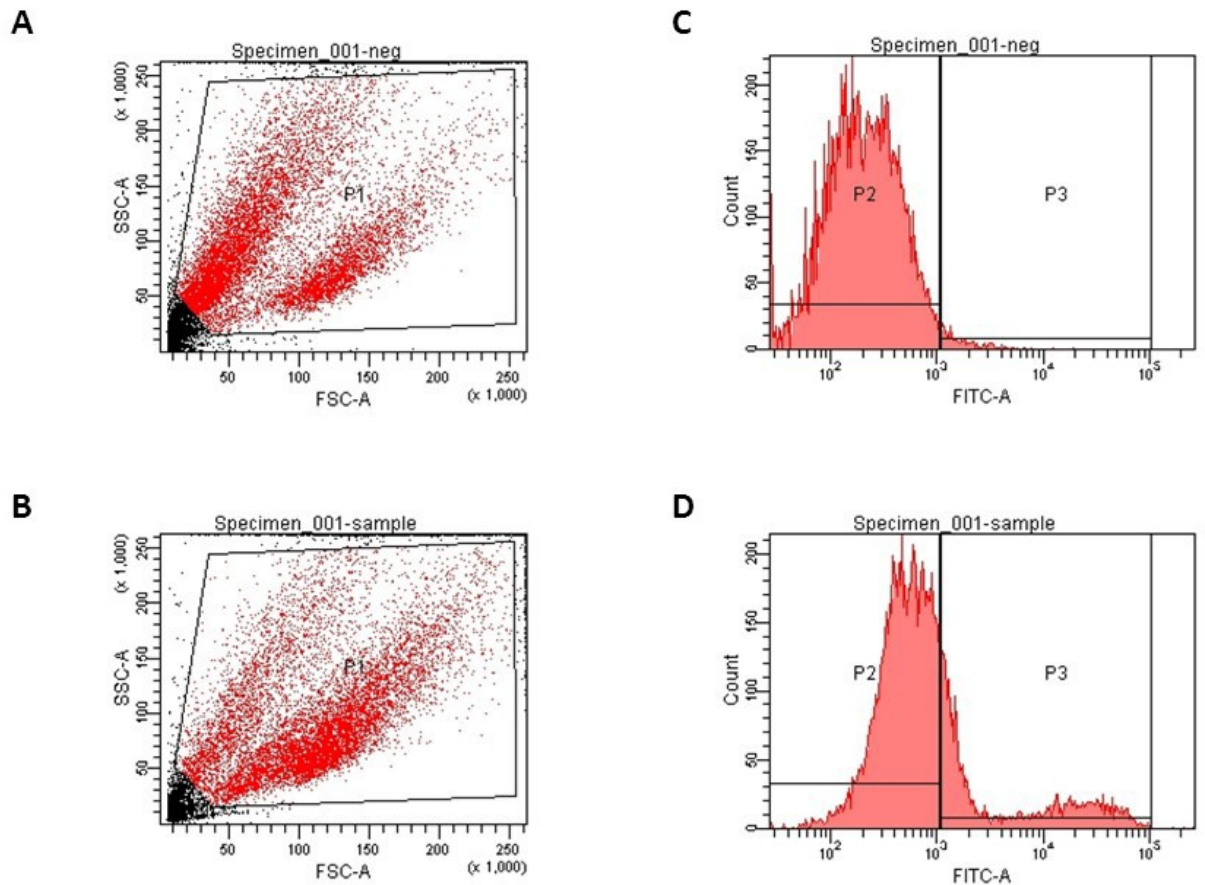


Figure 5.32 2D scatter plots and fluorescence intensity histograms of HSPA protein levels for the NHA cell lines post hypoxia treatment after 24 h recovery. Approximately 11% of NHA cells showed positive for HSPA. (**A**, negative, primary antibody omitted and **B**, sample) 2D scatter plot showing cell population of interest (P1), (**C**, negative, **D**, sample) fluorescent intensity histogram showing cells positive (P3) and negative (P2) for HSPA. Data values are for three independent experiments considering 10,000 events per sample.

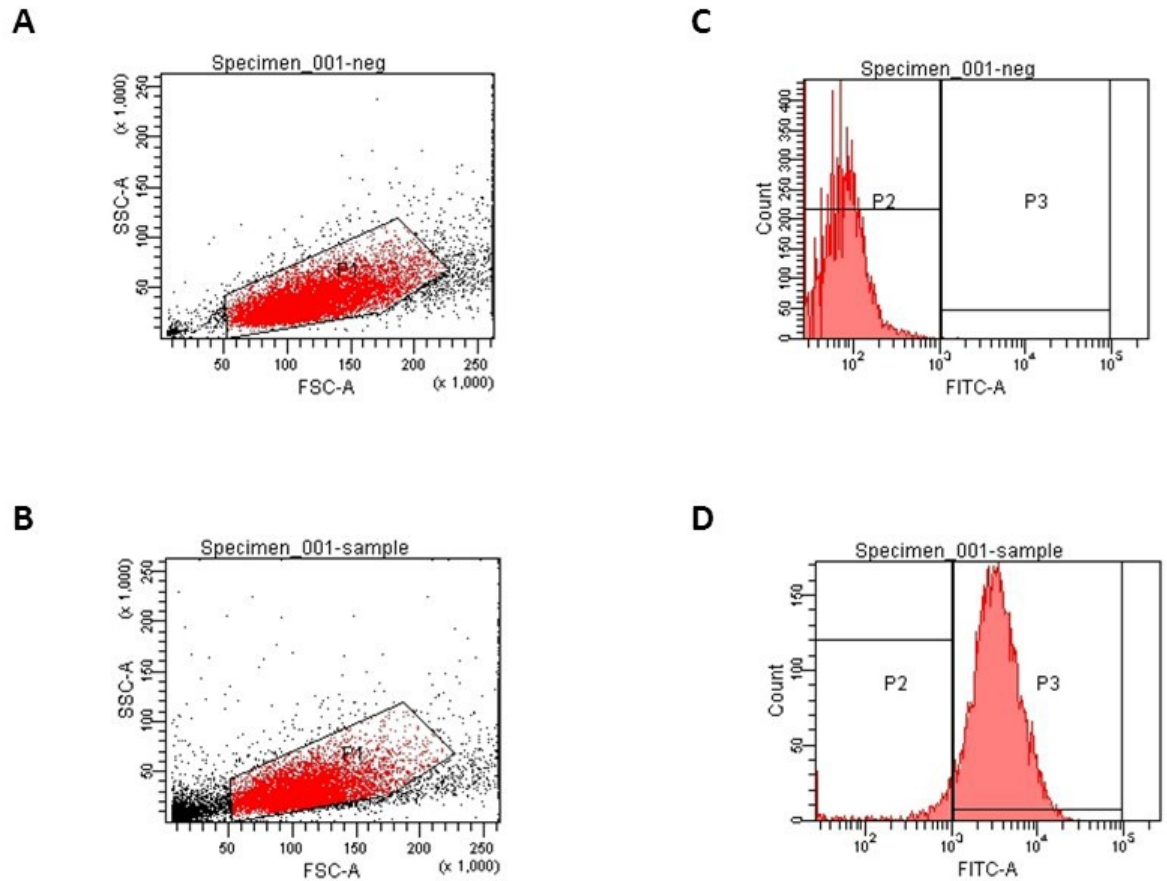


Figure 5.33 2D scatter plots and fluorescence intensity histograms of HSPA protein levels for the 1321N1 cell lines pre hypoxia treatment. Approximately 97% of 1321N1 glioma cells showed positive for HSPA. (**A**, negative, primary antibody omitted and **B**, sample) 2D scatter plot showing cell population of interest (P1), (**C**, negative, **D**, sample) fluorescent intensity histogram showing cells positive (P3) and negative (P2) for HSPA. Data values are for three independent experiments considering 10,000 events per sample.

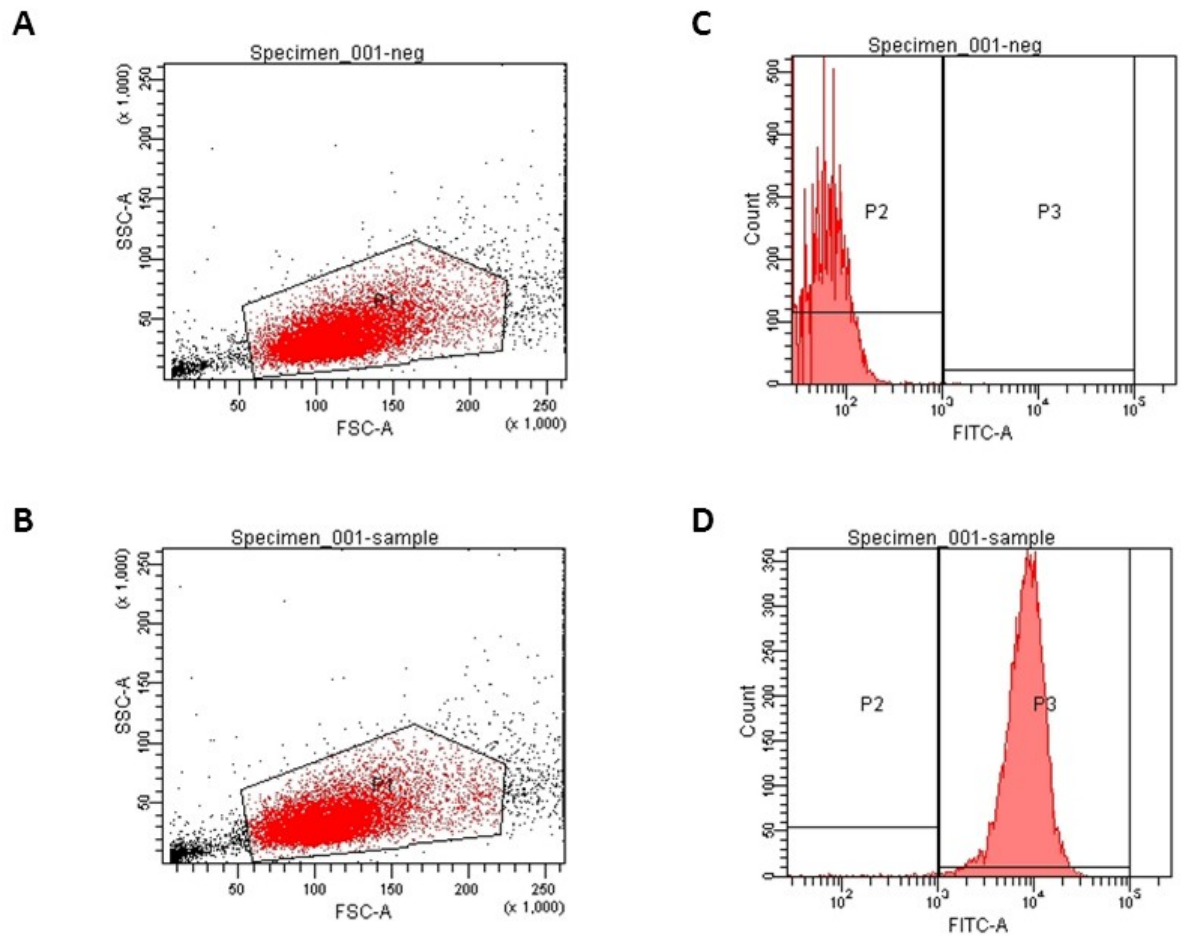


Figure 5.34 2D scatter plots and fluorescence intensity histograms of HSPA protein levels for the 1321N1 cell lines post hypoxia treatment after 0 h recovery. Approximately 99% of 1321N1 glioma cells showed positive for HSPA. (**A**, negative, primary antibody omitted and **B**, sample) 2D scatter plot showing cell population of interest (P1), (**C**, negative, **D**, sample) fluorescent intensity histogram showing cells positive (P3) and negative (P2) for HSPA. Data values are for three independent experiments considering 10,000 events per sample.

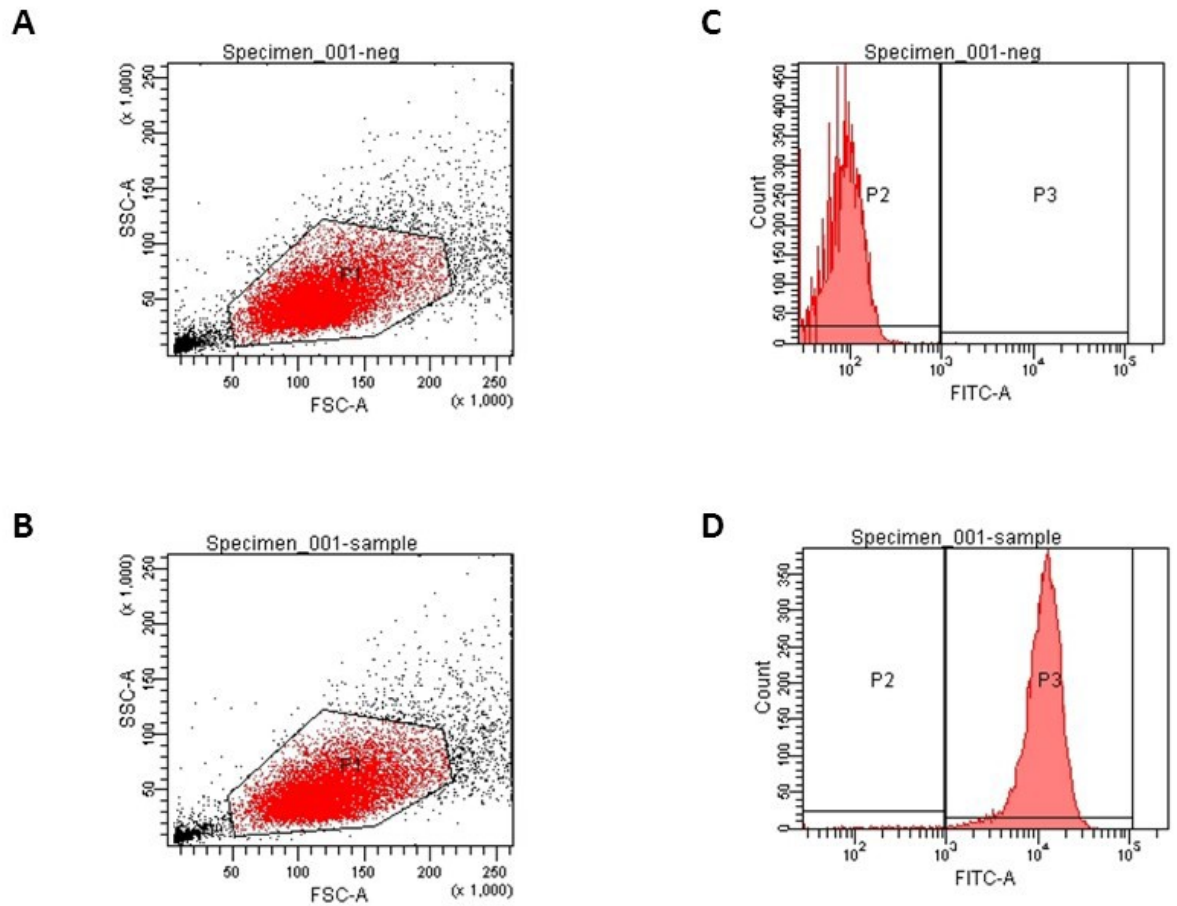


Figure 5.35 2D scatter plots and fluorescence intensity histograms of HSPA protein levels for the 1321N1 cell lines post hypoxia treatment after 3 h recovery. Approximately 99% of 1321N1 glioma cells showed positive for HSPA. (A, negative, primary antibody omitted and B, sample) 2D scatter plot showing cell population of interest (P1), (C, negative, D, sample) fluorescent intensity histogram showing cells positive (P3) and negative (P2) for HSPA. Data values are for three independent experiments considering 10,000 events per sample.

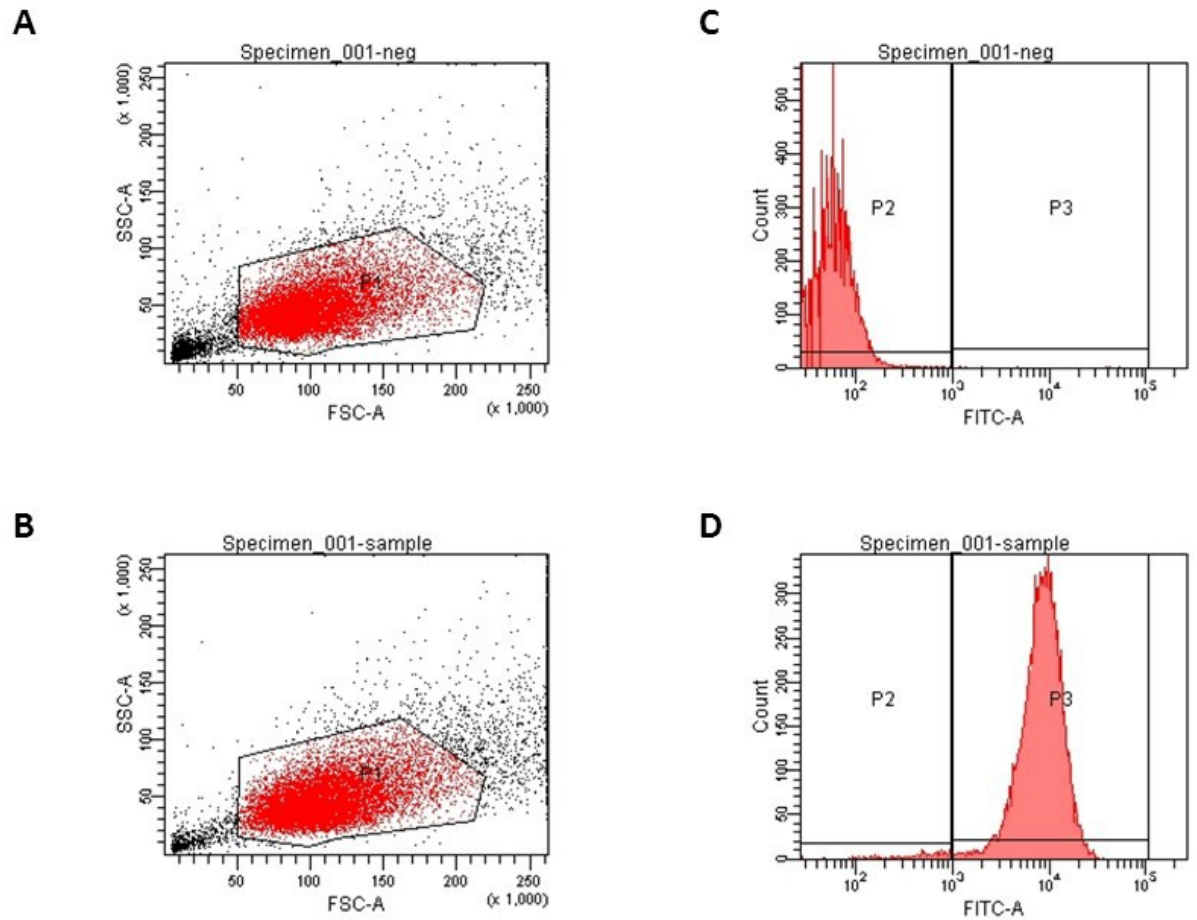


Figure 5.36 2D scatter plots and fluorescence intensity histograms of HSPA protein levels for the 1321N1 cell lines post hypoxia treatment after 6 h recovery. Approximately 99% of 1321N1 glioma cells showed positive for HSPA. (**A**, negative, primary antibody omitted and **B**, sample) 2D scatter plot showing cell population of interest (P1), (**C**, negative, **D**, sample) fluorescent intensity histogram showing cells positive (P3) and negative (P2) for HSPA. Data values are for three independent experiments considering 10,000 events per sample.

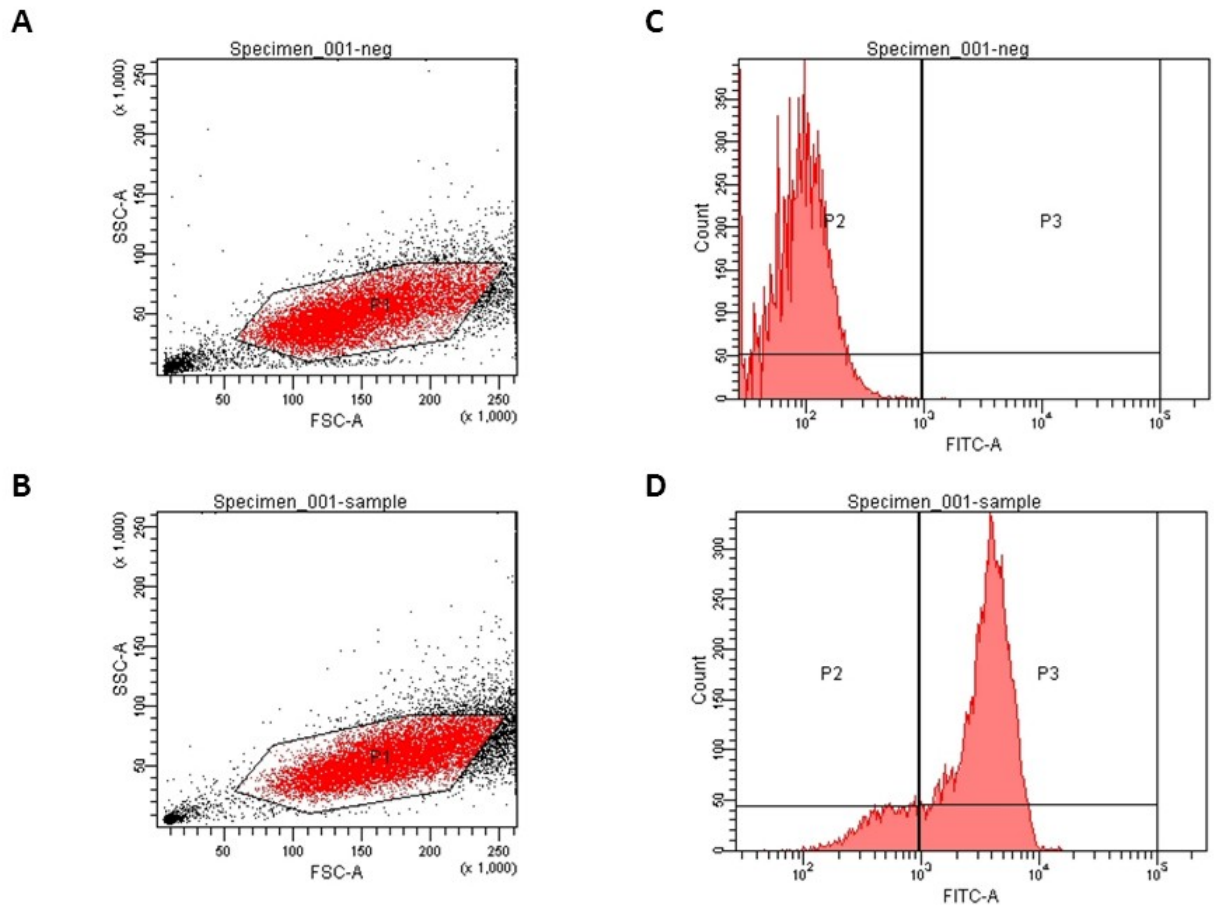


Figure 5.37 2D scatter plots and fluorescence intensity histograms of HSPA protein levels for the 1321N1 cell lines post hypoxia treatment after 24 h recovery. Approximately 94% of 1321N1 glioma cells showed positive for HSPA. (**A**, negative, primary antibody omitted and **B**, sample) 2D scatter plot showing cell population of interest (P1), (**C**, negative, **D**, sample) fluorescent intensity histogram showing cells positive (P3) and negative (P2) for HSPA. Data values are for three independent experiments considering 10,000 events per sample.

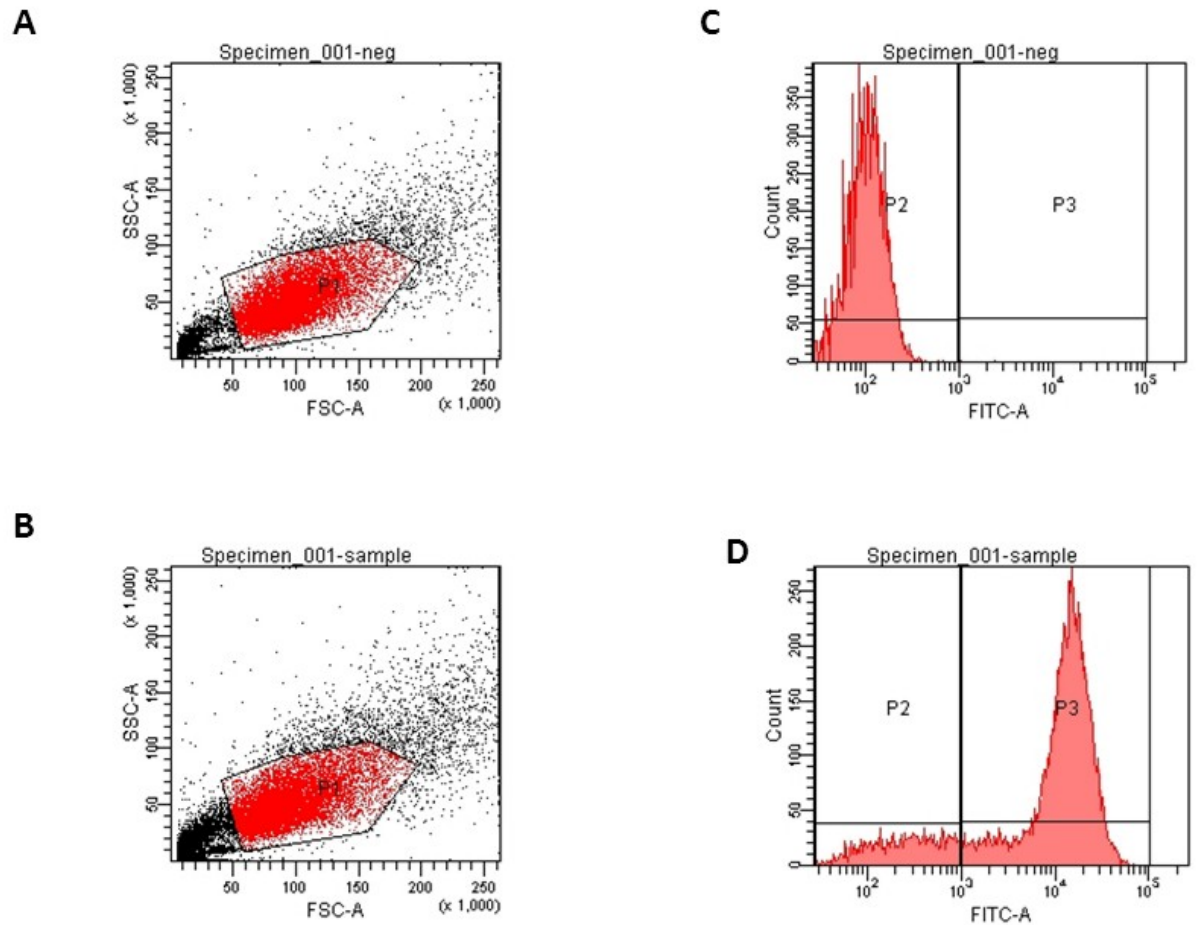


Figure 5.38 2D scatter plots and fluorescence intensity histograms of HSPA protein levels for the GOS-3 cell lines pre hypoxia treatment. Approximately 89% of GOS-3 glioma cells showed positive for HSPA. (**A**, negative, primary antibody omitted and **B**, sample) 2D scatter plot showing cell population of interest (P1), (**C**, negative, **D**, sample) fluorescent intensity histogram showing cells positive (P3) and negative (P2) for HSPA. Data values are for three independent experiments considering 10,000 events per sample.

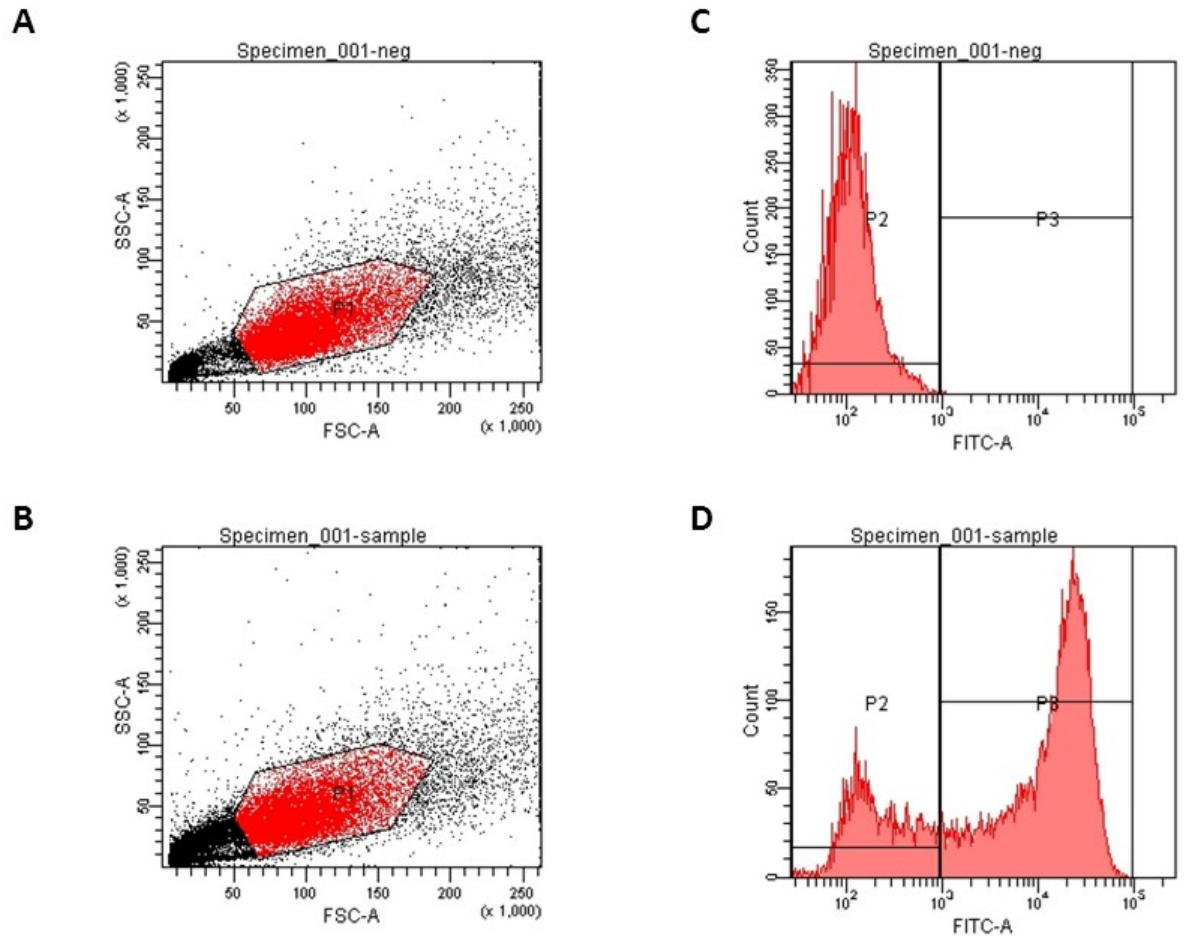


Figure 5.39 2D scatter plots and fluorescence intensity histograms of HSPA protein levels for the GOS-3 cell lines post hypoxia treatment after 0 h recovery. Approximately 73% of GOS-3 glioma cells showed positive for HSPA. (**A**, negative, primary antibody omitted and **B**, sample) 2D scatter plot showing cell population of interest (P1), (**C**, negative, **D**, sample) fluorescent intensity histogram showing cells positive (P3) and negative (P2) for HSPA. Data values are for three independent experiments considering 10,000 events per sample.

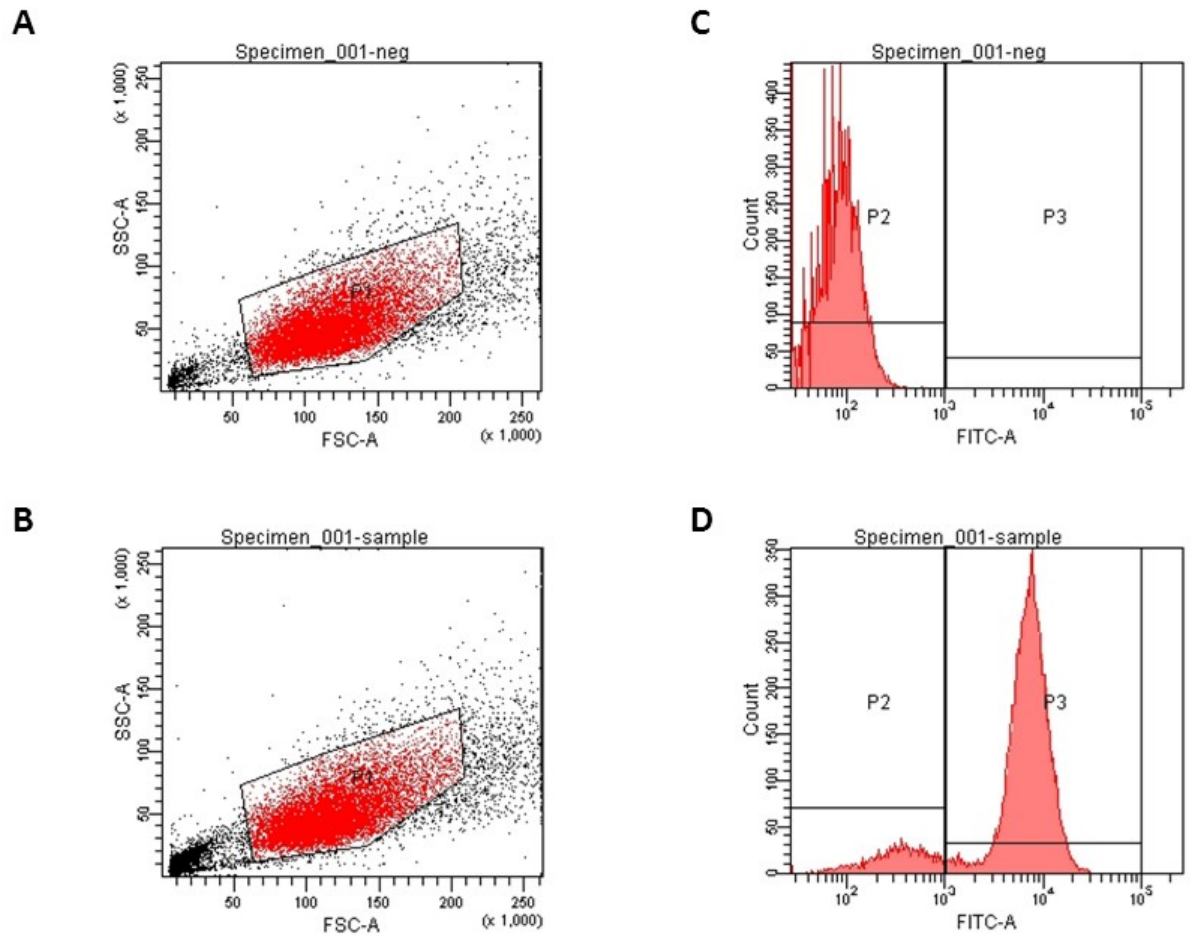


Figure 5.40 2D scatter plots and fluorescence intensity histograms of HSPA protein levels for the GOS-3 cell lines post hypoxia treatment after 3 h recovery. Approximately 92% of GOS-3 glioma cells showed positive for HSPA. (**A**, negative, primary antibody omitted and **B**, sample) 2D scatter plot showing cell population of interest (P1), (**C**, negative, **D**, sample) fluorescent intensity histogram showing cells positive (P3) and negative (P2) for HSPA. Data values are for three independent experiments considering 10,000 events per sample.

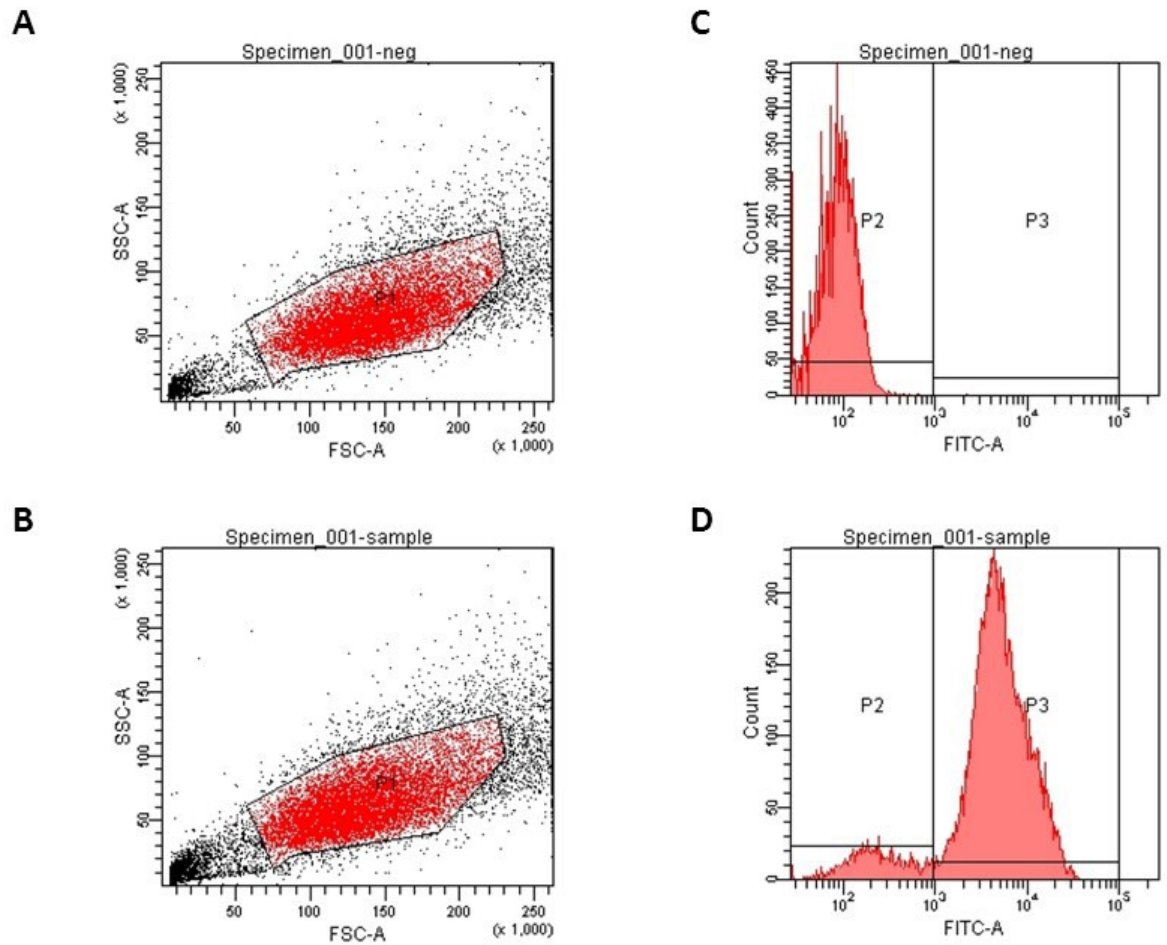


Figure 5.41 2D scatter plots and fluorescence intensity histograms of HSPA protein levels for the GOS-3 cell lines post hypoxia treatment after 6 h recovery. Approximately 92% of GOS-3 glioma cells showed positive for HSPA. (**A**, negative, primary antibody omitted and **B**, sample) 2D scatter plot showing cell population of interest (P1), (**C**, negative, **D**, sample) fluorescent intensity histogram showing cells positive (P3) and negative (P2) for HSPA. Data values are for three independent experiments considering 10,000 events per sample.

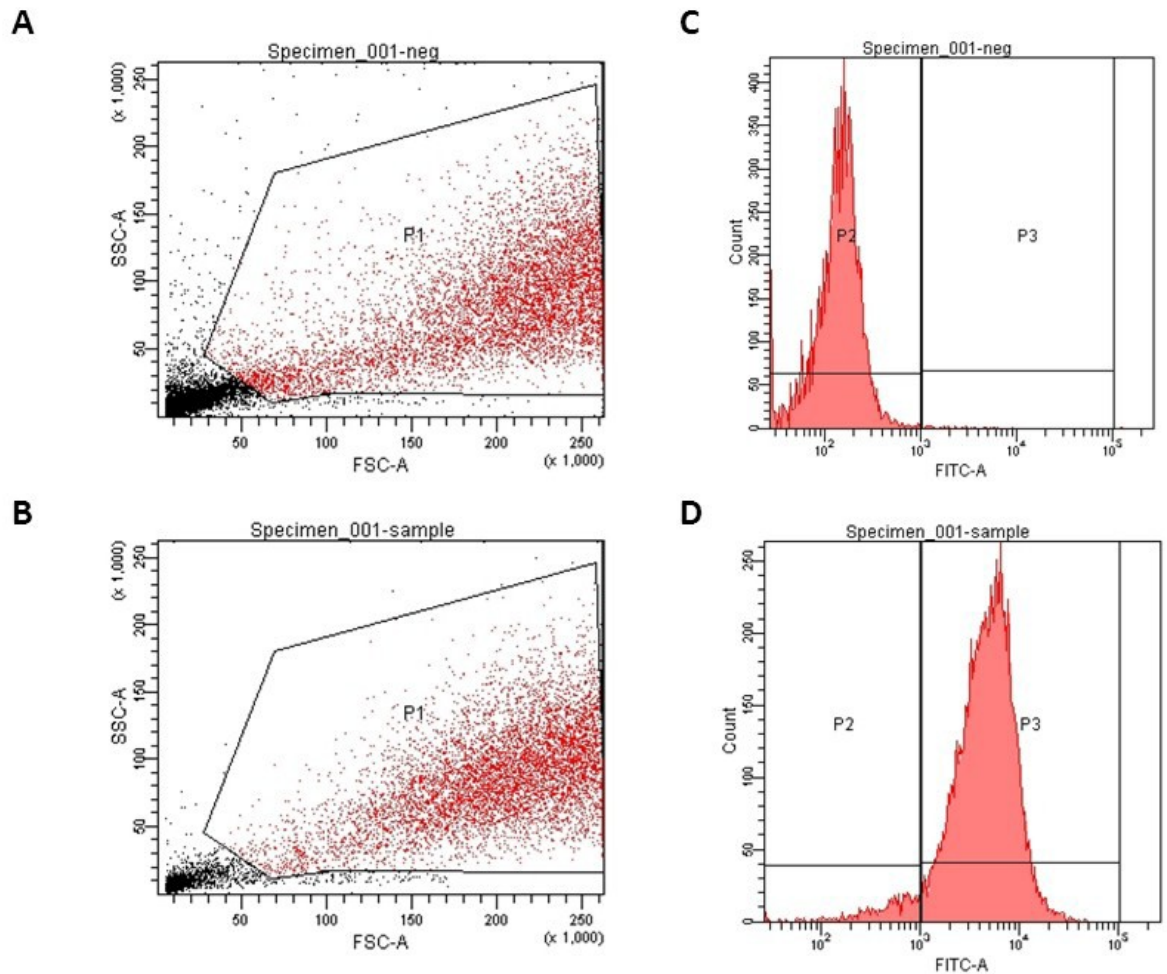


Figure 5.42 2D scatter plots and fluorescence intensity histograms of HSPA protein levels for the GOS-3 cell lines post hypoxia treatment after 24 h recovery. Approximately 97% of GOS-3 glioma cells showed positive for HSPA. (A, negative, primary antibody omitted and B, sample) 2D scatter plot showing cell population of interest (P1), (C, negative, D, sample) fluorescent intensity histogram showing cells positive (P3) and negative (P2) for HSPA. Data values are for three independent experiments considering 10,000 events per sample.

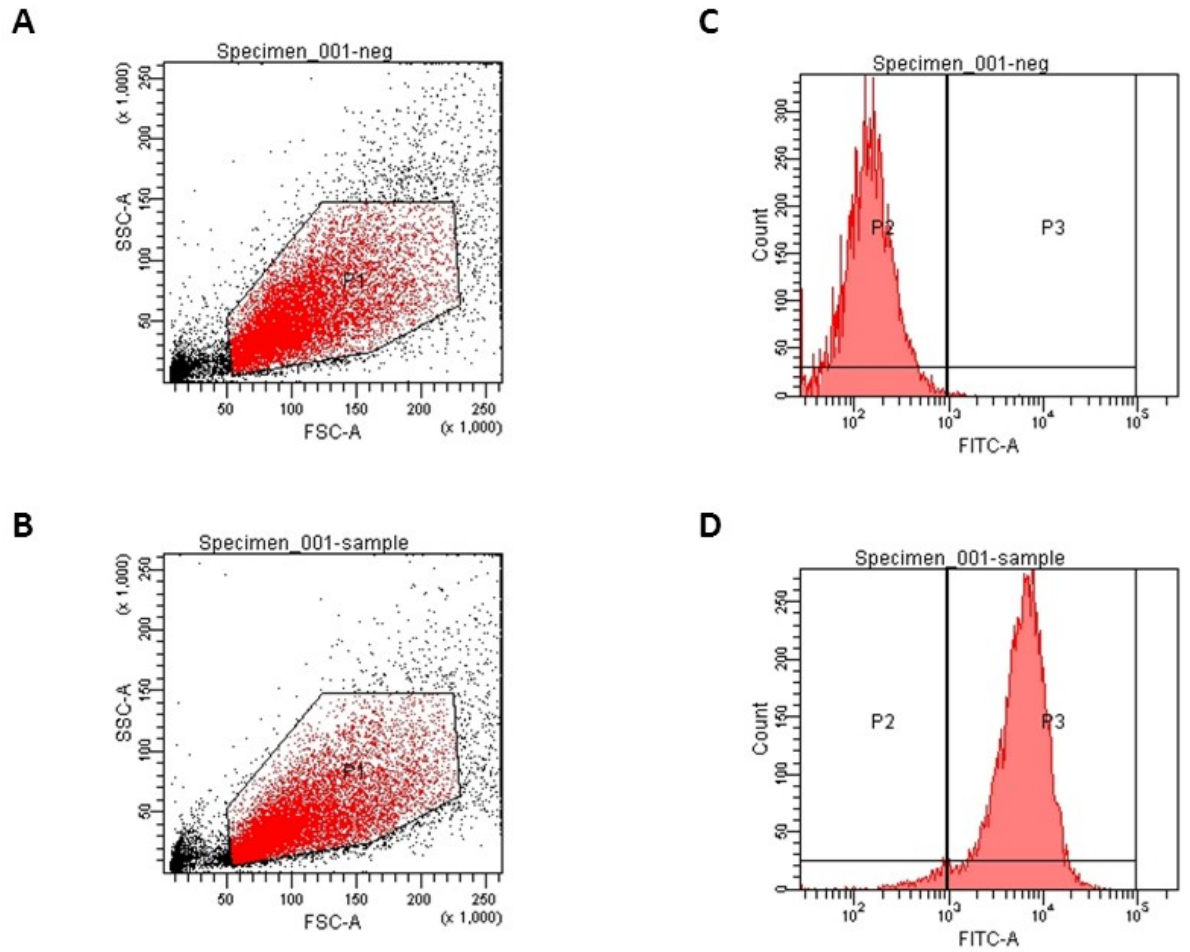


Figure 5.43 2D scatter plots and fluorescence intensity histograms of HSPA protein levels for the U87-MG cell lines pre hypoxia treatment. Approximately 97% of U87-MG glioma cells showed positive for HSPA. (**A**, negative, primary antibody omitted and **B**, sample) 2D scatter plot showing cell population of interest (P1), (**C**, negative, **D**, sample) fluorescent intensity histogram showing cells positive (P3) and negative (P2) for HSPA. Data values are for three independent experiments considering 10,000 events per sample.

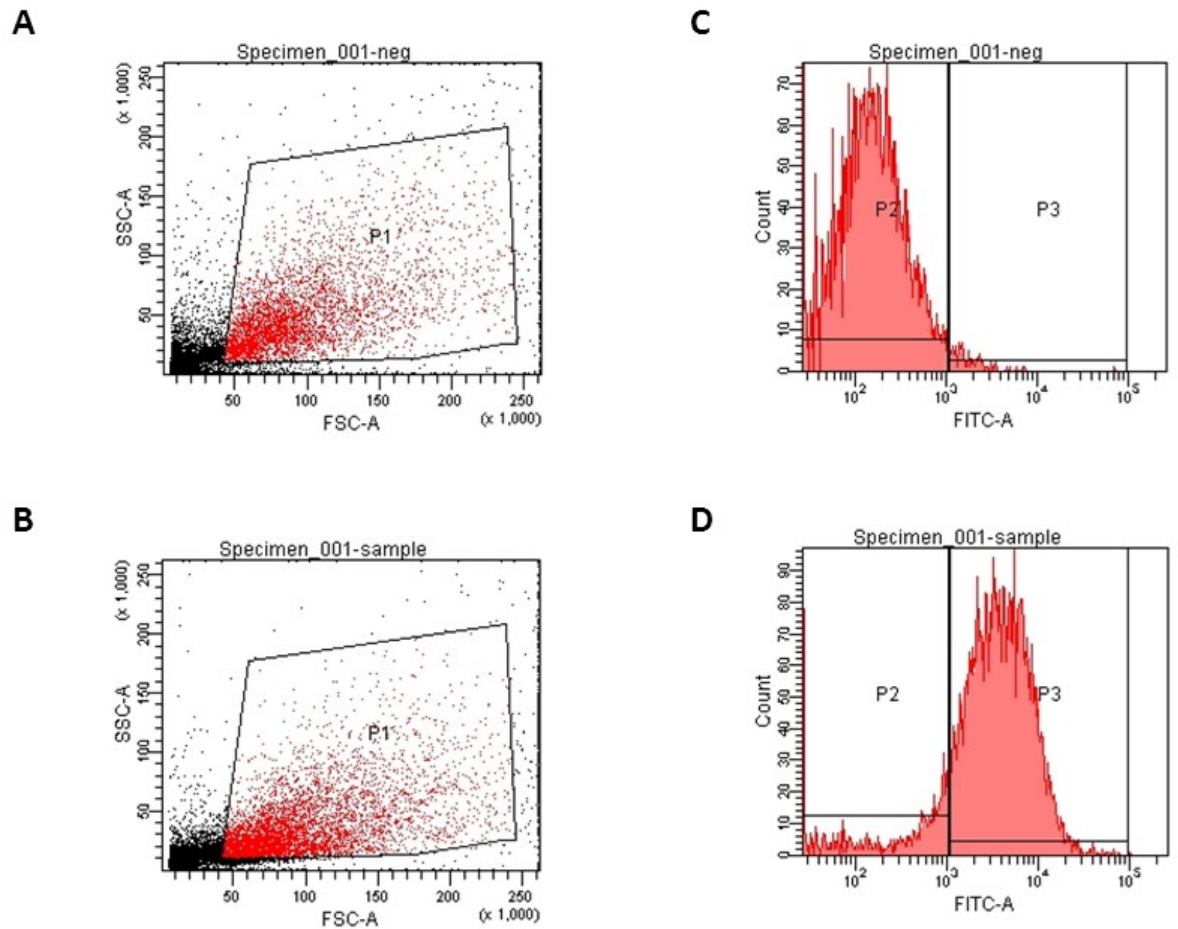


Figure 5.44 2D scatter plots and fluorescence intensity histograms of HSPA protein levels for the U87-MG cell lines post hypoxia treatment after 0 h recovery. Approximately 84% of U87-MG glioma cells showed positive for HSPA. (**A**, negative, primary antibody omitted and **B**, sample) 2D scatter plot showing cell population of interest (P1), (**C**, negative, **D**, sample) fluorescent intensity histogram showing cells positive (P3) and negative (P2) for HSPA. Data values are for three independent experiments considering 10,000 events per sample.

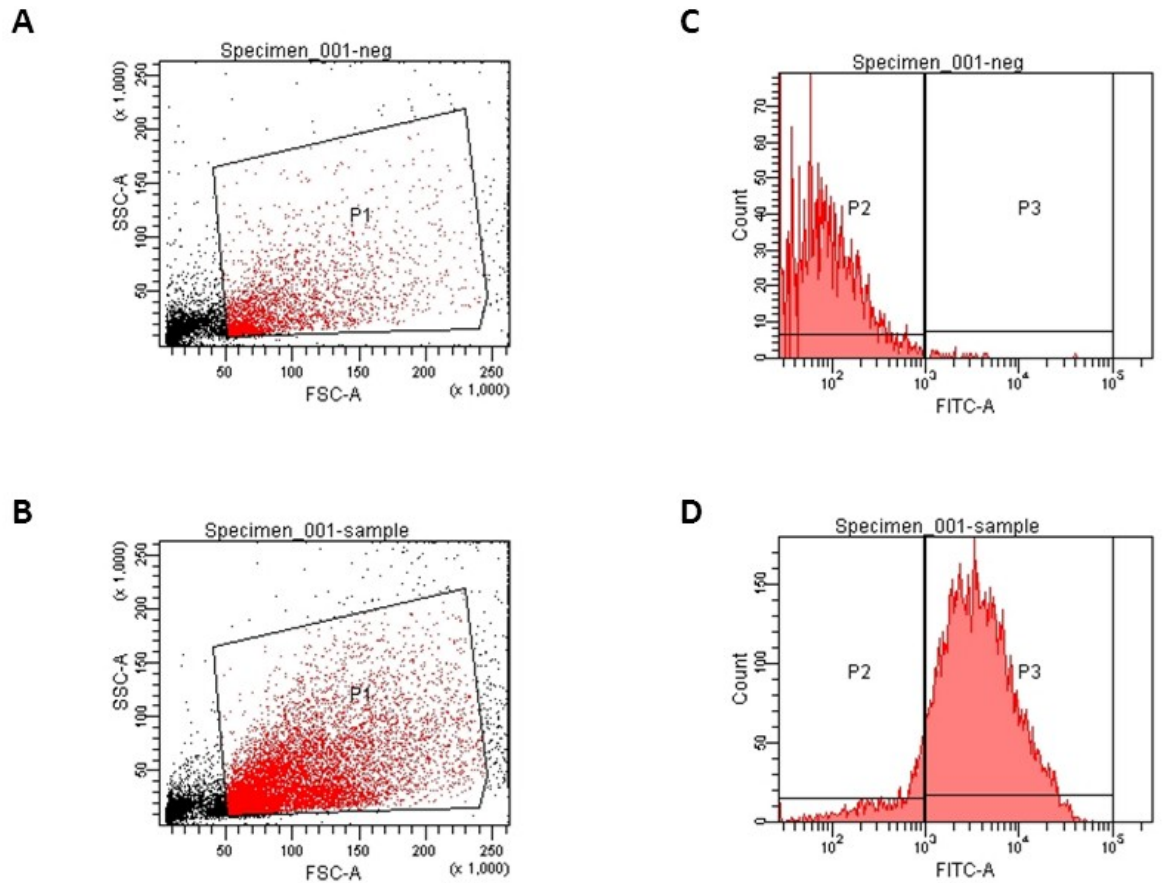


Figure 5.45 2D scatter plots and fluorescence intensity histograms of HSPA protein levels for the U87-MG cell lines post hypoxia treatment after 3 h recovery. Approximately 91% of U87-MG glioma cells showed positive for HSPA. (A, negative, primary antibody omitted and B, sample) 2D scatter plot showing cell population of interest (P1), (C, negative, D, sample) fluorescent intensity histogram showing cells positive (P3) and negative (P2) for HSPA. Data values are for three independent experiments considering 10,000 events per sample.

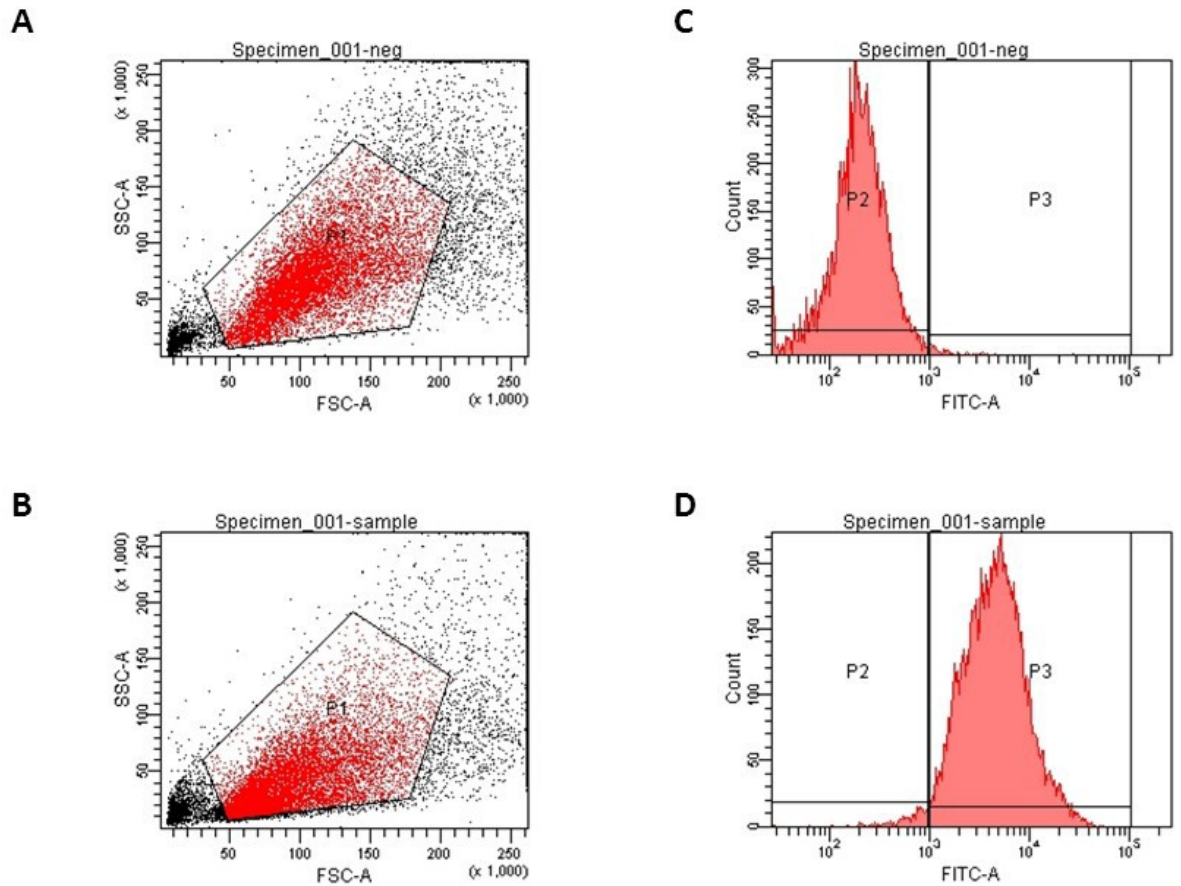


Figure 5.46 2D scatter plots and fluorescence intensity histograms of HSPA protein levels for the U87-MG cell lines post hypoxia treatment after 6 h recovery. Approximately 97% of U87-MG glioma cells showed positive for HSPA. (**A**, negative, primary antibody omitted and **B**, sample) 2D scatter plot showing cell population of interest (P1), (**C**, negative, **D**, sample) fluorescent intensity histogram showing cells positive (P3) and negative (P2) for HSPA. Data values are for three independent experiments considering 10,000 events per sample.

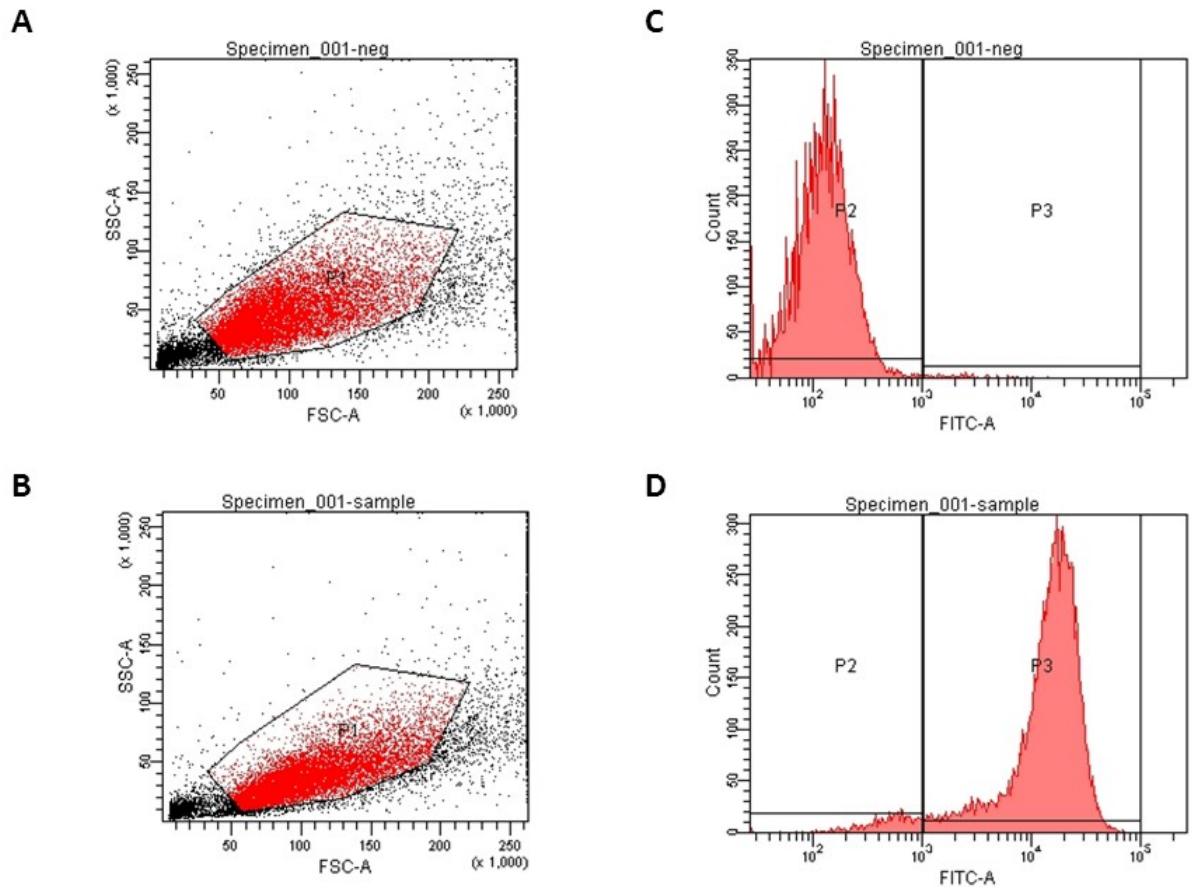


Figure 5.47 2D scatter plots and fluorescence intensity histograms of HSPA protein levels for the U87-MG cell lines post hypoxia treatment after 24 h recovery. Approximately 96% of U87-MG glioma cells showed positive for HSPA. (**A**, negative, primary antibody omitted and **B**, sample) 2D scatter plot showing cell population of interest (P1), (**C**, negative, **D**, sample) fluorescent intensity histogram showing cells positive (P3) and negative (P2) for HSPA. Data values are for three independent experiments considering 10,000 events per sample.

Results from this investigation show that *HSPA* is expressed at low levels in normal cells, but is highly expressed in cancer cell lines in pre- and post-hypoxia treatment. The average *HSPA* mRNA copy numbers in the three glioma cell lines for both pre- and post-hypoxia treatment were approximately 6 fold higher than the normal cell line.

As with *HSPA* mRNA, in both pre- and post-hypoxia treatment, high levels of HSPA protein were detected in the three glioma cell lines compared to low/barely detectable levels in the NHA cell line, indicating a direct correlation between *HSPA* mRNA and HSPA protein levels in glioma cell lines. High fluorescence intensity of HSPA observed in 1321N1, GOS-3 and U87-MG cells exposed to hypoxia showed a 3-fold increase compared to NHA cell line.

Again these results suggest that *HSPA* mRNA and HSPA protein levels in glioma may possibly be grade related, and therefore may be useful as a possible prognostic marker.

As expected, given that cancer is a form of cellular stress, HSPA protein was detected in both the cytoplasm and the nucleus of the three glioma cell lines under pre and post hypoxic conditions. Although HSPA protein was detected mainly in the cytoplasm in the normal (NHA) cell line pre-hypoxia, after hypoxia treatment migration of HSPA protein to the nucleus was observed.

Chapter 6

Effects of heat shock treatment on

***HSPA* gene expression in rat**

brain tissue

6.1 Gene Expression

HSPA expression is up-regulated in cells in response to heat shock and post-mortem conditions. The main research aims of this chapter was to measure and compare *HSPA* expression in normal and heat shocked post-mortem rat brain tissue and to characterise the possible “*de-novo*” expression of *HSPA* in response to severe heat shock.

Studies were undertaken using post-mortem brain tissue samples from aged-matched male Wistar rats (obtained from the Physiology Laboratory, University of Central Lancashire). All procedures conformed to the –UK Animals (Scientific Procedures) Act 1986 conforming to the –Principles of Laboratory Animal Care, 1985.

Rat brain tissue excised at 0, 3, 6, 12 and 24 h post sacrifice was subjected to mild heat shock at 0 h time course interval. For thermotolerance studies, brain tissue was subjected to mild heat shock at 0 h and again at 3, 6 and 24 h time course periods. Mild heat shock was conducted by immersion of the brain tissue, held in sterile 1.5 microfuge tubes, into a heated water bath at 42°C for a period of 10 min, after which brain tissue samples were stored at room temperature. Samples weighing approximately 50 mg were excised at timed intervals of 0, 3, 6, 12 and 24 h post sacrifice. Excised samples were immediately weighed and snap-frozen by immersion in liquid nitrogen, followed by grinding of the tissue to a fine powder using a sterile pestle and mortar, again under liquid nitrogen.

mRNA was isolated from post-mortem rat brain tissue, using mRNA Isolation Kit (Roche,UK) following the manufacturer’s protocol. The concentration and purity of mRNA was determined by ultraviolet spectrophotometry. Isolated mRNA (100 ng) was

transcribed to cDNA using 1st Strand cDNA Synthesis Kit for RT-PCR (AMV) (Roche, UK) following the manufacturer's protocol, which was then used as a template for qRT-PCR. Quantitative real-time PCR was used to evaluate the expression of *HSPA* and GAPDH as a control using FastStart DNA Master^{PLUS} SYBR Green 1 (Roche, UK).

Primers used for *HSPA* were 5' GTGTGGAGAGCCAAGAGGAG 3' (sense) and 5' TTTCCAAACTGGATCGAAGG 3' (antisense). For GAPDH, primers were 5' AGACAGCCGCATCTTCTTGT 3' (sense) and 5' CTTGCCGTGGGTAGAGTCAT 3' (antisense). All primers were designed using Primer3 software and manufactured by TIB MOLBIOL.

After an initial denaturation at 95°C for 10 min, the samples were subjected to 35 cycles of RT-PCR 95°C for 10 s, annealing temperature 56°C (*HSPA*) and 57°C (GAPDH) for 15 s, and 72°C for 15 s (Patel *et al.*, 2008). At the end of each cycle, the fluorescence emitted was measured in a single step in channel F1 (gain1). After the 35th cycle, the specimens were heated to 95°C and rapidly cooled to 65°C for 15 s. All heating and cooling steps were performed with a slope of 20°C / s. The temperature was subsequently raised to 95°C with a slope of 0.1°C / s and fluorescence was measured continuously (channel F1, gain1) to obtain data for the melting curve analysis. All PCR reactions were performed in triplicate and a negative control included, which contained primers with no DNA. All PCR products were analysed using gel electrophoresis stained and visualised using a gel analyser (SynGene, UK).

Expression of *HSPA* was measured in rat post-mortem brain tissue at post-mortem intervals 0, 3, 6, 12 and 24 h and at time course intervals of 0, 3, 6, 12 and 24 h within each post-mortem interval. Post sacrifice, the brain was sectioned in two. Half was used for control (non-heat shock) and half was subjected to mild heat shock at 0 h time course for 10 min at 42°C.

The expression of *HSPA* was also measured in rat post-mortem brain tissue at post-mortem intervals 0, 3, 6 and 24 h and at time course intervals of 0, 3, 6 and 24 h within each post-mortem interval to access the effect of thermotolerance. Post sacrifice, the brain was sectioned in two, and half was used as a control (non-heat shock) and half was subjected to mild heat shock at 0 h time course for 10 min at 42°C, and then again at 3, 12 and 24 h time course intervals. The brain tissue both control and after heat shock at the various post-mortem intervals and time course was used for experiments concerning gene expression and immunofluorescence. *GAPDH* was used as an internal standard throughout all RT-PCR experiments (Barber *et al.*, 2005).

6.2 Constitutive Expression

6.2.1 Rat Brain tissue

Transcript copy numbers of *HSPA* and *GAPDH* were evaluated using RT-PCR in rat post-mortem brain tissue at post-mortem intervals 0, 3, 6, 12 and 24 h and at time course intervals of 0, 3, 6, 12 and 24 h within each post-mortem interval, for both control (non-heat shock) and mild heat shock treatment samples. The primers and optimal temperatures used for the amplification of both genes are documented in Table 2.10 in section 2.5. All PCR experiments were carried out in triplicate for consistency and repeatability. For each gene analysed, a quantification graph was produced to confirm gene amplification. The resulting amplicons for *HSPA* and *GAPDH* were then visualized using agarose gel electrophoresis, when they were represented by bands of 156 and 265 bp respectively.

At 0 h and 3 h post-mortem interval at 0, 3, 6, 12 and 24 h time course, heat shocked brain tissue contained *HSPA* transcripts at a higher level compared to that of the non-

heat shocked brain tissue (Figure 6.1 and 6.2). At 6 h post-mortem interval *HSPA* transcribed higher in heat shocked brain tissue at time course 0, 3, 12 and 24 h, but lower at the 6 h time course than non-heat shocked brain tissue (Figure 6.3). At 12 h post-mortem interval *HSPA* transcribed higher in heat shocked brain tissue at time course 0 and 12 h, but lower at the 3, 6 and 24 h time course than non-heat shocked brain tissue (Figure 6.4). At 24 h post-mortem interval *HSPA* transcribed higher in heat shocked brain tissue at time course intervals; 0, 3 and 24 h, but lower at the 6 h and 12 h time course intervals than non-heat shocked brain tissue (Figure 6.5).

GAPDH expression level remained relatively consistent throughout each set of experiments confirming it as an ideal reference gene (Figures 6.6 – 6.10).

The mRNA copy number per 100 ng of extracted mRNA for both genes was calculated for each time course 0, 3, 6, 12 and 24 h within each post-mortem interval 0, 3, 6, 12 and 24 h for both non-heat shock and heat shock to monitor the gene expression level. mRNA copy numbers confirmed that at: 0 h post-mortem interval, *HSPA* was expressed at a higher level in heat shocked brain tissue at different time course intervals, with approximately 21 copies after 0 h recovery, with approximately 52 copies after 3 h recovery, with approximately 83 copies after 6 h recovery, with approximately 55 copies after 12 h recovery and approximately 31 copies after 24 h recovery compared to non-heat shocked brain tissue at different time course intervals, with approximately 19 copies after 0 h recovery, with approximately 38 copies after 3 h recovery, with approximately 55 copies after 6 h recovery, with approximately 36 copies after 12 h recovery and approximately 17 copies after 24 h recovery (Figure 6.1 and Table 6.1).

At 3 h post-mortem interval, *HSPA* was expressed at a higher level in heat shocked brain tissue at different time course intervals, with approximately 58 copies after 0 h

recovery, with approximately 53 copies after 3 h recovery, with approximately 15 copies after 6 h recovery, with approximately 45 copies after 12 h recovery and approximately 42 copies after 24 h recovery compared with non-heat shocked brain tissue at different time course intervals, with approximately 17 copies after 0 h recovery, with approximately 37 copies after 3 h recovery, with approximately 9 copies after 6 h recovery, with approximately 35 copies after 12 h recovery and approximately 36 copies after 24 h recovery (Figure 6.2 and Table 6.1).

At 6 h post-mortem interval, *HSPA* was expressed at a higher level in heat shocked brain tissue at different time course intervals, with approximately 19 copies after 0 h recovery, with approximately 34 copies after 3 h recovery, with approximately 21 copies after 12 h recovery and approximately 37 copies after 24 h recovery compared to non-heat shocked brain tissue at different time course intervals, with approximately 10 copies after 0 h recovery, with approximately 12 copies after 3 h recovery, with approximately 3 copies after 12 h recovery and approximately 17 copies after 24 h recovery. Expression was lower in heat shocked brain tissue after 6 h recovery, approximately 9 copies compared to non-heat shocked brain tissue after 6 h recovery, approximately 20 copies (Figure 6.3 and Table 6.1).

At 12 h post-mortem interval, *HSPA* was expressed at a higher level in heat shocked brain tissue at different time course intervals, with approximately 25 copies after 0 h recovery and approximately 67 copies after 12 h recovery compared to non-heat shocked brain tissue at different time course intervals, with approximately 18 copies after 0 h recovery and approximately 17 copies after 12 h recovery. Expression was lower in heat shocked brain tissue at different time course intervals, with approximately 38 copies after 3 h recovery, with approximately 23 copies after 6 h recovery and

approximately 30 copies after 24 h recovery compare to non-heat shocked brain tissue at different time course intervals, with approximately 57 copies after 3 h recovery, with approximately 65 copies after 6 h recovery and approximately 40 copies after 24 h recovery (Figure 6.4 and Table 6.1).

At 24 h post-mortem interval, *HSPA* was expressed at a higher level in heat shocked brain tissue at different time course intervals, with approximately 25 copies after 0 h recovery, with approximately 27 copies after 3 h recovery, with approximately 20 copies after 6 h recovery and approximately 23 copies after 24 h recovery compare to non-heat shocked brain tissue at different time course intervals, with approximately 12 copies after 0 h recovery, with approximately 2 copies after 3 h recovery, with approximately 13 copies after 6 h recovery and approximately 9 copies after 24 h recovery. Expression was lower in heat shocked brain tissue after 12 h recovery, approximately 4 copies compared to non-heat shocked brain tissue after 12 h recovery, approximately 4 copies (Figure 6.5, Table 6.1).

For *GAPDH*, mRNA copy numbers per 100 ng of extracted mRNA were relatively consistent throughout each PMI, time course in both non-heat shock and heat shocked brain tissue, with approximately 268,500 copies for non-heat shock and approximately 267,300 copies for heat shock, again confirming comparability of *HSPA* results (Figures 6.6 – 6.10 and Table 6.2).

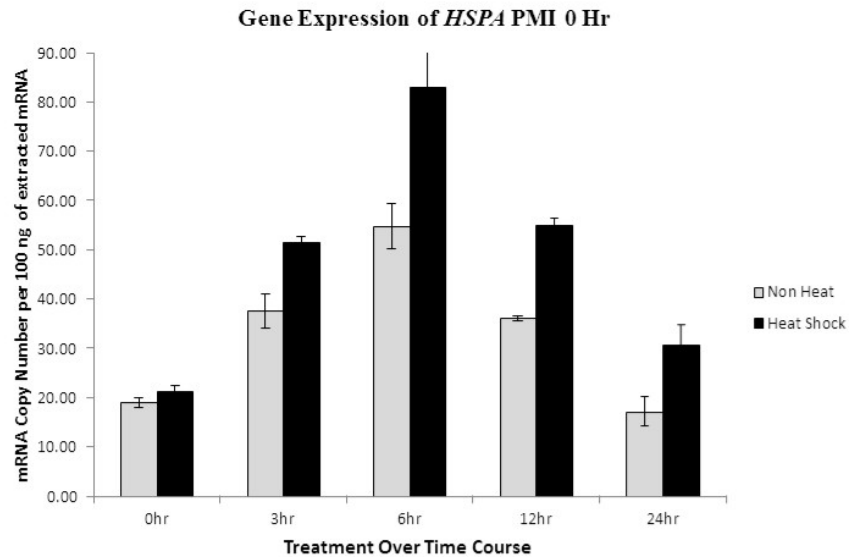
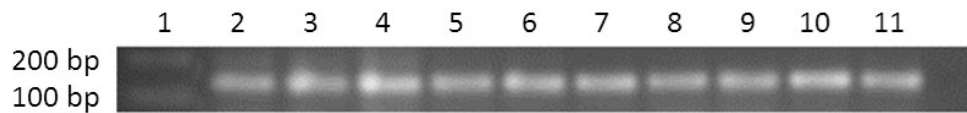


Figure 6.1 Transcription levels of *HSPA* mRNA in non-heat shock and heat shocked rat brain tissue at 0 h PMI. (A) agarose gel electrophoresis: Lane 1 represents the 100 bp molecular ladder; lanes 2, 4, 6, 8 and 10 represent amplicons from non-heat shocked rat brain tissue at time course intervals of 0, 3, 6, 12 and 24 h respectively. Lanes 3, 5, 7, 9 and 11 represent amplicons from heat shocked rat brain tissue at time course intervals of 0, 3, 6, 12 and 24 h respectively. (B) Histogram showing *HSPA* mRNA copy numbers for non-heat shock and heat shocked brain tissue at 0, 3, 6, 12 and 24 h time course intervals. Data values are the mean of three independent experiments, and the standard deviation from this mean is shown by the error bars.

Control samples show post-mortem effect, as *HSPA* transcripts increase over time.

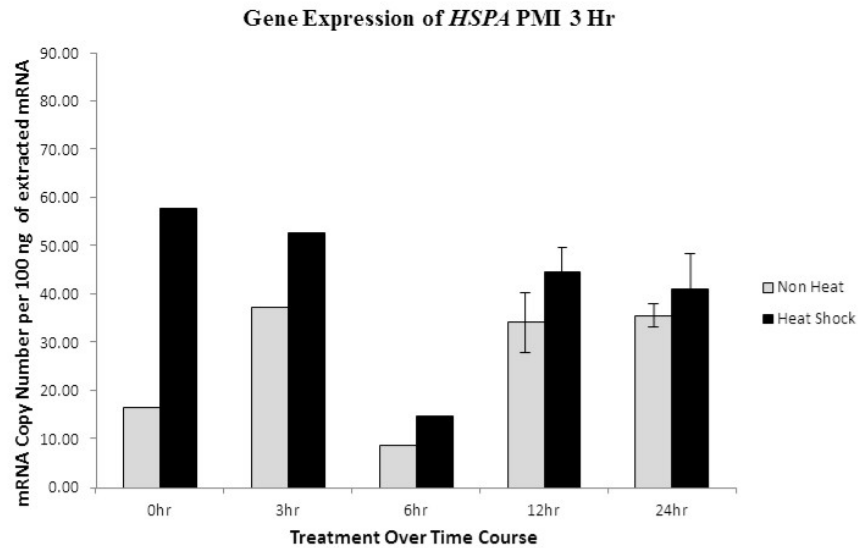
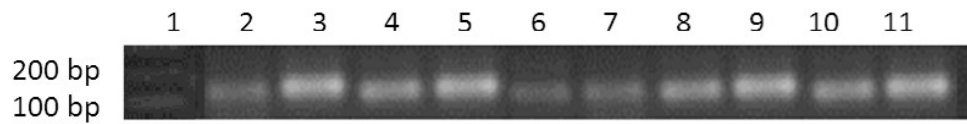


Figure 6.2 Transcription levels of *HSPA* mRNA in non-heat shock and heat shocked rat brain tissue at 3 h PMI. (A) agarose gel electrophoresis: Lane 1 represents the 100 bp molecular ladder; lanes 2, 4, 6, 8 and 10 represent amplicons from non-heat shocked rat brain tissue at time course intervals of 0, 3, 6, 12 and 24 h respectively. Lanes 3, 5, 7, 9 and 11 represent amplicons from heat shocked rat brain tissue at time course intervals of 0, 3, 6, 12 and 24 h respectively. (B) Histogram showing *HSPA* mRNA copy numbers for non-heat shock and heat shocked brain tissue at 0, 3, 6, 12 and 24 h time course intervals. Data values are the mean of three independent experiments, and the standard deviation from this mean is shown by the error bars. For both non-heat shock and heat shocked samples at time course intervals 0, 3 and 6 h no error bars are present as a 0 value standard deviation was calculated.

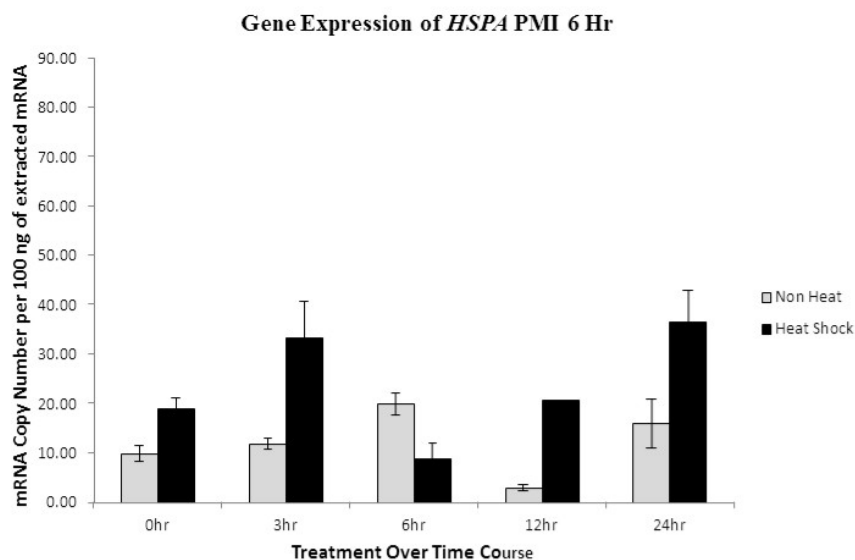
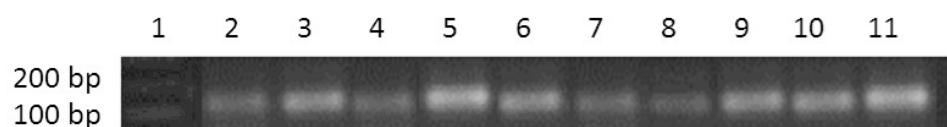


Figure 6.3 Transcription levels of *HSPA* mRNA in non-heat shock and heat shocked rat brain tissue at 6 h PMI. (A) Agarose gel electrophoresis: Lane 1 represents the 100 bp molecular ladder; lanes 2, 4, 6, 8 and 10 represent amplicons from non-heat shocked rat brain tissue at time course intervals of 0, 3, 6, 12 and 24 h respectively. Lanes 3, 5, 7, 9 and 11 represent amplicons from heat shocked rat brain tissue at time course intervals of 0, 3, 6, 12 and 24 h respectively. (B) Histogram showing *HSPA* mRNA copy numbers for non-heat shock and heat shocked brain tissue at 0, 3, 6, 12 and 24 h time course intervals. Data values are the mean of three independent experiments, and the standard deviation from this mean is shown by the error bars.

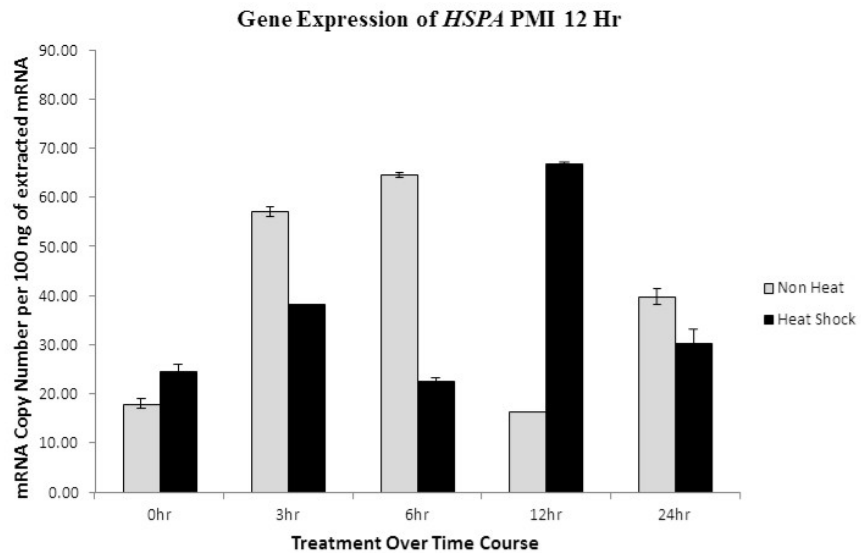
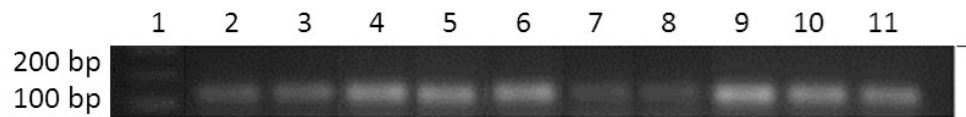


Figure 6.4 Transcription levels of *HSPA* mRNA in non-heat shock and heat shocked rat brain tissue at 12 h PMI. (A) Agarose gel electrophoresis: Lane 1 represents the 100 bp molecular ladder; lanes 2, 4, 6, 8 and 10 represent amplicons from non-heat shocked rat brain tissue at time course intervals of 0, 3, 6, 12 and 24 h respectively. Lanes 3, 5, 7, 9 and 11 represent amplicons from heat shocked rat brain tissue at time course intervals of 0, 3, 6, 12 and 24 h respectively. (B) Histogram showing *HSPA* mRNA copy numbers for non-heat shock and heat shocked brain tissue at 0, 3, 6, 12 and 24 h time course intervals. Data values are the mean of three independent experiments, and the standard deviation from this mean is shown by the error bars. At 3 h heat shock and 12 h non-heat shock no error bars are present as a 0 value standard deviation was calculated.

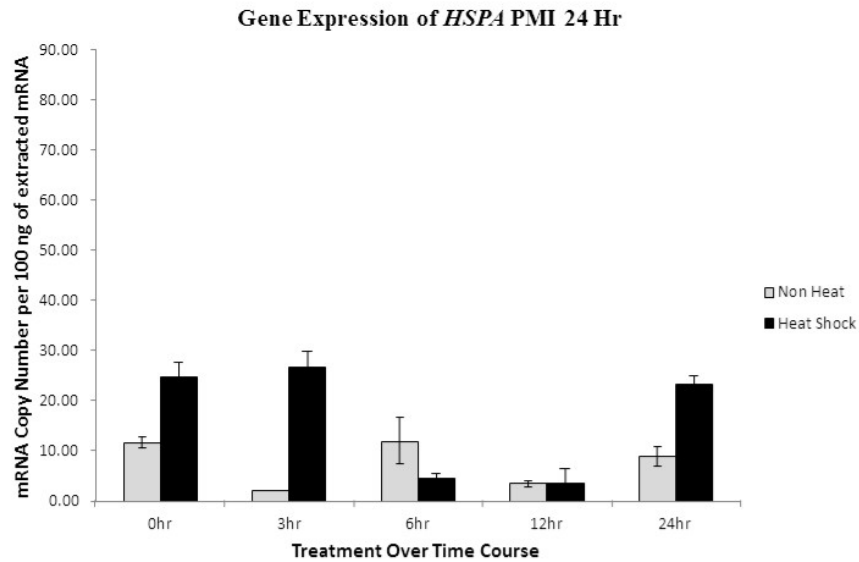
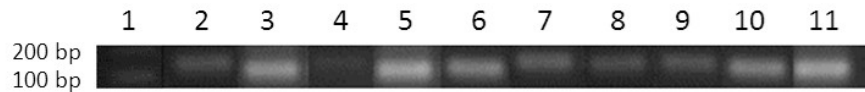


Figure 6.5 Transcription levels of *HSPA* mRNA in non-heat shock and heat shocked rat brain tissue at 24 h PMI. (A) Agarose gel electrophoresis: Lane 1 represents the 100 bp molecular ladder; lanes 2, 4, 6, 8 and 10 represent amplicons from non-heat shocked rat brain tissue at time course intervals of 0, 3, 6, 12 and 24 h respectively. Lanes 3, 5, 7, 9 and 11 represent amplicons from heat shocked rat brain tissue at time course intervals of 0, 3, 6, 12 and 24 h respectively. (B) Histogram showing *HSPA* mRNA copy numbers for non-heat shock and heat shocked brain tissue at 0, 3, 6, 12 and 24 h time course intervals. Data values are the mean of three independent experiments, and the standard deviation from this mean is shown by the error bars. At 3 h non-heat shock and 6 h heat shock no error bars are present as a 0 value standard deviation was calculated.

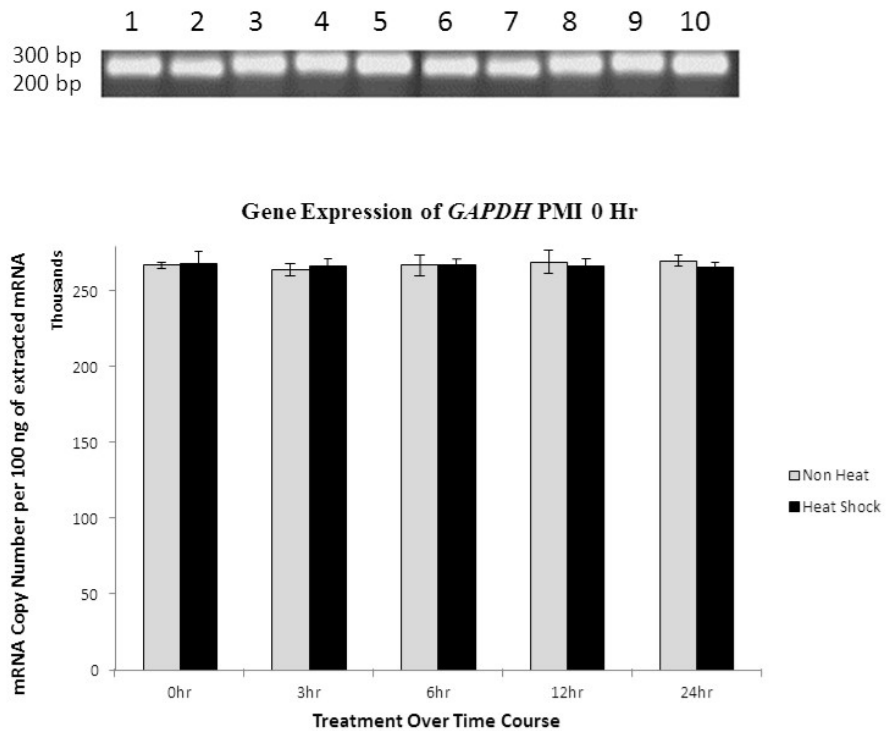


Figure 6.6 Transcription levels of *GAPDH* mRNA in non-heat shock and heat shocked rat brain tissue at 0 h PMI. (A) Agarose gel electrophoresis: Lane 1, 3, 5, 7 and 9 represent amplicons from non-heat shocked rat brain tissue at time course intervals of 0, 3, 6, 12 and 24 h respectively. Lanes 2, 4, 6, 8 and 10 represent amplicons from heat shocked rat brain tissue at time course intervals of 0, 3, 6, 12 and 24 h respectively. (B) Histogram showing *GAPDH* mRNA copy numbers for non-heat shock and heat shocked brain tissue at 0, 3, 6, 12 and 24 h time course intervals. Data values are the mean of three independent experiments, and the standard deviation from this mean is shown by the error bars.

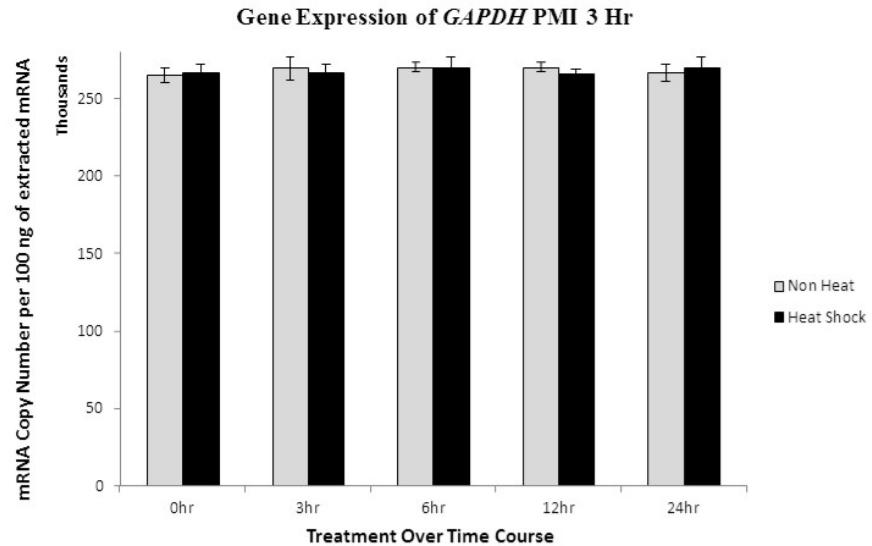
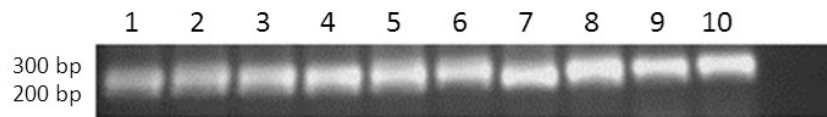


Figure 6.7 Transcription levels of *GAPDH* mRNA in non-heat shock and heat shocked rat brain tissue at 3 h PMI. (A) Agarose gel electrophoresis: Lane 1, 3, 5, 7 and 9 represent amplicons from non-heat shocked rat brain tissue at time course intervals of 0, 3, 6, 12 and 24 h respectively. Lanes 2, 4, 6, 8 and 10 represent amplicons from heat shocked rat brain tissue at time course intervals of 0, 3, 6, 12 and 24 h respectively. (B) Histogram showing *GAPDH* mRNA copy numbers for non-heat shock and heat shocked brain tissue at 0, 3, 6, 12 and 24 h time course intervals. Data values are the mean of three independent experiments, and the standard deviation from this mean is shown by the error bars.

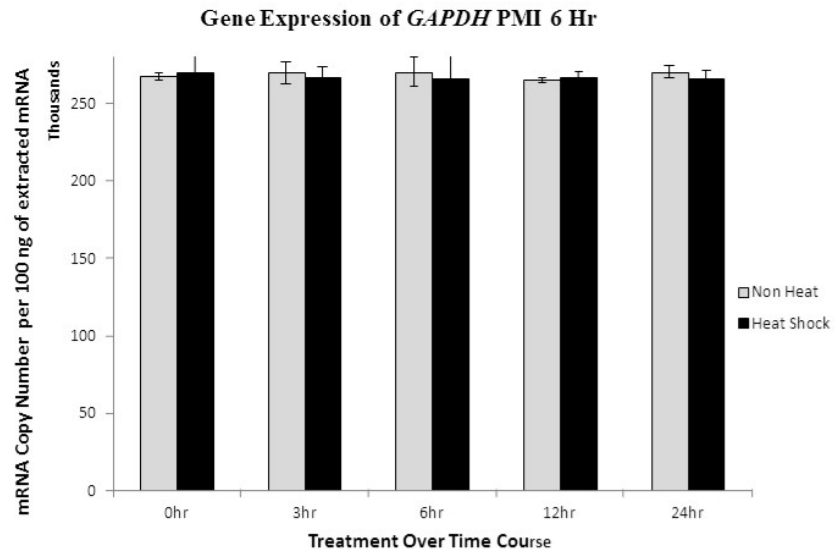
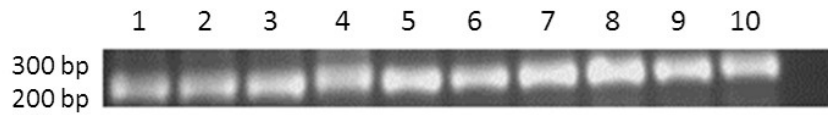


Figure 6.8 Transcription levels of *GAPDH* mRNA in non-heat shock and heat shocked rat brain tissue at 6 h PMI. (A) Agarose gel electrophoresis: Lane 1, 3, 5, 7 and 9 represent amplicons from non-heat shocked rat brain tissue at time course intervals of 0, 3, 6, 12 and 24 h respectively. Lanes 2, 4, 6, 8 and 10 represent amplicons from heat shocked rat brain tissue at time course intervals of 0, 3, 6, 12 and 24 h respectively. (B) Histogram showing *GAPDH* mRNA copy numbers for non-heat shock and heat shocked brain tissue at 0, 3, 6, 12 and 24 h time course intervals. Data values are the mean of three independent experiments, and the standard deviation from this mean is shown by the error bars.

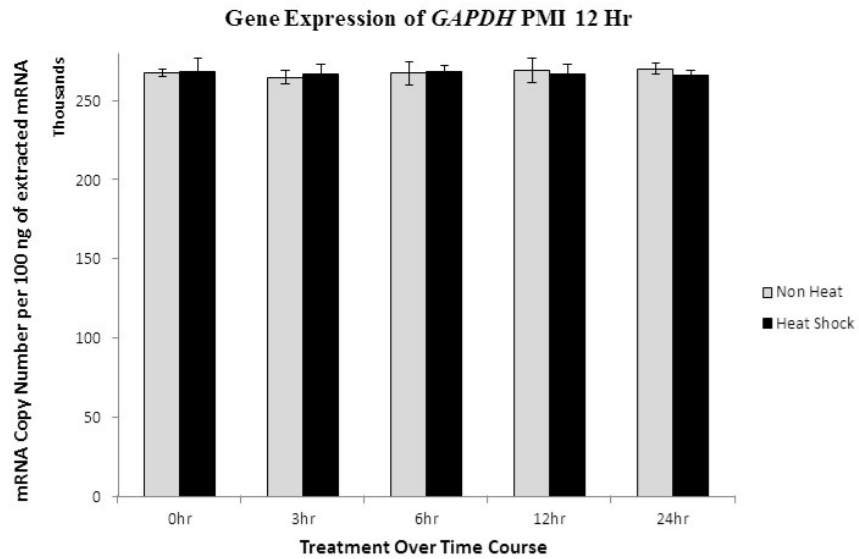
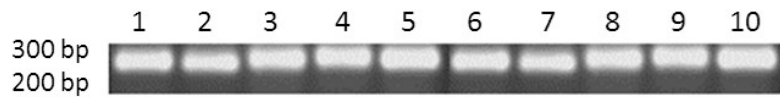


Figure 6.9 Transcription levels of *GAPDH* mRNA in non-heat shock and heat shocked rat brain tissue at 12 h PMI. (A) Agarose gel electrophoresis: Lane 1, 3, 5, 7 and 9 represent amplicons from non-heat shocked rat brain tissue at time course intervals of 0, 3, 6, 12 and 24 h respectively. Lanes 2, 4, 6, 8 and 10 represent amplicons from heat shocked rat brain tissue at time course intervals of 0, 3, 6, 12 and 24 h respectively. (B) Histogram showing *GAPDH* mRNA copy numbers for non-heat shock and heat shocked brain tissue at 0, 3, 6, 12 and 24 h time course intervals. Data values are the mean of three independent experiments, and the standard deviation from this mean is shown by the error bars.

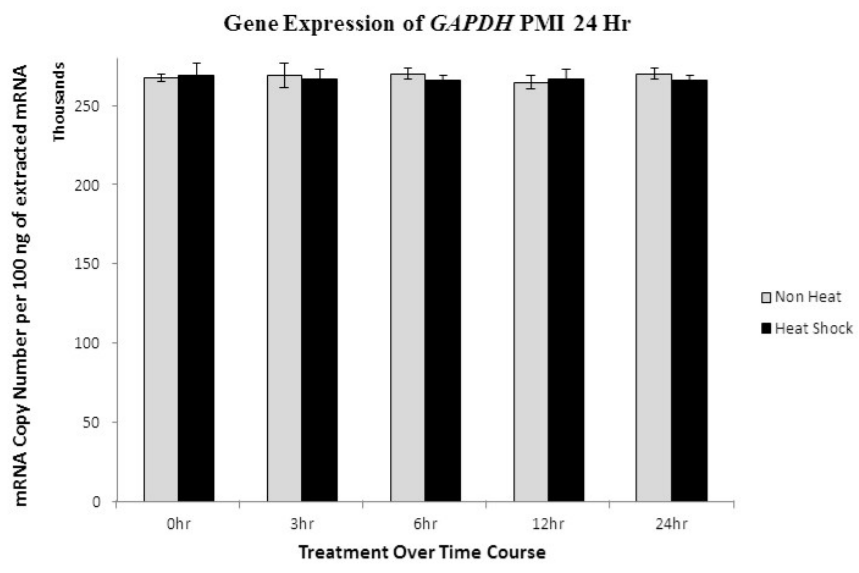
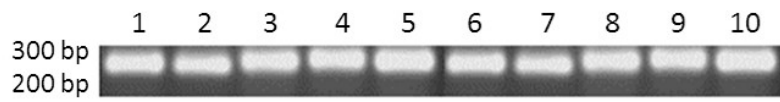


Figure 6.10 Transcription levels of *GAPDH* mRNA in non-heat shock and heat shocked rat brain tissue at 24 h PMI. (A) Agarose gel electrophoresis: Lane 1, 3, 5, 7 and 9 represent amplicons from non-heat shocked rat brain tissue at time course intervals of 0, 3, 6, 12 and 24 h respectively. Lanes 2, 4, 6, 8 and 10 represent amplicons from heat shocked rat brain tissue at time course intervals of 0, 3, 6, 12 and 24 h respectively. (B) Histogram showing *GAPDH* mRNA copy numbers for non-heat shock and heat shocked brain tissue at 0, 3, 6, 12 and 24 h time course intervals. Data values are the mean of three independent experiments, and the standard deviation from this mean is shown by the error bars.

6.2.2 Statistical Analysis

A three-way factorial mixed 5 (PMI: 0 h, 3 h, 6 h, 12 h, 24 h) x 2 (treatment: non-heat shock, heat shock) x 5 (time course: 0 h, 3 h, 6 h, 12 h, 24 h) ANOVA analysis of variance was performed to investigate differences of *HSPA* and *GAPDH* transcript copy numbers in rat brain tissue. The means and standard deviation are presented in Table 6.1 (*HSPA*) and Table 6.2 (*GAPDH*).

HSPA transcript copy numbers had a significant effect for time course [$F(4,17) = 443.06$, $P < .05$]; Wilks' Lambda = 0.010; partial eta squared = 0.990. *HSPA* transcript copy numbers had a significant effect between the interaction of: time course and PMI [$F(16,52.57) = 77.93$; $P < .05$], Wilks' Lambda = 0.000, partial eta squared = 0.914; time course and treatment [$F(4,17) = 47.30$; $P < .05$], Wilks' Lambda = 0.082, partial eta squared = 0.918; time course and PMI and treatment [$F(16,52.57) = 69.17$; $P < .05$], Wilks' Lambda = 0.000, partial eta squared = 0.906.

There was a statistically significant main effect in *HSPA* transcript copy numbers on the combined variables for PMI [$F(4,20) = 473.82$, $P < .05$]; partial eta squared (η_p^2) = 0.990; treatment [$F(1,20) = 431.83$, $P < .05$]; partial eta squared 0.956 and PMI and treatment [$F(4,20) = 45.76$, $P < .05$]; partial eta squared = 0.901.

When the results for the dependent variables were considered separately, there was a statistical significance in PMI at time course: 0 h [$F(4,20) = 208.28$, $P < .05$]; partial eta squared = .977; 3 h [$F(4,20) = 175.74$, $P < .05$]; partial eta squared = .972; 6 h [$F(4,20) = 271.82$, $P < .05$]; partial eta squared = .982; 12 h [$F(4,20) = 244.31$, $P < .05$]; partial eta squared = .980 and 24 h [$F(4,20) = 476.20$, $P < .05$]; partial eta squared = .855.

There was a statistical significance in treatment at time course: 0 h [$F(1,20) = 744.96$, $P < .05$]; partial eta squared = .973; 3 h [$F(1,20) = 124.37$, $P < .05$]; partial eta squared = .861; 12 h [$F(1,20) = 313.15$, $P < .05$]; partial eta squared = .940 and 24 h [$F(1,20) = 37.54$, $P < .05$]; partial eta squared = .652. There was a non-significant difference in treatment at time course 6 h [$F(1,20) = 2.70$, $P < .05$]; partial eta squared = .119.

There was a statistical significance in PMI and treatment at time course: 0 h [$F(4,20) = 166.73$, $P < .05$]; partial eta squared = .971; 3 h [$F(4,20) = 58.54$, $P < .05$]; partial eta squared = .921; 6 h [$F(4,20) = 75.95$, $P < .05$]; partial eta squared = .938; 12 h [$F(4,20) = 59.82$, $P < .05$]; partial eta squared = .923 and 24 h [$F(3,20) = 12.33$, $P < .05$]; partial eta squared = .712.

An independent-samples t-test was conducted to compare *HSPA* transcript copy numbers estimated marginal mean scores for non-heat shock and heat shock over time course by PMI (Figures 6.11 – 6.15).

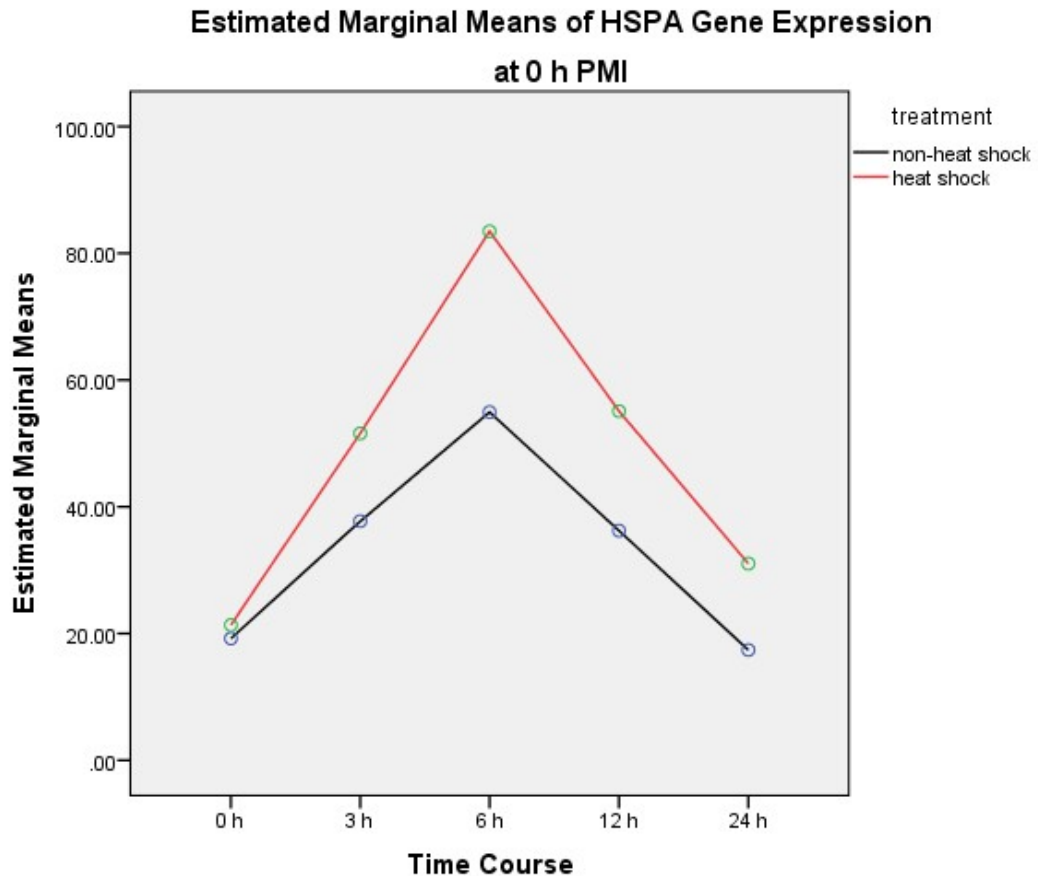


Figure 6.11 Estimated marginal means of *HSPA* transcript copy numbers at 0 h PMI. There was a non-significant difference in *HSPA* transcript copy numbers at 0 h PMI, 0 h time course between non-heat shock (MD = 19.21, SD = .922) and heat shock [MD 21.34, SD = 1.41; $t(4) = 2.181$, $P > .05$]. There was significantly lower *HSPA* transcript copy numbers at 0 h PMI, 3 h time course in non-heat shock (MD = 37.73, SD = .332) than heat shock [MD 51.57, SD = .986; $t(4) = 6.915$, $P = .002$]. There was significantly lower *HSPA* transcript copy numbers at 0 h PMI, 6 h time course in non-heat shock (MD = 54.94, SD = 4.47) than heat shock [MD 83.47, SD = 9.03; $t(4) = 4.903$, $P = .008$]. There was significantly lower *HSPA* transcript copy numbers at 0 h PMI, 12 h time course in non-heat shock (MD = 36.23, SD = .572) than heat shock [MD 55.10, SD = 1.58; $t(4) = 19.494$, $P < .05$]. There was significantly lower *HSPA* transcript copy numbers at 0 h PMI, 24 h time course in non-heat shock (MD = 17.40, SD = 2.79) than heat shock [MD 31.03, SD = 3.90; $t(4) = 4.921$, $P = .008$] (Table 6.1).

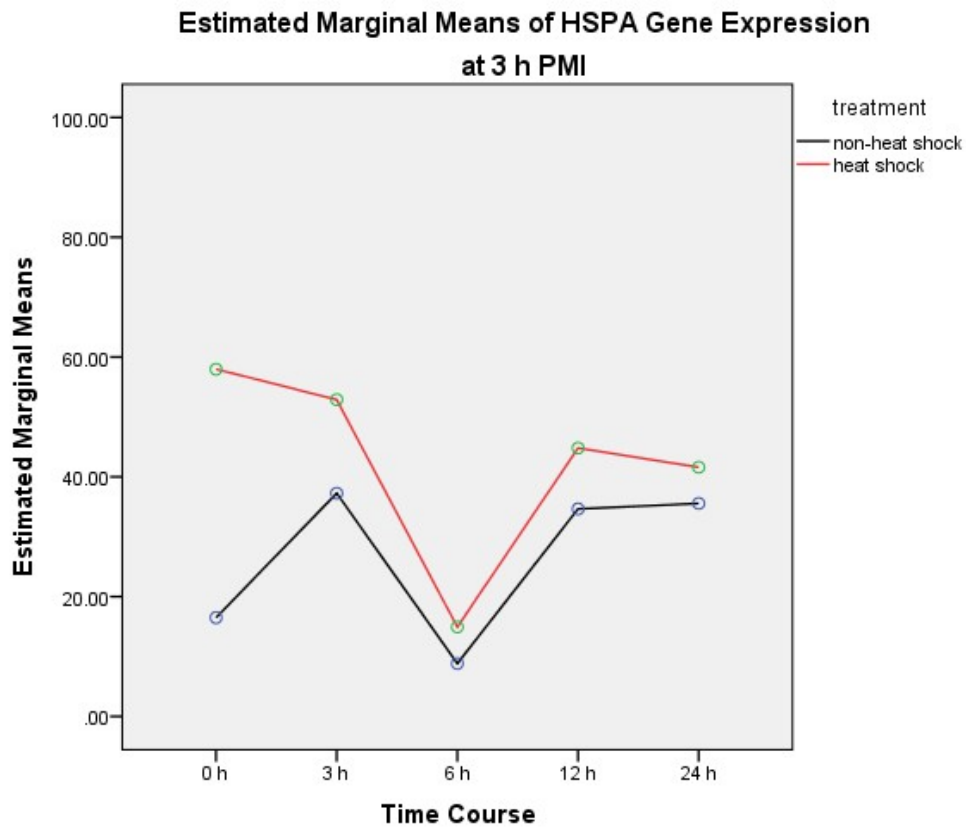


Figure 6.12 Estimated marginal means of *HSPA* transcript copy numbers at 3 h PMI. There was significantly lower *HSPA* transcript copy numbers at 3 h PMI, 0 h time course in non-heat shock (MD = 16.49, SD = .000) than heat shock [MD 57.96, SD = .000]. There was significantly lower *HSPA* transcript copy numbers at 3 h PMI, 3 h time course in non-heat shock (MD = 37.26, SD = .000) than heat shock [MD 52.89, SD = .000]. There was a non-significant difference in *HSPA* transcript copy numbers at 3 h PMI, 6 h time course between non-heat shock (MD = 8.83, SD = .000) and heat shock [MD 14.93, SD = .000]. There was a non-significant difference in *HSPA* transcript copy numbers at 3 h PMI, 12 h time course between non-heat shock (MD = 34.64, SD = 6.25) and heat shock [MD 44.80, SD = 5.08; $t(4) = 2.184$, $P > .05$]. There was a non-significant difference in *HSPA* transcript copy numbers at 3 h PMI, 24 h time course between non-heat shock (MD = 35.55, SD = 2.29) and heat shock [MD 41.59, SD = 7.51; $t(4) = 1.334$, $P > .05$] (Table 6.1).

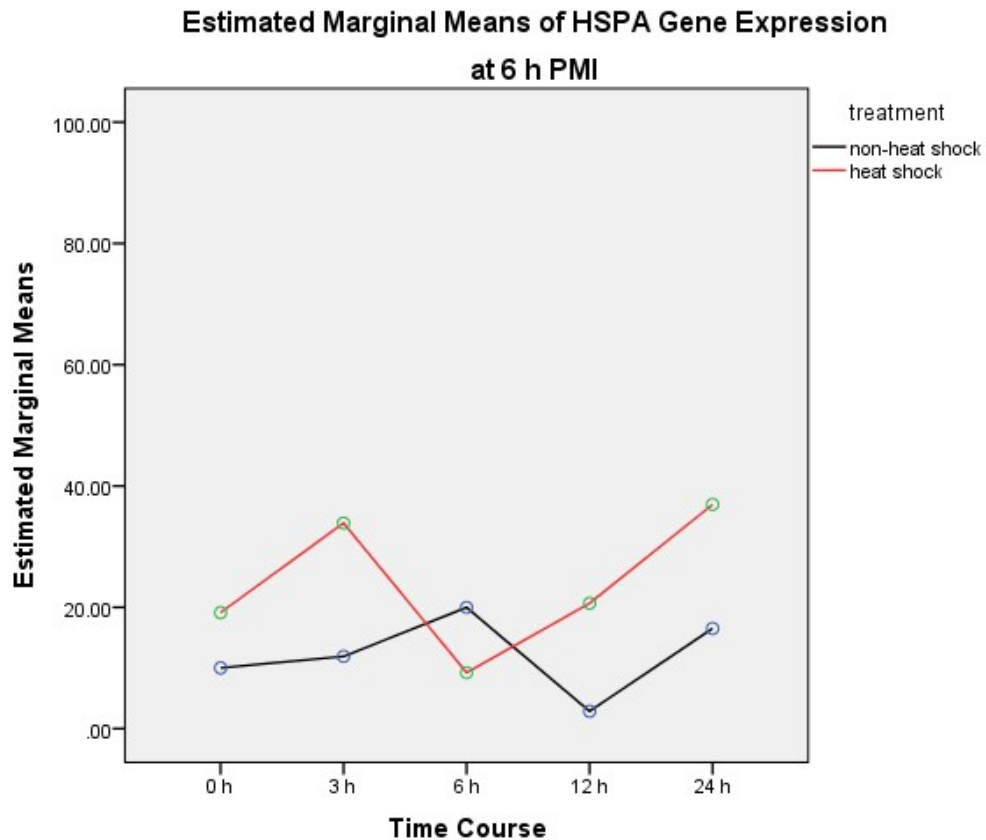


Figure 6.13 Estimated marginal means of *HSPA* transcript copy numbers at 6 h PMI. There was significantly lower *HSPA* transcript copy numbers at 6 h PMI, 0 h time course in non-heat shock (MD = 10.01, SD = 1.58) than heat shock [MD 19.13, SD = 2.07; $t(4) = 6.058$, $P = .004$]. There was significantly lower *HSPA* transcript copy numbers at 6 h PMI, 3 h time course in non-heat shock (MD = 11.91, SD = .943) than heat shock [MD 33.89, SD = 7.37; $t(4) = 5.124$, $P = .034$]. There was significantly higher *HSPA* transcript copy numbers at 6 h PMI, 6 h time course in non-heat shock (MD = 19.98, SD = 2.25) than heat shock [MD 9.22, SD = 2.95; $t(4) = 5.025$, $P = .007$]. There was significantly lower *HSPA* transcript copy numbers at 6 h PMI, 12 h time course in non-heat shock (MD = 2.86, SD = .496) than heat shock [MD 20.66, SD = .092; $t(4) = 81.08$, $P < .05$]. There was significantly lower *HSPA* transcript copy numbers at 6 h PMI, 24 h time course in non-heat shock (MD = 16.51, SD = 4.91) than heat shock [MD 36.96, SD = 6.14; $t(4) = 4.503$, $P = .011$]. (Table 6.1)

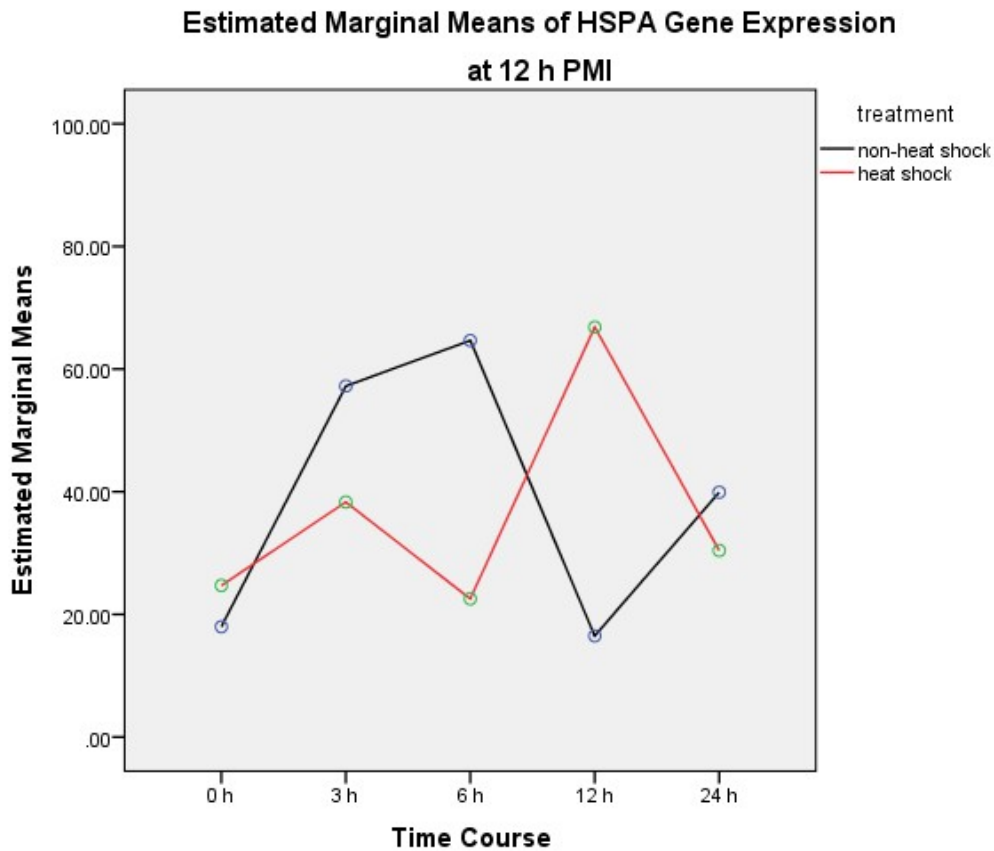


Figure 6.14 Estimated marginal means of *HSPA* transcript copy numbers at 12 h PMI. There was significantly lower *HSPA* transcript copy numbers at 12 h PMI, 0 h time course in non-heat shock (MD = 17.99, SD = .842) than heat shock [MD 24.71, SD = 1.24; $t(4) = 7.775$, $P = .001$]. There was significantly higher *HSPA* transcript copy numbers at 12 h PMI, 3 h time course in non-heat shock (MD = 57.23, SD = 1.01) than heat shock [MD 438.31, SD = .167; $t(4) = 31.998$, $P = .001$]. There was significantly higher *HSPA* transcript copy numbers at 12 h PMI, 6 h time course in non-heat shock (MD = 64.65, SD = .571) than heat shock [MD 22.54, SD = .782; $t(4) = 75.276$, $P < .05$]. There was significantly lower *HSPA* transcript copy numbers at 12 h PMI, 12 h time course in non-heat shock (MD = 16.49, SD = .000) than heat shock [MD 66.82, SD = .295; $t(4) = 296.06$, $P < .05$]. There was significantly higher *HSPA* transcript copy numbers at 12 h PMI, 24 h time course in non-heat shock (MD = 39.92, SD = 1.52) than heat shock [MD 30.41, SD = 2.77; $t(4) = 5.203$, $P = .007$] (Table 6.1).

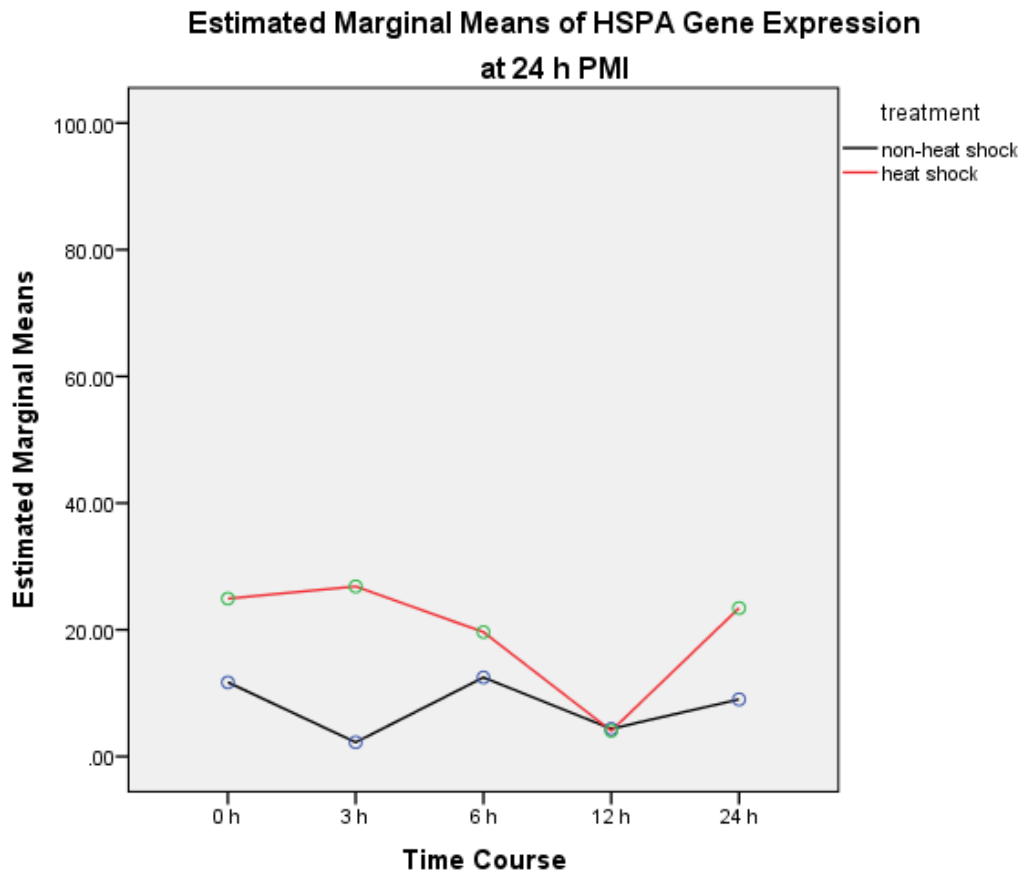


Figure 6.15 Estimated marginal means of *HSPA* transcript copy numbers at 24 h PMI. There was significantly lower *HSPA* transcript copy numbers at 24 h PMI, 0 h time course in non-heat shock (MD = 11.70, SD = 1.02) than heat shock [MD 24.93, SD = 2.98; $t(4) = 7.26$, $P = .002$]. There was significantly lower *HSPA* transcript copy numbers at 24 h PMI, 3 h time course in non-heat shock (MD = 2.24, SD = .000) than heat shock [MD 26.84, SD = 3.23; $t(4) = 13.183$, $P < .05$]. There was significantly lower *HSPA* transcript copy numbers at 24 h PMI, 6 h time course in non-heat shock (MD = 12.48, SD = 4.51) than heat shock [MD 19.64, SD = .010; $t(4) = 2.751$, $P < .05$]. There was a non-significant difference in *HSPA* transcript copy numbers at 24 h PMI, 12 h time course between non-heat shock (MD = 4.37, SD = 3.69) and heat shock [MD 4.05, SD = 2.86; $t(4) = .118$, $P > .05$]. There was significantly lower *HSPA* transcript copy numbers at 24 h PMI, 24 h time course in non-heat shock (MD = 9.02, SD = 1.95) than heat shock [MD 23.43, SD = 1.34; $t(4) = 10.56$, $P < .05$] (Table 6.1).

For *GAPDH* transcript copy numbers, had a non-significant effect for time course [F(4,17) = .270, P = .893]; Wilks' Lambda = 0.940; partial eta squared = 0.060. *GAPDH* transcript copy numbers had a non-significant effect between the interaction of: time course and PMI [F(16,52.57) = .280; P = .996], Wilks' Lambda = .779, partial eta squared = 0.061; time course and treatment [F(4,17) = 1.235; P = .333], Wilks' Lambda = 0.775, partial eta squared = 0.225; time course and PMI and treatment [F(16,52.57) = .763; P = .717], Wilks' Lambda = 0.528, partial eta squared = 0.147.

There was a non-significant effect in *GAPDH* transcript copy numbers on the combined variables for PMI [F(4,20) = .031, P = .998]; partial eta squared (η_p^2) = 0.006; treatment [F(1,20) = 1.044, P = .319]; partial eta squared 0.050 and PMI and treatment [F(4,20) = .055, P = .994]; partial eta squared = 0.011.

Post-hoc analyses using Tukey's HSD test indicated that all differences failed to reach significance.

When the results for the dependent variables were considered separately, there was a statistical non-significance in PMI at time course: 0 h [F(4,20) = .250, P = .906]; partial eta squared = .048; 3 h [F(4,20) = .293, P = .897]; partial eta squared = .055; 6 h [F(4,20) = .200, P = .935]; partial eta squared = .039; 12 h [F(4,20) = .365, P = .831]; partial eta squared = .068 and 24 h [F(4,20) = 0.000, P > .05]; partial eta squared = .000.

There was a statistical non-significance in treatment at time course: 0 h [F(1,20) = .783, P = .387]; partial eta squared = .038; 3 h [F(1,20) = .150, P = .703]; partial eta squared = .007; 6 h [F(1,20) = .769, P = .391]; partial eta squared = .037; 12 h [F(1,20) = .326, P = .574]; partial eta squared = .016 and 24 h [F(1,20) = 3.71, P = .068]; partial eta squared = .156.

There was a statistical non-significance in PMI and treatment at time course: 0 h [F(1,20) = .006, P > .05]; partial eta squared = .001; 3 h [F(1,20) = .293, P = .879]; partial eta squared = .055; 6 h [F(1,20) = .392, P = .812]; partial eta squared = .073; 12 h [F(1,20) = .456, P = .767]; partial eta squared = .083 and 24 h [F(1,20) = .942, P = .460]; partial eta squared = .159.

Overall inspection of the mean scores for *GAPDH* transcript copy numbers indicated no significant differences in PMI, time course and treatment (Table 6.2)

Table 6.1. Descriptive statistics showing the mean *HSPA* transcript copy numbers for untreated and treated brain tissue.

PMI	Treatment	N	Time Course									
			0 Hour		3 Hour		6 Hour		12 Hour		24 Hour	
			Mean	STD Dev.	Mean	STD Dev.	Mean	STD Dev.	Mean	STD Dev.	Mean	STD Dev.
0 Hour	Non	3	19.21	.923	37.73	3.32	54.94	4.47	36.23	.572	17.40	2.79
	Heat	3	21.34	1.41	51.57	.986	83.47	9.03	55.10	1.58	31.03	3.91
3 Hour	Non	3	16.49	.00	37.26	.00	8.83	.00	34.64	6.25	35.55	2.29
	Heat	3	57.96	.00	52.89	.00	14.93	.00	44.80	5.08	41.59	7.51
6 Hour	Non	3	10.01	1.58	11.91	.943	19.98	2.25	2.86	.497	16.51	4.91
	Heat	3	19.13	2.07	33.90	7.37	9.22	2.95	20.67	.092	36.96	6.14
12 Hour	Non	3	17.99	.84	57.23	1.01	64.65	.572	16.49	.00	39.92	1.52
	Heat	3	24.71	1.24	38.31	.167	22.54	.782	66.82	.295	30.41	2.78
24 Hour	Non	3	11.70	1.03	2.24	.00	12.48	4.51	4.37	3.69	9.02	1.95
	Heat	3	24.93	2.98	26.84	3.23	19.64	.010	4.05	2.86	23.43	1.34

Table 6.2. Descriptive statistics showing the mean *GAPDH* transcript copy numbers for untreated and treated brain tissue.

PMI	Treatment	N	Time Course									
			0 Hour		3 Hour		6 Hour		12 Hour		24 Hour	
			Mean	STD Dev.	Mean	STD Dev.	Mean	STD Dev.	Mean	STD Dev.	Mean	STD Dev.
0 Hour	Non	3	267595.53	2348.43	264904.33	4036.84	267652.60	7175.04	269709.77	7719.68	270333.27	3140.67
	Heat	3	269034.67	8198.82	266945.90	5354.84	268281.23	3116.86	266945.90	5354.84	266239.67	2348.43
3 Hour	Non	3	264904.33	4036.84	269709.77	7719.68	270333.27	3140.67	270333.27	3140.67	266949.90	5354.84
	Heat	3	266945.00	5353.81	266945.90	5354.84	269709.77	7719.68	266239.67	2348.43	269709.77	7719.68
6 Hour	Non	3	267595.53	2348.43	269709.77	7719.68	270333.27	3140.67	264904.33	4036.84	270333.27	3140.67
	Heat	3	269709.772	7719.68	266945.90	5354.84	266239.67	2348.43	266945.90	5354.84	266239.67	2348.43
12 Hour	Non	3	267595.43	2348.34	264904.33	4036.84	267652.60	7175.04	269709.77	7719.68	270333.27	3140.67
	Heat	3	269034.67	8198.82	266945.90	5354.84	268281.23	3116.86	266945.90	5354.84	266239.67	2348.43
24 Hour	Non	3	267595.53	2348.43	269709.77	7719.68	270333.27	3140.67	264904.33	4036.84	270333.27	3140.67
	Heat	3	269709.77	7719.68	266945.90	5354.84	266239.67	2348.43	266945.90	5354.84	266239.67	2348.43

Table 6.3. Statistical data from Tukey’s HSD test showing significance of *HSPA* transcript copy numbers between PMI. Any significant differences $P \leq 0.05$ are highlighted in bold.

(I) PMI	J (PMI)	Mean Difference (I – J)	Std. Error	Sig.
0	3	6.31	.793	.000
	6	22.69	.793	.000
	12	2.90	.793	.012
	24	26.93	.793	.000
3	6	16.38	.793	.000
	12	3.41	.793	.003
	24	20.62	.793	.000
6	12	19.79	.793	.000
	24	4.24	.793	.000
12	24	24.04	.793	.000

Post-hoc analyses using Tukey’s HSD test indicated significantly lower *HSPA* transcript copy numbers in 0 h PMI than in: 3 h PMI (MD = 6.31, $P < .05$); 6 h PMI (MD = 22.69, $P < .05$); 12 h PMI (MD = 0.012, $P < .05$) and 24 h PMI (MD = 26.93, $P < .05$). There was significantly lower *HSPA* transcript copy numbers in 3 h PMI than in: 6 h PMI (MD = 16.38, $P < .05$); 12 h PMI (MD = 3.41, $P = .003$) and 24 h PMI (MD = 20.62, $P < .05$). There was significantly lower *HSPA* transcript copy numbers in 6 h PMI than in: 12 h PMI (MD = 19.79, $P < .05$) and 24 h PMI (MD = 4.24, $P < .05$). There was significantly lower *HSPA* transcript copy numbers in 3 h PMI than in: 6 h PMI (MD = 16.38, $P < .05$); 12 h PMI (MD = 3.41, $P = .003$) and 24 h PMI (MD = 20.62, $P < .05$). There was significantly lower *HSPA* transcript copy numbers in 12 h PMI than in 24 h PMI (MD = 24.04, $P < .05$) (Table 6.3).

6.2.3 Rat Brain tissue - thermotolerance

Expression of *HSPA* and *GAPDH* in thermotolerant tissue was evaluated using RT-PCR in rat post-mortem brain tissue, at post-mortem intervals of 0, 3, 6 and 24 h and at time course intervals of 0, 3, 6 and 24 h within each post-mortem interval for both control (non-heat shock) and mild heat shock treated samples. The primers and optimal temperatures used for the amplification of both genes are documented in Table 2.10 in section 2.5. All PCR experiments were carried out in triplicate for consistency and repeatability. For each gene analysed, a quantification graph was produced to confirm gene amplification. The resulting amplicons for *HSPA* and *GAPDH* were then analysed using agarose gel electrophoresis, represented by bands of 156 and 265 bp respectively.

At 3 h, 6 and 24 h post-mortem interval at 0, 3, 6 and 24 h time course, heat shocked brain tissue transcribed *HSPA* at a higher level compared to that of the non-heat shocked brain tissue (Figure 6.17, 6.18 and 6.19). At 0 h post-mortem interval *HSPA* transcribed higher in heat shocked brain tissue at time course 0, 3 and 6 h, but lower at the 24 h time course than non-heat shocked brain tissue (Figure 6.17).

GAPDH expression level remained relatively consistent throughout each PMI, time course and non-heat shock and heat shocked brain tissue confirming it as an ideal reference gene (Figures 6.20 – 6.23).

The mRNA copy number per 100 ng of extracted mRNA for both genes was calculated for each time course 0, 3, 6 and 24 h within each post-mortem interval 0, 3, 6 and 24 h for both non-heat shock and heat shock to monitor the gene expression level. mRNA copy numbers confirmed that at: 0 h post-mortem interval, *HSPA* was expressed at a higher level in heat shocked brain tissue at different time course intervals; with

approximately 13 copies after 0 h recovery, with approximately 19 copies after 3 h recovery and approximately 4 copies after 6 h recovery compare to non-heat shocked brain tissue at different time course intervals; with approximately 2 copies after 0 h recovery, approximately 2 copies after 3 h recovery and approximately 16 copies after 6 h recovery. Expression was lower in heat shocked brain tissue after 24 h recovery, approximately 19 copies compare to non-heat shocked brain tissue after 24 h recovery, approximately 19 copies (Figure 6.16).

At 3 h post-mortem interval, *HSPA* was expressed at a higher level in heat shocked brain tissue at different time course intervals; with approximately 37 copies after 0 h recovery, with approximately 20 copies after 3 h recovery, with approximately 59 copies after 6 h recovery and approximately 20 copies after 24 h recovery compared to non-heat shocked brain tissue at different time course intervals; with approximately 2 copies after 0 h recovery, with approximately 10 copies after 3 h recovery, with approximately 19 copies after 6 h recovery and approximately 19 copies after 24 h recovery (Figure 6.17).

At 6 h post-mortem interval, *HSPA* was expressed at a higher level in heat shocked brain tissue at different time course intervals; with approximately 130 copies after 0 h recovery, with approximately 167 copies after 3 h recovery, with approximately 66 copies after 6 h recovery and approximately 63 copies after 24 h recovery compare to non-heat shocked brain tissue at different time course intervals; with approximately 30 copies after 0 h recovery, with approximately 47 copies after 3 h recovery, with approximately 50 copies after 6 h recovery and approximately 46 copies after 24 h recovery (Figure 6.18).

At 24 h post-mortem interval, *HSPA* was expressed at a higher level in heat shocked brain tissue at different time course intervals; with approximately 51 copies after 0 h recovery, with approximately 59 copies after 3 h recovery, with approximately 66 copies after 6 h recovery and approximately 121 copies after 24 h recovery compared to non-heat shocked brain tissue at different time course intervals; with approximately 44 copies after 0 h recovery, with approximately 31 copies after 3 h recovery, with approximately 43 copies after 6 h recovery and approximate 59 copies after 24 h recovery (Figure 6.19).

GAPDH expression level remained relatively consistent throughout each PMI, time course in both non-heat shock and heat shocked brain tissue again confirming comparability of *HSPA* results (Figures 6.20 – 6.23).

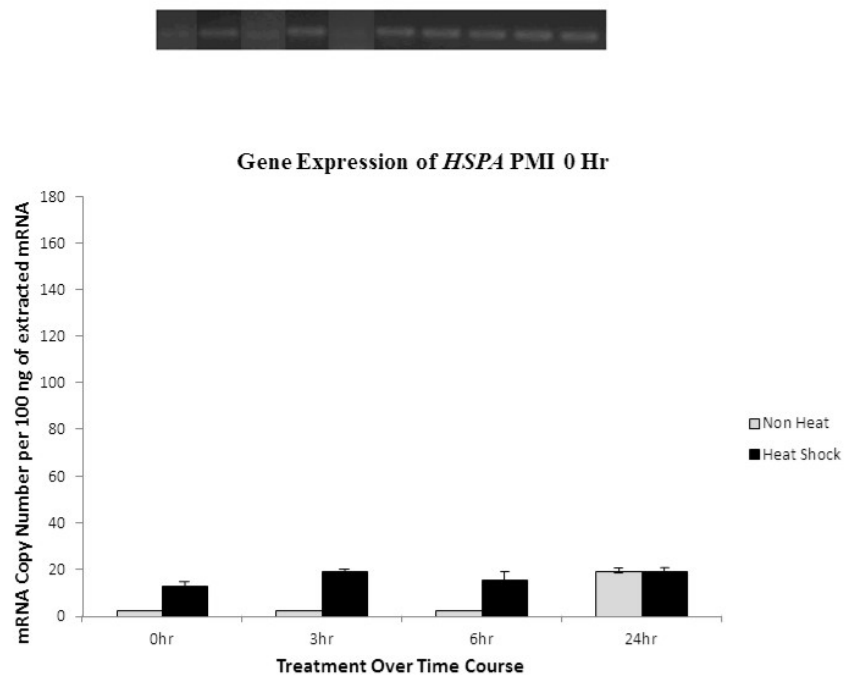


Figure 6.16 Transcription levels of *HSPA* mRNA in non-heat shock and heat shocked rat brain tissue at 0 h PMI. (A) Agarose gel electrophoresis: Lane 1, 3, 5 and 7 represent amplicons from non-heat shocked rat brain tissue at time course intervals of 0, 3, 6 and 24 h respectively. Lanes 2, 4, 6 and 8 represent amplicons from heat shocked rat brain tissue at time course intervals of 0, 3, 6 and 24 h respectively. (B) Histogram showing *HSPA* mRNA copy numbers for non-heat shock and heat shocked brain tissue at 0, 3, 6 and 24 h time course intervals. Data values are the mean of three independent experiments, and the standard deviation from this mean is shown by the error bars. At 0, 3 and 6 h non-heat shock no error bars are present as a 0 value standard deviation was calculated.

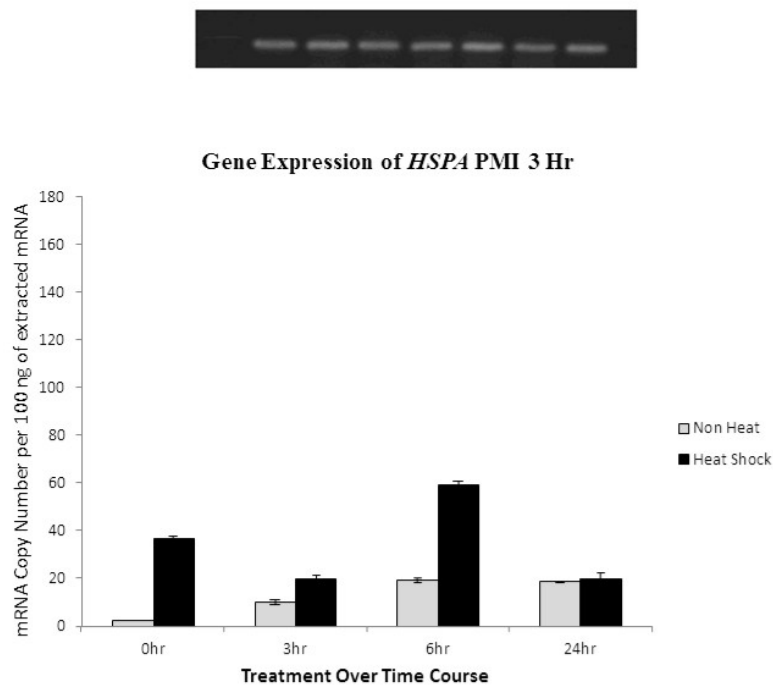


Figure 6.17 Transcription levels of *HSPA* mRNA in non-heat shock and heat shocked rat brain tissue at 3 h PMI. (A) Agarose gel electrophoresis: Lane 1, 3, 5 and 7 represent amplicons from non-heat shocked rat brain tissue at time course intervals of 0, 3, 6 and 24 h respectively. Lanes 2, 4, 6 and 8 represent amplicons from heat shocked rat brain tissue at time course intervals of 0, 3, 6 and 24 h respectively. (B) Histogram showing *HSPA* mRNA copy numbers for non-heat shock and heat shocked brain tissue at 0, 3, 6 and 24 h time course intervals. Data values are the mean of three independent experiments, and the standard deviation from this mean is shown by the error bars. At 0 h non-heat shock no error bars are present as a 0 value standard deviation was calculated.

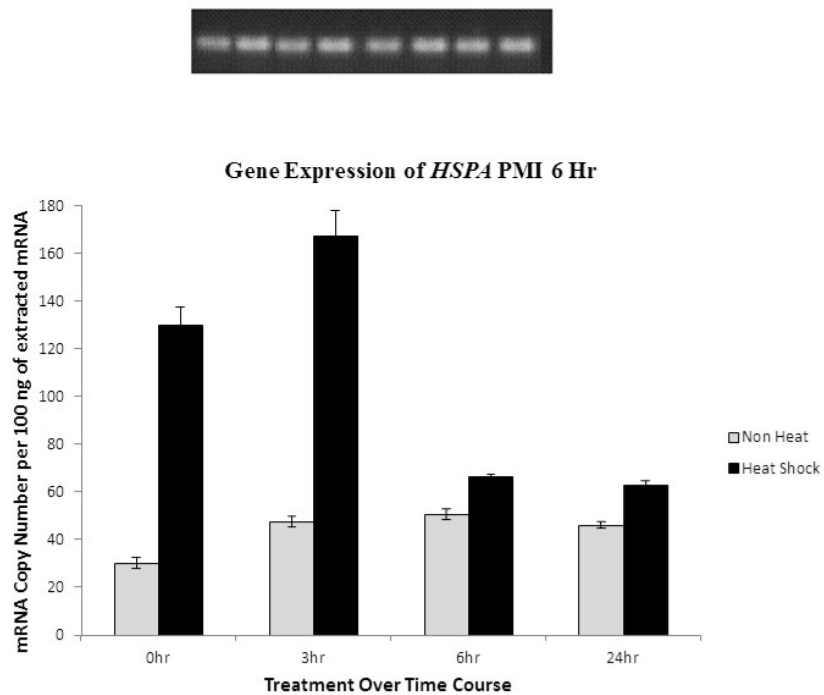


Figure 6.18 Transcription levels of *HSPA* mRNA in non-heat shock and heat shocked rat brain tissue at 6 h PMI. (A) Agarose gel electrophoresis: Lane 1, 3, 5 and 7 represent amplicons from non-heat shocked rat brain tissue at time course intervals of 0, 3, 6 and 24 h respectively. Lanes 2, 4, 6 and 8 represent amplicons from heat shocked rat brain tissue at time course intervals of 0, 3, 6 and 24 h respectively. (B) Histogram showing *HSPA* mRNA copy numbers for non-heat shock and heat shocked brain tissue at 0, 3, 6 and 24 h time course intervals. Data values are the mean of three independent experiments, and the standard deviation from this mean is shown by the error bars.

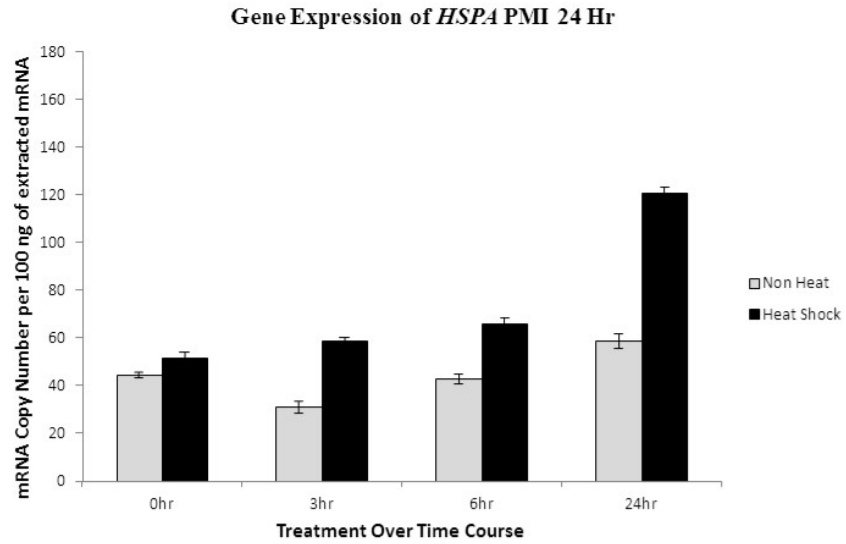
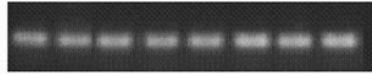


Figure 6.19 Transcription levels of *HSPA* mRNA in non-heat shock and heat shocked rat brain tissue at 24 h PMI. (A) Agarose gel electrophoresis: Lane 1, 3, 5 and 7 represent amplicons from non-heat shocked rat brain tissue at time course intervals of 0, 3, 6 and 24 h respectively. Lanes 2, 4, 6 and 8 represent amplicons from heat shocked rat brain tissue at time course intervals of 0, 3, 6 and 24 h respectively. (B) Histogram showing *HSPA* mRNA copy numbers for non-heat shock and heat shocked brain tissue at 0, 3, 6 and 24 h time course intervals. Data values are the mean of three independent experiments, and the standard deviation from this mean is shown by the error bars.

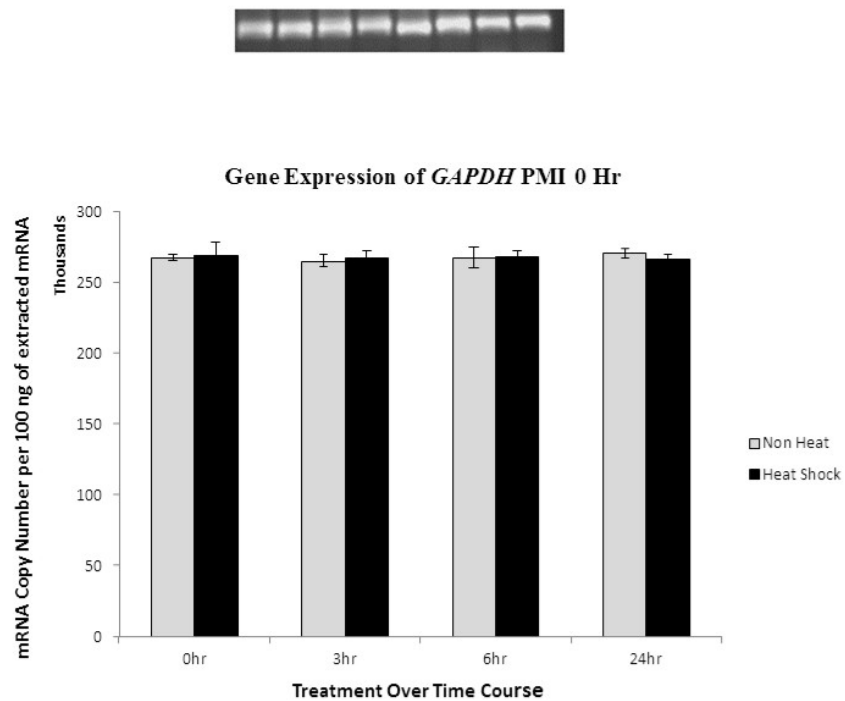


Figure 6.20 Transcription levels of *GAPDH* mRNA in non-heat shock and heat shocked rat brain tissue at 0 h PMI. (A) Agarose gel electrophoresis: Lane 1, 3, 5 and 7 represent amplicons from non-heat shocked rat brain tissue at time course intervals of 0, 3, 6 and 24 h respectively. Lanes 2, 4, 6 and 8 represent amplicons from heat shocked rat brain tissue at time course intervals of 0, 3, 6 and 24 h respectively. (B) Histogram showing *HSPA* mRNA copy numbers for non-heat shock and heat shocked brain tissue at 0, 3, 6 and 24 h time course intervals. Data values are the mean of three independent experiments, and the standard deviation from this mean is shown by the error bars.

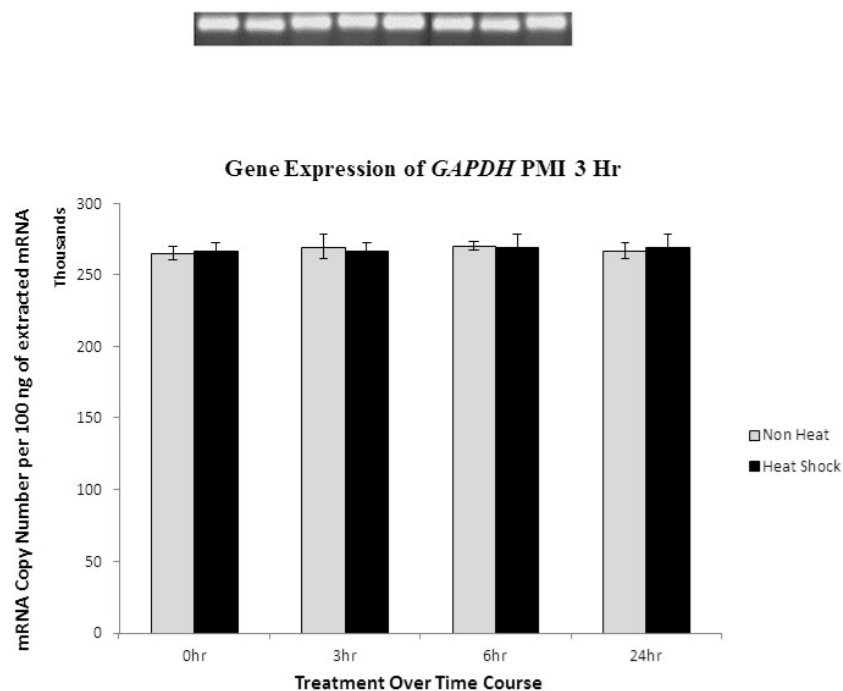


Figure 6.21 Transcription levels of *GAPDH* mRNA in non-heat shock and heat shocked rat brain tissue at 3 h PMI. (A) Agarose gel electrophoresis: Lane 1, 3, 5 and 7 represent amplicons from non-heat shocked rat brain tissue at time course intervals of 0, 3, 6 and 24 h respectively. Lanes 2, 4, 6 and 8 represent amplicons from heat shocked rat brain tissue at time course intervals of 0, 3, 6 and 24 h respectively. (B) Histogram showing *HSPA* mRNA copy numbers for non-heat shock and heat shocked brain tissue at 0, 3, 6 and 24 h time course intervals. Data values are the mean of three independent experiments, and the standard deviation from this mean is shown by the error bars.

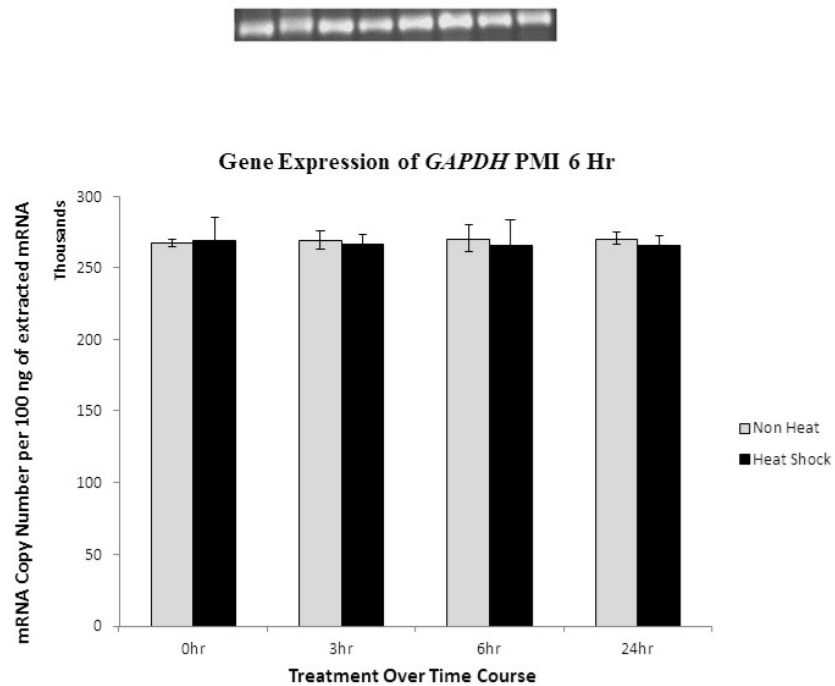


Figure 6.22 Transcription levels of *GAPDH* mRNA in non-heat shock and heat shocked rat brain tissue at 6 h PMI. (A) Agarose gel electrophoresis: Lane 1, 3, 5 and 7 represent amplicons from non-heat shocked rat brain tissue at time course intervals of 0, 3, 6 and 24 h respectively. Lanes 2, 4, 6 and 8 represent amplicons from heat shocked rat brain tissue at time course intervals of 0, 3, 6 and 24 h respectively. (B) Histogram showing *HSPA* mRNA copy numbers for non-heat shock and heat shocked brain tissue at 0, 3, 6 and 24 h time course intervals. Data values are the mean of three independent experiments, and the standard deviation from this mean is shown by the error bars.

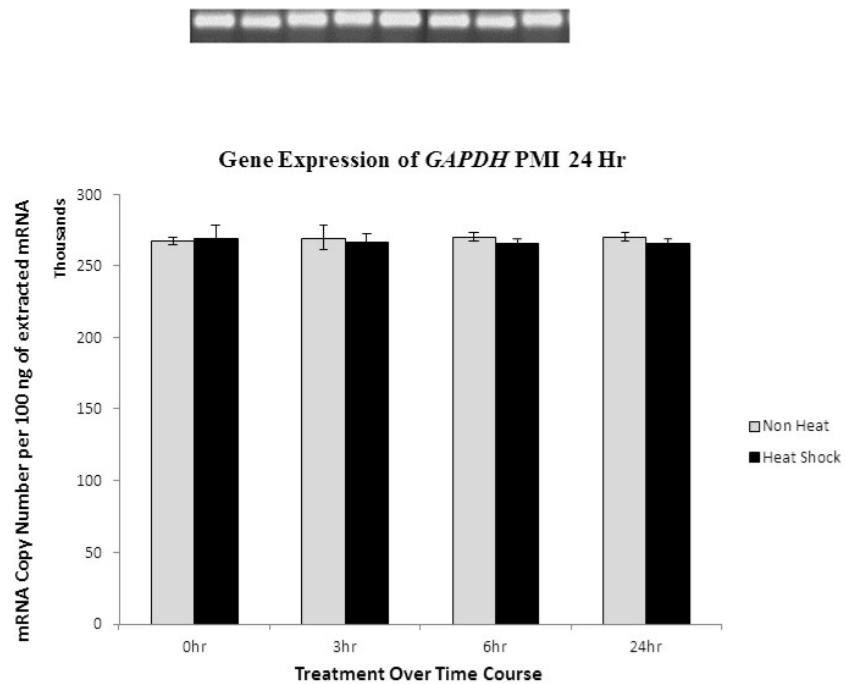


Figure 6.23 Transcription levels of *GAPDH* mRNA in non-heat shock and heat shocked rat brain tissue at 24 h PMI. (A) Agarose gel electrophoresis: Lane 1, 3, 5 and 7 represent amplicons from non-heat shocked rat brain tissue at time course intervals of 0, 3, 6 and 24 h respectively. Lanes 2, 4, 6 and 8 represent amplicons from heat shocked rat brain tissue at time course intervals of 0, 3, 6 and 24 h respectively. (B) Histogram showing *HSPA* mRNA copy numbers for non-heat shock and heat shocked brain tissue at 0, 3, 6 and 24 h time course intervals. Data values are the mean of three independent experiments, and the standard deviation from this mean is shown by the error bars.

6.2.4 Statistical Analysis

A three-way factorial mixed 4 (PMI: 0 h, 3 h, 6 h, 24 h) x 2 (treatment: non-heat shock, heat shock) x 4 (time course: 0 h, 3 h, 6 h, 24 h) ANOVA analysis of variance was performed to investigate differences of *HSPA* and *GAPDH* transcript copy numbers in rat brain tissue. The means and standard deviation are presented in Table 6.4 (*HSPA*) and Table 6.5 (*GAPDH*).

HSPA transcript copy numbers had a significant effect for time course [$F(3,14) = 108.67, P < .05$]; Wilks' Lambda = 0.041; partial eta squared = 0.959. *HSPA* transcript copy numbers had a significant effect between the interaction of: time course and PMI [$F(9,34.22) = 146.62; P < .05$], Wilks' Lambda = 0.000, partial eta squared = 0.949; time course and treatment [$F(3,14) = 50.74; P < .05$], Wilks' Lambda = 0.084, partial eta squared = 0.916; time course and PMI and treatment [$F(9,34.22) = 167.44; P < .05$], Wilks' Lambda = 0.000, partial eta squared = 0.954.

There was a statistically significant main effect in *HSPA* transcript copy numbers on the combined variables for PMI [$F(3,16) = 1809.72, P < .05$]; partial eta squared (η_p^2) = 0.997; treatment [$F(1,16) = 1982.83, P < .05$]; partial eta squared 0.992 and PMI and treatment [$F(3,16) = 265.01, P < .05$]; partial eta squared = 0.980.

When the results for the dependent variables were considered separately, there was a statistical significance in PMI at time course: 0 h [$F(3,16) = 680.86, P < .05$]; partial eta squared = .992; 3 h [$F(3,16) = 726.52, P < .05$]; partial eta squared = .993; 6 h [$F(3,16) = 759.73, P < .05$]; partial eta squared = .993 and 24 h [$F(3,16) = 2291.07, P < .05$]; partial eta squared = .998.

There was a statistical significance in treatment at time course: 0 h [$F(1,16) = 942.42$, $P < .05$]; partial eta squared = .983; 3 h [$F(1,16) = 695.39$, $P < .05$]; partial eta squared = .978; 6 h [$F(1,16) = 817.26$, $P < .05$]; partial eta squared = .981 and 24 h [$F(1,16) = 789.92$, $P < .05$]; partial eta squared = .980.

There was a statistical significance in PMI and treatment at time course: 0 h [$F(3,16) = 299.93$, $P < .05$]; partial eta squared = .983; 3 h [$F(3,16) = 241.46$, $P < .05$]; partial eta squared = .978; 6 h [$F(3,16) = 55.22$, $P < .05$]; partial eta squared = .912 and 24 h [$F(3,16) = 424.45$, $P < .05$]; partial eta squared = .988.

An independent-samples t-test was conducted to compare *HSPA* transcript copy numbers estimated marginal mean scores for non-heat shock and heat shock over time course by PMI (Figures 6.24 – 6.27).

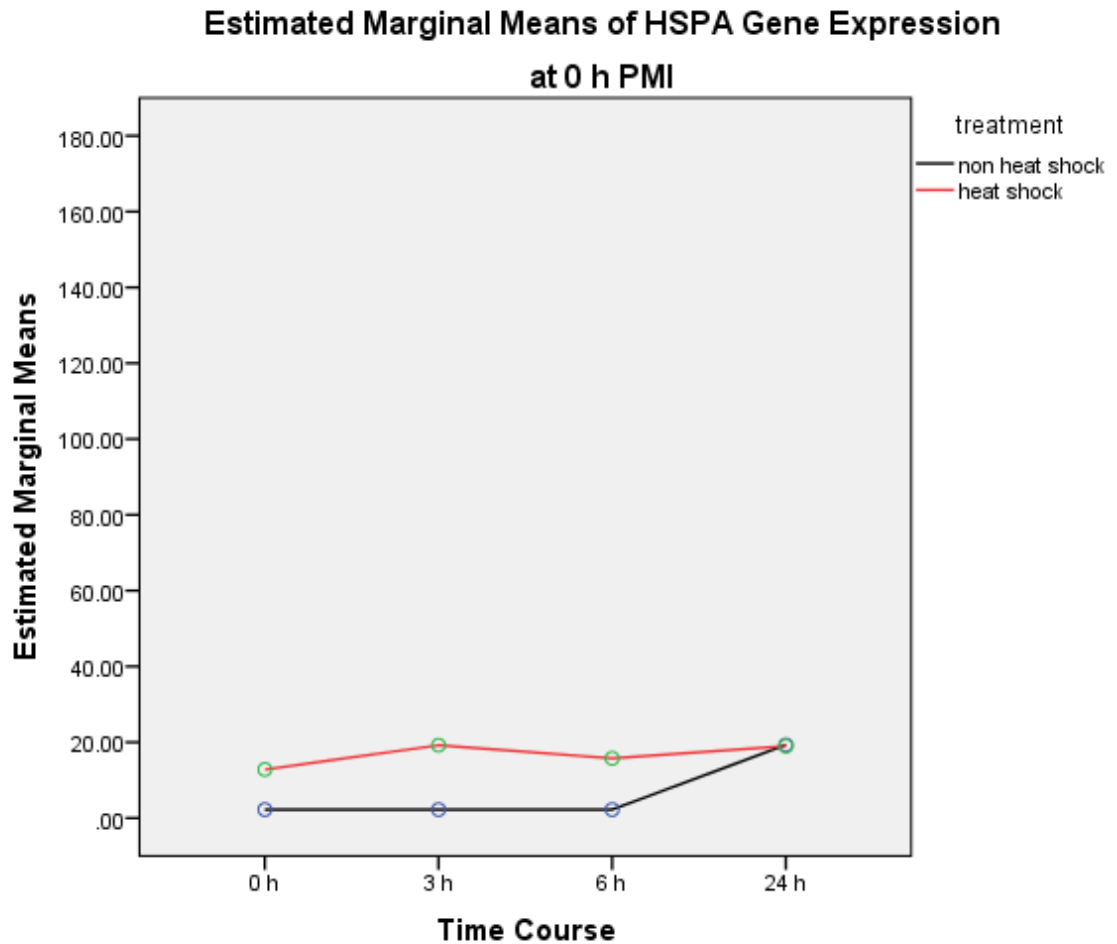


Figure 6.24 Estimated marginal means of *HSPA* transcript copy numbers at 0 h PMI. There was significantly lower in *HSPA* transcript copy numbers at 0 h PMI, 0 h time course in non-heat shock (MD = 2.24, SD = .00) than heat shock [MD 12.80, SD = 1.98; $t(4) = 9.258$, $P = .001$]. There was significantly lower *HSPA* transcript copy numbers at 0 h PMI, 3 h time course in non-heat shock (MD = 2.24, SD = .00) than heat shock [MD 19.20, SD = 0.526; $t(4) = 55.90$, $P < .05$]. There was significantly lower *HSPA* transcript copy numbers at 0 h PMI, 6 h time course in non-heat shock (MD = 2.24, SD = .00) than heat shock [MD 15.75, SD = 3.67; $t(4) = 6.38$, $P = .024$]. There was a non-significant difference in *HSPA* transcript copy numbers at 0 h PMI, 24 h time course between non-heat shock (MD = 19.31, SD = 0.84) and heat shock [MD 18.99, SD = 1.23; $t(4) = 0.372$, $P = .729$] (Table 6.4).

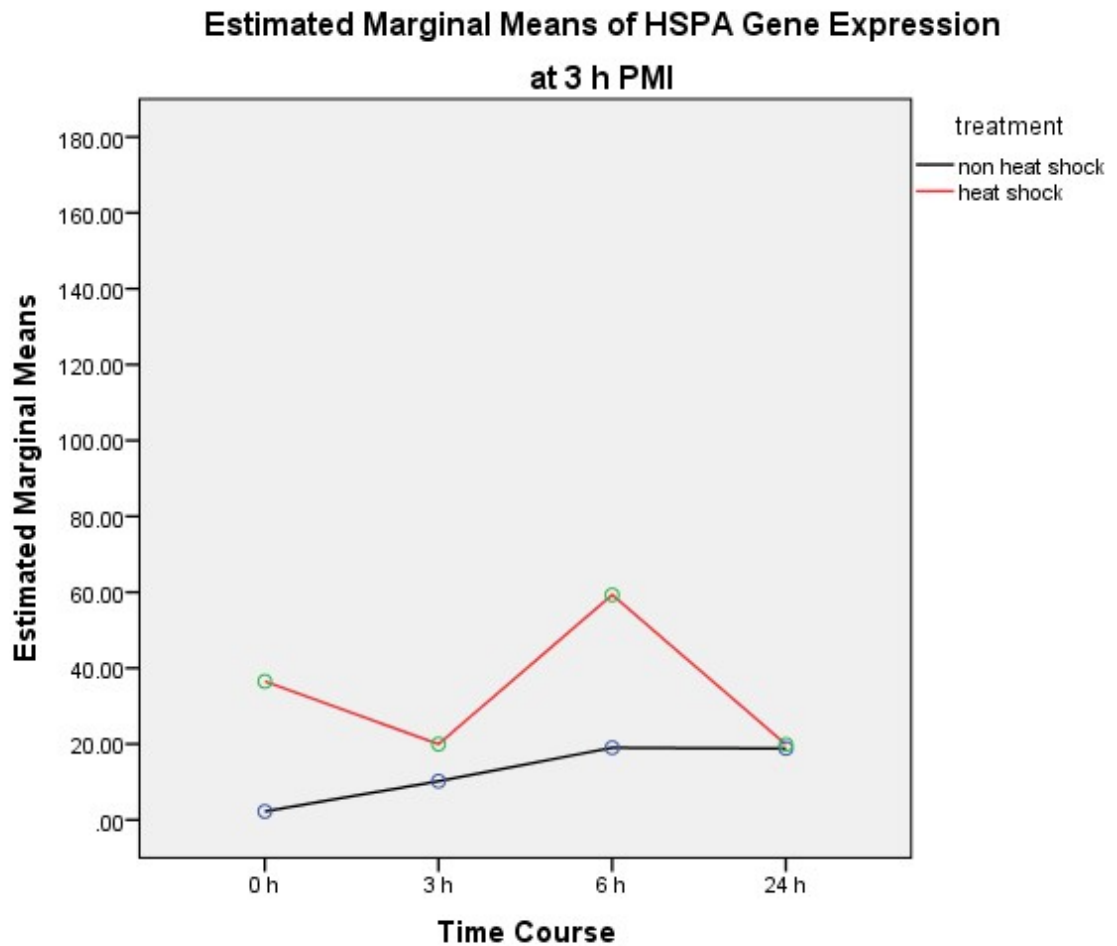


Figure 6.25 Estimated marginal means of *HSPA* transcript copy numbers at 3 h PMI. There was significantly lower *HSPA* transcript copy numbers at 3 h PMI, 0 h time course in non-heat shock (MD = 2.24, SD = .00) than heat shock [MD 36.51, SD = .647; $t(4) = 91.80$, $P < .05$]. There was significantly lower *HSPA* transcript copy numbers at 3 h PMI, 3 h time course in non-heat shock (MD = 10.21, SD = 1.03) than heat shock [MD 19.97, SD = 1.07; $t(4) = 11.40$, $P < .05$]. There was significantly lower *HSPA* transcript copy numbers at 3 h PMI, 6 h time course in non-heat shock (MD = 19.01, SD = .811) than heat shock [MD 59.30, SD = .785; $t(4) = 61.80$, $P < .05$]. There was a non-significant difference in *HSPA* transcript copy numbers at 3 h PMI, 24 h time course between non-heat shock (MD = 18.82, SD = .438) and heat shock [MD 19.90, SD = 1.70; $t(4) = 1.06$, $P = .388$] (Table 6.4).

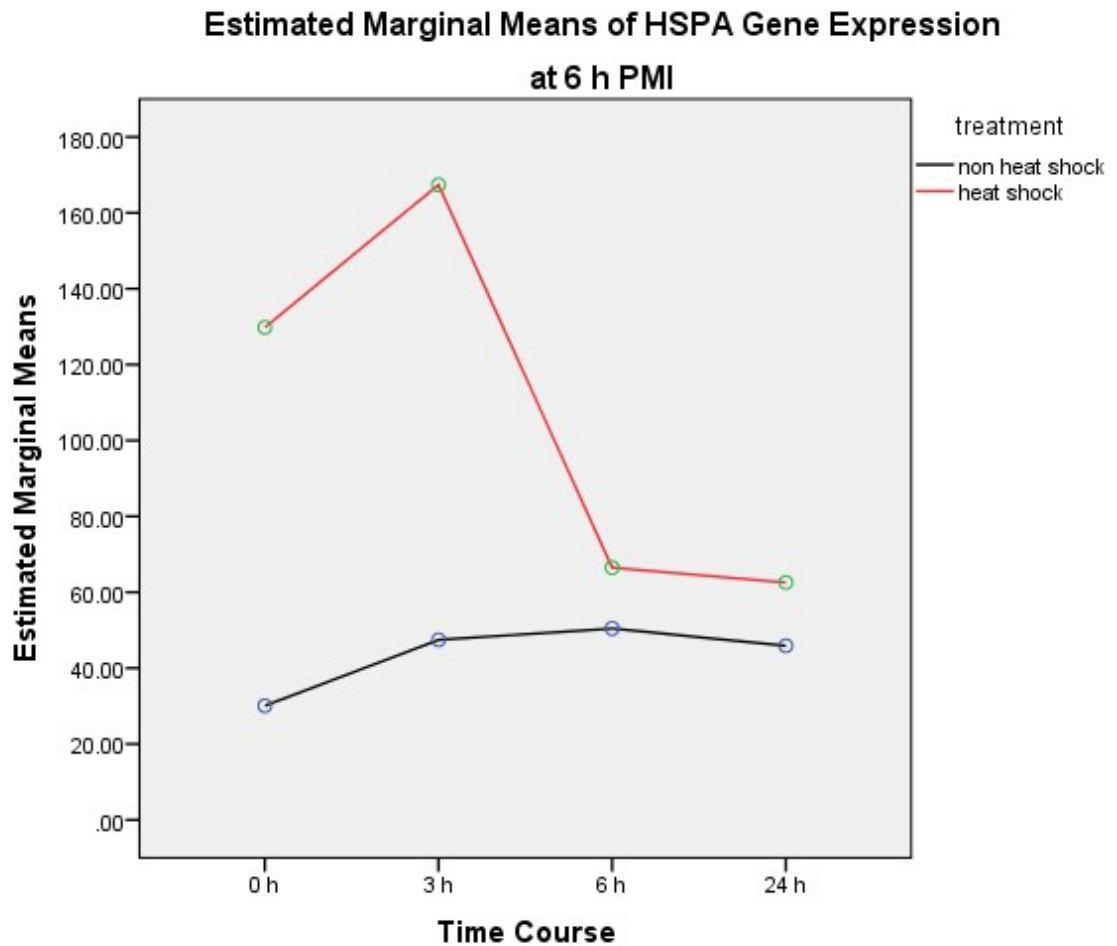


Figure 6.26 Estimated marginal means of *HSPA* transcript copy numbers at 6 h PMI. There was significantly lower *HSPA* transcript copy numbers at 6 h PMI, 0 h time course in non-heat shock (MD = 30.08, SD = 2.30) than heat shock [MD 129.81, SD = 7.59; $t(4) = 21.79$, $P < .05$]. There was significantly lower *HSPA* transcript copy numbers at 6 h PMI, 3 h time course in non-heat shock (MD = 47.45, SD = 2.07) than heat shock [MD 167.39, SD = 10.83; $t(4) = 18.84$, $P = .002$]. There was significantly lower *HSPA* transcript copy numbers at 6 h PMI, 6 h time course in non-heat shock (MD = 50.44, SD = 2.19) than heat shock [MD 66.48, SD = .878; $t(4) = 11.79$, $P < .05$]. There was significantly lower *HSPA* transcript copy numbers at 6 h PMI, 24 h time course in non-heat shock (MD = 45.89, SD = 1.01) than heat shock [MD 62.57, SD = 1.91; $t(4) = 13.41$, $P = .001$] (Table 6.4).

**Estimated Marginal Means of HSPA Gene Expression
at 24 h PMI**

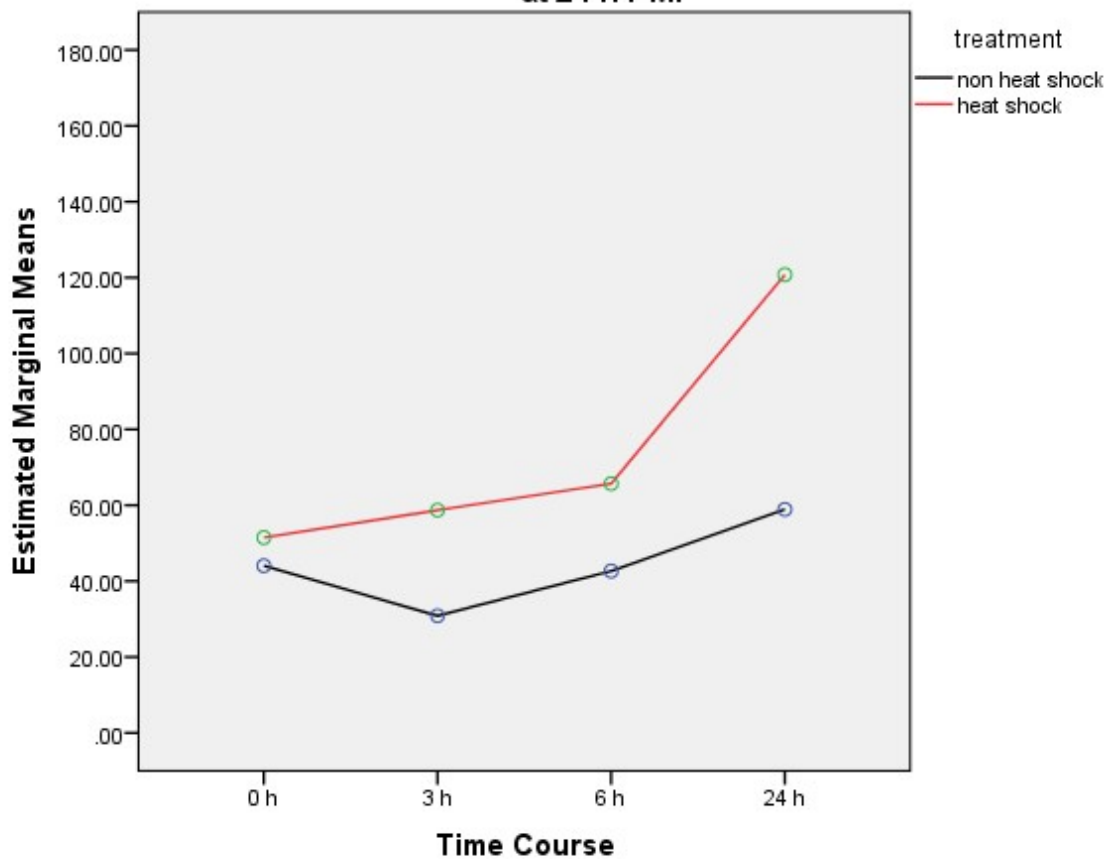


Figure 6.27 Estimated marginal means of *HSPA* transcript copy numbers at 24 h PMI. There was significantly lower *HSPA* transcript copy numbers at 24 h PMI, 0 h time course in non-heat shock (MD = 44.06, SD = 0.583) than heat shock [MD 51.47, SD = 2.45; $t(4) = 5.093$, $P = .029$]. There was significantly lower *HSPA* transcript copy numbers at 24 h PMI, 3 h time course in non-heat shock (MD = 30.86, SD = 2.49) than heat shock [MD 58.71, SD = 1.03; $t(4) = 17.88$, $P < .05$]. There was significantly lower *HSPA* transcript copy numbers at 24 h PMI, 6 h time course in non-heat shock (MD = 42.65, SD = 1.85) than heat shock [MD 65.68, SD = 2.82; $t(4) = 11.82$, $P = .001$]. There was significantly lower *HSPA* transcript copy numbers at 24 h PMI, 24 h time course in non-heat shock (MD = 58.90, SD = 3.06) than heat shock [MD 120.73, SD = 2.14; $t(4) = 28.71$, $P < .05$] (Table 6.4).

For *GAPDH* transcript copy numbers had a non-significant effect for time course [F(3,14) = .163, P = .920]; Wilks' Lambda = 0.966; partial eta squared = 0.034. *GAPDH* gene expression had a non-significant effect between the interaction of: time course and PMI [F(9,34.22) = .367; P = .943], Wilks' Lambda = .799, partial eta squared = 0.072; time course and treatment [F(3,14) = 1.020; P = .413], Wilks' Lambda = 0.821, partial eta squared = 0.179; time course and PMI and treatment [F(9,34.22) = .766; P = .717], Wilks' Lambda = 0.648, partial eta squared = 0.138.

There was a non-significant effect in *GAPDH* transcript copy numbers on the combined variables for PMI [F(3,16) = .085, P = .967]; partial eta squared (η_p^2) = 0.016; treatment [F(1,16) = 0.672, P = .424]; partial eta squared 0.040 and PMI and treatment [F(3,16) = .313, P = .815]; partial eta squared = 0.056.

Post-hoc analyses using Tukey's HSD test indicated that all differences failed to reach significance.

When the results for the dependent variables were considered separately, there was a statistical non-significance in PMI at time course: 0 h [F(3,16) = .336, P = .800]; partial eta squared = .059; 3 h [F(3,16) = .224, P = .879]; partial eta squared = .040; 6 h [F(3,16) = .259, P = .854]; partial eta squared = .046 and 24 h [F(3,16) = 0.00, P > .05]; partial eta squared = .000.

There was a statistical non-significance in treatment at time course: 0 h [F(1,16) = .719, P = .409]; partial eta squared = .043; 3 h [F(1,16) = .378, P = .547]; partial eta squared = .023; 6 h [F(1,16) = 1.244, P = .281]; partial eta squared = .072 and 24 h [F(1,16) = 2.022, P = .174]; partial eta squared = .112.

There was a statistical non-significance in PMI and treatment at time course: 0 h [F(3,16) = .005, P = > .999]; partial eta squared = .001; 3 h [F(3,16) = .224, P = .879];

partial eta squared.040; 6 h [F(3,16)435, P.731]; partial eta squared.075 and
24 h [F(3,16)1.050, P.398]; partial eta squared.164.

Table 6.4. Descriptive statistics showing the mean *HSPA* transcript copy numbers for untreated and treated brain tissue.

PMI	Treatment	N	Time Course							
			0 Hour		3 Hour		6 Hour		24 Hour	
			Mean	STD Dev.	Mean	STD Dev.	Mean	STD Dev.	Mean	STD Dev.
0 Hour	Non	3	2.24	.00	2.24	.00	2.24	.00	19.31	.837
	Heat	3	12.80	1.98	19.20	.526	15.75	3.67	18.99	1.24
3 Hour	Non	3	2.24	.00	10.21	1.03	19.02	.811	18.82	.437
	Heat	3	36.51	.647	19.97	1.07	59.30	.785	19.90	1.70
6 Hour	Non	3	30.08	2.30	47.45	2.07	50.44	2.19	45.89	1.01
	Heat	3	129.81	7.59	167.39	10.83	66.48	.878	62.57	1.91
24 Hour	Non	3	44.06	.583	30.86	2.49	42.65	1.85	58.90	3.06
	Heat	3	51.47	2.45	58.71	1.03	65.68	2.82	120.76	2.14

Table 6.5. Descriptive statistics showing the mean *GAPDH* transcript copy numbers for untreated and treated brain tissue.

PMI	Treatment	N	Time Course							
			0 Hour		3 Hour		6 Hour		24 Hour	
			Mean	STD Dev.	Mean	STD Dev.	Mean	STD Dev.	Mean	STD Dev.
0 Hour	Non	3	267595.53	2348.43	264904.33	4036.84	267652.60	7175.04	270333.27	3140.67
	Heat	3	269034.67	8198.82	266945.90	5354.84	268281.23	3116.86	266239.67	2348.43
3 Hour	Non	3	264904.33	4036.84	269709.77	7719.68	270333.27	3140.67	266945.90	5354.84
	Heat	3	266945.00	5353.81	266945.90	5354.84	269709.77	7719.68	269709.77	7719.68
6 Hour	Non	3	267595.53	2348.43	269709.77	7719.68	270333.27	3140.67	270333.27	3140.67
	Heat	3	269709.77	7719.68	266945.90	5354.84	266239.67	2348.43	266239.67	2348.43
24 Hour	Non	3	267595.53	2348.43	269709.77	7719.68	270333.27	3140.67	270333.27	3140.67
	Heat	3	269709.77	7719.68	266945.90	5354.84	266239.67	2348.43	266239.67	2348.43

Overall inspection of the mean scores for *GAPDH* transcript copy numbers indicated no significant differences in PMI, time course and treatment (Table 6.5)

Table 6.6. Statistical data from Tukey’s HSD test showing significance of *HSPA* transcript copy numbers between PMI. Any significant differences $P \leq 0.05$ are highlighted in bold.

(I) PMI	J (PMI)	Mean Difference (I – J)	Std. Error	Sig.
0	3	11.65	.990	.000
	6	63.42	.990	.000
	24	47.54	.990	.000
3	6	51.77	.990	.000
	24	35.89	.990	.000
6	24	35.89	.990	.000

Post-hoc analyses using Tukey’s HSD test indicated significantly lower *HSPA* transcript copy numbers in 0 h PMI than in: 3 h PMI (MD = 11.65, $P < .05$); 6 h PMI (MD = 63.42, $P < .05$) and 24 h PMI (MD = 47.54, $P < .05$). There was significantly lower *HSPA* transcript copy numbers in 3 h PMI than in: 6 h PMI (MD = 51.77, $P < .05$) and 24 h PMI (MD = 35.90, $P < .05$). There was significantly lower *HSPA* transcript copy numbers in 6 h PMI than in: 24 h PMI (MD = 15.88, $P < .05$) (Table 6.6).

6.3 Immunofluorescence

Under normal conditions HSPA protein in cells is localized in the cytoplasm, however under conditions of stress HSPA migrates to the nucleus. Immunofluorescence detection staining was carried out utilising a monoclonal primary HSPA antibody to identify the presence and localization of HSPA protein in post-mortem rat brain tissue for any comparable differences between control (unstressed) and under heat shock (stressed) conditions.

The tissue sections were initially fixed in freshly made 4% Paraformaldehyde (w/v) in PBS (0.1 M) for 15 min at room temperature, following which the excess paraformaldehyde was removed. The fixed tissue sections were permeabilized using Trypsin (0.025%) in aqueous calcium chloride (CaCl₂) (0.1%, pH 7.8) and incubated for 45 min at 37°C, then washed three times in warm PBS (0.1M). The sections were then incubated in blocking solution (0.1% PBS, 0.5% Tween 20, 0.1% Goat serum) for 30 min at room temperature, followed by overnight incubation at 4°C in the primary antibody for HSPA (Anti-Hsp70 antibody [BRM-22], Abcam,UK, dilution 1:200) to allow the antibody to bind and for permitted saturation to take place. After overnight incubation, the sections were washed with PBS three times for 5 min and incubated in a light sensitive Anti-mouse IgG FITC (Fluorescein Isothiocyanate) conjugated secondary detection antibody (Goat polyclonal Secondary Antibody to Mouse IgG - H&L FITC, Abcam, UK, dilution 1:200) diluted in blocking solution for 1 h at room temperature. The secondary antibody was removed followed by three consecutive washes with warm PBS (0.1 M). The sections were mounted under a cover slip using VECTASHIELD PI (0.01 M) (Propidium Iodide, Vector, USA) mounting medium. The tissue sections were then examined and images recorded using an Axiovert 200 LSM 510 laser scanning confocal microscope (Carl Zeiss, USA). Negative control cells from each sample

encountered identical preparations for immunofluorescence staining, except that the primary antibody was omitted.

HSPA antigens detected using an Anti-mouse IgG FITC conjugated secondary antibody were identified in the non-heat shock brain tissue, at 0 h post-mortem interval: in the cytoplasm at 0, 3 and 24 h time course, predominantly in the cytoplasm with a little fluorescence emitted from the nucleus at 6 h time course and in both cytoplasm and nucleus at 12 h time course (Figure 6.28). At 3 h post-mortem interval fluorescence was emitted: in the cytoplasm at 0 h time course and predominantly in the cytoplasm with a little fluorescence emitted from the nucleus at 3, 6, 12 and 24 h time course (Figure 6.29). At 6 h post-mortem interval fluorescence was emitted: in both the cytoplasm and nucleus at 0, 3 and 6 h time course and predominantly in the cytoplasm with a little fluorescence emitted from the nucleus at 12 and 24 h time course (Figure 6.30). At 12 h post-mortem interval fluorescence was emitted: in both the cytoplasm and nucleus at 0 h time course and predominantly in the cytoplasm with a little fluorescence emitted from the nucleus at 3, 6, 12 and 24 h time course (Figure 6.31). At 24 h post-mortem interval fluorescence was emitted predominantly in the cytoplasm with a little fluorescence emitted from the nucleus at 0, 3, 6, 12 and 24 h time course (Figure 6.32).

In heat shocked brain tissue HSPA protein was detected in both the cytoplasm and the nucleus for each time course 0, 3, 6, 12 and 24 h for each post-mortem interval 0, 3, 6, 12 and 24 h (Figures 6.33 – 6.37).

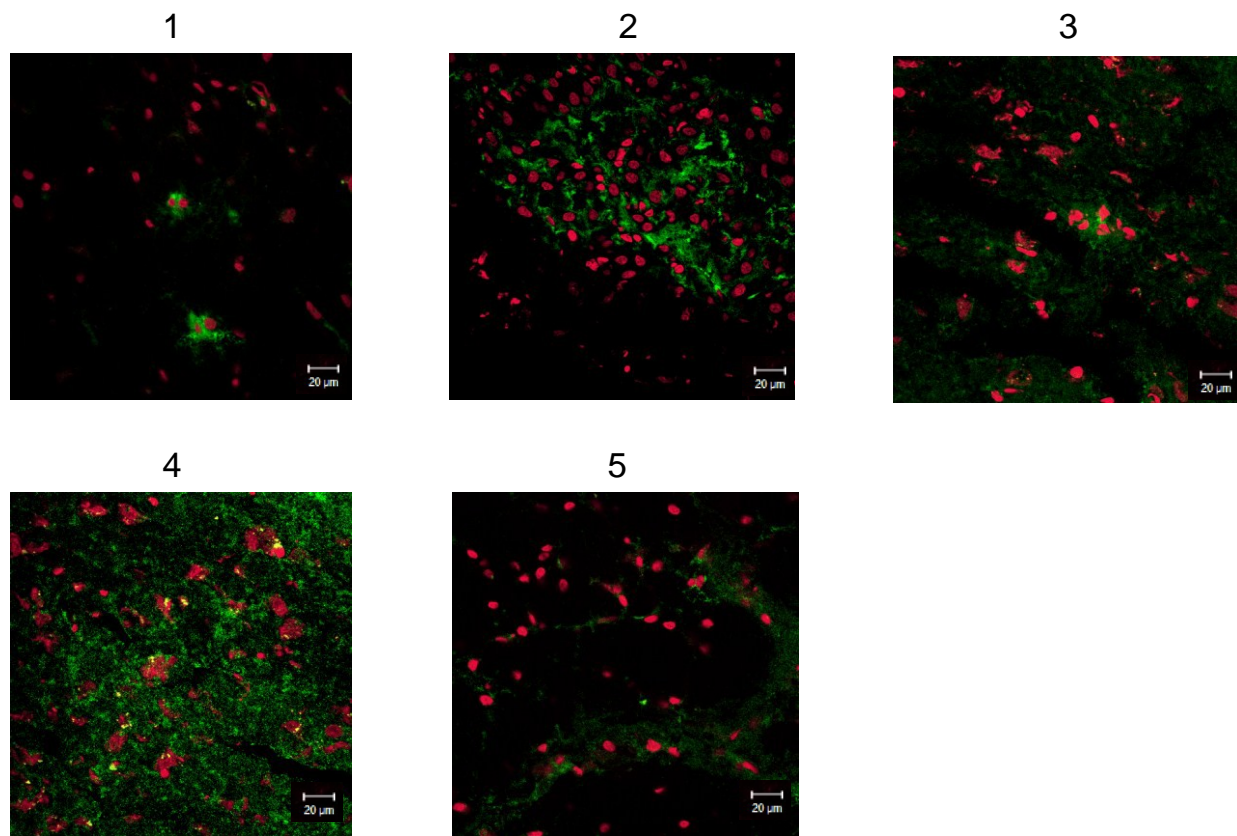


Figure 6.28 HSPA protein levels assessed using immunofluorescence in non-heat shocked rat brain tissue, PMI 0 h. (1) 0 h time course (2) 3 h time course (3) 6 h time course (4) 12 h time course (5) 24 h time course showing combined staining of nuclei labelled with propidium iodide (red) and primary antibody HSPA detected with Anti-mouse IgG FITC conjugated secondary antibody (green) Objective = x 40 magnification. Scale bar = 20μm.

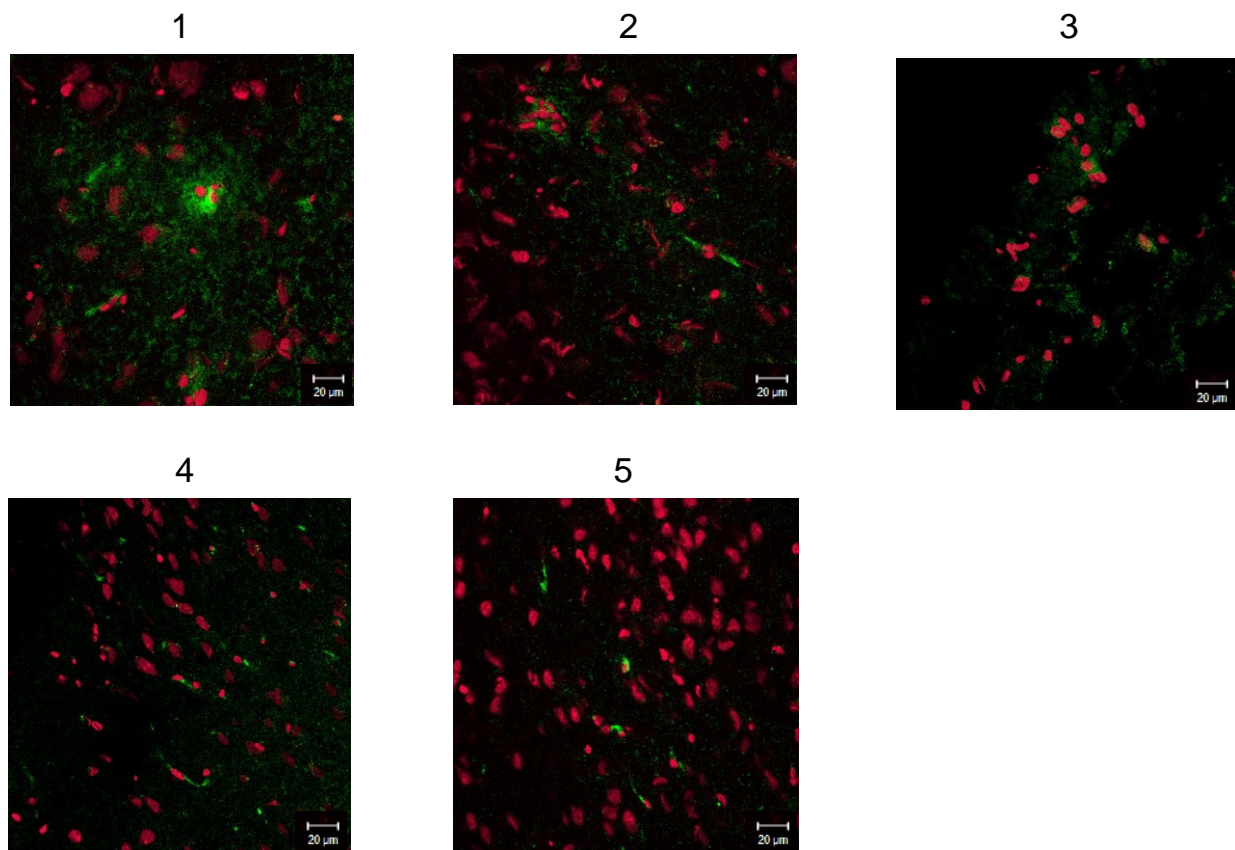


Figure 6.29 HSPA protein levels assessed using immunofluorescence in non-heat shocked rat brain tissue, PMI 3 h. (1) 0 h time course (2) 3 h time course (3) 6 h time course (4) 12 h time course (5) 24 h time course showing combined staining of nuclei labelled with propidium iodide (red) and primary antibody HSPA detected with Anti-mouse IgG FITC conjugated secondary antibody (green). Objective = x 40 magnification. Scale bar = 20μm.

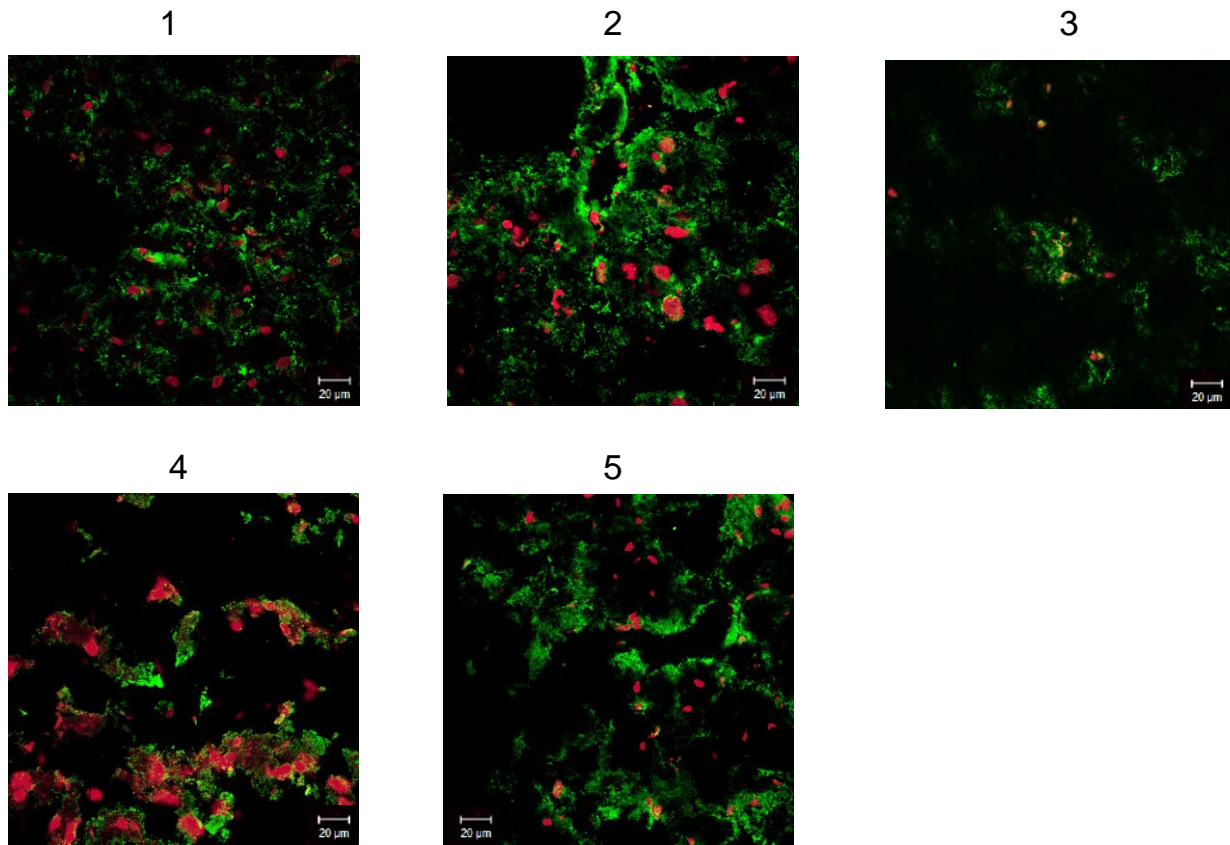


Figure 6.30 HSPA protein levels assessed using immunofluorescence in non-heat shocked rat brain tissue, PMI 6 h. (1) 0 h time course (2) 3 h time course (3) 6 h time course (4) 12 h time course (5) 24 h time course showing combined staining of nuclei labelled with propidium iodide (red) and primary antibody HSPA detected with Anti-mouse IgG FITC conjugated secondary antibody (green). Objective = x 40 magnification. Scale bar = 20 μ m.

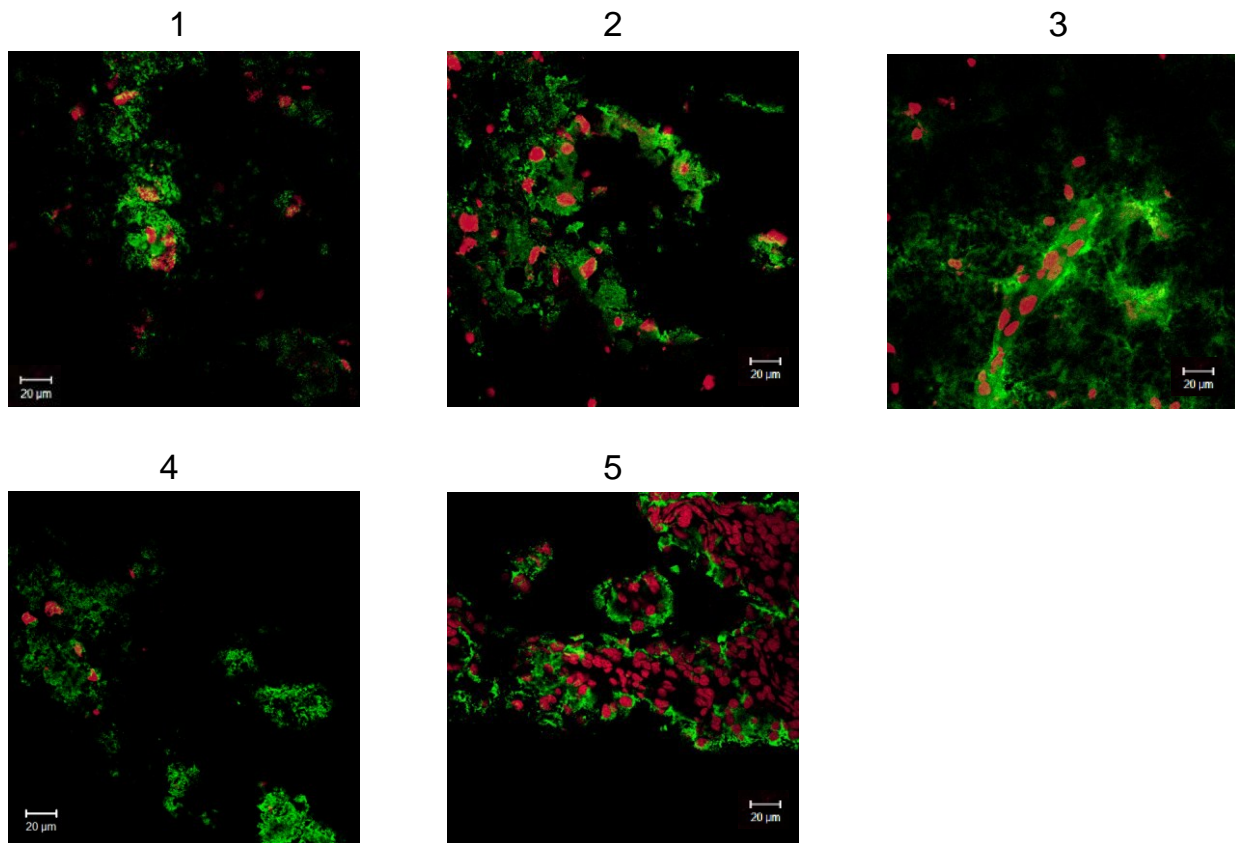


Figure 6.31 HSPA protein levels assessed using immunofluorescence in non-heat shocked rat brain tissue, PMI 12 h. (1) 0 h time course (2) 3 h time course (3) 6 h time course (4) 12 h time course (5) 24 h time course showing combined staining of nuclei labelled with propidium iodide (red) and primary antibody HSPA detected with Anti-mouse IgG FITC conjugated secondary antibody (green). Objective = x 40 magnification. Scale bar = 20μm.

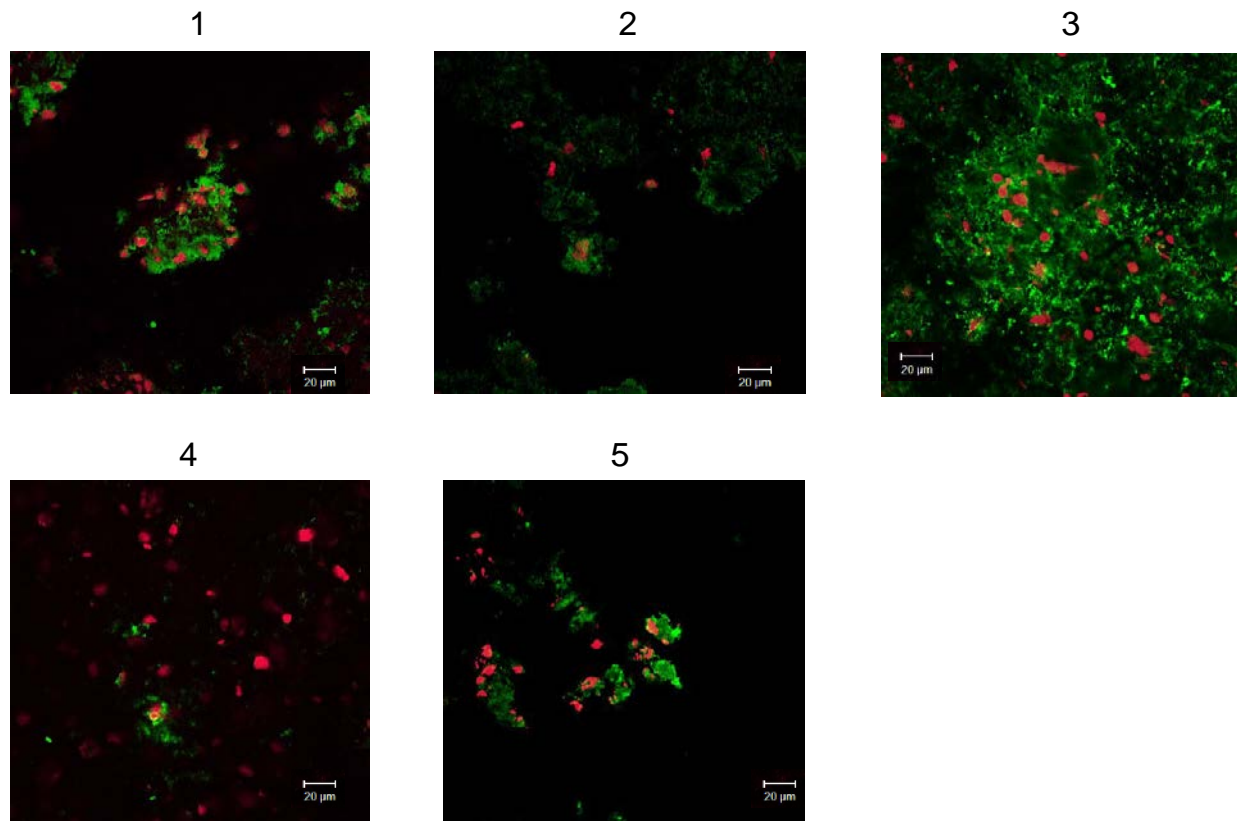


Figure 6.32 HSPA protein levels assessed using immunofluorescence in non-heat shocked rat brain tissue, PMI 24 h. (1) 0 h time course (2) 3 h time course (3) 6 h time course (4) 12 h time course (5) 24 h time course showing combined staining of nuclei labelled with propidium iodide (red) and primary antibody HSPA detected with Anti-mouse IgG FITC conjugated secondary antibody (green). Objective = x 40 magnification. Scale bar = 20μm.

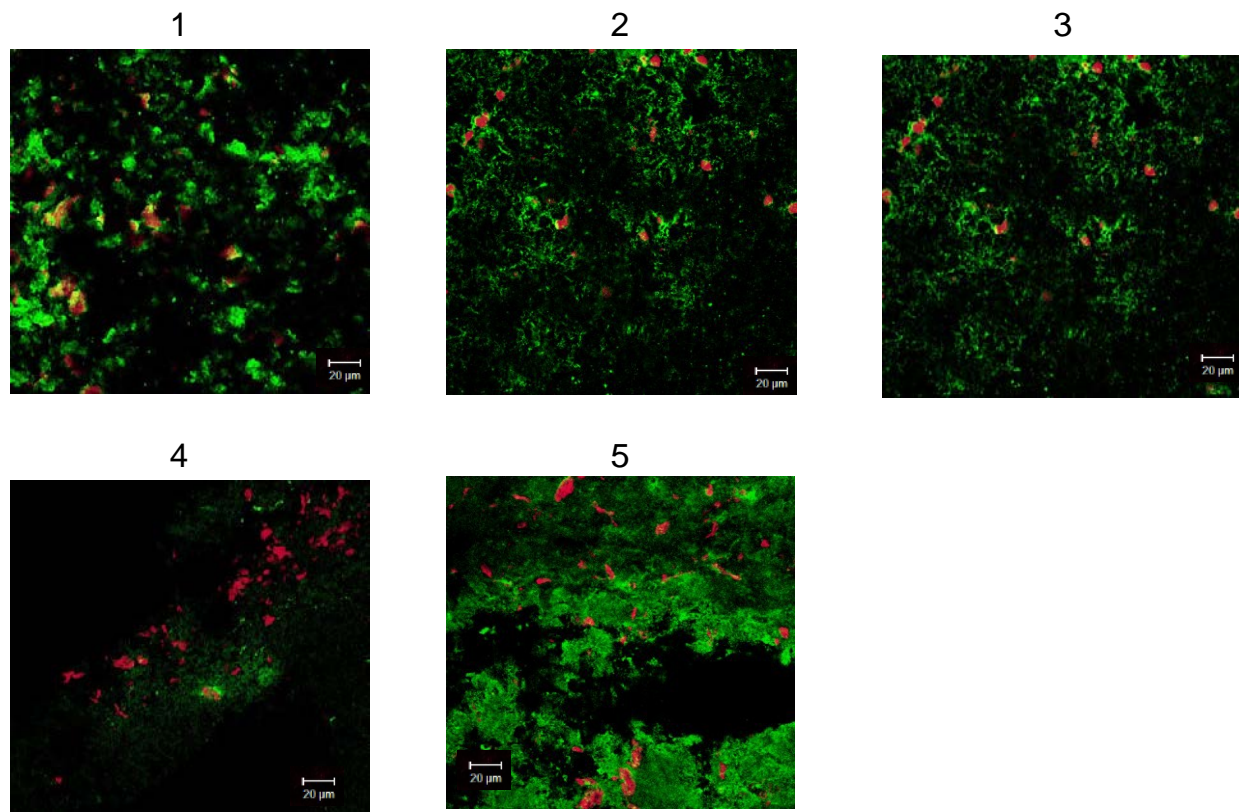


Figure 6.33 HSPA protein levels assessed using immunofluorescence in heat shocked rat brain tissue, PMI 0 h. (1) 0 h time course (2) 3 h time course (3) 6 h time course (4) 12 h time course (5) 24 h time course showing combined staining of nuclei labelled with propidium iodide (red) and primary antibody HSPA detected with Anti-mouse IgG FITC conjugated secondary antibody (green). Objective = x 40 magnification. Scale bar = 20 μ m.

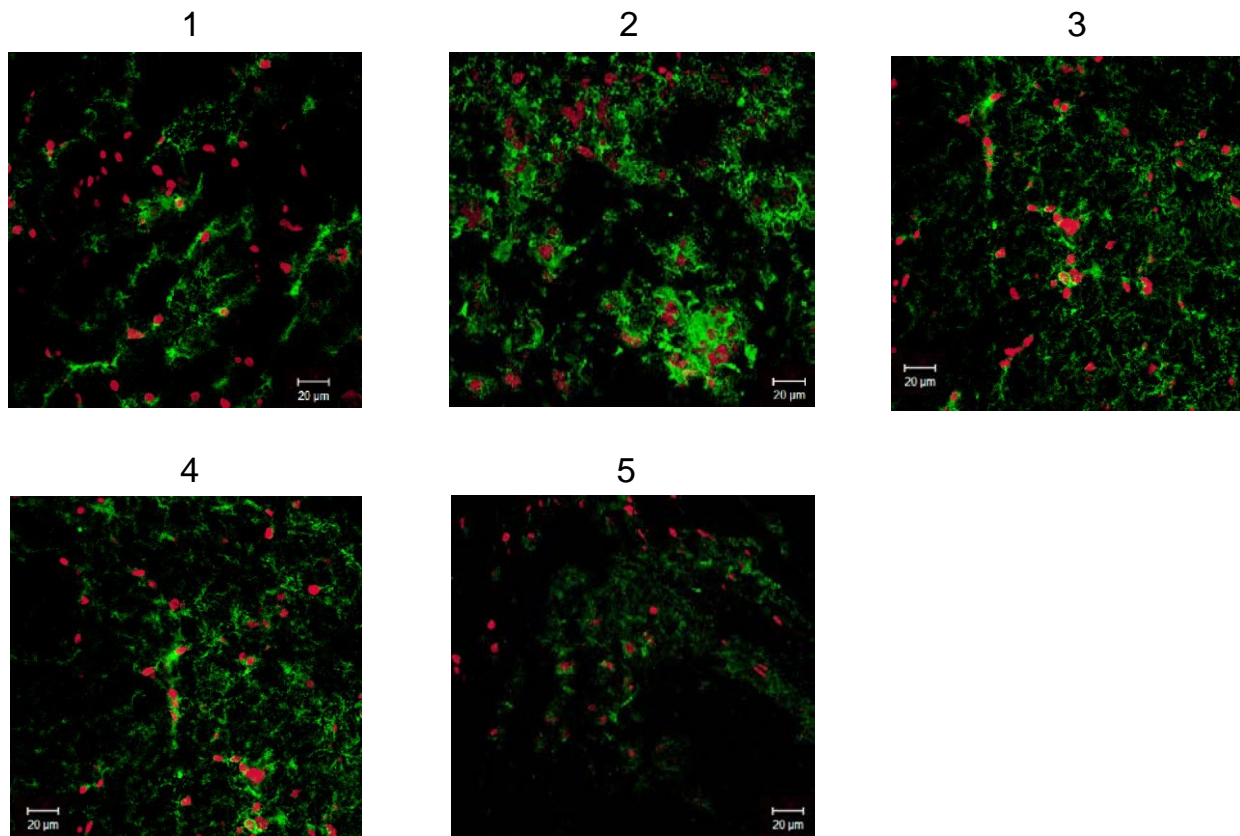


Figure 6.34 HSPA protein levels assessed using immunofluorescence in heat shocked rat brain tissue, PMI 3 h. (1) 0 h time course (2) 3 h time course (3) 6 h time course (4) 12 h time course (5) 24 h time course showing combined staining of nuclei labelled with propidium iodide (red) and primary antibody HSPA detected with Anti-mouse IgG FITC conjugated secondary antibody (green). Objective = x 40 magnification. Scale bar = 20 μ m.

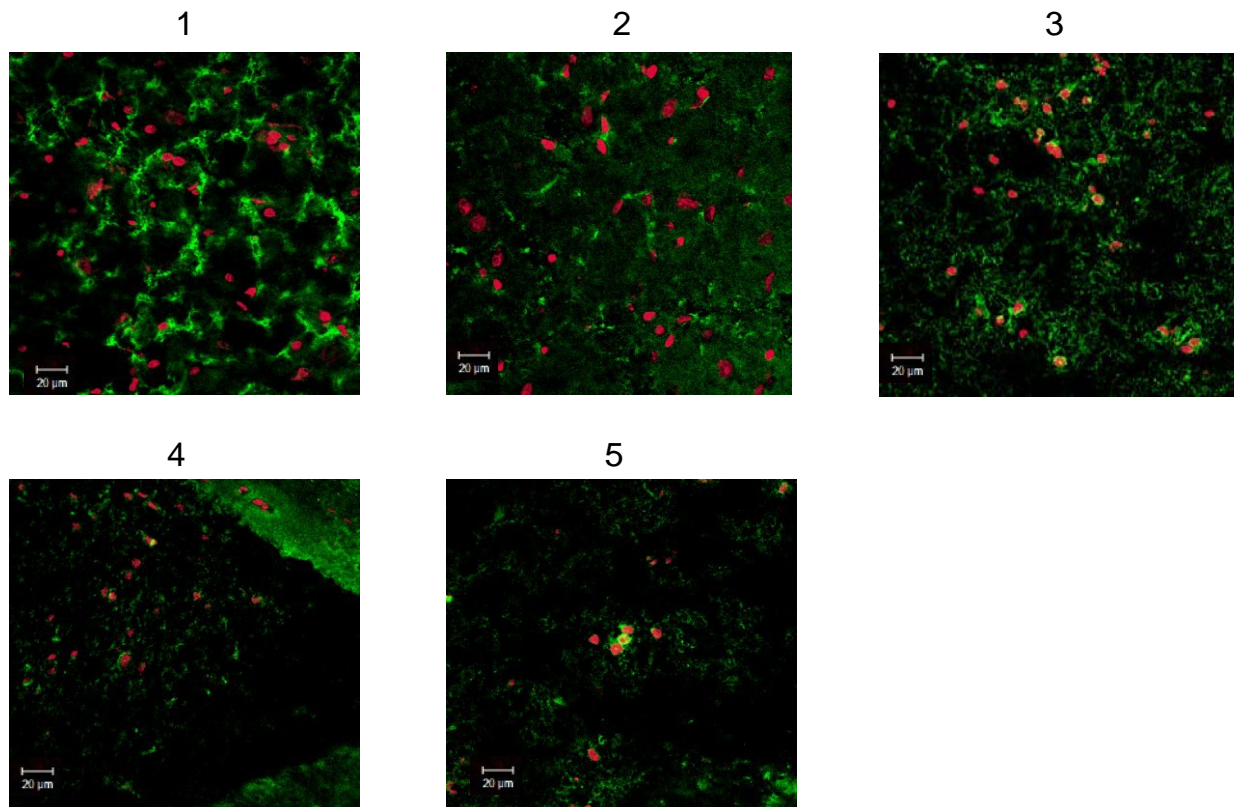


Figure 6.35 HSPA protein levels assessed using immunofluorescence in heat shocked rat brain tissue, PMI 6 h. (1) 0 h time course (2) 3 h time course (3) 6 h time course (4) 12 h time course (5) 24 h time course showing combined staining of nuclei labelled with propidium iodide (red) and primary antibody HSPA detected with Anti-mouse IgG FITC conjugated secondary antibody (green). Objective = x 40 magnification. Scale bar = 20μm.

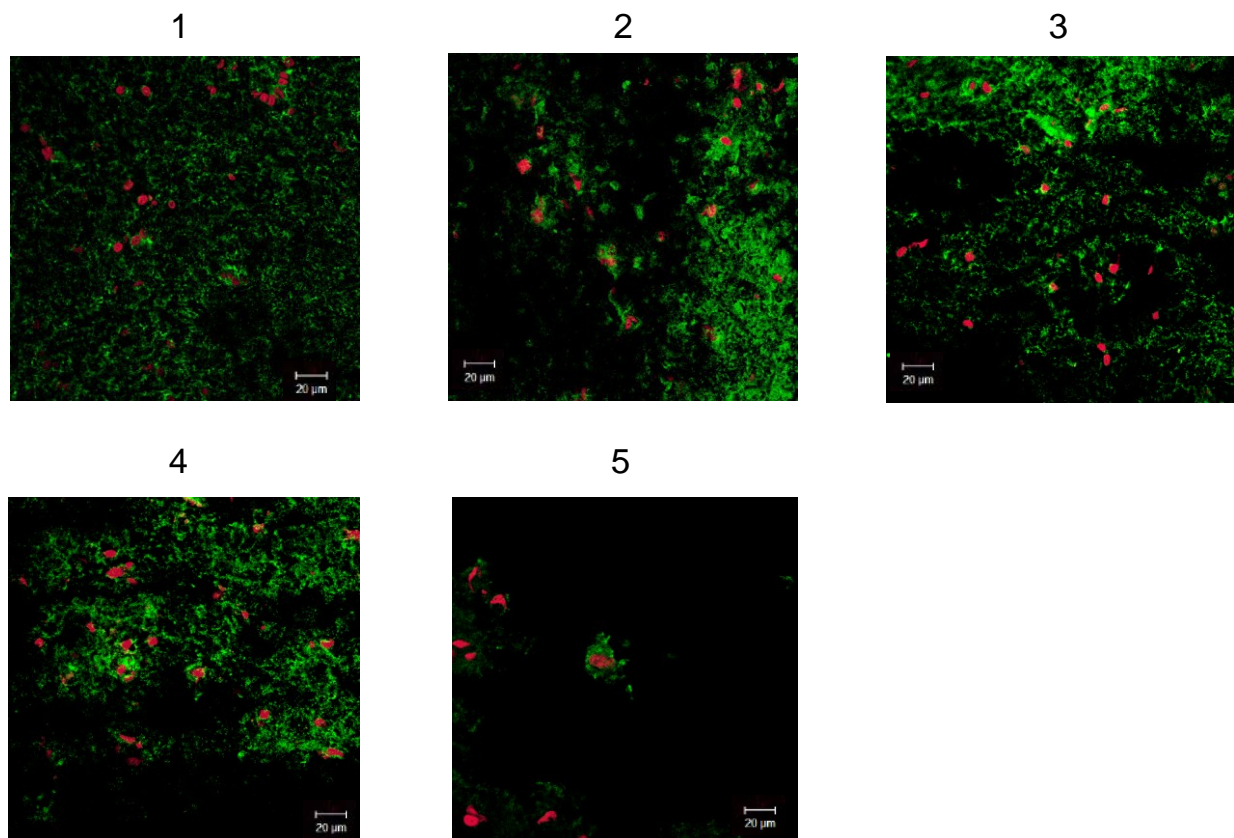


Figure 6.36 HSPA protein levels assessed using immunofluorescence in heat shocked rat brain tissue, PMI 12 h. (1) 0 h time course (2) 3 h time course (3) 6 h time course (4) 12 h time course (5) 24 h time course showing combined staining of nuclei labelled with propidium iodide (red) and primary antibody HSPA detected with Anti-mouse IgG FITC conjugated secondary antibody (green). Objective = x 40 magnification. Scale bar = 20 μ m.

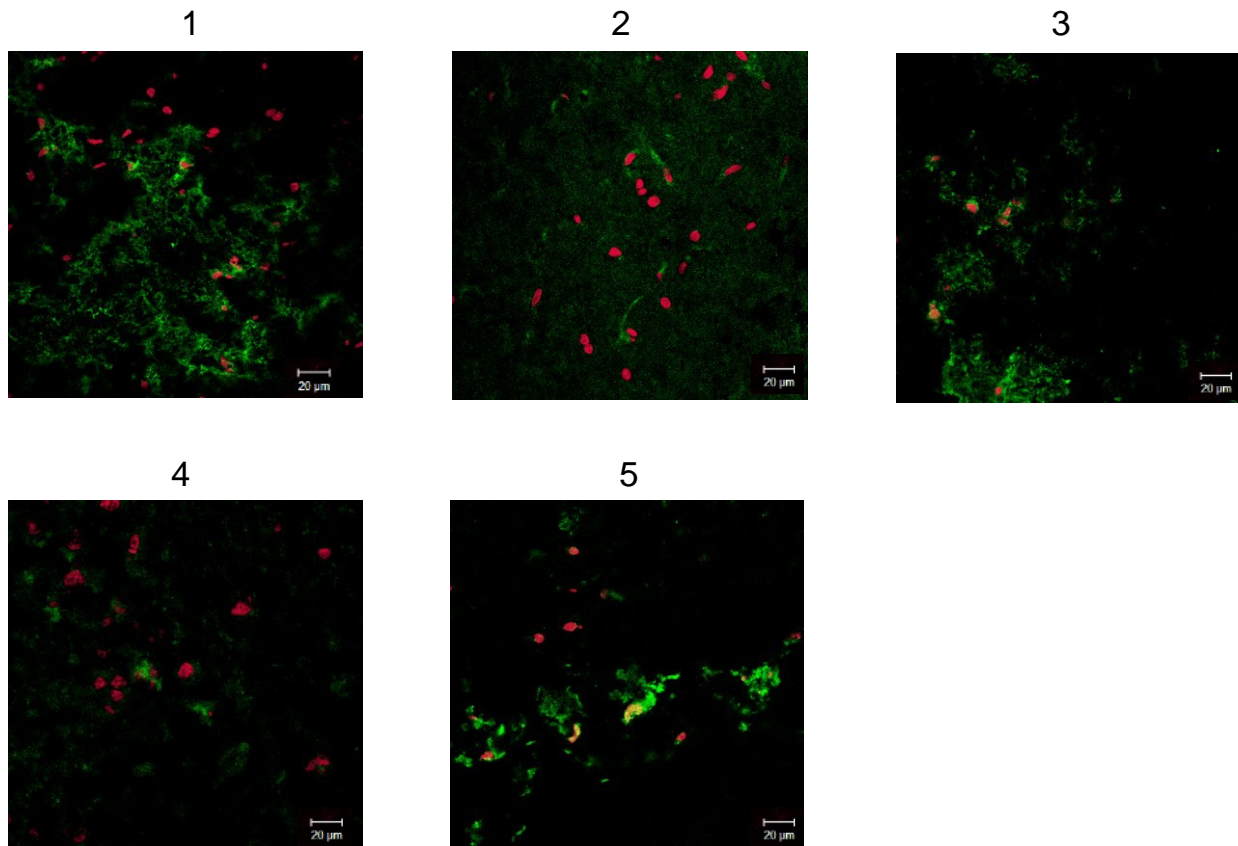


Figure 6.37 HSPA protein levels assessed using immunofluorescence in heat shocked rat brain tissue, PMI 24 h. (1) 0 h time course (2) 3 h time course (3) 6 h time course (4) 12 h time course (5) 24 h time course showing combined staining of nuclei labelled with propidium iodide (red) and primary antibody HSPA detected with Anti-mouse IgG FITC conjugated secondary antibody (green). Objective = x 40 magnification. Scale bar = 20 μ m.

Results from this investigation show that *HSPA* is expressed at low levels in normal brain tissue, but is highly expressed in brain tissue subjected to mild heat shock. In the non-heat shocked brain tissue, low level expression of *HSPA* was observed in the 0 h post-mortem interval at 0 h time course, followed by a gradual increase up to the 6 h time course interval, returning back to near basal levels at the 24 h time course interval. *HSPA* expression gradually decreased at 3 and 6 h post-mortem intervals however, *HSPA* transcripts substantially increased at the 12 h post-mortem interval. At the 24 h post-mortem interval *HSPA* transcripts were only present at low levels, below the initial basal levels observed at 0 h post-mortem 0 h time course interval. A higher level of *HSPA* expression was observed in samples taken at 0 h post-mortem that had been subjected to heat shock, compared to non-heat shock at each time course interval. *HSPA* transcripts were observed in the 0 h post-mortem interval at 0 h time course, followed by a gradual increase up to the 6 h time course interval, returning back to near basal levels at the 24 h time course interval. At 3 post-mortem, *HSPA* transcripts expressed high at 0 h time course with a gradual decline up to the 24 h time course. *HSPA* expression gradually decreased at 6 h post-mortem, however, as with non-heat shock, *HSPA* transcripts substantially increased at 12 h post-mortem. Again as with non-heat shock, *HSPA* transcripts were only present at low levels at the 24 h post-mortem interval, below or near to the initial basal levels observed at 0 h post-mortem 0 h time course interval.

The levels of *HSPA* transcripts in brain tissue that had been subjected to a mild heat shock, the first at 0 h time course followed by subsequent heat shocks at 3, 6 and 24 h time course intervals, showed a marked increase in *HSPA* expression in heat shocked brain tissue compared to non-heat shock within each post-mortem interval.

As expected, given that post-mortem and mild heat shock is a form of cellular stress, HSPA protein was detected in both the cytoplasm and the nucleus in all tissue samples at each post-mortem interval for both non-heat shock and heat shocked samples.

Chapter 7

Discussion

7.1. Discussion

7.1.1 Chapter 3 results

The target genes chosen for this study, *Homo sapiens* and *Rattus norvegicus* *HSPA*, both members of the heat shock protein family, are induced in response to various physiological and environmental stress conditions, or in response to certain diseases, such as cancer (Garrido *et al.*, 2006; Jolly and Morimoto, 2000; Lindquist, 1986; Morimoto, 1993; Powers *et al.*, 2009).

As discussed in chapter 3, section 3.3, the *HSPA* gene family contains three well characterized members: *HSPA1A*, *HSPA1B* and *HSPA1L*, which are located within the major histocompatibility complex class III region (MHC-III). In the human genome, they are located on the short arm of chromosome 6 (6p21.3), while in the rat genome, they are located on the short arm of chromosome 20 (20p12) (Milner and Campbell, 1990; Sargent *et al.*, 1989a; Sargent *et al.*, 1989). Although they contain similar nucleotide sequences, these three genes differ in their regulation. *HSPA1L* has no associated regulatory heat shock consensus sequence and is constitutively expressed at low levels, and is also induced by heat shock (Milner and Campbell, 1990). Therefore, this gene was excluded for the purposes of this study. Both *HSPA1A* and *HSPA1B* have been shown to encode identical protein products with 100% homology, and the genes also show 90% homology between their nucleotide sequences. Both have been shown to be expressed at high levels after heat shock, but only *HSPA1A* has been shown to be constitutively expressed at low levels (Milner and Campbell, 1990). After running a BLAST analysis for *HSPA1A* and *HSPA1B* and for the designed primers, results

indicated that both genes will be amplified at the same position and of the same product length for the designed primers (Appendix 9.26 and 9.27).

Studies have shown that, across a wide range of both human and rat tissues, the molecular integrity of 28S and 18S ribosomal RNAs and of some specific gene transcripts, such as interleukin-1 β (IL-1 β), can persist under post-mortem conditions for up to periods of 148 h in brain tissue (Inoue *et al*, 2002), making brain a suitable tissue for the purposes of this study. The molecular integrity of RNA is thus shown to be unlikely to change significantly in the early post-mortem period, up to 148 h in human and rat brain tissue, allowing the opportunity to elicit *de novo* gene expression of the *HSPA* gene in response to mild heat shock. Due to difficulties in obtaining post-mortem human brain tissue, rat brain tissue was chosen as an alternative source of tissue, and this was readily accessible from the Physiology Laboratory of this University. Sequence homology comparison between human and rat genes for *HSPA* indicated 73% homology between these two species for *HSPA* gene sequences and 96% homology for *HSPA* amino acid sequences, which also indicates that the rat is a comparable species to humans for the purposes of this study.

Primers for both *Homo sapiens* and *Rattus norvegicus* *HSPA* genes were designed using Primer 3 software. Melting curve analysis produced during RT-PCR showed only one defined peak indicating specific binding of primers to *HSPA*. This was confirmed by visualizing the resultant amplicons by agarose gel electrophoresis. Visualization of the amplicons showed the presence of a single band of the required product size. No primer-dimers or degradation were observed.

The choice of an appropriate internal standard is critical for quantitative protein and RNA analyses. Housekeeping genes are normally expressed in all cells and their expression levels should remain relatively constant under different experimental conditions. There is no single housekeeping gene that possesses stable expression levels under all experimental conditions. Therefore, it was necessary to characterize the suitability of any housekeeping gene chosen as an internal RNA control under particular experimental conditions where transcription effects are being tested. The chosen internal standard for this study was Glyceraldehyde-3-phosphate dehydrogenase (*GAPDH*), a housekeeping gene which encodes a glycolytic enzyme that possesses diverse functions that are independent of its role in glycolysis (Said *et al*, 2009, 2007; Sirover, 1999). *GAPDH* is a multifunctional enzyme reportedly over-expressed in many tumours and malignant cells (Said *et al*, 2009, 2007).

Literature has shown that *GAPDH* expression is regulated by a variety of different factors such as insulin (Nasrin *et al*, 1990); calcium (Chao *et al*, 1990) and hypoxia (Graven *et al*, 1994). The transcription factor hypoxia-inducible factor-1 alpha (HIF-1 α), which regulates the expression of genes involved in glucose supply, growth, metabolism, redox reactions and blood supply, is undetectable under normoxic conditions because it undergoes rapid ubiquitination and proteosomal degradation (Rapisarda *et al*, 2002). Hypoxia, which is the inadequate delivery of oxygen to tissue causes an imbalance between *oxygen* demand and energy supply, results in the transcription of HIF-1 regulated hypoxia induced genes (Cangul, 2004; Said *et al*, 2007). A number of the proteins encoded by these genes are involved in adaptive responses to hypoxia, such as angiogenesis, erythropoiesis, cell proliferation and cell survival (Said *et al*, 2007; Schmid *et al*, 1998). It has been suggested that *GAPDH* expression is regulated as a consequence of the hypoxic development of the cellular

environment *in vitro* and that *GAPDH* mRNA expression was regulated during hypoxic events (Graven *et al*, 1994; Graven and Farber, 1998; Said *et al*, 2005; Zhong and Simons, 1999).

There are two types of hypoxia: transient and chronic hypoxia. Transient hypoxia is a temporary reduction in oxygen availability. The inadequate vascular geometry relative to the volume of oxygen-consuming tumour cells creates diffusion-limited oxygen delivery, resulting in chronic hypoxia (Greco *et al*, 2003). The synthesis of HIF-1 is up-regulated in response to hypoxia. In general, tumours often contain hypoxic regions, since tumour vasculature is dysfunctional and unable to meet the metabolic needs of rapidly proliferating cancer cells (Hanahan and Folkman, 1996). The extent of hypoxic regions in a tumour tissue depends on the arrangement, blood flow rate and blood oxygen content of microvessels, and on the tissue's oxygen consumption rate (Said *et al*, 2007).

Studies undertaken by Said *et al*, (2007, 2009) compared the expression of *GAPDH* with 18S RNA in relation to HIF-1 α under different oxygen concentrations of severe hypoxia, normoxia and re-oxygenation in human glioblastoma, low-grade astrocytoma and normal brain tissue samples, together with human glioblastoma cell lines. These results did not indicate any correlation between hypoxia induced HIF-1 α protein over-expression and *GAPDH* regulation on mRNA and protein level *in vitro* in human glioblastoma cell lines. *GAPDH* was not significantly regulated under hypoxic conditions in a panel of human tumour cell lines *in vitro*, and the expression of the HIF-1 gene was not altered after substitution of the *GAPDH* by the 18S RNA band (Said *et al*, 2005). Extended studies by Said *et al*, (2009) indicated significant mRNA over-expression of known hypoxia-regulated genes in glioblastoma, compared to low-grade

astrocytoma (Said *et al*, 2007). It can be suggested that from these studies that the regulation of *GAPDH* mRNA synthesis as a response to the hypoxic development in the tumour cell environment *in vitro* and *in vivo* occurs as a cell-specific post-transcriptionally regulated event and that there is no hypoxia-dependent regulation of *GAPDH* in astrocytic tumours *in vivo*. It can therefore be concluded that *GAPDH* is a suitable reference gene for studies in normal and tumour brain tissue and cell lines under hypoxic conditions.

Results described in chapter 4 for *GAPDH* showed that mRNA copy numbers were relatively consistent in NHA (approximately 146,500 copies per sample) 1321N1, (approximately 144,500 copies per sample), GOS-3, (approximately 147,500 copies per sample) and U87-MG, (approximately 147,500 copies per sample), confirming the routine comparability of *HSPA* results (Table 4.1). For *GAPDH*, mRNA copy numbers were relatively consistent in all brain tissue samples, at approximately 143,700 copies per sample), again confirming the relative comparability of *HSPA* results (Figure 4.3 and Table 4.6).

Results described in chapter 5 for *GAPDH* showed that mRNA copy numbers were relatively consistent in NHA-, (approximately 148,300 copies per sample), 1321N1, (approximately 147,400 copies per sample), GOS-3, (approximately 147,400 copies per sample) and U87-MG, (approximately 147,300 copies per sample), again confirming the relative comparability of *HSPA* results (Figure 5.2 and Table 5.1).

One of the most important technical considerations in this study was the quality of the isolated mRNA. Cellular mRNA is less stable than DNA due to the ubiquitous nature and stability of RNases compared with DNases, and so RNA is more susceptible to spontaneous degradation. In addition to the intrinsic RNases already present in cells and

tissues, samples may become contaminated by RNases from other sources, such as bench surfaces and laboratory equipment, and therefore rigorous laboratory procedures for aseptic technique were required. During this study, contaminating RNase activity was precluded by careful preparation of reagents, aseptic handling of samples and use of equipment. During this study only RNase free pipette tips, microfuge tubes and RNase free water was used and all equipment was pre-treated with RNase-Zap, a commercial surface decontamination solution that destroys RNases on contact (Sigma, UK), prior to use.

mRNA isolated from NHA, 1321N1, GOS-3 and U87-MG cell lines and rat brain tissue samples showed little or no degradation or contamination. The overall A_{260} / A_{280} value for isolated mRNA ranged between 1.8 – 2.0 in the cell lines and 1.6 – 1.8 in the brain tissue samples, which was deemed acceptable for the purpose of this study.

The primary and secondary antibodies used for flow cytometry and immunofluorescence were obtained from Abcam, UK. The primary antibody Monoclonal Anti-Heat Shock Protein 70 (HSP70) reacts specifically with HSP70 and recognizes brain HSP70 in both human and rat. Immunofluorescent staining using this antibody has demonstrated a rapid and reversible accumulation of the HSP70 protein within the nucleus of heat-stressed (42°C, 1 hr.) human fibroblasts (Morimoto, 1998).

The secondary antibody Goat polyclonal Secondary Antibody to Mouse IgG - H&L FITC, was recommended by Abcam. No dilution factor was recommended for either antibody, and following a number of pilot trials with different dilutions, 1:200 (1 µl of antibody in 200 µl of blocking solution) was the most efficient and gave the best results.

This study had six main objectives:

1. To characterize the level of *HSPA* expression in normal human cell lines and normal human brain tissue compared to glioma cell lines and tumourous brain tissue.
2. To characterize the level of *HSPA* transcription in response to hypoxia in normal and glioma cell lines.
3. To characterize the level of *HSPA* transcription in post-mortem brain tissue.
4. To characterize the level of *HSPA* transcription in response to heat shock applied to the brain tissue in the early post-mortem period.
5. To characterize the level of *HSPA* transcription in response to multiple heat shocks applied to the brain tissue in the early post-mortem period.
6. Validate if *HSPA* can be used as an early post-mortem marker.

7.1.2 Chapter 4 and 5 results

HSPA is expressed at low levels in normal cells and tissues, but its expression is highly induced by cancer. The results from this study show that *HSPA* is expressed at high levels in pre and post hypoxia treated glioma cells. The average *HSPA* mRNA copy numbers in the three glioma cell lines were approximately 6 fold higher than the normal cell line and the average *HSPA* mRNA copy numbers in glioblastoma tissue were approximately 1.8 and 9 fold higher than in the low grade glioma and normal tissues, respectively. In cancer, *HSPA* expression is induced to assist the stabilization of native proteins (Rohde *et al*, 2005). On the other hand, *HSPA* mRNA levels in the untreated NHA cells were relatively low in comparison to hypoxia treated cells. This is in agreement with previous reports such as Rohde *et al*, (2005), where significantly higher expression was reported in cancer tissue in comparison to normal tissue, supporting the

notion that the increased expression of *HSPA* is associated with cellular stress (Rohde *et al*, 2005).

Although prolonged exposure to extreme stress conditions can result in cell and tissue death, induction of heat shock protein synthesis can afford cytoprotection and stress tolerance against stress-induced molecular damage. Heat shock protein synthesis is induced by numerous stress stimuli resulting in the accumulation of non-native proteins.

The heat shock response in mammalian cells involves the activation of heat shock factor 1 (HSF1) in response to the presence of non-native proteins which require the action of molecular chaperones. HSF1 is present in both stressed and unstressed cells. In unstressed cells HSF1 is found in the cytoplasm as an inert monomer bound to HSPA and therefore does not show any transcriptional activity. In a stressed state when non-native proteins are detected, HSF1 translocates to the nucleus and oligomerises into a trimer that becomes inducibly phosphorylated and binds to the heat shock element upstream of the *HSPA* gene, resulting in stress-induced transcription (Santoro, 2000).

Given that cancer is a form of cellular stress, it is to be expected that *HSPA* protein should be observed in both the cytoplasm and the nucleus of glioma and normal cell lines under pre and post hypoxic conditions. Although *HSPA* protein was detected mainly in the cytoplasm in the normal cell line, after hypoxia treatment, migration of *HSPA* to the nucleus was observed. Increased synthesis of heat shock proteins to a level proportional to that of non-native proteins results in *HSPA* relocating to the nucleus and binding to the HSF1 transcriptional transactivation domain, thereby blocking transcription of heat shock genes (Santoro, 2000).

As mentioned previously, *HSPA* is expressed at low levels in normal cells and tissues, but its expression is highly induced by cancer. Results from this study showed that *HSPA* is highly expressed at mRNA levels in pre and post hypoxia treated glioma cells. The average *HSPA* mRNA copy numbers in the three glioma cell lines were approximately 6 fold higher than the normal cell line in both pre- and post-hypoxia treatment. In glioma cancerous cells, *HSPA* is induced to assist the stabilization of native proteins in an effort to maintain its functionality (Rhode *et al*, 2005). On the other hand, *HSPA* mRNA levels in the untreated NHA cells were relatively low in comparison to hypoxic cells. A previous citation, Rohde *et al*, (2005), reported a significantly higher expression in breast cancer tissue in comparison to normal, supporting the notion that the increased expression of *HSPA* is associated with stress (Rhode *et al*, 2005)

High fluorescence intensity of *HSPA* observed in 1321N1, GOS-3 and U87-MG cells exposed to hypoxia showed a 3-fold increase compared to NHA cells, which suggests that hypoxia can activate HSF1 in many cell types, resulting in an increased expression of *HSPA*. Production of heat shock proteins in response to hypoxia depends on the cell type. In some endothelial cells, such as human microvascular (HMEC1), *HSPA* expression in response to hypoxia is down-regulated (Oehler *et al*, 2000). In contrast, *HSPA* expression is up-regulated in human hepatoma (HEP G2) (Patel *et al*, 1995) and human proximal tubular epithelial cells (Turman *et al*, 1997).

In neoplasms, *HSPA* expression has been associated in the regulation of apoptosis as a modulator of p53 function in the immune response against tumours and multidrug resistance (Ciocca *et al*, 1993; Soussi and Lozano, 2005). Increased *HSPA* expression enhances the resistance of cells to apoptosis which elevates immunity due to their

highly immunogenic properties. Thus, during carcinogenesis, the expression of heat shock proteins will be altered in many tumour types (Schmitt *et al*, 2007). High expression levels of HSPA protein were detected in the cytoplasm of bladder carcinomas, but no correlation was found between the expression level, grade of tumour, disease phase and patient outcome (Lebret *et al*, 2003).

Glioblastoma patient survival rate is considerably short, as indicated in Table 4.5 section 4.2.3. The survival period of patients from diagnosis to death ranged between 8 to 12 months with only one patient exceeding this period. The sample size used in this study indicating survival period across the patient sample data range is too small to make any significant conclusion. Future studies need to be undertaken using a larger sample base to include a larger variance of survival rate together with a wider range of cancer grade. However, from this initial study, the notion that expression of *HSPA* appears to be grade related is consistent with the results obtained in Figure 4.5.

Results from this part of the study showed that *HSPA* was similarly expressed at high levels in all three glioma cells lines *in vitro*, (Figure 4.1) however in the human brain tissue samples *HSPA* was predominantly expressed in malignant astrocytomas *in vivo* especially in glioblastomas (Figure 4.2), the most aggressive and phenotypically transformed of the gliomas. Although the results indicated an apparent grade related expression in the human brain tissue samples, this was not replicated in the three glioma cells lines. A possible explanation for this is that *in vitro* (cell lines) experiments, in cellular biology, are conducted outside of the organisms which do not correspond to the same conditions inside the organism (*in vivo*) which may lead to results that do not correspond to the same situation that arises in a living organism. For example, *in vivo*, tumour cells can release a variety of degradative enzymes, and enhanced proteolytic

activity which has been associated with tumour growth, angiogenesis and invasiveness (Yamamoto *et al*, 1996).

Significant differences were shown in *HSPA* mRNA expression levels between normal and the three glioma cells (Table 4.2), however no differences were observed at the protein level (Table 4.9), indicating that the level of *HSPA* protein did not directly correlate with the level of *HSPA* mRNA, suggesting *HSPA* expression in the glioma cell lines might be regulated either at the transcriptional level by a mechanism governing message stability or at the posttranscriptional level.

Although heat shock protein levels are not informative as diagnostic markers, they are useful biomarkers for carcinogenesis in some tissues (Ciocca and Calderwood, 2005). The high levels of *HSPA* expression detected in the majority of glioblastoma tissues, compared to low grade gliomas and normal tissues, may be taken as an indicator of its potential use as a biomarker for carcinogenesis in glioma. Elevated levels of *HSPA* have been related to malignancy, metastasis, poor prognosis and resistance to therapeutic strategies, including chemotherapy or radiation in glioblastoma, breast, bladder, endometrial and cervical carcinomas (Piura *et al*, 2002; Syrigos *et al*, 2003; Thanner *et al*, 2003). In contrast, a high level of *HSPA* expression has been associated with good prognosis in melanoma, pancreatic and renal carcinomas (Ricianadis *et al*, 2001; Sagol *et al*, 2002; Santarosa *et al*, 1997), suggesting possible tissue specificity.

Previous studies have shown that silencing of *HSPA* isoforms produces variable effects on cell viability, depending on the cell line used. Furthermore, silencing of one isoform heat shock cognate 70 (*HSPA8/HSC70*) leads to concurrent induction of the other isoform heat shock protein 72 (*HSPA/HSP72*) in glioblastoma, colon and ovarian cancer

cell lines (Powers *et al*, 2008). By silencing the *HSPA* isoforms, heat shock protein 90 (*HSPC1^a/HSP90*) function was modulated and also induced apoptosis in cancer cells. *HSPC1^a/HSP90* inhibition has been a promising target for cancer inhibition over the last decade. Thus, it can be postulated that a multi-target approach should be adopted modulating *HSPA* and *HSPC1^a/HSP90* function, for the future (Powers *et al*, 2009).

BAG1 and HSPA protein synthesis is up-regulated during the early post-mortem period (up to 4 hours) (Curcio *et al*, 2006; Torres *et al*, 2004). In cases of unexplained deaths one of the most important factors is accurate and precise determination of time since death, referred to as the post-mortem interval (PMI). Various methods are currently employed to determine PMI: temperature measurements post-mortem, biochemical markers and post-mortem muscle proteolysis (relaxation of muscles following rigor mortis). In many types of cancers, *HSPA* expression becomes dysregulated, resulting in elevated levels under stress conditions; furthermore, HSPA protects cancer cells from apoptosis (Calderwood, 2005). As HSPA1A protein is up-regulated in diseases such as cancer, Alzheimer's and Parkinson's disease (Petrucci *et al*, 2004), in order to use HSPA as an early post-mortem marker, the possible disease of the tissue also needs to be considered as a potential parameter.

7.1.3 Chapter 6 results

This part of the study had three main phases. Firstly, RNA was extracted from post-mortem rat brain tissue following post-mortem intervals of 0, 3, 6, 12 and 24 h at subsequent time course intervals of 0, 3, 6, 12 and 24 h, to determine when expression of *HSPA* was induced to characterise the persistence of *HSPA* transcripts in cells and as an indicator of *de novo* expression in these post mortem samples. The second part of

the study characterised the level of transcription in response to post-mortem cellular changes, and in response to heat shock applied to the rat brain tissue at 0 h time course interval within each post-mortem interval. The third part of this study characterised the levels of transcription in response to post-mortem cellular changes, and as a result of heat shock applied to the rat brain tissue at 0 h, and then again at 3, 6 and 24 h time course intervals within each post-mortem interval.

In the initial part of the study, it was determined that *HSPA* gene transcripts were present at each post-mortem interval (0, 3, 6, 12 and 24 h), which supported findings from previous literature (Blake *et al*, 1989; Inoue *et al*, 2002; Pardue *et al*, 2007). Low level expression of *HSPA* was observed in the 0 h post-mortem interval at 0 h time course (copy number $19.21 \pm .923$), followed by a gradual increase up to the 6 h time course interval (copy number 54.94 ± 4.47) and then returning to near basal levels at the 24 h time course interval (copy number 17.40 ± 2.79). No *HSPA* expression was expected at the 0 h time course interval, as *HSPA* is only induced by stress conditions, but, the low levels of *HSPA* transcripts may have resulted from induced stress during the initial sacrifice procedure of the rat and during the subsequent excision of the brain. As expected, *HSPA* expression gradually decreased at 3 and 6 h post-mortem intervals. However, *HSPA* transcripts substantially increased at the 12 h post-mortem interval by approximately 2 fold at 0 h time course, 6 fold at 3 h time course, 3 fold at 6 h time course, 3 fold at 12 h time course and 2.5 fold at 24 h time course. At the 24 h post-mortem interval *HSPA* transcripts were only present at low levels, below the initial basal levels observed at 0 h post-mortem 0 h time course interval.

In the second stage of this study, the levels of *HSPA* transcripts in brain tissue that had been subjected to a mild heat shock at the 0 h time course interval within each post-

mortem interval were compared to *HSPA* transcript levels in the non-heat shocked brain tissue. There was an increased level of *HSPA* expression following heat shock, although maximum levels of expression were seen at different time points through the post mortem period used in experiments. Maximum expression was observed at: 6 h within 0 h PMI; at 0 h within 3 h PMI; 24 h within 6 h PMI; 12 h within 12 h PMI and 3 h within 24 PMI. Under non-heat shock conditions, *HSPA* transcripts were observed in the 0 h post-mortem interval at 0 h time course (copy number 21.34 ± 1.41), followed by a gradual increase up to the 6 h time course interval (copy number 83.47 ± 9.03) returning back to near basal levels at the 24 h time course interval (copy number 31.03 ± 3.90). At the 3 post-mortem, *HSPA* transcripts expressed high at 0 h time course (copy number $57.96 \pm .00$) with a gradual decline up to the 24 h time course (copy number 41.59 ± 7.51). *HSPA* expression gradually decreased at the 6 h post-mortem interval, but as with non-heat shock, *HSPA* transcripts substantially increased at the 12 h post-mortem interval by approximately: 1.25 fold at 0 h time course, 1.25 fold at 3 h time course, 2 fold at 6 h time course, 3 fold at 12 h time course and 0 fold at 24 h time course. Again, as with non-heat shock, *HSPA* transcripts were only present at low levels at the 24 h post-mortem interval, below or near to the initial basal levels observed at 0 h post-mortem 0 h time course interval.

In the third stage of this study, the levels of *HSPA* transcripts in brain tissue that had been subjected to a mild heat shock, the first at 0 h time course followed by subsequent heat shocks at 3, 6 and 24 h time course intervals, were accessed to determine whether the application of subsequent heat shocks would increase *HSPA* expression in a thermotolerant state. In all cases there was a marked increase in *HSPA* expression in heat shocked brain tissue compared to non-heat shock. This phenomenon, known as thermotolerant preconditioning, is a cellular adaptation resulting from a single severe

non-lethal exposure to heat that allows cells to better survive subsequent potentially lethal heat stress episodes, and has been reported previously (Lindquist and Craig, 1988; Moseley, 1997; Pardue *et al*, 2007; Theodorakis and Morimoto, 1987; Theodorakis *et al*, 1999; Tolson and Roberts, 2005). The characteristics for thermotolerance are dependent on survival of the cell(s) exposed to an otherwise lethal heat stress, synthesis of heat shock proteins and a short duration of the thermotolerant state (Moseley, 1997). The response of cells to such stress conditions is dependent on the concentration of *HSPA* in the cell prior to stress and on the severity of the stress, based upon its intensity and duration (Lindquist and Craig, 1988; Mosser and Morimoto, 2004; Parsell and Lindquist, 1994).

HSPA is constitutively expressed under normal conditions and inducibly in response to cellular stress (Lindquist 1986). Under normal conditions, *HSPA* is constitutively expressed at relatively low but constant levels. Under conditions of stress, such as death or heat shock, weak hydrogen and van der Waals forces that hold cellular proteins in their conformational shape become weakened, resulting in protein denaturation, incorrect protein aggregation and mis-folding of newly synthesized proteins (Hartl and Hayer-Hartl, 2002; Nollen and Morimoto, 2002). Under such conditions, *HSPA* genes are induced in order to protect proteins and enhance cell survival (Calderwood *et al*, 2006; Mosser and Morimoto 2004; Powers *et al*, 2009). In addition to the above, *HSPA* plays a strong part in cytoprotection, allowing cells to adapt and to survive under hostile or otherwise lethal conditions (Calderwood *et al*, 2006; Mosser and Morimoto 2004; Parcellier *et al*, 2003; Powers *et al*, 2009).

The induction of *HSPA* production in response to stress conditions involves an increase in active heat shock factor 1 (HSF1) which is released from *HSPA* during an initial

stress, and subsequently binds to the heat shock element (HSE) in the *HSPA* gene promoter region (Fernandes *et al*, 1994; Morimoto *et al*, 1994; Wu *et al*, 1994,). Inducible transcription of the *HSPA* gene requires the *de novo* binding of the HSE by a heat shock transcription factor 1 (HSF1) protein, which is ubiquitously synthesised and plays a major role in the stress induced expression of the *HSPA* genes (de Thonel *et al*, 2011). *HSPA* synthesis is regulated at the transcriptional level by the heat shock factor 1 (HSF1) which assists, not only the long term induction of the *HSPA* gene, but also the regulation of gene expression and developmental processes (Morimoto, 1998; Sreedhar *et al*, 2004). This response protects the cells against further insults, and has been demonstrated in a number of *in vivo* and *in vitro* studies (Krishnan *et al*, 2006; Pespeni *et al*, 2005; Wagstaff *et al*, 1999). Although the production of heat shock proteins results in the protection of cells from the effects of further stresses, they are deemed toxic if present in the cells for any prolonged period (Theodorakis *et al*, 1999).

The brain tissue that was made thermotolerant by the application of multiple heat shocks contained lower levels of *HSPA* transcripts in the 0 and 3 post-mortem intervals compared to non-heat shock and to single heat shock, suggesting there is a regulation of *HSPA* synthesis that is dependent on the levels of *HSPA* existing within the cell (Kregel, 2002). Studies have demonstrated that inhibition of transcription during the conditioning heat stress allows the maintenance of thermotolerance (Bader *et al*, 1992). Induction of *HSPA* was rapid with high levels of the induced transcripts present at 6 h post-mortem intervals. Levels were substantially higher than those observed in non-heat shock and single heat shock samples, which supports work undertaken by Blake *et al*, (1990) and Theodorakis *et al*, (1999).

No significant differences were observed between the level of translation of *HSPA* mRNA in non-heat shock compared to the translation level in heat shocked tissue as shown in section 6.2.1. It can be concluded that heat shock is not necessary for the efficient translation of *HSPA* mRNA. Results from this study have shown that the transcription of the *HSPA* gene is rapidly and transiently activated in tissue subjected to a single heat shock. During heat shock, *HSPA* transcription levels rapidly increase and then decline after 6 h, section 6.2.1, Figure 6.1. The high levels of *HSPA* mRNA in the multiple heat shocked tissue is maintained through effects of message stability, due to the increase in heat shock factor (HSF) that is released from *HSPA* during the initial stress, which subsequently binds to the heat shock element (HSE) in the *HSPA* gene promoter region (Morimoto *et al*, 1994). Heat shock has an effect on the stability of *HSPA* mRNA. In non-heat shocked tissue, the half-life of *HSPA* mRNA, as stated by Theodorakis and Morimoto (1999), is approximately 50 min, but in heat shocked tissue the stability increases by at least 10-fold (Theodorakis and Morimoto, 1987). Previous studies have shown that *HSPA* mRNAs rapidly degrade during recovery from heat shock, which support the findings in this study (Blake *et al*, 1990; Pardue *et al*, 2007; Theodorakis *et al*, 1999; Theodorakis and Morimoto, 1987).

Tissue that was subjected to multiple heat shocks showed limited expression of *HSPA* compared to the single heat shock in the early post-mortem intervals 0 and 3 h. This could be due to a decrease in *HSPA* transcription and an increase in *HSPA* mRNA degradation, thus increasing cellular levels of *HSPA* in the recovery period, when returned to non-heat shock conditions 37°C. In contrast, during the heat shock period, no significant differences were observed in the levels of *HSPA* transcription in multiple heat shock compared to non-heat shock in the early post-mortem period 0 and 3 h. *HSPA* mRNA was observed to be less stable in multiple heat shocked tissue, compared

with the control non-heat shocked tissue. As stated by Theodorakis *et al*, (1999), a possible reason for this is that, under normal conditions, levels of *HSPA* mRNA are unstable, but during heat shock the mRNA becomes more stable due to mRNA degradation being affected by stress. In the tissue subjected to heat shock, mRNA degradation begins immediately after returning to non-heat shock conditions, and therefore it could be postulated that mRNA degradation is accelerated in tissue subjected to heat shock which would result in a reduced *HSPA* mRNA half-life.

Results have also shown that the levels of HSPALA proteins were higher in non-stressed and stressed (tumourous) human brain than those in non-stressed and stressed (heat shock) rat brain which supports the findings from Pardue *et al*, (2007). Consistent with the presence of the *HSPA* protein, *HSPA* mRNA levels were also found to be higher in non-stressed human brain than in non-stressed rat brain. This supports the overall conclusion by Pardue *et al*, (2007) that *HSPA/HSP70* protein levels in brain tissue are significantly higher in humans who die suddenly and are not subjected to agonal stresses pre-mortem, or from disease such as brain tumours, compared to rats that are either non-stressed pre-mortem or that have been subjected to heat shock post-mortem.

Given that death and heat shock are both forms of cellular stress, it is to be expected that *HSPA* protein was observed in both the cytoplasm and the nucleus of samples subjected to these conditions. *HSPA* protein was detected mainly in the cytoplasm in non-heat-shocked brain tissue in the early post-mortem period with gradual migration into the nucleus over time. In the heat shocked post-mortem brain tissue, *HSPA* protein was observed in both the cytoplasm and the nucleus. Increased synthesis of heat shock proteins in response to heat shock, results in *HSPA* relocalizing to the nucleus and

binding to the HSF1 transcriptional transactivation domain, thereby blocking transcription of heat shock genes (Santoro, 2000).

7.2 Summary

Overall, we may draw a number of conclusions from this study. Firstly, *GAPDH* showed relatively consistent expression in human normal and tumourous cell lines and tissue samples under normal and hypoxic conditions, and also in rat brain tissues at different post-mortem intervals under normal and heat shock conditions. For *Homo sapiens GAPDH*, the average transcript copy number for normal and tumourous cell lines was approximately 146,500 copies per 100 ng of extracted mRNA, and for normal and tumourous brain tissues samples this was similar at approximately 144,000 copies per sample. For *Rattus norvegicus GAPDH*, levels were higher than for human, with an average of 268,300 copies per 100 ng of extracted mRNA. This study supports previous literature (Barber *et al*, 2005; Said *et al*, 2005, 2007, 2009) in showing that the expression of *GAPDH* is not up or down regulated by post-mortem, cancer, hypoxic or heat shocked conditions, and therefore *GAPDH* is confirmed as a suitable candidate control gene for the purposes of this study.

Secondly, it was found that it was possible to isolate mRNA fragments from post mortem tissue up to 24 hours post mortem, which is in agreement with the previous report of Inoue *et al*. (2002).

Thirdly, *HSPA* is expressed at low levels in normal cell lines, at approximately 1,420 copies, and normal brain tissue samples, at approximately 200 copies, but its expression is highly induced by cancer in glioma cell lines, with approximately 5,360 copies and in glioma brain tissue samples, with approximately 1,600 copies, as shown in Figure 7.1.

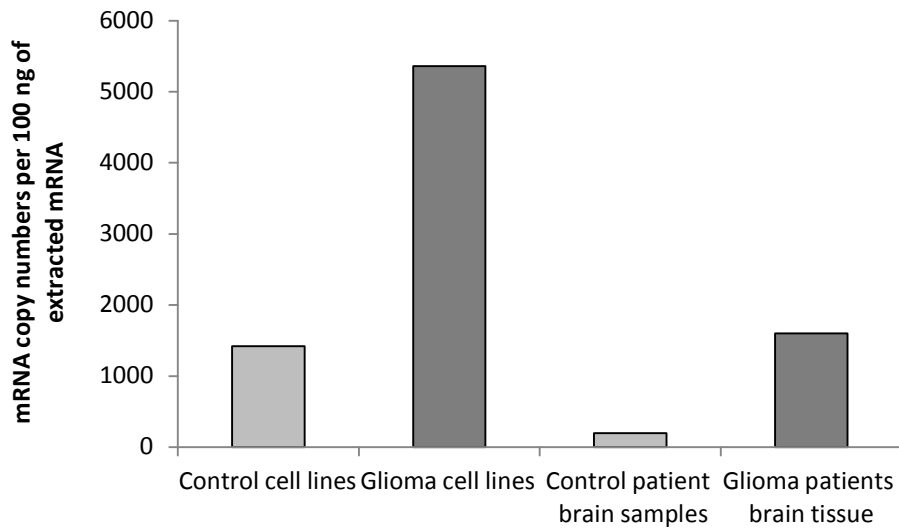


Figure 7.1 Histogram showing the average *HSPA* transcript levels from experiments using in control, glioma cell lines and v glioma brain tissue samples. *HSPA* can be seen to be more highly expressed in glioma cell lines and glioma brain tissue samples than in normal cell lines and normal brain tissue samples.

The results from this study also show that *HSPA* is expressed at low levels in pre and post hypoxia treated normal cells, (approximately 1,420 and 1,100 copies per 100 ng of extracted mRNA respectively) but is highly expressed in pre and post hypoxia treated glioma cells, (approximately 8,200 and 7,900 copies per 100 ng of extracted mRNA respectively), as shown in Figure 7.2.

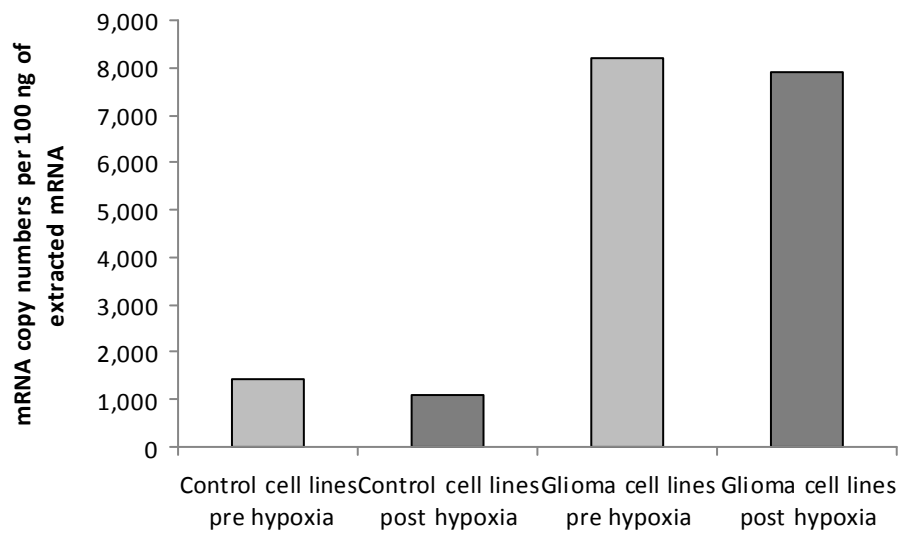


Figure 7.2 Histogram showing the average *HSPA* transcript levels in control and glioma cell lines under pre and post hypoxia conditions. *HSPA* can be seen to be more highly expressed in glioma cell lines under pre and hypoxia conditions compared to low *HSPA* expression in the normal cell lines under pre and post hypoxia conditions.

Hypoxia is a condition resulting from decreased cellular oxygen levels in tissues. In cellular hypoxia, tumours require additional blood vessels, a condition which is evident in many neoplasms. Hypoxia induces transcriptional activation of many genes that affect cellular metabolism and also promotes neoangiogenesis (the formation of new or recent blood vessels) (Duffy *et al*, 2003). Cells are able to sense and respond to

decreased oxygen levels through the conserved hypoxic response pathway involved in tumorigenesis. Exposure to decreased oxygen levels initiates the hypoxic response pathway by the regulated expression of hypoxia inducible transcription factor-1 (HIF-1). Many of the hypoxia-inducible genes are up-regulated during hypoxia, thus increasing oxygen transport to hypoxic tissues by promoting angiogenesis and also promoting cell proliferation and survival. However, failure to adapt to decreased oxygen levels will ultimately result in cell death via apoptosis (Bruick, 2003). Angiogenesis is associated with metastasis, and as tumours grow, some cells become detached from the tissues nutrient supply limiting the delivery of oxygen and nutrients to those cells (Duffy *et al*, 2003). This results in cellular hypoxia and metabolic stress inducing changes in transcriptional regulation, promoting growth of highly permeable blood vessels and facilitating the passage of tumour cells into the circulatory system. The response of cancer to hypoxia not only maintains the survival and growth of tumours, but also promotes tissue invasion and metastasis through angiogenesis (Duffy *et al*, 2003).

As predicted, HSPA protein was detected in both the cytoplasm and the nucleus of the three glioma cell lines under pre and post hypoxic conditions. Although HSPA protein was detected mainly in the cytoplasm in the normal (NHA) cell line pre-hypoxia, after hypoxia treatment, migration of HSPA protein to the nucleus was observed.

Although this research sheds light on the localisation and production of heat shock proteins in cells and supports a correlation between cancer and hypoxia environments, further research into glioma cells under hypoxic conditions is required to underpin the regulating mechanisms of HSPA in different cell types under such conditions. If cancer cells are expressing *HSPA* at high levels, then hypoxic conditions will have little or no further effect on these cells. Initially, tumours grow under non-hypoxic conditions, but

under hypoxic conditions, enhanced necrosis at the core of the tumour mass may be observed. Given that not all glioblastomas show the same degree of angiogenesis and necrosis, further research to address the localisation of HSPA in relation to a hematoxylin and eosin histology diagnosis (H and E) referring to angiogenesis and necrosis needs to be carried out. Furthermore, comparisons should be made between HSPA transcripts and protein levels after hypoxia with HIF to address whether cancer cells respond to hypoxia at HIF target gene levels. The glioma tissues indicate a correlation between *HSPA* expression and the grade of cancer, suggesting its possible application as a biomarker. This may also advocate the use of *HSPA* as a possible molecular target for therapy which may prolong glioma patient's survival in the future. However, different brain regions may show differences in *HSPA* levels, and thus additional work should be carried out to compare *HSPA* expression levels from various regions within the brain. The present study suggests that *HSPA* is up-regulated in glioma and it may be a suitable prognostic biomarker. .

HSPA was expressed at low levels in normal brain tissue, but was highly expressed in brain tissue subjected to mild heat shock. In the non-heat shocked brain tissue, low level expression of *HSPA* was observed in the 0 h post-mortem interval at 0 h time course, followed by a gradual increase up to the 6 h time course interval, and returning to near basal levels at the 24 h time course interval. *HSPA* expression gradually decreased at 3 and 6 h post-mortem intervals but, *HSPA* transcripts substantially increased at the 12 h post-mortem interval. At the 24 h post-mortem interval, *HSPA* transcripts were only detectable at low levels, below the initial basal levels observed at 0 h post-mortem 0 h time course interval. A higher level of *HSPA* expression was observed in samples taken at 0 h post-mortem which had been subjected to heat shock, compared to non-heat shocked samples at each time course interval. *HSPA* transcripts

were observed in the 0 h post-mortem interval at 0 h time course, followed by a gradual increase up to the 6 h time course interval, returning back to near basal levels at the 24 h time course interval. At 3 h post-mortem, *HSPA* transcripts were present at high levels at 0 h time course with a gradual decline up to the 24 h time course. *HSPA* expression gradually decreased at 6 h post-mortem but, as with non-heat shock, *HSPA* transcripts substantially increased at 12 h post-mortem. Again, as with non-heat shock, *HSPA* transcripts were only present at low levels at the 24 h post-mortem interval, below or near to the initial basal levels observed at 0 h post-mortem 0 h time course interval.

Furthermore, it is possible to induce the expression of heat shock genes in post mortem tissues, and this expression shows the preconditioning effect characteristic of the heat shock response. This phenomenon, known as thermotolerant preconditioning, is a cellular adaptation resulting from a single severe non-lethal exposure to heat that allows cells to better survive subsequent potentially lethal heat stress episodes, and has been reported previously (Lindquist and Craig, 1988; Moseley, 1997; Pardue *et al*, 2007; Theodorakis and Morimoto, 1987; Theodorakis *et al*, 1999; Tolson and Roberts, 2005). The levels of *HSPA* transcripts in brain tissue that had been subjected to a mild heat shock, the first at 0 h time course followed by subsequent heat shocks at 3, 6 and 24 h time course intervals, showed a marked increase in *HSPA* expression in heat shocked brain tissue compared to non-heat shock within each post-mortem interval. The response of cells to such stress conditions is dependent on the concentration of *HSPA* in the cell prior to stress and on the severity of the stress, based upon its intensity and duration (Lindquist and Craig, 1988; Mosser and Morimoto, 2004; Parsell and Lindquist, 1994).

The results from this study have shown that in the early post-mortem period, (0 h post-mortem), *HSPA* is expressed higher in tissue subjected to single and multiple heat shocks compared to non-heat-shock. However, in later post-mortem intervals, (3 - 24 h post-mortem intervals) results demonstrated some expression however results were inconsistent and somewhat irregular, with no predictive or reproducible patterns. Possible explanation for this could be that there were multiple factors involved in the stress experienced by cells, such as the initial sacrifice procedure by cervical dislocation, the excision of the brain and further damage to the tissues arising from the dissection of the brain. During this period, the cells are also under increased stress from circulatory failure which prevents the delivery of oxygen and removal of waste products of cellular respiration, resulting in anoxia, increased toxin levels and the functional activity of the cells. It is therefore possible that, during this period prior to experimental heat shock, *HSPA* will be up-regulated in response to these cellular changes. This could indicate that the response of the cells subjected to heat shock conditions was dependent on the initial concentration of *HSPA* in the cell prior to heat shock, based on the severity, intensity and duration of stress, (Lindquist and Craig, 1988; Mosser and Morimoto, 2001; Parsell and Lindquist, 1994). Although the production of *HSPA* assists in the protection of cells from the effects of further non-lethal or lethal stresses, they become toxic if they are present in cells for any prolonged period, which would result in cellular death (Theodorakis *et al*, 1999).

Again as expected, *HSPA* protein was detected in both the cytoplasm and the nucleus in all tissue samples at each post-mortem interval for both non-heat shock and heat shocked samples.

It can be concluded from the results of this part of the study that there is *-de novo* synthesis in post mortem brain tissue in response to the changes in cellular conditions during this time. It is possible to induce expression of *HSPA* following systemic death, using an external stimulus, such as heat shock, and that the induction of multiple heat shocks may be suggestive of a preconditioned protection from further stress. However, these initial studies would indicate that *HSPA* would be an unsuitable gene for its use as an early post-mortem marker. Therefore studies in the field of PMI using *HSPA* as an early post-mortem marker requires further investigation. The use of cell lines in replacement for tissue samples would eliminate initial pre stressful events, resulting in low or no detectable levels of *HPSAIA* transcripts. Also, based on the results from the normal and tumourous cell lines, it would be beneficial to include diseased subjects to address these findings.

Chapter 8

References

8.1 References

Abravaya K, Myers MP, Myrphy SP and Morimoto RI (1992) The human heat shock protein hsp70 interacts with HSF, the transcription factor that regulates heat shock gene expression. *Genes & Development*. **6**: 1153 – 1164.

Aldrian S, Trautinger F, Frohlich I, Berger W, Micksche M and Kindas-Mugge I (2002) Overexpression of HSP27 affects the metastatic phenotype of human melanoma cells in vitro. *Cell Stress Chaperones*. **2**: 177 – 185.

Althaus L and Henssge C (1999) Rectal temperature time of death nomogram: sudden changes of ambient temperature. *Forensic Science International*. **99 (3)**: 171 – 178.

Anderson S, Howard B, Hobbs GR and Bishop CP (2005) A method for determining the age of a bloodstain. *Forensic Science International*. **148**: 37–45.

Arunan E., Desiraju GR, Klein RA., Sadlej J., Scheiner S, Alkorta, I, Clary DC, Crabtree RH, Dannenberg JJ, Hobza P, Kjaergaard HG, Legon AC, Mennucci B. and Nesbitt DJ.(2011) Definition of the hydrogen bond. *Pure and Applied Chemistry*. **83**: 1637 – 1641.

Ashburner M. and Berendes HD (1978) in Ashburner,M. and Wright,T.R.F. (eds.), *The Genetics and Biology of Drosophila*, Vol. 2B, Academic Press, NY, pp. 315-395.

Ashburner M (1967) Gene activity dependent on chromosome synapsis in the polytene chromosomes of *Drosophila melanogaster*. *Nature*. **214**: 1159 – 1160.

Ashburner M (1970) Patterns of puffing activity in the salivary gland chromosomes of *Drosophila*. *Chromosoma*. **31**: 356 – 376.

Atalay M, Oksala NKJ, Lappalainen J, Laaksonen Chandan K, Sen CK and Roy S, (2009) Heat Shock Proteins in Diabetes and Wound Healing. *Current Protein Peptide Science*. **10**: 85 – 95.

Augusteyn RC (2004) Alpha-crystallin: a review of its structure and function. *Clinical and Experimental Optometry*. **87**: 356 – 366.

Babitzke P, Baker CS and Romeo T (2009) Regulation of translation initiation by RNA binding proteins. *Annual Review of Microbiology*. **63**: 27 – 44.

Baird NA, Turnbull DW and Johnson EA (2006) Induction of the heat shock pathway during hypoxia requires regulation of heat shock factor by hypoxia-inducible factor-1. *The Journal of Biological Chemistry*. **281 (50)**: 38675 – 38681.

Bakau B and Horwich AL (1998) The Hsp70 and Hsp60 chaperon machines, *Cell*. **92**: 351–366.

Baler R, Welch WJ and Voellmy R (1992) Heat Shock Gene Regulation by Nascent Polypeptides and Denatured Proteins HSP70 as a Potential Autoreulatory Factor. *Journal of Cell Biology*. **117**: 1151 – 1159.

Baler R, Dahl G and Voellmy R (1993) Activation of human heat shock genes is accompanied by heat shock factor 1 involves oligomerization, acquisition of DNA-binding activity, and nuclear localization and can occur in the absence of stress. *Molecular and Cellular Biology*. **13 (5)**: 1392 – 1407.

Ball TB, Plummer FT and Hayglass KT (2003). Improved mRNA quantification in Lightcycler RT-PCR. *International Archives of Allergy and Immunology*. **130**: 82 – 86.

Barber RD, Harmer DW, Coleman RA and Clark BJ (2005) GAPDH as a housekeeping gene: analysis of GAPDH mRNA expression in a panel of 72 human tissues. *Physiology Genomics*. **11: 21(3)**: 389 395.

Bauer M (2007) RNA in Forensic Science. *Forensic Science International: Genetics*. **1**: 69 – 74.

Bauer M, Polzin S, Gramlich I and Patzelt D (2003) Quantification of mRNA degradation as possible indicator of postmortem interval—a pilot study, *Legal Medicine*. **5**: 220 – 227.

Bauer M and Patzelt D (2003) Simultaneous RNA and DNA isolation from blood and semen stains, *Forensic Science International*. **136**: 76 – 78.

Beckmann RP, Mizzen LE and Welch WJ (1990) Interaction of Hsp 70 with newly synthesized proteins: implications for protein folding and assembly. *Science*. **248**: 850 – 854.

Behin A, Hoang-Xuan K, Carpentier AF and Delattre J (2003) Primary brain tumours in adults. *The Lancet*. **361**: 323 - 331.

Berendes HD (1965) Salivary gland function and chromosomal puffing patterns in *Drosophila hydei*. *Chromosoma*. **17**: 35 – 77.

Berendes HD (1968) Factors involved in the expression of gene activity in polytene chromosomes. *Chromosoma*. **24 (4)**: 418 – 437.

Besson U (2010) The cooling law and the search for a good temperature scale, from Newton to Dalton. *European Journal of Physics*. **32**: 343 – 354.

Braakman I and Bulleid NJ (2011) Protein folding and modification in the mammalian endoplasmic reticulum. *Annual Review of Biochemistry*. **7 (80)**: 71 – 99.

Brat DJ, Parisi JE, Kleinschmidt-DeMasters BK, Yachnis AT, Montine TJ, Boyer PJ, Powell SZ, Prayson RA and McLendon RE (2008) A Review of Changes Introduced by the WHO Classification of Tumours of the Central Nervous System, 4th Edition. *Archives of Pathology and Laboratory Medicine*. **132**: 993 – 1007.

Brocchieri L, Conway de Macario E and Macario Ajl (2008) HSP70 genes in the human genome: Conservation patterns predict a wide array of overlapping and specialized functions. *BMC Evolutionary Biology*. **8 (19)**: 1 – 20.

Bruick RK (2003) Oxygen sensing in the hypoxic response pathway: regulation of the hypoxia-inducible transcription factor. *Genes and Development*. **17**: 2614 – 2623.

- Buchner J (1999) HSP90 and Co. a holding or folding. *Trends in Biochemical Sciences*. **24 (4)**: 136 – 141.
- Bukau B and Horwich AL (1998) The Hsp70 and Hsp60 chaperone machines. *Cell*. **92**: 351 – 366.
- Butt E, Immier D, Meyer HE, Kotlyarov A, Laass K and Gaestel M (2001) Heat shock protein 27 is a substrate of cGMP-dependant protein kinase in intact human platelets: phosphorylation- induced actin polymerization caused HSP27 mutants. *Journal of Biological Chemistry*. **276 (10)**: 7108 – 7113.
- Calderwood SK, Theriault JR and Gong J (2005) Message in a bottle: Role of the 70-kDa heat shock protein family in anti-tumor immunity. *European Journal of Immunology*. **35**: 2518 – 2527.
- Calderwood SK, Khaleque Md A, Sawyer DB and Ciocca DR (2006) Heat shock proteins in cancer: chaperones of tumorigenesis. *TRENDS in Biochemical Sciences*. **31**: 164 - 172.
- Cangul H (2004) Hypoxia upregulates the expression of the NDRG1 gene leading to its overexpression in various human cancers. *BMC Genetics*. **5**: 27.
- Caplan AJ, Cyr DM, Douglas MG. (1992) YDJ1p facilitates polypeptide translocation across different intracellular membranes by a conserved mechanism. *Cell*. **71 (7)**: 1143–1155.

Cappello F, Di Stefano AD, Sabrina RF, Anzalone R, La Rocca G, D'Anna SE, Magno F, Donner CF, Balbi B and Zummo G (2006) HSP60 and HSP10 down-regulation predicts bronchial epithelial carcinogenesis in smokers with chronic obstructive pulmonary disease. *Cancer*. **107**: 2417 – 2424.

Chadli A, Bouhouche I, Sullivan W, Stensgard B, McMahon N, Catelli MG and Toft DO (2000) Dimerization and N-terminal domain proximity underlie the function of the molecular chaperone heat shock protein 90. *Proceedings of the National Academy of Sciences of the United States of America*. **97**: 12524 – 12529.

Chandana SR, Movva S, Arora M and Singh T (2008) Primary Brain Tumours in Adults. *American Family Physician*. **77**: 1423 – 1430.

Chao AT and Guild GM (1986) Molecular analysis of the ecdysterone-inducible 2B5 –early|| puff in *Drosophila melanogaster*. *The EMBO Journal*. **5**: 143 – 150.

Chao C C, Yam W C and Lin-Chao S (1990) Coordinated induction of two unregulated glucose-regulated protein genes by calcium ionophore: human BiP/GRP78 and GAPDH. *Biochemistry Biophysics Research Communication*. **171**: 431 – 438.

Charette SJ, Lavoie JN, Lambert H and Landry J (2000) Inhibition of DAXX – mediated apoptosis by heat shock protein 27. *Molecular and Cellular Biology*. **20**: 7602 – 7612.

- Cheetham ME and Caplan AJ (1998) Structure function and evolution of DnaJ: conservation and adaptation of chaperone function. *Cell Stress Chaperones*. **3**: 28 – 36.
- Chen B, Zhong D and Monteiro A (2006) Comparative genomics and evolution of the HSP90 family of genes across all kingdoms of organisms. *BMC Genomics*. **7**: 156.
- Cheng MY, Hartl FU and Norwich AL (1990) The mitochondrial chaperonin hsp60 is required for its own assembly. *Nature*. **348**: 455 – 458.
- Chenna R, Sugawara H, Koike T, Lopez R, Gibson TJ, Higgins DG and Thompson JD (2003) Multiple sequence alignment with the clustal series of programs. *Nucleic Acids Research*, **31**: 3497 – 3500.
- Christine R, Boudreau BS, Isaac A, Yang MD, Linda M and Liao MD (2005) Gliomas: advances in molecular analysis and characterization. *Surgical Neurology*. **64**: 286-294.
- Ciocca DR, Clark GM, Tandon AK, Fuqua SAW, Welch MJ and McGuire WL (1993) Heat shock protein hsp70 in patients with axillary lymph node-negative breast cancer: prognostic implications. *Journal of the National Cancer Institute*. **85**: 570 – 574.
- Ciocca DR, Oesterrich S, Chamness GC, McGuire WL and Fuqua SA (1993) Biological and clinical implications of heat shock protein 27,000 (HSP27) a review. *Journal of the National Cancer Institute*. **85 (19)**: 1570 – 1588.

Ciocca DR, Rozados VR, Carrion FDC, Gervasoni SI, Matar P and Scharovsky OG (2003) Hsp25 and Hsp70 in rodent tumors treated with doxorubicin and lovastatin. *Cell Stress and Chaperones*. **8**: 26 – 36.

Ciocca DR and Calderwood SK (2005) Heat shock proteins in cancer: diagnostics, prognostic, predictive, and treatment implications. *Cell Stress and Chaperones*. **12**: 86-103.

Corces V, Holmgren R, Freund R, Morimoto R and Meselson M (1980) Four heat shock proteins of *Drosophila melanogaster* coded within a 12-kilobase region in chromosome subdivision 67B. *Proceedings of the National Academy of Sciences of the United States of America*. **77**: 5390 – 5393.

Craig EA, McCarthy, B J (1980) Four *Drosophila* heat shock genes at 67B: characteristics of recombinant plasmids. *Nucleic Acids Research*. **8**: 4441 – 4457.

Craig EA, Weissman JS and Horwich AL (1994) Heat shock proteins and molecular chaperones: mediators of protein conformation and turnover in the cell. *Cell*. **78**: 365 – 372.

Csermely P, Schnaider T, Soti C, Prohaszka Z and Nardai G (1998) The 90-kDa molecular chaperone family: structure, function and clinical applications. A comprehensive review. *Pharmacology and Therapeutics*. **79**: 129 – 168.

Curcio C, Asheld JJ, Chabla JM, Ayubcha D, Hallas BH, Horowitz JM and Torres G (2006) Expression of BAG 1 in the Postmortem Brain. *Journal of Chemical Neuroanatomy*. **32**: 191-195.

Cyr DM and Douglas MG (1994) Differential regulation of HSP70 subfamilies by the eukaryotic DnaJ homologue Ydj1. *Journal of Biological Chemistry*. **269**: 9798 – 9804.

Cyr DM, Langer T and Douglas MG (1994) DnaJ-like proteins: molecular chaperones and specific regulators of HSP70. *Trends in Biochemical Sciences*. **19**: 176 – 181.

Cyr Dm (1995) Cooperation of the molecular chaperone Ydj1 with specific HSP70 homologs to suppress protein aggregation. *FEBS Letters*. **359**: 129 – 132.

Dang C and Jayasena S D (1996). Oligonucleotide inhibitors of taq DNA polymerase facilitate detection of low copy number targets by PCR. *Journal of Molecular Biology*. **264**: 268 - 278.

DiDomenico BJ, Bugaisky, GE and Lindquist S (1982) Heat shock and recovery are mediated by different translational mechanisms. *Proceedings of the National Academy of Sciences of the United States of America*. **79**: 6181 - 6185.

De Jong WW, Hendriks W, Mulders JWM and Bloemendal H (1989) Evolution of eye lens crystallins: the stress connection. *Trends in Biochemical Sciences*. 14365 - 14368.

- De Paepe ME, Mao Q, Huang C, Zhu D, Jackson CL and Hansen K (2002) Postmortem RNA and protein stability in perinatal human lungs. *Diagnostic Molecular Pathology*. : 170 – 176.
- De Thonel A, Mezger V and Garrido C (2011) Implication of heat shock factors in tumorigenesis: therapeutical potential. *Cancers*. **3**: 1158 – 1181.
- Dieffenbach CW, Lowe TMJ and Dveksler GS (1993) General Concepts for PCR Primer Design. *Genome Research*. **3**: S30 – S37.
- Doppler H, Storz P, Li J, Comb MJ and Toker A (2005) A phosphorylation state-specific anti-body recognises HSP27, a novel substrate of protein kinase D. *Journal of Biological Chemistry*. **280 (15)**: 15013 – 15019.
- Duffy JP, Eibl G, Reber HA and Hines OJ (2003) Influence of hypoxia and neoangiogenesis on the growth of pancreatic cancer. *Molecular Cancer*. **2**: 2 - 12.
- Ehrnsperger M, Gaber S, Gaestel M and Buchner J (1997) Binding of non-native proteins to HSP25 during heat shock creates a reservoir of folding intermediates for reactivation. *The EMBO Journal*. **16 (2)**: 221 – 229.
- Ellis RJ and Hemmingsen SM (1989) Molecular chaperons: proteins essential for the biogenesis of some macromolecular structures. *Trends in Biochemical Sciences*. **14**: 339 – 342.

Ellis RJ and van der Vies SM (1991) Molecular chaperones. *Annual Review of Biochemistry*. **60**: 321 – 347.

Ellis RJ (1993) The General Concept of Molecular Chaperones. *Philosophical Transactions of the Royal Society of London*. **339**: 257 – 261.

Fan C-Y, Lee S and Cyr DM (2003) Mechanisms for regulation of Hsp70 function by Hsp40. *Cell Stress and Chaperones*. **8**: 309 – 316.

Feder ME (1999) Heat shock proteins, molecular chaperones, and the stress response: Evolutionary and ecological physiology. *Annual Review of Physiology*. **61**: 243 – 282.

Fenstermacher D (2005) Introduction to Bioinformatics. *Journal of the American Society for Information Science and Technology*. **56**: 440 – 446.

Fernandes M, O'Brien T and Lis JT (1994) Structure and Regulation of Heat Shock Promoters. In the *Biology of Heat Shock Proteins and Molecular Chaperones* (ed. RI Morimoto, A Tissieres and G Georgopolis), pp. 375 – 393. Cold Spring Harbor Laboratory Press, Cold Spring Harbor, NY.

Feige U and Polla BS (1994) Heat shock proteins: the HSP70 family. *Experientia*. **50**: 979 – 986.

Fenton WA, Kashi Y, Furtak K and Horwich AL (1994) Residues in chaperonin GroEL required for polypeptide binding and release. *Nature*. **371**: 614 – 619.

Findly R C and Pederson T (1981) Regulated transcription of the genes for actin and heat shock proteins in cultured *Drosophila* cells. *Journal of Cell Biology*. **88**: 223 – 228.

Fink AL (1999) Chaperone-Mediated Protein Folding *Physiological Reviews*. **79**: 425 – 449.

Fountoulakis M, Hardmeier R, Hoger H and Lubec G (2001) Postmortem changes in the level of brain proteins. *Experimental Neurology*. **167**: 86 – 94.

Fraga D, Meulia T and Fenster S (2008) Real-time PCR. *Current Protocols for Essential Laboratory Techniques*. John Wiley and Sons Inc. Unit 10.2

Freeman BC, Myers MP, Schumacher R and Morimoto RI (1995) Identification of a regulatory motif in Hsp70 that affects ATPase activity, substrate binding and interaction with HDJ-1. *The EMBO Journal*. **14**: 2281 – 2292.

Friedman HS, Burger PC, Bigner SH, Trojanowski JQ, Brodeur GM, He XM, Wikstrand CJ, Kurtzberg J, Berens ME, Halperin EC and Bigner DD (1988) Phenotypic and genotypic analysis of a human medullablastoma cell line and transplantable xenograft (D341 Med) Demonstrating amplification of c-myc. *American Journal of Pathology*. **130**: 472 – 484.

Freshney R (1987). Culture of animal cells: A manual of basic technique. Alan R. Liss, Inc., New York. pp 117.

Fuse T (1991) Alterations in cytokinetics and heat shock protein (70 kDa) expression of glial cell by hyperthermia. *No to Shinkei*. **43**: 843 – 850.

Garnier C, Lafitte D, Tsvetkov PO, Barbier P, Leclerc-Devin J, Millot JM, Briand C, Makarov AA, Catelli MG and Peyrot V (2002) Binding of ATP to heat shock protein 90: evidence for an ATP-binding site in the C-terminal domain. *Journal of Biological Chemistry*. **5**: 12208 – 12214.

Garrido C, Fromentin A, Bonnotte B, Favre N, Moutet M, Arrigo A, Mehlen P and Solary E (1998) Heat shock protein 27 enhances the tumorigenicity of immunogenic rat colon carcinoma cells. *Cancer Research*. **58**: 5495 – 5499.

Garrido C, Ottavi P, Fromentin A, Hammann A, Arrigo AP, Chauffert B and Mehlen P (1997) HSP27 as a mediator of confluence-dependent resistance to cell death induced by anticancer drugs. *Cancer Research*. **57**: 2661 – 2667.

Garrido C (2002) Size matters: of the small HSP27 and its large oligomers. *Cell Death Differentiation*. **9**: 483 – 485.

Garrido C, Brunet M, Didelot C, Zermati Y, Schmitt E and Kroemer G (2006). Heat Shock Proteins 27 and 70, Anti-Apoptotic Proteins with Tumorigenic Properties. *Cell Cycle*. **5**: **22**, 2592 – 2601.

Gething MJ, Sambrook J. (1992) Protein folding in the cell. *Nature*. **355** (6): 33–45.

Giard DJ, Aaronson SA, Torado GJ, Arnstein P, Kersey JH, Dosik H and Parks WP (1973) In vitro cultivation of human tumors: establishment of cell lines derived from a series of solid tumors. *Journal of the National Cancer Institute*. **51 (5)**: 1417 – 1423.

Goggins M, Scott JM and Weir DG (1998) Regional differences in protein carboxymethylation in post-mortem human brain. *Clinical Science*. **94**: 677 – 685.

Gombos Z, Danihel L, Repiska V, Acs G and Furth E (2011) Expression of erythropoietin and its receptor increases colonic neoplastic progression: The role of hypoxia in tumorigenesis. *Indian Journal of Pathology and Microbiology*. **54 (2)**: 273 – 278.

Gopee NV and Howard PC (2007) A time course study demonstrating RNA stability in skin. *Experimental and Molecular Pathology*. **83**: 4-120.

Grammatikakis N, Vultur A, Ramana CV, Siganou A, Schweinfest CW, Watson DK and Raptis L (2002) The role of Hsp90N, a new member of the Hsp90 family, in signal transduction and neoplastic transformation. *The Journal of Biological Chemistry*. **277**: 8312 – 8320.

Graner MW, Cumming RI and Bigner DD (2007) The Heat Shock Response and Chaperones/Heat shock Protein in Brain Tumours: Surface Expression, Release, and Possible Immune Consequences. *The Journal of Neuroscience*. **27 (42)**: 11214-11227.

Graven K K, Troxler R F, Kornfield H, Panchenko M V and Farber H W (1994) Regulation of endothelial cell glyveraldehyde-3-phosphate dehydrogenase expression by hypoxia. *Journal of Biological Chemistry*. **269**: 24446 – 24453.

Graven K K and Farber H W (1998) Endothelial cell hypoxic stress proteins. *Journal of Laboratory and Clinical Medicine*. **132**: 456 – 463.

Greco O, Marples B, Joiner M C and Scott S D (2003) How to overcome (and exploit) tumour hypoxia for targeted gene therapy. *Journal of Cellular Physiology*. **197**: 312 – 325.

Green M, Schuetz TJ, Sullivan EK and Kingston RE (1995) A heat shock-responsive domain of human HSF1 that regulates transcription activation domain function. *Molecular and Cellular Biology*. **15**: 3354 – 3362.

Gress TM, Muller-Pillasch F, Weber C, Lerch MM, Freiss H, Buchler M, Beger HG and Adler G (1994) Differential expression of heat shock proteins in pancreatic carcinoma. *Cancer Research*. **54**: 547 – 551.

Guettouche T, Boellmarn F, Lane WS and Voellmy R (2005) Analysis of phosphorylation of human heat shock factor 1 in cells experiencing stress. *BMC Biochemistry*. **6**: 4

Gupta S and Knowlton AA (2002) Cytosolic heat shock protein 60, hypoxia, and apoptosis. *Circulation*. **106**: 2727 – 2733.

Guttman SD, Gorovsky MA (1979) Cilia regeneration in starved *tetrahymena*: an inducible system for studying gene expression and organelle biogenesis. *Cell*. **17**: 305 - 317.

Guzhova I, Kislyakova K, Moskaliova O, Fridlanskaa, Tytell M, Cheetham M, and Margulis B (2001) In vitro studies show that HSP70 can be released by glia and that exogenous Hsp70 can enhance neuronal stress tolerance. *Brain Research*. **914**: 66 -73.

Hanahan D and Folkman J (1996) Patterns and emerging mechanisms of the angiogenic switch during tumorigenesis. *Cell*. **86**: 353 – 364.

Hansen JJ, Bross P, Westergaard M, Nielsen MN, Eiberg H, Borglum AD, Mogensen J, Kristiansen K, Bolund L and Gregersen N (2003) Genomic structure of the human mitochondrial chaperonin genes: HSP60 and HSP10 are localised head to head on chromosome 2 separated by a bidirectional promoter. *Human Genetics*. **112**: 71 – 77.

Harrison CJ, Bohm AA and Nelson HCM (1994) Crystal structure of the DNA binding domain of the heat shock transcription factor. *Science*. **264**: 224 – 227.

Hartl FU and Hayer-Hartyl M (2009) Converging concepts of protein folding *in vitro* and *in vivo*. *Nature Structural and Molecular Biology*. **16**: 574 – 581

Hartl FU and Hayer-Hartyl M (2002) Molecular Chaperones in the Cytosol: from Nascent Chain to Folded Protein *Science*. **295**: 1852 – 1858.

Hartl FU (1996) Molecular Chaperones in Cellular Protein Folding. *Nature*. **381**: 573 – 579.

Hartl FU, Bracher A and Hayer-Hartl M (2011) Molecular chaperones in protein folding and proteostasis. *Nature*. **475**: 324 – 332.

He Q, Marjamaki M, Soini H, Mertsola J, Viljanen MK (1994) Primers are decisive for PCR primer design. *Biotechniques*. **31**: 1326 – 1330.

Heinrich M, Lutz-Bonengel S, Matt K and Schmidt U (2007) Real-time PCR detection of five different –endogenous control genell transcripts in forensic autopsy tissue. *Forensic Science International: Genetics*. **1**: 163 – 169.

Heinrich M, Matt K, Lutz-Bonengel S and Schmidt U (2007) Successful RNA extraction from various human postmortem tissues. *International Journal of Legal Medicine*. **121**: 136 – 142.

Henssge C (1988). Death time estimation in case work 1. The rectal temperature time of death nomogram. *Forensic Science International*. **38 (3-4)**: 209 – 236.

Henssge C and Madea B (2004) Estimation of the time since death in the early post-mortem period. *Forensic Science International*. **144**: 167 – 175.

Hermisson M, Strik H, Rieger J, Dichgans J, Meyermann R and Weller M (2000) Expression and functional activity of heat shock proteins in human gliomablastoma multiforme. *Neurology*. **54**: 1357 – 1365.

Holmgren RK, Livak K, Morimoto R, Freund R and Meselson M (1979) Studies of clones sequences from four *Drosophila* heat shock loci. *Cell*. **18**: 1359 – 1370.

Huang H, Colella S, Kurrer M, Yonekawa Y, Kleihues P and Ohgaki H (2000) Gene Expression Profiling of Low-Grade Diffuse Astrocytomas by cDNA Arrays. *Cancer Research*. **60**: 6868 – 6874.

Huang LE and Bunn HF (2003) Hypoxia-inducible factor and its biomedical relevance. *The Journal of Biological Chemistry*. **278 (22)**: 19575 – 19578.

Huet F, Ruiz C and Richards G (1993) Puffs and PCR: the in vivo dynamics of early gene expression during ecdysone responses in *Drosophila*. *Development*. **118**: 613 – 627.

Huott J, Roy G, Lambert P, Chretien P and Landry J (1991) Increased survival after treatments with anticancer agents of Chinese hamster cells expressing the human Mr 27,000 heat shock protein. *Cancer Research*. **51**: 5245 – 5252.

Ikematsu K, Takahashi H, Kondo T, Tsuda R and Nakasono I (2008) Temporal expression of immediate early gene mRNA during the supravital reaction in mouse brain and lung after mechanical asphyxiation. *Forensic Science International*. **179**: 152 – 156.

Inoue H, Kimura A and Tuji T (2002) Degradation profile of mRNA in a dead rat body: semi-quantification study. *Forensic Science International*. **130**: 127 – 132.

Isomoto H, Oka M, Yano Y, Kanazawa Y, Soda H, Terada R, Yasutake T, Nakayama T, Shikuma S, Takeshima F, Uono H, Murata I, Ohtsuka K and Kohno S (2003) Expression of heat shock protein (Hsp) 70 and Hsp 40 in gastric cancer. *Cancer Letters*. **198**: 219 – 228.

Itoh H, Komatsuda A, Ohtani H, Wakui H, Imai H, Sawada K, Otaka M, Ogura M, Suzuki A and Hamada F (2002) Mammalian HSP60 is quickly sorted into the mitochondria under conditions of dehydration. *European Journal of Biochemistry*. **269**: 5931 – 5938.

Jakob U, Lilie H, Meyer I and Buchner J (1995) Transient interaction of Hsp90 with early unfolding intermediates of citrate synthase. Implications for heat shock in vivo. *Journal of Biological Chemistry*. **270 (13)**: 7288 – 7294.

Jameel A, Skilton RA, Campbell TA, Chander SK, Coombes RC and Luqmani YA (1992) Clinical and biological significance of HSP89 α in human breast cancer. *International Journal of Cancer*. **50**: 409 – 415.

Jiang S, Seng S, Avraham H, Fu Y, Avraham S (2007). Process elongation of oligodendrocytes is promoted by the kelch-related protein MRP2/KLHL1. *Journal of Biological Chemistry*. **282**: 12319 – 12329.

Jindal S, Dundani AK, Singh B, Harley CB and Gupta RS (1989) Primary structure of a human mitochondrial protein homologous to the bacterial and plant chaperones and to

the 65 kilodalton mycobacterial antigen. *Molecular and Cellular Biology*. **9**: 2279 – 2283.

Johnson SA, Morgan DG and Finch CE (1986) Extensive post-mortem stability of RNA from rat and human brain. *Journal of Neuroscience Research*. **16**: 267 – 280.

Jolly C and Morimoto RI (2000) Role of the Heat Shock Response and Molecular Chaperones in Oncogenesis and Cell Death. *Journal of the National Cancer Institute*. **92**: 1564-1572.

Jones MD, James WS, Barasi S & Nokes LDM (1995) Postmortem electrical excitability of skeletal muscle: preliminary investigation of an animal model. *Forensic Science International*. **76 (2)**: 91 - 96.

Kaliszan M, Hauser R, Buczynski J, Jankowski Z, Raczynska K and Kernbach-Wighton G (2010) The potential use of the eye temperature decrease in determining the time of death in the early post-mortem period: studies in pigs. *The American Journal of Forensic Medicine and Pathology*. **31 (2)**: 162 – 164.

Kamel A and Abd-Elsalam (2003) Bioinformatic tools and guideline for PCR primer design. *African Journal of Biotechnology*. **2**: 91 – 95.

Kampinga HH, Hageman J, Vos MJ, Kubota H, Tanguay RM, Bruford EA, Chetham ME, Chen B and Hightower LE (2009) Guidelines for the Nomenclature of the Human Heat Shock Proteins. *Cell and Stress Chaperones*. **14**: 105 – 111.

Kanazawa Y, Isomoto H, Oka M, Yano Y, Soda H, Shikuwa S, Takeshima F, Omagari K, Mizuta Y, Murase K, Nakagoe T, Ohtsuka K and Kohno S (2003) Expression of heat shock protein (hsp) 70 and Hsp 40 in colorectal cancer. *Medical Oncology*. **20**: 157 – 164.

Kang EH, Kim DJ, Lee EY, Lee YJ, Lee EB and Sons YW (2009) Downregulation of heat shock protein 70 protects rheumatoid arthritis fibroblast-like synoviocytes from nitric oxide-induced apoptosis. *Arthritis Research and Therapy*. **11**: R130.

Kappe G, Franck E, Vershuure P, Boelens WC, Leunissen JA and De Jong WW (2003) The human genome encodes 10 α -crystallin-related small heat shock proteins HspB1-10. *Cell Stress Chaperones*. **8 (1)**: 53 – 61.

Kaufman BA, Newman SM, Hallberg RL, Slaughter CA, Perlman PS and Butow RA (2000) In organello formaldehyde crosslinking of proteins to mtDNA: identification of bifunctional proteins. *Proceedings of the National Academy of Sciences of the United States of America*. **97**: 7772 – 7777.

Kaufman BA, Kolesar P, Perlman PS and Butow RA (2003) A function for the mitochondrial chaperonin Hsp60 in the structure and transmission of mitochondrial DNA function in *Saccharomyces cerevisiae*. *The Journal of Cell Biology*. **163 (3)**: 457 – 461.

Kay HH, Zhu S and Tsoi S (2007) Hypoxia and Lactate Production in Trophoblast Cells. *Placenta*. **28**: 854 – 860.

Kelly PM and Schlesinger MJ (1982) The effect of amino acid analogues and heat shock on gene expression in chicken embryo fibroblasts. *Cell*. **15**: 1277 – 1286.

Khalil AA (2007) Biomarker discovery: A proteomic approach for brain cancer profiling. *Japanese Cancer Association*. **98**: 201 – 213.

Kim KK, Kim R and Kim S (1998) Crystal structure of a small heat shock protein. *Nature*. **394**: 595 – 599.

Kim TD (2000) PCR primer design: an inquiry-based introduction to bioinformatics on the World Wide Web. *Biochemistry and Molecular Biology Education*. **28**: 271 – 276.

Kleihues P and Cavenee K (2000) Genetics and Pathogenesis-tumours of the Nervous System. IARC Press, Lyon pp. 10 – 101.

Kleihues P, Louis DN, Scheithauer BW, Rorke LB, Reifenberger G, Burger PC and Cavenee WK (2002) The WHO classification of tumours of the nervous system. *Journal of Neuropathology and Experimental Neurology*. **61**: 215 – 225.

Koll H, Guiard B, Tassow J, Osterman J, Horwich A, Neupert W and Hartl FU (1992) Antifolding activity of HSP60 couples protein import into the mitochondrial matrix with export to the intermembrane space. *Cell*. **68**: 1163 – 1175.

Kothary RK and Candido EP (1982) Induction of a novel set of polypeptides by heat shock or sodium arsenite in cultured cells of rainbow trout: *Salmo gairdnerii*. *Canadian Journal of Biochemistry*. **60**: 47 - 55.

Kulikova T, Aldebert P, Althorpe N, Baker W, Bates K, Browne P, van den Broek A, Cochrane G, Duggan K, Eberhardt R, Faruque R, Garcia-Pastor M, Harte N, Kanz C, Leinonen R, Lin Q, Lombard V, Lopez R, Mancuso R, McHale M, Nardone F, Silventoinen V, Stoehr P, Stoesser G, Tuli M A, Tzouvara K, Vaughan R, Wu D, Zhu W and Apweiler R (2004) The EMBL Nucleotide Sequence Database. *Nucleic Acids Research*. **32 (1)**: 27 - 30

Kuliwaba JS, Fazzalari NL and Findlay DM (2005) Stability of RNA isolated from human trabecular bone at post-mortem and surgery. *Biochimica et Biophysica Acta*. **1740**: 1-11.

Kumar S and Nussinov R (1999) Salt bridge stability in monomeric proteins. *Journal of Molecular Biology*. **293 (5)**: 1241 – 1255.

Kumar S and Nussinov R (2002a) Close-range electrostatic interactions in proteins. *A European Journal of BioChemistry*. **3**: 604–617.

Landry J, Lambert H, Zhou M, Lavoie JN, Hickey E, Weber LA and Anderson CW (1992) HSP27 is phosphorylated at serines 78 and 82 by heat shock and mitogen-activated kinases that recognise the same amino acid motif as S6 Kinase II. *Journal of Biological Chemistry*. **267 (2)**: 794 – 803.

Lanneau D, de Thonel A, Maurel S, Didelot C and Garrido C (2007) Apoptosis Versus Cell Differentiation: Role of Heat Shock Proteins HSP90, HSP70 and HSP70. *Prion*. **1**: 53 – 60.

Laudenski K and Wyczechowska D (2006) The distinctive role of small heat shock proteins in oncogenesis. *Archives Immunologiae et Therapiae Experimentalis*. **54**: 103 – 111.

Laufen TU, Zuber A, Buchberger and Bukau B (1998). In: DnaJ proteins In: Molecular Chaperones in the Life Cycle of Proteins, edited by Fink AL, and Goto Y. New York: Dekker, p. 241-274.

Lebret T, Watson R, William G, Molinie V, O'Neil A, Gabriel C, Fitzpatrick JM and Botto H (2003) Heat shock proteins HSP27, HSP60, HSP70 and HSP90: Expression in bladder carcinoma. *Cancer*. **98**: 970 – 977.

Leenders HJ and Berendes (1972) The effect of changes in the respiratory metabolism upon genome activity in *Drosophila*: The induction of gene activity. *Chromosoma*. **37** (4): 433 – 444.

Li J and Lee AS (2006) Stress induction of GRP78/BiP and its role in cancer. *Current Molecular Medicine*. **6**: 45 – 54.

Li J, Qian X and Sha B (2009) Heat shock protein 40: Structural studies and their functional implications. *Protein Peptide Letters*. **16** (6): 606 – 612.

Lindquist S (1980) Varying patterns of protein synthesis in *Drosophila* during heat shock: Implications for regulation. *Developmental Biology*. **77**: 463 – 479.

Lindquist S (1980) Translational efficiency of heat-induced messages in *Drosophila melanogaster* cells. *Journal of Molecular Biology*. **137**: 151 – 158.

Lindquist S (1981) Regulation of protein synthesis during heat shock. *Nature*. **293**: 311 – 314.

Lindquist S, DiDomenico BJ, Bugaisky G, Kurtz S, Petko L and Sonoda S (1982) Heat shock regulation in *Drosophila* and yeast. In heat shock from bacteria to man. Cold Spring Harbor, New York: Cold Spring Harbor Press. pp 167 – 176.

Lindquist S (1986) The heat shock response. *Annual Review of Biochemistry*. **55**: 1151 – 1191.

Lindquist S and Craig EA (1988) The heat shock proteins. *Annual Review Genetics*. **22**: 631 – 677.

Liu J-S, Kuo S-R, Makhov AM, Cyr DM, Griffith JD, Broker TR and Chow LT (1998) Human Hsp70 and Hsp40 chaperone proteins facilitate human papillomavirus-11 E1 protein binding to the origin and stimulate cell-free DNA replication. *The Journal of Biological Chemistry*. **273**: 30707 – 30712.

Louis DN, Ohgaki H, Wiestler OD, Cavenee WK, Burger PC, Jouvet A, Scheithauer BW and Kleihues P (2007) The 2007 WHO classification of tumours of the central nervous system. *Acta Neuropathology*. **114**: 97 – 109.

Lowe WL,(1998) in JL Jameson (ed): Principles of Molecular Medicine. Totowa, NJ, Humana.

Luders J, Demand J, Papp O and Hohfeld J (2000b) Distinct isoforms of the cofactor BAG-1 differentially affect Hsc70 chaperone function. *Journal of Biological Chemistry*. **275**: 14817 – 14823.

Maarti HH (2004) Erythropoietin and the hypoxic brain, *Journal of Experimental Biology*. **207**: 3233–3242.

Madea B and Henssge C (1990) Electrical excitability of skeletal muscle post-mortem in casework. *Forensic Science International*. **47**: 207 – 227.

Madea B (1992) Estimating time of death from measurement of the electrical excitability of skeletal muscle *Journal of Forensic Science*. **32 (2)**: 117 – 129.

Madea B and Rodig A (2006) Time of death dependent criteria in vitreous humor – Accuracy of estimating the time since death. *Forensic Science International*. **164**: 87 – 92.

Maeda H, Zhu B, Ishikawa T and Michiue T (2010) Forensic molecular pathology of violent deaths. *Forensic Science International*. **203**: 83 – 92.

Mao Y, Deng A, Qu N and Wu Xueji (2006) ATPase Domain of HSP70 Exhibits Intrinsic ATP – ADP Exchange Activity. *Biochemistry*. **71**: 1222 – 1229.

Marcu MG, Schulte TW and Neckers LM (2000) *Journal of the National Cancer Institute*. **92**: 242 – 248.

Marshall T (1962) Estimating the time of death. The use of the cooling formula in the study of postmortem body cooling. *Journal of Forensic Science*. **7**: 189–210.

Mathur A and Agrawal YK (2011) An overview of methods used in estimation of time since death. *Australian Journal of Forensic Sciences*. 1 – 11.

Mayer MP, Rudiger S and Bukau B (2000) Molecular basis for interactions of the DnaK chaperone with substrates. *Biological Chemistry*. **381**: 877 – 885.

Mayer MP and Bukau B (2005) Hsp70 chaperones: Cellular functions and molecular mechanism. *Cellular and Molecular Life Sciences*. **62**: 670 – 684.

McAlister L, Strausberg A, Kulaga A and Finkelstein DB (1979) Altered patterns of protein synthesis induced by heat shock in yeast. *Current Genetics*. **1**: 63 – 74.

McClellan AJ, Tam S, Kaganovich D and Frydman J (2005) Protein quality control: chaperones culling corrupt conformations. *Nature*. **7**: 736 – 740.

Meyer P, Prodromou C, Hu B, Vaughan C, Roe SM, Panaretou B, Piper P and Pearl LH (2003) Structural and functional analysis of the middle segment of Hsp90: implications for ATP hydrolysis and client protein and cochaperone interactions. *Molecular Cell*. **11**: 647 – 656.

Miller M J, Xuong NH, Geiduschek EP (1979) A response of protein synthesis to temperature shift in yeast *Saccharomyces cerevisiae*. *Proceedings of the National Academy of Sciences of the United States of America*. **76**: 5222 – 5226.

Milner CM and Campbell RD (1990) Polymorphic analysis of the human MHC-linked HSP70 genes. *Immunogenetics*. **36**: 357 – 362.

Minami Y, Hohfeld J, Ohtsuka K and Hartl FU (1996) Regulation of the heat shock protein 70 reaction cycle by the mammalian DnaJ homolog, HSP40. *Journal of Biological Chemistry*. **271**: 19617 – 19624.

Miyata Y and Yahara I (1992) The 90-kDa heat shock protein, HSP90, binds and protects casein kinase II from self-aggregation and enhances its kinase activity *Journal of Biological Chemistry*. **267**: 7042 - 7047.

Mohammed K and Shervington A (2007). Can *CYP1A1* siRNA be an effective treatment for lung cancer? *Cellular and Molecular Biology Letters*. **13**: 240 – 249.

Mohammed K (2007). A study of gene expression in human normal and carcinogenic cell lines using qRT-PCR. Theses Collection 571.865/MOH University of Central Lancashire theses collection.

Morimoto RI (1993) Cells in stress: transcriptional activation of heat shock genes. *Science*. **259**: 1409 – 1410.

Morimoto RI, Tiseres A and Georgopoulos C (1994) Heat shock proteins in Biology and Medicine. Cold Spring Harbor, NY: Cold Spring Harbor Press.

Morimoto RI (1998) Regulation of the heat shock transcriptional response: cross talk between a family of heat shock factors, molecular chaperones, and negative regulators. *Genes and Development*. **12**: 3788 – 3796.

Morimoto R (2010) Shock and Age. *The Scientist*. **24**.

Moseley PL (1997) Heat Shock Proteins and Heat Adaptation of the Whole Organism. *Journal of Applied Physiology*. **83**: 1413 – 1417.

Mosser DD and Morimoto RI (2004) Molecular chaperones and the stress of oncogenesis. *Oncogene*. **23**: 2907 – 2918.

Mosser DD, Duchaine J and Massie B (1993) The DNA Activity of the Human Heat Shock Transcription Factor is Regulated in Vivo by HSP70. *Molecular and Cellular Biology*. **13**: 5427 – 5438.

Mukherjee T and Lakhota SC (1979) 3H-thymidine incorporation in the puff 93D and in chromocentric heterochromatin of heat shocked salivary glands of *D. melanogaster*. *Chromosoma*. **74**: 75 - 82.

Multhoff G and Hightower LE (1996) Cell surface expression of heat shock proteins and the immune response. *Cell Stress and Chaperones*. **1**: 167-176.

Multhoff G. (2007) Heat shock protein 70 (Hsp70): Membrane location, export and immunological relevance. *Methods*. **43**: 229 – 237.

Nakai A (1999) New aspects in the vertebrate heat shock factor system: HSF3 and HSF4. *Cell Stress and Chaperones*. **4 (2)**: 86 – 93.

Nakai A and Morimoto RI (1993) Characterization of a novel chicken heat shock transcription factor, heat shock factor 3, suggests a new regulatory pathway. *Molecular and Cellular Biology*. **13**: 1983 – 1997.

Nasrin N, Ercolani L, Denaro M, Kong X F, Kang I and Alexander M (1990) An insulin response element in the glyceraldehyde-3-phosphate dehydrogenase gene bind a nuclear protein induced by insulin in cultured cells and by nutritional manipulation in vivo. *Proceedings of the National Academy of Sciences of the United States of America*. **87**: 5273 – 5277.

Neidhardt FC, VanBogelen RA and Vaughn V (1984) The genetics and regulation of heat shock proteins. *Annual Review of Genetics*. **18**: 295 – 329.

Neuer A, Spandorfer SD, Giraldo P, Dieterle S, Rosenwaks Z and Witkin SS (2000). The role of heat shock proteins in reproduction. *Human Reproduction Update*. **6 (2)**: 149 – 159.

Newton I (1701) Scala graduum caloris, calorum descriptiones and signa. *Philosophical Transactions of the Royal Society of London*. **22**: 824 – 829.

Nollen EA and Morimoto RI (2002) Chaperoning signaling pathways: molecular chaperones as stress-sensing 'heat shock' proteins *Journal of Cell Science*. **115**: 2809 – 2816.

Nylandsted J, Brand K and Jaattela M (2000) Heat Shock Protein 70 is Required for the Survival of Cancer Cells. *Annals of the New York Academy of Sciences*. **926**: 122 – 125.

Oehler R, Schmierer B, Zellner M, Prohaska R and Roth E. (2000) Endothelial Cells Downregulate Expression of the 70 kDa Heat Shock Protein during Hypoxia. *Biochemical and Biophysical Research Communications*. **274**: 542 – 547.

Oesterreich S, Weng CN, Qui M, Hilsenbeck SG, Osbourne CK and Fuqua SW (1993). The small heat shock protein hsp27 is correlated with growth and drug resistance in human breast cancer cell lines. *Cancer Research*. **53**: 4443 – 4448.

Oesterreich S, Hilsenbeck SG, Ciocca DR, Allred DC, Clark GC, Chamness GC, Osbourne CJ and Fuqua SA (1996) The small heat shock protein HSP27 is not an independent prognostic marker in axillary lymph node-negative breast cancer patients. *Clinical Cancer Research*. **2**: 1199 – 1206.

Ogata M, Naito Z, Tanaka S, Moriyama Y and Asano G (2000) Overexpression and localization of heat shock proteins mRNA in pancreatic carcinoma. *Journal of Nippon Medical School*. **67**: 177 – 185.

Ohtsuka K and Hata M (2000) Mammalian HSP40/DNAJ homologs: cloning of novel cDNAs and a proposal for their classification and nomenclature. *Cell Stress Chaperones*. **5**: 98 – 112.

Olsvik PA, Lie KK, Jordal AE, Nilsen TO and Hordvik I (2005). Evaluation of potential reference genes in real-time RT-PCR studies of Atlantic Salmon. *Biomedical Central Molecular Biology*. **6**: 21 – 30.

Orosz A, Wisniewski J and Wu C (1996) Regulation of *Drosophila* heat shock factor trimerization: global sequence requirements and independence of nuclear localization. *Molecular and Cellular Biology*. **16 (12)**: 7018 – 7030.

Osipiuk J, Walsh MA, Freeman BC, Morimoto RI and Joachimiak A (1999) Structure of a new crystal form of human Hsp70 ATPase domain. *Acta Crystallographica*. **55**: 1105 – 1107.

Ostrowski LE, von Wronski MA, Bigner SH, Rasheed A, Schold SC, Brent TP, Mitra S and Bigner DD (1991) Expression of O6-methylguanine-DNA methyltransferase in malignant human glioma cell lines. *Carcinogenesis*. **12**: 1739 – 1744.

Palego L, Giromella A, Marazzita D, Borsini F, Naccarato G, Giannaccini G, Lucacchini A, Cassano GB and Mazzoni MR (1999) Effects of post mortem delay on serotonin and (+)8-OH-DPAT- mediated inhibition of adenylyl cyclase activity in rat and human brain tissues *Brain Research*. **816 (1)**: 165 - 174.

Pandley P, Farber R, Nakazawa A, Kumar S, Bharti A, Nalin C, Weichselbaum R, Kufe D and Kharbanda S (2000) Hsp27 functions as a negative regulator of cytochrome c-dependent activation of procaspase-3. *Oncogene*. **19 (16)**: 1975 – 1981.

Parcellier A, Schmitt E, Gurbuxani S, Seigneurin-Berny D, Pance A, Chantome A, Plenchette S, Khochbin S, Solary E and Garrido C (2003) HSP27 is an ubiquitin-binding protein involved in I- κ B α proteasomal degradation. *Molecular and Cellular Biology*. **16**: 5790 – 5802.

Parcellier A, Gurbuxani S, Schmitt E, Solary E and Garrido C (2003) Heat shock proteins, cellular chaperones that modulate mitochondrial cell death pathways. *Biochemical and Biophysical Research Communications*. **304**: 505 – 512.

Pardue S, Wang S, Miller MM and Morrison-Bogorad M (2007) Elevated levels of inducible heat shock 70 proteins in human brain. *Neurobiology of Aging*. **28**: 314-324.

Parsa C and Givard S (2008) Juvenile Pilocytic Astrocytomas do not Undergo Spontaneous Malignant Transformation: Grounds for Designation as Hamartomas. *British Journal of Ophthalmology*. **92**: 40 – 46.

Parsell DA and Lindquist S (1993) The function of heat-shock proteins in stress tolerance: degradation and reactivation of damaged proteins, *Annual Review of Genetics*. **27**: 437–496.

Parsell A, Kowal AS, Singer KM and Linquist S (1994) Protein disaggregation mediated by heat shock protein Hsp104. *Nature*. **372**: 475 – 478.

Patel B, Khaliq A, Jarvis-Evans J, Boulton M, Arrol S, Mackness M, and McLeod D (1995) Hypoxia induces HSP70 gene expression in human hepatoma (HEP G2) cells. *Biochemistry and Molecular Biology International*. **36**: 907 – 912.

Patel R, Shervington L, Lea R and Shervington A (2008) Epigenetic silencing of telomerase and a non-alkylating agent as a novel therapeutic approach for glioma. *Brain Research*. **1188**: 173 – 181.

Paul C, Maero F, Gonin S, Kretz-Remy C, Viot S and Arrigo Ap (2002) HSP27 as negative regulator of cytochrome C release. *Molecular and Cellular Biology*. **22 (3)**: 816 – 834.

Pearl LH and Prodromou C (2000) Structure and in vivo function of Hsp90. *Current Opinion in Structural Biology*. **10**: 46 – 51.1

Peteranderl R and Nelson HMC (1992) Trimerization of the heat shock transcription factor by a triple-stranded α -helical coiled-coil. *Biochemistry*. **31**: 12272 – 12276.

Petrucelli L, Dicson D, Kehoe K, Taylor J, Snyder H, Grover A, De Lucia M, McGowan E, Lewis J, Prihar G, Kim J, Dillmann WH, Browne SE, Hall A, Voellmy R, Tsuboi Y, Dawson TM, Wolozin B, Hardy J and Hutton M (2004) CHIP and Hsp70 regulate tau ubiquitination, degradation and aggregation. *Human Molecular Genetics*. **13**: 703 – 714.

Pfister G, Stroh CM, Perschinka H, Kind M, Knoflach M, Hinterdorfer P and Wick G (2005) Detection of HSP60 on the membrane surface of stressed human endothelial cells by atomic force and confocal microscopy. *Journal of Cell Science*. **118 (8)**: 1587 – 1594.

Piura B, Rabinovich A, Yavelsky V, Wolfson M (2002) Heat shock proteins and malignancies of the female genital tract. *Harefuah*. **141**: 962 – 972.

Pockley GA (2003) Heat shock proteins in health and disease: therapeutic targets or therapeutic agents? *Molecular Medicine*. 1 – 21.

Ponchel F, Toomes C, Bransfield K, Leong F T, Douglas S H, Field S L, Bell S M, Combaret V, Puisieux A, Mighell A J, Robinson P A, Inglehearn C F, Issacs J D and Markham A F (2003) Real-time PCR based on SYBR-Green I fluorescence: An alternative to the TaqMan assay for a relative quantification of gene rearrangements, gene amplifications and micro deletions. *BMC Biotechnology*. **3 (18)**: 1 – 13.

Powers MV and Workman P (2007) Inhibitors of the heat shock response: Biology and Pharmacology. *Federation of European Biochemical Societies*. **581**: 3758-3769.

Powers MV, Clarke PA, Workman P. (2008) Dual targeting of HSC70 and HSP72 inhibits HSP90 function and induces tumor-specific apoptosis. *Cancer Cell*. **14**: 250-62.

Powers MV, Clarke PA, Workman P. (2009) Death by chaperone: HSP90, HSP70 or both? *Cell Cycle*. **8**: 518-526.

Preece P and Cairns NJ (2003) Quantifying mRNA in postmortem human brain: influence of gender, age at death, postmortem interval brain pH, agonal state and inter-lobe mRNA variance. *Molecular Brain Research*. **118**: 60 – 71.

Prodromou C, Roe SM, O'Brien R, Ladbury JE, Piper PW and Pearl LH (1997a) Identification and structural characterization of the ATP/ADP-binding site in the Hsp90 molecular chaperone. *Cell*. **90**: 65 – 75.

Prodromou C and Pearl LH (2003). Structure and functional relationships of Hsp90. *Journal of Chemical Biology* **10**: 361 - 368. *Current Cancer Drug Targets*. **3**: 301 – 323.

Qian X, Hou W, Li Z and Sha BD (2002) Direct interactions between molecular chaperones Hsp70 and Hsp40. *Journal of Biochemistry*. **361**: 27 – 34.

Qiu XB, Shao YM, Miao S and Wang L (2006) The diversity of the DnaJ/Hsp40 family, the crucial partners for Hsp70 chaperones. *Cellular and Molecular Life Science*. **63**: 2560 – 2570.

Rabindran SK, Giorgi G, Clos J and Wu C. (1991) Molecular cloning and expression of a human heat shock factor HSF1. *Proceedings of the National Academy of Sciences of the United States of America*. **88**: 6906 – 6910.

Rabindran SK, Haroun RI, Clos J, Wisniewski J and Wu C. (1993) Regulation of heat shock factor trimer formation: Role of a conserved leucine zipper. *Science*. **259**: 230 – 234.

Rane MJ, Pan Y, Singh S, Powell DW, Wu R, Cummins T, Chen Q, McLeish KR and Klein JB (2003) Heat shock protein 27 controls apoptosis by regulating AKT activation. *Journal of Biological Chemistry*. **278 (30)**: 27828 – 27835.

Ranford JC, Coates AR and Henderson B (2000) Chaperonins are cell-signalling proteins: the unfolding biology of molecular chaperones. *Experimental Reviews in Molecular Medicine*. **2**: 1 – 17.

Rapisarda A, Uranchimeg B, Scudiero D A, Selby M, Sausville E A, Shoemaker R H and Melillo G (2002) Identification of small molecule inhibitors of hypoxia-inducible factor 1 transcriptional activation pathway. *Cancer Research*. **62**: 4316 – 4324.

Ricaniadis N, Katakaki A, Agnantis N, Androulakis G, Karakousis CP (2001) Long-term prognostic significance of HSP70, c-myc and HLA-DR expression in patients with malignant melanoma. *European Journal of Surgical Oncology*. **27**: 88 – 93.

Richards EH, Hickey E, Weber L, Master JR (1996) Effect of overexpression of the small heat shock protein HSP27 on the heat and drug sensitivities of human testis tumor cells. *Cancer Research*. **56**: 2446 – 2451.

Ritossa F. (1963) New puffs induced by temperature shocks, DNP and salicylate in salivary chromosomes of *D. melanogaster*. *Cellular and Molecular Life Sciences*. **12**: 571 - 573.

Ritossa F (1962) A new puffing pattern induced by heat shock and DNP in *Drosophila*. *Experimentia*. **18**: 571 – 573.

Ritossa F (1964) Behaviour of RNA and DNA synthesis at the puff level in salivary gland chromosomes of *Drosophila*. *Experimental Cell Research*. **36**: 515 – 523.

Ritossa F (1996) Discovery of the heat shock response. *Cell Stress Chaperones*. **1(2)**: 97 – 98.

Rohde M, Daugaard M, Jensen MH, Helin K, Nylandsted J and Jaattela M (2005) Members of the heat-shock protein 70 family promote cancer cell growth by distinct mechanisms. *Genes and Development*. **19**: 570 - 582.

Rose G, Fleming P, Banavar J and Maritan A (2006) "A backbone-based theory of protein folding". *Proceedings of the National Academy of Sciences of the United States of America*. **103 (45)**: 16623 –16633.

Sabucedo AJ and Furton KG (2003) Estimation of post-mortem interval using the protein marker cardiac Troponin I. *Forensic Science International*, **134**: 11 – 16.

Sagol O, Tuna B, Coker A (2002) Immunohistochemical detection of pS2 protein and heat shock protein-70 in pancreatic adenocarcinomas. Relationship with disease extent and patient survival. *Pathology Research and Practice*. **198**: 77 – 84.

Said H M, Katzer A, Flentje M and Voerdermark D (2005) Response of the plasma hypoxia marker osteopontin to in vitro hypoxia in human tumour cells. *Radiotherapy Oncology*. **76**: 200 – 205.

Said H M, Staab A, Hagemann C, Vince G H, Katzer A, Flentje M and Vordermark D (2007) Distinct patterns of hypoxic expression of carbonic anhydrase IX (CA IX) in human malignant glioma cell lines. *Journal of Neurooncology*. **81 (1)**: 27 – 38.

Said H M, Hagemann C, Sjojic J, Schoemig B, Vince G H, Flentje M, Roosen K and Vordermark D (2007) GAPDH is not regulated in human glioblastoma under hypoxic conditions. *BMC Molecular Biology*. **8 (55)**: 1 – 13.

Said H M, Polat B, Hagemann C, Anacker J, Flentje M and Vordermark D (2009) Absence of GAPDH regulation in tumour cells of different origin under hypoxic conditions in vitro. *BMC Research Notes*. **2: 8**

Sampson JH, Ashley DM, Archer GE Fuchs HE, Dranoff G, Hale LP and Bigner DD (1997) Characterization of a spontaneous murine astrocytoma and abrogation of its tumorigenicity by cytokine secretion. *Neurosurgery*. **41**: 1365 – 1373.

Santarosa M, Favaro D, Quaia M, Galligioni E (1997) Expression of heat shock protein 72 in renal cell carcinoma: possible role and prognostic implications in cancer patients. *European Journal of Cancer*. **33**: 873 – 877.

Santoro GM (2000) Heat Shock Factors and the Control of the Stress Response. *Biochemical Pharmacology*. **59**: 55 – 63.

Sarge KD, Murphy SP and Morimoto RI (1993) Activation of heat shock gene transcription by heat shock factor 1 involves oligomerization, acquisition of DNA-binding activity, and nuclear localization and can occur in the absence of stress. *Molecular and Cellular Biology*. **13**: 1392 – 1407.

Sargent CA, Dunham I, Trowsdale J and Campbell RD (1989). Human major histocompatibility complex contains genes for the major heat shock protein HSP70. *Proceedings of the National Academy of Sciences of the United States of America*. **86**: 1968 – 1972.

Sargent CA, Dunham I and Campbell RD (1989a). Identification of multiple HTF-island associated genes in the human major histocompatibility complex class III region. *The EMBO Journal*. **8**: 2305 – 2312.

Schlesinger MJ (1990) Heat shock proteins. *The Journal of Biological Chemistry*. **265** (21): 12111 – 12114.

Schleyer F (1963) Determinations of the time of death in the early postmortem interval, *Methods of Forensic Science*, **Vol. 2** (First Edition), Interscience Publishers, John Wiley and Sons, New York pp. 253 – 293.

Schmid D, Baici A, Gehring H, Christen P (1994). Kinetics of molecular chaperone action. *Science*. **263**: 971–973.

Schmid T, Zhou J and Brune B (1998) HIF-1 and P53: communication of transcription factors under hypoxia. *Journal of Cellular Molecular Medicine*. **8**: 423 – 431.

Schmitt E, Gehrman M, Brunet M, Multhoff G and Garrido C (2007) Intracellular and extracellular functions of heat shock proteins repercussions in cancer therapy. *Journal of Leukocyte Biology*. **81**: 15 – 27.

Schneider J, Jimenez E, Marenbach K, Romero H, Marx D and Meden H (1999) Immunohistochemical detection of HSP60-expression in human ovarian cancer. Correlation with survival in a series of 247 patients. *Anticancer Research*, **19**: 2141 – 2146.

Seidberg NA, Clark RSB, Zhang X, Lai Y, Chen M, Grahams SH, Kochanek PM, Watkins SC and Marion DW (2003) Alterations in inducible 72-kDa heat shock protein and the chaperone cofactor BAG-1 in human brain after head injury. *Journal of Neurochemistry*. **84**: 514 – 521.

Semenza GL (1999) Regulation of mammalian O₂ homeostasis by hypoxia-inducible factor 1. *Annual Reviews of Cell and Development Biology*. **15**: 551-578.

Serano RD, Pegram CN and Bigner DD (1980) Tumorigenic cell culture lines from a spontaneous VM/Dk murine astrocyte (SMA). *Acta Neuro-pathology*. **51**: 53 – 64.

Sevier CS and Kaiser CA (2002) Formation and transfer of disulphide bonds in living cells. *Nature Reviews Molecular and Cellular Biology*. **3**: 836 – 847.

Shamovsky I and Nudler E (2008) Visions and Reflections (Mini Review) New insights into the mechanism of heat shock response activation. *Cellular and Molecular Life Sciences*. **65**: 855 – 861.

Shaner L and Morano KA (2007). All in the family: atypical Hsp70 chaperones are conserved modulators of Hsp70 activity. *Cell Stress Chaperones*. **12**: 1 – 8.

Shervington A, Lu Chen, Patel R and Shervington L (2009) Telomerase down-regulation in cancer brain stem cell. *Molecular Cell Biochemistry*. **331**: 153 – 159.

Shervington A, Mohammed K, Patel R and Lea R (2007b). Identification of a novel co-transcription of *P450/IAI* with telomerase in A549. *Gene*. **388**: 110 – 116.

Shi Y, Kroeger PE and Morimoto RI (1995) The carboxyl-terminal transactivation domain of heat shock factor 1 is negatively regulated and stress responsive. *Molecular and Cellular Biology*. **15**: 4309 – 4318.

Shi Y, Mosser DD and Morimoto RI (1998) Molecular Chaperones as HSF1 Specific Transcriptional Repressors. *Genes and Development*. **12**: 654 – 666.

Shows TB, Alper CA, Bootsma D, Dorf M, Douglas T, Huisman T, Kit S, Klinger HP, Kozak C, Lalley PA, Lindsley D, McAlpine PJ, McDougall JK, Meera Khan P, Meisler M, Morton NE, Opitz JM, Partridge CW, Payne R, Roderick TH, Rubinstein P, Ruddle FH, Shaw M, Spranger JW and Weiss K (1987) International System for Human Gene Nomenclature. *Cytogenetics and Cell Genetics*. **25**: 96 – 116.

Silver N, Best S, Jiang J and Thein SL (2006) Selection of housekeeping genes for gene expression studies in human reticulocytes using real-time PCR. *BMC Molecular Biology*. **7**: (33).

Simiantonaki N, Asinghe CJ, Michel-Schmidt R, Peters K, Hermanns MI and Kirkpatrick CJ (2008) Hypoxia-induced epithelial VEGF-C/VEGFR-3 upregulation in carcinoma cell lines. *International Journal of Oncology*. **32**: 585 – 592.

Singh VK and Kumar A (2001) PCR Primer Design. *Molecular Biology Today*. **2**: 27 – 32.

Singh R, Kolvra S and Rattan SIS (2007) Genetics of human longevity with emphasis on the relevance of HSP70 as candidate gene. *Frontiers in Bioscience*. **12**: 4504 – 4513.

Sirove M A (1999) New insights into an old protein: the functional diversity of mammalian glyceraldehyde-3-phosphate dehydrogenase. *Biochemistry Biophysics ACTA*. **1432**: 159 – 184.

Smiley JK, Brown WC and Campbell JL (1992) The 66 kDa component of yeast SFI, stimulatory factor I, is hsp60. *Nucleic Acids Research*. **20**: 4913 – 4918.

Sorger PK and Nelson HCM (1989) Trimerization of a yeast transcriptional activator via a coiled-coil motif. *Cell*. **59**: 807 – 813.

Soti C, Racz A and Csermely P (2002) A nucleotide-dependent molecular switch controls ATP binding at the C-terminal domain of Hsp90. N-terminal nucleotide

binding unmask a C-terminal binding pocket. *Journal of Biological Chemistry*. **277**: 7066 – 7075.

Soussi T and Lozano G (2005) p53 mutation heterogeneity in cancer. *Biochemical and Biophysical Research Communications*. **331**: 834 – 842.

Sreedhar AS and Csermely P (2004) Heat shock proteins in the regulation of apoptosis: new strategies in tumor therapy A comprehensive review. *Pharmacology and Therapeutics*. **101**: 227 – 257.

Sreedhar AS, Kalmir E, Csermely P and Shen YF (2004) Hsp90 isoforms: functions, expression and clinical importance. *Federation of European Biochemical Societies*. **562**: 11 – 15.

Stefano L, Racchetti G, Bianco F, Passini N, Gupta RS, Bordignon PP and Meldolesi J (2009) The surface-exposed chaperone, Hsp60, is an agonist of the microglial TREM2 receptor. *Journal of Neurochemistry*. **110**: 284 – 294.

Stetler RA, Gan Y, Zhang W, Liou AK, Gao Y, Cao G and Chen J (2010) Heat Shock Proteins: Cellular and molecular mechanisms in the CNS. *Progress in Neurobiology*. **92** (2): 184 – 211.

Stokoe D, Engel K, Campbell DG, Cohen P and Gaestel M (1992) Identification of MAPKAP kinase 2 as a major enzyme responsible for the phosphorylation of the small mammalian heat shock proteins. *FEBS Letter*. **313** (3): 307 – 313.

Stuart JK, Myszka DG, Joss L, Mitchell RS, McDonald SM, Xie Z, Takayama S, Reed JC and Ely KR (1998) Characterization of interactions between anti-apoptotic protein BAG-1 and Hsc70 molecular chaperones. *Journal of Biological Chemistry*. **273**: 22506 – 22514.

Syrigos KN, Harrington KJ, Sekara E, Chatziyianni E, Syrigou EI, Waxman J (2003) Clinical significance of heat shock protein-70 expression in bladder cancer. *Urology*. **61**: 677 – 680.

Szabo A, Langer T, Schroder H, Flanagan J, Bukau B and Hartl FU (1994) The ATP hydrolysis-dependent reaction cycle of the *Escherichia coli* Hsp70 system – DnaK, DnaJ, and GrpE. *Proceedings of the National Academy of Sciences of the United States of America*. **91**: 10345 – 10349.

Takayama S, Bimston DN, Matsuzawa S, Freeman BC, Aime-sempé C, Xie Z, Morimoto RI and Reed JC (1997) BAG-1 modulates the chaperone activity of Hsp70/Hsc70. *The EMBO Journal*. **16**: 4887 – 4896.

Tanabe M, Kawazoe Y, Takeda S, Morimoto RI, Nagata K and Nakai A (1998) Disruption of the HSF3 gene results in the severe reduction of heat shock gene expression and loss of thermotolerance. *The EMBO Journal*. **17 (6)**: 1750 – 1758.

Thanner F, Sutterlin MW, Kapp M, Kristen P, Dietl J, Gassel AM, Müller T (2003) Heat-shock protein 70 as a prognostic marker in node-negative breast cancer. *Anticancer Research*. **23**: 1057 – 1062.

Thellin O, Zorzi W, Lakaye B, De Borman B, Coumans B, Hennen G, Grisar T, Igout A and Heinen E (1999) Housekeeping genes as internal standards: use and limits. *Journal of Biotechnology*. **8**: 291 – 295.

Theodorakis NG and Morimoto RI. (1987) Posttranscriptional Regulation of HSP70 Expression in Human Cells: Effects of Heat Shock, Inhibition of Protein Synthesis, and Adenovirus Infection on Translation and mRNA Stability. *Molecular and Cellular Biology*. **7**: 4357 - 4368.

Theodorakis NG, Drujan D and De Maio A (1999) Thermotolerant Cells Show an Attenuated Expression of HSP70 after Heat Shock. *The Journal of Biological Chemistry*. **274**: 12081-12086.

Thériault JR, Lambert H, Chávez-Zobel AT, Charest G, Lavigne P and Landry J (2004) Essential role of the N-terminal WD/EPF motif in the phosphorylation-activated protective function of mammalian Hsp27. *Journal of Biological Chemistry*. **279**: 23463 – 23471.

Thomas PJ, Qu BH, Pedersen PL (1995) Defective Protein Folding as a Basis of Human Disease. *Trends in Biochemical Sciences*. **20**: 456 – 459.

Tissieres A, Mitchell HK and Tracy UM (1974) Protein synthesis in salivary glands of *Drosophila melanogaster*: relation to chromosome puffs. *Journal of Molecular Biology*. **84**: 389 – 398.

Tolson JK and Roberts SM (2005) Manipulating Heat Shock Protein Expression in Laboratory Animals. *Methods*. **35**: 149 – 157.

Torres G, Hallas BH, Lorig EN, Strauss J and Horowitz JM (2004) Dynamic expression of molecular chaperones in structurally and functionally intact endothelial cell networks. *Preclinica*. **2**: 197 – 203.

Trautinger F, Kokesch C, Herbacek I, Knobler RM, Kindas-Mugge I (1997) Overexpression of the small heat shock protein, hsp 27 confers resistance to hyperthermia but not to oxidative stress and UV induced cell death in a stably transfected epidermal cell line' *Journal of Photochemistry and Photobiology*. **39**: 90 - 95.

Trivedi V, Gadhvi P, Chorawala M and Shah G (2010) Role of the heat shock proteins in immune response and immunotherapy for human cancer. *International Journal of Pharmaceutical Sciences Review and Research*. **2 (2)**: 59 – 62.

Tso C, Freije W, Day A, Chen Z, Merriman B, Perlina A, Lee Y, Dia E, Yoshimoto K, Mischel P, Liao L, Cloughesy T and Nelson S (2006) Distinct Transcriptional Profiles of Primary and Secondary Glioblastoma Subgroups. *Cancer Research*. **66**: 159 – 167.

Turman MA, Kahn DA, Rosenfeld, Apple CA and Bates CM (1997) Characterization of Human Proximal Tubular Cells after Hypoxic Preconditioning: Constitutive and Hypoxia-Induced Expression of Heat Shock Proteins HSP70 (A< B, and C), HSC70 and HSP90. *Biochemical and Molecular Medicine*. **60**: 49 – 58.

Uchiyama Y, Takeda N, Mori M and Terada K (2006) Heat Shock Protein 40/DjB1 Is Required for Thermotolerance in Early Phase. *Journal of Biochemistry*. **140**: 805 – 812.

Urushibara M, Kageyama Y, Akashi T, Yukihiro O, Takizawa T, Koike M and Kazunori K (2007) HSP60 may predict good pathological response to neoadjuvant chemoradiotherapy in bladder cancer. *Japanese Journal of Clinical Oncology*. **37**: 56 – 61.

Von Montfort R, Slingsby C and Vierling E (2001) Structure and function of the small heat shock protein alpha/crystalline family of molecular chaperones. *Advances in Protein Chemistry*. **59**: 105 – 156.

Voellmy R, Goldschmidt-Clermont M, Southgate R, Tissieres A, Lewis R and Gehring W (1981) A DNA segment isolated from chromosomal site 67B in *D. melanogaster* contains four closely linked heat shock genes. *Cell*. **23**: 261 - 270.

Vuister GW, Kim SJ, Wu C and Bax A (1994) NMR evidence for similarities between the DNA-binding regions of *Drosophila melanogaster* heat shock factor and the helix-turn-helix and HNF-3/forkhead families of transcription factors. *Biochemistry*. **33**: 10 – 16.

Vuister GW, Kim SJ, Orosz A, Marquardt J, Wu C and Bax A (1994) Solution structure of the DNA-binding domain of *Drosophila* heat shock transcription factor. *Nature Structural Biology*. **1**: 605 – 614.

Wang GL, Jiang B-H, Rue EA and Semenza GL (1995a) Hypoxia-inducible factor 1 is a basic-helix-loop-helix-PAS heterodimer regulated by cellular O₂ tension. *Proceedings of the National Academy of Sciences of the United States of America*. **92**: 5510 – 5514.

Wang X, Grammatikakis N, Siganou A and Calderwood SK (2003) Regulation of Molecular Chaperone Gene Transcription Involves the Serine Phosphorylation, 14-3-3 σ Binding, and Cytoplasmic Sequestration of Heat Shock Factor 1. *Molecular and Cellular Biology*. **23** (17): 6013 - 6026.

Wang XY, Arnouk H, Chen X, Kazim L, Repasky EA and Subjeck JR (2006) Extracellular targeting of endoplasmic reticulum chaperone glucose reagent protein 170 enhances tumor immunity to a poorly immunogenic melanoma. *Journal of Immunology*. **177**: 1543 – 1551.

Welch WJ (1993) Heat shock proteins functioning as molecular chaperones: their roles in normal and stressed cells. *Biological Sciences*. **339**: 327 – 333.

Westwood JT and Wu C (1993) Activation of *Drosophila* heat shock factor: Conformational change associated with a monomer-to-trimer transition. *Molecular and Cellular Biology*. **13**: 3481 – 3486.

White FP and Currie WR (1982) Heat shock regulation in *Drosophila* and yeast. In heat shock from bacteria to man. Cold Spring Harbor, New York: Cold Spring Harbor Press. pp 379 – 386.

Wiech H, Buchner J, Zimmermann R and Jakob U (1992) Hsp90 chaperones protein folding in vitro. *Nature*. **358**: 169 – 170.

Williams KJ, Cowen RL and Stratford IJ (2001) Hypoxia and oxidative stress in breast cancer Tumour hypoxia – therapeutic considerations. *Breast Cancer Research*. **3**: 328 – 331.

Wisniewski J, Orosz A, Allada R and Wu C (1996) The C-terminal region of *Drosophila* heat shock factor (HSF) contains a constitutively functional transactivation domain. *Nucleic Acids Research*. **24**: 367 – 374.

Wisniewska M, Karlberg T, Lehtio L, Johansson I, Kotenyova T, Moche M and Schuler H (2010) Crystal structures of the ATPase domains of four human Hsp70 isoforms: HSPA1L/Hsp70-hom, HSPA2/Hsp70-2, HSPA6/Hsp70B, and HSPA5/BiP/GRP78. *PLoS One*. **5 (1)**: 1 – 8.

Wu C, Clos J, Giorgi G, Haroun RI, Kim SJ, Rabindran SK, Westwood JT, Wisniewski J and Yim G (1994) Structure and Regulation of Heat Shock Promoters. In the *Biology of Heat Shock Proteins and Molecular Chaperones* (ed. RI Morimoto, A Tissieres and G Georgopoulos), pp. 395 – 416. Cold Spring Harbor Laboratory Press, Cold Spring Harbor, NY.

Wu C. (1995) Heat shock transcription factors: structure and regulation. *Annual Review of Cell and Developmental Biology*. **11**: 441 – 69.

Yamamori T, Ito K, Nakamura Y and Yura T (1978) Transient regulation of protein synthesis in *Escherichia coli* upon shift-up of growth temperature. *Journal of Bacteriology*. **134**: 1133 – 1140.

Yamamoto M, Mohanam S, Sawaya R, Fuller GN, Seiki M, Sato H, Gokaslan ZL, Liotta LA, Nicolson GL and Rao JS (1996) Differential expression of membrane-type matrix metalloproteinase and its correlation with gelatinase A activation in human malignant brain tumors *in Vivo* and *in Vitro*. *Cancer Research*. **56**: 384 – 392.

Yasojima K, McGeer EG and McGeer PL (2001) High stability of mRNAs postmortem and protocols for their assessment by RT-PCR. *Brain Research Protocols*. **8**: 132 – 136.

Young JC, Barral JM and Hartl FU (2003) More than folding: Localized functions of cytosolic chaperones. *Trends in Biochemical Sciences*. **28**: 541 – 547.

Yufu Y, Nishimura J and Nawata H (1992) High constitutive expression of heat shock protein 90 α in human acute leukemia cells. *Leukemia Research*. **16**: 597 – 605.

Zamecnik P (2005) From protein synthesis to genetic insertion, *Annual Review of Biochemistry*. **74**: 1 – 28.

Zhang Y, Murshid A, Prince T and Calderwood SK (2011) Protein kinase A regulates molecular chaperone transcription and protein aggregation. *PLoSone*. **6 (12)**: 1 – 8.

Zhao D, Ishikawa T, Quan L, Li DR, Michiue T, Yoshida C, Komatu A, Chen JH, Zhu BL and Maeda H (2009) Postmortem mRNA quantification for investigation of infantile death: a comparison with adult cases. *Legal Medicine*. **11**: S286 – S289.

Zhong T, Arndt KT. (1993) The yeast SIS1 protein, a DnaJ homolog, is required for the initiation of translation. *Cell*. **73(6)**: 1175 – 1186

Zhong H and Simmons J W (1999) Direct comparison of GAPDH, beta-actin, cyclophilin and 28S rRNA as internal standards for quantifying RNA levels under hypoxia. *Biochemistry Biophysics Research Communication*. **259**: 523 – 526.

Zuo J, Rungger D and Voellmy R (1995) Multiple layers of regulation of human heat shock transcription factor 1. *Molecular and Cellular Biology*. **15**: 4319 – 4330.

8.2 Websites

Creating Standard Curves with Genomic DNA or Plasmid DNA Templates for Use in Quantitative PCR

http://www6.appliedbiosystems.com/support/tutorials/pdf/quant_pcr.pdf

Dyes and fluorescence detection chemistry in qPCR

www.gene-quantification.com/chemistry.html

DOGS – Database of genome sizes

www.cbs.dtu.dk/databases/DOGS/index.html

European Bioinformatics Institute – ClustalW2, sequence alignment tool

<http://www.ebi.ac.uk/clustalw/>

Gene Cards – human gene database

<http://www.genecards.org>

Gene expression: transcription

www.users.rcm.com/.../T/Transcription.html

NanoDrop 1000 Spectrophotometer V3.7 User's Manual

<http://www.nanodrop.com/Library/nd-1000-v3.7-users-manual-8.5x11.pdf>

National Center for Biotechnology Information

<http://www.ncbi.nlm.nih.gov>

NCBI nucleotide database

<http://www.ncbi.nlm.nih.gov/entrez/query.fcgi?db=nucleotide&cmd=search&term>

Primer3 – PCR primer design tool

<http://frodo.wi.mit.edu>

The new WHO 2000 classification of brain tumours: imaging correlations

www.rad.usuhs.mil/rad/who/JPA.html

Chapter 9

Appendices

Appendix 9.1 Amino acid and gene sequence for *HSPA1A* *Homo sapiens* adapted from NCBI (<http://www.ncbi.nlm.nih.gov>)

NCBI Reference Sequence: NM_005345.5

Homo sapiens heat shock 70kDa protein 1A (HSPA1A), mRNA

LOCUS NM_005345 2445 bp mRNA linear PRI 20-DEC-2009
DEFINITION Homo sapiens heat shock 70kDa protein 1A (HSPA1A), mRNA.
ACCESSION NM_005345
VERSION NM_005345.5 GI:194248071

Amino Acid Sequence

```
/translation="MAKAAAIGIDLGTTYSCVGVFQHGKVEIIANDQGNRTTPSYVAF
TDTERLIGDAAKNQVALNPQNTVFDKRLIGRKFQDPVQSDMKHWPVQVINDGDKPK
VQVSYKGETKAFYPEEISSMVLTKMKEIAEAYLGYPVTNAVITVPAYFNDSQRQATKD
AGVIAGLNVLRINEPTAAAIAYGLDRTGKGERNVLIIFDLGGGTFDVSILTIDGIFE
VKATAGDTHLGGEDFDNRLVNHFVEEFKRKHKKDISQNKRAVRRRLRTACERAKRTLSS
STQASLEIDSLFEGIDFYTSITRARFEELCSDLFRSTLEPVEKALRDAKLDKAQIHDL
VLVGGSTRIPKVQKLLQDFFNDRDLNKSINPDEAVAYGAAVQAAILMGDKSENVQDLL
LLDVAPLSLGLTAGGVMTALIKRNSTIPTKQTQIFTTYSDNQPGVLIQVYEGERAMT
KDNLLGRFELSGIPPAPRGVPQIEVTFDIDANGILNVTATDKSTGKANKITITNDKG
RLSKEEIERMVQEAKEYKAEDVQRERVSAKNALESYAFNMKSAVEDEGLKGISEAD
KKKVLDKCQEVISWLDANTLAEKDEFEHKRKELEQVCNPIISGLYQGAGGPGPGGFGA
```

Gene Sequence

```
1 ataaaagccc aggggcaagc ggtccggata acggctagcc tgaggagctg
ctgcgacagt
61 ccactacctt tttcgagagt gactcccgtt gtcccaaggc ttcccagagc
gaacctgtgc
121 ggctgcaggc accggcgcgt cgagtttccg gcgtccggaa ggaccgagct
cttctcgcgg
181 atccagtgtt ccgtttccag cccccaatct cagagcggag ccgacagaga
gcaggggaacc
241 ggcattggcca aagccgcggc gatcggcacc gacctgggca ccactactc
ctgcgtgggg
301 gtgttccaac acggcaaggt ggagatcacc gccaacgacc agggcaaccg
caccaccccc
361 agctacgtgg ccttcacgga caccgagcgg ctcacgggg atgcggccaa
gaaccaggtg
421 gcgctgaacc cgcagaacac cgtgtttgac gcgaagcggc tgattggccg
caagttcggc
481 gaccgggtgg tgcagtcgga catgaagcac tggcctttcc aggtgatcaa
cgacggagac
```

541 aagcccaagg tgcaggtgag ctacaagggg gagaccaagg cattctacce
cgaggagatc
601 tcgtccatgg tgctgaccaa gatgaaggag atcgccgagg cgtacctggg
ctaccggtg
661 accaacgcgg tgatcacctg gccggcctac ttcaacgact cgcagcgcca
ggccaccaag
721 gatgcgggtg tgatcgcggg gctcaacgtg ctgcggatca tcaacgagcc
cacggccgcc
781 gccatcgctt acggcctgga cagaacgggc aagggggagc gcaacgtgct
catctttgac
841 ctgggggggg gcaccttoga cgtgtccatc ctgacgatcg acgacggcat
cttcgaggtg
901 aaggccacgg ccggggacac ccacctgggt ggggaggact ttgacaacag
gctggtgaac
961 cacttcgtgg aggagttaa gagaaaacac aagaaggaca tcagccagaa
caagcgagcc
1021 gtgaggcggc tgcgcaccgc ctgcgagagg gccaagagga ccctgtcgtc
cagcaccag
1081 gccagcctgg agatcgactc cctgtttgag ggcacgact tctacacgtc
catcaccagg
1141 gcgaggttcg aggagctgtg ctccgacctg ttccgaagca ccctggagcc
cgtggagaag
1201 gctctgcgcg acgccaagct ggacaaggcc cagattcacg acctggtcct
ggtcgggggc
1261 tccaccgcga tccccaaggt gcagaagctg ctgcaggact tcttcaacgg
gcgcgacctg
1321 aacaagagca tcaaccccgca cgaggctgtg gcctacgggg cggcgggtgca
ggcggccatc
1381 ctgatggggg acaagtccga gaacgtgcag gacctgctgc tgctggacgt
ggctcccctg
1441 tcgctggggc tggagacggc cggaggcgtg atgactgcc tgatcaagcg
caactccacc
1501 atccccacca agcagacgca gatcttcacc acctactccg acaaccaacc
cggggtgctg
1561 atccaggtgt acgagggcga gagggccatg acgaaagaca acaatctggt
ggggcgcttc
1621 gagctgagcg gcatccctcc ggccccagg ggcgtgcccc agatcgaggt
gaccttcgac
1681 atcgatgcca acggcatcct gaacgtcacg gccacggaca agagcaccgg
caaggccaac
1741 aagatcacca tcaccaacga caagggccgc ctgagcaagg aggagatcga
gcgcatggtg
1801 caggaggcgg agaagtacaa agcggaggac gaggtgcagc gcgagagggg
gtcagccaag
1861 aacgccctgg agtcctacgc cttcaacatg aagagcgccg tggaggatga
ggggctcaag
1921 ggcaagatca gcgaggcgga caagaagaag gtgctggaca agtgtcaaga
ggtcatctcg
1981 tggctggacg ccaacacctt ggccgagaag gacgagtttg agcacaagag
gaaggagctg
2041 gagcaggtgt gtaaccccat catcagcgga ctgtaccagg gtgccgggtg
tcccgggctt
2101 gggggcttcg gggctcaggg tcccaagga gggctctgggt caggccccac
cattgaggag
2161 gtagattagg ggcctttcca agattgctgt ttttgttttg gagcttcaag
actttgcatt
2221 tcctagtatt tctgtttgtc agttctcaat ttctgtgtt tgcaatggtg
aaattttttg
2281 gtgaagtact gaacttgctt tttttccggt ttctacatgc agagatgaat
ttatactgcc
2341 atcttacgac tttttcttct ttttaataca cttaactcag gccatttttt
aagttggtta
2401 cttcaaagta aataaacttt aaaattcaaa aaaaaaaaaa aaaaa

Appendix 9.2 Amino acid and gene sequence for *HSPA1B* *Homo sapiens* adapted from NCBI (<http://www.ncbi.nlm.nih.gov>)

NCBI Reference Sequence: NM_005346.4

Homo sapiens heat shock 70kDa protein 1B (HSPA1B), mRNA

LOCUS NM_005346 2551 bp mRNA linear PRI 26-SEP-2010
DEFINITION Homo sapiens heat shock 70kDa protein 1B (HSPA1B), mRNA.
ACCESSION NM_005346
VERSION NM_005346.4 GI:167466172

Amino Acid Sequence

```
/translation="MAKAAAIGIDLGTTYSCVGVFQHGKVEIIANDQGNRTTPSYVAF  
TDTERLIGDAAKNQVALNPQNTVFDKRLIGRKFQDPVVQSDMKHWPFQVINDGDKPK  
VQVSYKGETKAFYPEEISSMVLTKMKEIAEAYLGYPVTVNAVITVPAYFNDSQRQATKD  
AGVIAGLNVLRINEPTAAAIAYGLDRTGKGERNVLIIFDLGGGTFDVSILTIDDGIFE  
VKATAGDTHLGGEDFDNRLVNHVFVEEFKRKHKKDISQNKRAVRRLRTACERAKRTLSS  
STQASLEIDSLFEGIDFYTSITRARFEELCSDLFRSTLEPVEKALRDAKLDKAQIHDL  
VLVGGSTRIPKVQKLLQDFFNDRDLNKSINPDEAVAYGAAVQAAILMGDKSENVQDLL  
LLDVAPLSLGLLETAGGVM TALIKRNSTIPTKQTQIFTTYSDNQPGVLIQVYEGERAMT  
KDNLLGRFELSGIPPAPRGVPQIEVTFDIDANGILNVTATDKSTGKANKITITNDKG  
RLSKEEIERMVQEAKEYKAEDVQRERVSAKNALESYAFNMKSAVEDEGLKGI SEAD  
KKKVLDKCQEVISWLDANTLAEKDEFEHKRKELEQVCNPIISGLYQGAGGPGPGGFGA  
QGPKGSGSGPTIEEVD"
```

Gene Sequence

```
1 ggaaaacggc cagcctgagg agctgctgcg agggctccgct tcgtctttcg  
agagtgactc  
61 ccgcggtccc aaggctttcc agagcgaacc tgtgcggctg caggcaccgg  
cgtggtgagt  
121 ttccggcggt ccgaaggact gagctcttgt cgcggatccc gtccgccggt  
tccagcccc  
181 agtctcagag cggagcccac agagcagggc accggcatgg ccaaagccgc  
ggcgatcggc  
241 atcgacctgg gcaccaccta ctctgctg ggggtgttcc aacacggcaa  
ggtggagatc  
301 atcgccaacg accagggcaa ccgcaccacc cccagctacg tggccttcac  
ggacaccgag  
361 cggctcatcg gggatgcggc caagaaccag gtggcgctga acccgcagaa  
caccgtgttt  
421 gacgcgaagc ggctgatcgg ccgcaagttc ggcgaccgg tggtgcagtc  
ggacatgaag
```

481 cactggcctt tccaggtgat caacgacgga gacaagccca aggtgcaggt
 gagctacaag
 541 ggggagacca aggcattcta ccccgaggag atctcgtcca tgggtgctgac
 caagatgaag
 601 gagatcgccg aggcgtacct gggctacccg gtgaccaacg cggatgatcac
 cgtgccggcc
 661 tacttcaacg actcgcagcg ccaggccacc aaggatgcgg gtgtgatcgc
 ggggctcaac
 721 gtgctgcgga tcatcaacga gccacggcc gccgccatcg cctacggcct
 ggacagaacg
 781 ggcaaggggg agcgcaacgt gctcatcttt gacctgggcg ggggcacctt
 cgacgtgtcc
 841 atcctgacga tcgacgacgg catcttcgag gtgaaggcca cggccgggga
 caccacctg
 901 ggtggggagg actttgacaa caggctggtg aaccacttcg tggaggagtt
 caagagaaaa
 961 cacaagaagg acatcagcca gaacaagcga gccgtgaggc ggctgcgcac
 cgctgcgag
 1021 agggccaaga ggaccctgtc gtccagcacc caggccagcc tggagatcga
 ctccctgttt
 1081 gagggcatcg acttctacac gtccatcacc agggcgagggt tcgaggagct
 gtgctccgac
 1141 ctgttccgaa gcaccctgga gcccgaggag aaggctctgc gcgacgcaa
 gctggacaag
 1201 gccagattc acgacctggt cctggtcggg ggctccacc gcatacccaa
 ggtgcagaag
 1261 ctgctgcagg acttcttcaa cgggcgcgac ctgaacaaga gcatacaacc
 cgacgaggct
 1321 gtggcctacg gggcgccgggt gcaggcggcc atcctgatgg gggacaagtc
 cgagaacgtg
 1381 caggacctgc tgctgctgga cgtggctccc ctgtcgtggt ggctggagac
 ggccggaggc
 1441 gtgatgactg ccctgatcaa gcgcaactcc accatcccca ccaagcagac
 gcagatcttc
 1501 accacctact ccgacaacca acccggggtg ctgatccagg tgtacgaggg
 cgagagggcc
 1561 atgacgaaag acaacaatct gttggggcgc ttcgagctga gcggcatccc
 tccggccccc
 1621 aggggcgtgc cccagatcga ggtgaccttc gacatcgatg ccaacggcat
 cctgaacgtc
 1681 acggccacgg acaagagcac cggcaaggcc aacaagatca ccatcacaa
 cgacaagggc
 1741 cgcctgagca aggaggagat cgagcgcgatg gtgcaggagg cggagaagta
 caaagcggag
 1801 gacgaggtgc agcgcgagag ggtgtcagcc aagaacgccc tggagtccca
 cgcttcaac
 1861 atgaagagcg ccgtggagga tgaggggctc aagggaaga tcagcagggc
 ggacaagaag
 1921 aaggttctgg acaagtgtca agaggtcatc tcgtggctgg acgccaacac
 cttggccgag
 1981 aaggacgagt ttgagcacia gaggaaggag ctggagcagg tgtgtaacc
 catcatcagc
 2041 ggactgtacc agggtgccgg tggccccgg cctggcggct tcggggctca
 gggccccaa
 2101 ggaggtctg ggtcaggccc taccattgag gaggtggatt aggggccttt
 gttctttagt
 2161 atgtttgtct ttgaggtgga ctgttgggac tcaaggactt tgctgctggt
 ttcctatgtc
 2221 atttctgctt cagctctttg ctgcttcact tctttgtaaa gttgtaacct
 gatggtaatt
 2281 agctggcttc attatTTTTT tagtacaacc gatatgttca ttagaattct
 ttgcatttaa

```
2341 tgttgatact gtaaggggtgt ttcgttccct ttaaataaat caacactgcc
accttctgta
2401 cgagtttggt tgtttttttt tttttttttt ttttttgctt ggcgaaaaca
ctacaaaggc
2461 tgggaatgta tgtttttata atttgtttat ttaaataatga aaaataaaat
gttaaacttt
2521 aaaaaaaaaa aaaaaaaaaa aaaaaaaaaa a
//
```

Appendix 9.3 Amino acid and gene sequence for *HSPA1L* *Homo sapiens* adapted from NCBI (<http://www.ncbi.nlm.nih.gov>)

NCBI Reference Sequence: NM_005527.3

Homo sapiens heat shock 70kDa protein 1-like (HSPA1L), mRNA

LOCUS NM_005527 2550 bp mRNA linear PRI 20-SEP-2010
DEFINITION Homo sapiens heat shock 70kDa protein 1-like (HSPA1L), mRNA.
ACCESSION NM_005527
VERSION NM_005527.3 GI:124256495

Amino Acid Sequence

```
/translation="MATAKGIAIGIDLGTTYSCVGVFQHGKVEI IANDQGNRTTPSYV  
AFTDTERLIGDAAKNQVAMNPQNTVFDARLIGRKFNDPVVQADMKLWPFQVINEGGK  
PKVLVSYKGENKAFYPEEISSMVLTKLKETAEAF LGHPVTNAVITVPAYFNDSQRQAT  
KDAGVIAGLNLVRIINEPTAAAIAYGLDKGGQGERHVLI FDLGGGTFDVSILTIDDGI  
FEVKATAGDTHLGGEDFDNRLVSHFVEEFKRKHKKDISQNKRAVRRRLRTACERAKRTL  
SSSTQANLEIDSLEYEGIDFYTSITRARFEELCADLFRGTLEPVEKALRDAKMDKAKIH  
DIVLVGGSTRIPKVQRLQLQDYFNDRDLNKSINPDEAVAYGAAVQAA ILMGDKSEKVQD  
LLLLDVAPLSLGLTAGGVMTALIKRNSTIPTKQTQIFTTYSDNQPGVLIQVYEGERA  
MTKDNNLLGRFDLTGIPPAPRGVPQIEVTFDIDANGILNVTATDKSTGKVNKITITND  
KGRLSKEEIERMVLDAEKYKAEDDEVQREKIAAKNALESYAFNMKSVVSDEGLKGI SE  
SDKNKILDKCNELLSWLEVNQLAEKDEFDHRKRELEQMCNPIITKLYQGGCTGPACGT  
GYVPGRPATGPTIEEVD"
```

Gene Sequence

```
1 tttgaaaaa gattactgag ttggagccgt ctcaaatttg cagggagga  
cggggtgggg  
61 ggtgggggga ccccggttgt gcagtttgat attgagggag cccccaccta  
ctcgtggggg  
121 ctgcgtaatc tggacgtttc caaactgaag cgaaggcgtc gggagactag  
gcctcagaga  
181 accatggcta ctgccaaggg aatcgccata ggcacgacc tgggcaccac  
ctactcctgt  
241 gtgggggtgt tccagcacgg caaggtggag atcatcgcca acgaccaggg  
caaccgcacc  
301 acccccagct acgtggcctt cacagacacc gagcggctca ttggggatgc  
ggccaagaac  
361 caggtagcaa tgaatcccca gaacactggt tttgatgcta aacgtctgat  
cggcaggaaa  
421 tttaaatgatc ctgttgtaca agcagatatg aaactttggc cttttcaagt  
gattaatgaa
```

481 ggaggcaagc ccaaagtcct tgtgtcctac aaaggggaga ataaagcttt
 ctaccctgag
 541 gaaatctctt cgatggtatt gactaagttg aaggagactg ctgaggcctt
 tttgggccac
 601 cctgtcacca atgcagtgat taccgtgcca gcctatttca atgactctca
 acgtcaggct
 661 actaaggatg caggtgtgat tgctggactt aatgtgctaa gaatcatcaa
 tgagcccacg
 721 gctgctgcca ttgcctatgg tttagataaa ggaggtcaag gagaacgaca
 tgtcctgatt
 781 tttgatctgg gtggaggcac atttgatgtg tcaattctga ccatagatga
 tgggattttt
 841 gaggtaaagg cactgctgg ggacactcac ctgggtgggg aggactttga
 caacaggctt
 901 gtgagccact tcgtggagga gttcaagagg aacacaaaa aggacatcag
 ccagaacaag
 961 cgagccgtga ggcggctgcg caccgcctgc gagagggcca agaggacct
 gtcgtccagc
 1021 acccaggcca acctagaaat tgattcactt tatgaaggca ttgacttcta
 tacatccatc
 1081 accagagctc gatttgaaga gttgtgtgca gacctgttta ggggtacct
 ggagcctgta
 1141 gaaaaagcgc ttcgggatgc caagatggat aaggctaaaa tccatgacat
 tgttttagta
 1201 gggggctcca cccgcatccc caaggtgcag cggctgcttc aggactactt
 caatggacgt
 1261 gatctcaaca agagcatcaa ccctgatgag gccgtagcat atggggctgc
 ggtacaagca
 1321 gccatcctga tgggggacaa gtctgagaag gtacaggacc tgctgctgct
 ggacgtggct
 1381 cccctgtccc tggggctgga gacggctggg ggcgtgatga ctgcctgat
 aaagcgcaac
 1441 tccaccatcc ccaccaagca gacacagatt ttcaccacct actctgacaa
 ccaaccggg
 1501 gtgctgatcc aggtgtatga gggcgagagg gccatgacaa aggacaacaa
 cctgctgggg
 1561 cggtttgacc tgactggaat ccctccagca cccaggggag ttctcagat
 cgaggtgacg
 1621 tttgacattg atgccaatgg tattctcaat gtcacagcca cggacaagag
 caccggcaag
 1681 gtgaacaaga tcaccatcac caatgacaag ggccgcctga gcaaggagga
 gattgagcgc
 1741 atggttctgg atgctgagaa atataaagct gaagatgagg tccagagggg
 gaaaattgct
 1801 gcaaagaatg ccttagaatc ctatgctttt aacatgaaga gtgttgtag
 tgatgaaggt
 1861 ttgaagggca agattagtga gtctgataaa aataaaatat tggataaatg
 caacgagctc
 1921 ctttcgtggc tggaggtcaa tcaactggca gagaaagatg agtttgatca
 taagagaaag
 1981 gaattggagc agatgtgtaa ccctatcatc acaaaactct accaaggagg
 atgcactggg
 2041 cctgcctgcy gaacagggta tgtgcctgga aggctgcca caggccccac
 aattgaagaa
 2101 gtagattaat tctttttaga actgaagcat cctaggatgc ctctacatgt
 atttcattcc
 2161 cctcatcttc aaacatcatt attattcttg accagacctg aatctaagtt
 accatccctt
 2221 ggaaattctg gagaaggagt ctcatgcacc acctatcaca ctccctcaca
 tcctgtttct
 2281 gactttggaa tggactcagg aaaactagge ccctctttaa accgtgtgat
 gtatttgaat

```
2341 gtctggttatt tccagccacc ctaacattct tcttcctgtg tggatgctta
tttgtcaatc
2401 agtaaatttg ttcgtaaaga aaattacttc tggatatttag gctgtgaatg
taccttgaag
2461 gggagagttc atggagagag catgtgttct ctgattgtga ggtcactgtg
aatgattaaa
2521 ttggttaaggg taaagtaaaa aaaaaaaaaa
//
```

Appendix 9.4 Amino acid and gene sequence for *HSPA1A Rattus norvegicus* adapted from NCBI (<http://www.ncbi.nlm.nih.gov>)

NCBI Reference Sequence: NM_031971.2

Rattus norvegicus heat shock 70kD protein 1A (Hspa1a), mRNA

LOCUS NM_031971 4045 bp mRNA linear ROD 30-APR-2010
DEFINITION Rattus norvegicus heat shock 70kD protein 1A (Hspa1a), mRNA.
ACCESSION NM_031971
VERSION NM_031971.2 GI:260064044

Amino Acid Sequence

```
/translation="MAKKTAIGIDLGTTYSCVGVFQHGKVEIIANDQGNRTTPSYVAF
TDTERLIGDAAKNQVALNPQNTVFDARLIGRKFQDPVQSDMKHWPQVQVNDGDKPK
VQVNYKGENRSFYPEEISSMVLTKMKEIAEAYLGHPVTNAVITVPAYFNDSQRQATKD
AGVIAGLNVLRIINEPTAAAIAYGLDRTGKGERNVLIFDLGGGTFDVSILTIDDGIFE
VKATAGDTHLGGEDFDNRLVSHFVEEFKRKHKKDISQNKRAVRRRLRTACERAKRTLSS
STQASLEIDSLFEGIDFYTSITRARFEELCSDLFRGTLEPVEKALRDAKLDKAQIHDL
VLVGGSTRIPKVQKLLQDFFNDRDLNKSINPDEAVAYGAAVQAAIILMGDKSENVQDLL
LLDVAPLSLGLTAGGVM TALIKRNSTIPTKQTQTFTTYSNQPGLIQVYEGERAMT
RDNNLLGRFELSGIPPAPRGVPQIEVTFDIDANGILNVTATDKSTGKANKITITNDKG
RLSKEEIERMVQEAERYKAEDEVQRERVAAKNALESYAFNMKSAVEDEGLKGI SEAD
KKKVLDKCQEVISWLDSENTLAEKEEFVHKREELERVCNPIISGLYQGAGAPGAGGFGA
```

Gene Sequence

```
1 ccagggcatcc ttctctgagt ttctatcttt ctctcgattg taactcctct
cttcgacccat
61 caataccata ttcaaaaagg tcttgtctgc ctccgatttc agctcagact
aatttcagcc
121 actaatgtcc ctcaagagcc caacccatt ttttcttggt tgccaacacc
caaatccaga
181 attaaaactg gggttcctgt gtggagagcc aagaggagac ctaaggatgg
tggcttccac
241 tagaccacgt ctgtaaatca atcaaacctc agaaaattct tggccatta
aataagaacc
301 aactggaatt ccaggetcac ctggaatctc tacgccttcg atccagtttg
gaaaatttga
361 agtcgctgag cccctacgag tggggagctc caggaacatc caaactgagc
aactggggtt
```

421 cccccaccc cccaccccgc ccctcccggc aactttgagc ctcttctggg
acagatcctc
481 tgattcctaa ataagtccat gaggtcagag ttagcactgc cattgtaacg
cggctggagg
541 ggggtcacgt caccggacac gccccaggc acctcccttg ggtctcccaa
ggctaggaag
601 gggagttat aaccctaac tcgagcccca taatcagaac tgtgcgagtc
tgcaacccc
661 cacaaatcac aaccaactgt ccacaacacg gagctagcag tgacctttcc
tgtccattcc
721 actcaggcct cagtaatgcg tcgccatagc aacagtgtca acagcagcac
cagcaggtcc
781 cgccaccctc cccacagga atccgtcctt tccagctaac ccagatctg
tctggagagt
841 tctgaacagg ggcggaaccc tcaactccta ttactcaaag gaggcgggga
agctccaccc
901 gacgcgaaac tgctggaaga ttcttgccc caaggcctcc tcccgtcgc
tgattggccc
961 atgggagggg gggcggggcc ggaggaggct ccttaaaggc gcagggcggc
gcgcaggaca
1021 ccagattcct cctcttaatc tgacagaatc agtttctggt tccactcgca
gagaagcaga
1081 gaagcggagc aagcggcgcg ttccagaacc tcgggcaaga ccagcctctc
ccagagcatc
1141 cccaccgcga agcgcacact tctccagagc atccccagc ggagcgcacc
cttccccaga
1201 gcatccccgc cgccaagcgc aaccttccag aagcagagag cggcgacatg
gccaagaaaa
1261 cagcgatcgg catcgacctg ggcaccacct actcgtgctg gggcgtgttc
cagcacggca
1321 aggtggagat catcgccaac gaccagggca accgcacgac cccagctac
gtggccttca
1381 ccgacaccga gcggtcatc ggggacgccg ccaagaacca ggtggcgctg
aaccgcaga
1441 acaccgtgtt cgacgcgaag cggctgatcg gccgcaagtt cggcgacccg
gtggtgcagt
1501 cggacatgaa gcaactggccc ttccaggtgg tgaacgacgg cgacaagccc
aaggtgcagg
1561 tgaactacaa gggcgagaac cggtcgttct acccgaggga gatctcgtcc
atggtgctga
1621 ccaagatgaa ggagatcgcc gaggcgtacc tgggcccacc ggtgaccaac
gcggtgatca
1681 ccgtgcccgc ctacttcaac gactcgcagc ggcaggccac caaggacgcg
ggcgtgatcg
1741 cgggtctgaa cgtgctgcgg atcatcaacg agcccacggc ggccgccatc
gcctacgggc
1801 tggaccggac cggcaagggc gagcgcaacg tgctcatctt cgacctgggg
ggcggcacgt
1861 tcgacgtgtc catcctgacg atcgacgacg gcatcttcca ggtgaaggcc
acggcggggc
1921 acacgcacct gggcggggag gacttcgaca accggctggt gagccacttc
gtggaggagt
1981 tcaagaggaa gcacaagaag gacatcagcc agaacaagcg cgcggtgcgg
cgactgcgca
2041 cggcgtgcga gagggccaag aggacgtgt cgtccagcac ccaggccagc
ctggagatcg
2101 actctctgtt cgagggcatc gacttctaca cgtccatcac gcgggcgagg
ttcgaggagc
2161 tgtgctcgga cctgttccgc ggcacgctgg agcccgtgga gaaggcctg
cgcgacgcca
2221 agctggacaa ggcgcagatc cagcactggg tgctgggggg cggctcgacg
cgcatcccca

2281 aggtgcagaa gctgctgcag gacttcttca acgggcgcgga cctgaacaag
agcatcaatc
2341 cggacgagggc ggtggcctac ggggcgggcg tgcagggcggc catcctgatg
ggggacaagt
2401 cggagaacgt gcaggacctg ctgctgctgg acgtggcgcc gctgtcgctg
ggtctggaga
2461 ccgcgggcg gctgatgacg gcgctcatca agcgcaactc caccatcccc
accaagcaga
2521 cgcagacctt caccacctac tcggacaacc agcccgggggt gctgatccag
gtgtacgagg
2581 gcgagagggc catgacgcgc gacaacaacc tgctggggcg cttcgagttg
agcggcatcc
2641 cgccggctcc caggggcgtg ccccagatcg aggtgacctt cgacatcgac
gccaacggca
2701 tcctgaacgt cacggccact gacaagagca ccggcaaggc caacaagatc
accatcacca
2761 acgacaaggg ccgcctgagc aaggaggaga tcgagcgcag ggtgcaggag
gccgagcgct
2821 acaaggcgga ggacgaggtg cagcgcgaga ggggtggctgc caagaatgcg
ctcgagtctt
2881 atgccttcaa catgaagagc gccgtggagg acgagggctt caagggcaag
atcagcgagg
2941 ctgacaagaa gaaggtgctg gacaagtgcc aggaggtcat ctctggctg
gactctaaca
3001 cgctggctga gaaagaggag ttcgtgcaca agcgggagga gctggagcgg
gtgtgcaacc
3061 cgatcatcag cgggctgtat caggggtgcgg gtgctcccgg ggctggggggc
ttcggggccc
3121 aggcgcccga gggaggtctt gggctggggc ccaccatcga ggaggtggat
tagaggctct
3181 ttctggcgct ccaggtgtga tctaggagac agatgggtgg ccttgaggac
tttgggttat
3241 tgctgtttag gacattaact ccttcgctcg gtctgcaatc aagtcctagg
ttaaagcaaa
3301 ctgccttcca tttactctgt ggaatttcac gtgtgctttg cattcccagt
aaattagtag
3361 tgggagtggtg tctttgcaat agatataatt tcctgccttc aagtcagcac
tgcccccccc
3421 cccgaagtta tttcttttgc aggacagtca gagctatatt gatatagcaa
gaggtgtggt
3481 acaaaaacac caggacactg ttgagttcct ttgtgtttg actctcccct
ggcgacagt
3541 gttgaggcac tgttaagtca ggagctcagg ggccaccggg ggatcactga
aagctgagac
3601 tctgttgctt ctcccgtttg acactctggt gctttccttg catggtggct
cacctaaggc
3661 tgagactctt gttctccttc cctgtataat cttgcctggc cgttgcaact
gttccccagt
3721 gtgtgaactc ggagatgagt ttacaccacc actgttagtt cacgtttttt
gtttttacat
3781 aaccatcctg aactcaggtc aatTTTTact ggctatttga aaataaactt
caaaagaact
3841 tgccaggtct tgtgtctggt gtcttttgag gtcaggaatt gctgtgtatg
tcttacagat
3901 tggactacgc ttgactgaca ttttatggta agatgggggtg gggagcacc
agggactttg
3961 cattgggatc tgcttgtgtg agaaaaatga aagcagtcag agcaaataac
aaccagtccg
4021 gggctgaggt ctagtacagt gcaga
//

Appendix 9.5 Amino acid and gene sequence for *HSPA1B Rattus norvegicus* adapted from NCBI (<http://www.ncbi.nlm.nih.gov>)

NCBI Reference Sequence: NM_212504.1

Rattus norvegicus heat shock 70kD protein 1B (mapped) (Hspa1b), mRNA

LOCUS NM_212504 5918 bp mRNA linear ROD 20-JUN-2010
DEFINITION Rattus norvegicus heat shock 70kD protein 1B (mapped) (Hspa1b), mRNA.
ACCESSION NM_212504 XM_215309
VERSION NM_212504.1 GI:47059178

Amino Acid Sequence

```
/translation="MAKKTAIGIDLGTTYSCVGVFQHGKVEIIANDQGNRTTPSYVAF
TDTERLIGDAAKNQVALNPQNTVFDKRLIGRKFGDPVVQSDMKHWPQVVDGDKPK
VQVNYKGENRSFYPEEISSMVLTKMKEIAEAYLGHPVTNAVITVPAYFNDSQRQATKD
AGVIAGLNVLRIINEPTAAAIAYGLDRTGKGERNVLIIFDLGGGTFDVSILTIDGIFE
VKATAGDTHLGGEDFDNRLVSHFVEEFKRKHKKDISQNKRAVRRLRTACERAKRTLSS
STQASLEIDSLFEGIDFYTSITRARFEELCSDLFRGTLEPVEKALRDAKLDKAQIHDL
VLVGGSTRIPKVQKLLQDFFNDRDLNKSINPDEAVAYGAAVQAAILMGDKSENVQDLL
LLDVAPLSLGLLETAGGVMTALIKRNSTIPTKQTQTFTTYSDNQPGVLIQVYEGERAMT
RDNNLLGRFELSGIPPAPRGVPQIEVTFDIDANGILNVTATDKSTGKANKITITNDKG
RLSKEEIERMVQEAERYKAEDVQRERVAAKNALESYAFNMKSAVEDEGLKGISEAD
KKKVLDKCQEVISWLDSENTLAEKEEFVHKREELERV CNP IISGLYQGAGAPGAGGFGA
QAPKGGSGSGPTIEEVD"
```

Gene Sequence

```
1 gaattccagc acttgggtgt caaggctgga ggagcaagag ttaaggcta
gcctgggcta
61 catgagcccc tatthtggaaa aagaaaaaaa gaaataaaaa agttagaaaa
aagaaaaaat
121 gaaaacaaaa gatgtgtgcg tgtgtatgtg tgtgagagag agagacagtc
tctctctctc
181 tctctctctc tctctctctc tctctctctc tctctctctc tgtgtatgtg
tgtgtgtgag
241 acaattactc cctgctgtgg actgttacct cagaactaag actcctaatgc
aatctattct
```

301 ttttttaaaa aacaggctcg gggctgggga tttagctcag tggtagagcg
cttacctagg
361 aagcgcaagg ccctgggttc ggtccccagc tccgaaaaaa agaaccaaaa
aaaaaaaaaa
421 accaaaaaca aaaaaaaaaa acaaaaaaaaa acaaaacaaa acaggctcta
atgtagattg
481 ggctagcctc aaactcttca tctcctgcc tccccctcca aagcatgagg
actacagagg
541 tgggccacca taccagtaa cctcactctg tttcaagaca tctaactagg
gggtctttaa
601 ttcgtacacg gaaggaggag cccggaagaa gaaaaaggga catcactgac
agctaaacat
661 atttataatg agaggaggta ggggacagac aagggacgga aaggtgatgt
ctaggacaaa
721 aagctaacca cataaactag taggtgggtc ccgacacctc tgcttagggg
ctcacccaaa
781 agtcggagtt aacagcactg tgaggccaga tgctatcaga ggacaggaca
caccatctct
841 ccacctagga aaggtgaact gacaggggca gcagacacag aagaatcagc
aaactcttaa
901 gtcaaccctg aggttactac agcacagaat agaacagtgc ctggcaagga
gcagctgtgt
961 gaaggagaag ccaagcagcc atcctcagca ttcttcttct attaactttt
tgggacaggg
1021 tctgcctctg taacctaggc tgaccttgac tcgctgcagt ccctctgccc
caccctctac
1081 cgaaagtttt ttttttctc ctttctaatag ccaggctgcc gcctgaggca
aagggagcgg
1141 cttgcagcct ggcacggctg gtcgattaaa ccttgctctc cccgtcctgg
gacactttcc
1201 ttttttgggt cacaggctct cctaacaatga gaaccgagtg tttacacaat
gatgttcttt
1261 tgaaaaccgt gaaaactcca caggcgatgt acttgtagct taagcgtgac
ataaagacag
1321 caaagcgaat aaactatact gcaagatctc ttctctttcc ctatttaaac
ctaaaatgga
1381 gggagtgggg ggcagacaca gacaggcgag cattccacag gcgccccccc
cacgctgtca
1441 cttccaggca ggacceaatc acagacttct tagccaagcg ttatccctcc
cgttttgaga
1501 aactttctgc gtccgccatc ctgtaggaag aatttgtaca ccttaaactc
cctccctggg
1561 ctgattccca aatgtctctc accgcccagc actttcagga gctgaccctt
ctcagcttca
1621 catacagaga ccgctacctt gcgtcgccat ggcaaacactg tcacaaccgg
aacaagcact
1681 tcctaccacc cccgcctca ggaatccaat ctgtccagcg aagcccagat
ccgtctggag
1741 agttctggac aagggcggtg ccctcaacat ggattactca tgggagggcg
agaagctcta
1801 acagaccgga aactgctgga agattcctgg cccaaggcc tctcccgtc
cgctgattgg
1861 cccatgggag ggtgggcggg gccggaggag gctccttaa ggcgcagggc
ggcgcgcagg
1921 acaccagatt ctcctccta atctgacaga accagtttct ggttccactc
gcagagaagc
1981 agagaagcgg agcaagcggc gcgttccaga acctcgggca agaccagcct
ctcccagagc
2041 atccccaccg cgaagcgcaa ccttctccag agcatcccc agcggagcgc
acccttcccc
2101 agagcatccc cgccgccaa cgcaaccttc cagaagcaga gagcggcgac
atggccaaga

2161 aaacagcgat cggcatcgac ctgggcacca cctactcgtg cgtgggcgctg
 ttccagcacg
 2221 gcaaggtgga gatcatcgcc aacgaccagg gcaaccgcac gacccccagc
 tacgtggcct
 2281 tcaccgacac cgagcggctc atcggggacg ccgccaagaa ccaggtggcg
 ctgaaccgcg
 2341 agaacaccgt gttcgacgcg aagcggctga tcggccgcaa gttcggcgac
 ccggtggtgc
 2401 agtcggacat gaagcactgg cccttccagg tggatgaacga cggcgacaag
 cccaaggtgc
 2461 aggtgaacta caagggcgag aaccggctgt tctaccggga ggagatctcg
 tccatggtgc
 2521 tgaccaagat gaaggagatc gccgaggcgt acctgggcca cccggtgacc
 aacgcggtga
 2581 tcaccgtgcc cgcctacttc aacgactcgc agcggcaggc caccaaggac
 gcgggcgtga
 2641 tcgcggtctt gaacgtgctg cggatcatca acgagccac ggcggccgcc
 atcgctacg
 2701 ggctggaccg gaccggcaag ggcgagcgca acgtgctcat cttcgacctg
 gggggcggca
 2761 cgttcgacgt gtccatcctg acgatcgacg acggcatctt cgaggtgaag
 gccacggcgg
 2821 gcgacacgca cctgggcggg gaggacttcg acaaccggct ggtgagccac
 ttcgtggagg
 2881 agttcaagag gaagcacaag aaggacatca gccagaaca gcgcgcggtg
 cggcgactgc
 2941 gcacggcgtg cgagagggcc aagaggacgc tgtcgtccag caccaggcc
 agcctggaga
 3001 tcgactctct gttcgagggc atcgacttct acacgtccat cacgcgggcg
 cggttcgagg
 3061 agctgtgctc ggacctgttc cgcggcacgc tggagcccgt ggagaaggcc
 ctgcgcgacg
 3121 ccaagctgga caagggcgag atccacgacc tgggtgctggt gggcggctcg
 acgcgcaccc
 3181 ccaaggtgca gaagctgctg caggacttct tcaacgggcg cgacctgaac
 aagagcatca
 3241 atccggacga ggcgggtggc tacggggcgg cgggtgcaggc ggccatcctg
 atgggggaca
 3301 agtcggagaa cgtgcaggac ctgctgctgc tggacgtggc gccgctgctg
 ctgggtctgg
 3361 agaccgcggg cggcgtgatg acggcgtca tcaagcgcaa ctccaccatc
 cccaccaagc
 3421 agacgcagac cttcaccacc tactcggaca accagcccgg ggtgctgatc
 caggtgtacg
 3481 agggcgagag ggccatgacg cgcgacaaca acctgctggg gcgcttcgag
 ttgagcggca
 3541 tcccgcggc tcccaggggc gtgccccaga tcgaggtgac cttcgacatc
 gacgccaacg
 3601 gcatcctgaa cgtcacggcc actgacaaga gcaccggcaa ggccaacaag
 atcaccatca
 3661 ccaacgacaa gggccgcctg agcaaggagg agatcgagcg catggtgcag
 gaggccgagc
 3721 gctacaaggc ggaggacgag gtgcagcgcg agaggggtggc tgccaagaat
 gcgctcgagt
 3781 cctatgcctt caacatgaag agcgcctggg aggacgaggg tctcaagggc
 aagatcagcg
 3841 aggctgacaa gaagaaggtg ctggacaagt gccaggaggt catctcctgg
 ctggactcta
 3901 acacgctggc tgagaaagag gagttcgtgc acaagcggga ggagctggag
 cgggtgtgca
 3961 acccgatcat cagcgggctg tatcaggggtg cgggtgctcc cggggctggg
 ggcttcgggg

4021 cccagggcgcc caagggagggc tctggggtcgg ggcccacccat cgaggagggtg
gattagaggc
4081 ttttctggct ctcaggggtgt tggctagaga cagactcttg atggctgctg
gtgcacgatt
4141 cttatcaagt tactccttct ctccggagtt cagtttaaag ttacagcctt
ttatacggta
4201 attgatttga gtttggttaca ttttgatgct tcgtggggttt tttatatatt
caaattaagg
4261 ttgcatgttc tttgcgttta atctaagtag ctgtgtaaaa atgggtgttc
cttctgcga
4321 acacctcagc actgccaccc tgtgtacagt ttttctctg catccctaca
aactgagaaa
4381 aaaagttatc ttttgtaact taaacattca aaataaaatg ttacaagtat
gttttgcctg
4441 tgtgtatggt gggaggggcta atggattctg ggttcatgtg gatttcttag
ctttgcgatg
4501 acggggaaat ggggtttggg tactttgggtt agaagtgtgg gttttggggg
tggggattga
4561 gctcagtggg agagcgtctg cctaggaagc gcaaggccct gggttcggtc
cccagctccg
4621 aaaaaagaac caaaaaaaaa aaaagtgtgg gtttccagcg cagttatgca
gaaaatgcag
4681 gtattcgggt tgagggtagg actcattggg gggaacagta ggggtgggtg
gtagttgggg
4741 gtcagtggaa gagggactct tagggctatg atgactcagt tctcttagcc
ctccagggct
4801 gaaccagaac tgtttcccaa cttatgggtc gagacctctg ttggagtcag
acgaccttc
4861 cacagtggta gcctcggaca ttgaaaattg caggggttgt tgggtgtcgg
ttgggttttt
4921 gttttgtctt gttttgtttt tcaagacagg gtctctctgt gtagccctgg
ctggcctcga
4981 tttcggatcc acatgccttt cccaaacctg gcttccttat tacttttttt
ttttttttta
5041 agattttatt acttattata tataagtaca atgtagctgt cttcagagac
accagaagag
5101 ggcacagat cccattacag atggctgtga gccaccatgt ggttgctggg
atgtgaactc
5161 aggacctctt caagagcagt cagtgtctct aacttctgag ccctctctcc
agccctttat
5221 tactttttaga gatttcttac cagggtgccc tggctgtact tacactttct
ctttagctct
5281 gctgagcttt caattcacca gttccagacc acaccctga acccaccagc
tgaagacaac
5341 atgtcttgcct atctttttct ttcctttttg gggcagggat ggtctgtgtg
ttgtgtgtgt
5401 gagagacaga ggcagagaca tccttcccat gtagccctaa ctgagtcgga
agtcattatt
5461 tagaccaggc tgcctgact cctgtatctg cctctccaat ggattatggg
cacctgccac
5521 ctcaccact cactttatcc ccaggatccc cctccctctt cccaggcagt
aggctcggg
5581 atggagaaga ccacttacca tgtccatggc tcaaagaagc aggcagaacg
taggggaaag
5641 agttgctttc acctcaagcc tttggatcca tgggtgttca ttctagtggg
gtaatgcat
5701 cctttgagag ctgggggggtg tgggtcaaca gagatcgggt gctatgtgtg
catgaggccc
5761 gcaattcagt ccctggctcc atggagaacg aaccaatcag ttgggtgagg
tgtaaaccac
5821 atgtaatttt agcatgtcca aacagacagc ttaaggacat cctagggtaa
agaagtcttc
5881 agcaatagtt taattgaggc aattatgctc atgaattc

Appendix 9.6 Amino acid and gene sequence for *HSPAIL Rattus norvegicus* adapted from NCBI (<http://www.ncbi.nlm.nih.gov>)

NCBI Reference Sequence: NM_212546.4

Rattus norvegicus heat shock protein 1-like (Hspa1l), mRNA

LOCUS NM_212546 2632 bp mRNA linear ROD 27-NOV-2011
DEFINITION Rattus norvegicus heat shock protein 1-like (Hspa1l), mRNA.
ACCESSION NM_212546
VERSION NM_212546.4 GI:261824059

Amino Acid Sequence

```
/translation="MAANKGMAIGIDLGTTYSCVGVFQHGKVEIIANDQGNRTTTPSYV  
AFTDTERLIGDAAKNQVAMNPQNTVFDKRLIGRKFNDPVVQSDMKLWPFQVINEAGK  
PKVLVSYKGEKKAFYPEEISSMVLTKMKETAFAFLGHSVTNAVITVPAYFNDSQRQAT  
KDAGVIAGLNLVRIINEPTAAAIAYGLDKGSHGERHVLIFDLGGGTFDVSILTIDGDI  
FEVKATAGDTHLGGEDFDNRLVSHFVEEFKRKHKKDISQNKRAVRRRLRTACERAKRTL  
SSSTQANLEIDSLEYEGIDFYTSITRARFEELCADLFRGTLEPVEKSLRDAKMDKAKIH  
DIVLVGGSTRIPKVQKLLQDYFNDRDLNKSINPDEAVAYGAAVQAAILMGDKSEKVQD  
LLLLDVAPLSLGLTAGGVMTVLIKRNSTIPTKQTQIFTTYSDNQPGVLIQVYEGERA  
MTRDNNLLGRFDLTGIPPAPRGVPQIEVTFDIDANGILNVTAMDKSTGKANKITITND  
KGRLSKEEIERMVQEAERYKAEDEGQREKIAAKNALESYAFNMKSAVGDEGLKDKISE  
SDKKKILDKCSEVLSWLEANQLAEKEEFDHKRKELENMCNPIITKLYQSGCTGPTCAP  
GYTPGRAATGPTIEEVD"
```

Gene Sequence

```
1  cagaagaggc tcaaagttgc cgggaggggc ggggtggggg gtggggggaa  
ccccagttgc  
61  tcagtttggg tgttctctgga gctccccact cgtaggggct cagcgacttc  
aaattttcca  
121 aactggatcg aaggcgtaga gattccaggc ctcggaaaac catggctgct  
aataaaggaa  
181 tggccatagg catcgacctg ggcaccacct actcgtgcgt gggcgtgttc  
cagcacggca  
241 aggtggagat catcgccaac gaccagggca accgcacgac cccaagctac  
gtggcettca  
301 ccgacaccga gcggetcatc ggggacgccg ccaagaacca ggtggccatg  
aatccccaga
```

361 acactgtttt tgacgcaaaa cgtctaattg gcaggaagtt taatgatccc
gctgtgcagt
421 cggatatgaa gctgtggcca tttcaagtga tcaatgaagc gggcaagcct
aaggtgctgg
481 tgtcctacaa aggagagaag aaagccttct acccgaggga gatctcgtcc
atggtgctga
541 ccaagatgaa ggagactgca gaggcttttt tgggccacag tgtcaccaac
gctgtgatca
601 ccgtgccagc ctatttcaat gactcccaga gacaggccac taaagatgca
ggggtcatcg
661 caggactcaa cgtgctgca atcatcaatg agcccacagc gggggccatc
gcctacggct
721 tggataaagg aagtcacgga gagcggcacg tgctcatctt cgacctgggg
ggcggcacgt
781 tcgactgtc catcctgacg atcgacgacg gcatcttcga ggtgaaggcc
acggcgggcg
841 acacgcacct gggcggggag gacttcgaca accggctggg gagccacttc
gtggaggagt
901 tcaagaggaa gcacaagaag gacatcagcc agaacaagcg cgcggtgcbg
cgtctgcbg
961 cggcgtgca gaggccaag aggacgctgt cgtccagcac ccaggccaac
ctggagatcg
1021 actctctgta cgagggcatc gacttctaca cgtccatcac gcgggcgcbg
ttcgaggagc
1081 tgtgtgcaga cctatttaga ggcacgcttg agcccgtgga gaagtctctc
cgggacgcca
1141 agatggacaa ggctaaaatc catgacattg ttctagtagg gggctctacc
cgcacccaa
1201 aggtgcaaaa gctgcttcaa gactacttta atggacggga tctcaacaag
agtatcaatc
1261 ccgatgaggc ggtggcgtac ggagctgcag tccaggcagc tattttaatg
ggcgacaaat
1321 ctgaaaaagt acaggatttg cttttgttg acgtagctcc cctgtctcta
ggattggaga
1381 cagccggggg tgtgatgact gttctgatca agcgcgaactc caccatcccc
accaagcaga
1441 cgcagatctt caccacctac tcggacaacc agcccggggg gctgatccag
gtgtacgagg
1501 gcgagagggc catgacgcgc gacaacaacc tcctggggcg ctttgacctg
actggaatac
1561 cccctgcacc taggggtgtg cccagatcg aggtgacctt cgacatcgac
gccaacggga
1621 ttctcaacgt cacagccatg gacaagagca ccggcaaggc caacaagatc
accatcacca
1681 acgacaaggg ccgcttgagc aaggaggaga tcgagcgcg ggtgcaagag
gccgagcggg
1741 acaaggccga ggacgagggc cagagggaga agatcgctgc caaaaatgcc
ttagaatcgt
1801 atgcctttaa catgaagagc gctgtaggcg atgagggtct gaaggacaag
atcagcgagt
1861 ctgataaaaa gaaaatactg gataaatgca gtgaggctct ttctggctg
gaggccaacc
1921 agctggcgga gaaagaagag ttcgatcata aaagaaaaga gctggaaaac
atgtgcaacc
1981 ctatcatcac aaagctgtac cagagcggct gcacagggcc cacctgcgcbg
ccagggtata
2041 caccggcag ggctgccaca ggccccacca ttgaggaagt agattagcct
ttcccagaaa
2101 ggcaggggtgc taggggtgct ctaggcgaca tttattcacc tcccaacatc
actgtgattc
2161 ttgaaactgac tggacttgag cctaagtac catcctttgg gatctgatgc
agaaccacg

2221 gactccgcct ttccacgccc ccaccctctg atctatgac ctgaactgga
tctttagcac
2281 aaccaggccc ctctttgagc ctcgtgaaga atttgatgt ctgttattta
tcatccacac
2341 cccgcctttc acctccctgt gtggatgggt atttgtctct cagtaaattt
gttcccaaag
2401 gaaacgtctg tcacttttcg atttgttttag tcgagggcct tactgtatat
gtctagctga
2461 cctgacgctt accgcattgg ccaatttggc ccttaacttg cagcaatcct
cctgtctctg
2521 ccacctgaat ttcgagatta cggacctgca ccatcatgcc caacttgtga
tttttttttt
2581 ttgggaggca gggtttcttg aagcctaggt tagcctagaa cattctatac ac

Appendix 9.7 Amino acid and gene sequence for *GAPDH Homo sapiens* adapted from NCBI (<http://www.ncbi.nlm.nih.gov>)

NCBI Reference Sequence: NM_002046.3

Homo sapiens glyceraldehyde-3-phosphate dehydrogenase (GAPDH), mRNA

LOCUS NM_002046 1310 bp mRNA linear PRI 16-MAY-2010
DEFINITION Homo sapiens glyceraldehyde-3-phosphate dehydrogenase (GAPDH), mRNA.
ACCESSION NM_002046
VERSION NM_002046.3 GI:83641890

Amino Acid Sequence

/translation="MGKVKVGVNGFGRIGRLVTRAAFNSGKVDIVAINDPFIDLNYMV
YMFQYDSTHGKFHGTVKAENGLVINGNPITIFQERDPSKIKWGDAGAEYVVESTGVF
TTMEKAGAHLQGGAKRVIIISAPSADAPMFVMGVNHEKYDNSLKIIISNASCTTNCLAPL
AKVIHDNFGIVEGLMTTVHAITATQKTVDGPGSKLWRDGRGALQNIIPASTGAAKAVG
KVIPELNGKLTGMAFRVPTANVSVVDLTCRLEKPAKYDDIKKVVKQASEGPLKGILGY
TEHQVSSDFNSDTHSSTFDAGAGIALNDHFVKLISWYDNEFGYSNRVVDLMAHMASK

Gene Sequence

1 aaattgagcc cgcagcctcc cgcttcgctc tctgctcctc ctgttcgaca
gtcagccgca
61 tcttcttttg cgtcgccagc cgagccacat cgctcagaca ccatggggaa
ggtgaaggtc
121 ggagtcaacg gatttggtcg tattgggcgc ctggtcacca gggctgcttt
taactctggt
181 aaagtggata ttgttgccat caatgacccc ttcattgacc tcaactacat
ggtttacatg
241 ttccaatatg attccacca tggcaaattc catggcaccg tcaaggctga
gaacgggaag
301 cttgtcatca atggaaatcc catcaccatc ttccaggagc gagatccctc
caaatcaag
361 tggggcgatg ctggcgctga gtacgtcgtg gagtccactg gcgtcttcac
caccatggag
421 aaggctgggg ctcatctgca ggggggagcc aaaagggctca tcatctctgc
cccctctgct
481 gatgccccca tgctcgtcat ggggtgtaac catgagaagt atgacaacag
cctcaagatc
541 atcagcaatg cctcctgcac caccaactgc ttagcacccc tggccaagg
catccatgac
601 aactttggta tcgtggaagg actcatgacc acagtccatg ccatcactgc
caccagaag
661 actgtggatg gccctccgg gaaactgtgg cgtgatggcc gcggggctct
ccagaacatc

721 atccctgcct ctactggcgc tgccaaggct gtgggcaagg tcatccctga
gctgaacggg
781 aagctcactg gcatggcctt ccgtgtcccc actgccaacg tgtcagtgg
ggacctgacc
841 tgccgtctag aaaaacctgc caaatatgat gacatcaaga aggtggtgaa
gcaggcgtcg
901 gagggcccc tcaagggcat cctgggctac actgagcacc aggtggtctc
ctctgacttc
961 aacagcgaca cccactcctc cacctttgac gctggggctg gcattgcct
caacgaccac
1021 tttgtcaagc tcatttctg gtatgacaac gaatttggct acagcaacag
ggtggtggac
1081 ctcatggccc acatggcctc caaggagtaa gaccctgga ccaccagccc
cagcaagagc
1141 acaagaggaa gagagagacc ctcaactgctg gggagtccct gccacactca
gtccccacc
1201 aactgaatc tcccctcctc acagttgcca tgtagacccc ttgaagaggg
gaggggccta
1261 gggagccgca cttgtcatg taccatcaat aaagtaccct gtgctcaacc

Appendix 9.8 Amino acid and gene sequence for *GAPDH Rattus norvegicus* adapted from NCBI (<http://www.ncbi.nlm.nih.gov>)

NCBI Reference Sequence: NM_017008.3

Rattus norvegicus glyceraldehyde-3-phosphate dehydrogenase (Gapdh), mRNA

LOCUS NM_017008 1307 bp mRNA linear ROD 16-MAY-2010
DEFINITION Rattus norvegicus glyceraldehyde-3-phosphate dehydrogenase (Gapdh), mRNA.
ACCESSION NM_017008 XM_216453
VERSION NM_017008.3 GI:110347607

Amino Acid Sequence

```
/translation="MVKVGVNGFGRIGRLVTRAAFSCDKVDIVAINDPFIDLNYMVYM  
FQYDSTHGKFNGLTVKAENGLVINGKPIITIFQERDPANIKWGDAGAEYVVESTGVFTT  
MEKAGAHLKGGAKRVIIISAPSADAPMFVMGVNHEKYDNSLKIVSNASCTTNCLAPLAK  
VIHDNFGIVEGLMTTVHAIITATQKTVDGPGSLWRDGRGAAQNIIPASTGAAKAVGKV  
IPELNGLTGMFRVPTPNVSVVDLTCRLEKPAKYDDIKKVVKQAAEGPLKGLILGYTE  
DQVVSDFNSNSHSSTFDAGAGIALNDNFVKLISWYDNEYGYSNRVVDLMAYMASKE "
```

Gene Sequence

```
1 gggggctctc tgctcctccc tgttctagag acagccgcat cttcttgtagc  
agtgccagcc  
61 tcgtctcata gacaagatgg tgaaggctcgg tgtgaacgga tttggccgta  
tcggacgcct  
121 ggttaccagg gctgccttct cttgtgacaa agtggacatt gttgccatca  
acgaccctt  
181 cattgacctc aactacatgg tctacatggt ccagtatgac tctaccacg  
gcaagttaa  
241 cggcacagtc aaggctgaga atgggaagct ggtcatcaac gggaaacca  
tcaccatctt  
301 ccaggagcga gatcccgcta acatcaaagt gggatgatgct ggtgctgagt  
atgtcgtgga  
361 gtctactggc gtcttcacca ccatggagaa ggctggggct cacctgaagg  
gtggggccaa  
421 aagggtcatc atctccgccc cttccgctga tgccccatg tttgtgatgg  
gtgtgaacca  
481 cgagaaatat gacaactccc tcaagattgt cagcaatgca tctgcacca  
ccaactgctt  
541 agccccctg gccaaaggta tccatgacaa ctttggcatc gtggaagggc  
tcatgaccac  
601 agtccatgcc atcaactgcca ctcagaagac tgtggatggc ccctctggaa  
agctgtggcg  
661 tgatggcctg ggggcagccc agaacatcat ccctgcatcc actggtgctg  
ccaaggctgt
```

721 gggcaaggtc atcccagagc tgaacgggaa gctcactggc atggccttcc
gtgttcctac
781 ccccaatgta tccgttgtgg atctgacatg ccgcctggag aaacctgcca
agtatgatga
841 catcaagaag gtggtgaagc aggcggccga gggcccacta aaggcatcc
tgggctacac
901 tgaggaccag gttgtctcct gtgacttcaa cagcaactcc cattcttcca
cctttgatgc
961 tggggctggc attgctctca atgacaactt tgtgaagctc atttctggt
atgacaatga
1021 atatggctac agcaacaggg tggtagacct catggcctac atggcctcca
aggagtaaga
1081 aacctggac caccagccc agcaaggata ctgagagcaa gagagaggcc
ctcagttgct
1141 gaggagtccc catcccaact cagcccccaa cactgagcat ctccctcaca
attccatccc
1201 agaccccata acaacaggag gggcctgggg agccctccct tctctcgaat
accatcaata
1261 aagttcgctg caccctcaaa aaaaaaaaaa aaaaaaaaaa aaaaaaa

1 ACCAGGTGGCGCTGAACCCGCAAGAACCCGTGTTTGACGCGAAGCGGCTGATTGGCCGCA
472
2 ACCAGGTGGCGCTGAACCCGCAAGAACCCGTGTTTGACGCGAAGCGGCTGATCGGCCGCA
445
3 ACCAGGTAGCAATGAATCCCCAGAACACTGTTTTTGTATGCTAAACGTCTGATCGGCAGGA
418
***** ** **** * ***** ** ***** ** * * ***** ** * *
1 AGTTTCGGCGACCCGGTGGTGCAGTCGGACATGAAGCACTGGCCTTTCCAGGTGATCAACG
532
2 AGTTTCGGCGACCCGGTGGTGCAGTCGGACATGAAGCACTGGCCTTTCCAGGTGATCAACG
505
3 AATTTAATGATCCTGTTGTACAAGCAGATATGAAACTTTGGCCTTTTCAAGTGATTAATG
478
* ** **
1 ACGGAGACAAGCCCAAGGTGCAGGTGAGCTACAAGGGGGAGACCAAGGCATTCTACCCCG
592
2 ACGGAGACAAGCCCAAGGTGCAGGTGAGCTACAAGGGGGAGACCAAGGCATTCTACCCCG
565
3 AAGGAGGCAAGCCCAAAGTCCTTGTGTCTACAAGGGGGAGAATAAAGCTTTCTACCCCTG
538
* *****
1 AGGAGATCTCGTCCATGGTGTGACCAAGATGAAGGAGATCGCCGAGGCGTACCTGGGCT
652
2 AGGAGATCTCGTCCATGGTGTGACCAAGATGAAGGAGATCGCCGAGGCGTACCTGGGCT
625
3 AGGAAATCTCTTCGATGGTATTGACTAAGTTGAAGGAGACTGCTGAGGCCTTTTGGGCC
598
**** ***** ** ***** ***** ** ***** * *****
1 ACCCGGTGACCAACGCGGTGATCACCGTGCCGGCCTACTTCAACGACTCGCAGCGCCAGG
712
2 ACCCGGTGACCAACGCGGTGATCACCGTGCCGGCCTACTTCAACGACTCGCAGCGCCAGG
685
3 ACCCTGTACCAATGCAGTGATTACCGTGCCAGCCTATTTCAATGACTCTCAACGTCAGG
658
**** ** ***** ** ***** ***** ***** ***** ***** ** * * * * *
1 CCACCAAGGATGCGGGTGTGATCGCGGGGCTCAACGTGCTGCGGATCATCAACGAGCCCA
772
2 CCACCAAGGATGCGGGTGTGATCGCGGGGCTCAACGTGCTGCGGATCATCAACGAGCCCA
745
3 CTACTAAGGATGCAGGTGTGATTGCTGGACTIONAATGTGCTAAGAATCATCAATGAGCCCA
718
* ** ***** ***** **
1 CGGCCCGGCCATCGCCTACGGCCTGGACAGAACGGGCAAGGGGGAGCGCAACGTGCTCA
832
2 CGGCCCGGCCATCGCCTACGGCCTGGACAGAACGGGCAAGGGGGAGCGCAACGTGCTCA
805
3 CGGCTGCTGCCATTGCCTATGGTTTAGATAAAGGAGGTCAAGGAGAACGACATGTCCTGA
778
**** ** ***** *****
1 TCTTTGACCTGGGCGGGGGACCTTCGACGTGTCCATCCTGACGATCGACGACGGCATCT
892
2 TCTTTGACCTGGGCGGGGGACCTTCGACGTGTCCATCCTGACGATCGACGACGGCATCT
865
3 TTTTTGATCTGGGTGGAGGCACATTTGATGTGTCAATTCTGACCATAGATGATGGGATTT
838
* ***** ***** ** ***** **
1 TCGAGGTGAAGGCCACGGCCGGGGACACCCACCTGGGTGGGGAGGACTTTGACAACAGGC
952
2 TCGAGGTGAAGGCCACGGCCGGGGACACCCACCTGGGTGGGGAGGACTTTGACAACAGGC
925
3 TTGAGGTAAAGGCCACTGCTGGGGACACTCACCTGGGTGGGGAGGACTTTGACAACAGGC
898

```

* *****
1 TGGTGAACCACTTCGTGGAGGAGTTCAAGAGAAAACACAAGAAGGACATCAGCCAGAACA
1012
2 TGGTGAACCACTTCGTGGAGGAGTTCAAGAGAAAACACAAGAAGGACATCAGCCAGAACA
985
3 TTGTGAGCCACTTCGTGGAGGAGTTCAAGAGAAAACACAAAAAGGACATCAGCCAGAACA
958
* *****
1 AGCGAGCCGTGAGGCGCTGCGCACCGCTGCGAGAGGGCCAAAGAGGACCTGTCTGTCCA
1072
2 AGCGAGCCGTGAGGCGCTGCGCACCGCTGCGAGAGGGCCAAAGAGGACCTGTCTGTCCA
1045
3 AGCGAGCCGTGAGGCGCTGCGCACCGCTGCGAGAGGGCCAAAGAGGACCTGTCTGTCCA
1018
* *****
1 GCACCCAGGCCAGCCTGGAGATCGACTCCCTGTTTGAAGGCCATCGACTTCTACACGTCCA
1132
2 GCACCCAGGCCAGCCTGGAGATCGACTCCCTGTTTGAAGGCCATCGACTTCTACACGTCCA
1105
3 GCACCCAGGCCAACCTAGAAATTGATTCACTTTATGAAGGCATTGACTTCTATACATCCA
1078
* *****
1 TCACCAGGGCGAGGTTTCGAGGAGCTGTGCTCCGACCTGTTCCGAAGCACCTGGAGCCCG
1192
2 TCACCAGGGCGAGGTTTCGAGGAGCTGTGCTCCGACCTGTTCCGAAGCACCTGGAGCCCG
1165
3 TCACCAGGCTCGATTTGAAGAGTTGTGTGCAGACCTGTTTGGGGTACCCTGGAGCCTG
1138
* *****
1 TGGAGAAGGCTCTGCGCGACGCCAAGCTGGACAAGGCCAGATTACGACCTGGTCTGG
1252
2 TGGAGAAGGCTCTGCGCGACGCCAAGCTGGACAAGGCCAGATTACGACCTGGTCTGG
1225
3 TAGAAAAAGCGCTTCGGGATGCCAAGATGGATAAAGGCTAAAAATCCATGACATGTTTTAG
1198
* *****
1 TCGGGGGCTCCACCCGCATCCCCAAGGTGCAGAAGCTGCTGCAGGACTTCTTCAACGGGC
1312
2 TCGGGGGCTCCACCCGCATCCCCAAGGTGCAGAAGCTGCTGCAGGACTTCTTCAACGGGC
1285
3 TAGGGGGCTCCACCCGCATCCCCAAGGTGCAGCGGCTGCTTCAGGACTACTTCAATGGAC
1258
* *****
1 GCGACCTGAACAAGAGCATCAACCCCGACGAGGCTGTGGCCTACGGGGCGGCGGTGCAGG
1372
2 GCGACCTGAACAAGAGCATCAACCCCGACGAGGCTGTGGCCTACGGGGCGGCGGTGCAGG
1345
3 GTGATCTCAACAAGAGCATCAACCCCTGATGAGGCCGTAGCATATGGGGCTGCGGTACAAG
1318
* *****
1 CGGCCATCCTGATGGGGGACAAGTCCGAGAACGTGCAGGACCTGCTGCTGCTGGACGTGG
1432
2 CGGCCATCCTGATGGGGGACAAGTCCGAGAACGTGCAGGACCTGCTGCTGCTGGACGTGG
1405
3 CAGCCATCCTGATGGGGGACAAGTCTGAGAAGGTACAGGACCTGCTGCTGCTGGACGTGG
1378
* *****
1 CTCCCCTGTCGCTGGGGCTGGAGACGGCCGAGGGCGTATGACTGCCCTGATCAAGCGCA
1492
2 CTCCCCTGTCGCTGGGGCTGGAGACGGCCGAGGGCGTATGACTGCCCTGATCAAGCGCA
1465

```



```

1          AAAAAAAAAA-----
2445
2          CACTACAAAAGGCTGGGAATGTATGTTTTTATAATTTGTTTATTTAAATATGAAAAATAA
2508
3          ATGTACCTTGAAGGGGAGATTTCATGGAGAGAGCATGTGTTCTCTGATTGTGAGGTCACT
2507

```

*

```

1          -----
2          ATGTTAACTTTAAAAAAAAAAAAAAAAAAAAAAAAAAAAA 2513
GTGAATGATTAAATGGTAAGGGTAAAGTAAAAAAAAAAAAA 2550

```

KEY

- *|| Nucleotides are identical in all sequences in the alignment
- .|| Semi-conserved substitutions are observed
- :|| Conserved substitutions are observed

Appendix 9.15 Amino Acid Sequence Alignment for *HSPA1A* (1), *HSPA1B* (2) and *HSPA1L* (3) *Homo sapiens*

SeqA	NameLen(aa)	SeqB	NameLen(aa)	Score
1	1 624	2 2 641	100	
1	1 624	3 3 641	90	
2	2 641	3 3 641	89	


```

1      --MAKAAAIGIDLGTTYSCVGVFQHGKVEIIANDQGNRTTPSYVAFTDTERLIGDAAKNQ
58
2      --MAKAAAIGIDLGTTYSCVGVFQHGKVEIIANDQGNRTTPSYVAFTDTERLIGDAAKNQ
58
3      MATAKGIAIGIDLGTTYSCVGVFQHGKVEIIANDQGNRTTPSYVAFTDTERLIGDAAKNQ
60
      * _ . *****
1      VALNPQNTVFDAKRLIGRKFGDPVVQSDMKHWPFQVINDGDKPKVQVSYKGETKAFYPEE
118
2      VALNPQNTVFDAKRLIGRKFGDPVVQSDMKHWPFQVINDGDKPKVQVSYKGETKAFYPEE
118
3      VAMNPQNTVFDAKRLIGRKFNDPVVQADMKLWPFQVINEGGKPKVLVSYKGENKAFYPEE
120
      * *:***** _ . *****:*** *****:*_ **** ***** _ *****
1      ISSMVLTKMKEIAEAYLGYPVTNAVITVPAYFNDSQRQATKDAGVIAGLNVLRIINEPTA
178
2      ISSMVLTKMKEIAEAYLGYPVTNAVITVPAYFNDSQRQATKDAGVIAGLNVLRIINEPTA
178
3      ISSMVLTKLKETAEAFLGHPVTNAVITVPAYFNDSQRQATKDAGVIAGLNVLRIINEPTA
180
      *****:*** ** *:***:*****
1      AAIAYGLDRTGKGERNVLIFDLGGGTFDVSILTIDDGIFEVKATAGDTHLGGEDFDNRLV
238
2      AAIAYGLDRTGKGERNVLIFDLGGGTFDVSILTIDDGIFEVKATAGDTHLGGEDFDNRLV
238
3      AAIAYGLDKGGQGERHVLIFDLGGGTFDVSILTIDDGIFEVKATAGDTHLGGEDFDNRLV
240
      *****: *_:***:*****
1      NHFVEEFKRKHKKDISQNKRAVRRLRTACERAKRTLSSSTQASLEIDSLFEGIDFYTSIT
298
2      NHFVEEFKRKHKKDISQNKRAVRRLRTACERAKRTLSSSTQASLEIDSLFEGIDFYTSIT
298
3      SHFVEEFKRKHKKDISQNKRAVRRLRTACERAKRTLSSSTQANLEIDSLYEGIDFYTSIT
300
      . ***** _ . *****:*****
1      RARFEELCSDLFRSTLEPVEKALRDAKLDKAQIHDLVLVGGSTRIPKVQKLLQDFFNGRD
358
2      RARFEELCSDLFRSTLEPVEKALRDAKLDKAQIHDLVLVGGSTRIPKVQKLLQDFFNGRD
358
3      RARFEELCADLFRGTLEPVEKALRDAKMDKAKIHDIVLVGGSTRIPKVQRLLQDYFNGRD
360
      *****:*** _ . *****:***:***:*****:***:*****
1      LNKSINPDEAVAYGAAVQAAILMGDKSENVQDLLLLDVAPLSLGLETAGGVMTALIKRNS
418
2      LNKSINPDEAVAYGAAVQAAILMGDKSENVQDLLLLDVAPLSLGLETAGGVMTALIKRNS
418
3      LNKSINPDEAVAYGAAVQAAILMGDKSEKVQDLLLLDVAPLSLGLETAGGVMTALIKRNS
420
      *****:*****

```


Appendix 9.16 Gene Sequence for *HSPA1A* (1), *HSPA1B* (2) and *HSPA1L* (3) *Rattus norvegicus*

SeqA	NameLen(nt)	SeqB	NameLen(nt)	Score		
1	1	4045	2	2	5918	78
1	1	4045	3	3	2632	73
2	2	5918	3	3	2632	74

1	-----CCAG-----	5
2	GAA TTCAGCACTTGGGTGTCAAGGCTGGAGGAGCAAGAGTTTAAGGCTAGCCTGGGCTA	60
3	-----	
1	-----	
2	CATGAGCCCCTATTTGAAAAAGAAAAAAGAAATAAAAAGTTAGAAAAAGAAAAAT	120
3	-----	
1	-----	
2	GAAAAAAAAGATGTGTGCGTGTGTATGTGTGTGAGAGAGAGACAGTCTCTCTCTCTC	180
3	-----	
1	-----CATCCTTCTCTGAGTTTCTATCTTTCTCTCG-----	36
2	TCTCTCTCTCTCTCTCTCTCTCTCTCTCTCTCTCTCTCTGTGTATGTGTGTGTGTGAG	240
3	-----	
1	ATTGTA ACTCCT-----CTCTTCGACCATCAATACC	67
2	ACAATTA CTCCCTGCTGTGGACTGTTACCTCAGAACTAAGACTCTAATGCAATCTATTCT	300
3	-----	
1	ATATTCAAAAAGGT-----CTTGTCTG--	89
2	TTTTTTAAAAAACAGGCTCGGGGCTGGGGATTTAGCTCAGTGGTAGAGCGCTTACCTAGG	360
3	-----	
1	-----CCT-----CCGATTCAGCTCAGACTAATT-----	114
2	AAGCGCAAGGCCCTGGGTTCGGTCCCCAGCTCCGAAAAAAGAACCAAAAAAAAAAAAAA	420
3	-----	
1	-----TCAGCCACTAATGTC-----	129
2	ACCAAAACAAAAAAAAAAAAACAAAAAAAAACAAAACAAAACAGGCTCTAATGTAGATTG	480
3	-----	
1	-----CCTCAAGAGC-----CCAACCCCATTTTTTCTTGG-----	159
2	GGCTAGCCTCAAAC TCTTCATCTCTCTGCCTCCCCCTCCAAGCATGAGGACTACAGAGG	540
3	-----	
1	-----TTGCCAACCCAAATCCAGAATTA AA ACTGGGG-----	193
2	TGGGCCACCATACCCAGTAACCTCATACTGTTTCAAGACATCTA ACTAGGGGGTCTTTAA	600
3	-----	
1	-----TTCCTGTGTGGAG-AGCCAAGAG-----	215
2	TTCGTACACGGAAGGAGGAGCCCGAAGAAGAAAAAGGGACATCACTGACAGCTAAACAT	660
3	-----	
1	-----GAGACCTAAGGATGGTGGCTT-----	236

2 ATTTATAATGAGAGGAGGTAGGGGACAGACAAGGGACGGAAAGGTGATGTCTAGGACAAA 720
3 -----

1 -----CCACTAGACCACGTCTGTAATCAA-----TCAAACCTAAG 272
2 AAGCTAACCCATAACTAGTAGGTGGGTCCCCACACCTCTGCTTAGGGTCTCACC AAA 780
3 -----

1 A-----AAATCT 280
2 AGTCGGAGTTAACAGCACTGTGAGGCCAGATGCTATCAGAGGACAGGACACACCATCTCT 840
3 -----

1 TGGCCCATTAATAAGAACCAACTGGAATTCCAGGCTCA-----CCTGGAATCTCTACG 334
2 CCACCTAGGAAAGGTGAACTGACAGGGGCAGCAGACACAGAAGAATCAGCAAACCTCTAA 900
3 -----

1 -----CCTTCGATCCAGTTTGGAAAAATTGAAGTCGCTAGCCCCTACGA 379
2 GTCAAACCTGAGGTTACTACAGCACAGAATAGAACAGTGCCTGGCAAGGAGCAGCTGTGT 960
3 -----

1 GTGGGGAGCTCCAGGAA--CATCCAA----- 404
2 GAAGGAGAAGCCAAAGCAGCCATCCTCAGCATTCTTCTTCTATTAATCTTTTGGGACAGGG 1020
3 -----

1 -----CTGAGCAACTGGGGTT-----CCCCCAACCCCAACCCCGC 440
2 TCTGCCTCTGTAACTAGGCTGACCTTGACTCGCTGCAGTCCCTCTGCCCCACCTCTAC 1080
3 -----

1 C-----CCTCCCG-----CAA 452
2 CGAAAGTTTTTTTTTTCTCCTTTCTAATGCCAGGCTGCCCGCTGAGGC AAAGGAGCGG 1140
3 -----

1 CTTTGCCT-----CTT-----CTGGGACAGATCCT 479
2 CTTGCAGCCTGGCACGGTCGGTCGATTAAACCTTGCTCTCCCCGTCTGGGACACTTTCC 1200
3 -----

1 CTGATTCCTAAATAAGTCC-----ATGAGGTCAGAGT--TAGCACTG----- 519
2 TTTTTTGGGTACAGGTCCTCCTAACATGAGAACCGAGTGTTTACACAATGATGTTCTTT 1260
3 -----

1 -----CCATTGTAAACGGGCTGGAGGG----- 542
2 TGAAAACCGTGAAAACCTCCACAGGCGATGTACTTGTACGTTAAGCGTGACATAAAGACAG 1320
3 -----

1 -----GGTCACGTAC----- 553
2 CAAAGCGAATAAACTATACTGCAAGATCTCTTCTTTCCCTATTTAAACCTAAAAATGGA 1380
3 -----

1 -----CGGACAG-----CCCCAGGCACCTCCCTTGGGTCTCCC 588
2 GGGAGTGGGGGGCAGACACAGACAGGCGAGCATTCACAGGCGCCCCCCACG-CTGTC 1439
3 -----

1 AAGGCTAGGAAGGGGAGTTATAACCTTAACT--CGAGC-----CCCATAATCAG 637
2 ACTTCCAGGCAGGACCCAATCACAGACTTCTTAGCCAAGCGTTATCCCTCCCGTTTTGAG 1499
3 -----

1 -AACTGTGCGAGTCTGCGAACC-----CCACA 664


```

2      TTTCCACAGTGGTAGCCTCGGACATTGAAAATTGCAGGGGTTGTTGGTTGTCGGTTGGGT 4916
3      TCACCTCCCTGTGTGGATG-----GTTATTTG----- 2375
      * : ** : : : * . *                * : ***

1      -----TTCTCCT-----TCCCTGTATAATCTTGCCTGGCC 3701
2      TTTTGTTTTGTCTTGTTTTGTTTTCAAGACAGGGTCTCTCTGTGTAGCCCTGGCTGGCC 4976
3      -----TCTCTCAGTAAATTTG----- 2391
      * * * * : . * * . * *

1      -----GTTGCACTTG--TTCCCCAGTGTG----- 3723
2      TCGATTTTCGGATCCACATGCCTTTCCCAAACCTGGCTTCCTTATTACTTTTTTTTTTTTTT 5036
3      -----TTCCCAA----- 2398
      * * * * . *

1      -----TGAACTCGGAG----- 3734
2      TTTAAGATTTATTTACTTATTATATATAAGTACAATGTAGCTGTCTTCAGAGACACCAGA 5096
3      -----

1      -----ATGAGTTTACACCACA-----CTG---TTAGT 3759
2      AGAGGGCATCAGATCCCATTACAGATGGCTGTGAGCCACCATGTGGTTGCTGGGATTTGA 5156
3      -----AGG----- 2401
      : *

1      TCACG-----TTTTTTGTTTTTACATAACCATCCTGAACTCAGGTCAA 3802
2      ACTCAGGACCTCTTCAAGAGCAGTCACTGCTCTTAACTTCTGAGCCCTCTCTCCAGCCCT 5216
3      AAACG-----TCTGTCACTTTTCGATTTGTTTAG--TCGAGGGCCTT 2441
      : . : * .                * : * * * : . : : : * . * * :

1      TTTTFACTGG-----CTATTTGAAAATAAACTT----- 3830
2      TTATTACTTTTAGAGATTTCTTACCAGGTTGCCCTGGCTGTACTTACACTTTCTCTTTAG 5276
3      ACTGTATATG-----TCTAGCTGACCTGACGCTT----- 2470
      : : * * :                * * . * * : . : : * * * *

1      -----CAAAGAACTTGCCAG----- 3846
2      CTCTGCTGAGCTTTCAAATTCACAGTTCCAGACCACACCCCTGAACCCACCAGCTGAAGA 5336
3      -----ACCGCATGGCCAA----- 2484
      . . * * * . * * * .

1      -----GTCTTG-----TGTCTGTTGTCTTTTGGGTCAGGAAT-----TGCTGTGT 3887
2      CAACATGTCTTGCTATCTTTTTCTTTCTTTTGGGGCAGGGATGGTCTGTGTGTTGTGT 5396
3      -----TTTGGTCCTTAACTTGCAGCAAT-----CCTCCTGTCT 2517
      * * * * * * * : * * * . * * * * * * *

1      ATGT-----CTTACAGA----- 3899
2      GTGTGAGAGACAGAGGCAGAGACATCCTTCCCATGTAGCCCTAACTGAGTCGGAAGTCAT 5456
3      CTG-----CCACCTGAAT----- 2530
      * *                * * * . :

1      ---TTGGACTIONGCT-----TGACTIONGATTTTATGGTAAAGATGG----- 3936
2      TATTAGACCAGGCTGCCCTGACTCCTGTATCTGCCCTCTCCAATGGATTATGGGCACCTG 5516
3      ---TTCGAGATTACG-----GACCTGCACCATCATG----- 2558
      * * * * : . *                . * * * . : * :

1      -----
2      CCACCTCACCCACTCACTTTATCCCCAGGATCCCCCTCCCTCTTCCCAGGCAGTAGGTCT 5576
3      -----

1      ---GGTGGGGAG----- 3945
2      GGTGATGGAGAAGACCACTTACCATGTCCATGGCTCAAAGAAGCAGGCAGAACGTAGGGG 5636
3      -----

1      -----CACCCAGGGACTTTG----- 3960
2      AAAGAGTTGCTTTCACCTCAAGCCTTTGGATCCATGGGTGTTTCTTCTAGTGGGGTAAATG 5696
3      -----CCCAAC----- 2564
      * * . .

1      ---CATTGGGATCTGCTTG-TGTGAGAAAAATGAAAGCAG-----TCAG 4000

```

```

2      CCATCCTTTGAGAGCTGGGGGGTGTGGGTCAACAGAGATCGGTTGCTATGTGTGCATGAG 5756
3      -----TTGTGATTTTTTTTTTTTTGGGAGGCAGGGTTTCTTG----- 2600
          *** ** *          * **.*: . . . * . : *

1      ---AGCAAATAACAACCAG--TCCGGG-----GCTGAGGTCTAGT 4035
2      GCCCGCAATTCAGTCCCTGGCTCCATGGAGAACGAAccaATCAGTTGGGTGAGGTGTAAA 5816
3      --AAGCCTAGGTTAGCCTAG-----AACATTCTAT 2628
          .**.: : : **:. . * . * : . :

1      ACAGTG-----CAGA----- 4045
2      CCACATGTAATTTTAGCATGTCCAAACAGACACGTTAAGGACATCCTAGGGTAAAGAAGT 5876
3      ACAC----- 2632
          .**

1      -----
2      CTTCAGCAATAGTTTAATTGAGGCAATTATGCTCATGAATTC 5918
3      -----

```

KEY

- *|| Nucleotides are identical in all sequences in the alignment
- .| Semi-conserved substitutions are observed
- :| Conserved substitutions are observed

Appendix 9.17 Amino Acid Sequence for *HSPA1A* (1), *HSPA1B* (2) and *HSPA1L* (3)

Rattus norvegicus

CLUSTAL 2.0.12 multiple sequence alignment

SeqA	NameLen(nt)	SeqB	NameLen(nt)	Score	
1	1	2	2	641	100
1	1	3	3	641	80
2	2	3	3	641	80

```

1      --
MAKKTAIGIDLGTTYSCVGVFQHGKVEIIANDQGNRTTPSYVAFTDTERLIGDAAKNQ 58
2      --
MAKKTAIGIDLGTTYSCVGVFQHGKVEIIANDQGNRTTPSYVAFTDTERLIGDAAKNQ 58
3
MAANGMAIGIDLGTTYSCVGVFQHGKVEIIANDQGNRTTPSYVAFTDTERLIGDAAKNQ 60
      *
*****

1
VALNPQNTVFDAKRLIGRKFGDPVVQSDMKHWPFQVVNDGDKPKVQVNYKGENRSFYPEE 118
2
VALNPQNTVFDAKRLIGRKFGDPVVQSDMKHWPFQVVNDGDKPKVQVNYKGENRSFYPEE 118
3
VAMNPQNTVFDAKRLIGRKFNDPVVQSDMKLWPFQVINEAGKPKVLSYKGEKKAFYPEE 120
      ** : *****
* _ ***** : : *****

1
ISSMVLTKMKEIAEAYLGHPVTNAVITVPAYFNDSQRQATKDAGVIAGLNVLRIINEPTA 178
2
ISSMVLTKMKEIAEAYLGHPVTNAVITVPAYFNDSQRQATKDAGVIAGLNVLRIINEPTA 178
3
ISSMVLTKMKETAEAFLGHSVTNAVITVPAYFNDSQRQATKDAGVIAGLNVLRIINEPTA 180
      *****
*** : *** _ *****

1
AAIAYGLDRTGKGERNVLIFDLGGTFDVSILTIDDGIFEVKATAGDTHLGGEDFDNRLV 238
2
AAIAYGLDRTGKGERNVLIFDLGGTFDVSILTIDDGIFEVKATAGDTHLGGEDFDNRLV 238
3
AAIAYGLDKGSHGERHVLIFDLGGTFDVSILTIDDGIFEVKATAGDTHLGGEDFDNRLV 240
      ***** :
_ : *** : *****

1
SHFVEEFKRKHKKDISQNKRAVRLRTACERAKRTLSSSTQASLEIDSLFEGIDFYTSIT 298
2
SHFVEEFKRKHKKDISQNKRAVRLRTACERAKRTLSSSTQASLEIDSLFEGIDFYTSIT 298
3
SHFVEEFKRKHKKDISQNKRAVRLRTACERAKRTLSSSTQANLEIDSLYEGIDFYTSIT 300
      ***** : *****

1
RARFEELCSDLFRGTLEPVEKALRDAKLDKAQIHDLVLVGGSTRIPKVQKLLQDFFNGRD 358
2
RARFEELCSDLFRGTLEPVEKALRDAKLDKAQIHDLVLVGGSTRIPKVQKLLQDFFNGRD 358

```

3
RARFEELCADLFRGTLPEVKEKSLRDAKMDKAKIHDIVLVGGSTRIPKVQKLLQDYFNGRD 360

*****:*****:*****:***:***:*****:*****:*****

1
LNKSI^{DE}AVAYGAAVQAAILMGDKSEN^{VQ}DL^{LL}LDVAPLSL^{GLE}TAGG^{VT}ALIKRNS 418

2
LNKSI^{DE}AVAYGAAVQAAILMGDKSEN^{VQ}DL^{LL}LDVAPLSL^{GLE}TAGG^{VT}ALIKRNS 418

3
LNKSI^{DE}AVAYGAAVQAAILMGDKSEK^{VQ}DL^{LL}LDVAPLSL^{GLE}TAGG^{VT}ALIKRNS 420

*****:*****:*****:*****:*****

1
TIPTKQTQTFTTYS^{DN}QPGVLIQVYEGERAMTRD^{NN}LLGRFELSGIPPAPRGV^{PQ}IEVTF 478

2
TIPTKQTQTFTTYS^{DN}QPGVLIQVYEGERAMTRD^{NN}LLGRFELSGIPPAPRGV^{PQ}IEVTF 478

3
TIPTKQTQIFTTYS^{DN}QPGVLIQVYEGERAMTRD^{NN}LLGRFDLTGIPPAPRGV^{PQ}IEVTF 480

*****:*****:*****:*****:*****

1
DIDANGILNVTATDKSTGKANKITITNDKGR^{LS}SK^{EE}IERMVQEAERYKA^{ED}EVQRERVA 538

2
DIDANGILNVTATDKSTGKANKITITNDKGR^{LS}SK^{EE}IERMVQEAERYKA^{ED}EVQRERVA 538

3
DIDANGILNVTAMDKSTGKANKITITNDKGR^{LS}SK^{EE}IERMVQEAERYKA^{ED}EGQREKIAA 540

:

1
KNALESYAFNMKSAVEDEGLK^{GK}ISEADKKKVL^{DK}CQEVISW^{LD}SNTLAEKEEFVHKREE 598

2
KNALESYAFNMKSAVEDEGLK^{GK}ISEADKKKVL^{DK}CQEVISW^{LD}SNTLAEKEEFVHKREE 598

3
KNALESYAFNMKSAVGDEGLK^{DK}ISESDKKKIL^{DK}CEVLSW^{LE}ANQLAEKEEFDH^{KR}KE 600

***** *****:*****:*****:*****:*****:*****

***:*

1 LERVCNPIISGLYQAGAPGAGGFQA^{PK}GGSGSGPTIEEVD 641

2 LERVCNPIISGLYQAGAPGAGGFQA^{PK}GGSGSGPTIEEVD 641

3 LENMCNPIITKLYQ-SGCTGPTCAPGYTP-GRAATGPTIEEVD 641

:***:***:*. * .: * * :*:*****

KEY

- *|| Nucleotides are identical in all sequences in the alignment
- .|| Semi-conserved substitutions are observed
- :|| Conserved substitutions are observed

- MVFILAPW Non polar R-groups
- GNTSYQHC Polar R-groups
- KR Positively charged R-groups
- DE Negatively charged R-groups

Appendix 9.18 Gene Sequence Alignment for *HSPA1A* *Homo sapiens* v *Rattus norvegicus*

CLUSTAL 2.0.12 Multiple Sequence Alignments

SeqA	NameLen(nt)	SeqB	NameLen(nt)	Score
1	1	2	2	73

```

=====
1          -----
2          CCAGGCATCCTTCTCTGAGTTCTATCTTTCTCTCGATTGTA ACTCCTCTCTCGACCAT
60

1          -----
2          CAATACCATA TTCAAAAAGGCTTGTCTGCCTCCGATTTCA GCTCAGACTAA TTTTAGCC
120

1          -----
2          ACTAATGTCCCTCAAGAGCCCAACCCCATTTTTCTTGGTTGCCAACACCCAAATCCAGA
180

1          -----
2          ATTAAAAC TGGGTTCTGTGTGGAGAGCCAAGAGGAGACCTAAGGATGGTGGCTTCCAC
240

1          -----
2          TAGACCACGTCTGTA AATCAATCAAACCTAAGAAAATTC TTGGCCATTAAATAAGAACC
300

1          -----
2          AACTGGAA TTCCAGGCTCACCTGGAATCTCTACGCCTTCGATCCAGTTTGGAAAATTTGA
360

1          -----
2          AGTCGCTGAGCCCCCTACGAGTGGGGAGCTCCAGGAACATCCAAACTGAGCAA CTGGGGTT
420

1          -----
2          CCCCCACCCCCACCCCGCCCCTCCGGCAACTTTGAGCCTCTTCTGGGACAGATCCTC
480

1          -----
2          TGATTCC TAAATAAGTCCATGAGGTCAGAGTTAGCACTGCCATTGTAACGCGGCTGGAGG
540

1          -----
2          GGGGTCACGTCACCGGACACGCCCCAGGCACCTCCCTTGGGTCTCCCAAGGCTAGGAAG
600

1          -----
2          GGG AAGTTATAACCCTTA ACTCGAGCCCCATAATCAGAACTGTGCGAGTCTGCGAACCC
660

```



```

*****
1      ACAAGCGGAGGACGAGGTGCAGCGGAGAGGGTGTAGCCAAAGAACGCCCTGGAGTCCT
1876
2      ACAAGCGGAGGACGAGGTGCAGCGGAGAGGGTGGCTGCCAAAGATGCGCTCGAGTCCT
2880
****
1      ACGCCTTCAACATGAAGAGCGCCGTGGAGGATGAGGGGCTCAAGGGCAAGATCAGCGAGG
1936
2      ATGCCTTCAACATGAAGAGCGCCGTGGAGGACGAGGGTCTCAAGGGCAAGATCAGCGAGG
2940
*
1      CGGACAAGAAGAAGGTGCTGGACAAGTGTCAAGAGGTATCTCGTGGCTGGACGCCAACA
1996
2      CTGACAAGAAGAAGGTGCTGGACAAGTGCCAGGAGGTATCTCTGGCTGGACTCTAACA
3000
*
1      CCTTGGCCGAGAAGGACGAGTTTGTAGCACAAAGAGGAAGGAGCTGGAGCAGGTGTGTAACC
2056
2      CGCTGGCTGAGAAAGAGGAGTTTCGTGCACAAGCGGGAGGAGCTGGAGCGGGTGTGCAACC
3060
*
1      CCATCATCAGCGGACTGTACCAAGGTGCCGGTGGTCCCGGGCTGGGGGCTTCGGGGCTC
2116
2      CGATCATCAGCGGGCTGTATCAGGGTGCGGTGTCTCCCGGGCTGGGGGCTTCGGGGCCC
3120
*
1      AGGGTCCCAGGGAGGGTCTGGGTGAGGCCCAACATTGAGGAGGTAGATTAGGGGC-CT
2175
2      AGGCGCCCAAGGGAGGCTCTGGGTGCGGGCCCAACATCAGGAGGTGGATTAGAGGCTCT
3180
***
1      TTCCAAGATTGCTGTTTTTTGTTTGGAG-----CTTCAAGACTTTGCATTTCC
2222
2      TTCTGGCGCTCCAGGTGTGATCTAGGAGACAGATGGGTGGCCTTGAAGACTTTGGGTTAT
3240
***
1      C-----TAGTATTTCTGTTTGTCAAGTCTCAATT--TCCTGTGTTT--GCAA-
2265
2      TGTCGTTTAGGACATTAACCTCCTTCGTTCGGTCTGCAATCAAGTCCTAGGTTTAAAGCAA
3300
*
1      ---TGTGAAATTTTTTGGTGAAGTACTGAACTTGCTTTT--TTTCCGGTTTCTACATGC
2320
2      CTGCCTTCCATTTACTCTGTGGAATTTACGTTGTCTTTGCAATCCAGTAAATTAGTAC
3360
*
1      AGAGA-TGAATTTATACTGCCATCTTACGACTATTTCTTCTTTTAAATACACTTAATC-
2378
2      TGGGAGTGTGCTTTGCAATAGATATAAATTCCTGCCTTCAAGTCAGCACTGCCCCCCC
3420
*
1      ---AGGCCATTTTTTAAAGTTGGTACTTCAAAGTAAATAAACTT--TAAATTCAAAA
2432
2      CCCGAAGTTATTTCTTTTGCAGGACAGTCAGAGCTATATTGATATAGCAAGAGGTGTGTT
3480
*
1      AAAAAAAAAA-----
2445

```

```

2          AAAAAACACCAGGACACTGTTGAGTTCCTTTGTGTTTGGACTCTCCCCTGGGCGACAGT
3540
          * * * * * * *
1          -----
2          GTTGAGGCACCTGTTAAGTCAGGAGCTCAGGGGCCACCGGTGGATCACTGAAAAGCTGAGAC
3600
1          -----
2          TCTGTTGCTTCTCCCGTTTGAACACTCTGTTGCTTTCCTTGCAATGGTGGCTCACCTAAGGC
3660
1          -----
2          TGAGACTCTTGTTCCTTCCTGTATAATCTTGCCTGGCCGTTGCACCTGTTCCCCAGT
3720
1          -----
2          GTGTGAACTCGGAGATGAGTTTACACCACCACTGTTAGTTCACGTTTTTTGTTTTTACAT
3780
1          -----
2          AACCATCCTGAACTCAGGTCAATTTTTACTGGCTATTTGAAAATAAACTTCAAAGAAGT
3840
1          -----
2          TGCCAGGTCTTGTGCTGTTGTCTTTTGAAGTCAGGAATTGCTGTGTATGTCTTACAGAT
3900
1          -----
2          TGGACTACGCTTGACTGACATTTTATGGTAAGATGGGGTGGGGAGCACCCAGGGACTTTG
3960
1          -----
2          CATTGGGATCTGCTTGTGTGAGAAAAATGAAAGCAGTCAGAGCAAATAACAACCAAGTCCG
4020
1          -----
2          GGGCTGAGGTCTAGTACAGTGCAGA 4045

```

KEY

- *|| Nucleotides are identical in all sequences in the alignment
- .|| Semi-conserved substitutions are observed
- :|| Conserved substitutions are observed

Appendix 9.19 Amino Acid Sequence for HSPA1A Homo sapiens v Rattus norvegicus

CLUSTAL 2.0.12 multiple sequence alignment

```

SeqA NameLen(aa)  SeqB NameLen(aa)  Score
=====
1      1      641      2      2      641      96
=====

1      MAKAAAI GIDL GTTYSCVGVFQH GKVEIIANDQGNRTTPSYVAFTDTERLIGDAAKNQVA
60
2      MAKKTAIGIDL GTTYSCVGVFQH GKVEIIANDQGNRTTPSYVAFTDTERLIGDAAKNQVA
60
      *** :*****

1      LNPQNTVFD AKRLIGRKF G D PVVQSDMKHWP FQVINDGDKPKVQVSYKGETKAFYPEEIS
120
2      LNPQNTVFD AKRLIGRKF G D PVVQSDMKHWP FQVINDGDKPKVQVNYKGENRSFYPEEIS
120
      ***** :*****

1      SMVLTKMKEIAEAYLGPVTNAVITVPAYFNDSQRQATKDAGVIAGLNVLRIINEPTAAA
180
2      SMVLTKMKEIAEAYLGHVPTNAVITVPAYFNDSQRQATKDAGVIAGLNVLRIINEPTAAA
180
      ***** :*****

1      IAYGLDRTGKGERNVLIFDLGGGTFDVSILTIDDGIFEVKATAGDTHLGGEDFDNRLVNH
240
2      IAYGLDRTGKGERNVLIFDLGGGTFDVSILTIDDGIFEVKATAGDTHLGGEDFDNRLVSH
240
      *****

1      FVEEFKRKHKKDISQNKRAVRRRLTACERAKRTLSSSTQASLEIDSLFEGIDFYTSITRA
300
2      FVEEFKRKHKKDISQNKRAVRRRLTACERAKRTLSSSTQASLEIDSLFEGIDFYTSITRA
300
      *****

1      RFEELCSDLFRSTLEPVEKALRDAKLDKAQIHDLVLVGGSTRIPKVQKLLQDFFNGRDLN
360
2      RFEELCSDLFRGTLEPVEKALRDAKLDKAQIHDLVLVGGSTRIPKVQKLLQDFFNGRDLN
360
      *****

1      KSINPDEAVAYGAAVQAAIILMGDKSENVQDLLLDDVAPLSLGLTAGGVMTALIKRNSTI
420
2      KSINPDEAVAYGAAVQAAIILMGDKSENVQDLLLDDVAPLSLGLTAGGVMTALIKRNSTI
420
      *****

1      PTKQTQIFTTYSDNQPGVLIQVYEGERAMTKDNNLLGRFELSGIPPAPRGVPQIEVTFDI
480
2      PTKQTQTFTTYSDNQPGVLIQVYEGERAMTRDNNLLGRFELSGIPPAPRGVPQIEVTFDI
480
      *****

1      DANGILNVTATDKSTGKANKITITNDKGRLSKEEIERMVQEAEKYKAEDVQRERVSANK
540
2      DANGILNVTATDKSTGKANKITITNDKGRLSKEEIERMVQEAERYKAEDVQRERVAANK
540
      *****

1      ALESYAFNMKSAVEDEGLKGI SEADKKKVL D K CQEVISWLDANTLAEKDEFEHKRKELE
600
2      ALESYAFNMKSAVEDEGLKGI SEADKKKVL D K CQEVISWLD SNTLAEKEEFVHKREELE
600

```

*****:*****:***:***

```
1 QVCNPIISGLYQGAGGPGGGFGA 624
2 RVCNPIISGLYQGAGAPGAGGFGA 624
:*****_*_*_*****
```

KEY

- *|| Nucleotides are identical in all sequences in the alignment
- .|| Semi-conserved substitutions are observed
- :|| Conserved substitutions are observed

MVFILAPW	Non polar R-groups
GNTSYQHC	Polar R-groups
KR	Positively charged R-groups
DE	Negatively charged R-groups

Appendix 9.20 Gene Sequence Alignment for *HSPA1B* *Homo sapiens* v *Rattus norvegicus*

SeqA	NameLen(nt)	SeqB	NameLen(nt)	Score
1	1 2551	2	2 5918	78
1		-----		
2		GAATTCCAGCACTTGGGTGTCAAGGCTGGAGGCAAGAGTTTAAGGCTAGCCTGGGCTA		
60				
1		-----		
2		CATGAGCCCTATTTTGAAAAAGAAAACAAGAAATAAAAAATTAGAAAAAGAAAAAT		
120				
1		-----		
2		GAAACAAAAGATGTGTGCGTGTGTATGTGTGTGAGAGAGAGACAGTCTCTCTCTC		
180				
1		-----		
2		TCTCTCTCTCTCTCTCTCTCTCTCTCTCTCTCTCTCTCTGTGTATGTGTGTGTGAG		
240				
1		-----		
2		ACAATTACTCCCTGCTGTGGAAGTGTACCTCAGAAGTAAGACTCTAATGCAATCTATTCT		
300				
1		-----		
2		TTTTTTAAAAAACAGGCTCGGGGCTGGGATTTAGCTCAGTGGTAGAGCGCTTACCTAGG		
360				
1		-----		
2		AAGCGCAAGGCCCTGGGTTCCGTCCCCAGCTCCGAAAAAAGAACCAAAAAAAAAAAAAA		
420				
1		-----		
2		ACCAAAACAAAAAAAAAAAAACAAAAAAAAACAAACAAACAGGCTCTAATGTAGATTG		
480				
1		-----		
2		GGCTAGCCTCAAACCTCTTCACTCTCCTGCCTCCCCCTCCAAAGCATGAGGACTACAGAGG		
540				
1		-----		
2		TGGGCCACCATACCCAGTAACCTCATACTGTTTCAAGACATCTAACTAGGGGTCTTTAA		
600				
1		-----		
2		TTCGTACACGGAAGGAGGAGCCCGAAGAAAGAAAAGGGACATCACTGACAGCTAAACAT		
660				
1		-----		
2		ATTTATAATGAGAGGAGGTAGGGACAGACAAGGGACGGAAGGTGATGTCTAGGACAAA		
720				

1
2
780

AAGCTAACCCACATAAACTAGTAGGTGGGTCCCGACACCTCTGCTTAGGGTCTCACCCAAA

1
2
840

AGTCGGAGTTAACAGCACTGTGAGGCCAGATGCTATCAGAGGACAGGACACACCATCTCT

1
2
900

CCACCTAGGAAAGGTGAACTGACAGGGGCAGCAGACACAGAAGAATCAGCAAACCTCTTAA

1
2
960

GTCAACCCTGAGGTTACTACAGCACAGAATAGAACAGTGCCGGCAAGGAGCAGCTGTGT

1
2
1020

GAAGGAGAAAGCCAAGCAGCCATCCTCAGCATTCCTTCTTCTATTAACTTTTGGGACAGGG

1
2
1080

TCTGCCTCTGTAACCTAGGCTGACCTTGACTCGCTGCAGTCCCTCTGCCCCACCCTCTAC

1
2
1140

CGAAAGTTTTTTTTTTTCTCCTTTCTAATGCCAGGCTGCCGCTGAGGCAAGGGAGCGG

1
2
1200

CTTGCAAGCCTGGCACGGTCGGTCGATTAACCTTGCTCTCCCCGCTCTGGGACACTTTCC

1
2
1260

TTTTTTGGGTCACAGGTCCTCCTAACATGAGAACCGAGTGTACACAATGATGTTCTTT

1
2
1320

TGAAAACCGTGAAGAACTCCACAGGCGATGTACTTGTACGTTAAGCGTGACATAAAGACAG

1
2
1380

CAAAGCGAATAAACTATACTGCAAGATCTCTTCTCTTTCCCTATTTAAACCTAAAATGGA

1
2
1440

GGGAGTGGGGGGCAGACACAGACAGGCGAGCATTCACAGGCGCCCCCCCCACGCTGTCA

1
2
1500

CTTCCAGGCAGGACCCAATCACAGACTTCTTAGCCAAGCGTTATCCCTCCCGTTTTGAGA

1
2
1560

AACTTTCTGCGTCCGCCATCCTGTAGGAAGAAATTTGTACACCTTAAACTCCCTCCCTGGT

```

1 -----
2 CTGATTCCCAAATGTCTCTCACCGCCAGCATTTAGGAGCTGACCTTCTCAGCTTCA
1620

1 -----
2 CATACAGAGACCGCTACCTTGCCTCGCCATGGCAACACTGTCACAACCGGAACAAGCACT
1680

1 -----
2 TCCTACCACCCCCCGCCTCAGGAATCCAATCTGTCCAGCGAAGCCAGATCCGTCTGGAG
1740

1 -----
2 AGTTCTGGACAAGGGCGGTACCCCTCAACATGGATTACTCATGGAGGCGGAGAGCTCTA
1800

1 -----
2 ACAGACCCGAAACTGCTGGAAGATTCCTGGCCCCAAGGCCTCTCCGCTCGCTGATTGG
1860

1 -----
31 -----GGAAAACGGCC-----AGCCTGAGGAGCTGCTGCGA
2 CCCATGGGAGGGTGGGCGGGCCGGAGGAGGTCCTTAAAGGCGCAGGGCGGCGCAGG
1920
                *** * * * *          * *   * * * * *

1 GGGTCCGCTTCGTCTTTCGAGAGTACTCCCCGCGTCCCAAGGCTTTCCAG-AGCGAAC
90
2 ACACCAGATTCCCTCCTCTAATCTGACAGAACCAGTTCTGGTTCCACTCGCAGAGAAGC
1980
      * * * * * * * * *   * * * *   * * * * * * * * * *

1 TGTGCGGCTGCAGGCACCGCGTGTT--GAGTTTCCGGCG-----TTCCGAAG
136
2 AGAGAAGC-GGAGCAAGCGCGCGTTCCAGAACCTCGGGCAAGACCAGCCTCTCCCAGAG
2039
      * *   * * * * * * * * * * * * * * * * * * * * * * *

1 GACT-----GAGCTCTTGTCGCGGATCCC-----GTCCGCCGTTTCC
173
2 CATCCCCACCGCGAAGCGCAACCTTCTCCAGAGCATCCCCAGCGGAGCGCACCCTTCCC
2099
      *                * * * * * * * * * * * * * * * * * *

1 ---AGC-CCCCAGTCTCAGAGCGGAGCCAC---AGAGCAGGGCACCGCATGGCCAAA
225
2 CAGAGCATCCCCCGGCCAAGCGCAACCTTCCAGAAGCAGAGAGCGGGCGACATGGCCAAG
2159
      ***   *** * * * *   * * * * * * * * * * * * * * * * * *

1 GCCGCGGCGATCGGCATCGACCTGGGCACCACTACTCCTGCGTGGGGTGTTCAACAC
285
2 AAAACAGCGATCGGCATCGACCTGGGCACCACTACTCGTGCGTGGGCGTGTTCAGCAC
2219
      * * * * * * * * * * * * * * * * * * * * * * * * * * * *

1 GGCAAGGTGGAGATCATCGCCAACGACCAGGGCAACCGCACCACCCCAGCTACGTGGCC
345
2 GGCAAGGTGGAGATCATCGCCAACGACCAGGGCAACCGCACCACCCCAGCTACGTGGCC
2279
      * * * * * * * * * * * * * * * * * * * * * * * * * * * *

```

1
405
2
2339

1
465
2
2399

1
525
2
2459

1
585
2
2519

1
645
2
2579

1
705
2
2639

1
765
2
2699

1
825
2
2759

**

1
885
2
2819

**

1
945
2
2879

**

1
1005
2
2939

1
1065
2
2999

```

***** ** *****
1 ATCGACTCCCTGTTTGAGGGCATCGACTTCTACACGTCCATCACAGGGCGAGGTTGAG
1125
2 ATCGACTCTCTGTTGAGGGCATCGACTTCTACACGTCCATCACGCGGGCGGGTTCGAG
3059
***** *****
1 GAGCTGTGCTCCGACCTGTTCCGAAACACCTGGAGCCCGTGGAGAAGGCTCTGCGCGAC
1185
2 GAGCTGTGCTCCGACCTGTTCCGCGGCACGCTGGAGCCCGTGGAGAAGGCCCTGCGCGAC
3119
***** *****
1 GCCAAGCTGGACAAGGCCAGATTACGACCTGGTCTGGTGGGGGCTCCACCCGCATC
1245
2 GCCAAGCTGGACAAGGCCAGATCCACGACCTGGTCTGGTGGGGCGGCTCGACGCGCATC
3179
***** *****
1 CCCAAGGTGCAGAAGCTGCTGCAGGACTTCTTCAACGGGCGCGACCTGAACAAGAGCATC
1305
2 CCCAAGGTGCAGAAGCTGCTGCAGGACTTCTTCAACGGGCGCGACCTGAACAAGAGCATC
3239
***** *****
1 AACCCCGACGAGGCTGTGGCCTACGGGGCGGCGGTGCAGGCGGCCATCCTGATGGGGGAC
1365
2 AATCCGGACGAGGCGGTGGCCTACGGGGCGGCGGTGCAGGCGGCCATCCTGATGGGGGAC
3299
** ** *****
1 AAGTCCGAGAACGTGCAGGACCTGCTGCTGCTGGACGTGGCTCCCCTGTCGCTGGGGCTG
1425
2 AAGTCGGAGAACGTGCAGGACCTGCTGCTGCTGGACGTGGCGCCGCTGTCGCTGGGTCTG
3359
***** *****
1 GAGACGCGCCGAGGCGTGATGACTGCCCTGATCAAGCGCAACTCCACCATCCCCACCAAG
1485
2 GAGACGCGGGCGGCGTGATGACGGCGCTCATCAAGCGCAACTCCACCATCCCCACCAAG
3419
***** ** *****
1 CAGACGCAGATCTTACCACCTACTCCGACAACCAACCCGGGGTGCTGATCCAGGTGTAC
1545
2 CAGACGCAGACCTTACCACCTACTCGACAACCAAGCCGGGGTGCTGATCCAGGTGTAC
3479
***** *****
1 GAGGGCGAGAGGGCCATGACGAAAGACAACAATCTGTTGGGGCGCTTCGAGCTGAGCGGC
1605
2 GAGGGCGAGAGGGCCATGACGCGGACAACAACCTGCTGGGGCGCTTCGAGTTGAGCGGC
3539
***** *****
1 ATCCCTCCGGCCCCAGGGGCGTGCCCCAGATCGAGGTGACCTTCGACATCGATGCCAAC
1665
2 ATCCCGCCGGCTCCCAGGGGCGTGCCCCAGATCGAGGTGACCTTCGACATCGACGCCAAC
3599
***** *****
1 GGCATCCTGAACGTACGGCCACGGACAAGAGCACCGGC AAGGCCAACAAGATCACCATC
1725
2 GGCATCCTGAACGTACGGCCACTGACAAGAGCACCGGC AAGGCCAACAAGATCACCATC
3659
***** *****
1 ACCAACGACAAGGGCCGCTGAGCAAGGAGGATCGAGCGCATGGTGCAGGAGGCGGAG
1785

```

2 ACCAACGACAAGGGCCGCCTGAGCAAGGAGGAGATCGAGCGCATGGTGCAGGAGGCCGAG
3719

1 AAGTACAAAGCGGAGGACGAGGTGCAGCGGAGAGGGTGTAGCCAAGAACGCCCTGGAG
1845
2 CGCTACAAGGCGGAGGACGAGGTGCAGCGGAGAGGGTGGCTGCCAAGAATGCGCTCGAG
3779

1 TCCTACGCCTTCAACATGAAGAGCGCCGTGGAGGATGAGGGCTCAAGGGCAAGATCAGC
1905
2 TCCTATGCCTTCAACATGAAGAGCGCCGTGGAGGACGAGGGTCTCAAGGGCAAGATCAGC
3839

1 GAGGCGGACAAGAAGGTTCTGGACAAGTGTCAGAGGTCACTCTGGCTGGACGCC
1965
2 GAGGCTGACAAGAAGGTTGCTGGACAAGTGCCAGGAGGTCACTCTGGCTGGACTCT
3899

1 AACACCTTGGCCGAGAAGGACGAGTTTGAAGCAAGAGGAAAGGAGCTGGAGCAGGTGTGT
2025
2 AACACGCTGGCTGAGAAAGAGGAGTTCTGTGCAAGCGGGAGGAGCTGGAGCGGGTGTGC
3959

1 AACCCCATCATCAGCGGACTGTACCAGGGTGCCGGTGGTCCCGGGCCTGGCGGCTTCGGG
2085
2 AACCCGATCATCAGCGGGTGTATCAGGGTGCCGGTGTCCCGGGCCTGGGGCTTCGGG
4019

1 GCTCAGGGTCCCAGGGAGGGTCTGGGTACAGCCCTACCATTGAGGAGGTGGATTAGGGG
2145
2 GCCCAGGCGCCCAGGGAGGCTCTGGGTCCGGGCCACCATCGAGGAGGTGGATTAGAGG
4079
** *****

1 CCTTTGT--TCTTTAGTATGTTTGTCTTTGAGGTGGACTGTTG--GGACTCAAGGACTTT
2201
2 CTTTCTGGCTCTCAGGGTGTGG--CTAGAGACAGACTCTTGATGGCTGCTGGTGCACG
4137
* * * * *

1 GCTGCTGTTTTCTATGTCAATTTCTGCTTCAGCTC--TTTGCTGCTTCACTTCTTTGTAA
2259
2 ATTCTTATCAAGTTACTCCTTCTCT-CCGGAGTTAGTTTAAAGTTACAGCCTTTTATA
4196
* * * * *

1 AGTTGT-AACTGA--TGGTA-ATTAGCTGGCTTCAATTATTTTTGTAGTACAACCGATA
2314
2 GGTAATTGATTTGAGTTTGTACATTTTGTATGCTCGTGGTTTTTTA-TATATTCAAT
4255
* * * * *

1 TGTTCAATTAGAATTCTTTGCATTTAATGTTGATA-CTGT----AAGGGTGTTCGTTCC
2368
2 TAAGGTTGCATGTTCTTTGCGTTTAACTAAGTAGCTGTGTAAAAATGGTGTTCCTTCC
4315
* * * * *

1 CTTTAAATGAATCAACACTGCCACCTTCTGTACGAGTTTGTGTTTTTTTTTTTTTTTT
2428
2 -TGCGAACCTCAGCACTGCCACCCTGTGTAC-AGTTTTTCTTGCATCCCTACAAAC
4373
* * * * *

2 TGA^{||}ACTCAGGACCTCTTCAAGAGCAGTCAGTGCTCTTAACTTCTGAGCCCTCTCTCCAGC
5213

1 -----
2 CCTTTATTACTTTTAGAGATTTCTTACCAGGTTGCCCTGGCTGTACTTACACTTTCTCTT
5273

1 -----
2 TAGCTCTGCTGAGCTTTCAATTCACCAGTTCCAGACCACACCCCTGAACCCACCAGCTGA
5333

1 -----
2 AGACAACATGTCTTGCTATCTTTTTCTTTCCTTTTTGGGGCAGGGATGGTCTGTGTGTTG
5393

1 -----
2 TGTGTGTGAGAGACAGAGGCAGAGACATCCTTCCCATGTAGCCCTAACTGAGTCGGAAGT
5453

1 -----
2 CATTATTTAGACCAGGCTGCCCTGACTCCTGTATCTGCCTCTCCAATGGATTATGGGCAC
5513

1 -----
2 CTGCCACCTCACCCACTCACTTTATCCCCAGGATCCCCCTCCCTCTTCCCAGGCAGTAGG
5573

1 -----
2 TCTGGTGATGGAGAAGACCACTTACCATGTCCATGGCTCAAAGAAGCAGGCAGAACGTAG
5633

1 -----
2 GGGAAAGAGTTGCTTTACCTCAAGCCTTTGGATCCATGGGTGTTTATTCTAGTGGGGTA
5693

1 -----
2 ATGCCATCCTTTGAGAGCTGGGGGTGTGGGTCAACAGAGATCGGTTGCTATGTGTGCAT
5753

1 -----
2 GAGCCCGCAATTCAGTCCCTGGCTCCATGGAGAACGAACCAATCAGTTGGGTGAGGTGT
5813

1 -----
2 AAACCACATGTAATTTTAGCATGTCCAAACAGACACGTTAAGGACATCCTAGGGTAAAGA
5873

1 -----
2 AGTCTTCAGCAATAGTTTAAATGAGGCAATTATGCTCATGAATTC 5918

KEY

- *|| Nucleotides are identical in all sequences in the alignment
- .|| Semi-conserved substitutions are observed
- :|| Conserved substitutions are observed

Appendix 9.21 Amino Acid Sequence for *HSPA1B* *Homo sapiens* v *Rattus norvegicus*

SeqA	Name	Len(aa)	SeqB	Name	Len(aa)	Score
1		1	2		2	96
1		641	2		641	96
1		60				
2		60				
1		120				
2		120				
1		180				
2		180				
1		240				
2		240				
1		300				
2		300				
1		360				
2		360				
1		420				
2		420				
1		480				
2		480				
1		540				
2		540				
1		600				
2		600				

MAKAAAIGIDLGTTYSCVGVFQHGKVEIIANDQGNRTTPSYVAFTDTERLIGDAAKNQVA
 MAKKTAIGIDLGTTYSCVGVFQHGKVEIIANDQGNRTTPSYVAFTDTERLIGDAAKNQVA
 *** :*****
 LNPQNTVFDKRLIGRKFDPVQSDMKHWPQVINDGDKPKVQVSYKGETKAFYPEEIS
 LNPQNTVFDKRLIGRKFDPVQSDMKHWPQVVDGDKPKVQVNYKGENRSFYPEEIS
 *****:*****.****.:*****
 SMVLTMKKEIAEAYLGPVTVNAVITVPAYFNDSQRQATKDAGVIAGLNVLRIINEPTAAA
 SMVLTMKKEIAEAYLGHPTNAVITVPAYFNDSQRQATKDAGVIAGLNVLRIINEPTAAA
 *****:*****
 IAYGLDRTGKGERNVLIFDLGGGTFDVSILTIDDGIFEVKATAGDTHLGGEDFDNRLVNH
 IAYGLDRTGKGERNVLIFDLGGGTFDVSILTIDDGIFEVKATAGDTHLGGEDFDNRLVSH
 *****.*
 FVEEFKRKHKKDISQNKRAVRRRLRTACERAKRTLSSSTQASLEIDSLFEGIDFYTSITRA
 FVEEFKRKHKKDISQNKRAVRRRLRTACERAKRTLSSSTQASLEIDSLFEGIDFYTSITRA

 RFEELCSDLFRSTLEPVEKALRDAKLDKAQIHDLVLVGGSTRIPKVQKLLQDFFNGRDLN
 RFEELCSDLFRGTLEPVEKALRDAKLDKAQIHDLVLVGGSTRIPKVQKLLQDFFNGRDLN
 *****.*
 KSINPDEAVAYGAAVQAAIILMGDKSENVQDLLLLDVAPLSLGLTAGGVMTALIKRNSTI
 KSINPDEAVAYGAAVQAAIILMGDKSENVQDLLLLDVAPLSLGLTAGGVMTALIKRNSTI

 PTKQTQIFTTYSDNQPGVLIQVYEGERAMTKDNNLLGRFELSGIPPAPRGVQIEVTFDI
 PTKQTQFTTTYSDNQPGVLIQVYEGERAMTRDNNLLGRFELSGIPPAPRGVQIEVTFDI
 *****:*****
 DANGILNVTATDKSTGKANKITITNDKGRLSKEEIERMVQEAERYKAEDEVQRERVAKN
 DANGILNVTATDKSTGKANKITITNDKGRLSKEEIERMVQEAERYKAEDEVQRERVAKN
 *****:*****:
 ALESYAFNMKSAVEDEGLKGISEADKKKVLKQEVISWLDANTLAEKDEFVHKRKELE
 ALESYAFNMKSAVEDEGLKGISEADKKKVLKQEVISWLDANTLAEKEEFVHKREELE
 *****:*****:***

Appendix 9.23 Amino Acid Sequence for *HSPA1L* *Homo sapiens* v *Rattus norvegicus*

SeqA	Name	Len(aa)	SeqB	Name	Len(aa)	Score
1		641	2		641	94
=====						
1	MATAK	GIAIG	IDLGT	TYS	CVGVF	QHGKVEIIANDQGNRTTPSYVAFTDTERLIGDAAKNQ 60
2	MAANK	GMAIG	IDLGT	TYS	CVGVF	QHGKVEIIANDQGNRTTPSYVAFTDTERLIGDAAKNQ 60
				** :		
** : *****						
1	VAMNP	QNTVF	DAKRL	IGRKF	NDP	VVQADMKLWPFQVINEGGPKVLSYKGENKAFYPEE 120
2	VAMNP	QNTVF	DAKRL	IGRKF	NDP	VVQSDMKLWPFQVINEAGPKVLSYKGEKKAFYPEE 120
***** : ***** . ***** : *****						
1	ISSMV	LTKL	KETA	EAF	LGH	PVTNAVITVPAYFNDSQRQATKDAGVIAGLNVLRIINEPTA 180
2	ISSMV	LTKM	KETA	EAF	LGH	SVTNAVITVPAYFNDSQRQATKDAGVIAGLNVLRIINEPTA 180
***** : ***** . ***** : *****						
1	AAIAY	GLDK	GGQ	GER	HVL	IFDLGGGTFDVSILTIDDGIFEVKATAGDTHLGGEDFDNRLV 240
2	AAIAY	GLDK	GSH	GER	HVL	IFDLGGGTFDVSILTIDDGIFEVKATAGDTHLGGEDFDNRLV 240
***** . : *****						
1	SHFV	EEFK	RKH	KKDIS	QNKRA	VRRLRTACERAKRTLSSTQANLEIDSLYEGIDFYTSIT 300
2	SHFV	EEFK	RKH	KKDIS	QNKRA	VRRLRTACERAKRTLSSTQANLEIDSLYEGIDFYTSIT 300

1	RARFE	ELCAD	LFRGT	LEP	VEKAL	RDAMDKAKIHDIVLVGGSTRIPKVQRLQDYFNDRD 360
2	RARFE	ELCAD	LFRGT	LEP	VEKSL	RDAMDKAKIHDIVLVGGSTRIPKVQKLLQDYFNDRD 360
***** : ***** : *****						
1	LNKS	INP	DEAV	AYGAA	VQAAIL	MGDKSEKVQDLLLLDVAPLSLGLTAGGVM TALIKRNS 420
2	LNKS	INP	DEAV	AYGAA	VQAAIL	MGDKSEKVQDLLLLDVAPLSLGLTAGGVM TVLIKRNS 420
***** . *****						
1	TIPTK	QTQI	FTTYS	DNQP	GVLIQ	VYEGERAMTKDNNLLGRFDLTGIPPAPRGVPQIEVTF 480
2	TIPTK	QTQI	FTTYS	DNQP	GVLIQ	VYEGERAMTRDNNLLGRFDLTGIPPAPRGVPQIEVTF 480

Appendix 9.24 Gene Sequence Alignment for *GAPDH Homo sapiens v Rattus norvegicus*

CLUSTAL 2.0.12 multiple sequence alignment

```

SeqA NameLen(nt)  SeqB NameLen(nt)  Score
=====
1      1    1310      2      2    1307      84
=====

1      AAATTGAGCCCGAGCCTCCCCTTCGCTCTCTGCTCCTCC-TGTTTCGACAGTCAGCCGC
59
2      -----GGGGGCTCTCTGCTCCTCCCTGTTCTAGAGACAGCCGC
38
                                     ***** * * * *****

1      ATCTTCTTTTGCCTGCCAGCCGAGCCACATCGCTCAGACACCATGGGGAAGGTGAAGGT
119
2      ATCTTCTTGTGCAGTGCCAGCCTCGTCTCAT-----AGACA-----AGATGGTGAAGGT
87
                                     ***** * * * *****

1      CGGAGTCAAACGGATTTGGTTCGTATTGGGCGCCTGGTACCAGGGCTGCTTTTAACTCTGG
179
2      CGGTGTGAACGGATTTGGCCGTATCGGACGCCTGGTTACCAGGGCTGCCTTCTTTGTGA
147
                                     *** * * ***** * * ***** * * *

1      TAAAGTGGATATTGTTGCCATCAATGACCCCTTCATTGACCTCAACTACATGGTTTACAT
239
2      CAAAGTGGACATTGTTGCCATCAACGACCCCTTCATTGACCTCAACTACATGGTCTACAT
207
                                     ***** ***** ***** *****

1      GTTCCAATATGATTCCACCCATGGCAAATTCATGGCACCGTCAAGGCTGAGAACGGGAA
299
2      GTTCCAGTATGACTCTACCCACGGCAAGTTCACGGCACAGTCAAGGCTGAGAAATGGGAA
267
                                     ***** * * * ***** ***** ***** *****

1      GCTTGTCAATGGAATCCCATCACCATCTTCCAGGAGCGAGATCCCTCCAAAATCAA
359
2      GCTGGTCAATCAACGGGAAACCCATCACCATCTTCCAGGAGCGAGATCCCGCTAACATCAA
327
                                     *** ***** * * * ***** ***** ***** * * *

1      GTGGGGCGATGCTGGCGCTGAGTACGTCGTGGAGTCCACTGGCGTCTTACCACCATGGA
419
2      ATGGGGTATGCTGGTGTGAGTATGTCGTGGAGTCTACTGGCGTCTTACCACCATGGA
387
                                     ***** ***** ***** ***** ***** *****

1      GAAGGCTGGGGCTCATTGCAAGGGGGAGCCAAAAGGGTCATCATCTCTGCCCCCTCTGC
479
2      GAAGGCTGGGGCTCACCTGAAGGGTGGGGCCAAAAGGGTCATCATCTCCGCCCTTCCGC
447
                                     ***** * * * ***** ***** ***** ***** * * *

1      TGATGCCCCATGTTTCGTCATGGGTGTGAACCATGAGAAGTATGACAACAGCCTCAAGAT
539
2      TGATGCCCCATGTTTGTGATGGGTGTGAACACGAGAAATATGACAACCCCTCAAGAT
507
                                     ***** * * * ***** ***** ***** *****

1      CATCAGCAATGCCTCCTGCACCACCAACTGCTTAGCACCCCTGGCCAAGGTCAATCCATGA
599

```

2 TGTCAGCAATGCATCCTGCACCACCAACTGCTTAGCCCCCTGGCCAAGGTCATCCATGA
567 *****

1 CAACTTTGGTATCGTGGAAAGACTCATGACCACAGTCCATGCCATCACTGCCACCCAGAA
659
2 CAACTTTGGCATCGTGGAAAGGCTCATGACCACAGTCCATGCCATCACTGCCACTCAGAA
627 *****

1 GACTGTGGATGGCCCTCCGGGAAACTGTGGCGTGATGGCCGCGGGGCTCTCCAGAACAT
719
2 GACTGTGGATGGCCCTCTGGAAGCTGTGGCGTGATGGCCGTGGGGCAGCCAGAACAT
687 *****

1 CATCCCTGCCTCTACTGGCGTGCCAAGGCTGTGGGCAAGGTCATCCCTGAGCTGAACGG
779
2 CATCCCTGCATCCACTGGTGCTGCCAAGGCTGTGGGCAAGGTCATCCAGAGCTGAACGG
747 *****

1 GAAGCTCACTGGCATGGCCTTCCGTGTCCCACTGCCAACGTGTCAGTGGTGGACCTGAC
839
2 GAAGCTCACTGGCATGGCCTTCCGTGTTCCCTACCCCAATGTATCCGTTGTGGATCTGAC
807 *****

1 CTGCCGTCTAGAAAACCTGCCAAATATGATGACATCAAGAAGGTGGTGAAGCAGGCGTC
899
2 ATGCCGCTGAGAAAACCTGCCAAGTATGATGACATCAAGAAGGTGGTGAAGCAGGCGGC
867 *****

1 GGAGGGCCCCCTCAAGGGCATCCTGGGCTACACTGAGCACCAGGTGGTCTCCTCTGACTT
959
2 CGAGGGCCCACTAAAGGGCATCCTGGGCTACACTGAGGACCAGGTGTCTCCTGTGACTT
927 *****

1 CAACAGCGACACCCACTCCTCCACCTTTGACGCTGGGGCTGGCATTGCCCTAACGACCA
1019
2 CAACAGCAACTCCATTCTCCACCTTTGATGCTGGGGCTGGCATTGCTCTCAATGACAA
987 *****

1 CTTTGTCAAAGCTCATTTCCTGGTATGACAAAGAAATTTGGCTACAGCAACAGGGTGGTGA
1079
2 CTTTGTGAAGCTCATTTCCTGGTATGACAAATGAAATATGGCTACAGCAACAGGGTGGTGA
1047 *****

1 CCTCATGGCCACATGGCCTCCAAGGAGTAAGAC-CCCTGGACCACCAGCCCCAGCAAGA
1138
2 CCTCATGGCCTACATGGCCTCCAAGGAGTAAGAAACCTGGACCACCAGCCCCAGCAAGG
1107 *****

1 GCAC-AAGAGGAAGAGAGAGACCCTCA-CTGCTGGGGAGTCCCTGCCACACTCAGTCCCC
1196
2 ATACTGAGAGCAAGAGAGAGGCCCTCAGTTGCTGAGGAGTCCCATCCCAACTCAGCCCC
1167 *****

1 CACCACACTGAATCTCCCCTCCTCACAGTTGCCATGTAGACCCCTTGAAGAGGGGAGGGG
1256
2 CA--ACACTGAGCATCTCC--CTCACAAATCCATCCAGACCCCAATAACAACAGGAGGGG
1223 *****

```

1          CCTAGGGAGCCGCACCTTGTCATG--TACCATCAATAAAGTACCCTGTGC--TCAACC--
1310
2          CCTGGGGAGCCCTCCCTTCTCTCGAATACCATCAATAAAGTTCGCTGCACCCTCAAAAAA
1283
          ***  *****      *****  **  *  *****  *****  *  ***  *  *****

1          -----
2          AAAAAAAAAAAAAAAAAAAAAAAAAA 1307

```

KEY

- *|| Nucleotides are identical in all sequences in the alignment
- .|| Semi-conserved substitutions are observed
- :|| Conserved substitutions are observed

Appendix 9.25 Amino Acid Sequence for *GAPDH Homo sapiens v Rattus norvegicus*

CLUSTAL 2.0.12 multiple sequence alignment

```

SeqA NameLen(aa)  SeqB NameLen(aa)  Score
=====
1      1      335      2      2      333      93
=====

1      MGKVKVGVNGFGRIGRLVTRAAFNSGKVDIVAINDPFIDLNYMVYMFQYDSTHGKFGHTV
60
2      --MVKVGVNGFGRIGRLVTRAAFSCKVDIVAINDPFIDLNYMVYMFQYDSTHGKFNQTV
58
          ***** . . ***** : ***

1      KAENGLVINGNPITIFQERDPSKIKWGDAGAEYVVESTGVFTTMEKAGAHLQGGAKRVI
120
2      KAENGLVINGKIPITIFQERDPANIKWGDAGAEYVVESTGVFTTMEKAGAHLKGGAKRVI
118
          ***** : ***** : ***** : *****

1      ISAPSADAPMFVMGVNHEKYDNSLKIIISNASCTTNCLAPLAKVIHDFNGIVEGLMTTVHA
180
2      ISAPSADAPMFVMGVNHEKYDNSLKIVSNASCTTNCLAPLAKVIHDFNGIVEGLMTTVHA
178
          ***** : *****

1      ITATQKTVDGPGSKLWRDGRGALQNIIPASTGAAKAVGKVIPELNGKLTGMAFRVPTANV
240
2      ITATQKTVDGPGSKLWRDGRGAAQNIIPASTGAAKAVGKVIPELNGKLTGMAFRVPTPNV
238
          ***** ***** . **

1      SVVDLTCRLEKPAKYDDIKKVVKQASEGPLKGILGYTEHQVSSDFNSDTHSSTFDAGAG
300
2      SVVDLTCRLEKPAKYDDIKKVVKQAAEGPLKGILGYTEDQVVSDFNSNSHSSTFDAGAG
298
          ***** : ***** . **** . **** : *****

1      IALNDHFVKLISWYDNEFGYSNRVVDLMAHMASK- 334
2      IALNDNFVKLISWYDNEYGYSNRVVDLMAYMASKE 333
          ***** : ***** : ***** : *****

```

KEY

- *|| Nucleotides are identical in all sequences in the alignment
- .|| Semi-conserved substitutions are observed
- :|| Conserved substitutions are observed

MVFILAPW Non polar R-groups
GNTSYQHC Polar R-groups
KR Positively charged R-groups
DE Negatively charged R-groups

Appendix 9.26 BLAST analysis showing sequences producing significant alignments for HSPA1A:

<u>Accession</u>	<u>Description</u>	<u>Max score</u>	<u>Total score</u>	<u>Query coverage</u>	<u>E value</u>	<u>Max ident</u>	<u>Links</u>
Transcripts							
NM_005345.5	Homo sapiens heat shock 70kDa protein 1A (HSPA1A), mRNA	4516	4516	100%	0.0	100%	U E G M
NM_005346.4	Homo sapiens heat shock 70kDa protein 1B (HSPA1B), mRNA	3801	3801	88%	0.0	99%	U E G M
NM_005527.3	Homo sapiens heat shock 70kDa protein 1-like (HSPA1L), mRNA	1620	1620	73%	0.0	83%	U E G M
NM_002155.3	Homo sapiens heat shock 70kDa protein 6 (HSP70B') (HSPA6), mRNA	1580	1580	73%	0.0	83%	U E G M
NM_021979.3	Homo sapiens heat shock 70kDa protein 2 (HSPA2), mRNA	1524	1524	74%	0.0	82%	U E G M
NR_024151.1	Homo sapiens heat shock 70kDa protein 7 (HSP70B) (HSPA7), non-coding RNA	1474	1474	73%	0.0	82%	E G M

Appendix 9.27 BLAST analysis showing sequences producing significant alignments for HSPA designed primers:

<u>Accession</u>	<u>Description</u>	<u>Max score</u>	<u>Total score</u>	<u>Query coverage</u>	<u>E value</u>	<u>Max ident</u>	<u>Links</u>
Transcripts							
NM_005346.4	Homo sapiens heat shock 70kDa protein 1B (HSPA1B), mRNA	42.1	82.3	100%	0.027	100%	U E G M
NM_005345.5	Homo sapiens heat shock 70kDa protein 1A (HSPA1A), mRNA	42.1	82.3	100%	0.027	100%	U E G M
NM_001254.3	Homo sapiens cell division cycle 6 homolog (S. cerevisiae) (CDC6), mRNA	34.2	34.2	52%	6.5	95%	U E G M
NM_021979.3	Homo sapiens heat shock 70kDa protein 2 (HSPA2), mRNA	34.2	66.4	82%	6.5	100%	U E G M
NR_024151.1	Homo sapiens heat shock 70kDa protein 7 (HSP70B) (HSPA7), non-coding RNA	34.2	34.2	42%	6.5	100%	E G M
NM_002155.3	Homo sapiens heat shock 70kDa protein 6 (HSP70B') (HSPA6), mRNA	34.2	34.2	42%	6.5	100%	U E G M
NM_022473.1	Homo sapiens zinc finger protein 106 homolog (mouse) (ZFP106), mRNA	32.2	32.2	40%	26	100%	U E G M
NM_033044.3	Homo sapiens microtubule-actin crosslinking factor 1 (MACF1), transcript variant 2, mRNA	32.2	32.2	40%	26	100%	M
NM_012090.4	Homo sapiens microtubule-actin crosslinking factor 1 (MACF1), transcript variant 1, mRNA	32.2	32.2	40%	26	100%	U G M *
NM_006391.2	Homo sapiens importin 7 (IPO7), mRNA	30.2	30.2	57%	101	91%	U E G M

Accession	Description	<u>Max score</u>	<u>Total score</u>	<u>Query coverage</u>	<u>E value</u>	<u>Max ident</u>	Links
NM_018411.4	Homo sapiens hairless homolog (mouse) (HR), transcript variant 2, mRNA	30.2	30.2	37%	101	100%	
NM_005144.4	Homo sapiens hairless homolog (mouse) (HR), transcript variant 1, mRNA	30.2	30.2	37%	101	100%	